



ROLES OF REGULATORY RNAs IN BACTERIAL PATHOGENS

EDITED BY: Olga Soutourina and Florence Hommais
PUBLISHED IN: *Frontiers in Microbiology*



frontiers

Frontiers eBook Copyright Statement

The copyright in the text of individual articles in this eBook is the property of their respective authors or their respective institutions or funders. The copyright in graphics and images within each article may be subject to copyright of other parties. In both cases this is subject to a license granted to Frontiers.

The compilation of articles constituting this eBook is the property of Frontiers.

Each article within this eBook, and the eBook itself, are published under the most recent version of the Creative Commons CC-BY licence.

The version current at the date of publication of this eBook is CC-BY 4.0. If the CC-BY licence is updated, the licence granted by Frontiers is automatically updated to the new version.

When exercising any right under the CC-BY licence, Frontiers must be attributed as the original publisher of the article or eBook, as applicable.

Authors have the responsibility of ensuring that any graphics or other materials which are the property of others may be included in the CC-BY licence, but this should be checked before relying on the CC-BY licence to reproduce those materials. Any copyright notices relating to those materials must be complied with.

Copyright and source acknowledgement notices may not be removed and must be displayed in any copy, derivative work or partial copy which includes the elements in question.

All copyright, and all rights therein, are protected by national and international copyright laws. The above represents a summary only. For further information please read Frontiers' Conditions for Website Use and Copyright Statement, and the applicable CC-BY licence.

ISSN 1664-8714

ISBN 978-2-88976-538-6

DOI 10.3389/978-2-88976-538-6

About Frontiers

Frontiers is more than just an open-access publisher of scholarly articles: it is a pioneering approach to the world of academia, radically improving the way scholarly research is managed. The grand vision of Frontiers is a world where all people have an equal opportunity to seek, share and generate knowledge. Frontiers provides immediate and permanent online open access to all its publications, but this alone is not enough to realize our grand goals.

Frontiers Journal Series

The Frontiers Journal Series is a multi-tier and interdisciplinary set of open-access, online journals, promising a paradigm shift from the current review, selection and dissemination processes in academic publishing. All Frontiers journals are driven by researchers for researchers; therefore, they constitute a service to the scholarly community. At the same time, the Frontiers Journal Series operates on a revolutionary invention, the tiered publishing system, initially addressing specific communities of scholars, and gradually climbing up to broader public understanding, thus serving the interests of the lay society, too.

Dedication to Quality

Each Frontiers article is a landmark of the highest quality, thanks to genuinely collaborative interactions between authors and review editors, who include some of the world's best academicians. Research must be certified by peers before entering a stream of knowledge that may eventually reach the public - and shape society; therefore, Frontiers only applies the most rigorous and unbiased reviews.

Frontiers revolutionizes research publishing by freely delivering the most outstanding research, evaluated with no bias from both the academic and social point of view. By applying the most advanced information technologies, Frontiers is catapulting scholarly publishing into a new generation.

What are Frontiers Research Topics?

Frontiers Research Topics are very popular trademarks of the Frontiers Journals Series: they are collections of at least ten articles, all centered on a particular subject. With their unique mix of varied contributions from Original Research to Review Articles, Frontiers Research Topics unify the most influential researchers, the latest key findings and historical advances in a hot research area! Find out more on how to host your own Frontiers Research Topic or contribute to one as an author by contacting the Frontiers Editorial Office: frontiersin.org/about/contact

ROLES OF REGULATORY RNAs IN BACTERIAL PATHOGENS

Topic Editors:

Olga Soutourina, UMR9198 Institut de Biologie Intégrative de la Cellule (I2BC),
France

Florence Hommais, Université Claude Bernard Lyon 1, France

Citation: Soutourina, O., Hommais, F., eds. (2022). Roles of Regulatory RNAs in
Bacterial Pathogens. Lausanne: Frontiers Media SA.
doi: 10.3389/978-2-88976-538-6

Table of Contents

04	<i>Editorial: Roles of Regulatory RNAs in Bacterial Pathogens</i>
	Florence Hommais and Olga Soutourina
07	<i>AtxA-Controlled Small RNAs of Bacillus anthracis Virulence Plasmid pXO1 Regulate Gene Expression in trans</i>
	Ileana D. Corsi, Soumita Dutta, Ambro van Hoof and Theresa M. Koehler
31	<i>RNA-Mediated Control in Listeria monocytogenes: Insights Into Regulatory Mechanisms and Roles in Metabolism and Virulence</i>
	Agata Krawczyk-Balska, Magdalena Ładziak, Michał Burmistrz, Katarzyna Ścibek and Birgitte H. Kallipolitis
49	<i>Three Ribosomal Operons of Escherichia coli Contain Genes Encoding Small RNAs That Interact With Hfq and CsrA in vitro</i>
	Thomas Søndergaard Stenum, Mette Kongstad, Erik Holmqvist, Birgitte Kallipolitis, Sine Lo Svenningsen and Michael Askvad Sørensen
67	<i>Transfer RNA-Derived Fragments, the Underappreciated Regulatory Small RNAs in Microbial Pathogenesis</i>
	Zhongyou Li and Bruce A. Stanton
76	<i>OmpA, a Common Virulence Factor, Is Under RNA Thermometer Control in Yersinia pseudotuberculosis</i>
	Daniel Scheller, Christian Twittenhoff, Franziska Becker, Marcel Holler and Franz Narberhaus
87	<i>An Inventory of CiaR-Dependent Small Regulatory RNAs in Streptococci</i>
	Nancy Jabbour and Marie-Frédérique Lartigue
100	<i>RNA Chaperones Hfq and ProQ Play a Key Role in the Virulence of the Plant Pathogenic Bacterium Dickeya dadantii</i>
	Simon Leonard, Camille Villard, William Nasser, Sylvie Reverchon and Florence Hommais
116	<i>Riboregulation in the Major Gastric Pathogen Helicobacter pylori</i>
	Alejandro Tejada-Arranz and Hilde De Reuse
126	<i>Assembling the Current Pieces: The Puzzle of RNA-Mediated Regulation in Staphylococcus aureus</i>
	Laura Barrientos, Noémie Mercier, David Lalaouna and Isabelle Caldelari
133	<i>The Small Protein YmoA Controls the Csr System and Adjusts Expression of Virulence-Relevant Traits of Yersinia pseudotuberculosis</i>
	Katja Böhme, Ann Kathrin Heroven, Stephanie Lobedann, Yuzhu Guo, Anne-Sophie Stolle and Petra Dersch
154	<i>Diversity and Versatility in Small RNA-Mediated Regulation in Bacterial Pathogens</i>
	Brice Felden and Yoann Augagneur
179	<i>The Small RNA ErsA Impacts the Anaerobic Metabolism of Pseudomonas aeruginosa Through Post-Transcriptional Modulation of the Master Regulator Anr</i>
	Silvia Ferrara, Riccardo Carrubba, Silvia Santoro and Giovanni Bertoni



Editorial: Roles of Regulatory RNAs in Bacterial Pathogens

Florence Hommais¹ and Olga Soutourina^{2,3*}

¹ Université de Lyon, Université Claude Bernard Lyon 1, INSA-Lyon, CNRS, UMR5240 MAP, Villeurbanne, France, ² Université Paris-Saclay, CEA, CNRS, Institute for Integrative Biology of the Cell (I2BC), Gif-sur-Yvette, France, ³ Institut Universitaire de France (IUF), Paris, France

Keywords: metabolism, physiology and virulence control, diversity of regulatory RNAs, RNA-based mechanisms, plant, human, animal pathogens, host-pathogen interactions

Editorial on the Research Topic

Roles of Regulatory RNAs in Bacterial Pathogens

Since the discovery of the first regulatory RNAs in bacteria, the amount of data on potential RNA regulators has been consistently increasing, particularly over the last couple of years. Recent technical advances have led to the identification of a large number of highly diverse regulatory RNAs, as well as their potential targets. While not all of their biological roles and molecular mechanisms of action are known, we have begun to appreciate their importance in regulatory networks governing bacterial physiology and infectious processes. In bacterial pathogens, non-coding RNAs have been recently identified as central players reprogramming gene expression in response to environmental constraints in order to adapt bacterial physiology and metabolism to host conditions. This Research Topic is focused on the role of regulatory RNAs from bacterial pathogens and is dedicated to the memory of Brice Felden and his contributions to the field of bacterial small RNAs (sRNAs). We have collected 12 excellent papers encompassing 6 original research articles and 6 reviews covering different aspects of RNA-based regulation in pathogens, which belong to both Gram-positive and Gram-negative bacteria. While many of them are focusing on human and animal pathogens including extracellular (*Helicobacter pylori*, *Yersinia pseudotuberculosis*, *Pseudomonas aeruginosa*, *Bacillus anthracis*), intracellular (*Listeria monocytogenes*), and opportunistic pathogens (*Staphylococcus aureus*, *Streptococci*), one study also presents results on a phytopathogenic bacterium (*Dickeya dadantii*).

A review by Felden and Augagneur provides a good overview of the diversity of pathophysiological and metabolic processes targeted by RNAs and the diversity of the RNAs themselves in terms of their genomic location, biogenesis, and mode of action. Recent studies extended the boundaries of regulatory RNA classes with novel mechanisms of action and biogenesis that are constantly discovered. They suggest a broad definition of bacterial sRNA as any RNA molecule that interacts with other actors to regulate gene expression.

Four review papers in this Research Topic are devoted to riboregulation in a particular pathogen with a specific focus on Gram-positive pathogens for three of them. First, Tejada-Arranz and De Reuse covered different aspects of RNA-based regulatory mechanisms in an important Gram-negative gastric pathogen *H. pylori*. With only a few transcriptional regulators described in this pathogen, the posttranscriptional level occupies a major but original position in the control of gene expression for efficient colonization of the hostile acidic environment inside the stomach.

OPEN ACCESS

Edited and reviewed by:

Marc Strous,
University of Calgary, Canada

*Correspondence:

Olga Soutourina
olga.soutourina@
universite-paris-saclay.fr

Specialty section:

This article was submitted to
Microbial Physiology and Metabolism,
a section of the journal
Frontiers in Microbiology

Received: 07 April 2022

Accepted: 26 April 2022

Published: 15 June 2022

Citation:

Hommais F and Soutourina O (2022)
Editorial: Roles of Regulatory RNAs in
Bacterial Pathogens.
Front. Microbiol. 13:915005.
doi: 10.3389/fmicb.2022.915005

The absence of well-described Hfq and ProQ chaperones suggests that *H. pylori* do not follow the general rules established in model bacteria like *Escherichia coli* and *Salmonella*. The authors also highlight the role of riboregulation in persister formation via toxin-antitoxin mechanisms and in phase variation.

Second, the review by Krawczyk-Balska et al. summarizes 20 years of research on the RNA-mediated regulation of virulence and metabolism in *L. monocytogenes* starting from the identification of the thermosensor at the 5'UTR of the gene-encoding master regulator of virulence, PrfA. A number of unique regulatory mechanisms were discovered in this pathogen including rare examples among Gram-positive bacteria of RNA chaperone Hfq-associated RNAs (LhrA, LhrB, and LhrC1-5), the first evidence for riboswitch-derived sRNA SreA acting *in trans* to inhibit *prfA* mRNA translation, new dual-function long antisense RNAs named excludons acting both as *cis*-antisense RNAs and mRNAs, and finally, the secreted RNAs that modulate the innate immune response in the host through the interaction with the RNA sensor RIG-I.

In *S. aureus*, regulatory RNAs are placed together with transcriptional regulators at the center of the regulatory network ensuring successful adaptation of this opportunistic pathogen to various infection sites. Besides the well-described RNA III, the review by Barrientos et al. assembles the pieces of the puzzle from our current knowledge of riboregulation governing metabolism, stress responses, and virulence. The authors discussed the future challenges to fill the gaps in this regulatory puzzle to understand the significance of recent data on different sRNA interconnections and to identify new RNA-binding proteins important for RNA metabolism and action in *S. aureus*.

In addition to these reviews, several investigators in this Research Topic addressed the role of sRNAs in complex regulatory networks orchestrating the control of virulence factor expressions during the different stages of bacterial infection. They highlighted the interconnection of transcriptional regulation by transcriptional factors and post-transcriptional regulation by sRNAs. The role of sRNAs controlled by the two-component system CiaRH in bacterial adaptation, virulence, and resistance to antibiotics and to the host immune system is discussed in the review by Jabbour and Lartigue. These sRNAs are conserved in the *Streptococcus* genus. The authors present a comprehensive inventory for this class of sRNAs, named csRNAs, and addressed open questions on the presence and role of multiple homologous sRNAs in the CiaRH regulons. Among the original research articles, Corsi et al. characterized two regulatory sRNAs whose expression is dependent upon the master virulence regulator of *B. anthracis* AtxA, and Böhme et al. demonstrated the control of the sRNA CsrC by YmoA, a member of the Hha family in *Y. pseudotuberculosis*. The expression of virulence factors is in close association with stress adaption. In this area, Ferrara et al. characterized an sRNA named ErsA, suggesting its role in the regulation of the master regulator of anaerobiosis in *P. aeruginosa*, whereas Scheller et al. described an RNA thermometer in the 5'UTR of the *Y. pseudotuberculosis ompA* transcript involved in

the host-body temperature-dependent control of this outer membrane protein known as an important virulence factor. Finally, the study by Leonard et al. on *D. dadantii* strains defective for the RNA chaperones Hfq and ProQ suggests that sRNAs would regulate targets during the different steps of the infection process. The lack of these well-characterized RNA chaperones in some bacterial groups or their questionable role in the majority of Gram-positive bacteria suggests the involvement of additional proteins in sRNA-based regulations (Tejada-Arranz and De Reuse; Barrientos et al.; Felden and Augagneur).

The RNA-mediated host-pathogen crosstalk could even be deeper. Li and Stanton discuss the underappreciated role of extracellular vesicles (EVs) for the transfer of sRNAs, especially tRNA fragments, and the role of EVs in the inter- and intra-kingdom communications without direct cell-cell contact. Based on results obtained in *P. aeruginosa* and *H. pylori*, the authors propose that tRNA fragment products delivered into the host cells by EVs would allow them to hijack the host immune response to enhance pathogen survival and that this mechanism would be widespread. Indeed, recent studies explored the secRNome of major Gram-negative and Gram-positive pathogens including secreted RNAs and vesicle-derived RNAs that could modulate the host immune response as a new mechanism for host-pathogen interactions (Lécrivain and Beckmann, 2020).

In addition to house-keeping tRNAs as a potential source of regulatory RNAs (Lalaouna et al., 2015; Li and Stanton), Stenum et al. described three sRNAs named RrA, RrB, and RrF generated from tRNA-linked repeats located downstream from the 5S gene within the ribosomal operons *rrnA*, *rrnB*, and *rrnD* in *E. coli*. Despite modest phenotypic effects of deletion or overexpression of these sequences in *E. coli*, their conservation in different Enterobacteria, including pathogenic species, suggests a role for these sRNAs in the fine-tuned regulation of growth phase-related processes. In eukaryotes, together with numerous tRNA-derived fragments controlling important cellular processes, several functional miRNAs have been identified as co-transcribed with rRNA primary transcripts. Further studies will define the function of these newly described bacterial sRNAs derived from ribosomal operons.

The regulatory RNA genes can be located not only in bacterial chromosomes but also within mobile genetic elements, including prophage-, pathogenicity island- and plasmid-associated RNAs. As an example, Corsi et al. characterized two sRNAs named XrrA and XrrB encoded from the virulence pXO1 plasmid of *B. anthracis*. These sRNAs are highly conserved upon closely related species carrying pXO1-like plasmids, and despite their plasmid loci, these regulatory RNAs control multiple target genes on the chromosome, placing these RNAs at the center of the crosstalk between genetic elements of *B. anthracis*. This is the second example of plasmid-transcribed regulatory sRNA controlling chromosomal-encoded targets relating to virulence suggesting such regulation could be widespread.

CONCLUDING REMARKS AND PERSPECTIVES

All original research and review articles in this Research Topic highlight the importance of RNA-based mechanisms in bacterial pathogens. Numerous new facets of these regulations shaping the adaptive and pathogenic processes both in the bacterium and in its host remain to be explored, generating several directions for future research. Among them, future studies should address questions about the roles of RNAs in the regulatory crosstalk of bacterial pathogens with their hosts and within complex microbial communities focusing on the interactions of sRNAs with both the bacterial and host RNA-binding proteins, the role of RNAs in persister formation, in phase variation, and in the interplay between mobile genetic elements, and the bacterial chromosomes that question evolutionary aspects of regulatory RNA transfer and maintenance. Furthermore, regulatory RNA integration into complex genetic circuits and impact of cellular compartmentation on sRNA regulation should be investigated. Such accumulating knowledge should provide an excellent basis for innovative therapeutic approaches targeting both protein and RNA components of regulatory networks to

control pathogen development and dissemination of adaptive traits within bacterial populations.

AUTHOR CONTRIBUTIONS

FH and OS wrote the manuscript. Both authors contributed to the article and approved the submitted version.

FUNDING

This work was supported by grants from the University of Lyon 1, the CNRS, the University Paris-Saclay, the Institute for Integrative Biology of the Cell, the DIM-1HEALTH regional Ile-de-France program (LSP Grant No. 173403), the CNRS-RFBR PRC 2019 (Grant Nos. 288426 and 19-54-15003), and the Institut Universitaire de France.

ACKNOWLEDGMENTS

We are grateful to all authors that contributed their work to this Research Topic and the experts that provided their reviews for the manuscripts submitted, and the editorial support of the Journal.

REFERENCES

- Lalaouna, D., Carrier, M.-C., Semsey, S., Brouard, J.-S., Wang, J., Wade, J. T., et al. (2015). A 3' External transcribed spacer in a tRNA transcript acts as a sponge for small RNAs to prevent transcriptional noise. *Mol. Cell* 58, 393–405. doi: 10.1016/j.molcel.2015.03.013
- Lécrivain, A.-L., and Beckmann, B. M. (2020). Bacterial RNA in extracellular vesicles: A new regulator of host-pathogen interactions? *Biochim. Biophys. Acta* 1863, 194519. doi: 10.1016/j.bbagr.2020.194519

Conflict of Interest: The authors declare that the research was conducted in the absence of any commercial or financial relationships that could be construed as a potential conflict of interest.

Publisher's Note: All claims expressed in this article are solely those of the authors and do not necessarily represent those of their affiliated organizations, or those of the publisher, the editors and the reviewers. Any product that may be evaluated in this article, or claim that may be made by its manufacturer, is not guaranteed or endorsed by the publisher.

Copyright © 2022 Hommais and Soutourina. This is an open-access article distributed under the terms of the Creative Commons Attribution License (CC BY). The use, distribution or reproduction in other forums is permitted, provided the original author(s) and the copyright owner(s) are credited and that the original publication in this journal is cited, in accordance with accepted academic practice. No use, distribution or reproduction is permitted which does not comply with these terms.



AtxA-Controlled Small RNAs of *Bacillus anthracis* Virulence Plasmid pXO1 Regulate Gene Expression *in trans*

Ileana D. Corsi^{1,2}, Soumita Dutta¹, Ambro van Hoof^{1,2} and Theresa M. Koehler^{1,2*}

¹ Department of Microbiology and Molecular Genetics, McGovern Medical School, The University of Texas Health Science Center at Houston, Houston, TX, United States, ² MD Anderson Cancer Center UTHealth Graduate School of Biomedical Sciences, The University of Texas, Houston, TX, United States

OPEN ACCESS

Edited by:

Ruiting Lan,
University of New South Wales,
Australia

Reviewed by:

Franz Narberhaus,
Ruhr-University Bochum, Germany
Olga Soutourina,
UMR 9198 Institut de Biologie
Intégrative de la Cellule (I2BC), France

*Correspondence:

Theresa M. Koehler
Theresa.M.Koehler@uth.tmc.edu

Specialty section:

This article was submitted to
Evolutionary and Genomic
Microbiology,
a section of the journal
Frontiers in Microbiology

Received: 24 September 2020

Accepted: 11 December 2020

Published: 15 January 2021

Citation:

Corsi ID, Dutta S, van Hoof A and
Koehler TM (2021) AtxA-Controlled
Small RNAs of *Bacillus anthracis*
Virulence Plasmid pXO1 Regulate
Gene Expression *in trans*.
Front. Microbiol. 11:610036.
doi: 10.3389/fmicb.2020.610036

Small regulatory RNAs (sRNAs) are short transcripts that base-pair to mRNA targets or interact with regulatory proteins. sRNA function has been studied extensively in Gram-negative bacteria; comparatively less is known about sRNAs in Firmicutes. Here we investigate two sRNAs encoded by virulence plasmid pXO1 of *Bacillus anthracis*, the causative agent of anthrax. The sRNAs, named “XrrA and XrrB” (for pXO1-encoded regulatory RNA) are abundant and highly stable primary transcripts, whose expression is dependent upon AtxA, the master virulence regulator of *B. anthracis*. sRNA levels are highest during culture conditions that promote AtxA expression and activity, and sRNA levels are unaltered in Hfq RNA chaperone null-mutants. Comparison of the transcriptome of a virulent Ames-derived strain to the transcriptome of isogenic sRNA-null mutants revealed multiple 4.0- to >100-fold differences in gene expression. Most regulatory effects were associated with XrrA, although regulation of some transcripts suggests functional overlap between the XrrA and XrrB. Many sRNA-regulated targets were chromosome genes associated with branched-chain amino acid metabolism, proteolysis, and transmembrane transport. Finally, in a mouse model for systemic anthrax, the lungs and livers of animals infected with *xrrA*-null mutants had a small reduction in bacterial burden, suggesting a role for XrrA in *B. anthracis* pathogenesis.

Keywords: anthrax, transcription, sRNA, RNA-seq, *Bacillus*, gene expression, plasmid, *anthracis*

INTRODUCTION

Eukaryotic and bacterial organisms have evolved mechanisms employing specialized RNA molecules to modulate gene expression. The microRNAs (miRNAs) of eukaryotic cells are non-coding RNAs of 21 to 24 nucleotides that serve as mRNA-targeting templates to guide the function of miRNA-associated proteins (Grishok et al., 2001; Song et al., 2003; Vaucheret et al., 2004). Upon target recognition, these proteins, collectively referred to as Argonaute proteins, induce mRNA decay or inhibit mRNA translation initiation (Pillai et al., 2004; Filipowicz et al., 2005; Wu and Xie, 2006). Similar to miRNAs, bacterial cells employ small regulatory RNAs (sRNAs) between 50 and 500 nucleotides long to modulate gene expression

by direct base-pairing with target mRNAs or direct interaction with regulatory proteins (Gottesman and Storz, 2011). sRNAs base-pair with mRNAs using short complementary sequences, leading to modulation of transcription termination, translation initiation, and/or mRNA decay. Protein-interacting sRNAs mimic specific nucleic acid structures or sequence motifs recognized by RNA- or DNA-binding regulators, resulting in titration of such regulators from their normal target sites.

Similar to miRNA association with Argonaute proteins in eukaryotes to affect function, mRNA-targeting sRNAs of bacteria can partner with RNA-binding proteins. The most-well studied RNA chaperone that participates in sRNA-mediated regulation is the hexameric Hfq protein (Wassarman et al., 2001; Møller et al., 2002). Hfq forms a donut-like structure with three RNA-binding surfaces, binding an sRNA and its cognate mRNA target at separate faces of the protein and allowing complementary sequences to come into proximity and base-pair at the rim of the protein (Schumacher et al., 2002; Link et al., 2009; Panja et al., 2013). In many bacterial species, deletion of *hfq* results in shortened half-lives of sRNAs and impaired sRNA-mediated regulation (Vytvytska et al., 1998; Sledjeski et al., 2001; Lenz et al., 2004; Deng et al., 2012; Santiago-Frangos et al., 2016).

Mounting evidence suggests that sRNAs can function as important virulence regulators in a number of bacterial pathogens. In *Pseudomonas aeruginosa*, a Gram-negative pathogen, two RNA-binding proteins, RsmA and RsmF, positively regulate genes involved in planktonic lifestyle while repressing genes involved in biofilm formation. Several sRNAs of the Rsm system titrate RsmA and RsmF to allow induction of biofilm formation (Vakulskas et al., 2015; Miller et al., 2016; Janssen et al., 2018). sRNAs also control virulence in some Gram-positive bacteria. An Hfq-independent sRNA of *Staphylococcus aureus*, RNAIII, allows translation of the mRNA encoding alpha-hemolysin while inhibiting expression of the repressor of toxin (*rot*) gene. In *Listeria monocytogenes*, the LhrA sRNA base-pairs to and represses translation of the *chiA* mRNA, which encodes chitinase A (Nielsen et al., 2011). Mutants deleted for *chiA* are defective in liver and spleen colonization of mice in a listeriosis model (Chaudhuri et al., 2013). Hfq stabilizes LhrA and facilitates the base-pairing interaction with *chiA*.

Knowledge of sRNA-mediated regulation is limited in the *Bacillus cereus sensu lato* species, a group of closely-related Gram-positive pathogens. Only one sRNA has been described in detail. In the YBT-1518 strain of the insect and nematode pathogen *Bacillus thuringiensis*, the BtsR1 sRNA silences expression of a cry toxin, which mediates killing of the host, by inhibiting translation initiation (Peng et al., 2018). Bioinformatic analysis of microarray data obtained from *Bacillus cereus* strain ATCC14579 grown in AgNO₃ stress predicts expression of several hundred sRNAs from intergenic regions along the genome (Sridhar and Gayathri, 2019). However, whether these sRNAs are functional remains unknown. *B. thuringiensis* and the mammalian pathogen *B. anthracis* harbor homologs of the SR1 sRNA found in multiple *Bacillus* species (Gimpel et al., 2012). *In vitro* transcribed *B. thuringiensis* SR1 was found to interact with a homolog of the *Bacillus subtilis* *ahrC* transcript, which encodes a regulator that activates

transcription of arginine catabolism operons (Heidrich et al., 2006; Gimpel et al., 2012). Interaction between *B. anthracis* SR1 and the *ahrC* homolog of this bacterium has not been experimentally confirmed.

Here, we report the first investigation of sRNA function in *B. anthracis*, the causative agent of anthrax. The *B. anthracis* genome is comprised of a 5-Mbp circular chromosome and two virulence plasmids, pXO1 and pXO2, 182 and 94 kbp in length, respectively. pXO1 carries the three anthrax toxin genes *pagA* (protective antigen), *cya* (edema factor), and *lef* (lethal factor), as well as *atxA*, encoding the *trans*-acting anthrax toxin activator AtxA. pXO2 carries the glutamic-acid-capsule biosynthesis operon *capBCADE* and genes for two functional paralogs of AtxA, the proteins AcpA and AcpB. AtxA positively regulates expression of the three toxin genes as well as the *acpA* gene (Dai et al., 1995; Drysdale et al., 2004). In turn, the AcpA protein positively regulates expression of the capsule biosynthesis operon, which aids in immune evasion (Drysdale et al., 2005). Read-through of a weak terminator hairpin at the end of the capsule biosynthesis operon transcript leads to transcription of the downstream *acpB* gene, which in turn positively regulates the operon in a feed-forward loop (Drysdale et al., 2005). The AtxA protein and its paralogs are members of an emerging class of virulence regulators designated PRD-containing virulence regulators (PCVRs), so termed due to the presence of phosphoenolpyruvate phosphotransferase system - regulated domains (PRDs) in their protein structures (Hondorp et al., 2013; Raynor et al., 2018).

A study comparing the transcriptome of the attenuated *B. anthracis* strain Ames 35 (pXO1⁺, pXO2⁻) to an isogenic *atxA*-null mutant revealed two unannotated transcripts encoded by pXO1. The transcripts, initially designated sRNA1 and sRNA2, were highly expressed in the parent strain and showed greatly reduced expression in the *atxA* mutant (McKenzie et al., 2014). Our own recent RNA-seq analysis confirmed expression of these transcripts in the fully virulent *B. anthracis* Ames strain (pXO1⁺, pXO2⁺) (Raynor et al., 2018). Culture of *B. anthracis* in toxin-inducing conditions resulted in high level expression of the transcripts. Expression of both putative sRNAs was abolished in an $\Delta atxA \Delta acpA \Delta acpB$ strain and complementation of exogenously expressed AtxA restored sRNA expression (Raynor et al., 2018). The pXO1 loci of the sRNAs and the tight regulation by AtxA suggest a relationship between sRNA-mediated regulation and virulence.

Of further interest, while about half of all bacterial genomes sequenced contain an *hfq* gene (Sun et al., 2002), and most of those species harbor a single copy of *hfq* in the chromosome, *B. anthracis* has three Hfq homologs. Two of the *hfq* genes, *hfq1* and *hfq2*, are located on the chromosome. The third *hfq* gene, *hfq3*, is located on pXO1, the plasmid encoding the predicted sRNAs. Hfq2 and Hfq3, but not Hfq1, are functional when expressed in *Escherichia coli* (Vrentas et al., 2015). Hfq2 and Hfq3 form hexamers *in vitro*, while Hfq1 purifies as a monomer (Vrentas et al., 2015). Our *B. anthracis* RNA-seq data indicate that the chromosome-borne *hfq2* is positively regulated by AtxA (Raynor et al., 2018). AtxA-mediated positive control of both the sRNAs and Hfq2, and the predicted functionality of Hfq2 and

Hfq3, suggest roles for the sRNAs and Hfq proteins in *B. anthracis* gene regulation.

In this study, we designated the sRNAs previously described as sRNA2 and sRNA1 (McKenzie et al., 2014) as “XrrA” and “XrrB” (for pXO1-encoded regulatory RNA). We mapped the loci and assessed expression and function of XrrA and XrrB in *B. anthracis*. We constructed deletion mutants $\Delta xrrA$, $\Delta xrrB$, and $\Delta xrrA\Delta xrrB$ in an Ames strain background and compared gene expression of these mutants to that of the Ames-derived parent strain using RNA-seq. We tested for effects of the three Hfq chaperones of *B. anthracis* on sRNA half-life and assessed virulence of sRNA mutant strains using a murine model of systemic anthrax. XrrA and XrrB are the first regulatory RNAs experimentally examined in *B. anthracis* and are shown here to regulate metabolic and virulence gene expression in this pathogen.

MATERIALS AND METHODS

Growth Conditions

Escherichia coli strains were grown in 5 ml of Luria-Bertani (LB) (Bertani, 1951) broth at 30 or 37°C, as indicated. For RNA isolation, *B. anthracis* strains were cultured in 25 ml of brain heart infusion (BHI, Becton, Dickson and Company, Franklin Lakes, NJ, United States) broth at 30°C overnight before sub-culturing into 25 ml of casamino acids medium supplemented with 0.1% w/v of glucose (CA) (Thorne and Belton, 1957; Hadjifrangiskou et al., 2007) or LB medium at a starting OD₆₀₀ of 0.08. *B. anthracis* sub-cultures were grown at 37°C in air (CA-Air or LB-Air) or in 5% atmospheric CO₂ (CA-CO₂ or LB-CO₂; medium supplemented with 0.8% sodium bicarbonate). All cultures were incubated with shaking at 200 r.p.m. Expression of recombinant XrrA in the $\Delta xrrA$ strain was induced by addition of 500 μ M IPTG to the medium at early exponential phase. For growth curves, *B. anthracis* strains were sub-cultured at a starting OD₆₀₀ of 0.08 into a 26-well plate containing 1 ml of CA medium per well. Cultures were grown in a Biotek SynergyH1 microplate reader (Biotek, Winooski, VT, United States) at 37°C in 5% atmospheric CO₂ with continuous orbital shaking at 355 c.p.m. Absorbance measurements were taken hourly for 18 h. LB agar was used for growth of all strains on solid media. Media contained antibiotics when appropriate: carbenicillin (100 μ g ml⁻¹) and erythromycin (150 μ g ml⁻¹) for *E. coli*, and erythromycin (10 μ g ml⁻¹), and spectinomycin (100 μ g ml⁻¹) for *B. anthracis*.

Strain Construction

Strains used in this study are listed on Table 1. Oligonucleotide primers used in polymerase chain reactions (PCR) are listed in Supplementary Table 1. The fully virulent Ames strain (pXO1⁺, pXO2⁺), the Ames-derived UTA37, and isogenic mutants of these strains were used to determine the effect of *atxA* and *acpA* deletions on XrrA and XrrB expression, the effect of deleting *xrrA* and *xrrB* on the transcriptome of *B. anthracis*, and for validation of XrrA-mediated control of the *inhA1* target. The Ames-derived parent strain UTA37 contains a recombinant *atxA* gene at the native pXO1 locus that encodes a functional

TABLE 1 | *Bacillus anthracis* strains and plasmids.

Strains or Plasmids	Relevant characteristics ^{a,b}	Source
Strains		
Ames	<i>B. anthracis</i> (pXO1 ⁺ , pXO2 ⁺)	Ivins et al., 1990
UTA5	Ames-derivative, <i>inhA1::specR</i>	Pflughoeft et al., 2014
UTA22	Ames-derivative, $\Delta atxA$	Dale et al., 2018
UTA37	Ames-derivative with <i>atxA-FLAG</i> expressed from the native locus	Raynor et al., 2018
UTA38	UTA37-derivative, $\Delta xrrB$	This work
UTA39	UTA37-derivative, $\Delta xrrA$	This work
UTA41	UTA37-derivative, $\Delta xrrA\Delta xrrB$	This work
UTA44	Ames-derivative, $\Delta acpA$	Raynor et al., 2018
ANR-1	<i>B. anthracis</i> (pXO1 ⁺ , pXO2 ⁻)	Welkos et al., 2001
UT434	ANR-1-derivative, $\Delta xrrB$	This work
UT435	ANR-1-derivative, $\Delta xrrA$	This work
UT436	ANR-1-derivative, $\Delta xrrA\Delta xrrB$	This work
UT440	ANR-1-derivative, $\Delta hfq1$	This work
UT437	ANR-1-derivative, $\Delta hfq2$	This work
UT438	ANR-1-derivative, $\Delta hfq3$	This work
UT471	ANR-1-derivative, $\Delta hfq1\Delta hfq2\Delta hfq3$	This work
Plasmids		
pHY304	Heat-sensitive vector used for deletion of indicated loci by homologous recombination; <i>Ern</i> ^r	Ho et al., 1989
pUTE657	Expression vector with IPTG-inducible <i>lac</i> operon promoter; <i>Spec</i> ^r	Pflughoeft et al., 2011
pUTE1205	pUTE657-derived expression vector containing <i>xrrA</i> sequence under the control of the <i>lac</i> operon promoter; <i>Spec</i> ^r	This work

^a Δ mutants were created by markerless deletion of coding sequences using pHY304-derived constructs.

^b *Ern*^r indicates resistance to erythromycin.

AtxA protein with a FLAG tag at the C-terminus of the protein. This strain has been used to monitor AtxA protein levels, and AtxA expression and function is unchanged from Ames (Raynor et al., 2018). The attenuated ANR-1 strain (pXO1⁺, pXO2⁻) and isogenic mutants were used for all other experiments. *E. coli* strains TG1 and GM2163 were hosts for general cloning and plasmid constructions using standard methods (Marrero and Welkos, 1995).

Markerless sRNA deletions ($\Delta xrrA$, $\Delta xrrB$, $\Delta xrrA\Delta xrrB$) in the Ames and ANR-1 backgrounds, and *hfq* deletions ($\Delta hfq1$, $\Delta hfq2$, $\Delta hfq3$, $\Delta hfq1\Delta hfq2\Delta hfq3$) in the ANR-1 background were made by homologous recombination as described previously (Ho et al., 1989; Raynor et al., 2018). Briefly, the pHY304 plasmid contains a heat-sensitive origin of replication and an erythromycin resistance marker to select for allelic recombination (Chaffin et al., 2005). Two-kb DNA constructs containing target gene flanking sequences 1-kb upstream and 1-kb downstream from the gene locus were created using PCR and gene-specific primers listed in Supplementary Table 1. The resulting plasmids were electroporated into *B. anthracis*. Plasmid-containing isolates were grown in 25 ml of BHI broth at the non-permissive temperature of 41°C in the presence of erythromycin. Cultures were sub-cultured into 25 ml

of fresh BHI broth with no erythromycin at a starting OD₆₀₀ of 0.08 and grown at 30°C. Deletion mutants were verified by PCR and sequencing. The $\Delta xrrA\Delta xrrB$ and $\Delta hfq1\Delta hfq2\Delta hfq3$ mutants were created by sequentially deleting each gene using one pHY304-derived shuttle vector at a time. Gene deletions were confirmed using PCR.

To create a $\Delta xrrA$ -null mutant complemented with *xrrA*, the gene was amplified from the native locus using PCR with *xrrA*-specific primers, and ligated into pUTE657 downstream of the *lac* operon promoter such that *xrrA* transcription is IPTG-inducible. The resulting construct, named pUTE1205, was electroporated into the $\Delta xrrA$ Ames strain, creating strain UTA39 (pUTE1205). Plasmid-containing isolates were confirmed by PCR using pUTE657-specific primers.

Newly-created mutants were grown in 25 ml of Phage Assay (PA) broth at 30°C for 72 h to induce spore formation, and spores were prepared as previously described (Thorne, 1968). Spores were finally stored at 4°C in a suspension of 5 ml of sterile water and strain names were assigned as listed on Table 1.

RNA Isolation

RNA isolation was performed as described previously (Raynor et al., 2018). Briefly, *B. anthracis* strains were cultured in CA-CO₂, CA-Air, LB-CO₂, or LB-Air as indicated. At early stationary phase (OD₆₀₀ = 1.0–1.5), cells from 10-ml samples were centrifuged at 10,000 × *g* for 15 min. Cell pellets were resuspended in 500 µl of PBS followed by an equivalent volume of saturated acid phenol (pH 4.3) (Fisher Bioreagents, Fair Lawn, NJ, United States) at 65°C. Samples were homogenized in screw cap tubes containing 400 µl of 0.1-mm diameter zirconia/silica beads (BioSpec Products, Bartlesville, OK, United States) by bead beating in a Mini Beadbeater (BioSpec Products, Bartlesville, OK, United States). Samples were beaten twice for 1 min, with a 5-min incubation at 65°C between homogenizations. Samples were centrifuged at 16,000 × *g* for three min at 4°C. The aqueous phase was collected and the phenol extraction repeated. Following centrifugation, the aqueous phase was mixed with one-third volume of chloroform and incubated at room temperature for 10 min prior to centrifugation at 16,000 × *g* for 15 min at 4°C. To precipitate the RNA from the final aqueous phase, 20 ng of glycogen, one-tenth volume of 3 M sodium acetate, and 3 volumes of 100% ice-cold ethanol were added to the samples. RNA was precipitated at –80°C for one h to overnight. Samples were centrifuged at 16,000 × *g* for 30 min at 4°C. The resulting pellet was washed twice with ice-cold 75% ethanol before resuspending in DEPC-treated sterile water. RNA was quantified using a Nanodrop Spectrophotometer ND-1000.

Northern Blotting

Expression of *XrrA*, *XrrB*, 5S rRNA load control, 16S rRNA, 23S rRNA, and *rpsO* mRNA was determined using northern blot analysis. To detect *XrrA*, *XrrB*, 5S rRNA, and *rpsO* mRNA 3–10 µg of total RNA was denatured for 5 min at 95°C in Gel Loading Buffer II (Invitrogen, Carlsbad, CA, United States) and subjected to electrophoresis on an 8% polyacrylamide – 8 M urea gel. To determine the length of the sRNAs, 12 ng of biotinylated sRNA ladder (Kerafast, Boston, MA, United States) was added to

the first lane of the gel. To detect 16S rRNA and 23S rRNA, 3 µg of total RNA was denatured as described above and subjected to electrophoresis on a 1% agarose – 1.5% formaldehyde gel. Size-separated RNA was then transferred to an Amersham Hybond-N nylon membrane (GE Healthcare, Little Chalfont, United Kingdom) via capillary transfer in 50 mM NaOH. After overnight transfer, RNA was crosslinked to the membrane by UV light exposure and subsequently incubated in NorthernMax Prehybridization/Hybridization Buffer (Invitrogen, Carlsbad, CA, United States) at 42°C. Biotinylated DNA probes were used to detect expression of the RNAs. The probes were generated by PCR using the indicated primers (Supplementary Table 1) and the resulting double-stranded DNA templates were subjected to random biotin-labeling by incorporation of biotin-11-dUTP with Klenow enzyme (Thermo Scientific, Waltham, MA, United States). Hybridization of RNA with the respective biotin-labeled DNA probes was detected using the North2South Chemiluminescent Hybridization and Detection Kit (Thermo Scientific, Waltham, MA, United States) according to manufacturer's instructions.

5' and 3' Rapid Amplification of cDNA Ends (RACE)

RACE analysis was performed as described previously with modifications (Bensing et al., 1996; Argaman et al., 2001). RNA Adapter sequences and oligonucleotide primers used in RACE are listed in Supplementary Table 1. To precisely map the 5' and 3' ends of *XrrA* and *XrrB*, RNA samples isolated from ANR-1 were treated with 30 units of DNase I (New England Biolabs, Ipswich, MA, United States) for 30 min at 37°C to remove potential DNA contamination. RNA was recovered from the DNAase treatment and all subsequent reactions using the RNA Clean and Concentrator Kit (Zymo Research, Irvine, CA, United States), according to kit instructions.

For 5' RACE, 5-µg samples of RNA were treated with 20 units of RNA 5' Polyphosphatase (5'PP, Lucigen, Middleton, WI, United States) at 37°C for 1 h. This reaction removes the 5' triphosphate of primary RNA transcripts, leaving a 5' monophosphate which is then ligated to the 3'-OH group of the 5' RNA Adapter. The treated RNA was ligated to the 5' RNA Adapter by incubation with 500 pmoles of the adapter, 100 units of T4 RNA Ligase I (New England Biolabs, Ipswich, MA, United States) and 150 µM ATP at 16°C overnight. One microgram of the resulting ligated RNA was used to synthesize cDNA using a locus-specific internal primer for *XrrA* or *XrrB* and the Super Script III Reverse Transcriptase Kit (Invitrogen, Carlsbad, CA, United States). Finally, an aliquot of the cDNA synthesis reaction was used to perform PCR using the same locus-specific primer for either *XrrA* or *XrrB* and a 5' Adapter-specific primer. PCR products were visualized by 1.5% agarose gel electrophoresis. Products of interest were excised from the gel and recovered using the DNA Clean and Concentrator Kit (Zymo Research, Irvine, CA, United States), according to kit instructions. Recovered PCR products were assessed using Sanger sequencing employing both PCR primers (Genewiz, South Plainfield, NJ, United States).

For 3' RACE, 15- μ g samples of RNA were treated with 20 units of Calf Intestinal Alkaline Phosphatase (CIP, New England Biolabs, Ipswich, MA, United States) for one h at 37°C. This reaction removes 3' phosphate groups from the ends of RNA. The 3'-OH group of RNA in the sample was ligated to the 3' RNA Adapter, which contains a 5' monophosphate modification. The adapter also contains an inverted deoxythymidine at the 3' to prevent self-ligation of the adapter during the ligation reaction. CIP-treated RNA was incubated with 500 pmol of the 3' RNA Adapter, 100 units of T4 RNA ligase and 150 μ M ATP at 16°C overnight. One microgram of the resulting RNA was used to perform cDNA synthesis, using an adapter-specific primer for first strand synthesis with the Super Script III Reverse Transcriptase Kit (Invitrogen, Carlsbad, CA, United States). Finally, an aliquot of the cDNA synthesis reaction was used to perform a PCR, using the 3' RNA Adapter-specific primer and a gene-specific internal primer for either *XrrA* or *XrrB*. PCR products were visualized and sequenced as described above.

Determination of *XrrA* and *XrrB* 5' End Phosphate Groups

Primary transcripts are 5' tri-phosphorylated, while processed secondary transcripts are 5' mono-phosphorylated. To determine if *XrrA* and *XrrB* are primary transcripts, total RNA isolated from ANR-1 was subjected to RNA 5' Polyphosphatase treatment as described above followed by Terminator Exonuclease (TEX, Lucigen, Middleton, WI, United States) treatment, in which 3- μ g samples of RNA were incubated with one unit of TEX enzyme at 30°C for 3 h. TEX specifically degrades RNA with a 5' monophosphate. Total RNA from ANR-1 was divided into four treatment groups. The control sample TEX⁻ 5'PP⁻ received no treatments. The TEX⁺ 5'PP⁻ sample was treated with TEX alone, while the TEX⁻ 5'PP⁺ sample was treated with RNA 5' Polyphosphatase alone. Finally, the TEX⁺ 5'PP⁺ sample was first treated with RNA 5' Polyphosphatase, followed by TEX treatment. All RNA was recovered from reactions using the RNA Clean and Concentrator Kit (Zymo Research, Irvine, CA, United States), according to the manufacturer's instructions. RNA samples were subjected to northern blot analysis as described above. sRNA signal was normalized to the TEX-resistant 5S rRNA signal (Patrick et al., 2009; Ferrara et al., 2017). Relative sRNA levels were calculated as a fraction of the TEX⁻ 5'PP⁻ control sample. The experiment was performed in triplicate and an analysis of variance (ANOVA) paired with Tukey's multiple comparison analysis was used to determine significance between treatments, with an adjusted *p*-value cut-off of 0.05. As a control for TEX-mediated degradation, levels of the TEX-sensitive 16S rRNA and 23S rRNA (Fleischmann and Rocha, 2018; Lalaouna et al., 2019) in the treated samples were detected by northern blotting as described above.

Construction of Next-Generation Sequencing (NGS) Libraries and RNA Sequencing

Total RNA from Ames strains UTA37 (Parent), UTA38 (Δ *xrrB*), UTA39 (Δ *xrrA*), UTA41 (Δ *xrrA* Δ *xrrB*) was isolated from

cultures grown in CA-CO₂ in triplicate, using saturated phenol:chloroform extraction as described above. RNA was quantified using a QubitFluorometer (Thermo Scientific, Waltham, MA, United States) and RNA quality was checked using an Agilent 2100 Bioanalyzer (Agilent Technologies, Santa Clara, CA, United States). One microgram of pure and quality-checked RNA from each sample was subjected to rRNA removal using the Ribo-Zero kit (Epicentre, Madison, WI, United States), according to manufacturer's instructions. The rRNA-free RNA was fragmented into ~200–400 nt fragments using divalent cations and heat (Breslow and Huang, 1991). The fragments were primed with random hexamers and Superscript II reverse transcriptase enzyme (Invitrogen, Carlsbad, CA, United States) was used for first strand synthesis of cDNA. Double-stranded cDNA was generated using DNA polymerase I and remaining RNA was removed by RNase treatment. The 5' ends of the ds-cDNA were phosphorylated using T4 polynucleotide kinase (New England Biolabs, Ipswich, MA, United States) and the 3' ends were adenylated using Taq enzyme (New England Biolabs, Ipswich, MA, United States). The cDNA end modifications allow for ligation to double stranded Tru-seq Illumina Adapters, which contain monophosphate modifications at the 5' ends and thymidine overhangs at the 3' ends. The Adapters contain short sequences for binding to the sequencer flow cell oligos and indexing of pooled libraries. They also contain sequences for primers used for PCR enrichment of the library and to initiate sequencing by synthesis. The quality of the prepared libraries was verified using an Agilent 2100 Bioanalyzer before loading the libraries into the flow cell of a NextSeq550 sequencer. Sequencing by synthesis was performed to generate 75 bp paired-end reads. Two 130M-read sequencing runs were performed and an average of 31M reads per sample was obtained.

RNA Sequencing Bioinformatic Analysis

All bioinformatic analysis was performed using the publicly available Galaxy web resource¹ (Afgan et al., 2018). Triplicate paired-end fastq.gz raw read files for each strain for each of the two sequencing runs were uploaded to Galaxy and converted into fastqsanger files using FASTQ Groomer (Blankenberg et al., 2010). This conversion allows read files to be processed and analyzed on Galaxy. The quality of the reads was assessed using FastQC (Andrews, 2010). Low quality bases and Illumina Adapter sequences were removed using Trim Galore! Galaxy Version 0.6.3 (Krueger, 2012). A second round of FastQC analysis was done to verify the removal of low-quality bases and Illumina Adapter sequences. Trimmed reads were aligned to the complete Ames Ancestor genome (NCBI accession numbers AE017334.2 for chromosome, AE017336.2 for pXO1, and AE017335.3 for pXO2) using the GCF_000008445.1_ASM844v1_genomic.fna FASTA file obtained from the NCBI website. Bowtie2 Galaxy Version 2.3.4.3 (Langmead and Salzberg, 2012) with default parameters was used to align the paired-end reads to the genome. On average, 97% of all the reads in each sample mapped to the reference genome. BAM files obtained from mapped reads from each of the two sequencing runs were

¹<https://usegalaxy.org/>

pooled using Convert, Merge, Randomize Galaxy Version 2.4.0.0 (Barnett et al., 2011), resulting in a single BAM file per triplicate per strain. The Cufflinks/Cuffcompare/CuffDiff pipeline (Trapnell et al., 2010) was used for transcript assembly using the GCF_000008445.1_ASM844v1_genomic.gff reference annotation file from NCBI, count the number of reads mapped to each annotated transcript, and calculate differential transcript expression between the strains. The Fragments Per Kilobase of transcript per Million mapped reads (FPKM) values per assembled transcript were obtained and differential expression was calculated as the log₂ (fold-change) in FPKM values between the parent strain and each mutant strain, with an adjusted p-value cut-off for significance of 0.01. The Cufflinks/Cuffcompare/CuffDiff pipeline had a lower limit of 0.00005 for p-value reporting. Genes differentially regulated in the $\Delta xrrA$ and $\Delta xrrA\Delta xrrB$ mutants with a fold-change of ≥ 4.0 compared to the parent strain were assigned gene ontology terms based on annotation of the encoded proteins according to the UniProt web database (The UniProt Consortium, 2019). BamCoverage Galaxy Version 3.3.2.0.0 (Ramírez et al., 2016) was used to create BigWig files for visualization of read coverage over the genome on Integrative Genomics Viewer (IGV) (Thorvaldsdóttir et al., 2013). The RNA-seq data discussed in this publication have been deposited in the NCBI Gene Expression Omnibus (GEO) (Edgar et al., 2002) and are accessible through GEO Series accession number GSE152356².

Validation of XrrA-Mediated *inhA1* Regulation Using qPCR

Expression of the XrrA-regulated *inhA1* transcript was assessed using qPCR analysis. The Ames-derived UTA37 (Parent), UTA39 ($\Delta xrrA$), UTA39 (pUT1205) (*xrrA* complementation), and the previously published UTA5 (*inhA1*-null) (Pflughoeft et al., 2014) strains were grown in CA-CO₂ as described above. RNA samples extracted from these strains were treated with 30 units of DNase I (New England Biolabs, Ipswich, MA, United States) for 30 min at 37°C to remove potential DNA contamination. RNA was recovered from the DNase treatment using the RNA Clean and Concentrator Kit (Zymo Research, Irvine, CA, United States). cDNA synthesis was performed using random heptamers and the Super Script III Reverse Transcriptase Kit (Invitrogen, Carlsbad, CA, United States). The resulting cDNA was recovered from the synthesis reaction using the DNA Clean and Concentrator Kit (Zymo Research, Irvine, CA). cDNA samples were subjected to qPCR analysis using *inhA1*-specific primers. The *gyrB* gene, which encodes DNA gyrase subunit B, was used as a reference gene. cDNA and primers were mixed with the SsoAdvanced Universal SYBR Green Supermix (Bio-Rad, Hercules, CA, United States) in duplicate reactions per strain. No reverse transcriptase (NRT) RNA and no template (NTC) water controls were also included. qPCR CT values and melt-curve data were recorded using a CFX96 Real-Time System C1000 Touch Thermal Cycler (Bio-Rad, Hercules, CA, United States). CT values of the duplicate reactions were averaged. The Δ CT values were calculated by subtracting the reference gene *gyrB*

CT values from those of *inhA1*. The log₁₀ relative expression [$2^{(-\Delta CT)}$] was calculated for each gene of interest.

sRNA:mRNA Complementarity and sRNA Secondary Structure *in silico* Analyses

The XrrA and XrrB sequences were entered into the TargetRNA2 webserver (Kery et al., 2014) and aligned to the *B. anthracis* Ames ancestor chromosome (NCBI accession number AE017334.2), pXO1 plasmid (NCBI accession number AE017336.2), and pXO2 plasmid (NCBI accession number AE017335.3) using default parameters. TargetRNA2 takes into account conservation of sRNA sequences, predicted secondary structure of the sRNAs, predicted secondary structure of potential mRNA targets, and the hybridization energy of the sRNA:mRNA interaction and outputs a list of potential targets ranked by hybridization energy, with an adjusted p-value cut-off of 0.05 for each interaction. The TargetRNA2 list of potential targets was compared to the list of sRNA-regulated transcripts obtained from RNA-seq analysis. Transcripts exhibiting a fold-change of ≥ 4.0 in at least one sRNA-null strain and exhibiting complementarity with the sRNA sequences are reported in Table 4. To determine the most likely predicted secondary structure of XrrA and XrrB, the sRNA sequences were entered into the mfold webserver (Zuker, 2003) and analyzed under default parameters.

sRNA Half-Life Determinations

The parent strain ANR-1 and the *hfq*-null mutants ($\Delta hfq1$, $\Delta hfq2$, $\Delta hfq3$, $\Delta hfq1\Delta hfq2\Delta hfq3$) were grown in CA-CO₂ in triplicate until exponential phase (OD₆₀₀ = 0.6–0.8). After collection of a 750- μ l sample (time zero), rifampicin (200 μ g ml⁻¹) was added to stop transcription. Culture samples were taken at 2, 4, 8, 16, 32, and 45 min post rifampicin addition. Immediately after collection, each sample was mixed with saturated phenol (pH = 4.3) at 65°C and cells were lysed immediately by bead-beating. RNA was extracted from all samples using phenol:chloroform extraction and ethanol precipitation as described above. RNA (3 μ g per sample) was subjected to northern blotting, probing for XrrA, XrrB, and 5S rRNA as described above. To validate the half-life determination protocol, the previously known half-life of the *rpsO* transcript, encoding 30S ribosomal protein S15, was determined in the parent strain by probing for *rpsO* using northern blotting. sRNA signal was normalized to 5S rRNA signal per sample for each of the three replicates. sRNA decay over time was calculated as a percent of the signal at time point zero. A linear regression model was fit to the decay data and the slope of the decay lines was used to calculate the half-lives in each replicate per each strain. An analysis of variance (ANOVA) paired with Tukey's multiple comparison analysis was used to determine significance between the parent strain half-life and each mutant strain half-life, with an adjusted p-value cut-off of 0.05.

Preparation of Vegetative Cells for Mouse Infection

Spores of the ANR-1 strain, the $\Delta xrrA$ mutant, and the $\Delta xrrA\Delta xrrB$ mutant ($\sim 10^7$ CFU) were incubated in 1 ml of BHI

²<https://www.ncbi.nlm.nih.gov/geo/query/acc.cgi?acc=GSE152356>

at 37°C for 1 h with shaking at 200 r.p.m. The entire outgrowth was transferred into 25 ml of fresh CA medium supplemented with 0.8% sodium bicarbonate. Cultures were incubated in 5% atmospheric CO₂ at 37°C with shaking at 200 r.p.m. for 4 h. At an OD₆₀₀ of 0.4–0.6, cells were harvested using a 0.22 µm pore filter unit and washed twice with 25 ml Dulbecco's phosphate-buffered saline without calcium or magnesium (DPBS, Sigma-Aldrich, St. Louis, MO, United States). Cells were finally resuspended in 25 ml of DPBS and diluted to the desired colony forming unit (CFU) concentration, which was verified by plating the inocula on LB agar plates. The inocula were loaded into 1-ml syringes with 27-gauge needles in a final volume of 100 µl.

Mouse Infections and Organ CFU Determination

All mouse protocols were approved by The University of Texas Health Science Center Institutional Animal Care and Use Committee. Mice were housed in a veterinary-supervised vivarium and had access to unlimited food and water. Seven-week-old female A/J mice, purchased from Jackson Laboratory (Bar Harbor, ME, United States), were sedated prior to infection with 0.1 mg/kg of acepromazine injected intraperitoneally. Mice were infected intravenously via the tail-vein with 100 µl of DPBS containing ~10⁵ CFU. Fifteen mice were infected with the ANR-1 parent strain, ten mice were infected with the $\Delta xrrA$ mutant, and nine mice were infected with the $\Delta xrrA \Delta xrrB$ mutant. The mice were followed for a period of 11 days and monitored for signs of infection. Moribund mice were sacrificed using CO₂ asphyxiation, death was verified using cervical dislocation as a secondary method, and time of death was recorded. The liver, lung, spleen, and kidney of sacrificed mice were collected, weighed, and homogenized in 1 ml of DPBS via bead-beating with 2.3-mm diameter zirconia beads (BioSpec Products, Bartlesville, OK, United States). Tissues were homogenized for 1 min, incubated on ice for 1 min, and then homogenized for an additional minute using a Mini Beadbeater (BioSpec Products, Bartlesville, OK, United States). Homogenates were diluted serially and plated on LB agar. Following overnight incubation at 37°C, CFU per gram of tissue was calculated. Survival data were plotted on a Kaplan–Meier curve. An Analysis of Variance (ANOVA), followed by Tukey's multiple comparisons test was used to calculate significance between CFU organ burden of mice infected with different strains.

RESULTS

Transcript Mapping of XrrA and XrrB

We previously investigated regulatory functions of the *B. anthracis* PCVRs, AtxA, AcpA, and AcpB, using RNA-seq to compare gene expression by the Ames parent strain (pXO1⁺, pXO2⁺), an isogenic PCVR-null mutant ($\Delta atxA \Delta acpA \Delta acpB$), and strains of the PCVR-null mutant complemented with the individual PCVRs (Raynor et al., 2018). While most of the data revealed sequences mapping to annotated loci of the Ames ancestor genome, our RNA-seq read maps showed PCVR-regulated expression of two unannotated loci on the

pXO1 virulence plasmid. The apparent high expression level of these RNAs, and the lack of previous annotation suggested that these loci may represent small regulatory RNAs.

To quantify RNAs associated with these loci and verify PCVR-mediated regulation, we re-analyzed raw paired-end reads from Raynor et al. (2018) [raw paired-end reads accessible at NCBI GEO database (Edgar et al., 2002), accession number GSE152357] using the Galaxy web resource for bioinformatic analysis (Afgan et al., 2018) (Figure 1A). We designated the two loci as XrrA and XrrB. In the Ames parent strain, XrrA had 4.5M fragments per kilobase of transcript per million mapped reads (FPKM), while XrrB had 2M FPKM. For comparison, the toxin gene *lef* had 2076 FPKM in the parent strain. XrrA is located within the IS1627 boundaries of the 35-kb pathogenicity island on pXO1, that contains *atxA* and all three anthrax toxin genes. XrrB is located downstream of the pathogenicity island, in proximity to the adhesin gene *bslA*. The $\Delta atxA \Delta acpA \Delta acpB$ mutant, deleted for all PCVRs, exhibited reduced sRNA-associated reads. Expression of both sRNAs was restored upon complementation of the triple-null strain with AtxA, while expression of XrrB was also restored upon complementation with AcpA. The third regulator, AcpB had no effect on XrrA or XrrB expression (Figure 1A).

The RNA sequencing performed by Raynor et al. (2018) was not stranded. We performed Rapid Amplification of cDNA Ends (RACE) experiments to determine the directions of XrrA and XrrB transcription and to precisely map the 5' and 3' ends of the sRNAs. Our RACE analysis indicated that XrrA is transcribed from the leading DNA strand, with 5' and 3' ends mapping to pXO1 coordinates 131,385 and 131,566, respectively. XrrB is transcribed from the lagging DNA strand of pXO1, with 5' and 3' ends mapping to pXO1 coordinates 105,925 and 105,702, respectively. Figure 1B illustrates the loci of the sRNAs with nucleotides corresponding to the 5' ends of the sRNAs shown as +1. The lengths of the sRNAs as discerned from our RACE analysis are 182 nt for XrrA and 224 nt for XrrB, in agreement with the predicted lengths from the RNA-seq studies.

We used the ORFinder tool from NCBI to search for ATG-initiated open reading frames (ORFs) within the sequences obtained from the RACE analysis. There were no apparent ORFs in XrrB. The XrrA sequence contained a 63 nt ORF with an ATG initiating at pXO1 coordinate 131,488, predicted to encode a 20-amino acid peptide. However, no apparent ribosomal binding site (RBS) could be found upstream of the ORF sequence. Overall, the data indicate that XrrA and XrrB are likely to be non-coding small RNAs.

Small regulatory RNAs may be transcribed from stand-alone promoters to form primary transcripts or result from 5' or 3' processing of longer RNA transcripts. Visualization of the 5' and 3' RACE PCR products of XrrA and XrrB on an agarose gel showed single bands (Supplementary Figure 1), indicating the formation of a single 5' and a single 3' RACE product per sRNA. Moreover, genes adjacent to both ends of the sRNA loci on pXO1 appear to be transcribed in opposite direction from the sRNAs (Figure 1B), making it unlikely that the sRNAs are co-transcribed with other genes. RNA folding predictions using the mFold web server (Zuker, 2003) suggest

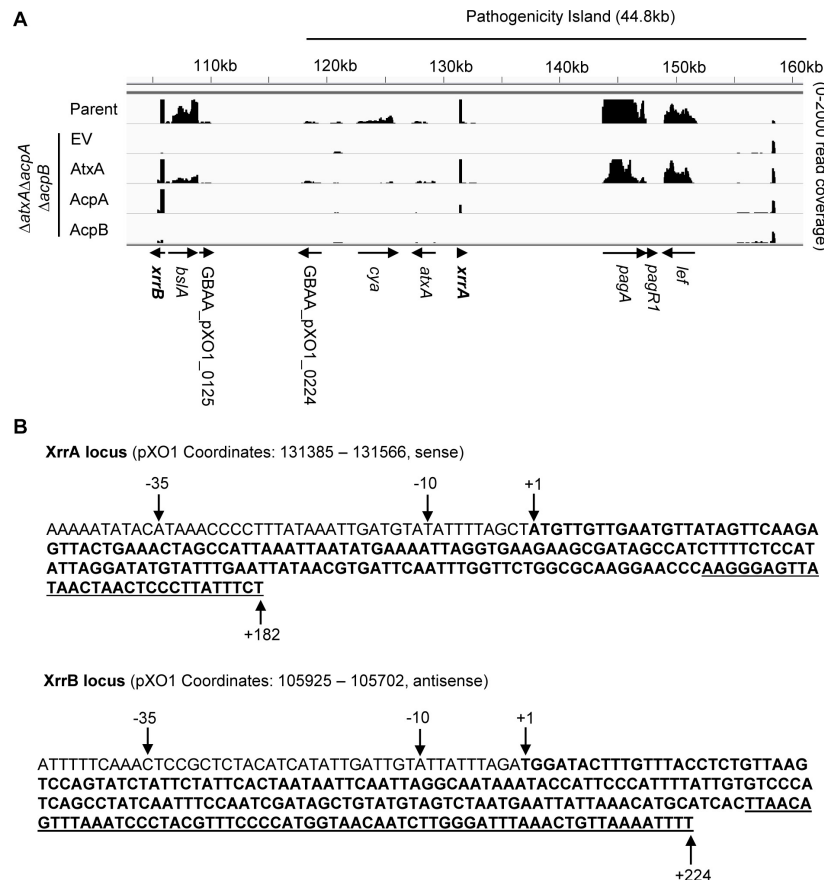


FIGURE 1 | Sequences and PCVR-mediated regulation of sRNA loci on pXO1. **(A)** Read map of the virulence plasmid pXO1, focused on the 44.8 kb pathogenicity island, shows effect of individual PRD-containing virulence regulators (PCVRs) on RNA abundance. RNA-seq data from Raynor et al. (2018) was used to generate read map of gene expression for the Ames parent strain, the Δ atxA Δ acpA Δ acpB strain expressing empty vector (EV), and the individual PCVR complementations in the Δ atxA Δ acpA Δ acpB background. Genes showing apparent regulation by the PCVRs are labeled and direction of transcription is indicated with arrows. XrrA (sense) and XrrB (antisense) are indicated in bold. The boundaries of the pXO1 pathogenicity island, defined by inverted IS1627 elements, are indicated above the read map. **(B)** Sequences and transcriptional direction of the sRNA loci suggested by RNA-seq were confirmed by precise mapping of the 5' and 3' ends using RACE. Transcriptional start sites are indicated as +1. The 3' termini of the transcripts are indicated (+182 for XrrA, +224 for XrrB), and the entire sRNA sequence is shown in bold. Predicted Rho-independent terminator sequences, according to mfold webserver, are underlined. The -10 and -35 nucleotides are shown upstream of the transcriptional start. RACE analysis was repeated 2–3 times per end per sRNA to confirm precise mapping.

that both sRNAs form a 3' hairpin loop followed by a run of uridines (Figure 1B and Supplementary Figures 2, 3), which is indicative of Rho-independent terminators for both XrrA and XrrB. Together, these observations suggest that the sRNAs are primary transcripts.

Primary transcripts in bacteria have a 5' tri-phosphate group, while secondary transcripts have a 5' mono-phosphate group. To test whether XrrA and XrrB possess a 5' tri-phosphate group, we isolated RNA from the ANR-1 strain, treated it with Terminator Exonuclease (TEX), and performed northern blot analysis (Figure 2). The TEX enzyme specifically degrades transcripts with a 5' monophosphate. XrrA (Figure 2A) and XrrB (Figure 2B) were resistant to TEX-mediated degradation. 5S rRNA was used as a load control and as a negative control for TEX-mediated degradation because it is resistant to degradation by TEX (Patrick et al., 2009; Ferrara et al., 2017; Fleischmann and Rocha, 2018; Lalaouna et al., 2019). As a positive control for

TEX-mediated degradation, levels of the TEX-sensitive 16S rRNA and 23S rRNA were assessed. We observed clear degradation of the 16S and 23S rRNAs, but not 5S rRNA, for TEX-treated samples. To confirm that protection of the sRNAs from TEX was due to a tri-phosphate modification at their 5' ends, we treated RNA with RNA 5' Polyphosphatase (5'PP), which removes the gamma and beta phosphates from the 5' end of primary transcripts, leaving a 5' mono-phosphate. Treatment with 5'PP followed by TEX treatment resulted in degradation of both XrrA (Figure 2A) and XrrB (Figure 2B), confirming that protection from TEX was due to the presence of a tri-phosphate at the 5' ends of the sRNAs. Importantly, treatment with 5'PP alone did not cause sRNA degradation. There was no significant difference in XrrA (Figure 2C) and XrrB (Figure 2D) levels in only TEX-treated and only 5'PP-treated samples. XrrA (Figure 2C) and XrrB (Figure 2D) levels in the 5'PP-TEX-treated samples were significantly reduced compared to all other treatments.

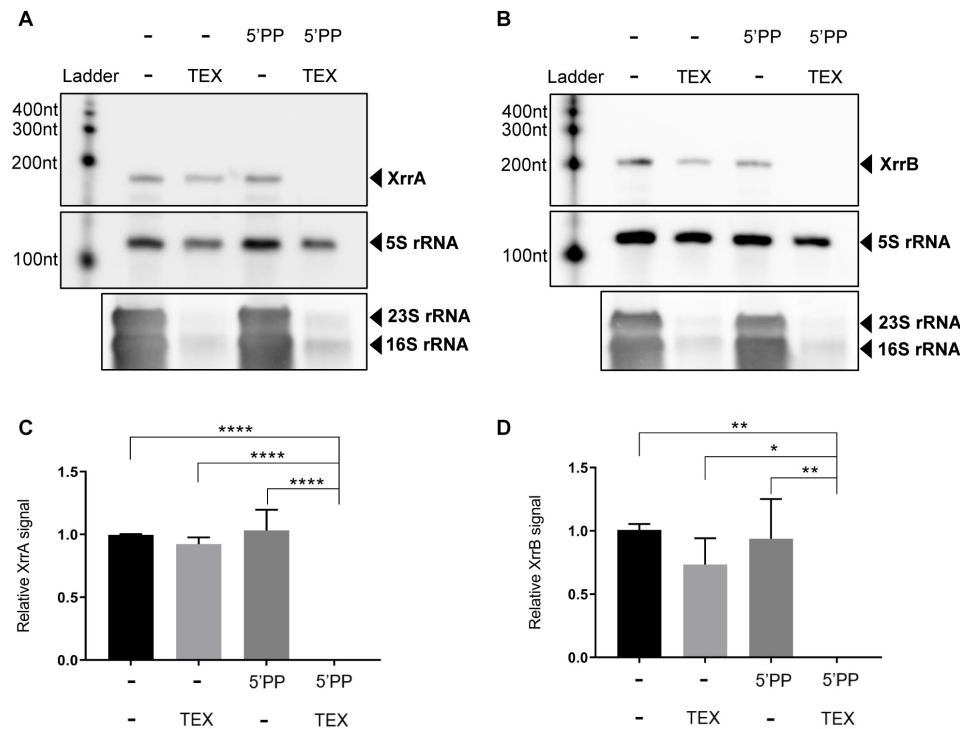


FIGURE 2 | Characterization of XrrA and XrrB 5' ends. To discern the type of 5'phosphate modification on XrrA and XrrB 5' ends, total RNA from the parent strain ANR-1 grown in CA-CO₂ was treated with RNA 5' Polyphosphatase enzyme (5'PP), and/or Terminator exonuclease enzyme (TEX) in the combinations shown. 5'PP removes the gamma and beta phosphates from primary transcripts with a 5' triphosphate, leaving a 5' monophosphate. TEX preferentially degrades transcripts with a 5' monophosphate. Total RNA was treated, as indicated, followed by northern blotting to probe for (A) XrrA and (B) XrrB signal. As a positive control for TEX-mediated degradation, levels of 23S and 16S rRNAs were also assessed. The northern blots shown are representative images of three biological replicates. (C) XrrA and (D) XrrB levels from the three biological replicates were normalized to the TEX-resistant 5S rRNA load control signal and averaged per treatment. The standard deviation in sRNA signal per treatment is shown. Analysis of variance (ANOVA) followed by Tukey's multiple comparison test was used to determine significance. * indicates < 0.05; ** indicates < 0.01; **** indicates < 0.0001.

These data indicate that XrrA and XrrB are primary transcripts originating from stand-alone promoters.

sRNA Expression in Cultures Grown in Conditions That Influence AtxA Expression and Activity

Data from previous reports indicate that XrrA and XrrB transcript levels are positively regulated by AtxA (McKenzie et al., 2014; Raynor et al., 2018). To further explore AtxA-mediated control of XrrA and XrrB, we asked whether sRNA expression patterns are influenced during culture conditions that affect AtxA expression and activity. Transcript levels of *atxA* in cultures grown in minimal media containing glucose are higher than levels in cultures grown in rich media (Chiang et al., 2011). Several reports have described a positive effect of CO₂/bicarbonate on anthrax toxin production (Koehler et al., 1994; Dai et al., 1995; Hammerstrom et al., 2011). Elevated CO₂/bicarbonate levels in media enhance dimerization of AtxA (Hammerstrom et al., 2011), which is required for its activity (Hammerstrom et al., 2015).

We cultured cells at 37°C in the semi-defined minimal medium CA, which contains 0.1% w/v of glucose, or the

rich complex medium LB with no added glucose. CA and LB cultures were incubated shaking in air (CA-Air, LB-Air) or in 5% CO₂ (with 0.8% sodium bicarbonate added to the medium) (CA-CO₂, LB-CO₂). sRNA expression was assessed in the Ames parent strain using northern blotting (Figure 3). Representative northern blots are shown in Figure 3A (XrrA) and Figure 3B (XrrB). Averages of three biological replicates are represented in Figure 3C (XrrA) and Figure 3D (XrrB). Overall, expression patterns for the two sRNAs were similar. sRNA levels were elevated when cultures were incubated in CA medium, relative to LB, and when media were supplemented with 0.8% sodium bicarbonate and incubated in 5% atmospheric CO₂, relative to media lacking the sodium bicarbonate supplement and incubated in air. XrrA and XrrB levels were 16- and 22-fold higher in cultures grown in CA-CO₂ compared to LB-Air, respectively. When cultured in air, XrrA and XrrB levels were 7.0-fold greater in CA compared to LB. The CO₂ effect was apparent in both media. XrrA and XrrB levels were 3.0-fold greater in CA-CO₂ compared to CA-Air. XrrA and XrrB levels were elevated 7.0- and 11-fold, respectively, in LB-CO₂ compared to LB-Air. Finally, for both sRNAs, expression levels were 2.0-fold higher in cultures grown in CA-CO₂ compared to cultures grown in LB-CO₂.

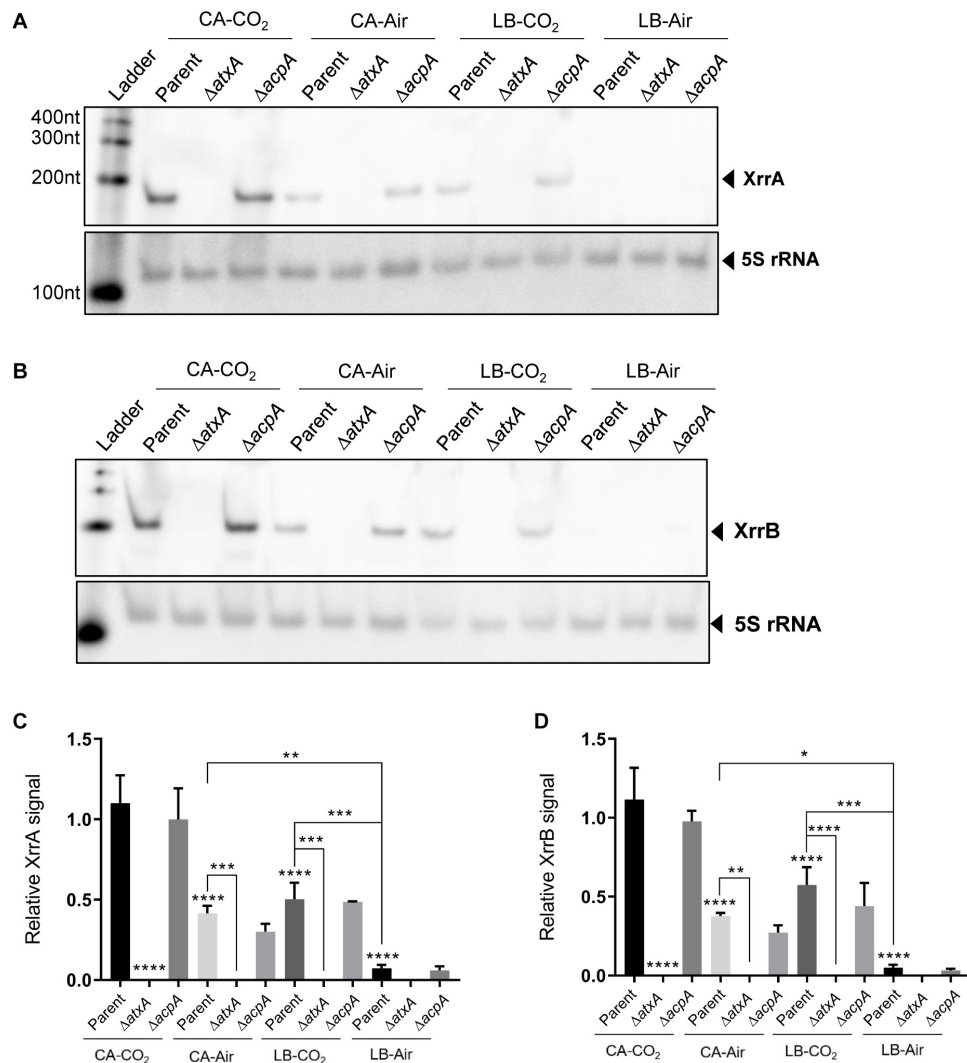


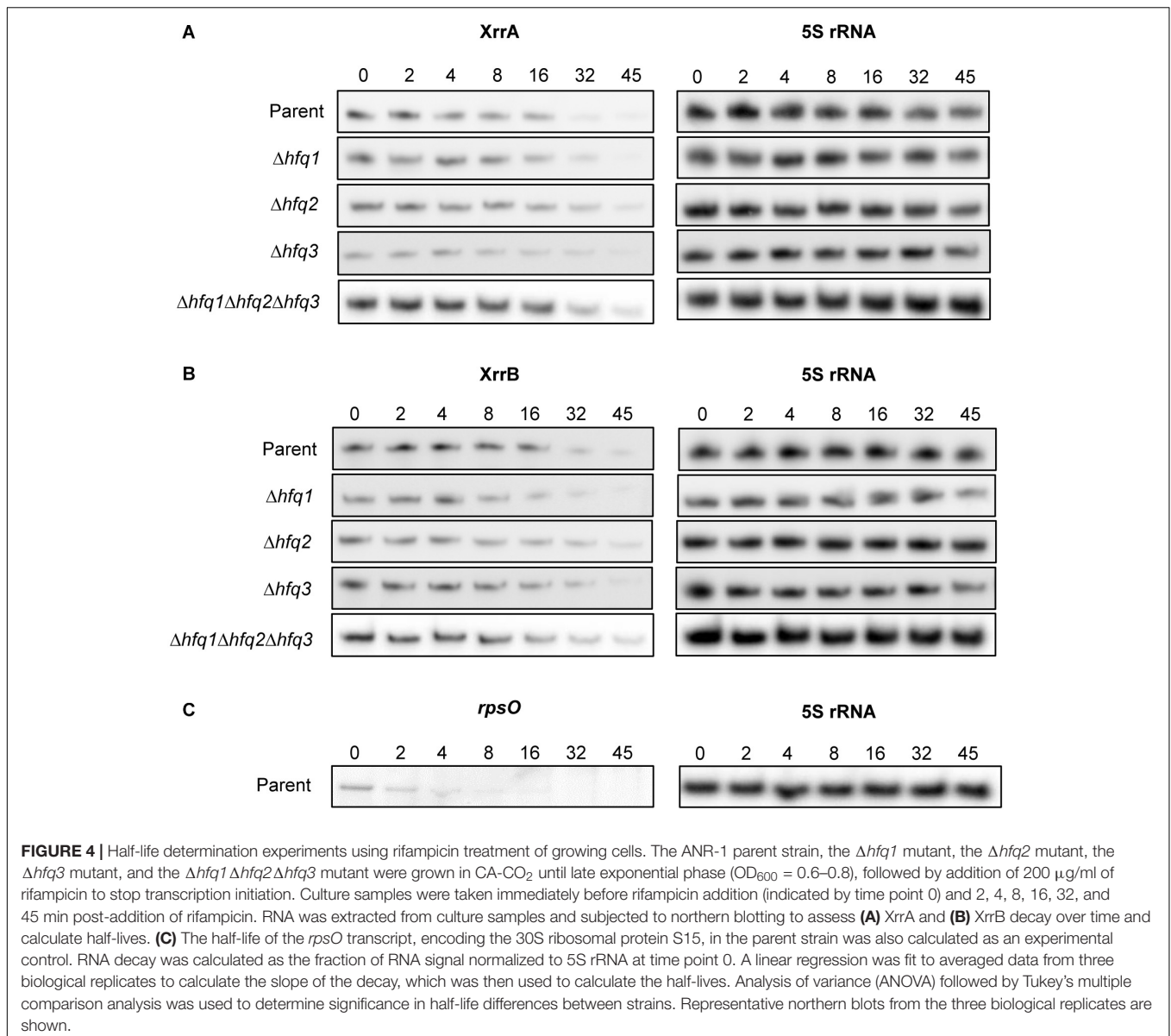
FIGURE 3 | AtxA-mediated control of XrrA and XrrB, and influence of growth conditions that affect AtxA expression and activity on sRNA expression. Total RNA from the Ames parent strain, the $\Delta atxA$ mutant, and the $\Delta acpA$ mutant was extracted from cultures grown in the indicated conditions until early stationary phase ($OD_{600} = 1.0$ – 1.5). Cultures were grown in CA or LB medium and exposed to 5% atmospheric CO₂ or air during growth. Expression of (A) XrrA and (B) XrrB was assessed using northern blotting, and the 5S rRNA signal was used as a load control. A representative northern blot from three biological replicates is shown. (C) XrrA and (D) XrrB levels from the three biological replicates were normalized by 5S rRNA and averaged. The standard deviation in sRNA signal per sample is shown. Analysis of variance (ANOVA) followed by Tukey's multiple comparison test was used to determine significance. * indicates < 0.05 ; ** indicates < 0.01 ; *** indicates < 0.001 ; **** indicates < 0.0001 . Asterisks directly above bars indicate significance of comparison between that bar and the "Parent CA-CO₂" condition. Additional comparisons between conditions are shown linked by brackets, with respective significance indicated by asterisks above the brackets.

Deletion of *atxA* resulted in no detectable sRNA expression in all the conditions tested (Figure 3). Notably, although previously reported RNA-seq data suggested that AcpA positively affected XrrB expression (Raynor et al., 2018), in our experiments deletion of *acpA* did not alter XrrB levels compared to the parent strain. In the previous study (Raynor et al., 2018), AcpA control of XrrB was observed when an $\Delta atxA \Delta acpA \Delta acpB$ strain was complemented with AcpA. Our studies using an *acpA*-null mutant carrying the native *atxA* gene suggest that XrrB is responsive to AtxA in the absence of AcpA. Together, the data indicate that XrrA and XrrB are primarily regulated by AtxA, and that sRNA expression patterns mimic the

atxA-dependent expression of *B. anthracis* virulence factors such as the anthrax toxin genes.

sRNA Half-Life in Parent and hfq-Null Strains

In some bacteria, sRNAs are stabilized by the RNA-chaperone Hfq. Interactions with Hfq lead to protection against RNases and facilitate base-pairing with mRNA targets. The *B. anthracis* genome includes three genes predicted to encode Hfq proteins. Two of these proteins, Hfq1 and Hfq2, are encoded on the chromosome, while a third protein, Hfq3, is encoded on pXO1



(Vrentas et al., 2015). Positive control of the pXO1-encoded sRNAs and the chromosome-encoded Hfq2 by AtxA (McKenzie et al., 2014; Raynor et al., 2018), and the previously reported functionality of Hfq2 and Hfq3 in *E. coli* (Vrentas et al., 2015; Keefer et al., 2017), indicate potential relationships between the sRNAs and Hfq proteins of *B. anthracis*.

A common feature of Hfq-dependent sRNAs is the presence of Rho-independent terminators at the 3' ends of the transcripts (Otaka et al., 2011). The 3' oligoU tails of these sRNAs are often bound by Hfq (Sauer and Weichenrieder, 2011; Ishikawa et al., 2012). Given that XrrA and XrrB are predicted to form Rho-independent terminators (Supplementary Figures 2, 3), we asked whether the *B. anthracis* Hfq chaperones influenced XrrA and XrrB stability. We constructed isogenic deletion mutants for the *hfq* genes ($\Delta hfq1$, $\Delta hfq2$, $\Delta hfq3$, and $\Delta hfq1 \Delta hfq2 \Delta hfq3$) and measured the sRNA half-lives in parent and mutant strains when

cultured in toxin-inducing conditions (Figure 4). XrrA and XrrB had similar half-lives in the parent strain. The half-life of XrrA was 20 ± 1.1 min (Figure 4A and Table 2), while the half-life of XrrB was 21 ± 1.5 min (Figure 4B and Table 2). Deletion of the *B. anthracis hfq* genes had no statistically significant effects on sRNA stability, although there was a slight trend toward extension of sRNA half-life in some mutants. To validate our RNA stability assay, we tested the stability of the *rpsO* transcript, which encodes a ribosomal protein of the small sub-unit of the ribosome. The *B. subtilis rpsO* transcript has been reported to be approximately 4 min (Yao and Bechhofer, 2010). In our experimental conditions, the half-life of the *B. anthracis rpsO* transcript was 2.1 ± 1.2 min (Figure 4C and Table 2). Overall, these data indicate that when *B. anthracis* is cultured in optimal conditions for toxin gene expression, XrrA and XrrB are highly stable, Hfq-independent sRNAs.

TABLE 2 | sRNA half-lives in the parent and *hfq*-null strains.

Strain	XrrA Half-life (minutes) ^a	XrrB Half-life (minutes) ^a	<i>rpsO</i> Half-life (minutes) ^a
Parent	20 ± 1.1	21.2 ± 1.5	2.1 ± 1.2
$\Delta hfq1$	20.4 ± 0.9	20.2 ± 0.2	
$\Delta hfq2$	25.1 ± 4.4	23 ± 3.4	
$\Delta hfq3$	24.7 ± 4.6	21.4 ± 3.4	
$\Delta hfq1 \Delta hfq2 \Delta hfq3$	23 ± 1.6	25.2 ± 2.3	

^aHalf-lives reported are the average of three biological replicates, shown in minutes. Standard deviation in sRNA and *rpsO* mRNA half-lives is indicated as \pm minutes.

sRNA Regulons and Loci of sRNA-Regulated Genes

To determine sRNA-controlled genes of *B. anthracis*, we compared the transcriptomes of *xrrA*- and *xrrB*-null mutants to that of a parent strain using RNA-seq. We constructed sRNA-null mutants in a virulent Ames (pXO1⁺, pXO2⁺) background. We compared the transcriptome of UTA37 (Raynor et al., 2018) with that of the isogenic mutants UTA38 ($\Delta xrrB$), UTA39 ($\Delta xrrA$), and UTA41 ($\Delta xrrA \Delta xrrB$). Cultures were grown to early stationary phase in CA-CO₂, which allows high level expression of the sRNAs (Figure 3). RNA was extracted and subjected to Illumina sequencing.

Deletion of *xrrA* and *xrrB* had distinct effects on *B. anthracis* gene expression (Figure 5). Deletion of *xrrA* resulted in 50 transcripts showing a ≥ 4.0 -fold change in expression compared to the parent strain; expression of 12 transcripts was reduced in the $\Delta xrrA$ mutant, while 38 transcripts were elevated in the mutant (Figure 5A). In contrast, deletion of *xrrB* led to one transcript having a ≥ 4.0 -fold change in expression compared to the parent strain (Figure 5B). The transcript, encoded by the gene GBAA_0594, was decreased in the $\Delta xrrB$ mutant. Interestingly, deletion of both sRNAs in the $\Delta xrrA \Delta xrrB$ mutant affected a greater number of transcripts than the combined total number of transcripts affected in the $\Delta xrrA$ and $\Delta xrrB$ mutants. In the $\Delta xrrA \Delta xrrB$ mutant, levels of 116 transcripts were affected with a fold-change of ≥ 4.0 (Figure 5C). Ninety-seven of these transcripts were increased in the mutant, while 19 transcripts were decreased. Our analysis detected one apparent operon and nine bicistronic transcripts amongst all transcripts affected by sRNA deletions (Supplementary Table 2). The apparent operon (*hom1-thrC-thrB*) encodes enzymes involved in threonine biosynthesis and its expression was elevated in the $\Delta xrrA$ and $\Delta xrrA \Delta xrrB$ mutants (Supplementary Table 2). Eight of the nine bicistronic transcripts were elevated in sRNA mutant strains. One bicistronic transcript (GBAA_2366-GBAA_2367) was decreased in the $\Delta xrrA$ and $\Delta xrrA \Delta xrrB$ mutants (Supplementary Table 2).

Most sRNA-regulated genes uncovered in this study were located on the *B. anthracis* chromosome. Of all transcripts exhibiting a fold-change of ≥ 4.0 , only four were associated with genes on pXO1. Three of these genes encode hypothetical proteins with no ascribed functions (Supplementary Table 2). These transcripts were encoded by the GBAA_pXO1_0022, GBAA_pXO1_0153, and GBAA_pXO1_0171 genes. GBAA_pXO1_0022 was the only affected pXO1 gene not located

within the plasmid pathogenicity island. Expression of all three of these genes was affected in both the $\Delta xrrA$ and $\Delta xrrA \Delta xrrB$ strains. The fourth sRNA-regulated pXO1 gene was *lef*, encoding the lethal factor component of the anthrax toxin, located within the pXO1 pathogenicity island. Interestingly, expression of the *lef* transcript was reduced 4.7-fold in the $\Delta xrrA \Delta xrrB$ mutant and unaffected in the single deletion strains. Finally, there were no pXO2-encoded transcripts regulated by the sRNAs having a fold-change of ≥ 4.0 compared to the parent.

Overlap Between sRNA Regulons

Table 3 lists transcripts that were most highly-regulated (≥ 16 -fold-change) by the individual sRNAs and transcripts that were regulated by both sRNAs. Supplementary Table 2 is an expanded version of Table 3, listing transcripts that were regulated ≥ 4.0 -fold by individual sRNAs and transcripts regulated by both sRNAs. The transcript encoded by GBAA_0594 was the only transcript affected in all sRNA deletion mutants with a ≥ 4.0 fold-change (Figure 5 and Supplementary Table 2). GBAA_0594 was also the sole transcript that showed a fold-change of ≥ 4.0 in the $\Delta xrrB$ mutant (Figure 5B).

Given that XrrA regulated many more transcripts than XrrB, and that deletion of both *xrrA* and *xrrB* resulted in even further changes to transcript expression, we compared the XrrA and XrrAXrrB regulons obtained from RNA-seq analysis (Figure 6). To visualize overlap between sRNA regulons, we plotted transcripts exhibiting a significant fold-change of ≥ 4.0 in at least one mutant strain as a scatterplot (Figure 6A). We found that most transcripts affected in the $\Delta xrrA \Delta xrrB$ mutant were also affected in the $\Delta xrrA$ mutant. All transcripts were regulated in the same direction, either increased or decreased expression, in both strains (Figure 6A). In addition, for most of the regulated genes, the fold-changes in the $\Delta xrrA$ mutant and the $\Delta xrrA \Delta xrrB$ mutant were comparable. The data indicate that for most transcripts, regulatory effects observed in the double mutant likely result from deletion of *xrrA*. Nevertheless, we observed some transcripts that exhibited non-significant changes in expression in the $\Delta xrrA$ mutant but were significantly altered in the $\Delta xrrA \Delta xrrB$ mutant. To confirm that these transcripts were affected only in the double null mutant, we directly compared transcript expression in the $\Delta xrrA$ and $\Delta xrrA \Delta xrrB$ mutants (Figure 6B). Indeed, we found 11 transcripts for which expression was affected ≥ 4.0 -fold in the $\Delta xrrA \Delta xrrB$ mutant but were not affected ≥ 4.0 -fold in the $\Delta xrrA$ mutant. Together, the data suggest distinct regulatory roles for XrrA, as well as some functional overlap between XrrA and XrrB, as evidenced by the increased number of XrrB-regulated targets in the *xrrA-xrrB*-null background.

Notably, our data show that the sRNAs do not regulate expression of each other or *atxA*. Northern blot analysis of XrrA and XrrB in sRNA-null strains showed comparable levels of XrrA expression in the parent and $\Delta xrrB$ mutant (Supplementary Figure 4). Similarly, XrrB levels were comparable in the parent and $\Delta xrrA$ mutant (Supplementary Figure 4).

Most-Highly sRNA-Regulated Targets

RNA-seq data uncovered GBAA_0594 as the only transcript controlled by XrrB in the presence of XrrA

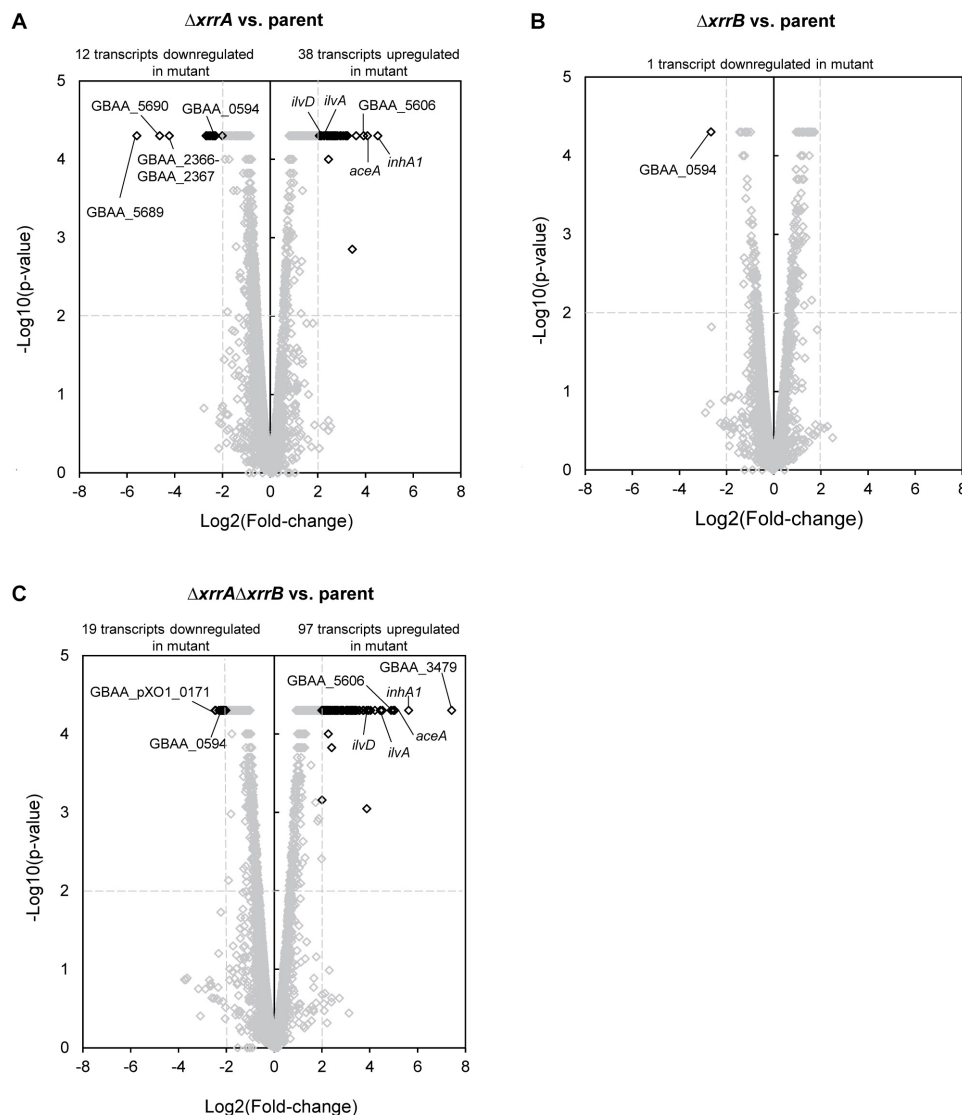


FIGURE 5 | Transcriptomic analysis of sRNA-null mutants compared to the parent strain. The Ames-derived UTA37 parent strain, UTA38 ($\Delta xrrB$), UTA39 ($\Delta xrrA$), and UTA41 ($\Delta xrrA\Delta xrrB$) were grown in CA-CO₂ to early stationary phase (OD₆₀₀ = 1.0–1.5) and RNA was extracted for RNA-seq analysis. Volcano plots show the effect of (A) $\Delta xrrA$ deletion, (B) $\Delta xrrB$ deletion, and (C) $\Delta xrrA\Delta xrrB$ deletion on RNA abundance, compared to the parent strain. Transcripts that showed significantly different expression levels are highlighted in black. Transcripts that did not show a significant difference in expression are shown in gray. The p -value cutoff was 0.01, which corresponds to a $-\log_{10}(p\text{-value})$ of 2, and the $\log_2(\text{fold-change})$ cutoff was ≥ 2.0 , which represents a fold-change of ≥ 4.0 . Significance and fold-change thresholds are indicated by dashed lines. Transcripts of interest are labeled.

(Figure 5B). GBAA_0594 is predicted to encode a putative transcriptional regulator of the ArsR-family. These regulators typically bind DNA in the presence of metal cofactors (Ren et al., 2017). Expression of GBAA_0594 was reduced in the $\Delta xrrB$ mutant compared to the parent strain, with a fold-change of 6.3 (Figure 5B and Supplementary Table 2). This transcript was also decreased in the $\Delta xrrA$ and $\Delta xrrA\Delta xrrB$ mutants, with fold-changes of 5.7 and 5.4, respectively (Figure 5 and Supplementary Table 2). Decreased levels of GBAA_0594 in the $xrrB$ -null did not result in changes in expression of other transcripts in this mutant,

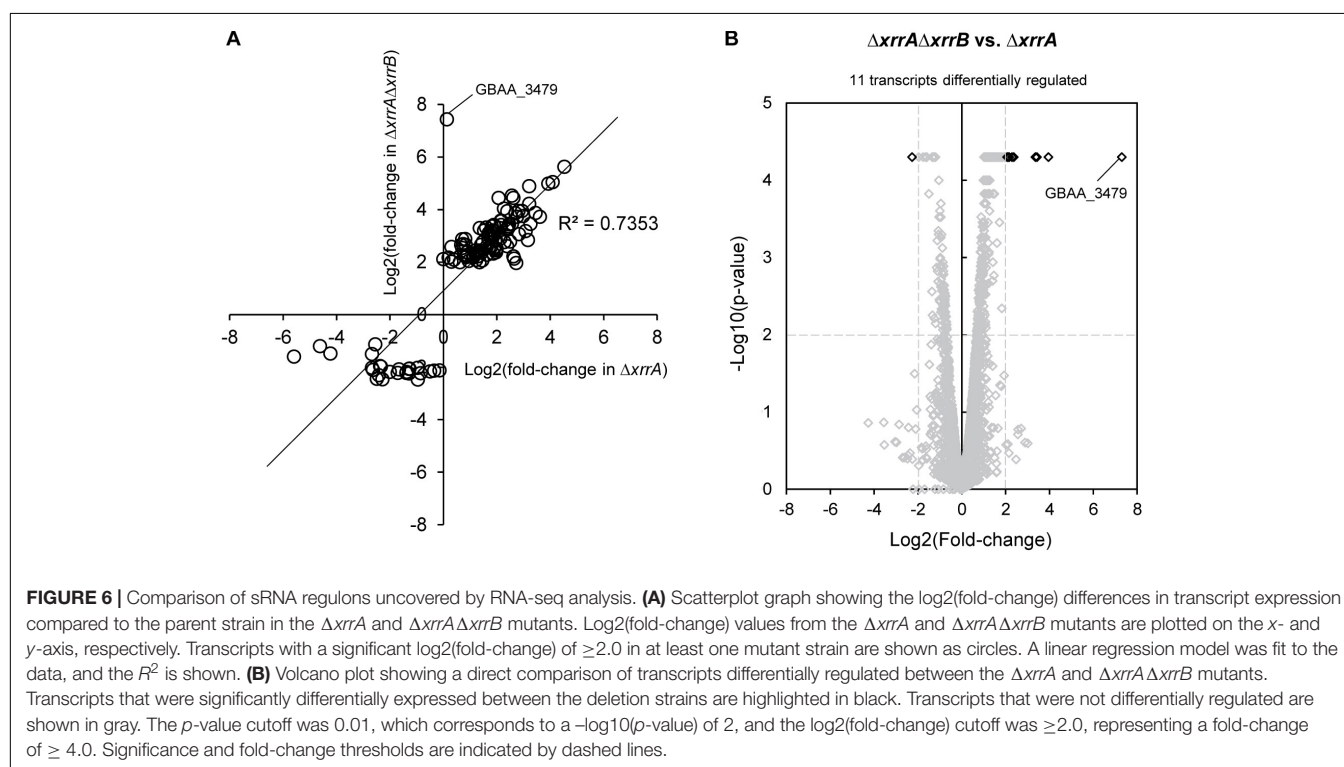
suggesting that the encoded protein may not function as a transcriptional regulator, at least in the growth conditions tested.

Overall, XrrA regulated many more genes than XrrB. One of the most highly XrrA-regulated transcripts is encoded by the *inhA1* gene (Figure 5A). *InhA1* is a secreted protease that mediates processing of *B. anthracis* proteins and breakdown of host proteins during infection (Pflughoeft et al., 2014; Terwilliger et al., 2015). Expression of *inhA1* was elevated 23-fold in the $\Delta xrrA$ mutant compared to the parent strain (Table 3), suggesting that XrrA represses expression of *inhA1*. The transcript was also differentially regulated in the $\Delta xrrA\Delta xrrB$,

TABLE 3 | Transcripts most highly regulated and co-regulated by the sRNAs.

Transcript tag	Gene name(s)	Function	Log2(fold-change) ^a		
			$\Delta xrrA$	$\Delta xrrB$	$\Delta xrrA\Delta xrrB$
GBAA_3479		Putative ArsR-family transcriptional regulator	–	–	+7.43
GBAA_1295	<i>inhA1</i>	Immune inhibitor metalloprotease	+4.52	+1.02	+5.63
GBAA_1132	<i>aceA</i>	Isocitrate lyase	+4.08	–	+5.05
GBAA_5606		Putative aminopeptidase	+3.92	–	+4.99
GBAA_2827		Putative chitin binding protein	+3.21	+0.98	+4.89
GBAA_1854	<i>ilvA</i>	Threonine ammonia-lyase	+2.56	–	+4.53
GBAA_4149		Putative hydrolase	+2.62	–	+4.44
GBAA_2633		Putative cysteine deoxygenase	+2.06	–	+4.44
GBAA_3709-GBAA_3710	<i>hutG-hutI</i>	Formiminoglutamate-imidazolonepropionase	+3.21	–	+4.22
GBAA_1853	<i>ilvD</i>	Dihydroxy-acid dehydratase	+2.26	–	+4.04
GBAA_2366-GBAA_2367		Hypothetical protein-putative oxalate:formate antiporter	–4.23	–	–1.48
GBAA_5690		Putative holin	–4.63	–	–1.2
GBAA_5689		Putative membrane protein	–5.6	–	–1.6

^aHyphens indicate a non-significant difference in transcript expression.



with a fold-change of 50 (Table 3). Deletion of *XrrB* had a 2.0-fold effect on *inhA1* expression, indicating a synergistic effect of the sRNAs on *inhA1* expression.

XrrA also appears to regulate enzymes of the glyoxylate cycle. This cycle is a variation of the tricarboxylic acid (TCA) cycle that allows some organisms, including bacteria, to bypass decarboxylation steps of the TCA cycle to synthesize succinate from acetyl-coA (Kornberg and Madsen, 1989). The two enzymes, isocitrate lyase and malate synthase, are encoded by the *aceA* and *aceB* genes, respectively. Expression of *aceA* was increased in the $\Delta xrrA$ and $\Delta xrrA\Delta xrrB$ mutants, with

fold-changes of 17 and 33, respectively (Figure 5 and Table 3). Expression of *aceB* was elevated 7.9- and 13-fold in the $\Delta xrrA$ and $\Delta xrrA\Delta xrrB$ mutants (Supplementary Table 2).

Deletion of *xrrA* also affected genes predicted to be involved in branched-chain amino acid (BCAA) biosynthesis, transport, and catabolism. Previous reports have indicated AtxA-mediated repression of BCAA biosynthesis operons and BCAA transporter genes (Bourgogne et al., 2003; Raynor et al., 2018). According to our own RNA-seq data, the two most highly sRNA-regulated BCAA-related genes were *ilvA* and *ilvD*, which encode enzymes of the BCAA biosynthesis pathway (Figure 5 and Table 3).

The *ilvA* gene encodes an enzyme that catalyzes the first step of isoleucine biosynthesis from threonine, while *ilvD* encodes an enzyme utilized in the biosynthesis of all three BCAAs. The *ilvA* transcript increased 5.9-fold in the $\Delta xrrA$ mutant (Figure 5A and Table 3). Interestingly, in the $\Delta xrrA\Delta xrrB$ mutant the *ilvA* transcript increased 23-fold compared to the parent (Figure 5C and Table 3). The *ilvD* transcript displayed similar effects, with the double sRNA deletion having a greater effect on expression than the single *xrrA* deletion (Figure 5 and Table 3). Interestingly, deletion of *xrrB* alone did not affect *ilvA* or *ilvD* expression. XrrA also regulated other enzymes of the BCAA biosynthesis operons of *B. anthracis*, as well as enzymes involved in threonine biosynthesis (*hom1-thrC-thrB*) (Supplementary Table 2). Threonine serves as a precursor for isoleucine biosynthesis. At least one gene predicted to be involved in BCAA transport, *brnQ3*, was regulated by XrrA. Based on sequence conservation, BrnQ3 is predicted to function as a sodium-dependent transmembrane transporter of BCAAs. The transcript was differentially regulated 3.7-fold in the $\Delta xrrA$ mutant, and 9.1-fold in the $\Delta xrrA\Delta xrrB$ mutant (Supplementary Table 2). Expression of genes encoding enzymes involved in BCAA catabolism was also impacted. Transcript levels of the *bfbAa*, *bfbB*, and *bfbAb* genes, encoding components of the branched-chain alpha-keto dehydrogenase complex, were reduced in the $\Delta xrrA$ mutant, suggesting that XrrA positively influences expression of BCAA catabolism while at the same time repressing BCAA biosynthesis and transport (Supplementary Table 2).

The most highly sRNA-regulated transcript in *B. anthracis* according to our RNA-seq analysis was GBAA_3479, which encodes a second putative ArsR-family transcriptional regulator. Interestingly, expression of GBAA_3479 was only affected in the $\Delta xrrA\Delta xrrB$ mutant (Figure 6 and Table 3). Expression of GBAA_3479 was increased 172-fold in this mutant. Overall, the data indicate that XrrA primarily functions to repress expression of targets, and that at least one target requires both XrrA and XrrB for regulation.

Given that *inhA1* was the most-highly regulated target controlled by a single sRNA, we sought to confirm XrrA-mediated regulation of *inhA1*. We used qPCR to compare relative *inhA1* levels in the Ames-derived parent strain UTA37, the $\Delta xrrA$ mutant UTA39, and UTA39 complemented with pUT1205 containing *xrrA* under the control of an IPTG-inducible promoter. The *inhA1*-null (*inhA1::specR*) mutant UTA5 was used as control for primer specificity. In agreement with our RNA-seq analysis, the qPCR data (Supplementary Figure 5) showed that *inhA1* expression was elevated 10- to 15-fold in the *xrrA*-null mutant compared to the parent. Moreover, exogenous complementation of *xrrA* lowered *inhA1* expression to levels similar to the parent strain. These data confirm XrrA-mediated regulation of *inhA1* and validate our RNA-seq data.

Gene Ontology Analysis of sRNA Regulons

We performed gene ontology analysis of genes regulated by the sRNAs. Since XrrB regulated a single target, we chose

to focus on classification of genes affected ≥ 4.0 -fold in the $\Delta xrrA$ and $\Delta xrrA\Delta xrrB$ mutants according to their predicted biological function (Figure 7). Hypothetical proteins of unknown function comprised 21% of the XrrA regulon (Figure 7A). Interestingly, genes encoding proteins predicted to be involved in oligopeptide transport represented approximately 7% of the XrrA regulon. These included GBAA_0656, GBAA_0658, and GBAA_0852, which are predicted to be ABC-type transporters (Supplementary Table 2). Transcripts from these genes appear to be repressed by XrrA. BCAA biosynthesis genes represented an additional 7% of the XrrA regulon. About 5% of the XrrA-affected genes are involved in proteolysis (Figure 7A). These included *inhA1*, GBAA_5606, and *calY*. The *calY* gene encodes camelysin, a cell surface-bound metalloprotease involved in virulence in *B. cereus* (Grass et al., 2004; Candela et al., 2019). An additional 5% of the XrrA regulon consists of genes associated with histidine catabolism, including genes of the *histidine utilization* (*hut*) operon. The *hutG-hutI* transcript was regulated 9.3-fold in the $\Delta xrrA$ strain (Table 3) and the *hutU* transcript was regulated 5.4-fold in this strain (Supplementary Table 2).

For genes whose expression was altered in the $\Delta xrrA\Delta xrrB$ mutant, 38% were genes encoding hypothetical proteins with no ascribed functions (Figure 7B). Interestingly, approximately 7% of the genes of the XrrAXrrB regulon encode proteins that mediate oxidation-reduction reactions (Figure 7B). These included genes encoding ubiquinone, menaquinol, and putative cytochromes (Supplementary Table 2). BCAA biosynthesis genes represented 6.3% of the XrrAXrrB regulon, and proteolysis genes represented 5.6%. Regulation of transcription was a biological process represented only in the XrrAXrrB regulon (3.2%), in part given by control of the putative transcriptional regulator GBAA_3479 in the $\Delta xrrA\Delta xrrB$ mutant only. Other represented biological processes included histidine catabolism, transmembrane transport, and chitin catabolism.

In silico Analysis of Complementarity Between the sRNAs and mRNA Targets

A common mechanism of sRNA function is direct base-pairing with mRNA targets to control aspects of translation and/or transcript decay. Base-pairing to the mRNA target often occurs via a short, imperfect region of complementarity often referred to as the seed region (Gottesman and Storz, 2011). We asked whether the sRNAs displayed any complementarity to sRNA-regulated mRNA transcripts uncovered in this study. To find potential interactions between the sRNAs and mRNAs, we used the TargetRNA2 webserver (Kery et al., 2014). sRNA sequences uncovered by RACE analysis were entered to the TargetRNA2 webserver and aligned to the *B. anthracis* chromosome. Transcripts displaying a fold-change of ≥ 4.0 in at least one sRNA-null strain and showing complementarity to the sRNAs are listed in Table 4. We found seven XrrA-regulated transcripts that had complementarity to XrrA. For four of the transcripts, XrrA was predicted to interact at the translational start site of the mRNA, suggesting that XrrA may influence translation of these transcripts. The transcripts *inhA1*, GBAA_0656, and GBAA_4468 are negatively regulated

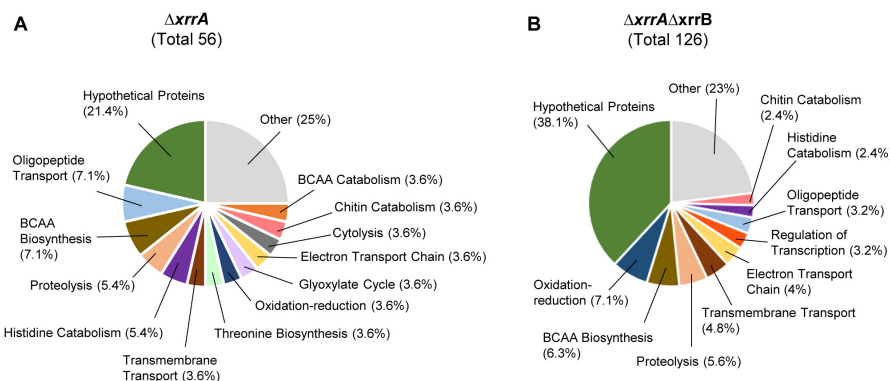


FIGURE 7 | Gene ontology analysis of genes of which expression was affected in the $\Delta xrrA$ and $\Delta xrrA\Delta xrrB$ strains. Genes that were differentially regulated in the (A) $\Delta xrrA$ and (B) $\Delta xrrA\Delta xrrB$ mutants with a fold-change of ≥ 4.0 compared to the parent strain were categorized based on biological processes. Pie charts show the total number of differentially regulated genes and the percentage of those genes that belong to a gene ontology category based on biological processes. Hypothetical proteins represent genes with unknown functions or no putative functions based on gene sequence analysis. The colored sections of the pie charts represent biological process categories associated with more than 2% of the strain regulons. Categories associated with 2% or less of the regulons are shown in gray and labeled as “other.”

TABLE 4 | Regions of complementarity between the sRNAs and sRNA-regulated mRNA transcripts.

sRNA sequence ^a	sRNA start ^b	sRNA end ^b	mRNA ^c	mRNA sequence ^{a,d}	mRNA start ^e	mRNA end ^e	Energy ^f	p-value ^g
XrrA								
Seed region # 1								
aGUCAUUGAGAAcUUGAu	34	17	<i>asnO2</i>	aUAGUAAACUCUuAACU	−72	−56	−11.97	0.008
Seed region # 2								
CCUCu UUUCUACCG-AUagCGa	92	72	GBAA_4468	GGAG-GGAGAUGGC CaUG gaGC	−14	+7	−13.21	0.003
uAUACCUCUUUUCUaCCg	96	79	GBAA_5301	uUAUGGAGAAAAGGaGG	−27	−11	−14.83	0.001
aUACCUCUUUUCUaCCc	95	80	GBAA_0656	gGUGGAGAAAGuu AUG a	−12	+4	−11.58	0.01
Seed region # 3								
aUCCCCUCAAUcAAUaUu	177	160	GBAA_3451	aGGGGGAGUUA-UUAU Au	−15	+2	−14.81	0.001
uCUUJaUCCCCUCa	182	169	<i>hutU</i>	uGAGAAaAGGGGAGa	−21	−8	−13.72	0.002
U-CUUUAUCCCUc	182	170	<i>inha1</i>	AgGAAUAAGGG Au	−12	+2	−11.54	0.01
XrrB								
AUGGUaCCCCUUUg	194	180	GBAA_2549	UACUAaGGGGGAAa	−19	−6	−13.7	0.002

^a Complementarity between sequences is shown in uppercase letters. Dashes indicate a break in the complementarity region.

^b Indicates start and end of complementarity region on the sRNA, relative to the sRNA transcriptional start site.

^c Transcripts exhibiting a fold-change of ≥ 4.0 in at least one sRNA-null strain were selected for analysis.

^d Nucleotides that are part of the translational start codon of the mRNA are shown in bold.

^e Indicates start and end of complementarity region on the mRNA, relative to the mRNA translational start site.

^f Thermodynamic energy (kcal/mol) of hybridization between sRNA and mRNA, as calculated by TargetRNA2.

^g Indicates probability that the sRNA and mRNA interaction occurs by chance (p-value cutoff was 0.05), as calculated by TargetRNA2.

by XrrA (Table 4 and Supplementary Table 2). Thus base-pairing with XrrA may result in inhibition of translation, leading to mRNA decay due to reduced ribosomal occupancy. On the other hand, GBAA_3451 is positively regulated by XrrA (Supplementary Table 2), suggesting that the base-pairing interaction may result in enhanced translation of the transcript. For the remaining 3 transcripts, XrrA was predicted to interact further upstream in the 5' UTR. For *hutU*, which encodes urocanate hydratase and is negatively regulated by XrrA (Supplementary Table 2), base-pairing with XrrA is predicted to occur eight nucleotides upstream of the translational start site, suggesting that XrrA may block the RBS

of *hutU* to inhibit translation. The remaining two transcripts, GBAA_5301 and *asnO2*, are predicted to base-pair with XrrA further upstream in their respective 5'UTRs. Such interactions could affect secondary structure and stability of the transcripts, resulting in changes to the rate of mRNA decay. Overall, our data suggest that XrrA is likely to function as a base-pairing sRNA.

Interestingly, the seven mRNA transcripts that showed complementarity to XrrA were all targeted by one of three seed regions on XrrA. These regions included sections of XrrA that are predicted to be at least partially single-stranded (Supplementary Figure 2). The predicted secondary structure of XrrA suggests

formation of three hairpin loops: the 3' terminator described earlier, a major hairpin encompassing most of the XrrA sequence, and a minor hairpin directly preceding the predicted terminator (**Supplementary Figure 2**). Seed region #1, which encompasses nucleotides +17 and +34 in relation to the transcriptional start site, as well as seed region #2, which includes nucleotides +72 to +96, are found along the major hairpin of XrrA. Both regions include loops of single-stranded nucleotides that would be available to mediate initial interaction with mRNA targets. One transcript is predicted to be targeted by seed region #1, while three transcripts had predicted complementarity to seed region #2 (**Table 4**). The third seed region was located between nucleotides +160 and +182 and is found within the 3' hairpin terminator of XrrA. Three transcripts are predicted to base-pair with XrrA at this region, including the highly-regulated *inhA1* (**Table 4**).

XrrB showed limited complementarity to sRNA targets. There was no complementarity found to GBAA_0594, the only transcript differentially regulated in the $\Delta xrrB$ mutant by a ≥ 4.0 fold-change. Instead, we found that XrrB is predicted to interact with GBAA_2549, at the 5' UTR of the transcript (**Table 4**). Interestingly, expression of this transcript increases 10-fold in the $\Delta xrrA\Delta xrrB$ mutant, and only 3.5- and 2.0-fold in the $\Delta xrrA$ and $\Delta xrrB$ mutants, respectively, suggesting a synergistic effect of the sRNAs by an unknown mechanism. Given that XrrB is predicted to base-pair with GBAA_2549 at the 5' UTR, repression of this transcript in the $\Delta xrrA\Delta xrrB$ mutant may be, at least in part, given by decreased stability of the transcript upon interaction with XrrB.

The predicted structure of XrrB was similar to that of XrrA. This sRNA is also predicted to form three hairpins along its sequence (**Supplementary Figure 3**). These included the 3' hairpin terminator, an initial hairpin located at the 5' end of XrrB, and a major hairpin between the 5' and 3' hairpins, occluding a long stretch of XrrB sequence in a double-stranded structure. Interestingly, complementarity to GBAA_2549 was found at the 3' terminator of XrrB, further illustrating the molecular similarities between XrrA and XrrB.

To further validate the base-pairing predictions, we used IntaRNA as an additional RNA-RNA interaction program (Busch et al., 2008). IntaRNA confirmed five of the seven predicted interactions between XrrA and target mRNA sequences obtained from TargetRNA2, including at least one base-pairing interaction per predicted seed region. Additionally, IntaRNA predicted a base-pairing interaction between XrrB and the GBAA_2549 mRNA, which was also predicted by TargetRNA2.

Role of sRNAs in *B. anthracis* Virulence in a Mouse Model for Systemic Anthrax

In a murine model for systemic anthrax in which complement-deficient A/J mice are infected intravenously with pXO1⁺ pXO2⁻ strains of *B. anthracis*, deletion of *atxA* leads to complete attenuation of virulence (Dai et al., 1995; Dale et al., 2012). Considering that the sRNAs are positively controlled by AtxA, we sought to determine if sRNA expression influences virulence in this model (**Figure 8**). We chose to infect mice

with the pXO1⁺ pXO2⁻ ANR-1 strain and isogenic $\Delta xrrA$, and $\Delta xrrA\Delta xrrB$ mutants. XrrA regulates more targets than XrrB, including many genes exhibiting AtxA-regulated expression. The $\Delta xrrA\Delta xrrB$ mutant displayed additional effects on gene expression, including highly increased expression of a putative transcriptional regulator. Mice were infected with vegetative cells of the parent and mutant strains and monitored for up to 11 days. Time to death was recorded, and organ tissues were collected for assessment of infection burden. As shown in **Figure 8A**, there was no statistical difference in the time to death for the parent- and mutant-infected mice. All parent-infected mice and most mutant-infected mice succumbed to infection within the 11-day period. One $\Delta xrrA$ -infected and one $\Delta xrrA\Delta xrrB$ -infected mouse survived. These surviving mice presented no symptoms and were sacrificed at the end of the experiment.

We determined the bacterial burden in organ tissues extracted from all mice that succumbed to infection and in tissues from mice that were sacrificed on day 11. For parent-infected mice, we recovered an average of approximately 10^8 CFU per gram of tissue from the spleen and liver, and approximately 10^9 CFU per gram of tissue from the lungs and kidney. The surviving mutant-infected mice had no detectable CFU in their organ tissue, but all other mice that succumbed to the infection had recoverable levels of CFU. There was no difference in bacterial burden in the kidneys (**Figure 8D**) and spleens (**Figure 8E**) of parent-infected and mutant-infected mice. However, there was a statistically significant decrease in bacterial burden of the liver (**Figure 8B**) and lung (**Figure 8C**) for the $\Delta xrrA$ mutant compared to the parent strain. Mice that succumbed to infection with the $\Delta xrrA\Delta xrrB$ mutant also showed a statistically significant decrease in the number of bacteria in the lung (**Figure 8C**), however, the number of bacteria in the liver (**Figure 8B**) was comparable to that observed for mice infected with the parent strain. The data suggest that de-regulation of XrrA targets leads to a small decrease in colonization of certain host tissues at time of death. Finally, we note that although previous reports have shown that deletion of *atxA* has minimal effects on *in vitro* growth (Dai et al., 1995; Dale et al., 2012), we observed no significant differences in growth rate between the ANR-1 parent strain and the sRNA-null mutants when cultured in CA-CO₂ (**Supplementary Figure 6**).

DISCUSSION

In this work, we provide experimental evidence for sRNA-mediated regulation in the mammalian pathogen *B. anthracis*. The *xrrA* locus is within the 44.8-kb pathogenicity island on the virulence plasmid pXO1. The *xrrB* locus is also on pXO1, just outside of the pathogenicity island. In a previous study reporting expression of these sRNAs, it was proposed that the boundaries of pXO1 pathogenicity island be expanded to include *xrrB* (McKenzie et al., 2014). Sequence analysis using the NCBI Basic Local Alignment Search Tool (BLAST), indicates a high degree of conservation of the sRNA loci across *B. anthracis* strains and in closely-related species carrying pXO1-like plasmids. The *B. anthracis* Ames strain XrrA and XrrB sequences are 99–100%

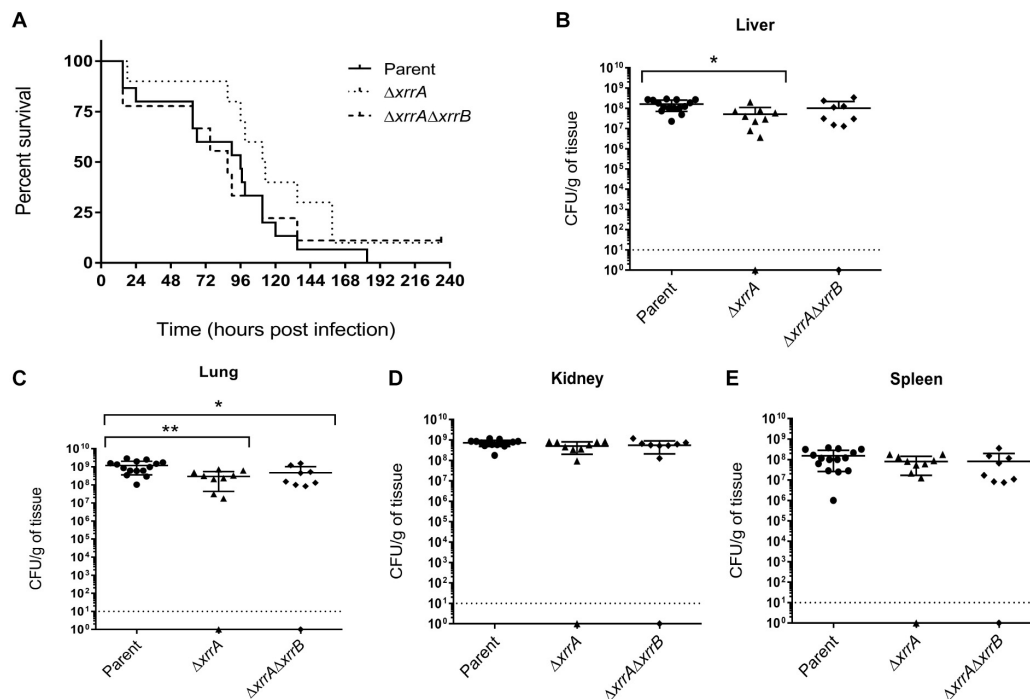


FIGURE 8 | Effect of sRNA deletions on virulence of *B. anthracis* in a murine model for systemic anthrax. Seven-week-old female A/J mice were infected intravenously via the tail-vein with $\sim 10^5$ CFU of the ANR-1 parent strain ($n = 15$), the $\Delta xrrA$ mutant ($n = 10$), or the $\Delta xrrA\Delta xrrB$ mutant ($n = 9$). Mice were monitored for a period of 11 days. Moribund mice were sacrificed, time of death recorded, and liver, lung, kidney, and spleen were collected for CFU determinations to measure organ infection burden. **(A)** Survival analysis using the Kaplan-Meier estimate was used to determine significance between survival of ANR-1-infected and sRNA-null-infected mice. One $\Delta xrrA$ -infected mouse, and one $\Delta xrrA\Delta xrrB$ -infected mouse survived the 11-day period. All other mice succumbed to the infection. CFU/g of tissue of **(B)** liver, **(C)** lung, **(D)** kidney, and **(E)** spleen per infecting strain was calculated. The limit of detection is shown as a dashed line at 10^1 CFU. The surviving $\Delta xrrA$ -infected and $\Delta xrrA\Delta xrrB$ -infected mice showed no detectable CFU in the collected organs and are shown below the limit of detection at 10^0 . Analysis of variance (ANOVA) followed by Tukey's multiple comparisons analysis was used to determine significance between the CFU/g of tissue of each organ for ANR-1-infected, $\Delta xrrA$ -infected, and $\Delta xrrA\Delta xrrB$ -infected mice. * indicates < 0.05 ; ** indicates < 0.01 .

identical to the corresponding sRNAs of all other pXO1⁺ *B. anthracis* strains deposited in the NCBI genome database. The sRNA sequences are also highly conserved (99–100% identical) in the pXO1-like plasmids pBCXO1 and pCI-XO1, found in *B. cereus* strain G9241 and *B. cereus biovar anthracis* strain CI, respectively. Sequences surrounding the sRNA loci in these plasmids, as well as the anthrax toxin and *atxA* genes, are also 99–100% identical to the corresponding sequences on pXO1. These *B. cereus* strains carrying pXO1-like plasmids cause anthrax-like disease (Hoffmaster et al., 2006; Brézillon et al., 2015). The presence of both sRNAs either in proximity or within the classical pXO1 pathogenicity island, and the high degree of conservation of these loci on pXO1 plasmids, suggest co-acquisition of sRNA loci with virulence genes.

Most reports of sRNA expression and function have concerned chromosome-encoded sRNAs. Of the relatively few plasmid-encoded sRNAs that have been reported, most belong to a specific family of regulatory small RNAs called antisense RNAs. These antisense RNAs are encoded in the DNA strand directly opposite to their cognate mRNA target, resulting in long stretches of perfect complementarity between the sRNA and the target (Georg et al., 2009; Güell et al., 2009). Antisense RNAs often regulate plasmid carriage by participating in

toxin-antitoxin systems and control of plasmid conjugation. Typically antisense RNAs can only base-pair to one mRNA target (van Biesen et al., 1993; Fozo et al., 2010; Arthur et al., 2011). On the other hand, chromosome-encoded sRNAs typically belong to the *trans*-encoded RNA family. These sRNAs are transcribed from a location in the bacterial genome that is distant from their cognate mRNA target and mediate base-pairing via a short seed region (Gottesman and Storz, 2011). Thus, *trans*-encoded sRNAs can typically base-pair to multiple mRNA targets using the same seed region. Despite the plasmid loci of XrrA and XrrB, together these regulatory RNAs control multiple target genes on the chromosome. Expression of a few pXO1-encoded transcripts is altered in sRNA-null mutants, but the sequences of these targets do not indicate antisense function of the sRNAs. Our data indicate that XrrA and XrrB are rare examples of *trans*-encoded sRNAs located on a plasmid. These observations place these RNAs, particularly XrrA, at the center of crosstalk between two of the *B. anthracis* genetic elements. We know of only one other report of a virulence plasmid-encoded sRNA regulating chromosomal genes; QfsR, encoded by the tumor inducing (Ti) plasmid of *Agrobacterium fabrum*, controls polycistronic mRNAs of chromosome genes involved in flagella synthesis

and Ti plasmid genes associated with conjugative transfer (Diel et al., 2019).

In addition to the locations of the sRNAs on pXO1, PCVR control of XrrA and XrrB suggests a relationship between the regulatory RNAs and virulence. Our northern blotting data, as well as previous RNA-seq studies (McKenzie et al., 2014; Raynor et al., 2018), indicate that AtxA is the major regulator of XrrA and XrrB expression. While our previous report indicated that artificially expressing AcpA in the $\Delta atxA\Delta acpA\Delta acpB$ strain allowed XrrB expression (Raynor et al., 2018), here we determined that deletion of *acpA* does not affect XrrB expression, indicating a dominant role for AtxA in transcriptional control of XrrB. The crystal structure of AtxA contains two helix-turn-helix domains proximal to the amino-terminus, indicative of DNA-binding activity (Hammerstrom et al., 2015; McCall et al., 2019), and a recent report demonstrated AtxA binding to DNA sequences 5' of *pagA*, an anthrax toxin gene (McCall et al., 2019). Nevertheless, consensus sequences for AtxA-binding to promoter regions of target genes have not been identified. We utilized the MEME suite web server (Bailey et al., 2009) to analyze sequences in the promoter regions of XrrA and XrrB and to compare them to sequences upstream of other AtxA-regulated genes. No consensus sequences were apparent despite our data showing that sRNA expression is dependent upon AtxA. It is possible that AtxA does not directly control *xrrA* and *xrrB* expression, as has been postulated for other genes in the AtxA regulon (Raynor et al., 2018).

Other examples of relationships between PCVRs and sRNAs have been reported. In *Streptococcus pyogenes*, the *multiple* gene activator Mga is a PCVR crucial for expression of virulence factors such as M-protein, streptococcal peptidases, and fibronectin-binding protein (Ribardo and McIver, 2006; Hondorp et al., 2013). Interestingly, expression of the *mga* gene itself is influenced by two sRNAs. The Mga-activating regulatory sRNA MarS was identified in a bioinformatic screen and found to influence expression of virulence factors of *S. pyogenes* (Pappesch et al., 2017). Deletion of *marS* leads to reduced levels of *mga* transcript. A second sRNA, RivX, also positively influences expression of Mga (Roberts and Scott, 2007). RivX is co-transcribed with a second PCVR of *S. pyogenes*, the regulator RivR. Despite co-regulation, RivX and RivR function in independent regulatory pathways and do not influence expression of each other (Roberts and Scott, 2007). In contrast to sRNA control of *mga* transcription, *atxA* transcript levels are unaffected by XrrA and XrrB. Rather, AtxA positively controls sRNA expression. To our knowledge, our study is the first report of PCVR-mediated regulation of sRNAs.

Our half-life determination experiments suggest that XrrA and XrrB are highly stable. Many sRNAs are stabilized by RNA chaperones such as Hfq. While Hfq plays a major role in sRNA function in Gram-negative bacteria, contributions of Hfq to sRNA-mediated regulation vary between species in Gram-positive bacteria. We found that XrrA and XrrB stability is unaffected by deletion of any of the *B. anthracis* *hfq* genes. Interestingly, evidence for RNA chaperones other than Hfq has emerged in recent years. The highly conserved bacterial ProQ protein, first studied in *E. coli*, stabilizes sRNAs

and facilitates base-pairing to mRNA targets, similarly to Hfq (Olejniczak and Storz, 2017). The RNA-binding protein CsrA, which regulates carbon catabolism by influencing mRNA translation and decay, facilitates interactions between sRNAs and their mRNA targets in *B. subtilis* (Müller et al., 2019). Another highly conserved protein, YbeY, influences expression of sRNAs in *E. coli* and accumulation of sRNAs in the plant symbiont *Sinorhizobium meliloti* (Pandey et al., 2011, 2014). It is possible that the sRNAs of *B. anthracis* are stabilized by proteins other than Hfq. The molecular features of XrrA and XrrB may also provide stability. In Gram-positive bacteria, the endonucleolytic enzyme RNase Y mediates the first rate-limiting internal cleavage of transcripts, followed by processive degradation mediated by exonucleases (Mohanty and Kushner, 2016). Additionally, 5' to 3' exonucleolytic decay may be initiated by the 5' exonuclease complex RNase J1/J2 (Even et al., 2005; Bechhofer, 2011). The catalytic activity of RNases Y and J1/J2 is enhanced by a 5' monophosphate group at the 5' of transcripts (Even et al., 2005; Li de la Sierra-Gallay et al., 2008; Shahbadian et al., 2009; Bandyra et al., 2012; De Lay and Gottesman, 2012). Our data indicate that both XrrA and XrrB are primary transcripts, each with a 5' triphosphate group. Thus, the sRNAs are predicted to be protected from RNase Y-mediated endonucleolytic cleavage and RNase J1/J2-mediated 5' exonucleolytic decay. Moreover, the predicted hairpin terminators at the sRNA 3' ends would confer protection against 3' exonucleolytic decay. Additionally, most of the sRNA sequences are predicted to be occluded by extensive secondary structure, which would further protect the sRNAs from RNase Y, which requires single-stranded structure for cleavage. Initiation of XrrA and XrrB decay in *B. anthracis* would likely be dependent on endonucleases that specifically target double-stranded regions on RNA, such as RNase III, which has a minor role in bulk RNA turnover compared to RNase Y and RNase J1/J2 (Durand et al., 2012). While RNA decay has not been studied directly in *B. anthracis*, we infer from RNA decay mechanisms of other species that XrrA and XrrB are highly stable due in part to their 5' and 3' end characteristics and their extensive secondary structure.

Our RNA-seq data show that multiple transcripts are affected by deletion of *xrrA* alone. Given that seven of those transcripts are predicted to directly interact with XrrA, it is likely that this sRNA functions by base-pairing. We found three predicted seed regions on XrrA, predicted to contain short single-stranded regions. Initial base-pairing between these regions and the mRNA targets could result in rearrangement of the XrrA secondary structure, revealing further single-stranded stretches to complete base-pairing along the entire seed region. Furthermore, levels of some transcripts are altered in the sRNA double-deletion, but are unaffected in single sRNA-null mutants, suggesting some functional overlap between XrrA and XrrB. Particularly, expression of the GBAA_3479 transcript predicted to encode a member of the ArsR family of transcriptional regulators, was highly increased in the double-null only, suggesting that both sRNAs are required for regulation of this target. We

found no sequence complementary between the sRNAs and GBAA_3479, so direct base-pairing to GBAA_3479 by both sRNAs seems unlikely. The additional 10 transcripts that were altered only in the double mutant may be responsive to the GBAA_3479 gene product.

It is possible that the sRNAs may also function as protein-interacting sRNAs and compete for interaction with the same regulatory protein(s). There are several examples of multiple sRNAs titrating the same proteins. For example, the multiple sRNAs of the *P. aeruginosa* Rsm system titrate the regulatory proteins RsmA and RsmF (Vakulskas et al., 2015; Miller et al., 2016; Janssen et al., 2018). Interactions between the sRNAs and regulatory proteins of *B. anthracis* could account for the apparent overlapping functions of XrrA and XrrB. Future experiments will test for direct base-pairing between the sRNAs and target gene sequences, as well as for sRNA-protein interactions.

Gene ontology analysis suggests at least two groups of XrrA-regulated genes that are of particular interest for a pathogen that survives in multiple host tissues. First, XrrA regulates expression of several proteases, including InhA1, CalY, and the putative aminopeptidase GBAA_5606. Second, XrrA also regulates expression of predicted amino acid transporters, including the predicted BCAA transporter BrnQ3, and the predicted oligopeptide transporters GBAA_0656, GBAA_0658, and GBAA_0852. Co-regulation of these targets by XrrA suggests a link between expression of proteases during an infection and acquisition of amino acids for growth and survival, in agreement with a previously proposed model (Terwilliger et al., 2015). In collaboration with Terwilliger et al. (2015) we reported that *B. anthracis* requires valine for growth in a synthetic medium designed to mimic human serum (BSM medium). In our experiments, synthesis of the InhA1 protease allowed *B. anthracis* to grow in BSM lacking valine, likely due to acquisition of valine from proteolysis of serum proteins (Terwilliger et al., 2015). If indeed valine and other amino acids can be obtained from the breakdown of host proteins by InhA1, the resulting oligopeptides would enter *B. anthracis* cells via membrane-bound oligopeptide importers or permeases. XrrA-mediated control of both InhA1 and predicted BCAA and oligopeptide transporters, as shown in work reported here, further supports the model for acquisition of BCAAs and other nutrients from proteolyzed host proteins.

Although we did not observe sRNA-associated growth rate, colony morphology, or sporulation when parent and mutant strains were cultured in various media (data not shown), we predicted that altered expression of the large and diverse XrrA regulon would affect *B. anthracis* pathogenesis in an animal model for anthrax. Although our animal experiments did not reveal changes in time to death, the *xrrA*-null mutant showed reduced numbers of bacteria in the murine liver and lungs at time of death. A relationship between the model for BCAA acquisition and tissue-specific differences in colonization is worthy of speculation. Quantification of BCAA concentrations in the blood and lungs of humans and pigs suggest varying levels of BCAA availability, such that BCAA levels are higher

in blood than in lungs (Subashchandrabose et al., 2009; Kaiser and Heinrichs, 2018). Additionally, activity of the first two enzymes involved in BCAA catabolism is highest in human liver and skeletal muscle tissues, leading to high utilization and low accumulation of BCAAs (Holeček, 2018). Thus, liver and lung niches appear to be BCAA-poor. Given that BCAA availability varies across host niches within the mammalian host, tight regulation of BCAA acquisition could be a determinant of pathogen success. *B. anthracis*, which replicates to high titers in the blood and can colonize virtually all host tissues, may need to fine-tune degradation of host proteins for uptake of host-derived BCAAs according to nutrient availability in different niches. While this model requires further exploration, our data indicate that XrrA co-regulates amino acid transport, amino acid biosynthesis, and protease expression, and that dysregulation of these XrrA targets leads to decreased bacterial abundance in BCAA-poor host niches.

XrrA and XrrB are the first reported sRNAs of *B. anthracis* and are rare examples of plasmid-borne *trans*-acting sRNAs. Also, to our knowledge XrrA and XrrB are the only sRNAs reported to be controlled by a PCVR. Together, these highly expressed stable sRNAs play significant roles in regulatory crosstalk between the pXO1 virulence plasmid and the *B. anthracis* chromosome. The large XrrA regulon controls expression of genes associated with *B. anthracis* virulence and metabolic genes that may be important for bacterial-host interaction. Future work will focus on the molecular basis for sRNA function, including investigations of potential RNA and/or protein interacting partners of XrrA and XrrB, and studies of the function of specific sRNA-controlled genes in *B. anthracis* physiology and virulence.

DATA AVAILABILITY STATEMENT

The datasets presented in this study can be found in online repositories. The names of the repository/repositories and accession number(s) can be found in the article/Supplementary Material.

ETHICS STATEMENT

The animal study was reviewed and approved by Institutional Biosafety and Animal Welfare Committees of the University of Texas Health Science Center – Houston.

AUTHOR CONTRIBUTIONS

IC and TK contributed to the conception and design of the study. IC, SD, AV, and TK contributed to data acquisition, analysis, and interpretation of the data. IC and TK wrote the article. All authors contributed to the article and approved the submitted version.

FUNDING

This work was supported by National Institute of Allergy and Infectious Diseases R01 AI33537 and R21 AI151313 to TK. AV was supported by R01 GM099790 and GM130147 from the National Institute of General Medicine.

ACKNOWLEDGMENTS

We thank the University of Texas Medical Branch (UTMB) Next Generation Sequencing Core Facility for library preparation and sequencing of RNA samples. We thank Nicholas De Lay, Ph.D., for sharing his RACE protocol.

REFERENCES

- Afgan, E., Baker, D., Batut, B., van den Beek, M., Bouvier, D., and Cech, M. (2018). The Galaxy platform for accessible, reproducible and collaborative biomedical analyses: 2018 update. *Nucleic Acids Res.* 46, W537–W544. doi: 10.1093/nar/gky379
- Andrews, S. (2010). *FastQC A Quality Control tool for High Throughput Sequence Data*. URL: <http://www.bioinformatics.babraham.ac.uk/projects/fastqc/>
- Argaman, L., Hershberg, R., Vogel, J., Bejerano, G., Wagner, E. G., Margalit, H., et al. (2001). Novel small RNA-encoding genes in the intergenic regions of *Escherichia coli*. *Curr. Biol.* 11, 941–950. doi: 10.1016/S0960-9822(01)00270-6
- Arthur, D. C., Edwards, R. A., Tsutakawa, S., Tainer, J. A., Frost, L. S., and Glover, J. N. (2011). Mapping interactions between the RNA chaperone FinO and its RNA targets. *Nucleic Acids Res.* 39, 4450–4463. doi: 10.1093/nar/gkr025
- Bailey, T. L., Boden, M., Buske, F. A., Frith, M., Grant, C. E., Clementi, L., et al. (2009). MEME SUITE: tools for motif discovery and searching. *Nucleic Acids Res.* 37, W202–W208. doi: 10.1093/nar/gkp335
- Bandyra, K. J., Said, N., Pfeiffer, V., Góna, M. W., Vogel, J., and Luisi, B. F. (2012). The seed region of a small RNA drives the controlled destruction of the target mRNA by the endoribonuclease RNase E. *Mol. Cell.* 47, 943–953. doi: 10.1016/j.molcel.2012.07.015
- Barnett, D. W., Garrison, E. K., Quinlan, A. R., Strömberg, M. P., and Marth, G. T. (2011). BamTools: a C++ API and toolkit for analyzing and managing BAM files. *Bioinformatics* 27, 1691–1692. doi: 10.1093/bioinformatics/btr174
- Bechhofer, D. H. (2011). *Bacillus subtilis* mRNA decay: new parts in the toolkit. *Wiley Interdisc. Rev. RNA* 2, 387–394. doi: 10.1002/wrna.66
- Bensing, B. A., Meyer, B. J., and Dunne, G. M. (1996). Sensitive detection of bacterial transcription initiation sites and differentiation from RNA processing sites in the pheromone-induced plasmid transfer system of *Enterococcus faecalis*. *Proc. Natl. Acad. Sci. U S A.* 93, 7794–7799. doi: 10.1073/pnas.93.15.7794
- Bertani, G. (1951). Studies on lysogenesis. I. The mode of phage liberation by lysogenic *Escherichia coli*. *J. Bacteriol.* 62, 293–300. doi: 10.1128/JB.62.3.293-300.1951
- Blankenberg, D., Gordon, A., Von Kuster, G., Coraor, N., Taylor, J., and Nekrutenko, A. (2010). Manipulation of FASTQ data with Galaxy. *Bioinformatics* 26, 1783–1785. doi: 10.1093/bioinformatics/btq281
- Bourgogne, A., Drysdale, M., Hilsenbeck, S. G., Peterson, S. N., and Koehler, T. M. (2003). Global effects of virulence gene regulators in a *Bacillus anthracis* strain with both virulence plasmids. *Infect. Immun.* 71, 2736–2743. doi: 10.1128/iai.71.5.2736-2743.2003
- Breslow, R., and Huang, D. L. (1991). Effects of metal ions, including Mg^{2+} and lanthanides, on the cleavage of ribonucleotides and RNA model compounds. *Proc. Natl. Acad. Sci. U S A.* 88, 4080–4083. doi: 10.1073/pnas.88.10.4080
- Brezillon, C., Haustant, M., Dupke, S., Corre, J. P., Lander, A., Franz, T., et al. (2015). Capsules, toxins and AtxA as virulence factors of emerging *Bacillus cereus* biovar *anthracis*. *PLoS Negl. Trop. Dis.* 9:e0003455. doi: 10.1371/journal.pntd.0003455
- Busch, A., Ritcher, A. S., and Backofen, R. (2008). IntaRNA: efficient prediction of bacterial sRNA targets incorporating target site accessibility and seed regions. *Bioinformatics* 24, 2849–2856. doi: 10.1093/bioinformatics/btn544
- Candela, T., Fagerlund, A., Buisson, C., Gilois, N., Kolstø, A. B., Økstad, O. A., et al. (2019). CalY is a major virulence factor and a biofilm matrix protein. *Mol. Microbiol.* 111, 1416–1429. doi: 10.1111/mmi.14184
- Chaffin, D. O., Mentele, L. M., and Rubens, C. E. (2005). Sialylation of Group B streptococcal capsular polysaccharide is mediated by *cpsK* and is required for optimal capsule polymerization and expression. *J. Bacteriol.* 187, 4615–4626. doi: 10.1128/JB.187.13.4615-4626.2005
- Chaudhuri, S., Gantner, B. N., Ye, R. D., Cianciotto, N. P., and Freitag, N. E. (2013). The *Listeria monocytogenes* ChiA chitinase enhances virulence through suppression of host innate immunity. *mBio* 4, e617–e612. doi: 10.1128/mBio.00617-12
- Chiang, C., Bongiorno, C., and Perego, M. (2011). Glucose-dependent activation of *Bacillus anthracis* toxin gene expression and virulence requires the carbon catabolite protein CcpA. *J. Bacteriol.* 193, 52–62. doi: 10.1128/JB.01656-09
- Dai, Z., Sirard, J. C., Mock, M., and Koehler, T. M. (1995). The *atxA* gene product activates transcription of the anthrax toxin genes and is essential for virulence. *Mol. Microbiol.* 16, 1171–1181. doi: 10.1111/j.1365-2958.1995.tb02340.x
- Dale, J. L., Raynor, M. J., Dwivedi, P., and Koehler, T. M. (2012). cis-Acting elements that control expression of the master virulence regulatory gene *atxA* in *Bacillus anthracis*. *J. Bacteriol.* 194, 4069–4079. doi: 10.1128/JB.00776-12
- Dale, J. L., Raynor, M. J., Ty, M. C., Hadjifrangiskou, M., and Koehler, T. M. (2018). A dual role for the *Bacillus anthracis* master virulence regulator AtxA: control of sporulation and anthrax toxin production. *Front. Microbiol.* 9:482. doi: 10.3389/fmicb.2018.00482
- De Lay, N., and Gottesman, S. (2012). RNase E finds some sRNAs stimulating. *Mol. Cell.* 47, 825–826. doi: 10.1016/j.molcel.2012.09.007
- Deng, Z., Meng, X., Su, S., Liu, Z., Ji, X., Zhang, Y., et al. (2012). Two sRNA RyhB homologs from *Yersinia pestis* biovar *microtus* expressed *in vivo* have differential Hfq-dependent stability. *Res. Microbiol.* 163, 413–418. doi: 10.1016/j.resmic.2012.05.006
- Diel, B., Dequivre, M., Wisniewski-Dyé, F., Vial, L., and Hommais, F. (2019). A novel plasmid-transcribed regulatory sRNA, QfsR, controls chromosomal polycistronic gene expression in *Agrobacterium fabrum*. *Env. Microbiol.* 21, 3063–3075. doi: 10.1111/1462-2920.14704
- Drysdale, M., Bourgogne, A., and Koehler, T. M. (2005). Transcriptional analysis of the *Bacillus anthracis* capsule regulators. *J. Bacteriol.* 187, 5108–5114. doi: 10.1128/JB.187.15.5108-5114.2005
- Drysdale, M., Bourgogne, A., Hilsenbeck, S. G., and Koehler, T. M. (2004). *atxA* controls *Bacillus anthracis* capsule synthesis via *acpA* and a newly discovered regulator, *acpB*. *J. Bacteriol.* 186, 307–315. doi: 10.1128/jb.186.2.307-315.2004
- Durand, S., Gillet, L., Bessières, P., Nicolas, P., and Condon, C. (2012). Three Essential Ribonucleases—RNase Y, J1, and III—Control the Abundance of a Majority of *Bacillus subtilis* mRNAs. *PLoS Genet.* 8:e1002520. doi: 10.1371/journal.pgen.1002520

We also thank past and present members of the Koehler laboratory, Malik Raynor, Ph.D., Naomi Bier, Ph.D., and Jung-Hyeob Roh, Ph.D. for their intellectual contributions. The content of this publication is solely the responsibility of the authors and does not necessarily represent the official views of the National Institute of Allergy and Infectious Diseases or the NIH.

SUPPLEMENTARY MATERIAL

The Supplementary Material for this article can be found online at: <https://www.frontiersin.org/articles/10.3389/fmicb.2020.610036/full#supplementary-material>

- Edgar, R., Domrachev, M., and Lash, A. E. (2002). Gene Expression Omnibus: NCBI gene expression and hybridization array data repository. *Nucleic Acids Res.* 30, 207–210. doi: 10.1093/nar/30.1.207
- Even, S., Pellegrini, O., Zig, L., Labas, V., Vinh, J., Bréchemmiller-Baey, D., et al. (2005). Ribonucleases J1 and J2: two novel endoribonucleases in *B. subtilis* with functional homology to *E. coli* RNase E. *Nucleic Acids Res.* 33, 2141–2152. doi: 10.1093/nar/gki505
- Ferrara, S., Falcone, M., Macchi, R., Bragonzi, A., Girelli, D., Cariani, L., et al. (2017). The PAPI-1 pathogenicity island-encoded small RNA PesA influences *Pseudomonas aeruginosa* virulence and modulates pyocin S3 production. *PLoS One* 12:e0180386. doi: 10.1371/journal.pone.0180386
- Filipowicz, W., Jaskiewicz, L., Kolb, F. A., and Pillai, R. S. (2005). Post-transcriptional gene silencing by siRNAs and miRNAs. *Curr. Opin. Struct. Biol.* 15, 331–341. doi: 10.1016/j.sbi.2005.05.006
- Fleischmann, J., and Rocha, M. A. (2018). Nutrient depletion and TOR inhibition induce 18S and 25S ribosomal RNAs resistant to a 5'-phosphate-dependent exonuclease in *Candida albicans* and other yeasts. *BMC Mole. Biol.* 19:102. doi: 10.1186/s12867-018-0102-y
- Fozo, E. M., Makarova, K. S., Shabalina, S. A., Yutin, N., Koonin, E. V., and Storz, G. (2010). Abundance of type I toxin-antitoxin systems in bacteria: searches for new candidates and discovery of novel families. *Nucleic Acids Res.* 38, 3743–3759. doi: 10.1093/nar/gkq054
- Georg, J., Voss, B., Scholz, I., Mitschke, J., Wilde, A., and Hess, W. R. (2009). Evidence for a major role of antisense RNAs in cyanobacterial gene regulation. *Mol. Syst. Biol.* 5:305. doi: 10.1038/msb.2009.63
- Gimpel, M., Preis, H., Barth, E., Gramzow, L., and Brantl, S. (2012). SR1—a small RNA with two remarkably conserved functions. *Nucleic Acids Res.* 40, 11659–11672. doi: 10.1093/nar/gks895
- Gottesman, S., and Storz, G. (2011). Bacterial small RNA regulators: versatile roles and rapidly evolving variations. *Cold Spring Harb. Perspect. Biol.* 3:a003798. doi: 10.1101/cshperspect.a003798
- Grass, G., Schierhorn, A., Sorkau, E., Müller, H., Rücknagel, P., Nies, D. H., et al. (2004). Camelysin is a novel surface metalloproteinase from *Bacillus cereus*. *Infect. Immun.* 72, 219–228. doi: 10.1128/iai.72.1.219-228.2004
- Grishok, A., Pasquinelli, A. E., Conte, D., Li, N., Parrish, S., Ha, I., et al. (2001). Genes and mechanisms related to RNA interference regulate expression of the small temporal RNAs that control *C. elegans* developmental timing. *Cell* 106, 23–34. doi: 10.1016/s0092-8674(01)00431-7
- Güell, M., van Noort, V., Yus, E., Chen, W. H., Leigh-Bell, J., and Michalodimitrakis, K. (2009). Transcriptome complexity in a genome-reduced bacterium. *Science* 326, 1268–1271. doi: 10.1126/science.1176951
- Hadjifrangiskou, M., Chen, Y., and Koehler, T. M. (2007). The alternative sigma factor sigma^H is required for toxin gene expression by *Bacillus anthracis*. *J. Bacteriol.* 189, 1874–1883. doi: 10.1128/JB.01333-06
- Hammerstrom, T. G., Horton, L. B., Swick, M. C., Joachimiak, A., Osipiuk, J., and Koehler, T. M. (2015). Crystal structure of *Bacillus anthracis* virulence regulator AtxA and effects of phosphorylated histidines on multimerization and activity. *Mol. Microbiol.* 95, 426–441. doi: 10.1111/mtm.12867
- Hammerstrom, T. G., Roh, J. H., Nikonowicz, E. P., and Koehler, T. M. (2011). *Bacillus anthracis* virulence regulator AtxA: oligomeric state, function and CO₂-signalling. *Mol. Microbiol.* 82, 634–647. doi: 10.1111/j.1365-2958.2011.07843.x
- Heidrich, N., Chinali, A., Gerth, U., and Brantl, S. (2006). The small untranslated RNA SR1 from the *Bacillus subtilis* genome is involved in the regulation of arginine catabolism. *Mol. Microbiol.* 62, 520–536. doi: 10.1111/j.1365-2958.2006.05384.x
- Ho, S. N., Hunt, H. D., Horton, R. M., Pullen, J. K., and Pease, L. R. (1989). Site-directed mutagenesis by overlap extension using the polymerase chain reaction. *Gene* 77, 51–59. doi: 10.1016/0378-1119(89)90358-2
- Hoffmaster, A. R., Hill, K. K., Gee, J. E., Marston, C. K., De, B. K., and Popovic, T. (2006). Characterization of *Bacillus cereus* isolates associated with fatal pneumonias: strains are closely related to *Bacillus anthracis* and harbor *B. anthracis* virulence genes. *J. Clin. Microbiol.* 44, 3352–3360. doi: 10.1128/JCM.00561-06
- Holeček, M. (2018). Branched-chain amino acids in health and disease: metabolism, alterations in blood plasma, and as supplements. *Nutr. Metab.* 15:33. doi: 10.1186/s12986-018-0271-1
- Hondorp, E. R., Hou, S. C., Hause, L. L., Gera, K., Lee, C. E., and McIver, K. S. (2013). PTS phosphorylation of Mga modulates regulon expression and virulence in the Group A *streptococcus*. *Mol. Microbiol.* 88, 1176–1193. doi: 10.1111/mtm.12250
- Ishikawa, H., Otaka, H., Maki, K., Morita, T., and Aiba, H. (2012). The functional Hfq-binding module of bacterial sRNAs consists of a double or single hairpin preceded by a U-rich sequence and followed by a 3' poly(U) tail. *RNA* 18, 1062–1074. doi: 10.1261/rna.031575.111
- Ivins, B. E., Welkos, S. L., Knudson, G. B., and Little, S. F. (1990). Immunization against anthrax with aromatic compound-dependent (Aro-) mutants of *Bacillus anthracis* and with recombinant strains of *Bacillus subtilis* that produce anthrax protective antigen. *Infect. Immun.* 58, 303–308. doi: 10.1128/IAI.58.2.303-308.1990
- Janssen, K. H., Diaz, M. R., Gode, C. J., Wolfgang, M. C., and Yahr, T. L. (2018). RsmV, a Small Noncoding Regulatory RNA in *Pseudomonas aeruginosa* That Sequesters RsmA and RsmF from Target mRNAs. *J. Bacteriol.* 200, 277–218. doi: 10.1128/JB.00277-18
- Kaiser, J. C., and Heinrichs, D. E. (2018). Branching Out: Alterations in Bacterial Physiology and Virulence Due to Branched-Chain Amino Acid Deprivation. *mBio* 9, 1188–1118. doi: 10.1128/mBio.01188-18
- Keefer, A. B., Asare, E. K., Pomerantsev, A. P., Moayeri, M., Martens, C., Porcella, S. F., et al. (2017). *In vivo* characterization of an Hfq protein encoded by the *Bacillus anthracis* virulence plasmid pXO1. *BMC Microbiol.* 17:63. doi: 10.1186/s12866-017-0973-y
- Kery, M. B., Feldman, M., Livny, J., and Tjaden, B. (2014). TargetRNA2: identifying targets of small regulatory RNAs in bacteria. *Nucleic Acids Res.* 42, W124–W129. doi: 10.1093/nar/gku317
- Koehler, T. M., Dai, Z., and Kaufman-Yarbray, M. (1994). Regulation of the *Bacillus anthracis* protective antigen gene: CO₂ and a trans-acting element activate transcription from one of two promoters. *J. Bacteriol.* 176, 586–595. doi: 10.1128/jb.176.3.586-595.1994
- Kornberg, H. L., and Madsen, N. B. (1989). Synthesis of C4-dicarboxylic acids from acetate by a "glyoxylate bypass" of the tricarboxylic acid cycle. 1957. *Biochim. Biophys. Acta* 1000, 275–277. doi: 10.1016/0006-3002(57)90268-8
- Krueger, F. (2012). *Trim Galore! Quality and adapter trimmer of reads*. URL: https://www.bioinformatics.babraham.ac.uk/projects/trim_galore/
- Lalouna, D., Baude, J., Wu, Z., Tomasini, A., Chicher, J., Marzi, S., et al. (2019). RsaC sRNA modulates the oxidative stress response of *Staphylococcus aureus* during manganese starvation. *Nucleic Acids Res.* 47, 9871–9887. doi: 10.1093/nar/gkz728
- Langmead, B., and Salzberg, S. L. (2012). Fast gapped-read alignment with Bowtie 2. *Nat. Methods* 9, 357–359. doi: 10.1038/nmeth.1923
- Lenz, D. H., Mok, K. C., Lilley, B. N., Kulkarni, R. V., Wingreen, N. S., and Bassler, B. L. (2004). The small RNA chaperone Hfq and multiple small RNAs control quorum sensing in *Vibrio harveyi* and *Vibrio cholerae*. *Cell* 118, 69–82. doi: 10.1016/j.cell.2004.06.009
- Li de la Sierra-Gallay, I., Zig, L., Jamalli, A., and Putzer, H. (2008). Structural insights into the dual activity of RNase J. *Nat. Struct. Mol. Biol.* 15, 206–212. doi: 10.1038/nsmb.1376
- Link, T. M., Valentin-Hansen, P., and Brennan, R. G. (2009). Structure of *Escherichia coli* Hfq bound to polyribadenylate RNA. *Proc. Natl. Acad. Sci. U S A.* 106, 19292–19297. doi: 10.1073/pnas.0908744106
- Marrero, R., and Welkos, S. L. (1995). The transformation frequency of plasmids into *Bacillus anthracis* is affected by adenine methylation. *Gene* 152, 75–78. doi: 10.1016/0378-1119(94)00647-b
- McCall, R. M., Sievers, M. E., Fattah, R., Ghirlando, R., Pomerantsev, A. P., and Leppä, S. H. (2019). *Bacillus anthracis* Virulence Regulator AtxA Binds Specifically to the *pagA* Promoter Region. *J. Bacteriol.* 201, e569–e519. doi: 10.1128/JB.00569-19
- McKenzie, A. T., Pomerantsev, A. P., Sastalla, I., Martens, C., Ricklefs, S. M., Virtanova, K., et al. (2014). Transcriptome analysis identifies *Bacillus anthracis* genes that respond to CO₂ through an AtxA-dependent mechanism. *BMC Genom.* 15:229. doi: 10.1186/1471-2164-15-229
- Miller, C. L., Romero, M., Karna, S. L., Chen, T., Heeb, S., and Leung, K. P. (2016). RsmW, *Pseudomonas aeruginosa* small non-coding RsmA-binding RNA upregulated in biofilm versus planktonic growth conditions. *BMC Microbiol.* 16:155. doi: 10.1186/s12866-016-0771-y

- Mohanty, B. K., and Kushner, S. R. (2016). Regulation of mRNA Decay in Bacteria. *Annu. Rev. Microbiol.* 70, 25–44. doi: 10.1146/annurev-micro-091014-104515
- Møller, T., Franch, T., Højrup, P., Keene, D. R., Bächinger, H. P., Brennan, R. G., et al. (2002). Hfq: a bacterial Sm-like protein that mediates RNA-RNA interaction. *Mol. Cell* 9, 23–30. doi: 10.1016/s1097-2765(01)00436-1
- Müller, P., Gimpel, M., Wildenhain, T., and Brantl, S. (2019). A new role for CsrA: promotion of complex formation between an sRNA and its mRNA target in *Bacillus subtilis*. *RNA Biol.* 16, 972–987. doi: 10.1080/15476286.2019.1605811
- Nielsen, J. S., Larsen, M. H., Lillebæk, E. M., Bergholm, T. M., Christiansen, M. H., Boor, K. J., et al. (2011). A small RNA controls expression of the chitinase ChiA in *Listeria monocytogenes*. *PLoS One* 6:e19019. doi: 10.1371/journal.pone.0019019
- Olejniczak, M., and Storz, G. (2017). ProQ/FinO-domain proteins: another ubiquitous family of RNA matchmakers? *Mol. Microbiol.* 104, 905–915. doi: 10.1111/mmi.13679
- Otake, H., Ishikawa, H., Morita, T., and Aiba, H. (2011). PolyU tail of rho-independent terminator of bacterial small RNAs is essential for Hfq action. *Proc. Natl. Acad. Sci. U S A.* 108, 13059–13064. doi: 10.1073/pnas.1107050108
- Pandey, S. P., Minesinger, B. K., Kumar, J., and Walker, G. C. (2011). A highly conserved protein of unknown function in *Sinorhizobium meliloti* affects sRNA regulation similar to Hfq. *Nucleic Acids Res.* 39, 4691–4708. doi: 10.1093/nar/gkr060
- Pandey, S. P., Winkler, J. A., Li, H., Camacho, D. M., Collins, J. J., and Walker, G. C. (2014). Central role for RNase YbeY in Hfq-dependent and Hfq-independent small-RNA regulation in bacteria. *BMC Genom.* 15:121. doi: 10.1186/1471-2164-15-121
- Panja, S., Schu, D. J., and Woodson, S. A. (2013). Conserved arginines on the rim of Hfq catalyze base pair formation and exchange. *Nucleic Acids Res.* 41, 7536–7546. doi: 10.1093/nar/gkt521
- Pappesch, R., Warnke, P., Mikkat, S., Normann, J., Wisniewska-Kucper, A., and Huschka, F. (2017). The Regulatory Small RNA MarS Supports Virulence of *Streptococcus pyogenes*. *Sci. Rep.* 7:12241. doi: 10.1038/s41598-017-12507-z
- Patrick, K. L., Shi, H., Kolev, N. G., Ersfeld, K., Tschudi, C., and Ullu, E. (2009). Distinct and overlapping roles for two Dicer-like proteins in the RNA interference pathways of the ancient eukaryote *Trypanosoma brucei*. *PNAS* 106, 17933–17938. doi: 10.1073/pnas.0907766106
- Peng, D., Luo, X., Zhang, N., Guo, S., Zheng, J., Chen, L., et al. (2018). Small RNA-mediated Cry toxin silencing allows *Bacillus thuringiensis* to evade *Caenorhabditis elegans* avoidance behavioral defenses. *Nucleic Acids Res.* 46, 159–173. doi: 10.1093/nar/gkx959
- Pflughoeft, K. J., Sumbly, P., and Koehler, T. M. (2011). *Bacillus anthracis* sin locus and regulation of secreted proteases. *J. Bacteriol.* 193, 631–639. doi: 10.1128/JB.01083-10
- Pflughoeft, K. J., Swick, M. C., Engler, D. A., Yeo, H. J., and Koehler, T. M. (2014). Modulation of the *Bacillus anthracis* secretome by the immune inhibitor A1 protease. *J. Bacteriol.* 196, 424–435. doi: 10.1128/JB.00690-13
- Pillai, R. S., Artus, C. G., and Filipowicz, W. (2004). Tethering of human Ago proteins to mRNA mimics the miRNA-mediated repression of protein synthesis. *RNA* 10, 1518–1525. doi: 10.1261/rna.7131604
- Ramirez, F., Ryan, D. P., Grünig, B., Bhardwaj, V., Kilpert, F., Richter, A. S., et al. (2016). deepTools2: a next generation web server for deep-sequencing data analysis. *Nucleic Acids Res.* 44, W160–W165. doi: 10.1093/nar/gkw257
- Raynor, M. J., Roh, J. H., Widen, S. G., Wood, T. G., and Koehler, T. M. (2018). Regulons and protein-protein interactions of PRD-containing *Bacillus anthracis* virulence regulators reveal overlapping but distinct functions. *Mol. Microbiol.* doi: 10.1111/mmi.13961
- Ren, S., Li, Q., Xie, L., and Xie, J. (2017). Molecular Mechanisms Underlying the Function Diversity of ArsR Family Metallorepressor. *Crit. Rev. Eukaryot. Gene. Expr.* 27, 19–35. doi: 10.1615/CritRevEukaryotGeneExpr.2016018476
- Ribardo, D. A., and McIver, K. S. (2006). Defining the Mga regulon: Comparative transcriptome analysis reveals both direct and indirect regulation by Mga in the Group A streptococcus. *Mol. Microbiol.* 62, 491–508. doi: 10.1111/j.1365-2958.2006.05381.x
- Roberts, S. A., and Scott, J. R. (2007). RivR and the small RNA RivX: the missing links between the CovR regulatory cascade and the Mga regulon. *Mol. Microbiol.* 66, 1506–1522. doi: 10.1111/j.1365-2958.2007.06015.x
- Santiago-Frangos, A., Kavita, K., Schu, D. J., Gottesman, S., and Woodson, S. A. (2016). C-terminal domain of the RNA chaperone Hfq drives sRNA competition and release of target RNA. *Proc. Natl. Acad. Sci. U S A.* 113, E6089–E6096. doi: 10.1073/pnas.1613053113
- Sauer, E., and Weichenrieder, O. (2011). Structural basis for RNA 3'-end recognition by Hfq. *Proc. Natl. Acad. Sci. U S A.* 108, 13065–13070. doi: 10.1073/pnas.1103420108
- Schumacher, M. A., Pearson, R. F., Møller, T., Valentin-Hansen, P., and Brennan, R. G. (2002). Structures of the pleiotropic translational regulator Hfq and an Hfq-RNA complex: a bacterial Sm-like protein. *EMBO J.* 21, 3546–3556. doi: 10.1093/emboj/cdf322
- Shahbadian, K., Jamalli, A., Zig, L., and Putzer, H. (2009). RNase Y, a novel endoribonuclease, initiates riboswitch turnover in *Bacillus subtilis*. *EMBO J.* 28, 3523–3533. doi: 10.1038/emboj.2009.283
- Sledjeski, D. D., Whitman, C., and Zhang, A. (2001). Hfq is necessary for regulation by the untranslated RNA DsrA. *J. Bacteriol.* 183, 1997–2005. doi: 10.1128/JB.183.6.1997-2005.2001
- Song, J. J., Liu, J., Tolia, N. H., Schneiderman, J., Smith, S. K., Martienssen, R. A., et al. (2003). The crystal structure of the Argonaute2 PAZ domain reveals an RNA binding motif in RNAi effector complexes. *Nat. Struct. Biol.* 10, 1026–1032. doi: 10.1038/nsb1016
- Sridhar, J., and Gayathri, M. (2019). Transcriptome based Identification of silver stress responsive sRNAs from *Bacillus cereus* ATCC14579. *Bioinformation* 15, 474–479. doi: 10.6026/97320630015474
- Subashchandrabose, S., LeVeque, R. M., Wagner, T. K., Kirkwood, R. N., Kiupel, M., and Mulks, M. H. (2009). Branched-chain amino acids are required for the survival and virulence of *Actinobacillus pleuropneumoniae* in swine. *Infect. Immun.* 77, 4925–4933. doi: 10.1128/IAI.00671-09
- Sun, X., Zhulin, L., and Wartell, R. M. (2002). Predicted structure and phyletic distribution of the RNA-binding protein Hfq. *Nucleic Acids Res.* 30, 3662–3671. doi: 10.1093/nar/gkf508
- Terwilliger, A., Swick, M. C., Pflughoeft, K. J., Pomerantsev, A., Lyons, C. R., Koehler, T. M., et al. (2015). *Bacillus anthracis* Overcomes an Amino Acid Auxotrophy by Cleaving Host Serum Proteins. *J. Bacteriol.* 197, 2400–2411. doi: 10.1128/JB.00073-15
- The UniProt Consortium. (2019). UniProt: a worldwide hub of protein knowledge. *Nucleic Acids Res.* 47, D506–D515. doi: 10.1093/nar/gky1049
- Thorne, C. B. (1968). Transduction in *Bacillus cereus* and *Bacillus anthracis*. *Bacteriol. Rev.* 32, 358–361.
- Thorne, C. B., and Belton, F. C. (1957). An agar-diffusion method for titrating *Bacillus anthracis* immunizing antigen and its application to a study of antigen production. *J. Gen. Microbiol.* 17, 505–516. doi: 10.1099/00221287-17-2-505
- Thorvaldsdóttir, H., Robinson, J. T., and Mesirov, J. P. (2013). Integrative Genomics Viewer (IGV): high-performance genomics data visualization and exploration. *Brief Bioinform.* 14, 178–192. doi: 10.1093/bib/bbs017
- Trapnell, C., Williams, B. A., Pertea, G., Mortazavi, A., Kwan, G., van Baren, M. J., et al. (2010). Transcript assembly and quantification by RNA-Seq reveals unannotated transcripts and isoform switching during cell differentiation. *Nat. Biotechnol.* 28, 511–515. doi: 10.1038/nbt.1621
- Vakulskas, C. A., Potts, A. H., Babitzke, P., Ahmer, B. M., and Romeo, T. (2015). Regulation of bacterial virulence by Csr (Rsm) systems. *Microbiol. Mol. Biol. Rev.* 79, 193–224. doi: 10.1128/MMBR.00052-14
- van Biesen, T., Söderbom, F., Wagner, E. G., and Frost, L. S. (1993). Structural and functional analyses of the FinP antisense RNA regulatory system of the F conjugative plasmid. *Mol. Microbiol.* 10, 35–43. doi: 10.1111/j.1365-2958.1993.tb00901.x
- Vaucheret, H., Vazquez, F., Crété, P., and Bartel, D. P. (2004). The action of ARGONAUTE1 in the miRNA pathway and its regulation by the miRNA pathway are crucial for plant development. *Genes Dev.* 18, 1187–1197. doi: 10.1101/gad.1201404
- Vrentas, C., Ghirlando, R., Keefer, A., Hu, Z., Tomczak, A., and Gittis, A. G. (2015). Hfq in *Bacillus anthracis*: Role of protein sequence variation in the structure and function of proteins in the Hfq family. *Protein Sci.* 24, 1808–1819. doi: 10.1002/pro.2773
- Vytvytska, O., Jakobsen, J. S., Balcunaite, G., Andersen, J. S., Baccarini, M., and von Gabain, A. (1998). Host factor I, Hfq, binds to *Escherichia coli* ompA mRNA in a growth rate-dependent fashion and regulates its stability. *Proc. Natl. Acad. Sci. U S A.* 95, 14118–14123. doi: 10.1073/pnas.95.24.14118

- Wassarman, K. M., Repoila, F., Rosenow, C., Storz, G., and Gottesman, S. (2001). Identification of novel small RNAs using comparative genomics and microarrays. *Genes Dev.* 15, 1637–1651. doi: 10.1101/gad.901001
- Welkos, S., Little, S., Friedlander, A., Fritz, D., and Fellows, P. (2001). The role of antibodies to *Bacillus anthracis* and anthrax toxin components in inhibiting the early stages of infection by anthrax spores. *Microbiology* 147, 1677–1685. doi: 10.1099/00221287-147-6-1677
- Wu, J., and Xie, X. (2006). Comparative sequence analysis reveals an intricate network among REST, CREB and miRNA in mediating neuronal gene expression. *Genome Biol.* 7:R85. doi: 10.1186/gb-2006-7-9-r85
- Yao, S., and Bechhofer, D. H. (2010). Initiation of decay of *Bacillus subtilis* rpsO mRNA by endoribonuclease RNase Y. *J. Bacteriol.* 192, 3279–3286. doi: 10.1128/JB.00230-10
- Zuker, M. (2003). Mfold web server for nucleic acid folding and hybridization prediction. *Nucleic Acids Res.* 31, 3406–3415. doi: 10.1093/nar/gkg595
- Conflict of Interest:** The authors declare that the research was conducted in the absence of any commercial or financial relationships that could be construed as a potential conflict of interest.
- Copyright © 2021 Corsi, Dutta, van Hoof and Koehler. This is an open-access article distributed under the terms of the Creative Commons Attribution License (CC BY). The use, distribution or reproduction in other forums is permitted, provided the original author(s) and the copyright owner(s) are credited and that the original publication in this journal is cited, in accordance with accepted academic practice. No use, distribution or reproduction is permitted which does not comply with these terms.



RNA-Mediated Control in *Listeria monocytogenes*: Insights Into Regulatory Mechanisms and Roles in Metabolism and Virulence

Agata Krawczyk-Balska^{1*}, Magdalena Ładziak¹, Michał Burmistrz¹, Katarzyna Ścibek¹ and Birgitte H. Kallipolitis²

¹ Department of Molecular Microbiology, Biological and Chemical Research Centre, Faculty of Biology, University of Warsaw, Warsaw, Poland, ² Department of Biochemistry and Molecular Biology, University of Southern Denmark, Odense, Denmark

OPEN ACCESS

Edited by:

Olga Soutourina,
UMR 9198 Institut de Biologie
Intégrative de la Cellule (I2BC), France

Reviewed by:

Svetlana Chabelskaya,
Institut National de la Santé et de la
Recherche Médicale (INSERM),
France

Soraya Chaturongakul,
Mahidol University, Thailand

*Correspondence:

Agata Krawczyk-Balska
akra@biol.uw.edu.pl

Specialty section:

This article was submitted to
Microbial Physiology and Metabolism,
a section of the journal
Frontiers in Microbiology

Received: 29 October 2020

Accepted: 16 March 2021

Published: 14 April 2021

Citation:

Krawczyk-Balska A, Ładziak M,
Burmistrz M, Ścibek K and
Kallipolitis BH (2021) RNA-Mediated
Control in *Listeria monocytogenes*:
Insights Into Regulatory Mechanisms
and Roles in Metabolism
and Virulence.
Front. Microbiol. 12:622829.
doi: 10.3389/fmicb.2021.622829

Listeria monocytogenes is an intracellular pathogen that is well known for its adaptability to life in a broad spectrum of different niches. RNA-mediated regulatory mechanisms in *L. monocytogenes* play important roles in successful adaptation providing fast and versatile responses to a changing environment. Recent findings indicate that non-coding RNAs (ncRNAs) regulate a variety of processes in this bacterium, such as environmental sensing, metabolism and virulence, as well as immune responses in eukaryotic cells. In this review, the current knowledge on RNA-mediated regulation in *L. monocytogenes* is presented, with special focus on the roles and mechanisms underlying modulation of metabolism and virulence. Collectively, these findings point to ncRNAs as important gene regulatory elements in *L. monocytogenes*, both outside and inside an infected host. However, the involvement of regulatory ncRNAs in bacterial physiology and virulence is still underestimated and probably will be better assessed in the coming years, especially in relation to discovering the regulatory functions of 5' and 3' untranslated regions and excludons, and by exploring the role of ncRNAs in interaction with both bacterial and host proteins.

Keywords: non-coding RNAs, post-transcriptional regulation, metabolism, virulence, *Listeria monocytogenes*

INTRODUCTION

Listeria monocytogenes is an intracellular, Gram-positive pathogen, responsible for foodborne infections called listerioses in humans and different animal species. This bacterium is well known for its adaptability to life in a broad spectrum of different niches, ranging from soil or wastewater to the cytoplasm of infected mammalian cells. *L. monocytogenes* is widely distributed in the environment owing to its ability to survive in different stress conditions, including pH variations, low temperature and high salt concentration (Ferreira et al., 2014). Infection with *L. monocytogenes* starts with the ingestion of contaminated food. In the intestine, *L. monocytogenes* invades epithelial cells as a result of the interaction of bacterial surface proteins with appropriate eukaryotic receptors. After crossing the intestinal barrier, *L. monocytogenes* enters into macrophage cells and is transported via blood to the liver and spleen. When the host's cell-mediated response is impaired, *L. monocytogenes* multiplies in these organs and subsequently spreads through the blood to different

organs, often crossing placental and blood-brain barriers, leading to septicemia, meningitis and miscarriage in the case of pregnant women (McLauchlin et al., 2004; Liu et al., 2007). *L. monocytogenes* has the ability to invade the host's cells, multiply inside them and spread from cell to cell owing to tightly regulated expression of genes encoding virulence factors (Cossart, 2011).

The regulation of gene expression has a pivotal role in the virulence of *L. monocytogenes* and the ability of this bacterium to survive in different stress conditions. Proper changes in gene expression programs are indispensable in allowing saprophytic growth, stress response and resistance to extreme conditions, or triggering virulence properties. Numerous studies have documented the importance of protein regulators in the coordination of the infection process. The master coordinator of transcription of the virulence genes of *L. monocytogenes* is transcriptional regulator PrfA (positive regulatory factor A), which belongs to the superfamily of cyclic AMP receptor proteins (Crp) (Renzoni et al., 1999; Reniere et al., 2016). Other regulators of expression of virulence and virulence-associated genes are the alternative sigma factor Sigma B (Dorey et al., 2019), two-component signal transduction systems CesRK, LisRK, and VirRS, as well as the nutrient-responsive regulator CodY (Cotter et al., 1999; Kallipolitis et al., 2003; Mandin et al., 2005; Lobel et al., 2015). While knowledge about protein-mediated control of *L. monocytogenes* gene expression to environmental changes has been acquired over many decades, recent studies have shown that pathogenesis and stress adaptation of this bacterium are also regulated post-transcriptionally by ncRNA molecules. Generally, ncRNAs can be divided into five main categories. The first category contains small regulatory RNAs encoded *in trans* relative to the genes they regulate (*trans* ncRNAs). Some *trans* ncRNAs mainly act through interactions with proteins, whereas others control gene expression through base pairing with RNA transcripts (Storz et al., 2011). The base pairing *trans* ncRNAs affect the translation and/or stability of mRNAs originating from different sites in the genome. They show incomplete complementarity with their targets and thus can interact with multiple mRNAs. The interaction of *trans* ncRNAs with target mRNAs in bacteria is often mediated by the RNA chaperone Hfq (Christiansen et al., 2006). The second category contains *cis*-acting regulatory RNAs encoded from the 5' regions of the genes they regulate (*cis* ncRNAs). They fold into two alternative RNA structures that terminate or antiterminate transcription of downstream genes. The rearrangements of *cis* ncRNA structures are coupled with translation of small ORFs within their sequences. The third category comprises antisense RNAs (asRNAs), including long antisense RNAs (lasRNAs). These molecules are encoded on the opposite strand relative to the genes they regulate, which makes them perfectly complementary to the target mRNA. Hybridization of asRNAs to target mRNAs often affects their stability and/or translational activity (Waters and Storz, 2009; Wurtzel et al., 2012). The recently discovered excludon corresponds to a genomic locus encoding a lasRNA (Wurtzel et al., 2012). The transcription of an excludon inhibits expression of the gene encoded on the opposite strand and also ensures expression of the downstream operon. The fourth category, viewed by some as the simplest form of RNA

regulatory elements, are *cis*-encoded and *cis*-acting molecules, which undergo conformational changes upon binding a specific ligand (riboswitches) or in response to temperature change (thermosensors). Bacterial riboswitches and thermosensors are located mainly in the 5' untranslated regions (UTRs) and less frequently in the 3' UTRs of the genes that they control (Waters and Storz, 2009). Conformational changes in riboswitches and thermosensors located in 5' UTR regions lead to premature transcription termination, arrest of translation initiation or both (Waters and Storz, 2009). Finally, the fifth category is comprised of 5' and 3' UTRs, whose regulatory mechanism relies on base pairing with other RNA transcripts.

While this general classification of ncRNAs is widely accepted and very useful due to its simplicity, mounting evidence suggests that ncRNAs are versatile regulators which can act by more than just a single mechanism as will be shown in this review.

Research devoted *sensu stricto* to riboregulation in *L. monocytogenes* began in 2002. At that time, it was discovered that the 5' UTR of *prfA* switches between a structure active at high temperatures and inactive at low ones. This mechanism is driven by a thermosensor, which regulates the expression of *prfA*, thereby controlling the virulence properties of *L. monocytogenes* (Johansson et al., 2002). Over the next several years, other ncRNAs of *L. monocytogenes* were discovered. The first identified and characterized small ncRNAs of *L. monocytogenes* were LhrA, LhrB and LhrC1-5 interacting with chaperone Hfq (Christiansen et al., 2006). Shortly after, further ncRNAs, i.e., RliA, RliB, RliC, RliD, RliE, RliF, RliG, RliH, RliI, and SbrA were identified using classical methods of molecular biology and bioinformatics (Mandin et al., 2007; Nielsen et al., 2008). During this time, the SreA and SreB riboswitches, which can act as *trans* ncRNAs to inhibit translation of *prfA* mRNA, were also discovered (Loh et al., 2009). The biggest scientific breakthrough in the discovery of riboregulatory elements in *L. monocytogenes* took place in 2009, when Toledo-Arana and coworkers presented the first study of the whole transcriptome of this bacterium. From that moment on, an enormous number of new ncRNAs was discovered, and in a few cases, their function and mechanisms of action was revealed. In this research, genomic tiling arrays was applied to compare the whole transcriptome of *L. monocytogenes* during growth in different physiologically relevant conditions including infection-relevant ones, i.e., whole human blood and the intestinal lumen of mice. Investigation of the transcriptome changes allowed understanding of the switching of *L. monocytogenes* from saprophytism to virulence. These studies led to the identification of 50 ncRNAs, of which 29 were novel ncRNAs with sizes from 77 to 534 nucleotides (nt), including seven asRNAs. Furthermore, comprehensive information about changes in the expression of ncRNAs in different conditions was provided (Toledo-Arana et al., 2009). In the same year another study was performed by Oliver and coworkers, who applied a high-throughput RNA sequencing method with Illumina Genome Analyzer. This study allowed the identification of 67 *L. monocytogenes* ncRNAs expressed in stationary phase of growth, with 60 molecules being previously described (Oliver et al., 2009). Another NGS (next generation sequencing) method, i.e., 454 pyrosequencing was used by

Mraheil et al. (2011), in which sequencing of small RNA (below 500 nt) isolated from bacteria growing inside infected macrophages was carried out. This study led to the identification of 150 ncRNAs, whereof almost half had not been previously described (Mraheil et al., 2011). In the following year, NGS was applied to compare the transcriptomes of pathogenic *L. monocytogenes* with non-pathogenic *Listeria innocua* under various growth conditions (Wurtzel et al., 2012). The results of this study revealed the presence of 113 ncRNAs and 70 asRNAs in *L. monocytogenes*, of which 33 ncRNAs and 53 asRNAs had not been previously identified. This research also led to the identification of new lasRNAs that can act as asRNAs and mRNAs. Such a dual function for a lasRNA transcript was first described in *L. monocytogenes* for the lasRNA regulating flagellum biosynthesis (Toledo-Arana et al., 2009). This type of lasRNA was named an excludon. Another study that used a high-throughput SOLiD sequencing platform led to the discovery of 172 as yet undescribed ncRNAs candidates isolated from intracellularly and extracellularly growing *L. monocytogenes* (Behrens et al., 2014). This method led to the identification of nine new asRNAs and additionally revealed that four asRNAs are potentially longer than previously thought and could form lasRNAs (Behrens et al., 2014). In another whole transcriptomic study of *L. monocytogenes* under intracellular and extracellular growth conditions, a semiconductor sequencing technology and bioinformatic analysis pipeline was applied to identify 741 putative ncRNAs in *L. monocytogenes*, 441 of which had never

been described before. One of the newly identified lasRNAs was a very long transcript of about 5,400 nt, fully complementary to a region from *lmo2677* up to *lmo2680* and partially to *kdpB* (Wehner et al., 2014). The described progress in the discovery of ncRNAs in *L. monocytogenes* is shown in **Figure 1**. Altogether, a huge number of candidates for riboregulatory elements in *L. monocytogenes* have been identified throughout the last decade, and their number has been increasing in line with the progress in sequencing technology. Although the number of potential regulatory RNAs identified varies in different works, it is assumed that *L. monocytogenes* possesses more than 55 riboswitches, 100 asRNAs and 150 putative *trans* and *cis* ncRNAs (Schultze et al., 2014; Lebreton and Cossart, 2017). However, in spite of the rapid increase in the number of newly identified regulatory RNAs, their function and mechanism of action is poorly understood. Interestingly, recent studies have shown that ncRNAs are secreted by *L. monocytogenes* into the cytoplasm of infected cells where they modulate the innate immune response through interaction with the RNA sensor RIG-I (Frantz et al., 2019). Therefore, these molecules besides being potent regulators of gene expression, could also play a role as virulence effectors of *L. monocytogenes*. Furthermore, except for the classic riboregulatory elements, recent research has revealed that canonical mRNA can also be involved in regulatory base-pairing interactions extending riboregulatory mechanisms in *L. monocytogenes* beyond non-coding elements (Ignatov et al., 2020; Peterson et al., 2020). In this review, we focus on

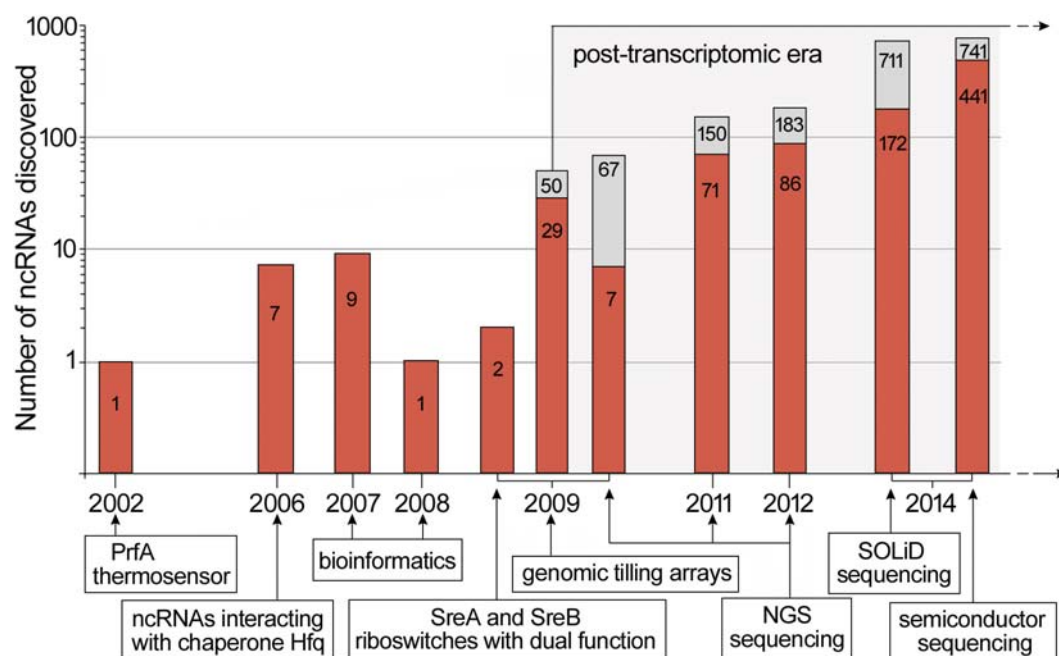


FIGURE 1 | Discovery timeline of ncRNAs in *L. monocytogenes*. New ncRNAs discovered are marked in red while the total number of ncRNAs discovered is indicated in gray. For high-throughput RNA analysis, the data represents putative riboregulatory candidates. Below the timeline, key scientific breakthroughs and novel methods applied in ncRNAs discovery are shown. The timeline is based on data presented in Johansson et al. (2002); Christiansen et al. (2006); Mandin et al. (2007); Nielsen et al. (2008); Loh et al. (2009); Oliver et al. (2009); Toledo-Arana et al. (2009); Mraheil et al. (2011); Wurtzel et al. (2012); Behrens et al. (2014), and Wehner et al. (2014).

the riboregulators of *L. monocytogenes* which, besides being consistently identified in high-throughput studies, have been characterized in low-throughput analyses, providing summarized data on their physiological role and, when available, mechanism of action. The detailed characteristics of these riboregulators are presented in **Table 1**.

TRANS REGULATORY ncRNAs

LhrA

LhrA was identified as an ncRNA interacting with the chaperone Hfq of *L. monocytogenes*. The LhrA transcript is known to be present throughout the growth phase, reaching a maximum level at the onset of the stationary phase, which suggests a role for LhrA during transition from exponential to stationary phase of growth (Christiansen et al., 2006). Notably, the stability of LhrA is highly dependent on the presence of the Hfq chaperone (Christiansen et al., 2006). LhrA is highly conserved among *Listeria* species, and it seems to appear exclusively in the genus *Listeria*. *In silico* studies predicted the secondary structure of LhrA to contain four stem-loops and a well preserved single stranded, 21 nt long motif, which is responsible for base pairing between this ncRNA and its targets. The first identified target for LhrA was *lmo0850*, which encodes a protein of unknown function. The regulation is dependent on Hfq, which facilitates base pairing between LhrA and a region upstream from the start codon of *lmo0850* mRNA, leading to inhibition of translation followed by a decrease in mRNA stability (Nielsen et al., 2010). Further transcriptomic microarray-based studies showed that inactivation of *lhrA* influences the expression level of more than 300 genes in *L. monocytogenes*. Additionally, this study allowed for the identification of two other genes directly regulated by LhrA, i.e., *lmo0302* and *chiA*, encoding a hypothetical protein and a chitinase, respectively. Similarly to regulation of *lmo0850*, these genes are downregulated by LhrA at the posttranscriptional level and the regulation is Hfq-dependent (Nielsen et al., 2011). So far, the dependency on Hfq for efficient binding of LhrA to its targets represents a unique example of Hfq chaperone involvement in ncRNA-mRNA interaction and posttranscriptional regulation in Gram-positive bacteria. A recent study revealed that transfection of eukaryotic cells with LhrA triggers moderate IFN- β induction suggesting the involvement of LhrA in modulating the immune response during infection of the host organism (Frantz et al., 2019).

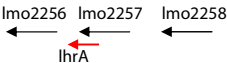
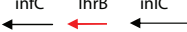
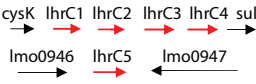
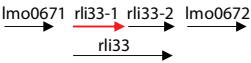


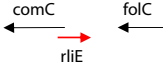


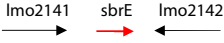

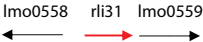


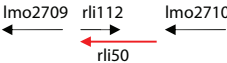
LhrC Family (LhrC1-5, Rli33-1, and Rli22)

The LhrC is a multicopy ncRNA family, which comprises seven homologous ncRNAs, ranging from 105 to 121 nt in length. Notably, this ncRNA family holds the highest number of siblings reported so far. The first discovered members of this family were LhrC1-5 owing to their ability to interact with Hfq (Christiansen et al., 2006). LhrC1-5 arises from two different locations within the *L. monocytogenes* genome, i.e., *lhrC1-4* located between genes *cysK* and *sul*, while *lhrC5* resides between *lmo0946* and *lmo0947* (**Table 1**). Deletion of *lhrC1-5* results in increased susceptibility of *L. monocytogenes* to the β -lactam antibiotic

cefuroxime (Sievers et al., 2014), leads to decreased survival of *L. monocytogenes* in macrophage cells (Sievers et al., 2015), and impairs the adaptation of *L. monocytogenes* to excess of heme (dos Santos et al., 2018). While initially five LhrCs were discovered, further studies led to expanding the LhrC family to seven members based on the discovery of two additional ncRNAs, namely Rli22 and Rli33-1, that are structurally and functionally related to LhrC1-5, although they do not possess the ability to interact with the Hfq (Mollerup et al., 2016). Rli22 is encoded from the intergenic region of *lmo0028* and *lmo0029*, and Rli33-1 was initially identified as part of a larger transcript, designated Rli33, encoded from the intergenic region of *lmo0671* and *lmo0672* (Toledo-Arana et al., 2009). A more recent study identified two individual ncRNAs, Rli33-1 and Rli33-2, which suggests either the presence of an internal transcription start site (TSS) or an unknown RNA processing mechanism of Rli33 (Mraheil et al., 2011). Deletion of the *rli33-1* gene resulted in decreased survival of *L. monocytogenes* in macrophage cells and led to attenuation of *L. monocytogenes* virulence in murine and insect models of infection (Mraheil et al., 2011). Despite their structural similarity, different LhrCs have expression patterns that vary to some extent from one another (Mollerup et al., 2016). Cell envelope stress was shown to induce the expression of LhrC1-5 and Rli22 via the LisRK two-component system. Rli33-1 expression is upregulated in response to osmotic stress and during stationary growth phase in a Sigma B-dependent manner. Rli22 was found to be upregulated in bacteria inside the intestinal lumen of mice (Toledo-Arana et al., 2009). On the contrary, Rli22 is the only representative of the LhrC family which is not upregulated during growth inside macrophages (Mraheil et al., 2011). All seven ncRNAs were shown to be expressed after exposure to blood (Toledo-Arana et al., 2009; **Table 1**).

To date, six targets for LhrCs have been identified. Five of these target genes encode surface proteins required for full virulence of *L. monocytogenes*. For three targets the mechanism of regulation has been studied in detail. The most important features and regulatory mechanisms of ncRNAs from the LhrC family are presented in **Figure 2**. The first target is *lapB* (*lmo1666*), which encodes a cell wall anchored adhesin. The second one is *oppA* (*lmo2349*) that encodes a substrate-binding protein of an oligopeptide transporter. The third target is *tcsA* (*lmo1388*), which encodes a CD4+ T cell-stimulating antigen. In two cases, the ncRNAs exert a negative effect on translation: for *lapB* and *oppA*, the LhrCs are known to act by direct base pairing to the ribosome binding site (RBS), leading to inhibition of translation followed by mRNA degradation (Sievers et al., 2014, 2015) (see **Figure 2A**). In the case of *tcsA*, the LhrC-binding site is located far upstream of the Shine-Dalgarno (SD) region in the 5' UTR of the mRNA. Notably, the LhrCs act by promoting degradation of *tcsA* mRNA and do not affect the translation of this transcript (Sievers et al., 2015; Ross et al., 2019; **Figure 2A**). In addition to the three targets described above, the LhrCs are known to control the expression of genes involved in heme uptake and utilization: *lmo2186* and *lmo2185*, encoding the heme-binding proteins Hbp1 and Hbp2, respectively, and *lmo0484*, encoding a heme oxygenase-like protein. Using *in vitro* binding assays, it was shown that the LhrCs interact with mRNAs encoded

TABLE 1 | Characteristics of non-coding RNAs of *L. monocytogenes*.

Name	Size (nt)	Genome locus ^a	Conditions that induce [↑] or repress [↓] expression ^b	Involvement in particular processes/relevant comment	References
Trans regulatory ncRNAs					
LhrA	268		Early stationary phase of growth ↑	Transition from log to stationary phase; Chitinolytic activity; Induction IFN-β	Christiansen et al., 2006; Nielsen et al., 2010, 2011; Frantz et al., 2019
LhrB	140		ND	ND	Christiansen et al., 2006
LhrC1-5	110–114		Cefuroxime ↑ High osmolarity ↑ Bile ↑ Acid ↑ Ethanol ↑ Blood ↑ Intracellular growth in macrophages ↑ Hemin stress ↑	Resistance to cefuroxime; Virulence; Heme toxicity	Toledo-Arana et al., 2009; Mraheil et al., 2011; Sievers et al., 2014, 2015; Mollerup et al., 2016; dos Santos et al., 2018; Ross et al., 2019
Rli33-1 (LhrC6)	121		Intracellular growth in macrophages ↑ Blood ↑ Stationary phase of growth ↑ High osmolarity ↑	Virulence	Toledo-Arana et al., 2009; Mraheil et al., 2011; Mollerup et al., 2016
Rli22 (LhrC7)	105		Intestinal lumen ↑ Blood ↑ Cefuroxime ↑	ND	Toledo-Arana et al., 2009; Mollerup et al., 2016
RliB	360		Intestinal lumen ↑ Blood ↑ Low oxygen conditions ↑	Virulence; Related to CRISPR in a PnpA-dependent manner	Mandin et al., 2007; Toledo-Arana et al., 2009; Mraheil et al., 2011; Sesto et al., 2014
RliE	223		ND	ND	Mandin et al., 2007
RliI	239		Stationary phase of growth ↑	ND	Mandin et al., 2007; Dar et al., 2016
SbrA	70		High osmolarity ↑ ethanol ↑ Stationary phase of growth ↑	ND	Nielsen et al., 2008; Toledo-Arana et al., 2009
SbrE (Rli47)	515		Stationary phase of growth ↑ Intestinal lumen ↑ Intracellular growth in macrophages ↑ Oxidative stress ↑ Growth with other bacteria ↑	Inhibition of growth through repressing isoleucine biosynthesis	Oliver et al., 2009; Toledo-Arana et al., 2009; Mraheil et al., 2011; Mujahid et al., 2012; Marinho et al., 2019; Anast and Schmitz-Esser, 2020
Rli27	131		Intestinal lumen ↑ Blood ↑ Intracellular growth in epithelial cells ↑	Survival in blood plasma	Toledo-Arana et al., 2009; Quereda et al., 2014, 2016
Rli31	144		Intracellular growth in macrophages ↑	Virulence; Lysozyme resistance	Toledo-Arana et al., 2009; Mraheil et al., 2011; Burke et al., 2014; Dar et al., 2016; Burke and Portnoy, 2016
Rli32	147		Intracellular growth in macrophages ↑	Virulence; oxidative stress response; resistance to cefuroxime; Strong IFN-β induction	Mraheil et al., 2011; Burke et al., 2014; Grubaugh et al., 2018; Frantz et al., 2019
Rli38	369		Stationary phase of growth ↑ Blood ↑ Oxidative stress ↑	Virulence	Toledo-Arana et al., 2009
Rli50	306		ND	Virulence; IFN-β induction	Toledo-Arana et al., 2009; Mraheil et al., 2011; Frantz et al., 2019

(Continued)

TABLE 1 | Continued

Name	Size (nt)	Genome locus ^a	Conditions that induce [↑] or repress [↓] expression ^b	Involvement in particular processes/relevant comment	References
Cis regulatory ncRNAs					
Rli53	207		Intracellular growth in macrophages [↑]	Lincomycin resistance	Toledo-Arana et al., 2009; Mraheil et al., 2011; Dar et al., 2016
Rli59	214		Intestinal lumen [↑] blood [↑] Intracellular growth in macrophages [↓]	ND	Toledo-Arana et al., 2009; Dar et al., 2016
Rli60	247		Low BCAA concentration [↑]	Control of BCAA biosynthesis; virulence; stress adaptation; biofilm formation; IFN- β induction	Toledo-Arana et al., 2009; Peng et al., 2016a,b; Brenner et al., 2018; Frantz et al., 2019
lasRNA (excludon)					
Anti0677 (excludon)	2900		Stationary phase of growth [↑]	Control of motility	Toledo-Arana et al., 2009
Riboswitches and thermosensors					
PrfA thermosensor	127		37°C [↑] infection [↑]	Virulence	Johansson et al., 2002
SAM riboswitch 229 (SreA)			Exponential phase of growth [↑] Stationary phase of growth [↓] SAM [↑] Intracellular growth in macrophages [↓] Intestinal lumen [↑] blood [↑]	Virulence	Loh et al., 2009; Mraheil et al., 2011
Lysine riboswitch (LysRS)	198		Lysine [↑] Intracellular growth in macrophages [↓]	ND	Toledo-Arana et al., 2009; Mraheil et al., 2011
Vitamin B ₁₂ riboswitch of AspocR	230		Intestinal lumen [↑] Propanediol [↑]	Propanediol utilization; Vitamin B ₁₂ biosynthesis	Toledo-Arana et al., 2009; Mellin et al., 2013
Vitamin B ₁₂ riboswitch of Rli55	200		Blood [↑] Intracellular growth in macrophages [↓]	Ethanolamine utilization; Virulence	Toledo-Arana et al., 2009; Mraheil et al., 2011; Mellin et al., 2014
CspA thermosensor	101		26°C or below [↑]	Cold stress tolerance	Schmid et al., 2009; Ignatov et al., 2020
regulatory 5' UTR					
hly	NA		37°C [↑] Infection [↑]	Virulence	Peterson et al., 2020
regulatory 3' UTR					
hly	NA		37°C [↑] Infection [↑]	Virulence	Ignatov et al., 2020

^aArrows indicate the sense of the gene on the genome; data acc. to Toledo-Arana, modified; indicate localization of a riboswitch.

^b[↑] – Positive fold changes represent higher transcript levels in stress compared to stressless conditions while [↓] – negative fold changes represent higher transcript levels in stressless versus stress conditions. BCAA, branched-chain amino acids; SAM, S-adenosylmethionine; IFN- β , β -interferon; '–', no changes in expression were detected; ND, not determined; NA, not applicable.

from *lmo2186*, *lmo2185*, and *lmo0484*, and for *lmo0484* it was confirmed that the LhrC-binding site overlaps with the AG-rich SD region of the mRNA. Furthermore, LhrC1–5 down-regulate the expression of *lmo0484* at the posttranscriptional level in response to the cell wall-acting antibiotic cefuroxime through base pairing to the RBS, leading to inhibition of translation (dos Santos et al., 2018). While LhrC1–5 are known to interact with the chaperone Hfq, the interaction between LhrC and mRNAs

has been shown so far to be Hfq-independent. A common feature of each LhrC family member is a structure that contains two stem loops (named stem loop A and terminator loop) joined by a single stranded stretch. Each LhrC family member contains two highly conserved UCCC motifs located in loop A and the single stranded stretch. LhrC1–5 contain an additional UCCC motif in the terminator loop. These motifs have been shown to be responsible for the interaction between these ncRNAs and their

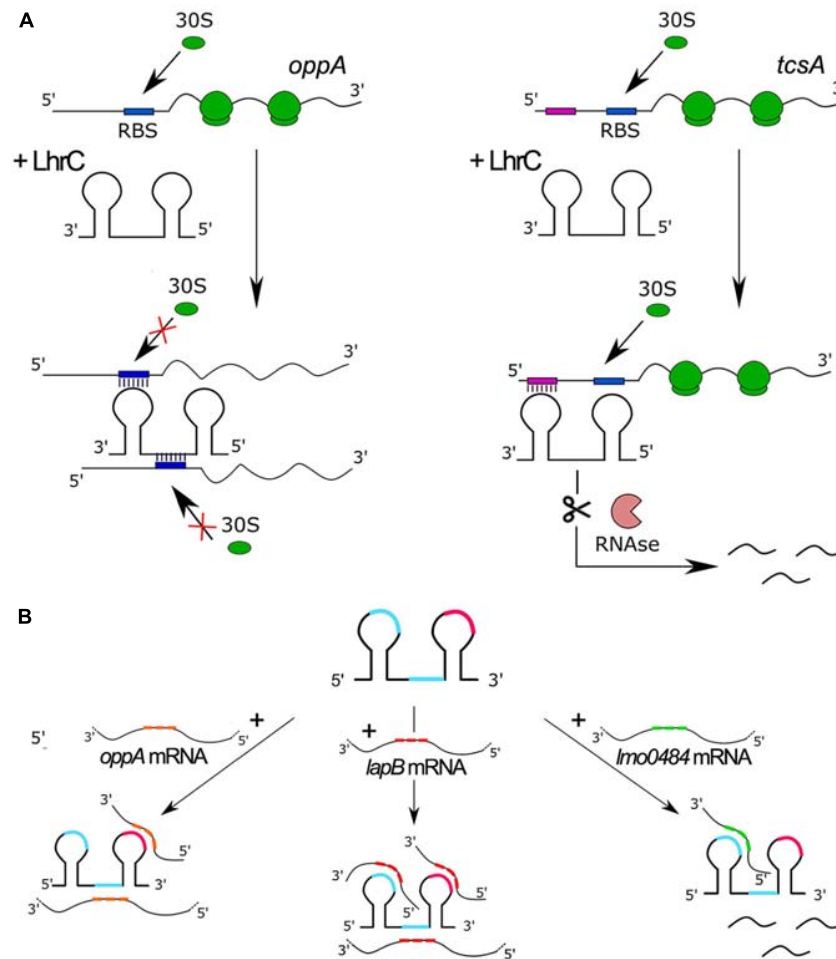


FIGURE 2 | Features and regulatory mechanisms of ncRNAs from the LhrC family. **(A)** Model of LhrC regulation of *oppA* (left) and *tcsA* (right). The LhrC ncRNAs repress *oppA* expression by directly base pairing to the RBS, leading to ribosome occlusion and repression of translation. In contrast, the LhrC ncRNAs repress *tcsA* expression by base pairing to a sequence far upstream of the RBS leading to degradation of *tcsA* mRNA without directly affecting translation. **(B)** Model of LhrCs and LhrC-target mRNA interactions. Each LhrC molecule possesses two different sites containing a UCCC motif located in loop A and the single-stranded region (blue). LhrC1-5 have an additional UCCC motif in the terminator loop (pink). CU-rich sequences are capable of binding to the AG-rich SD region of target mRNAs *oppA*, *lapB*, and *lmo0484*. One LhrC molecule may bind three *lapB* mRNAs, two *oppA* mRNAs or one *lmo0484* mRNA, and the target mRNAs show different binding preferences for the individual UCCC motifs.

target mRNA sequences. Despite general similarity, the structure of the stem loops of Rli22 and Rli33-1 is slightly different from the structure of LhrC1-5. Interestingly, LhrC uses a different number of its UCCC motifs when pairing with different partners (see **Figure 2B**). For example, all three motifs in LhrC4 are capable of binding *lapB* mRNA, two are required for binding *oppA* mRNA, whereas only one is sufficient for efficient binding of *lmo0484* mRNA (Sievers et al., 2014, 2015; dos Santos et al., 2018). The unusually high number of binding sites of LhrC is considered to be a way of amplifying a weak input signal into a strong output response. Multiple binding sites may also accelerate the regulatory effect of LhrC, by binding multiple mRNAs at the same time. Additionally, different flanking regions adjacent to the UCCC motifs provide LhrC with a high degree of flexibility in terms of binding to SD regions of various target mRNAs.

RliB

RliB displays five repeats of 29 nt spaced by 35–36 nt, strikingly resembling CRISPR (Clustered Regularly Interspaced Short Palindromic Repeats) elements present in many prokaryotes and archaea (Mandin et al., 2007). RliB is conserved at the same genomic locus in *L. monocytogenes* strains and also in other *Listeria* species (Mandin et al., 2007; Sesto et al., 2014). The deletion of *rliB* led to faster colonization of the livers of infected mice, indicating that RliB is involved in controlling virulence (Toledo-Arana et al., 2009; **Table 1**). A bioinformatic analysis was applied in an attempt to identify the targets of this ncRNA and this allowed prediction of three bicistronic transcripts as putative RliB targets, from which *lmo2104-lmo2105*, encoding the ferrous iron transport proteins FeoA and FeoB, respectively, was further analyzed (Mandin et al., 2007). The study revealed

a weak complex formation ability between RliB and *lmo2104* and an increase of the *lmo2104-lmo2105* mRNA levels in *L. monocytogenes* as a consequence of overexpression of RliB, suggesting that an interaction of RliB with *lmo2104-lmo2105* mRNA may occur *in vivo* (Mandin et al., 2007). Further studies focused on the initially observed similarity of RliB to CRISPR elements and revealed that RliB is an atypical member of the CRISPR family, whose processing does not depend on *cas* (CRISPR-associated) genes (Sesto et al., 2014). Interestingly, an endogenously encoded polynucleotide phosphorylase (PNPase) with both 3′–5′ exonuclease and 3′ polymerase activities, has been identified as the enzyme responsible for processing of RliB-CRISPR into a 280 nt mature form. The PNPase-dependent processing of RliB-CRISPR is observed both in the *cas*-less *L. monocytogenes* strains and in those encoding a complete set of *cas* genes elsewhere in the genome. Functional studies revealed that RliB-CRISPR has DNA interference activity for which it requires the presence of both PNPase and the *cas* genes belonging to CRISPR-I (Sesto et al., 2014). These results indicate the involvement of RliB in the defense of *L. monocytogenes* against bacteriophage infection in strains carrying *cas* genes, however, the role of RliB in *cas*-less strains remains unknown. It is speculated that RliB-CRISPR's *cas*-independent activity might rely on RNA interference that could be involved in controlling the formation of viral particles and lysis of the bacterial cell, transcription-dependent DNA targeting or gene expression silencing at the posttranscriptional level (Sesto et al., 2014). However, these hypotheses, as well as the discovery of the regulatory mechanism of RliB in *L. monocytogenes* virulence, require further research.

RliI

The *rliI* gene is conserved in *L. innocua* and *Listeria ivanovii* species. The expression of *rliI* in *L. monocytogenes* does not change under conditions related to the infection process but it increases in the stationary phase of growth (Mandin et al., 2007; Toledo-Arana et al., 2009). Three putative bicistronic transcripts have been predicted as RliI targets, i.e., *lmo2660-lmo2659* encoding a transketolase and a ribulose-phosphate epimerase, *lmo1035-lmo1036* encoding a beta-glucoside transporter subunit of a PTS system and a beta-glucosidase, and *lmo2124-lmo2123* encoding components of a maltodextrin ABC transporter system. In each case, pairing of RliI with the 3′ ends of the target bicistronic mRNAs is anticipated (Mandin et al., 2007; Table 1). Among the anticipated mRNAs targets, binding of RliI with the *lmo1035-lmo1036* transcript has been examined and proven. Furthermore, it has been observed that overexpression of RliI in *L. monocytogenes* decreases the level of *lmo1035-lmo1036* mRNA, which suggests that RliI promotes the degradation of this transcript (Mandin et al., 2007). More recently, term-seq analysis, which maps the 3′-termini of RNA transcripts on a genome-wide scale, revealed that RliI is a putative conditional-terminator of the downstream gene *lmo2760* encoding an ABC transporter ATP-binding protein. This observation strongly suggests the role of RliI as a *cis* regulator (Dar et al., 2016). While the predicted function of the RliI targets suggests that this ncRNA is involved in controlling

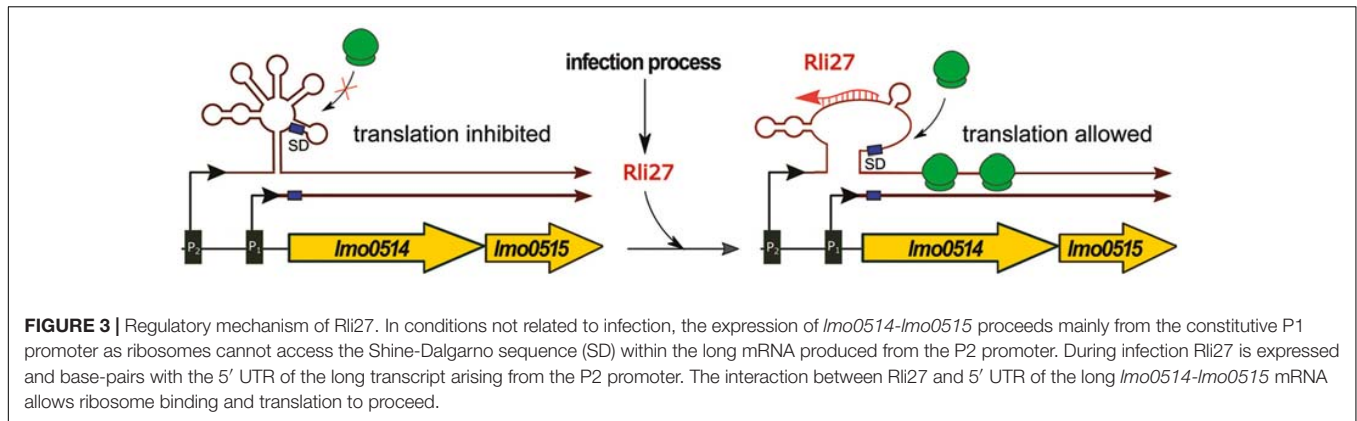
sugar metabolism and transport, the physiological role of RliI remains unknown.

SbrE (Rli47)

The SbrE ncRNA is highly conserved among *L. monocytogenes* strains. In addition to *L. monocytogenes*, *sbrE* was also detected in the genomes of *L. innocua* and *Listeria welshimeri* (Mraheil et al., 2011). It was shown that SbrE affects the expression of the *lmo0636-lmo0637* operon (Mujahid et al., 2012). The Lmo0636 protein is predicted to be a DNA binding protein of the RrF2 family and Lmo0637 was annotated as an UbiE/COQ5 family methyltransferase. Additionally, in a mutant lacking *sbrE* a diminished level of Lmo2094, which is a metal ion binding class II aldolase/adducin domain protein, was observed. Studies of a *sbrE* deficient strain showed no significant effect of SbrE on growth in acid stress, salt stress, glucose-limiting conditions, or low temperature. Furthermore, the susceptibility of the *sbrE* mutant strain to infection with *Listeria* phages was comparable to the wild type strain (Mujahid et al., 2012). However, recent studies revealed that SbrE interacts with the SD region of the *ilvA* mRNA, which encodes threonine deaminase, an enzyme required for branched-chain amino acid biosynthesis (Marinho et al., 2019). Subsequent investigations revealed that in a mutant lacking the *sbrE* gene, both *ilvA* transcript levels and threonine deaminase activity were increased and the mutant also displayed a shorter growth lag in isoleucine-depleted growth media. These data indicate that SbrE acts to inhibit growth of *L. monocytogenes* under harsh conditions, through repression of isoleucine biosynthesis (Marinho et al., 2019). Furthermore, global transcriptional analyses revealed that SbrE is involved in modulation of amino acid metabolism and that the SbrE regulon largely overlaps with that of CodY, further establishing a possible role of Rli47 in the global regulation of metabolism during stress conditions (Marinho et al., 2019).

Rli27

Rli27 is exclusive for the genus *Listeria*, with no orthologs found in other bacteria. Rli27 is responsible for the posttranscriptional regulation of *lmo0514*; the interaction region for Rli27 is located in the 5′ UTR of the target mRNA. Lmo0514 is an internalin-like protein with LPXTG motif, which is required for survival of *L. monocytogenes* in plasma (Quereda et al., 2016). It was shown that the abundance of Lmo0514 increases during infection of eukaryotic cells. The *lmo0514* gene was found to be transcribed from two promoters resulting in two mRNAs, containing a shorter and longer 5′ UTR sequence, respectively (Figure 3). The latter one, which contains the Rli27 interaction site, is detected exclusively in intracellular bacteria. Interaction between Rli27 and *lmo0514* long 5′ UTR mRNA has no effect on the transcript level of *lmo0514*, but results in increased translation. These observations suggest that the regulation is based on altering the secondary structure of the 5′ UTR that in turn leads to increased accessibility of the SD sequence (Quereda et al., 2014) (see Figure 3). Notably, the intracellular-specific translation of an alternative transcript, controlled by Rli27, is the only example



described so far of positive regulation by *trans* ncRNAs in *L. monocytogenes*.

Rli31

While Rli31 is highly abundant and expressed in all growth phases of *L. monocytogenes*, its transcription increases significantly during the infection of macrophage cells. Deletion of *rli31* results in decreased lysozyme resistance, decreased survival of *L. monocytogenes* in macrophages, and attenuation of virulence in insect and murine models of infection (Mraheil et al., 2011; Burke et al., 2014). Decreased mRNA levels of *pgdA* and *pbpX* (encoding peptidoglycan deacetylase and putative carboxypeptidase, respectively) were observed in the *rli31* mutant strain. However, Rli31 does not show any sequence complementarity to *pgdA* or *pbpX* transcripts, suggesting that Rli31 regulates expression of these genes in an indirect way (Burke et al., 2014). Rli31 was also proposed to function as the transcriptional attenuator of *lmo0559* encoding a Mg^{2+}/Co^{2+} transporter, but this putative *cis*-regulation was not studied in detail (Dar et al., 2016). A further genetic screen for Rli31 target genes revealed that Rli31 binds the 5' UTR of *spoVG* mRNA, as well as SpoVG protein (Table 1). However, despite its binding properties, Rli31 does not regulate SpoVG mRNA or protein abundance (Burke and Portnoy, 2016). Notably, SpoVG is a global regulator involved in lysozyme resistance, motility and virulence of *L. monocytogenes* and is itself able to bind various ncRNAs *in vitro* (Burke and Portnoy, 2016). Furthermore, inactivation of *rli31* and *spoVG* results in an opposite effect on lysozyme resistance and virulence, suggesting the existence of an antagonistic regulatory relationship between them. The molecular mechanism of Rli31 regulation and its link to SpoVG definitely requires further investigation.

Rli32

Gene *rli32* is highly conserved in *L. monocytogenes*. The expression of Rli32 is stable in different conditions, including the intestinal lumen and whole human blood, but increases during infection of macrophage cells (Toledo-Arana et al., 2009; Mraheil et al., 2011). It has been shown that expression of Rli32 strongly depends on the transcriptional regulator of virulence VirR (Grubaugh et al., 2018). Furthermore, Rli32

holds the ability to bind to protein SpoVG, but the biological significance of this interaction remains unknown (Burke and Portnoy, 2016). More recently, a secRNome analysis of RNAs secreted by *L. monocytogenes* led to identification of Rli32 among ncRNAs that are secreted into the host cytoplasm following infection with *L. monocytogenes*, with strong β -interferon (IFN- β) inducing properties. The observed IFN- β expression triggered by Rli32 depends mainly on the presence of RIG-I (retinoic acid inducible gene I), and it was postulated that Rli32 is a ligand recognized by the RIG-I receptor (Frantz et al., 2019). Deletion of *rli32* results in decreased survival of *L. monocytogenes* in macrophages and increased resistance to the beta-lactam antibiotic cefuroxime. By contrast, the overexpression of Rli32 promotes intracellular bacterial growth and decreased resistance to cefuroxime. Additionally, *L. monocytogenes* overexpressing Rli32 is more resistant to H_2O_2 and exhibits increased catalase activity (Frantz et al., 2019). Comparative transcriptome analysis revealed that deletion of *rli32* led to the downregulation of ncRNA Rli60 and genes *lmo1627-lmo1633*, corresponding to the complete tryptophan operon, while the overexpression of Rli32 resulted in elevated expression of ncRNAs LhrC1-4, *lmo1958* and *lmo1960* encoding ferrichrome ABC transporter permease components, and operon *lmo2181-lmo2186* encoding heme-binding proteins Hbp1 and Hbp2, and components of a ferrichrome ABC transport system (Frantz et al., 2019). Especially intriguing seems the link between Rli32 and LhrC1-4, since inactivation of *rli32* and *lhrC1-4* results in an opposite effect on cefuroxime resistance. The molecular regulatory mechanism of Rli32 and its link to LhrC1-4 requires further investigation.

Rli38

Rli38 is absent in non-pathogenic *L. innocua* and its expression is at least partially dependent on Sigma B (Toledo-Arana et al., 2009). Three putative mRNAs have been predicted as Rli38 targets, i.e., *lmo1956* (*fur*), *lmo0460*, and *lmo2752*. Notably, two of these genes encode proteins with roles in virulence: the transcriptional repressor Fur corresponds to the global iron uptake regulator and *lmo0460* is a membrane associated lipoprotein belonging to internalin family proteins. While the details of the interaction of Rli38 with its putative mRNA targets remain unknown, a functional analysis has shown that deletion of

the *rli38* gene leads to attenuation of *L. monocytogenes* virulence in the murine model of infection, thus confirming the postulated importance of Rli38 in pathogenesis (Toledo-Arana et al., 2009).

Rli50

Rli50 was first reported to be 176 nt in length (Toledo-Arana et al., 2009), but further studies revealed that the length of the Rli50 transcript is 306 nt (Mraheil et al., 2011). Moreover, it partially overlaps with Rli112 encoded from the opposite strand (Table 1). Rli50 shares homology with another ncRNA – Rli28 that is encoded from the region between *lmo0470* and *lmo0471* genes. Bioinformatic analysis showed that the chromosomal locus including *rli28* (*lmo0459*–*lmo0479*) has a different GC-content, which together with the presence of a IS3 family transposase gene (*lmo0464*) in this region led to speculation that horizontal gene transfer might be involved in chromosomal spreading of these regulatory RNAs (Mraheil et al., 2011). The Rli50 transcript level was slightly higher in extracellular versus intracellular conditions, but noteworthy, Rli50 is one of the most highly transcribed ncRNAs in *L. monocytogenes* under intracellular conditions. Deletion of the *rli50* gene resulted in decreased survival of *L. monocytogenes* in macrophage cells and led to attenuation of *L. monocytogenes* virulence in murine and insect models of infection. The attenuated virulence phenotype can be at least partially justified by the observed IFN- β induction in cells transfected with Rli50, which suggests the involvement of Rli50 in modulating the immune response during infection (Frantz et al., 2019). *In silico* studies showed that both Rli50 and Rli28 could pair with the mRNA of *lmo0549*, which shows similarity to an internalin-like gene. In addition, Rli50 is predicted to bind other ncRNAs such as Rli44, which suggests the existence of a regulatory network based on interaction between ncRNAs (Toledo-Arana et al., 2009). However, these putative interactions require experimental confirmation.

CIS REGULATORY ncRNAs

Rli53

Initially, Rli53 was annotated as a conserved *cis* regulatory ncRNA located in the 5' UTR of *lmo0919* (Table 1). However, it has also been hypothesized that Rli53 might function as a riboswitch, with an open state when *L. monocytogenes* resides in the intestinal lumen and a closed state in blood (Toledo-Arana et al., 2009). Recent term-seq studies revealed that Rli53 forms two alternative RNA structures that terminate or antiterminate the transcription of the downstream *lmo0919* gene, in response to the presence of the translation-inhibiting antibiotic lincomycin. In the absence of the antibiotic, transcription is terminated prematurely leading to the formation of a 207 nt Rli53 transcript. However, in the presence of the antibiotic, termination of Rli53 in the 5' UTR of *lmo0919* is diminished, leading to increased transcription of *lmo0919* encoding an ABC transporter providing resistance to lincomycin (Dar et al., 2016). The predicted structure of Rli53 displays a conserved anti-antiterminator/antiterminator arrangement overlapping with a three-amino-acid ORF, which is translated in *L. monocytogenes*. Detailed functional studies revealed that the Rli53 regulatory

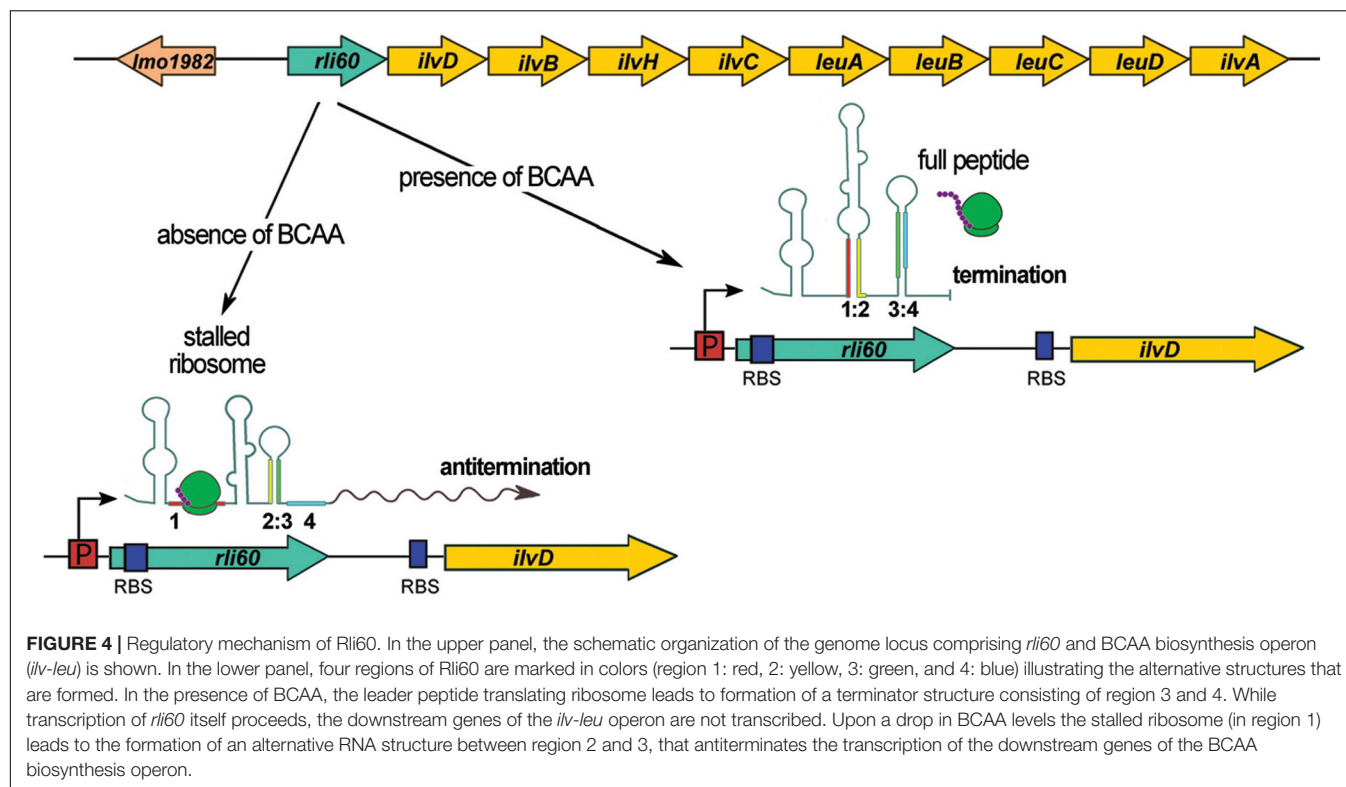
mechanism relies on transcription attenuation mediated by lincomycin-inhibited ribosomes, which stall on the three-amino-acid ORF. This causes a shift of the riboregulator structure from a closed to an open state leading to induced expression of the full-length *lmo0919* mRNA that provides resistance to lincomycin (Dar et al., 2016).

Rli59

Rli59 is a conserved *cis* regulatory ncRNA with a small ORF within its sequence (Toledo-Arana et al., 2009). Similar to Rli53, termination of Rli59 in the 5' UTR of *lmo1652* is hampered by sub-lethal doses of translation-inhibiting antibiotics and leads to increased transcription of *lmo1652* encoding an ABC transporter with unknown function. However, the physiological effect of this regulation remains unknown, and furthermore regulation in this case is more permissive since Rli59 responds to different translation inhibiting antibiotics including lincomycin, erythromycin and chloramphenicol (Dar et al., 2016). While details concerning Rli59 regulation are missing, it is postulated that similarly to Rli53, Rli59 would control the level of *lmo1652* transcription via a mechanism of translation-coupled ribosome-mediated attenuation (Dar et al., 2016).

Rli60

Rli60 is encoded from the region upstream of *ilvD*, which is the first gene of the branched-chain amino acids (BCAA) biosynthesis operon *ilv-leu* (see Figure 4). Rli60 was predicted to function as a riboswitch with increased transcription in blood (Toledo-Arana et al., 2009) or as a ncRNA with a small ORF within its sequence (Mraheil et al., 2011). Other studies have suggested a role for Rli60 in stress adaptation, biofilm formation and virulence of *L. monocytogenes*, by a mechanism that is not known (Peng et al., 2016a,b). Recent studies revealed that *rli60* is co-transcribed with *ilvD* under BCAA limiting conditions, whereas under rich BCAA conditions a shorter transcript (~200 nt) representing only Rli60 RNA is produced (Brenner et al., 2018; Figure 4). Of note, transcription of *ilvD* depends solely on transcription of *rli60* as *ilvD* does not possess a promoter on its own, meaning that transcription of *ilvD* is driven from the promoter located upstream of *rli60*. Detailed studies revealed that in low concentration of BCAA *rli60* is transcribed, forming two alternative RNA structures that terminate or antiterminate the transcription of the downstream *ilv-leu* genes. Transcription attenuation is dictated by a 13-amino-acid leader peptide rich in BCAA, which is translated ribosomally, implying that this mode of regulation corresponds to classical translation-coupled ribosome-mediated attenuation (Figure 4). Thus, Rli60 functions as a ribosome-mediated attenuator that regulates BCAA biosynthesis genes *in cis* and it is important for shutting down BCAA production even under BCAA depletion. This regulatory mechanism is crucial for virulence, as it ensures low level of the internal pools of BCAA, which is the signal for direct binding of the CodY regulator in the coding sequence of *prfA*. In turn, CodY activates the transcription of *prfA* and thereby stimulates the expression of virulence genes (Lobel et al., 2015; Brenner et al., 2018). Whether the 200 nt Rli60 ncRNA produced in BCAA rich condition functions as a *trans* acting regulator remains unknown. However, a recent study revealed

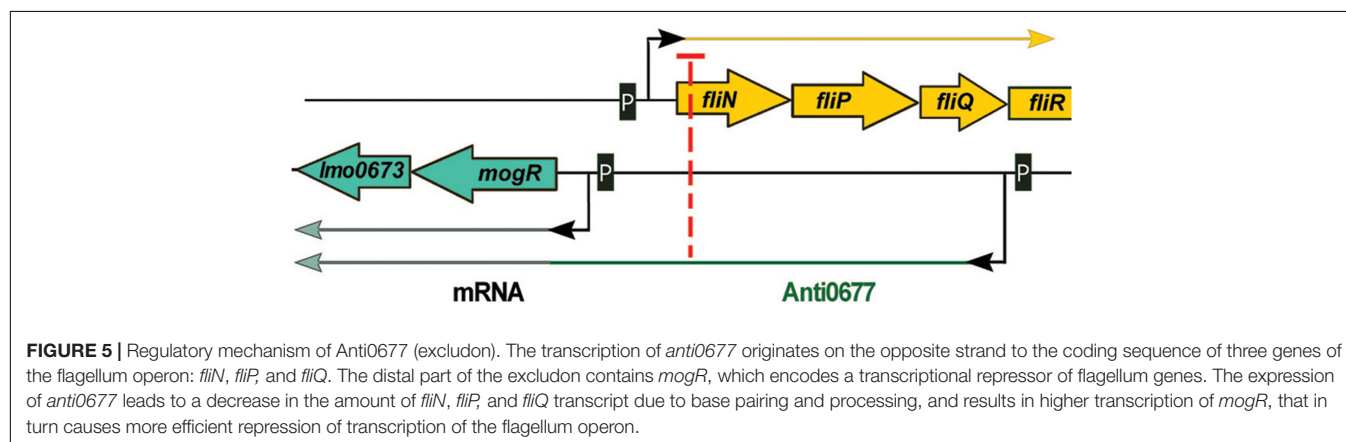


that transfection of eukaryotic cells with Rli60 triggers moderate IFN- β induction (Frantz et al., 2019), suggesting that this ncRNA could have an additional role during infection that relies on modulating the immune response.

lasRNAs (EXCLUDONS)

Anti0677 is an example of a unique class of lasRNA transcripts called excludons. These lasRNAs contain the mRNA sequence of a gene and an exceptionally long 5' or 3' UTR. The UTR region overlaps other genes transcribed on the opposite strand, affecting their expression. The transcription of *anti0677* originates on the opposite strand to the coding sequence of three genes of the

flagellum operon: *fliN*, *fliP*, and *fliQ* and the distal part of the excludon contains the coding sequence of the *mogR* gene, which encodes a transcriptional repressor of flagellum genes (Table 1 and Figure 5). The *mogR* gene is transcribed from two promoters: transcription from the first, located just upstream of the start codon, generates a 1,200 nt transcript, whereas the second promoter is Sigma B dependent and drives transcription of a 2,900 nt Anti0677 excludon (Toledo-Arana et al., 2009). While the shorter *mogR* transcript is generated constitutively, *anti0677* was observed to be highly expressed during the stationary phase of growth. The expression of *anti0677* has a dual regulatory effect on the expression of the flagellum operon. First, it leads to higher transcription of *mogR*, that in turn causes more efficient repression of transcription of the flagellum operon. Second,



it leads to a decrease in the amount of *fliN*, *fliP*, and *fliQ* transcript of flagellum operon due to base pairing and processing (Figure 5). Regarding a proposed action, the overexpression of *anti0677* was shown to impair motility (Toledo-Arana et al., 2009). While *Anti0677* was the first described excludon of *L. monocytogenes*, further transcriptomic studies revealed the existence of additional excludons in this bacterium, i.e., *Anti0605*, *Anti1846*, and *Anti0424* (Wurtzel et al., 2012). The transcription of *anti0605* inhibits expression of *lmo0605* encoding a MatE-family multidrug efflux pump and simultaneously leads to expression of *lmo0606* encoding a transcriptional regulator and two downstream genes (*lmo0607* and *lmo0608*) encoding an ABC-type multidrug transport system. Transcription of *anti1846* originates from the opposite strand relative to the coding sequence of *lmo1846* encoding an efflux pump from the MatE family. The distal part of the excludon contains the coding sequence of the downstream *lmo1845*, *lmo1844*, and *lmo1843* encoding xanthine-uracil permease, lipoprotein signal peptidase and ribosomal subunit synthase, respectively. It has been suggested that the *anti1846* might lead to expression of the permease while expression of the efflux pump is repressed. In the case of *anti0424*, it has been shown that this excludon includes genes involved in importing and metabolizing fructose (*lmo0425* and *lmo0428*) whereas its 5' UTR overlaps, in the antisense orientation, with a glucose-specific permease (*lmo0424*). While functional studies are missing for these excludons, it is suggested that they may represent a common mechanism of linking regulation of physically adjacent genes that have opposing functions (Wurtzel et al., 2012).

RIBOSWITCHES AND THERMOSENSORS

PrfA Thermosensor

The PrfA thermosensor is a 127 nt riboregulator covering 115 nt of the 5' UTR and 12 nt of the coding sequence of *prfA*, which encodes the master virulence regulator of *L. monocytogenes*. At environmental temperatures (30°C or below), the thermosensor element creates a stable hairpin structure which blocks the access of the ribosome to the SD sequence of *prfA* mRNA and therefore inhibits translation initiation. An increase of temperature to 37°C melts the stem-loop structure allowing the ribosome to access the SD sequence, resulting in translation of the *prfA* mRNA (Johansson et al., 2002; Table 1). The temperature-dependent control of *prfA* translation has a pivotal role in the virulence of *L. monocytogenes* as during infection of the host organism, the temperature rises to 37°C, opens the stem-loop and unmasks the translation initiation site. Consequently, PrfA is produced, which results in the transcription of the PrfA-dependent virulence genes.

SreA Riboswitch

The SreA riboswitch, termed for SAM (S-adenosyl-methionine) riboswitch elements, is located upstream from, and in orientation consistent with, *lmo2419*, *lmo2418*, and *lmo2417* which encode proteins related to an ABC-transporter system potentially

involved in methionine uptake (Figure 6 and Table 1). Interestingly, the SreA riboswitch exhibits dual function. First, SreA acts as a riboswitch to regulate *in cis* the expression of the *lmo2419-lmo2417* operon in a SAM-dependent manner. During growth in rich nutrient conditions, ensuring a high intracellular concentration of SAM, binding of the metabolite to the aptamer leads to premature termination of the operon transcription and formation of a truncated 229 nt transcript representing SreA alone. Contrary, during growth at low nutrient conditions, reflecting the absence of SAM, a full-length polycistronic transcript of around 2800 nt is produced (Loh et al., 2009). Therefore, in relation to regulation of the *lmo2419-lmo2417* operon, SreA exhibits a default structure and mechanism of action like other SAM riboswitches. Notably, in addition to the *in cis* activity of SreA on transcriptional regulation, the riboswitch can give rise to an ncRNA with *in trans* regulatory properties. More specifically, it was shown that SreA can base-pair, *in trans*, with the distal part of the 5' UTR region of *prfA* mRNA. The interaction, which takes place approximately 80 nt upstream of the SD site of *prfA*, masks the SD sequence and impedes translation initiation (Loh et al., 2009). Thus, SreA acts as a dual riboregulator controlling the transcription of the downstream genes *in cis*, and furthermore, it acts *in trans* on distally located mRNAs, like *prfA* (Figure 6). Worth mentioning is that PrfA is a transcriptional activator of SreA expression. Therefore, SreA as a *trans* ncRNA constitutes part of a negative feedback loop on the expression of the main virulence regulator in *L. monocytogenes*. While the physiological effect of *sreA* inactivation was not examined, it is postulated that, according to the observed regulatory function on *prfA*, it is involved in virulence control. In agreement with this, SreA ncRNA is transcribed in the intestinal lumen and in blood (Toledo-Arana et al., 2009), therefore giving rise to *trans* regulatory activity of SreA in these conditions related to pathogenesis. On the other hand, a decreased level of the SreA ncRNA was observed during infection of macrophages (Mraheil et al., 2011), which suggests that SreA-mediated modulation of *prfA* expression changes at different stages of the infection process. Additionally, inactivation of *sreA* led to an increased level of *lmo2230* mRNA and decreased level of *lmo0049* mRNA. However, the regulatory mechanism of SreA on these mRNAs was not examined and therefore remains unknown. Notably, in addition to SreA, *L. monocytogenes* has six additional putative SAM riboswitches, from which SreB was shown to prevent *in trans* translation of *prfA* as well (Loh et al., 2009). SreB was also shown to restore the expression of *lmo2230*, but not that of *lmo0049* (Loh et al., 2009), suggesting that despite high similarity, the individual SAM riboswitches may differ in their ability to interact with mRNA targets.

LysRS

The LysRS riboswitch, encoded between *lmo0798* and *lmo0799*, possesses a dual function. First, depending on the environmental conditions, the riboswitch acts as a terminator of transcription for the upstream gene *lmo0799*. The second regulatory mechanism of LysRS depends on the presence of lysine. Binding of the metabolite to the riboswitch leads to an alteration of its structure and results in transcription termination of the downstream

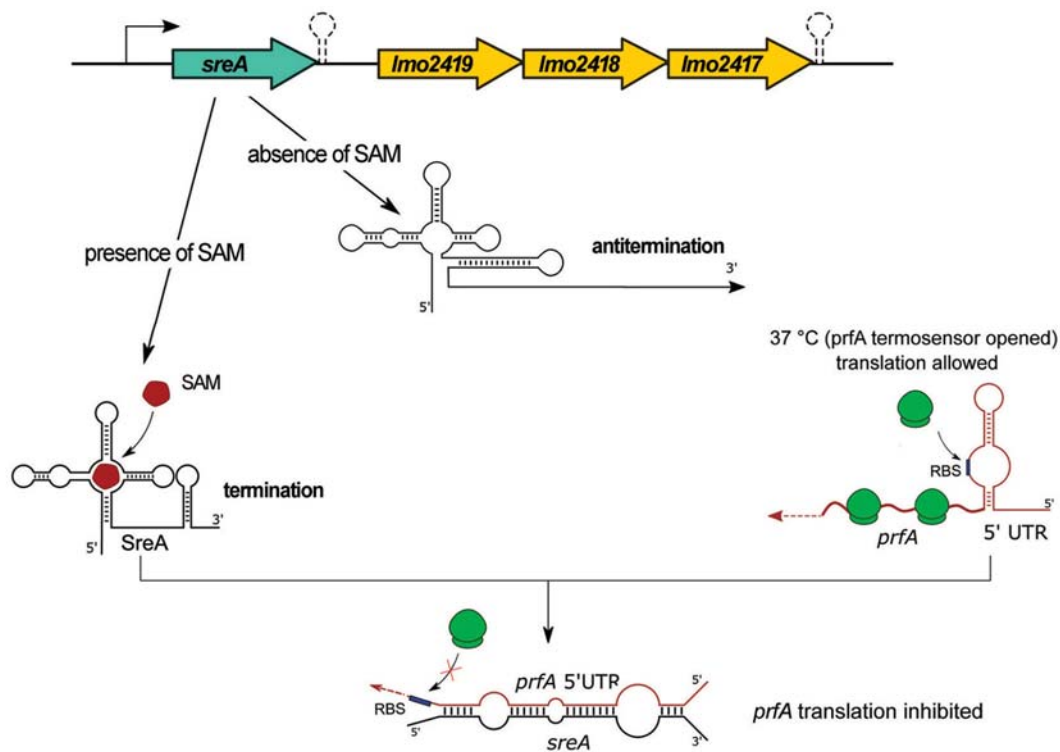


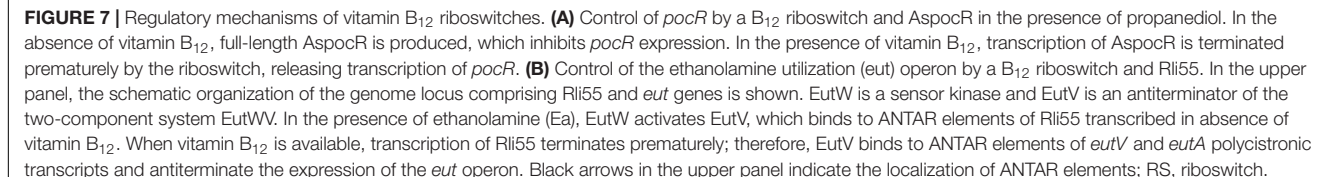
FIGURE 6 | Regulatory mechanisms of the SreA riboswitch. The upper panel illustrates the schematic organization of the genome locus comprising the SAM riboswitch SreA and the *lmo2419-lmo2417* operon. In the absence of SAM the riboswitch element forms an antitermination structure that allows transcription of the downstream genes. Binding of SAM to the riboswitch alters its conformation, a terminator structure is formed, and downstream genes are not synthesized. The SreA small RNA, which is the product of a terminated riboswitch, base-pairs *in trans* with the 5' UTR of *prfA* and blocks access of ribosomes to the SD sequence, which results in the inhibition of translation of *prfA*.

gene *lmo0798* encoding a lysine transporter (Table 1). Notably, when lysine is absent, an anti-terminator structure is formed, which allows for transcription of the lysine transporter gene. Interestingly, in the absence of lysine a small transcript is generated, corresponding to LysRS alone (Toledo-Arana et al., 2009). The expression of *lysRS* proceeds from a Sigma B-dependent promoter, and its transcription increases in the presence of lysine and is strongly repressed during growth of *L. monocytogenes* in macrophages (Toledo-Arana et al., 2009; Mraheil et al., 2011). While the regulatory mechanism of LysRS is solved, its importance for *L. monocytogenes* physiology remains to be examined.

Vitamin B₁₂ Riboswitch of AspocR

A vitamin B₁₂-dependent riboswitch is positioned between *lmo1149* and *lmo1150*, the latter encoding the transcriptional regulator PocR (Table 1). Initially, this riboswitch was annotated as ncRNA Rli39 and it was hypothesized to function as a riboswitch that terminates the transcription of *lmo1149* (Toledo-Arana et al., 2009). However, further research revealed that the riboswitch is transcribed as part of, and controls transcription of, an antisense RNA to *pocR* (AspocR) in a vitamin B₁₂-dependent manner (Mellin et al., 2013; Figure 7A). Notably, AspocR encompasses as well the previously identified RliH and taking

into account that no TSS was identified for RliH, this ncRNA is anticipated to be a processed fragment of AspocR (Mandin et al., 2007; Wurtzel et al., 2012; Mellin et al., 2013). Binding of vitamin B₁₂ to the riboswitch leads to premature termination of *aspocR* transcription and the arising of a truncated 230 nt transcript. In the absence of vitamin B₁₂, a full length AspocR transcript of 1,400 nt is produced, which inhibits *pocR* expression by an antisense mechanism (Figure 7A). PocR positively regulates expression of the *pdu* genes involved in propanediol utilization, as well as the *cob* genes responsible for biosynthesis of vitamin B₁₂, in response to the presence of propanediol. These regulatory functions of PocR are linked, as propanediol catabolism requires vitamin B₁₂ as a cofactor. The observed vitamin B₁₂ riboswitch-dependent antisense regulation of *pocR* ensures that *pdu* genes are expressed only when both the substrate and the cofactor are available. It is ensured by only partial repression of *pocR* by AspocR in response to the presence of propanediol but in unavailability of vitamin B₁₂. In such conditions, the arising level of PocR is sufficient to activate expression of the *cob* genes and synthesis of B₁₂ cofactor, while propanediol catabolism genes are repressed. Therefore, the vitamin B₁₂ riboswitch and AspocR serve as fine-tuning riboregulators integrating signals on propanediol and vitamin B₁₂ availability (Mellin et al., 2013). While the regulatory mechanism of the riboswitch relies



fucose (Toledo-Arana et al., 2009; Mellin et al., 2013). While the effects of the vitamin B₁₂ riboswitch or full length AspocR on pathogenesis of *L. monocytogenes* have not been examined, it is anticipated that the riboregulator plays a role in this process as propanediol catabolism is important for the pathogenesis of many intestinal pathogens (Mellin et al., 2013).

The vitamin B₁₂-dependent riboswitch is positioned upstream of Rli55 which is a ncRNA located in the close vicinity of the *eut* operon responsible for ethanolamine utilization (Toledo-Arana et al., 2009; Mellin et al., 2014; **Figure 7B**). Binding of vitamin B₁₂ to the riboswitch leads to premature termination of Rli55 transcription, resulting in a short, 200 nt transcript,

while in the absence of vitamin B₁₂, a full-length transcript of around 450 nt is produced (Mellin et al., 2014). Further analysis revealed that full-length Rli55 contains a structural motif similar to ANTAR (amiR and nasR transcriptional antiterminator regulator) elements. This motif corresponds to a binding site for the EutV antiterminator of a two-component system, EutVW, which is responsible for the upregulation of the *eut* operon. The *eut* genes require both ethanolamine and vitamin B₁₂ to be transcribed. In the presence of ethanolamine alone, EutV is bound and sequestered by the ANTAR element of Rli55. Conversely, in the presence of ethanolamine and vitamin B₁₂, *rli55* transcription terminates prematurely downstream from the riboswitch, and therefore it is transcribed without an ANTAR element. This transcript cannot bind EutV, and thus allows EutV to bind ANTAR elements of *eut* mRNAs and antiterminate *eut* expression (Figure 7B; Mellin et al., 2014). As enzymes of the ethanolamine utilization pathway use vitamin B₁₂ as a cofactor, Rli55 prevents expression of the *eut* locus in the absence of B₁₂, thereby ensuring that the *eut* genes are expressed only in the presence of both substrate and cofactor. Deletion of the vitamin B₁₂ riboswitch of Rli55 led to significantly reduced virulence; in contrast, deletion of the whole *rli55* sequence had no effect on virulence. Notably, Rli55 is the only ncRNA described so far in *L. monocytogenes* which regulates the expression of genes by the mechanism of the protein sequestration.

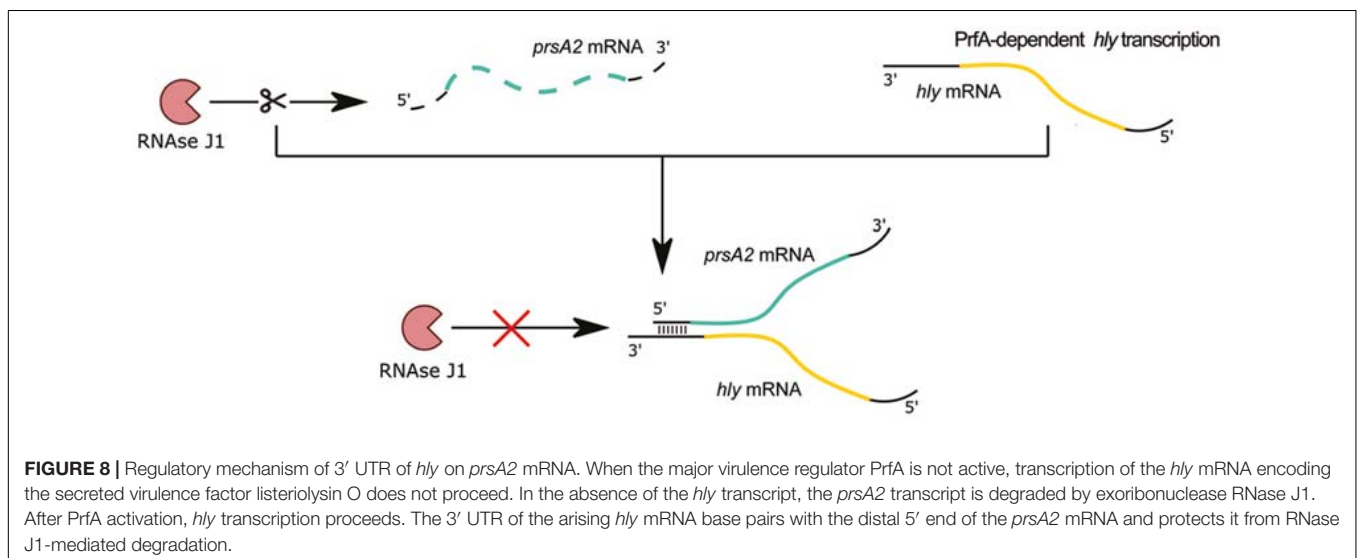
CspA Thermosensor

CspA thermosensor is a 101 nt riboregulator located in the 5' UTR of gene *cspA* encoding cold shock protein A (Table 1). At 37°C, the 5' UTR creates a stable hairpin structure in the region of the SD sequence, making it unavailable for ribosome binding and therefore preventing translation initiation of *cspA*. A decrease of temperature to 30°C or below leads to the formation of a stable hairpin structure at the distal part of the 5' UTR whereas the region containing the SD sequence becomes available for ribosome binding and thus translation

of the *cspA* mRNA may proceed (Ignatov et al., 2020). The rearrangements of the thermosensor structure occur both *in vivo* and *in vitro*, indicating that a temperature change itself is sufficient to initiate conformational changes of the riboregulator. While the physiological role of thermosensor-driven control of *cspA* expression was not examined, it can be assumed that this regulatory mechanism is important for *L. monocytogenes* cold adaptation since CspA was shown to play an important role in cold stress tolerance (Schmid et al., 2009).

REGULATORY 5' AND 3' UTRs

Recent studies revealed non-canonical posttranscriptional regulation, in which the 5' and 3' UTRs of *hly* mRNA are involved (Ignatov et al., 2020; Peterson et al., 2020; Table 1). The *hly* gene encodes listeriolysin O (LLO); a secreted pore-forming cytotoxin that is a key virulence factor of *L. monocytogenes* (Cossart, 2011). LLO promotes rupture of the host phagosome membrane and therefore enables bacterial escape into the cytoplasm, where bacteria replicate and undergo cell-to-cell spreading. While the expression and activity of LLO is indispensable for *L. monocytogenes* virulence, it must be precisely regulated to ensure efficient escape of bacteria from a phagosome and to minimize cytotoxicity during growth inside the cytoplasm of infected cells. Recent work discovered that mRNA of *hly* forms an extensive secondary structure between the 5' UTR comprising the RBS and a region encoding the PEST domain of LLO which is located near the N-terminus. The formation of this secondary mRNA structure is responsible for downregulation of LLO synthesis during bacterial growth (Peterson et al., 2020). Disruption of the interaction between the 5' UTR-PEST sequence of *hly* mRNA did not change the level of *hly* mRNA but led to an increase of LLO. Further analysis revealed that this interaction is crucial for diminishing the cytotoxicity level during infection of host cells and therefore is important for *L. monocytogenes* virulence. Notably, 5' UTR driven regulation of *hly* expression



is observed only for growing bacteria. However, more details concerning the dependency of this regulatory mechanism on growth phase remain to be elucidated.

The 3' UTR of *hly* mRNA is also involved in posttranscriptional gene regulation. In studies devoted to the discovery of RNA-RNA and RNA-protein interactions, *prsA2* mRNA, encoding peptidyl-prolyl isomerase responsible for the folding of secreted proteins at the bacterial surface, was identified as the RNA target of posttranscriptional regulation by *hly* mRNA (Ignatov et al., 2020). Detailed studies revealed that the distal part of the 5' UTR of *prsA2* mRNA directly interacts *in trans* with the 3' UTR of full length *hly* mRNA. Disruption of the interaction between *hly* and *prsA2* mRNAs led to a reduction of *prsA2* mRNA level and protein abundance of PrsA2 but did not change *hly* mRNA level or the amount of LLO. The *hly-prsA2* interaction does not influence ribosome binding to the SD sequence of *prsA2* mRNA, but instead affects the stability of *prsA2* mRNA. Further analysis revealed that interaction with *hly* mRNA protects *prsA2* mRNA from degradation by RNase J1 (Figure 8), and that the *hly-prsA2* interaction is important for *L. monocytogenes* virulence (Ignatov et al., 2020). Of note, the PrsA2 surface chaperone was shown to promote secretion and stability of LLO (Zemansky et al., 2009), therefore *hly*-driven regulation of *prsA2* constitutes a posttranscriptional mechanism ensuring efficient secretion and activity of the regulator. Notably, the *hly-prsA2* interaction is the first described riboregulatory function of a 3' UTR in *L. monocytogenes*.

CONCLUDING REMARKS

The transcriptomic studies of recent years revealed the expression of a huge number of ncRNAs in *L. monocytogenes*. However, the biological functions and regulatory mechanisms of most ncRNAs remain unknown. Despite this fragmentary picture of the regulatory properties of the ncRNAs, recent research on RNA-mediated regulation in *L. monocytogenes* clearly points to ncRNAs being crucial contributors to virulence and stress adaptation. Strikingly, the vast majority of regulatory RNAs studied thus far are important for virulence. Moreover, through their regulatory functions at various stages of pathogenesis, these elements ensure successful infection by *L. monocytogenes*. In the intestinal lumen, effective growth of bacteria is ensured by vitamin B₁₂ riboswitch-driven regulation (Mellin et al., 2014). In the blood, ncRNAs like the LhrCs and Rli27 contribute to resistance to heme toxicity and promote dissemination to deep lying organs (Quereda et al., 2016; dos Santos et al., 2018). Finally, in the intracellular phase of infection, efficient phagosome escape and low cytotoxicity inside the cytoplasm is ensured by riboregulatory elements involved in the control of LLO activity (Ignatov et al., 2020; Peterson et al., 2020). Importantly, multiple ncRNAs are known to regulate genes encoding cell envelope-associated proteins with virulence functions, such as *lapB*, *tcsA*, *hbp1*, *hbp2*, and *lmo0514* (Sievers et al., 2014; Quereda et al., 2014; Sievers et al., 2015; dos Santos et al., 2018; Ross et al., 2019). Furthermore, ncRNAs involved in regulation of amino acid

biosynthesis genes, such as *ilvA* and *ilvD*, have been found to affect virulence (Brenner et al., 2018; Marinho et al., 2019). These findings indicate that riboregulators play important roles during infection by controlling *sensu stricto* virulence factors and by modulating the expression of genes involved in immune evasion, iron acquisition, and general metabolism. While the significance of iron transport and metabolism in the pathogenesis of *L. monocytogenes* is well known (Lechowicz and Krawczyk-Balska, 2015), recent research also points to a link between amino acid availability and virulence, as exemplified by increased virulence gene expression in response to a decrease in BCAA availability (Lobel et al., 2015). Therefore, adequate adjustments of different metabolic pathways is clearly important for establishing a successful infection, and ncRNAs appear to play important roles in these regulatory processes. Regulatory links between different metabolic pathways and the virulence program of *L. monocytogenes* can be achieved due to the versatility of ncRNAs. For example, the LhrC ncRNAs control the level of proteins belonging to different functional categories, such as amino acid and peptide transport, iron transport and metabolism, and surface proteins involved in virulence (Sievers et al., 2014; Sievers et al., 2015; dos Santos et al., 2018). Furthermore, SAM-dependent downregulation of *prfA* by SreA during growth in rich nutrient conditions also illustrates the important role of riboregulatory elements in the cross-coordination of virulence with metabolic pathways, and furthermore illustrates the complexity of riboregulation in this pathogen (Loh et al., 2009). This complexity is clearly manifested by the ability of regulatory RNAs to integrate complex metabolic stimuli, such as availability of different carbon sources and cofactors, into regulatory networks as exemplified by AspocR and Rli55 vitamin B₁₂ riboswitches (Mellin et al., 2013, 2014). Presently, the complexity of regulation involving ncRNAs might be underestimated, as evidenced by the recently described Rli32-dependent changes in LhrC1-4 and Rli60 expression, which strongly suggests the existence of a regulatory network comprising multiple ncRNAs (Frantz et al., 2019). Intriguingly, multiple ncRNAs have been recently reported to modulate the innate immune response through interaction with host sensor RIG-I, suggesting that riboregulatory elements act to link and fine-tune the expression of both bacterial and host genes as a part of *L. monocytogenes*' virulence strategies (Frantz et al., 2019).

Noteworthy, studies of riboregulation in *L. monocytogenes* have led to the definition of new concepts in prokaryotic gene regulation, such as the excludon, and disclosure of the versatility of riboswitches (Loh et al., 2009; Toledo-Arana et al., 2009; Wurtzel et al., 2012). However, further studies are required to explain the molecular basis and physiological role of unexplored post-transcriptional regulators. Such studies represent a demanding task, considering that riboregulators often represent fine-tuning, subtle modulation instead of all-or-nothing regulation. Notably, the regulatory function of most 5' and 3' UTRs is waiting to be revealed. Similarly, most excludons and their roles in adaptation to environmental conditions are still unknown. With a few exceptions, very little is known about RNA chaperones, such as Hfq, and other RNA binding proteins

in *L. monocytogenes* (Jorgensen et al., 2020). So far, LhrA is the only example of an Hfq-dependent regulatory ncRNA in *L. monocytogenes*. Clearly, additional RNA binding proteins and their RNA partners remain to be uncovered in this bacterium. Furthermore, RNA-mediated regulation is triggered in response to changing environmental conditions, therefore the exploration of riboregulation demands linking to – and understanding of – the influence of specific environmental cues. Finally, an emerging theme in the field of riboregulation is the role of bacterial RNAs as virulence effectors modulating the expression of host genes during infection. In *L. monocytogenes*, the role of riboregulators in pathogen-host interactions most likely will continue being at the center of attention in the coming years.

REFERENCES

- Anast, J. M., and Schmitz-Esser, S. (2020). The transcriptome of *Listeria monocytogenes* during co-cultivation with cheese rind bacteria suggests adaptation by induction of ethanolamine and 1, 2-propanediol catabolism pathway genes. *PLoS One* 15:e0233945. doi: 10.1371/journal.pone.0233945
- Behrens, S., Widder, S., Mannala, G. K., Qing, X., Madhugiri, R., Kefer, N., et al. (2014). Ultra deep sequencing of *Listeria monocytogenes* sRNA transcriptome revealed new antisense RNAs. *PLoS One* 9:e83979. doi: 10.1371/journal.pone.0083979
- Brenner, M., Lobel, L., Borovok, I., Sigal, N., and Herskovits, A. A. (2018). Controlled branched-chain amino acids auxotrophy in *Listeria monocytogenes* allows isoleucine to serve as a host signal and virulence effector. *PLoS Genet.* 14:e1007283. doi: 10.1371/journal.pgen.1007283
- Burke, T. P., and Portnoy, D. A. (2016). SpoVG is a conserved RNA-binding protein that regulates *Listeria monocytogenes* lysozyme resistance, virulence, and swarming motility. *mBio* 7:e00240. doi: 10.1128/mBio.00240-16
- Burke, T. P., Loukitcheva, A., Zemansky, J., Wheeler, R., Boneca, I. G., and Portnoy, D. A. (2014). *Listeria monocytogenes* is resistant to lysozyme through the regulation, not the acquisition, of cell wall-modifying enzymes. *J. Bacteriol.* 196, 3756–3767. doi: 10.1128/JB.02053-14
- Christiansen, J. K., Nielsen, J. S., Ebersbach, T., Valentin-Hansen, P., Søgaard-Andersen, L., and Kallipolitis, B. H. (2006). Identification of small Hfq-binding RNAs in *Listeria monocytogenes*. *RNA* 12, 1383–1396. doi: 10.1261/rna.49706
- Cossart, P. (2011). Illuminating the landscape of host-pathogen interactions with the bacterium *Listeria monocytogenes*. *Proc. Natl. Acad. Sci. U.S.A.* 108, 19484–19491. doi: 10.1073/pnas.1112371108
- Cotter, P. D., Emerson, N., Gahan, C. G. M., and Hill, C. (1999). Identification and disruption of lisRK, a genetic locus encoding a two-component signal transduction system involved in stress tolerance and virulence in *Listeria monocytogenes*. *J. Bacteriol.* 181, 6840–6843.
- Dar, D., Shamir, M., Mellin, J. R., Koutero, M., Stern-Ginossar, N., Cossart, P., et al. (2016). Term-seq reveals abundant ribo-regulation of antibiotics resistance in bacteria. *Science* 352:aad9822. doi: 10.1126/science.aad9822
- Dorey, A., Marinho, C., Piveteau, P., and O'Byrne, C. (2019). Role and regulation of the stress activated sigma factor sigma B (σ B) in the saprophytic and host-associated life stages of *Listeria monocytogenes*. *Adv. Appl. Microbiol.* 106, 1–48. doi: 10.1016/bs.aambs.2018.11.001
- dos Santos, P. T., Menendez-Gil, P., Sabharwal, D., Christensen, J.-H., Brunhede, M. Z., Lillebæk, E. M. S., et al. (2018). The small regulatory RNAs LhrC1–5 contribute to the response of *Listeria monocytogenes* to heme toxicity. *Front. Microbiol.* 9:599. doi: 10.3389/fmicb.2018.00599
- Ferreira, V., Wiedmann, M., Teixeira, P., and Stasiewicz, M. J. (2014). *Listeria monocytogenes* persistence in food-associated environments: epidemiology, strain characteristics, and implications for public health. *J. Food Prot.* 77, 150–170. doi: 10.4315/0362-028X.JFP-13-150
- Frantz, R., Teubner, L., Schultze, T., La Pietra, L., Müller, C., Gwozdinski, K., et al. (2019). The secRNome of *Listeria monocytogenes* harbors small noncoding RNAs that are potent inducers of Beta interferon. *mBio* 10:e01223-19. doi: 10.1128/mBio.01223-19

AUTHOR CONTRIBUTIONS

AK-B and BK contributed to conception and design of the manuscript. AK-B wrote the first draft of the manuscript. AK-B, MŁ, and MB wrote sections of the manuscript. KŚ prepared figures. All authors contributed to manuscript revision, read, and approved the submitted version.

FUNDING

This work was supported by a grant no. 2015/18/E/NZ6/00643 from the National Science Center, Poland.

- Grubaugh, D., Regeimbal, J. M., Ghosh, P., Zhou, Y., Lauer, P., Dubensky, T. W., et al. (2018). The VirAB ABC transporter is required for VirR regulation of *Listeria monocytogenes* virulence and resistance to nisin. *Infect. Immun.* 86, e00901–17. doi: 10.1128/IAI.00901-17
- Ignatov, D., Vaitkevicius, K., Durand, S., Cahoon, L., Sandberg, S. S., Liu, X., et al. (2020). An mRNA-mRNA interaction couples expression of a virulence factor and its chaperone in *Listeria monocytogenes*. *Cell Rep.* 30, 4027–4040.e7. doi: 10.1016/j.celrep.2020.03.006
- Johansson, J., Mandin, P., Renzoni, A., Chiaruttini, C., Springer, M., and Cossart, P. (2002). An RNA thermosensor controls expression of virulence genes in *Listeria monocytogenes*. *Cell* 110, 551–561. doi: 10.1016/s0092-8674(02)00905-4
- Jorgensen, M. G., Pettersen, J. S., and Kallipolitis, B. H. (2020). sRNA-mediated control in bacteria: an increasing diversity of regulatory mechanisms. *Biochim. Biophys. Acta Gene Regul. Mech.* 1863:194504. doi: 10.1016/j.bbagr.2020.194504
- Kallipolitis, B. H., Ingmer, H., Gahan, C. G., Hill, C., and Søgaard-Andersen, L. (2003). CesRK, a two-component signal transduction system in *Listeria monocytogenes*, responds to the presence of cell wall-acting antibiotics and affects beta-lactam resistance. *Antimicrob. Agents Chemother.* 47, 3421–3429. doi: 10.1128/aac.47.11.3421-3429.2003
- Lebreton, A., and Cossart, P. (2017). RNA- and protein-mediated control of *Listeria monocytogenes* virulence gene expression. *RNA Biol.* 14, 460–470. doi: 10.1080/15476286.2016.1189069
- Lechowicz, J., and Krawczyk-Balska, A. (2015). An update on the transport and metabolism of iron in *Listeria monocytogenes*: the role of proteins involved in pathogenicity. *Biomaterials* 28, 587–603. doi: 10.1007/s10534-015-9849-5
- Liu, D., Lawrence, M. L., Ainsworth, A. J., and Austin, F. W. (2007). Toward an improved laboratory definition of *Listeria monocytogenes* virulence. *Int. J. Food Microbiol.* 118, 101–115. doi: 10.1016/j.ijfoodmicro.2007.07.045
- Lobel, L., Sigal, N., Borovok, I., Belitsky, B. R., Sonenshein, A. L., and Herskovits, A. A. (2015). The metabolic regulator CodY links *Listeria monocytogenes* metabolism to virulence by directly activating the virulence regulatory gene *prfA*. *Mol. Microbiol.* 95, 624–644. doi: 10.1111/mmi.12890
- Loh, E., Dussurget, O., Gripenland, J., Vaitkevicius, K., Tiensuu, T., Mandin, P., et al. (2009). A trans-acting riboswitch controls expression of the virulence regulator PrfA in *Listeria monocytogenes*. *Cell* 139, 770–779. doi: 10.1016/j.cell.2009.08.046
- Mandin, P., Fsihi, H., Dussurget, O., Vergassola, M., Milohanic, E., Toledo-Arana, A., et al. (2005). VirR, a response regulator critical for *Listeria monocytogenes* virulence. *Mol. Microbiol.* 57, 1367–1380. doi: 10.1111/j.1365-2958.2005.04776.x
- Mandin, P., Repoila, F., Vergassola, M., Geissmann, T., and Cossart, P. (2007). Identification of new noncoding RNAs in *Listeria monocytogenes* and prediction of mRNA targets. *Nucleic Acids Res.* 35, 962–974. doi: 10.1093/nar/gkl1096
- Marinho, C. M., Dos Santos, P. T., Kallipolitis, B. H., Johansson, J., Ignatov, D., Guerreiro, D. N., et al. (2019). The σ B-dependent regulatory sRNA Rli47 represses isoleucine biosynthesis in *Listeria monocytogenes* through a direct interaction with the *ilvA* transcript. *RNA Biol.* 16, 1424–1437. doi: 10.1080/15476286.2019.1632776

- McLauchlin, J., Mitchell, R. T., Smerdon, W. J., and Jewell, K. (2004). *Listeria monocytogenes* and listeriosis: a review of hazard characterisation for use in microbiological risk assessment of foods. *Int. J. Food Microbiol.* 92, 15–33. doi: 10.1016/S0168-1605(03)00326-X
- Mellin, J. R., Koutero, M., Dar, D., Nahori, M.-A., Sorek, R., and Cossart, P. (2014). Riboswitches. Sequestration of a two-component response regulator by a riboswitch-regulated noncoding RNA. *Science* 345, 940–943. doi: 10.1126/science.1255083
- Mellin, J. R., Tiensuu, T., Bécavin, C., Gouin, E., Johansson, J., and Cossart, P. (2013). A riboswitch-regulated antisense RNA in *Listeria monocytogenes*. *Proc. Natl. Acad. Sci. U.S.A.* 110, 13132–13137. doi: 10.1073/pnas.1304795110
- Møllerup, M. S., Ross, J. A., Helfer, A.-C., Meistrup, K., Romby, P., and Kallipolitis, B. H. (2016). Two novel members of the LhrC family of small RNAs in *Listeria monocytogenes* with overlapping regulatory functions but distinctive expression profiles. *RNA Biol.* 13, 895–915. doi: 10.1080/15476286.2016.1208332
- Mraheil, M. A., Billion, A., Mohamed, W., Mukherjee, K., Kuenne, C., Pischmarov, J., et al. (2011). The intracellular sRNA transcriptome of *Listeria monocytogenes* during growth in macrophages. *Nucleic Acids Res.* 39, 4235–4248. doi: 10.1093/nar/gkr033
- Mujahid, S., Bergholz, T. M., Oliver, H. F., Boor, K. J., and Wiedmann, M. (2012). Exploration of the role of the non-coding RNA SbrE in *L. monocytogenes* stress response. *Int. J. Mol. Sci.* 14, 378–393. doi: 10.3390/ijms14010378
- Nielsen, J. S., Larsen, M. H., Lillebæk, E. M. S., Bergholz, T. M., Christiansen, M. H. G., Boor, K. J., et al. (2011). A small RNA controls expression of the chitinase ChiA in *Listeria monocytogenes*. *PLoS One* 6:e19019. doi: 10.1371/journal.pone.0019019
- Nielsen, J. S., Lei, L. K., Ebersbach, T., Olsen, A. S., Klitgaard, J. K., Valentin-Hansen, P., et al. (2010). Defining a role for Hfq in Gram-positive bacteria: evidence for Hfq-dependent antisense regulation in *Listeria monocytogenes*. *Nucleic Acids Res.* 38, 907–919. doi: 10.1093/nar/gkp1081
- Nielsen, J. S., Olsen, A. S., Bonde, M., Valentin-Hansen, P., and Kallipolitis, B. H. (2008). Identification of a σ^B -dependent small noncoding RNA in *Listeria monocytogenes*. *J. Bacteriol.* 190, 6264–6270. doi: 10.1128/JB.00740-08
- Oliver, H. F., Orsi, R. H., Ponnala, L., Keich, U., Wang, W., Sun, Q., et al. (2009). Deep RNA sequencing of *L. monocytogenes* reveals overlapping and extensive stationary phase and sigma B-dependent transcriptomes, including multiple highly transcribed noncoding RNAs. *BMC Genomics* 10:641. doi: 10.1186/1471-2164-10-641
- Peng, Y.-L., Meng, Q.-L., Qiao, J., Xie, K., Chen, C., Liu, T.-L., et al. (2016a). The regulatory roles of ncRNA Rli60 in adaptability of *Listeria monocytogenes* to environmental stress and biofilm formation. *Curr. Microbiol.* 73, 77–83. doi: 10.1007/s00284-016-1028-6
- Peng, Y.-L., Meng, Q.-L., Qiao, J., Xie, K., Chen, C., Liu, T.-L., et al. (2016b). The roles of noncoding RNA Rli60 in regulating the virulence of *Listeria monocytogenes*. *J. Microbiol. Immunol. Infect.* 49, 502–508. doi: 10.1016/j.jmii.2014.08.017
- Peterson, B. N., Portman, J. L., Feng, Y., Wang, J., and Portnoy, D. A. (2020). Secondary structure of the mRNA encoding listeriolysin O is essential to establish the replicative niche of *L. monocytogenes*. *Proc. Natl. Acad. Sci. U.S.A.* 117, 23774–23781. doi: 10.1073/pnas.2004129117
- Quereda, J. J., García-Del Portillo, F., and Pucciarelli, M. G. (2016). *Listeria monocytogenes* remodels the cell surface in the blood-stage. *Environ. Microbiol. Rep.* 8, 641–648. doi: 10.1111/1758-2229.12416
- Quereda, J. J., Ortega, ÁD., Pucciarelli, M. G., and García-del Portillo, F. (2014). The *Listeria* small RNA Rli27 regulates a cell wall protein inside eukaryotic cells by targeting a long 5'-UTR variant. *PLoS Genet.* 10:e1004765. doi: 10.1371/journal.pgen.1004765
- Reniere, M. L., Whiteley, A. T., and Portnoy, D. A. (2016). An in vivo selection identifies *Listeria monocytogenes* genes required to sense the intracellular environment and activate virulence factor expression. *PLoS Pathog.* 12:e1005741. doi: 10.1371/journal.ppat.1005741
- Renzoni, A., Cossart, P., and Dramsi, S. (1999). PrfA, the transcriptional activator of virulence genes, is upregulated during interaction of *Listeria monocytogenes* with mammalian cells and in eukaryotic cell extracts. *Mol. Microbiol.* 34, 552–561. doi: 10.1046/j.1365-2958.1999.01621.x
- Ross, J. A., Thorsing, M., Lillebæk, E. M. S., Teixeira Dos Santos, P., and Kallipolitis, B. H. (2019). The LhrCsRNAs control expression of T cell-stimulating antigen TcsA in *Listeria monocytogenes* by decreasing tcsA mRNA stability. *RNA Biol.* 16, 270–281. doi: 10.1080/15476286.2019.1572423
- Schmid, B., Klumpp, J., Raimann, E., Loessner, M. J., Stephan, R., and Tasara, T. (2009). Role of cold shock proteins in growth of *Listeria monocytogenes* under cold and osmotic stress conditions. *Appl. Environ. Microbiol.* 75, 1621–1627. doi: 10.1128/AEM.02154-08
- Schultze, T., Izar, B., Qing, X., Mannala, G. K., and Hain, T. (2014). Current status of antisense RNA-mediated gene regulation in *Listeria monocytogenes*. *Front. Cell Infect. Microbiol.* 4:135. doi: 10.3389/fcimb.2014.00135
- Sesto, N., Touchon, M., Andrade, J. M., Kondo, J., Rocha, E. P. C., Arraiano, C. M., et al. (2014). A PNPase dependent CRISPR system in *Listeria*. *PLoS Genet.* 10:e1004065. doi: 10.1371/journal.pgen.1004065
- Sievers, S., Lund, A., Menendez-Gil, P., Nielsen, A., Storm Møllerup, M., Lambert Nielsen, S., et al. (2015). The multicopy sRNA LhrC controls expression of the oligopeptide-binding protein OppA in *Listeria monocytogenes*. *RNA Biol.* 12, 985–997. doi: 10.1080/15476286.2015.1071011
- Sievers, S., Sternkopflillebæk, E. M., Jacobsen, K., Lund, A., Møllerup, M. S., Nielsen, P. K., et al. (2014). A multicopy sRNA of *Listeria monocytogenes* regulates expression of the virulence adhesin LapB. *Nucleic Acids Res.* 42, 9383–9398. doi: 10.1093/nar/gku630
- Storz, G., Vogel, J., and Wassarman, K. M. (2011). Regulation by small RNAs in bacteria: expanding frontiers. *Mol. Cell* 43, 880–891. doi: 10.1016/j.molcel.2011.08.022
- Toledo-Arana, A., Dussurget, O., Nikitas, G., Sesto, N., Guet-Revillet, H., Balestrino, D., et al. (2009). The *Listeria* transcriptional landscape from saprophytism to virulence. *Nature* 459, 950–956. doi: 10.1038/nature08080
- Waters, L. S., and Storz, G. (2009). Regulatory RNAs in bacteria. *Cell* 136, 615–628. doi: 10.1016/j.cell.2009.01.043
- Wehner, S., Mannala, G. K., Qing, X., Madhugiri, R., Chakraborty, T., Mraheil, M. A., et al. (2014). Detection of very long antisense transcripts by whole transcriptome RNA-Seq analysis of *Listeria monocytogenes* by semiconductor sequencing technology. *PLoS One* 9:e108639. doi: 10.1371/journal.pone.0108639
- Wurtzel, O., Sesto, N., Mellin, J. R., Karunker, I., Edelheit, S., Bécavin, C., et al. (2012). Comparative transcriptomics of pathogenic and non-pathogenic *Listeria* species. *Mol. Syst. Biol.* 8:583. doi: 10.1038/msb.2012.11
- Zemansky, J., Kline, B. C., Woodward, J. J., Leber, J. H., Marquis, H., and Portnoy, D. A. (2009). Development of a mariner-based transposon and identification of *Listeria monocytogenes* determinants, including the peptidyl-prolyl isomerase PrsA2, that contribute to its hemolytic phenotype. *J. Bacteriol.* 191, 3950–3964. doi: 10.1128/JB.00016-09

Conflict of Interest: The authors declare that the research was conducted in the absence of any commercial or financial relationships that could be construed as a potential conflict of interest.

Copyright © 2021 Krawczyk-Balska, Ładziak, Burmistrz, Ścibek and Kallipolitis. This is an open-access article distributed under the terms of the Creative Commons Attribution License (CC BY). The use, distribution or reproduction in other forums is permitted, provided the original author(s) and the copyright owner(s) are credited and that the original publication in this journal is cited, in accordance with accepted academic practice. No use, distribution or reproduction is permitted which does not comply with these terms.



Three Ribosomal Operons of *Escherichia coli* Contain Genes Encoding Small RNAs That Interact With Hfq and CsrA *in vitro*

Thomas Søndergaard Stenum¹, Mette Kongstad¹, Erik Holmqvist^{2†}, Birgitte Kallipolitis³, Sine Lo Svenningsen^{1*} and Michael Askvad Sørensen^{1*}

OPEN ACCESS

Edited by:

Olga Soutourina,
UMR 9198 Institut de Biologie
Intégrative de la Cellule (I2BC), France

Reviewed by:

Branislav Vecerek,
Institute of Microbiology, Academy
of Sciences of the Czech Republic
(ASCR), Czechia
Franz Narberhaus,
Ruhr University Bochum, Germany

*Correspondence:

Michael Askvad Sørensen
MAS@bio.ku.dk
Sine Lo Svenningsen
SLS@bio.ku.dk

† Present address:

Erik Holmqvist,
Department of Cell and Molecular
Biology, Uppsala University, Uppsala,
Sweden

Specialty section:

This article was submitted to
Microbial Physiology and Metabolism,
a section of the journal
Frontiers in Microbiology

Received: 04 November 2020

Accepted: 09 April 2021

Published: 11 May 2021

Citation:

Stenum TS, Kongstad M,
Holmqvist E, Kallipolitis B,
Svenningsen SL and Sørensen MA
(2021) Three Ribosomal Operons
of *Escherichia coli* Contain Genes
Encoding Small RNAs That Interact
With Hfq and CsrA *in vitro*.
Front. Microbiol. 12:625585.
doi: 10.3389/fmicb.2021.625585

¹ Department of Biology, University of Copenhagen, Copenhagen, Denmark, ² Institute for Molecular Infection Biology, University of Würzburg, Würzburg, Germany, ³ Department of Biochemistry and Molecular Biology, University of Southern Denmark, Odense, Denmark

Three out of the seven ribosomal RNA operons in *Escherichia coli* end in dual terminator structures. Between the two terminators of each operon is a short sequence that we report here to be an sRNA gene, transcribed as part of the ribosomal RNA primary transcript by read-through of the first terminator. The sRNA genes (*rrA*, *rrB* and *rrF*) from the three operons (*rrnA*, *rrnB* and *rrnD*) are more than 98% identical, and pull-down experiments show that their transcripts interact with Hfq and CsrA. Deletion of *rrA*, *B*, *F*, as well as overexpression of *rrB*, only modestly affect known CsrA-regulated phenotypes like biofilm formation, *pgaA* translation and *glgC* translation, and the role of the sRNAs *in vivo* may not yet be fully understood. Since *RrA*, *B*, *F* are short-lived and transcribed along with the ribosomal RNA components, their concentration reflect growth-rate regulation at the ribosomal RNA promoters and they could function to fine-tune other growth-phase-dependent processes in the cell. The primary and secondary structure of these small RNAs are conserved among species belonging to different genera of Enterobacteriales.

Keywords: sRNA, CsrA, Hfq, ribosomal RNA operon, dual terminators

INTRODUCTION

Bacterial small regulatory RNAs (sRNA) are major post-transcriptional regulators of gene expression. Mechanistically, the majority of these sRNAs act by base pairing to complementary sequences in mRNA targets, thereby altering translation initiation rates and/or mRNA stability (Wagner and Romby, 2015). Association rates between sRNAs and their target RNAs are often strongly increased by the presence of the homohexameric RNA chaperone Hfq, which binds both RNAs and facilitates base pairing (Santiago-Frangos and Woodson, 2018). Many sRNAs are involved in the rapid reorganization of bacterial gene expression as a response to various types of stresses (recently reviewed in Holmqvist and Wagner, 2017). However, sRNAs that are expressed in the absence of an acute stress have also been described, including anti-toxin sRNAs (reviewed in Brantl and Jahn, 2015), the sRNAs ChiX and Spot 42 which regulate different aspects of carbohydrate metabolism (Møller et al., 2002; Rasmussen et al., 2009; Beisel and Storz, 2011) and MgrR (Moon and Gottesman, 2009), a regulator of lipopolysaccharide composition. The sRNAs

CsrB and CsrC are expressed in response to the accumulation of end-metabolism products at the entry to stationary phase (Lawhon et al., 2002; Gonzalez Chavez et al., 2010). In contrast to base-pairing sRNAs, CsrB/C act by sequestering a single protein target, the global regulator CsrA. This small (7 kDa) homodimeric RNA-binding protein acts by binding at or close to ribosome binding sites (RBS) in a myriad of different mRNAs (Potts et al., 2017). Targets of CsrA include mRNAs encoding proteins involved in carbon metabolism (Liu et al., 1995), biofilm formation (Jackson et al., 2002), motility (Wei et al., 2001), quorum sensing, and virulence (Altier et al., 2002). CsrB and CsrC function by mimicking CsrA targets and carry ~18 and nine motifs for CsrA binding, respectively (Liu et al., 1997; Weilbacher et al., 2003). As a consequence, they antagonize CsrA by sequestering it away from its lower-affinity mRNAs targets, thereby decreasing the effective concentration of CsrA. More recent, similar activities on CsrA have been described for two additional sRNAs in *E. coli*; McaS (Jorgensen et al., 2013) and GadY (Parker et al., 2017), both of which are believed to contain two binding sites for CsrA. Unlike CsrB/C, both McaS and GadY also regulate gene expression independent of CsrA (Opdyke et al., 2004; Jorgensen et al., 2012; Thomason et al., 2012).

While the majority of characterized sRNAs from *E. coli* are transcribed from intergenic regions (IGRs) under the control of a dedicated promoter, several reports suggest that a substantial number of sRNAs are generated from 5' or 3' untranslated regions (UTRs) by RNase-dependent mRNA processing (Kawano et al., 2005; Chao et al., 2012; Miyakoshi et al., 2015). Additionally, the *glyW-cysT-leuZ* transcript, which is processed to give rise to tRNA^{glyW}, tRNA^{cysT} and tRNA^{leuZ}, also generates the sRNA 3'-ETS^{leuZ} (Lalaouna et al., 2015). This sRNA, which is generated by RNase E-dependent processing, base-pairs to two other sRNAs, RyhB and RybB. The pairing neutralizes transcriptional noise from the *ryhB* and *rybB* genes and counteracts potential regulatory outcomes of inadvertent expression of the corresponding sRNAs. The 3'-ETS^{leuZ} is the first functional tRNA-derived fragment (tRF) described in bacteria. However, numerous tRFs have been reported in eukaryotes, where they control multiple different cellular processes, including genome stability (Martinez et al., 2017; Schorn et al., 2017), cell-cell signaling (Baglio et al., 2015), response to viral infection (Yeung et al., 2009) and stress responses (Emara et al., 2010; Saikia et al., 2014).

In the present study, we have investigated the family of so-called tRNA-linked repeats (TLRs) from *E. coli*. The TLRs are a class of sequences located in tRNA or ribosomal RNA (rRNA) operons. Since the first description of TLRs in 1978 (Egan and Landy, 1978), a total of 22 TLR genes have been identified (Rudd, 1999), which are distributed between ten different loci on the *E. coli* K-12 chromosome, each locus harboring one to five TLRs. A striking feature common to all TLRs is that 18–19 bp of their 3'-end is identical to the 3'-end of the tRNA or rRNA gene that is located immediately upstream of the TLR (Figure 1). Regarding TLR functionality, one of the TLRs found in the pre-tRNA transcript *tyrT-tyrV* was initially reported to be involved in recovery from amino acid starvation (Bösl and Kersten, 1991). However, this claim was later retracted as the

phenotype was shown to originate from a nearby open reading frame (Bösl and Kersten, 1994). Thus far, the TLRs have no known function. In the following, we present evidence that the three TLRs located downstream from rRNA operon A (*rrA*), B (*rrB*) and D (*rrF*), respectively, are transcribed, processed, and bind the post-transcriptional regulators Hfq and CsrA. We present evidence that these novel sRNAs may act as regulators to fine-tune CsrA activity.

MATERIALS AND METHODS

Culture Growth and Media

The study was carried out in *E. coli* K-12 MAS1081 (MG1655 *rph⁺ gatC⁺ glpR⁺*). All strains used in the study are listed in **Supplementary Table 1**. Unless otherwise noted, all cultures were grown in MOPS minimal medium (Neidhardt et al., 1974) at 37°C shaking at 160 rpm and were grown exponentially for at least ten generations before start of the experiment to obtain balanced growth. Antibiotics were added as described for each experiment.

RNA Purification and Northern Blotting

Culture aliquots were harvested into 1/4 vol ice-cold stop solution (95% ethanol, 5% phenol) (Bernstein et al., 2002). Subsequently RNA was purified using hot phenol and flash freezing in liquid nitrogen as in Fessler et al. (2020). Briefly: Stopped culture aliquots were centrifuged 2 min at 20,000 g and resuspended in 0.1 vol cold 0.3 M sucrose, 0.01 M NaOAc pH 4.5 followed by addition of 0.1 vol 2% SDS 0.01 M NaOAc pH 4.5. Phenol (saturated with water) was added to the liquid phase at a 1:1 ratio, the tubes were vortexed and incubated 3 min at 65°C. After freezing 15 sec in liquid N₂ and centrifugation at 20,000 g for 5 min, the water phase was transferred to new tubes and the phenol extraction was repeated. If the RNA was used in an enzymatic reaction after purification, a chloroform extraction step was included. The RNA was ethanol-precipitated, washed by 96% ethanol, air dried at room temperature and dissolved in 10 mM NaOHAc, 1 mM EDTA. For northern blots, RNA was mixed 1:1 with loading buffer (0.1 M NaOAc (pH 5.0), 8 M urea, 0.05% (w/v) bromophenol blue and 0.05% (w/v) xylene cyanol) and size-separated on denaturing 0.4 mm thick polyacrylamide gels using 1 × TBE buffer (90 mM Tris, 90 mM boric acid and 2 mM EDTA). The RNA was electroblotted onto Hybond-N membranes (GE Healthcare) (1.5 V/cm, 1.5 h) in 40 mM Tris-acetate (pH 8.1), 2 mM EDTA. After UV-crosslinking (0.12 J/cm²) the membranes were pre-hybridized (1 h, rotating at 42°C) in hybridization solution (0.9 M NaCl, 0.05 M NaH₂PO₄ (pH 7.7), 5 mM EDTA, 5 × Denhardt's solution (0.1% BSA, 0.1% Ficoll 400, 0.1% polyvinylpyrrolidone), 0.5% (w/v) SDS and 100 mg/ml sheared, denatured salmon sperm DNA). Probe hybridization was done by adding 30 pmol of oligo-DNA, 5'-end labeled with ³²P (overnight, rotating at 42°C). Subsequently, membranes were washed several times with 0.3 M NaCl, 30 mM sodium citrate, 0.1% SDS at 42°C. Radioactive signals were quantified on a PhosphorImager (Typhoon-GE Healthcare) using ImageQuant software as previously described

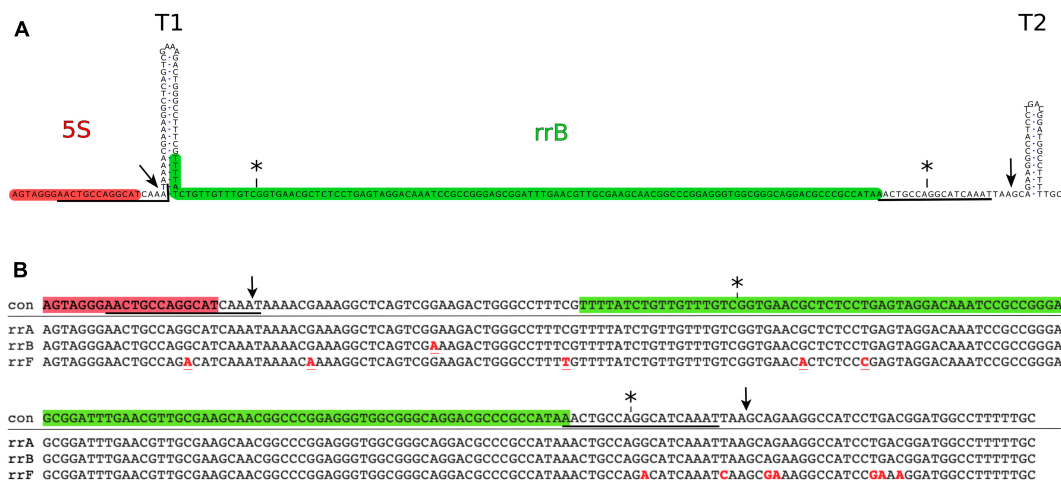


FIGURE 1 | Genomic position of the *rrB* sequence and alignment of *rrA*, *rrB*, and *rrF*. **(A)** The *rrB* sequence found in *rrmB*. The 3'-end of the mature 5S transcript (highlighted in red) is followed by two transcriptional terminators (T1 and T2). An 18 base pair sequence (underlined) overlapping the 3'-end of the 5S gene, is found twice in the sequence with a spacing of 150 bp. The predominant form of RrB found on Hfq (RrB^{short}) is highlighted in green (see also **Figures 2, 3**). The asterisks (*) above the sequence indicate the ends of the annotated version of *rrB* (Ecogene; Zhou and Rudd, 2012) and the arrows indicate the ends found by S1 mapping of the longer transcript (**Figure 3**). **(B)** Alignment of the sequences found in the 3'-end of three out of seven rRNA operons in *E. coli*: *rrnA* (*rrA*), *rrmB* (*rrB*) and *rrmD* (*rrF*). con: consensus. Symbols are as in **Figure 1A**, red font indicates sequence differences compared to the consensus sequence.

(Sørensen, 2001; Stenum et al., 2017) and in case of very low signals (e.g., **Figure 2C**) the signal found in the estimated position of a band was used. Before re-probing, membranes were stripped by washing several times with 98°C, 15 mM NaCl, 1.5 mM sodium citrate, 0.1% SDS, until no more radioactive signal could be detected by a Geiger-Müller tube. Probe sequences used in this study are listed in **Supplementary Table 4**.

Hfq Pull-Down Assay

RNAs that bind Hfq were isolated using an *E. coli* strain, where the *hfq* allele was tagged with a biotinylation sequence (Hfq_{bio}). We chose this tag as it is not positively charged, to reduce the risk that the tag might unspecifically bind negatively charged RNA. Hfq_{bio} was biotinylated by the biotin ligase BirA, and biotin's high-affinity binding to avidin was used for purifying Hfq_{bio} (Kay et al., 2009). To ensure full biotinylation of Hfq_{bio} we introduced the plasmid pBirA where *birA* is under the control of an IPTG-inducible promoter. We found that production of sufficient BirA was achieved without induction of transcription by IPTG.

Wildtype and Hfq_{bio} cells both containing the pBirA plasmid were grown exponentially in MOPS medium supplemented with; 15 µg/ml chloramphenicol, 0.2% glucose, 10 µg/ml uracil, 50 µM biotin, at 37°C for at least 10 generations. At OD₄₃₆ = 0.8 the cells were pelleted and washed in medium without biotin, re-suspended in 2 ml lysis buffer (50 mM Tris-HCl pH 7.5, 50 mM NaCl, 5% glycerol), lysed by sonication and centrifuged (20,000 g, 60 min). Total RNA was prepared from an aliquot of the cleared lysate, and the remaining lysate was transferred to fresh tubes containing 300 µl equilibrated SoftLink™ Avidin Resin (Promega) and left overnight rotating at 4°C. Then, the resin was washed four times in lysis buffer as above and RNA was harvested

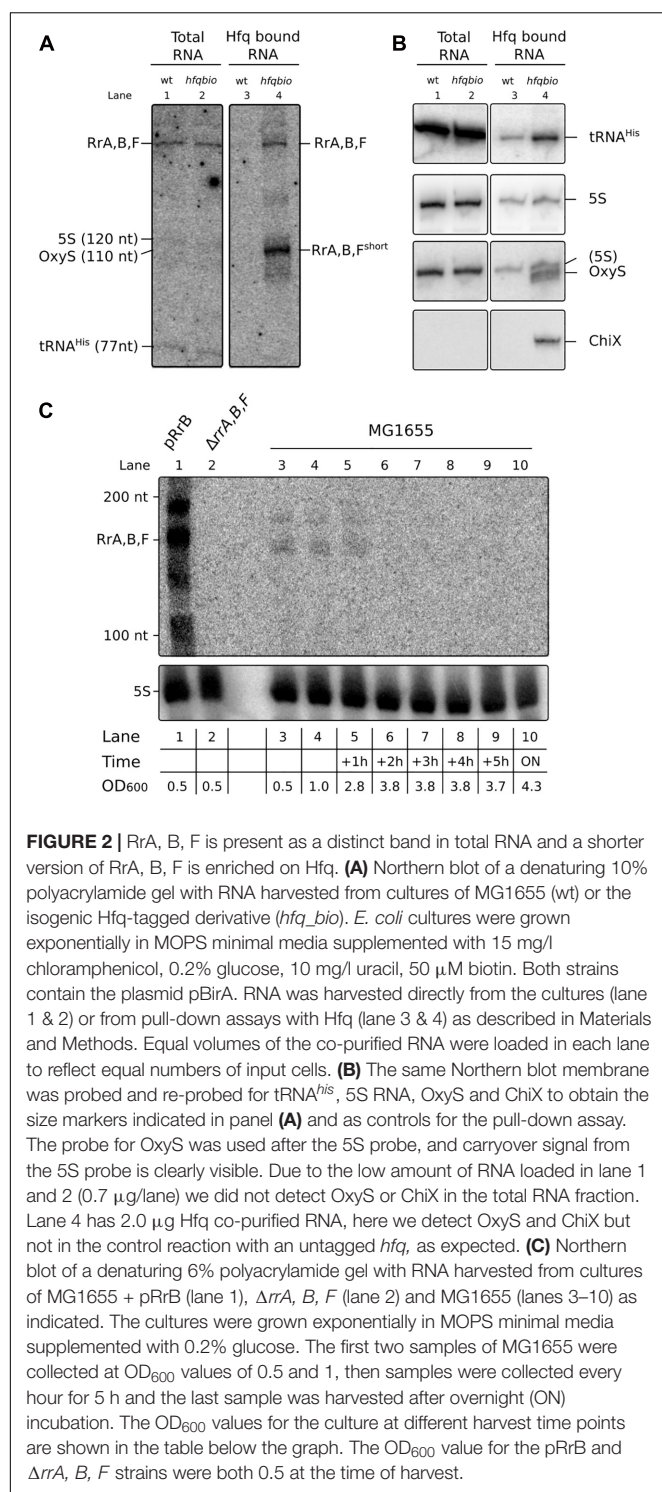
by phenol extraction and ethanol precipitation. For total RNA and the Hfq-bound RNA, RNA corresponding to 0.05 and 10% of the total culture volume respectively (approximately 2,000 ng for Hfq-bound RNA from the Hfq_{Bio} strain and 700 ng for total RNA samples), was used for analysis by northern blotting.

S1 Nuclease Mapping

Briefly, a [γ -³²P]-ATP end-labeled DNA oligo antisense to the TLR area of interest was hybridized to total RNA and single-stranded overhangs were removed by addition of S1 nuclease. The resulting fragments were visualized on a denaturing polyacrylamide gel. If the synthetic oligo extends beyond the end of the target RNA, the position of the end can be determined by the number of nucleotides removed from the DNA oligo. S1 nuclease was used to map the RrB transcript of a strain harboring the plasmid pTSS1. RNA was harvested by hot phenol 1 h after IPTG induction. One pmol of 5'-end [³²P]-labeled probe was hybridized to 30 µg of total RNA from the strain of interest. Hybridization was done in 50% formamide, 20 mM HEPES, 0.5 mM EDTA, 0.2 M NaCl, 0.05% (w/v) SDS and performed overnight in a thermocycler (68°C for 10 min, then the temperature was lowered to 54°C and decreased 1°C every 30 min until reaching 20°C). Digestion was performed by adding 300 µl 0.28 M NaCl, 50 mM NaOAc pH 4.6, 4.5 mM ZnSO₄ along with 300 U/ml S1 nuclease (Thermo Fisher Scientific) and incubating at RT for 60 min. Samples were phenol/CHCl₃ extracted, ethanol precipitated, size separated by electrophoresis on 7 M urea, 10% polyacrylamide sequencing gels and detected by autoradiography.

Circular RACE Mapping

Circular RACE was used to map the isoform of RrB enriched on Hfq. Briefly, RNA purified from the Hfq_{bio} purification



experiment was circularized using RNA ligase, reverse transcribed using random hexamer primers, PCR amplified twice using nested sets of *RrA*, *B*, *F*-specific primers, and subjected to deep sequencing. The site of circularization thus reveals both ends of the transcript. Mapping was carried out essentially as described by McGrath (2011) omitting the TAP

treatment: 500 ng of RNA co-purified with Hfq was circularized in 1 \times buffer by adding T4 RNA ligase. Reverse transcription was carried out using Super Script III RT (Thermo Fischer) and primed by random hexamer oligos. The area of interest was amplified twice by PCR with two different sets of specific primers (cRACE rrB-2 1F + cRACE rrB-2 1R and cRACE rrB-2 2F + cRACE rrB-2 2R, see **Supplementary Table 3**). The PCR-library was sequenced on an Illumina Mi-seq by 300 bp paired-end sequencing. The resulting sequences were merged and subsequently listed by abundance. All reads that could not be merged were left out of the analysis.

RNA Stability During Rifampicin Treatment

Cultures were grown exponentially at 37°C, shaking at 160 rpm for at least 10 generations in MOPS medium supplemented with 0.2% glucose and 10 μ g/ml uracil. At an OD₄₃₆ of 0.7, 3 \times 15 ml culture aliquots were collected (time 0 min) and rifampicin was added to the remaining culture to a final concentration of 100 μ g/ml. Aliquots of 15 ml were collected at 2.5, 5, 10, and 20 min post rifampicin treatment. Five percent spike-in culture overexpressing tRNA^{selC} was added to each sample aliquot as in Stenum et al. (2017). RNA was harvested using TRI-reagent (Sigma), as described by the manufacturer. The RNA was size-separated on polyacrylamide gels, northern blotted and probed as described above. RrB^{short} transcript levels were normalized to the tRNA^{selC} level for each sample.

Structure Probing

The structure of RrB was investigated *in vitro* with and without Hfq.

Reactions (10 μ l) containing 0.1 pmol of 5'-end [γ -³²P] ATP-labeled transcript and 50 nM unlabeled *E. coli* tRNA were incubated with different concentrations of hexameric Hfq (Hfq₆) (3, 1.5, and 0 μ M) at 37°C for 100 min along with the relevant cleavage buffer. For Pb²⁺ cleavage: 1 \times Structural Probing Buffer (Ambion AM2237), Pb²⁺ was added to a final concentration of 10 mM and samples incubated 1 min at 37°C. Control (C1) was without Hfq and Pb²⁺. RNaseIII cleavage: 1 \times Short Cut MnCl₂ buffer (New England Biolabs) and 0.002 units Short Cut RNaseIII (New England Biolabs), samples were incubated 20 min at 37°C. Control (C2) was without Hfq and RNaseIII. Control T1: 1 \times Structural Probing Buffer (Ambion AM2237), sample was incubated at 95°C for 1 min, transferred to 37°C for 1 min. After addition of 0.05 U RNase T1 (Ambion AM2237) the sample was incubated at 37°C for 5 min. OH ladder: 1 \times Alkaline Hydrolysis Buffer (Ambion AM2237), sample was incubated at 95°C for 5 min. All samples were cooled by addition of 200 μ l ice-cold H₂O and transferred to ice. The digested RNA was phenol extracted, ethanol precipitated, resuspended in 1 \times loading buffer II (Ambion AM2237), and separated on an 8% polyacrylamide/urea/TBE gel. Radioactive signal from the dried gel was visualized on a PhosphorImager (Typhoon -GE Healthcare). Hfq protein used for all *in vitro* experiments was a kind gift from Anders Boysen.

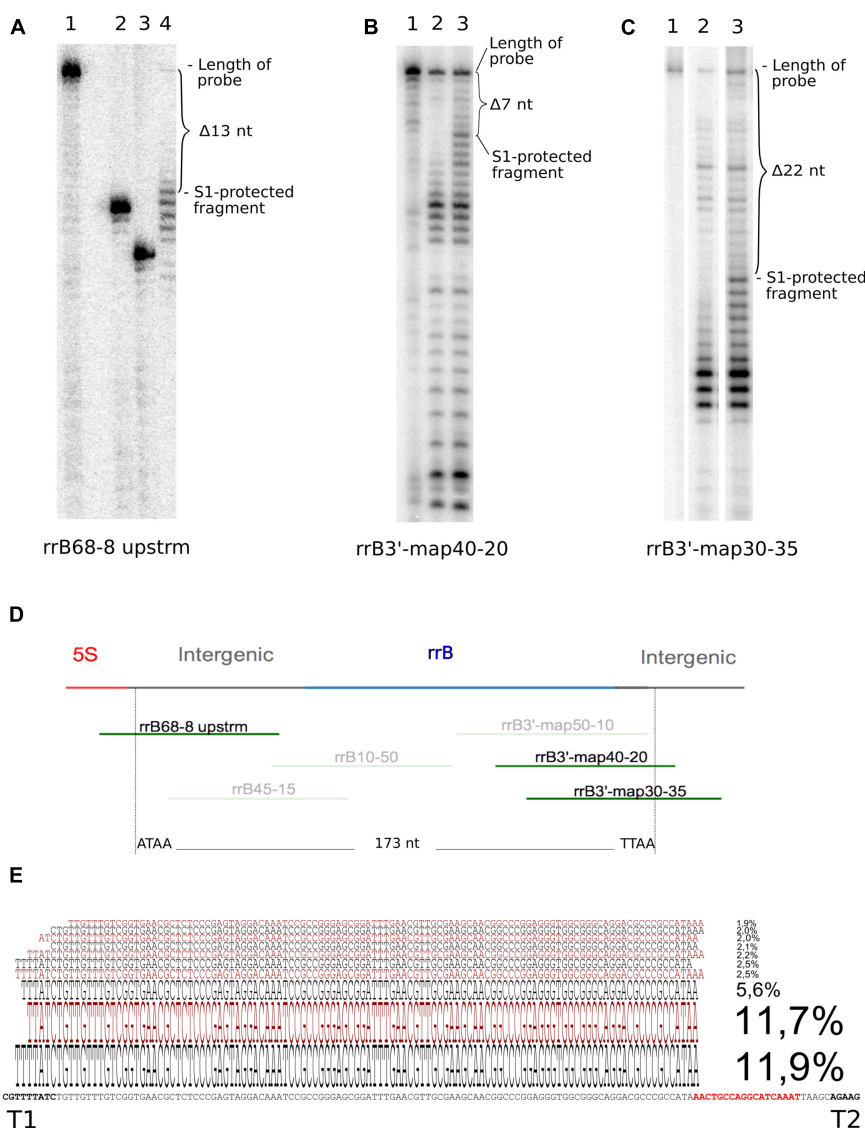


FIGURE 3 | Determination of 5' and 3' ends of RrB by S1 nuclease analysis and of RrB^{short} by circular RACE. In the S1 nuclease mapping analysis (**A–C**) the ³²P-labeled probe DNA was visualized by autoradiography of 10% poly-acrylamide sequencing gels. (**A**) mapping of the 5'-end using probe rrB68-8upstrm [shown in panel (**D**)] and total RNA from an IPTG-induced culture of MG1655 + pRrB over-expressing truncated '*rrfB* and *rrB*'. The S1-protected fragment (lane 4) is 13 nt shorter than the untreated probe (lane 1). The exact number of nucleotides removed was determined by loading two labeled oligos as size markers [lane 2 (rrB54-8 upstrm) and 3 (rrB50-8 upstrm), probe rrB68- 8upstrm truncated by 14 and 18 nt respectively]. (**B**) probe rrB3'-map40-20 was hybridized to total RNA from an IPTG-induced culture of $\Delta 22$ TLR + pRrB-RrB over-expressing *rrfB* and *rrB*. The S1 protected band was shortened by 7 nt (lane 3) compared to the untreated probe (lane 1). Lane 2 shows a similar experiment using total RNA from the strain $\Delta 22$ TLR harboring empty vector (pJFR1). (**C**) Probe rrB3'-map30-35 was hybridized to total RNA from MG1655 + pRrB-RrB over-expressing *rrfB* and *rrB*. The S1 protected band was shortened by 22 nt (lane 3) compared to the untreated probe (lane 1). Lane 2 shows a similar experiment using total RNA from the strain $\Delta 22$ TLR harboring empty plasmid. (**D**) Map of the probes used for the experiments shown in panels (**A–C**). Top line represents the genomic map; *rrfB* (5S) is shown in red, the intergenic sequences in gray and the annotated version of *rrB* in blue. Probe sequences are presented as green lines and probes shown in transparent colors were also used for mapping but detected no ends. The vertical broken lines denote the two ends detected in this study. (**E**) Circular RACE mapping of the RrB sequences that co-precipitated with Hfq. The ten most abundant RrB^{short} sequences detected by circular RACE and deep sequencing are aligned to the genomic sequence. The size of the characters correlates with their relative abundance, which is also stated as a percentage of total merged reads ($n = 4722$). Bold characters highlight the two terminators T1 and T2 and the direct repeat, which is also found at the 3'-end of the mature 5S RNA is highlighted in red (see Figure 1).

MS2 Affinity Purification, RNA-Seq and MS-MS

Affinity purification of MS2-tagged RNAs was done either with *in vivo* expressed RNA or *in vitro* transcripts that were added

to the cell lysate. The 115 bp RrB^{short} sequence, mapped as the most abundant variant pulled down with Hfq (**Figure 3**) was cloned into the plasmid pNS21 using PCR amplifying RrB^{short} with either *NheI* or *XbaI* restriction sites on the ends.

Purified PCR fragments were restriction digested with either *NheI* or *XbaI* and ligated into the pNS21 plasmid cut with the corresponding restriction enzyme, resulting in RrB^{short} 3'-fused to MS2 (*NheI* digestion) or RrB^{short} 5'-fused to MS2 (*XbaI* digestion), respectively. The transcripts from the resulting plasmids are terminated by the *rra* terminator originally found in *Vibrio* species. Transcription from the plasmids is under control of the P_{LacO-1} promoter. As the strains used for affinity purification harbor only the chromosomal copy of *lacI*, expression from these plasmids should be constitutive. This was verified by northern blotting (Supplementary Figure 4). Cell lysates of the strain *hfq*-FLAG (JVS814) harboring the different MS2-aptamer expressing plasmids, were prepared by growing cells in LB with 100 µg/ml ampicillin, to an OD₆₀₀ of 1.0. Cell pellets corresponding to 50 OD₆₀₀ units were resuspended in 800 µl of buffer A (20 mM Tris-HCl pH 8.0, 150 mM KCl, 1 mM MgCl₂, 1 mM DTT) and lysed by addition of glass beads (0.1 mm), flash freezing in liquid N₂ and shaking at 30 Hz for 10 min. Lysates were cleared by centrifugation (30 min 16,000 g, 4°C). Lysates corresponding to 2 and 0.5 OD₆₀₀ units of cell culture were used to prepare RNA and protein, respectively. Before addition of lysate, the affinity chromatography columns (Bio-Spin #732-6008, Bio-Rad) were prepared by adding 100 µl amylose resin (New England Biolabs, #E8021S), washing three times with 2 ml buffer A and subsequently adding 200 pmol of MS2-MBP recombinant protein (a gift from the Jörg Vogel group). All steps of the affinity chromatography were done at 4°C. Following addition of the lysate, the columns were washed four times with 2 ml buffer A, and the RNA-protein complexes were eluted with 900 µl buffer A containing 12 mM maltose. RNA was purified using phenol-chloroform, followed by ethanol precipitation with the addition of 1 µl GlycoBlue (ThermoFisher). Protein was harvested from the organic phase by acetone precipitation. RNA was subjected to next generation sequencing on the Illumina platform at the University of Würzburg. Proteins were detected and quantified by mass spec at the mass spec facility at University of Würzburg, see Supplementary Methods.

Input Into Invenire CsrB/C Family RNA Prediction Algorithm

The web version of Invenire sRNA found at <http://markov.math.umb.edu/inveniresrna/> was used for the analysis. The dataset included the 85 sRNAs, 22 TLR sequences, and 2217 intergenic regions (<1,000 bp) annotated in the Ecogene database¹ on November 24, 2017. In addition, 578 sequence peaks identified experimentally as CsrA binding sites by CLIP-seq (Potts et al., 2017) were included in the analysis.

In vitro Transcription and Electrophoretic Mobility Shift Assay

Binding of RNAs to CsrA was examined using electrophoretic mobility shift assay (EMSA) with recombinant CsrA-3xFLAG (Supplementary Tables 1, 2) and *in vitro* transcribed RNA. DNA templates for *in vitro* transcription were made by PCR using

pRrB, pRrB-3GGA and pCsrB (see Supplementary Tables 1, 2) as template for RrB, RrB-3GGA and CsrB, respectively. All primers used in the study are listed in Supplementary Table 3. Transcription was performed overnight at room temperature using the MEGAscript T7 transcription kit (ThermoFisher). The resulting RNA was treated with TurboDNase (ThermoFisher) (0.1 unit/µl, 30 min at 37°C), gel-purified from denaturing polyacrylamide gels, dephosphorylated using calf intestinal alkaline phosphatase (30 min at 37°C) and 5' radiolabeled using T4 polynucleotide kinase and [γ -³²P] ATP. After each step the RNA was phenol extracted once, chloroform extracted twice and ethanol precipitated. Binding reactions contained 100 mM KCl, 10 mM MgCl₂, 2 mM DTT, 7.5% glycerol, 0.1 U SUPERase-IN RNase inhibitor (ThermoFisher), 2 ng total yeast RNA, 120 pM labeled RNA and 0–1,600 nM CsrA-3xFLAG in a 10 µl reaction. Samples were incubated 10 min at 37°C and separated on 8% native polyacrylamide gels using 1x TBE as buffer. Radioactive signals were detected on a PhosphorImager (Typhoon -GE Healthcare). The CsrA-3xFLAG was purified from the strain CsrA-3xFLAG carrying the plasmid pBAD-RBS-csrA:3xFLAG as described by Jorgensen et al. (2013).

Construction of Deletion Mutants

For λ Red recombineering, we used a MAS1081-derivative strain (MAS1080) harboring the λ RED prophage [λ cI₈₅₇ Δ (cro-bioA)] imported from strain HME68 (Sawitzke et al., 2007) by P1 transduction. Deletion mutations were constructed in this strain as described (Sawitzke et al., 2007). For each deletion, a *cat-sacB* cassette was first inserted at the desired genomic region by selecting for chloramphenicol resistance and confirming by PCR. The cassette was then replaced by a DNA fragment designed to yield deletion of 107 bp, 103 bp and 103 bp for *rrnA*, *rrnB* and *rrnD*, respectively, by counter-selection of the cassette by sucrose tolerance and confirmation by PCR and DNA sequencing. The deletions roughly match the annotated TLR sequences, including all GGA motifs found in RrA, B, F. For reasons outside the scope of this study, the DNA fragments were constructed so that the TLR sequence was replaced with a tRNA gene in two out of the three deletion sites (see Supplementary Table 1).

To obtain an *E. coli* mutant where the λ Red recombination enzymes had not been expressed, and thereby reduce the risk of undesired genome mutations, each mutated locus was then moved to an otherwise wildtype strain by P1 transduction first of each *cat-sacB* cassette and next of the locus carrying a deletion. P1 transduction was done as described by Miller (1972).

Biofilm Measurements

Biofilm was measured in microtiter plates using peg-lids (Nunc-TSP, cat. no. 445497) and crystal violet staining. Cultures were grown in 96-well flat-bottom microtiter plates. Ten microliter outgrown culture was used to inoculate each well containing 150 µl YT media (per liter: 8 g tryptone, 5 g yeast extract and 5 g NaCl) supplemented with 100 µl/ml ampicillin and 1 mM IPTG for strains carrying plasmids. The outer-most wells on the plates were not used, as the results from these were found to fluctuate more than average. Plates were incubated at 37°C for 48 h (no

¹ www.ecogene.org

shaking) to ensure all cultures were completely outgrown. After incubation the pegs were washed once in wash buffer (25 mM Tris pH 7.5, 100 mM NaCl) and placed in 0.01% crystal violet for 15 min. Then, the pegs were washed three times in wash buffer and transferred to a fresh microtiter plate containing 180 μ l 96% ethanol in each well. When the crystal violet was completely dissolved, the A_{590} of each well was measured along with the OD_{600} of each well of the growth plate. The optical densities from the growth plate were used to normalize the absorbance signals from the stained biofilm.

Motility Measurements

Mobility was measured on soft agar plates. One microliter outgrown culture was used to inoculate each plate by injection of 1 μ l culture halfway into the agar in the center of the plate. Plates contained YT media (per liter: 8 g tryptone, 5 g yeast extract and 5 g NaCl) + 0.3% agar, and were supplemented with 100 μ l/ml ampicillin and 1 mM IPTG for strains carrying plasmids. The plates were incubated approx. 16 h at 37°C before the spread of the bacteria was measured. Measurements were repeated several times with approximately 2 h in between to compensate for differences in the growth rates of different strains.

Translational Reporters

The *glgC-gfp* in-frame fusion was constructed by replacing the *NsiI-NheI* fragment of pXG10-SF (Supplementary Table 2) with the 5'UTR and first 30 nucleotides of the *glgC* coding sequence by restriction digestion and ligation. The *pgaA-lacZ* in-frame fusion was made by cloning the promoter of *lacI* along with a *NheI* restriction site into pGH253-kan (Supplementary Table 2) by replacing the *EcoRI-BamHI* fragment. Subsequently, the 5'UTR and first 30 nucleotides of the *pgaA* coding sequence was inserted using *BamHI-NheI* digestion. All primers used in the study are listed in Supplementary Table 3.

Beta-Galactosidase Measurement

Beta-Galactosidase (β -gal) activity was measured from overnight cultures harboring the translational fusion *pgaA-lacZ*, grown in test tubes in YT media (per liter: 8 g tryptone, 5 g yeast extract and 5 g NaCl) supplemented with 15 μ g/ml kanamycin. The β -gal activity was measured using the fluorescent substrate 4-methylumbelliferone *b*-D-galactopyranoside (MUG), as described (Li et al., 2018). OD_{600} of the cultures was measured and used to normalize the corresponding β -gal values.

GFP Measurements

Fluorescence of GFP was measured from strains harboring the *glgC-gfp* translational fusion. Cultures were grown in MOPS minimal media supplemented with 0.2% glucose, 15 μ g/ml chloramphenicol and 100 μ g/ml ampicillin when needed, at 37°C shaking at 300 rpm in 96-well black microtiter plates with clear, flat bottoms (Costar) in a plate reader (Synergy H1, Biotek). OD_{600} and GFP fluorescence (excitation 470 nm and emission 510 nm) was measured simultaneously every 10 min. The values for GFP were normalized to the corresponding values for OD_{600} . The normalized data was plotted against time and the area under

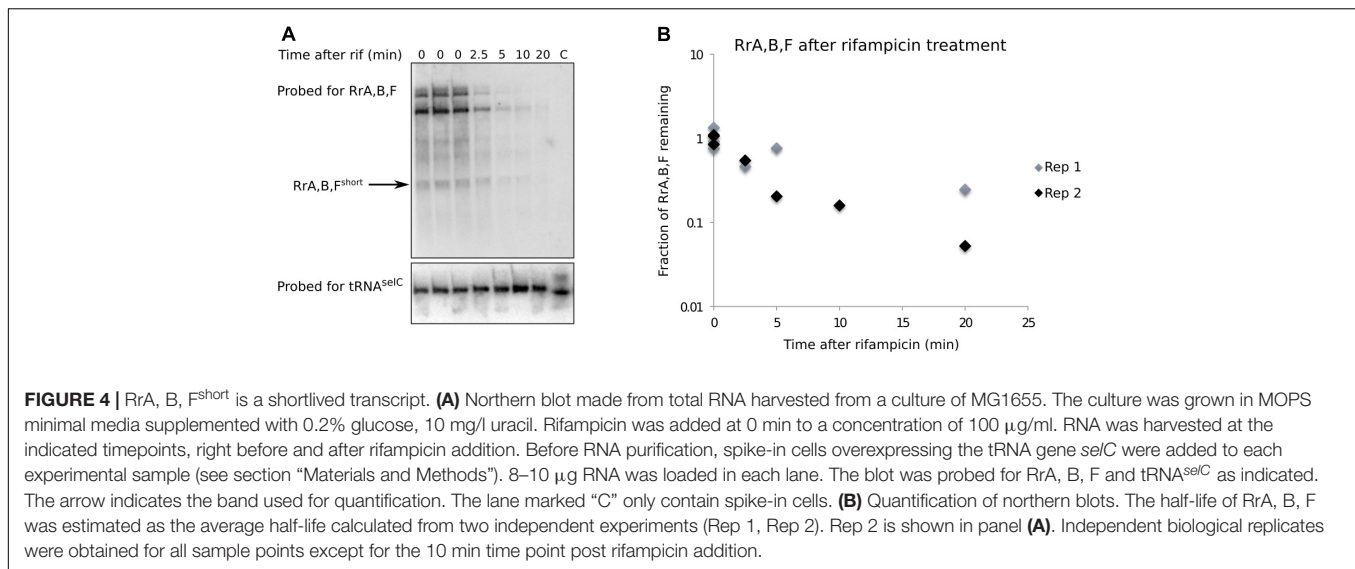
the curve was calculated as a measure of relative GFP expression. The same amount of data points were used for each strain and only data where cultures were growing exponentially was used in the analysis.

RESULTS

Expression of RrA, B, F and Interaction With Hfq

Three out of seven ribosomal RNA (rRNA) operons from *E. coli* contain a sequence from the TLR-family downstream from the 5S gene (Supplementary Figure 1). These three sequences, named *rrA*, *rrB* and *rrF* respectively, are very similar in sequence (Figure 1). Furthermore, their location downstream of 5S, and their sequence, is highly conserved in many species of the Enterobacteriales, suggesting a specific role for these sequences and structures (Supplementary Figure 2).

We hypothesized that the sequences may function as sRNAs. To begin testing this hypothesis we first examined whether RNA molecules of defined sizes could be detected after processing of the primary *rrn* transcripts. Total RNA harvested from exponentially growing *E. coli* K-12 cultures was subjected to northern blot analysis. To detect RrA, RrB and RrF, here collectively referred to as RrA, B, F, we used a single probe, which is expected to detect all three sequences since they only differ at a few positions. As shown in Figure 2A (lane 1 and 2), a distinct band of 150–200 nt was observed, confirming that RrA, B, F can be detected after processing of the primary transcript. The size of the RrA, B, F RNA was estimated based on re-probing of the membrane for transcripts of known sizes (Figures 2A,B) and comparison to an RNA ladder (Figure 2C). Next, we asked whether the RrA, B, F RNAs interact with the RNA chaperone Hfq, like many well-characterized *E. coli* sRNAs (Bilusic et al., 2014). To enable pull-down of Hfq and analysis of co-purified RNAs, a biotinylation sequence (Beckett et al., 2008) was inserted in the chromosomal *hfq* gene. The C-terminally tagged Hfq protein (Hfq_{bio}) is functional, as shown by intact repression of an mRNA target by an Hfq-dependent sRNA in the tagged strain (Supplementary Figure 3). After affinity purification of Hfq_{bio} using a streptavidin resin, co-precipitated RNA was analyzed by northern blot analysis. Detection of the known Hfq-binding sRNAs OxyS and ChiX only in the co-precipitated RNA verified that Hfq-binding RNAs had been enriched in the Hfq pull-down assay (Figure 2B). Interestingly, the pull-down revealed that a shorter form of RrA, B, F (RrA, B, F^{short}) was highly enriched on Hfq in addition to the band detected in total RNA (Figure 2A, lane 4). Further, to verify the identity of the bands on our northern blots found by the RrA, B, F, probe, we made a blot containing RNA from a strain overexpressing RrB from pRrB, a strain deleted for *rrA*, *B*, *F*, and several samples from the wildtype strain harvested at different stages of growth (Figure 2C). The blot verifies the identity of the bands and shows that RrA, B, F are only detected during exponential growth, where the rRNA operons are actively transcribed. During stationary phase, the transcriptional activity of rRNA operons is absent or very low (Baracchini and Bremer, 1991) but the 5S, 16S and 23S RNAs



are stable molecules. Therefore the 5S rRNA detected during stationary phase in **Figure 2C** was transcribed during growth and serves as a qualitative loading control.

The ends of the longer RNA species were mapped using S1 nuclease protection assay (Berk and Sharp, 1977). As this assay was not sensitive enough to detect chromosomally expressed RrA, B, F, we used a strain overexpressing the 5S gene *rrfB* along with *rrB* from a plasmid. The S1 protected fragments are displayed in **Figures 3A–C**. Several bands spaced with one nucleotide intervals are seen, which is a common observation when using S1 nuclease transcript mapping (Green and Roeder, 1980; Aiba et al., 1981; Brosius et al., 1982) and is probably due to “end-nibbling” (Shenk et al., 1975). Thus, we define the transcript ends based on the longest protected bands. For the 5′ end the probe was shortened by 13 nt (**Figure 3A**). For the 3′ end the two different probes were shortened by 7 nt (**Figure 3B**) and 22 nt (**Figure 3C**), respectively. They both predict the same end. The 5′ end of RrB was detected 3 nt downstream of the mature 3′ end of the 5S transcript (see **Figures 1, 3A**). This site has been described as the initial RNase E processing site of the pre-5S RNA (Roy et al., 1983; Li and Deutscher, 1995) suggesting that the 5′ end of RrB is generated by RNase E cleavage. The 3′ end of RrB was detected 13 nt downstream of its annotated 3′ end (**Figure 1**). This 3′ end was verified using two different probes (**Figures 3B,C**). These results predict that the most abundant RrA, B, F transcript in total RNA has a length of 173 nt, which is in good agreement with the northern blots shown in **Figures 2A,C**. We also carried out S1 analysis with probes antisense to the area between the two observed ends to detect any alternative transcript ends, but could not detect any (data not shown, the probes are shown in **Figure 3D**).

To determine the ends of the Hfq-enriched shorter version of RrA, B, F (RrA, B, F^{short}) we used the circular RACE method (McGrath, 2011), coupled with next generation sequencing. As this method is PCR-based it requires substantially less input RNA than the S1 nuclease assay. Circular RACE yielded a variety of sequences mapping to *rrA*, *B*, *F*, of which the ten most

abundant are shown in **Figure 3E**. The most abundant reads predict the Hfq-associated RrA, B, F^{short} transcript to be 113–115 nt in length. This is in accordance with our observations from northern blots (**Figure 2**).

To detect the RrA, B, F^{short} fragment in the total RNA fraction, we carried out another northern blot analysis using substantially more total RNA per lane than the one presented in **Figure 2A**. This blot showed three different species of the RrA, B, F RNA (**Figure 4A**): the 115 nt RrA, B, F^{short} , the 173 nt fragment, and a longer version. We suspect that the longer version represents a processing intermediate that includes the T2 terminator sequence. Thus, the RrA, B, F^{short} is not uniquely seen in the RNA fraction co-precipitating with Hfq but can also be detected in the total RNA fraction.

A short half-life of the RrA, B, F RNA could explain its low abundance relative to the rRNA transcripts expressed from the same operons and the absence of signal from stationary phase cells (**Figure 2C**). We measured the half-life of RrA, B, F^{short} by monitoring the levels of RrA, B, F^{short} upon transcription initiation blocking by addition of rifampicin to a culture in balanced growth (**Figure 4**). Indeed, we found that the half-life of RrA, B, F^{short} was ~2.5 min, which is very short relative to the rRNA transcripts that are stable on the time scale of hours during exponential growth (Piir et al., 2011).

Taken together, we conclude that the RrA, B, F RNAs can be detected in exponentially growing cells as at least two transcripts of ~173 and ~115 nt that appear to interact with Hfq and that the shorter variant RrA, B, F^{short} has a half-life of about 2–3 min. The presence of RrA, B, F is therefore dependent on active rRNA transcription.

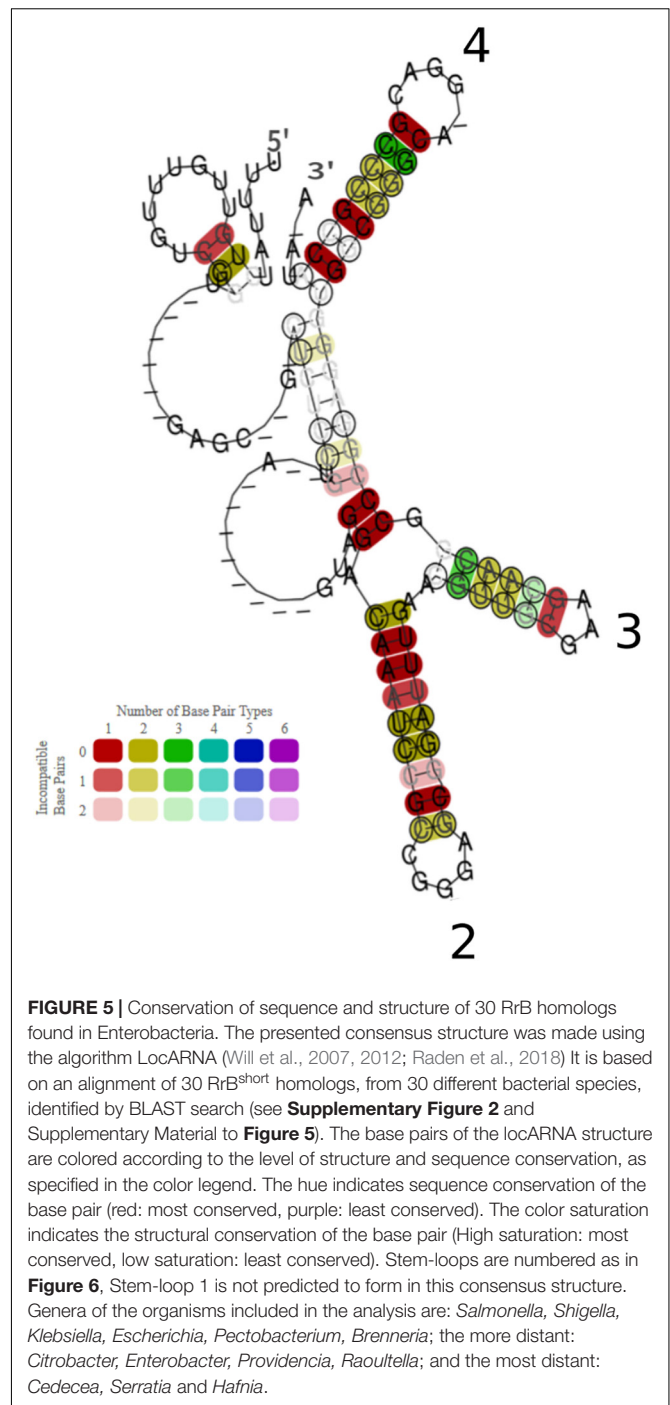
The Structure of RrA, B, F Is Conserved Within the Order of Enterobacteriales

In order to assess the conservation of RrA, B, F between species we did a BLAST search² with *rrB* and the sequences

²<https://blast.ncbi.nlm.nih.gov/Blast.cgi>

surrounding the locus as input (see **Supplementary Figure 2** and **Supplementary Material**). Both the sequence and the location of the *rrB* downstream of the gene encoding 5S was found to be conserved in at least 31 species from 12 genera, all belonging to the order of Enterobacteriales (**Supplementary Figure 2**). To evaluate the structural conservation of the RrA, B, F homologs we used the locARNA algorithm (Will et al., 2007, 2012; Raden et al., 2018) to predict a consensus structure (**Figure 5**). The consensus structure shows a high degree of structural conservation, particularly in the three stem loop structures named 2-4 in the figure, which could indicate a conserved function of the RNA.

We speculated that the enrichment of RrA, B, F^{short} in RNA that had co-precipitated with Hfq could be due to a role for Hfq in chaperoning the correct folding of RrA, B, F, as shown for other RNAs (Geissmann and Touati, 2004; Soper and Woodson, 2008; Bordeau and Felden, 2014; Hoekzema et al., 2019). In this case, we would expect to see differences in the RrA, B, F^{short} structure with and without Hfq. To experimentally investigate the structure of the 115 nt RrB^{short} RNA, we performed RNA structure probing in the presence or absence of Hfq (**Figure 6**). As shown in **Figure 1B**, RrA^{short} and RrB^{short} are identical in sequence, and differ by only two nucleotides from RrF^{short}. We therefore expect RrA, B, F^{short} to serve identical functions, and arbitrarily chose the 115 nt long RrB^{short} from the *rrnB* operon for these experiments. An *in vitro* transcript of the RNA was incubated with increasing concentrations of Hfq, followed by exposure to the RNA cleavage agent Pb²⁺ that primarily hydrolyzes single-stranded RNA (Ciesiolka et al., 1998), or the endoribonuclease RNase III that predominantly hydrolyzes double-stranded RNA with a strong preference for helices of sufficient length (Robertson, 1990). Fragmented RNA was size-separated on a polyacrylamide gel and visualized by autoradiography (**Figure 6A**). In general, only subtle changes in the fragment pattern were observed upon Hfq addition (**Figure 6A**). The most notable Hfq-induced change was found in the Pb²⁺-treated samples at the apparent single-stranded region at nt 63-64, 66-68. This sequence displayed reduced hydrolysis by Pb²⁺ in the presence of Hfq (**Figure 6A**). In contrast, nt 53-56 showed slightly enhanced Pb²⁺ cleavage, upon addition of Hfq. Finally, nt 48-50 displayed slightly enhanced RNase III cleavage after incubation with Hfq (**Figure 6A**). The change in cleavage pattern observed at nt 63-68 as a consequence of Hfq addition could be interpreted as direct binding of Hfq in the area, leading to protection from Pb²⁺-induced cleavage. Alternatively, the main outcome of interaction with Hfq may be a structural rearrangement that allows the region around nt 63-68 to engage in intramolecular base-pairing. The structure probing data do not allow us to distinguish between these two potential effects of Hfq. To pursue the hypothesis that Hfq may facilitate a structural rearrangement of the region, we used the algorithm Mfold (Zuker, 2003)³ to predict the most thermodynamically favorable RrB^{short} structure with (**Figure 6B**) and without (**Figure 6C**) the constraint of a single-stranded region from nt 63-68 (open red triangles). The predicted structure



for RrB^{short} in the absence of the constraint (**Figure 6C**) forms stem loop #2 predicted by the consensus structure (**Figure 5**), whereas the predicted structure given the structural constraint of a single-stranded region from nt 63-68, does not (**Figure 6B**). The structure shown in **Figure 6B** is not the energetically most favorable one. This leads us to suggest that Hfq could be involved in folding of the RrA, B, F in order for the RNA to attain its most thermodynamically favorable structure, namely that shown

³<http://unafold.rna.albany.edu/?q=mfold>

in **Figure 6C**, which shows the consensus stem-loop structure (stem loop #2) predicted by locARNA.

RrB Binds to CsrA *in vitro*

In order to identify potential interaction partners of RrA, B, F besides Hfq, we used MS2 affinity purification coupled with either mass spectrometry or RNA sequencing (Said et al., 2009; Corcoran et al., 2012; Lalaoua et al., 2015). Here, an RNA of interest is expressed as a fusion with an MS2-aptamer sequence, to allow purification of *in vivo* formed RNA-RNA or RNA-protein complexes using immobilized MS2 protein (Bardwell and Wickens, 1990; Said et al., 2009). We constructed plasmid-borne versions of RrB^{short}, MS2-tagged at either the 5'-end or the 3'-end and affinity-purified the RNAs. Expression and purification of the tagged RNAs was verified by northern blotting (**Supplementary Figure 4**). RNAs co-purifying with RrB^{short} were identified by deep RNA sequencing (RNA-seq) and co-purifying proteins were

identified by mass spectrometry. The results were compared to results for affinity purification of the MS2 RNA alone. While no specific enrichment was reproducibly detected in the RNA-seq analysis (data not shown), several proteins were specifically enriched in pull-downs with MS2-tagged RrB^{short}, the most strongly enriched protein being the RNA-binding post-transcriptional regulator CsrA (**Table 1**). Somewhat surprising, Hfq was not found among the enriched proteins. We verified that RrB^{short} binds Hfq *in vitro* by electrophoretic mobility shift assay (EMSA). The EMSA analysis showed that RrB^{short} bound Hfq *in vitro* but with substantially lower affinity than the established Hfq-binding sRNA OxyS (**Supplementary Figure 5**). We will return to this point in section "Discussion."

The canonical CsrA binding motif identified both in *S. typhimurium* (Holmqvist et al., 2016) and *E. coli* (Dubey et al., 2005; Potts et al., 2017) contains a GGA sequence located in the loop of a stem-loop structure. Interestingly, the RrA, B, F^{short} sequences have five GGA sequences, two of which are predicted to be located in the loops of stem-loop structures by the mfold and LocaRNA structure prediction algorithms (**Figures 5, 6**). Intriguingly, the structure probing experiments shown in **Figure 6A** suggest that the potential CsrA binding motif in loop 2 is only formed after interaction with Hfq.

The machine-learning-based algorithm InvenireSRNA (Fakhry et al., 2017) is designed to predict sRNAs of the CsrB/C family. To gauge how RrA, B, F rank in this algorithm compared to other *E. coli* non-coding RNAs, we provided the algorithm with a total of 2902 sequences, including all annotated *E. coli* sRNA sequences, the 22 TLR sequences, all sequences identified as CsrA-binding peaks from CLIP-seq data (Potts et al., 2017),

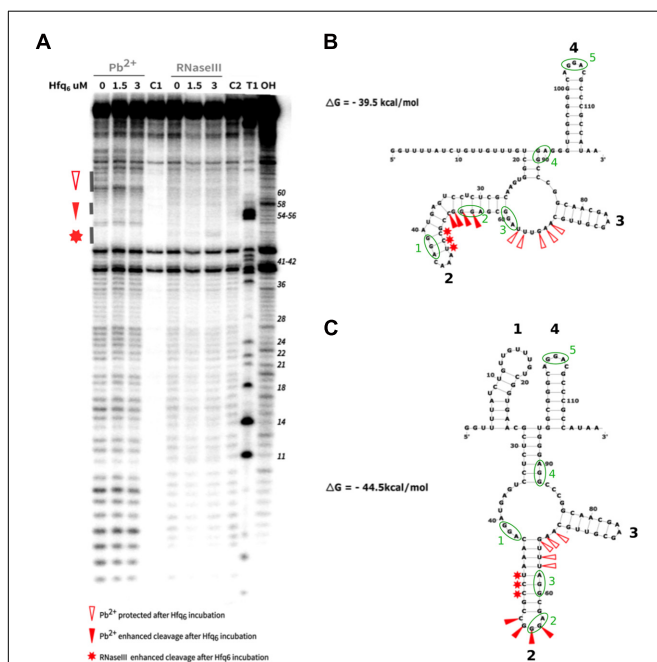


FIGURE 6 | Structure probing of RrB^{short} with and without Hfq. The RrB^{short} *in vitro* transcript was incubated with 0, 1.5, or 3 μM of Hfq₆ before addition of the cleavage agent. The partly digested RNA was size-separated on a denaturing 8% polyacrylamide gel. An autoradiogram of the gel is shown in panel (A). C1 indicates the transcript in Pb²⁺-buffer without addition of Pb²⁺, C2 indicates the transcript in RNase III-buffer without addition of RNase III. T1 indicates the heated transcript treated with RNase T1 and OH indicates the transcript heated in alkaline buffer. Gray bars on the left side of the gel mark areas of Pb²⁺ protection, Pb²⁺ enhancement and RNase III enhancement. The nucleotide number with respect to the 5' end is indicated at the right side of the gel. Intense bands at position 39 and 43 in all lanes can probably be attributed to background hydrolysis of the purified transcript before the analysis since they are abundant in all lanes. The structure of RrB^{short} was predicted by mfold with the constraint of a single-stranded region at nt 63-68 (B) or without any constraints (C). The predicted free energies of the structures are indicated. Triangles and stars mark Hfq-dependent structural changes as indicated. GGA sequence motifs are marked by green ellipses; see section "RrB binds to CsrA *in vitro*."

TABLE 1 | Proteins identified by MS2-affinity purification to co-purify with RrB^{short}.

Protein	MS2-RrB		RrB-MS2		Average
	#1	#2	#1	#2	
csrA	8,68	6,83	5,80	3,55	6,22
gapA	1,04	1,88	6,03	3,49	3,11
rluC	4,75	3,75	1,28	1,98	2,94
rpsM	3,81	2,60	4,75	0,13	2,82
rpsS	6,40	2,71	1,40		2,63
sucA	2,79	1,85	2,62	2,33	2,40
deaD	-0,05	5,04		3,85	2,21
rpsA	3,90	4,14			2,01
gpmA			7,72		1,93
dnaK	1,01		2,84	3,56	1,85
hfq	-1,81	-2,29	-7,24	-4,91	-4,06

RrB^{short} was tagged with the MS2 sequence at either the 5'-end (MS2-RrB) or the 3'-end (RrB-MS2). The co-purifying proteins were identified and quantified by mass spec. The table presents the ten proteins most highly enriched on average, in these pull downs compared to pull downs using the MS2 transcript alone. The data for Hfq is also included. The numbers in the table represent the log2-transformed ratio of intensities between the sample and the MS2 transcript alone, after normalization to the total number of fragments analyzed in each sample. Color tones represent the degree of co-purification: red color (positive values) indicates relative more peptides co-purifying with RrB compared to the MS2 transcript alone, whereas blue color (negative values) indicates less co-purification.

and finally all intergenic regions of *E. coli* shorter than 1,000 bp. The results show that CsrB and CsrC both score high as expected (Table 2), while McaS and GadY both have low probability scores, suggesting that the features that make the latter acceptable binding partners for CsrA are not picked up by the algorithm. In accordance with the MS2-purification and structure prediction, RrA^{short}, RrB^{short} and RrF^{short} are predicted to bind CsrA with high probability and, remarkably, rank among the 16 highest scoring sequences in the analysis (Table 2). Notably, the remaining 19 members of the TLR family located in tRNA operons all obtained a probability score of <0.01, suggesting RrA, B, F are unique among the TLR family in their affinity for CsrA.

To further validate the binding between RrB^{short} and CsrA we conducted EMSAs. *In vitro* transcribed RrB^{short} was incubated with increasing amounts of purified CsrA-3xFLAG and separated on non-denaturing gels. As seen in Figure 7A, an RrB^{short}-CsrA complex is observed from a concentration of 50 nM CsrA, and a complete shift is seen at 100–200 nM CsrA. At higher concentrations of CsrA, several complexes with higher molecular weights are visible. The number of different band sizes suggests that RrB^{short} has multiple binding sites for CsrA, which is expected based on our RNA structure predictions (Figures 5, 6). The binding relationship between CsrA and RrB^{short} is therefore complex but a first approximation of an overall K_D from our

data in Figure 7A is around 100 nM. We repeated the binding experiment using a mutant version of RrB^{short}, where three GGA sequences have been changed to “UUU” (number 1, 2 and 5 on Figure 6C), which includes the two motifs found in loops of stem structures. By only mutating the three GGA motifs found in single stranded regions, we do not expect this to have any consequences for the secondary structure of the RNA. The affinity for CsrA is clearly lower for this mutant compared to the wildtype RrB^{short} as the mutant does not show any shift within the tested range of CsrA concentrations. Note that part of the RNA is degraded at the highest CsrA concentration. We attribute this to residual activity of the RNase that was added during CsrA purification, see materials and methods. To further probe the specificity of RrB^{short} to CsrA we did competition binding experiments where a preformed CsrA-RrB^{short} complex (CsrA at 200 nM, RrB^{short} at 120 pM) was challenged with increasing concentrations of the unlabeled competitors RrB^{short}, RrB^{short}-3GGA and CsrB (Figure 7B). CsrB is believed to have ~18 CsrA binding sites (Liu et al., 1997), a K_D around 1 nM of binding to CsrA (Weilbacher et al., 2003) and thus we expect it to be a more efficient competitor than RrB^{short}. This is indeed what we observe, CsrB fully competes off the labeled RrB^{short} at a concentration of 3.13 nM, whereas a concentration of 50 nM is needed in the self-competition with RrB^{short}. RrB^{short}-3GGA show significantly less competition and is not able to fully compete the labeled RrB^{short} off CsrA within the range of concentrations tested.

With these binding assays we clearly show that RrB^{short} binds CsrA *in vitro* and that this interaction relies on the predicted binding sites located in single-stranded regions. The two remaining GGA motifs in the mutant RNA RrB^{short}-3GGA do not efficiently bind CsrA on their own. We suspect that these low affinity GGA sites may require nearby high affinity sites in order to bind CsrA, this type of binding has previously been described for the CsrA homolog RsmE (Duss et al., 2014).

In combination, our results from MS2 affinity purification, structure prediction, the InvenireSRNA algorithm, and the EMSAs strongly suggest that RrB^{short}, and likely RrA, B, F^{short}, specifically interact with the post-transcriptional regulator CsrA.

Phenotypic Effects of Altered RrA, B, F Levels

We next asked whether RrA, B, F might act by sequestering CsrA, similarly to the effects of CsrB, CsrC, GadY and McaS. To this end, we constructed an *E. coli* mutant deleted for the chromosomal copies of *rrA*, *B*, *F* (see Materials and Methods). Additionally, to overexpress *rrB* in a fashion that would presumably allow normal processing of RrB^{short}, we cloned the *rrB* sequence including the 3'-half of the adjacent 5S gene and both terminators (T1 and T2) into a modified pUC18 plasmid (pJFR1, see Supplementary Table 2) to make pRrB.

Putative effects of RrB expression on the activity of CsrA were investigated by monitoring several CsrA-regulated phenotypes: growth rate, biofilm formation, motility, and post-transcriptional repression of the CsrA-regulated genes *pgaA* (Wang et al., 2005) and *glgC* (Baker et al., 2002). As a positive control, we moved

TABLE 2 | Transcripts predicted to regulate CsrA by the algorithm InvenireSRNA (Fakhry et al., 2017).

RNA	Probability score
CsrB sRNA	0.9997
csrB chip-SEQ	0.9977
speA chip-SEQ	0.9507
glyQ_ysaB	0.9505
setA_leuD	0.8794
OmpX chip-SEQ	0.872
lhr_grxD	0.8634
tatE_lipA	0.8518
CsrC sRNA	0.8435
zapB chip-SEQ	0.8308
csrC chip-SEQ	0.7979
ybhH_ybhI	0.7439
glTD chip-SEQ	0.7013
yqfE_argP	0.6407
RrA, B ^{short}	0.6245
RrF ^{short}	0.5833
McaS	0.005
GadY	0.0003

The input into InvenireSRNA was all annotated sRNAs, the 22 TLR sequences, all sequences identified as peaks in a comprehensive CsrA CHIP-seq experiment (Potts et al., 2017) and all intergenic regions of *E. coli* shorter than 1,000 bp (2902 sequences in total). The table displays the 16 highest-scoring transcripts from the analysis, and the sRNAs McaS and GadY, along with the associated probability scores. Intergenic regions are named by the two genes flanking them, separated by “_” and CHIP-seq peaks by addition of “chip-SEQ” to the gene name. Note that CsrB/C are present twice as they are included as full-length sequences from the list of sRNAs and as peak regions from the CHIP-seq data.

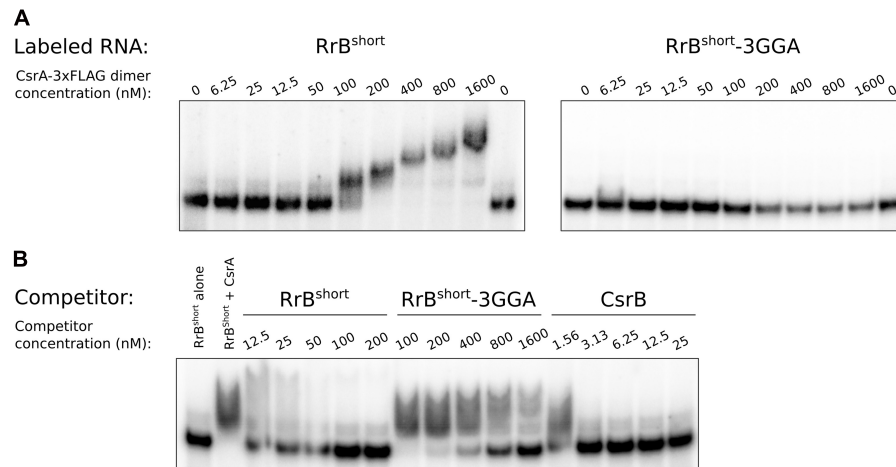


FIGURE 7 | Electrophoretic mobility shift assays (EMSA) of RrB^{short} with CsrA. EMSA with 120 pM *in vitro* transcribed RNA and increasing concentration of CsrA-3xFLAG, as indicated. **(A)** EMSA of ³²P-labeled RrB^{short} and an RrB^{short} mutant (RrB^{short}-3GGA) where three out of five GGA motifs were replaced with 'UUU', mixed with increasing concentration of CsrA-3xFLAG, as indicated. **(B)** A competition assay with ³²P-labeled RrB^{short} (120 pM), CsrA (200 nM) and increasing concentration of the *in vitro* transcribed unlabeled RNAs: RrB^{short}, RrB^{short}-3GGA and the well-known CsrA-binding RNA CsrB. Note the differences in concentrations between the different competitor RNAs. The first lane contains no CsrA in any of the experiments. The stated CsrA concentrations refer to the concentrations of the homodimer.

a previously characterized *csrA::kan* allele (Romeo et al., 1993) into our wildtype strain (which is otherwise isogenic to the $\Delta rrA, B, F$ strain). The *csrA::kan* allele encodes a truncated version of CsrA which is known to have strongly reduced CsrA activity (Romeo et al., 1993). The results of these analyses are presented in **Figure 8**. In general, if RrA, B, F regulate CsrA activity in a manner similar to CsrB, we expect the phenotype of overexpression of *rrB* to display a similar tendency to that of the *csrA::kan* allele. Neither deletion nor overexpression of the *rrA, B, F* significantly affected the growth rate in minimal glucose medium (**Figure 8A**). For comparison, *E. coli* harboring a truncated CsrA have been reported to grow at approximately half the growth rate of the wildtype strain when glucose is the carbon source (Morin et al., 2016). The mutants lacking or overexpressing the *rrA, B, F* were also tested for motility on soft agar plates. Neither overexpression nor deletion of the *rrA, B, F* affected motility (**Figure 8B**). In contrast, the *csrA::kan* strain was severely impaired for motility as previously described (Romeo et al., 1993), although we note that this phenotype in our hands was very variable between replicate experiments.

CsrA is a negative regulator of PGA (poly- β -1,6-*N*-acetyl-d-glucosamine)-mediated biofilm formation (Wang et al., 2005). In agreement with this, we found that the *csrA::kan* strain produces more biofilm than wildtype as measured by crystal violet staining (**Figure 8C**). The $\Delta rrA, B, F$ strain also formed significantly more biofilm than the wildtype. However, overexpression of RrB also showed somewhat increased biofilm formation, although the difference from the strain carrying the empty vector control was not statistically significant.

In connection with biofilm, translation of the *pgaABCD* mRNA, encoding the machinery for synthesis and transport of PGA, is known to be strongly repressed by CsrA

(Wang et al., 2005). Indeed, we found > 20-fold higher activity of β -galactosidase from a *pgaA-lacZ* fusion in the presence of CsrB overexpression than in the wildtype strain (**Figure 8D**). A modest increase in β -galactosidase activity was also observed in the $\Delta rrA, B, F$ mutant. Again, overexpression of RrB resulted in a phenotype similar to that of the $\Delta rrA, B, F$ mutant, pointing to a surprisingly similar effect on the *pgaA-lacZ* fusion of decreasing and increasing the RrA, B, F levels. There is good correlation between our data on biofilm formation and our data on the *pgaA-lacZ* fusion for all the strains (**Figures 8C,D**), as would be expected for CsrA-dependent regulation of biofilm (Wang et al., 2005).

Lastly, we tested the expression of GFP from a plasmid-borne translational *glgC-gfp* fusion during exponential growth, the growth phase where RrA, B, F accumulated (**Figure 2C**). The *glgCAP* operon encodes enzymes involved in glycogen metabolism, and is known to be repressed by CsrA (Baker et al., 2002). CsrB overexpression increases *glgC-gfp* expression substantially, while we observed slightly more GFP signal both upon deletion and overexpression of *rrA, B, F* (**Figure 8E**). In summary, we only observed minor phenotypic effects of changes in the expression of RrA, B, F. The RrA, B, F RNAs appear to modestly influence biofilm formation and expression from the CsrA-controlled *pgaA* and *glgC* mRNAs, but all three assays showed the same curious trend, namely that both deletion of *rrA, B, F* and overexpression of *rrB* resulted in a change consistent with modestly reduced CsrA activity. A plausible explanation for this unexpected similarity of phenotypes would be if RrB RNA expressed from the vector was processed into a form that exerted a different action on the tested properties than chromosomally expressed RrB. To address this hypothesis, we also tested expression of the *glgC-gfp* fusion in the presence of the pKK3535

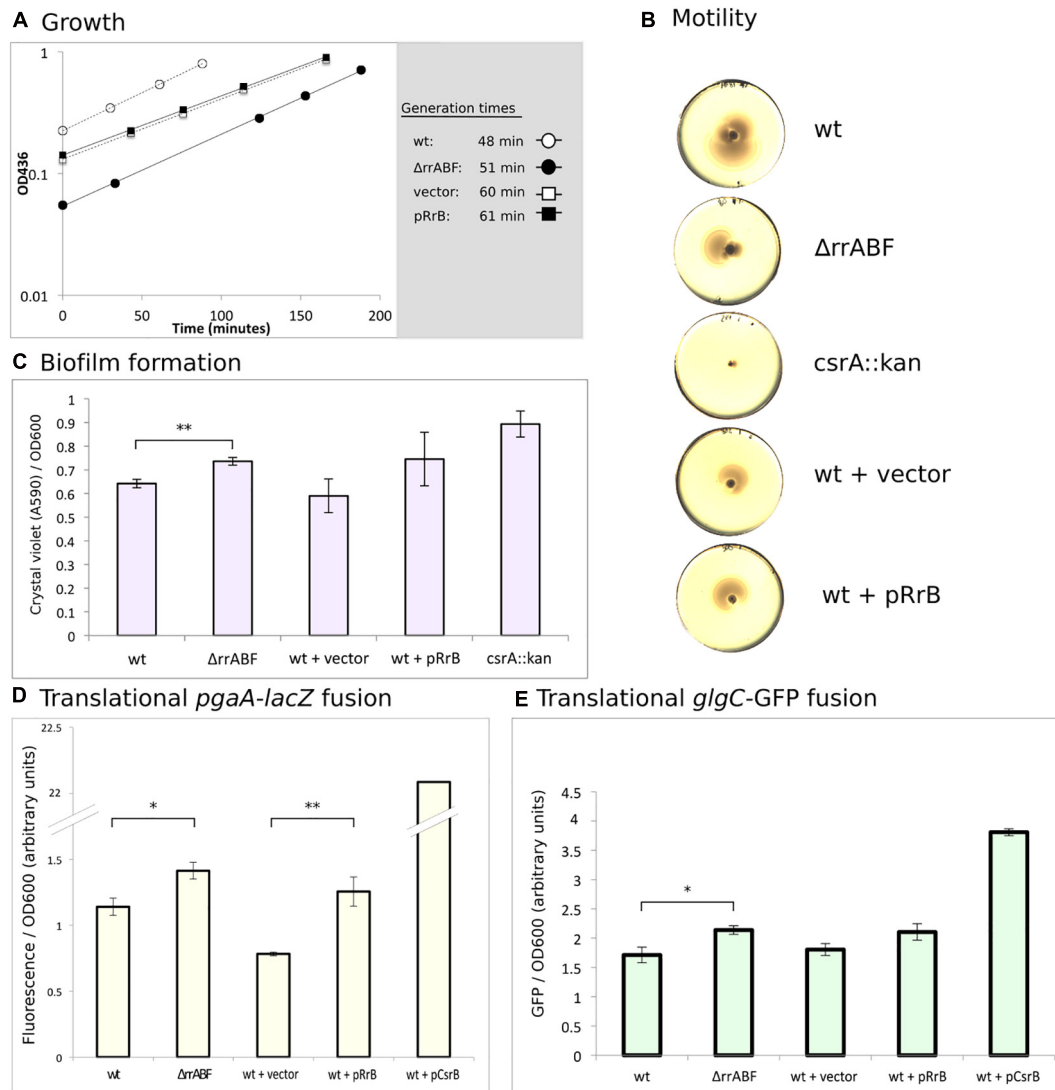


FIGURE 8 | Phenotypes of deletion and overexpression of the *rrA*, *B*, *F* genes. **(A)** Growth of the four indicated strains. Cultures were grown in MOPS minimal media supplemented with 0.2% glucose and 100 μ g/ml ampicillin for strains harboring plasmids. The indicated generation times were calculated as the average of two independent replicates. **(B)** Motility of the indicated strains was assayed on soft YT agar (0.3%) plates. Color and contrast of the photo has been manipulated to more clearly visualize the zone of bacterial growth. **(C)** Amount of biofilm formed on “peg-lids” by the indicated strains was quantified using crystal violet staining and absorbance measurements. **(D)** Quantification of the fluorescence produced by cleavage of 4-methylumbelliferyl- β -D-galactopyranoside (MUG) by β -galactosidase for outgrown cultures of the indicated strains. All strains carried a plasmid with a translational fusion of the *pgaA* leader to *lacZ* (pTSS36). **(E)** Quantification of GFP-signal for strains growing in exponential phase. All strains carried the translational fusion of the *glgC* leader to *sf-gfp* on a plasmid (pTSS16). In all cases, statistical probability was calculated using a two-sided student's *t*-test and is indicated (* $P < 0.05$, ** $P < 0.01$).

plasmid that contains the entire *rrnB* operon, including *rrB*. Although the rRNA operon promoters are feedback-controlled and thus difficult to overexpress, this plasmid was expected to cause a relative increase in RrB levels, because the pKK3535 plasmid is responsible for approximately 50% of total rRNA synthesis even in the presence of the seven chromosomal rRNA operons (Steen et al., 1986). As shown in **Supplementary Figure 5**, overexpression of the *rrnB* operon resulted in increased *glgC-gfp* expression, and was thus consistent with reduced CsrA activity under this condition. In our hands, however, the strains containing pKK3535 had impaired growth rates

(see **Supplementary Figure 6A**) and thus we did not pursue additional experiments with this plasmid.

The Concentration of RrA, B, F Increases Upon Translational Halt

The very modest effects of RrA, B, F on CsrA-controlled phenotypes suggest that if there is a physiological consequence of RrA, B, F interaction with CsrA then we might not have examined it under the proper growth conditions. In *E. coli*, rRNA expression is controlled by the second messenger ppGpp

(Zhang and Bremer, 1995). A decrease in ppGpp levels leads to increased rRNA expression (as observed upon treatment with antibiotics specifically blocking translation (Kurland and Maaløe, 1962; Muto et al., 1975)). To test whether the ppGpp effect also applies to *rrA*, *B*, *F*, we induced translational arrest, either by chloramphenicol addition, or by expression of the toxin MazF, and investigated the level of RrA, B, F by northern blot analysis at several time points after induction. Chloramphenicol blocks translation by binding to ribosomes and inhibiting the peptidyl transferase activity (Das et al., 1966) while MazF leads to translational arrest by disrupting ribosome biogenesis and cleaving mRNAs (Culviner and Laub, 2018), thereby removing the template for translation. In both cases of translational arrest, we detect a strong increase in RrA, B, F transcript levels 20–80 min after the treatment (**Figure 9**). As an independent indicator of transcription from the rRNA operons, we also investigated the level of tRNA^{Glu}. This tRNA is exclusively expressed from genes located in four rRNA operons (*rrnB*, *rrnC*, *rrnE*, *rrnG*), so we expected its expression pattern to resemble that of RrA, B, F. Indeed, the level of tRNA^{Glu} also increases during translational arrest, albeit not nearly to the same extent as RrA, B, F (**Figure 9**).

DISCUSSION

We identify three small genes that are co-transcribed from rRNA operons and processed to transcripts of defined lengths that bind the post-transcriptional regulator CsrA both *in vitro* and *in vivo*. As the transcription rate of rRNA is strictly correlated with the growth rate of *E. coli* (Potrykus et al., 2011), it is tempting to speculate that such short-lived sRNAs transcribed along with rRNA could function to align growth-rate-regulated transcription rates with other growth-phase-dependent processes in the cell, such as those regulated by CsrA. The relatively short half-life of RrA, B, F compared to other sRNAs makes biological sense if their abundance should reflect the transcriptional activity of the rRNA operons in real time.

We find a modest effect of overexpression of *rrB* on three of the CsrA-regulated phenotypes tested (**Figure 8**). The phenotypes observed upon overexpression of *rrB* agree with those expected from a mutant with modestly reduced CsrA activity. Such an apparent inhibition of CsrA upon overexpression of *rrB* could be due to binding of RrB to CsrA, resulting in regulation by titration in the classical way first described for CsrB/C. Direct binding between CsrA and RrB^{short} is experimentally supported by the results of our RNA affinity purification and EMSA analyses as well as theoretically supported by the InvenireSRNA prediction and the presence of consensus CsrA-binding motifs in the RrB^{short} structure. The fact that deletion of the *rrA*, *B*, *F* genes showed similar phenotypes to RrB overexpression is then counterintuitive (see **Figure 8**). Potentially, the chromosomally encoded form of RrB could fulfill a function for which the version of RrB expressed from our multicopy plasmid has a dominant negative effect (overriding the phenotype of the wildtype allele), in which case similar phenotypes of the chromosomal *rrA*, *B*, *F* deletions and the RrB overexpression could be expected.

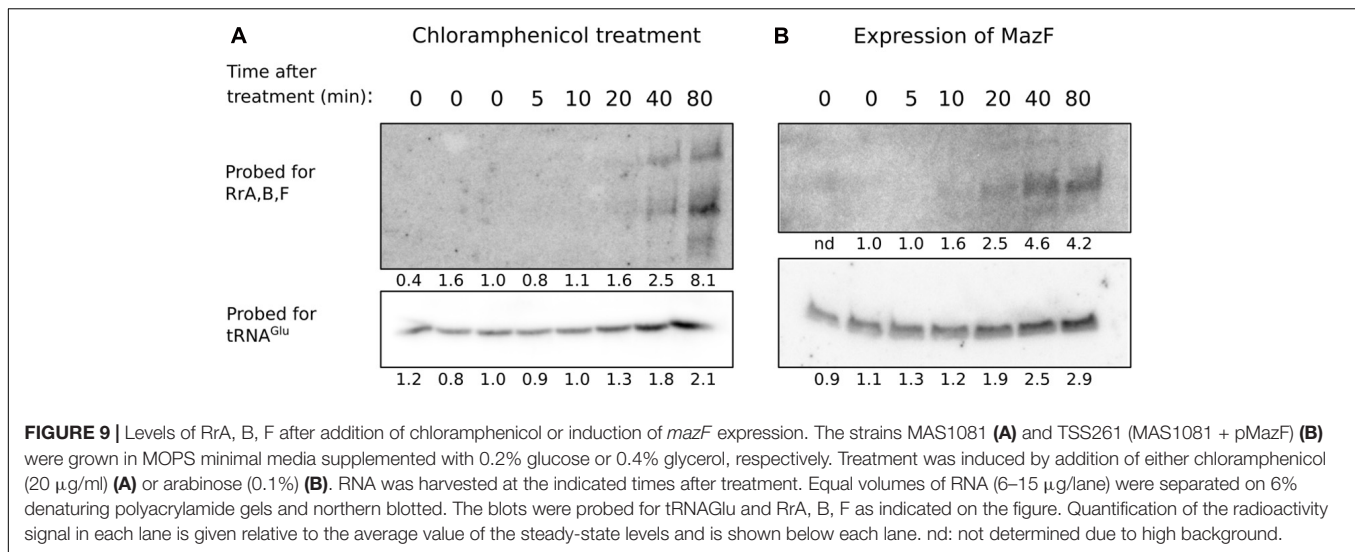
The curious effect of RrB overexpression was investigated further by introducing a plasmid expressing the entire *rrnB* operon (**Supplementary Figure 6**), which confirmed the results obtained by specific overexpression of RrB (**Figure 8E**). Since overexpression of *rrB* by two different cloning tactics affected the *glgC-gfp* fusion similarly, we conclude that deletion and overexpression of RrB both result in phenotypes consistent with reduced CsrA activity, but cannot currently provide a mechanistic explanation for this curious observation.

While we have demonstrated an interaction between the RrA, B, F RNAs and CsrA, deletion and overexpression of *rrA*, *B*, *F* show only modest changes of the CsrA-related phenotypes tested in this study. We want to note that CsrA is the major hub in a regulatory network with many inputs (Romeo and Babitzke, 2018). For that reason, one might not expect that the absence, or presence in excess, of RrA, B, F would lead to prominent phenotypes, but merely fine tuning of the activity of CsrA. Further, EMSA analyses (**Figure 7**) showed that CsrB totally competed RrB^{short} off CsrA at a ten-fold lower concentration than RrB^{short} itself (**Figure 7B**). This shows that CsrB is a higher-affinity CsrA binding partner than RrA, B, F and that we therefore might expect small effects, if any, of changes to the RrA, B, F levels in situations where CsrA-regulation by CsrB/C is at play.

Our northern analysis shows that RrA, B, F are most abundant when the rRNA operons are expressed, namely during exponential growth (**Figure 2C**), and especially upon treatments that lower ppGpp production by arresting translation (**Figure 9**). During translational halt, RrA, B, F levels increased more than the tRNA^{Glu}, which is also expressed solely from rRNA operons. This difference in the extent of induction could either mean that there is differential expression of the genes in the rRNA operons upon translational arrest, or, more likely, translational arrest may result in increased stability of the RrA, B, F sRNAs relative to tRNA^{Glu} by an unknown mechanism. Our data do not allow us to distinguish between these possibilities. Nevertheless, the experiments show that conditions exist in which the abundance of the RrA, B, F RNAs increase substantially. If they play a greater role in cell physiology than the fine-tuning of CsrA-regulated phenotypes shown in **Figure 8**, their impact should maybe be sought under such conditions, or at least under conditions where CsrB/C concentrations are low but the transcription rate of rRNA is high.

We find that *rrA*, *B*, *F* is well conserved in various different genera of bacteria including numerous pathogenic species. It is well known that growth-phase-dependent regulation is important for bacterial virulence (Dalebroux and Swanson, 2012; Kitamoto et al., 2016). Thus, if RrA, B, F is used as an indicator of growth rate in the cell, it could also potentially have a regulatory effect on the pathogenesis of these virulent strains.

A hallmark of all the members of the TLR family found in *E. coli* is the presence of a short (18–19 bp) repeated sequence identical to the 3'-end of the mature tRNA or rRNA from the same operon. For the tRNA or rRNA this 3'-end sequence is important for processing (reviewed in Mackie, 2013). The 3'-end of the 173-nt form of RrB was mapped 3 nt downstream of the repeated sequence that is identical to the final 18 bp of mature 5S RNA. As this repeated sequence and structure is known to be important for the RNase E cleavage immediately



downstream of 5S, we suggest that the repeat in the RrB 3'-end is also recognized by RNase E, and that this explains the function of the repeated sequence.

RrB^{short} was enriched on Hfq in the co-purification experiment (Figure 2), and showed specific binding to Hfq by EMSA analysis (Supplementary Figure 5), which could suggest a role for Hfq in folding or processing of RrB. Hfq could affect folding and the kinetics of the processing but is not essential for processing since RrB^{short} was also observed in a Δ hfq mutant (Supplementary Figure 7). Alternatively, the enrichment could reflect that RrB^{short} functions as a base-pairing sRNA to regulate one or more target RNAs, chaperoned by Hfq. GadY (Parker et al., 2017) and McaS (Jorgensen et al., 2013) are two recent examples of dual function sRNAs that can both function to bind and titrate out CsrA, and function as generic Hfq-dependent base-pairing sRNAs to regulate target mRNAs. Although we cannot rule out either option, we favor the former option, namely that Hfq participates in the folding or processing of RrB, which is also supported by our structure probing with and without Hfq (Figure 6). If Hfq assisted with pairing of RrB^{short} to a target RNA(s), we would have expected to detect the binding between RrB^{short} and Hfq in the mass spectrometry analysis of the proteins co-purifying with RrB^{short}, and the RNA-seq analysis could have revealed the target RNA(s). On the other hand, if the role of Hfq is to facilitate the refolding or processing of RrB, then the affinity of Hfq for the refolded product RrB^{short} need not be very high, why we speculate that competing binders with higher affinity, like the abundant CsrA protein, may have excluded binding of Hfq to RrB^{short} in the MS2-RNA affinity purification experiments.

The *rrA*, *B*, *F* genes are found downstream of the gene encoding 5S in three out of seven rRNA operons of *E. coli*. These three operons are furthermore the only three that contain two terminator sequences (T₁ and T₂), whereas the remaining four rRNA operons have a single terminator (Supplementary Figure 1; Lesnik et al., 2001). The significance of the dual terminators is not clear and has been puzzling since its

discovery (Brosius et al., 1981; Brosius, 1984; Ghosh et al., 1991; Orosz et al., 1991). The termination efficiencies of each of the terminators from the *rrnB* operon have been measured. T₁ was measured to terminate 87% of transcripts while T₂ terminated 100% of transcripts (Orosz et al., 1991). As the *rrA*, *B*, *F* genes are located between the two terminators we suggest that this dual terminator arrangement could serve the purpose of regulating the expression of *rrA*, *B*, *F*. In this way, the expression of *rrA*, *B*, *F* will be directly linked to expression of rRNA and growth rate, but they would be expressed at a lower level than the rRNA, which are among the most highly transcribed genes in the cell. We point out that the dual terminators of ribosomal operon B, including the *rrB* gene, are among the most highly used transcription terminator sequences on plasmids for cloning and protein expression (Denèfle et al., 1987; Andrews et al., 1996; Rogers et al., 2015; Wille et al., 2015; Engstrom and Pfleger, 2017). Our demonstration that the RrA, B, F molecules can interact with at least two pleiotropic regulatory proteins in *E. coli* (Hfq and CsrA), warrants careful consideration of whether expression of such putative sRNAs from a high copy number plasmid is desirable for a given application.

Several studies on eukaryotic organisms have identified potential miRNAs transcribed as part of rRNA primary transcripts (Wei et al., 2013; Chak et al., 2015; Asha and Soniya, 2017), and the murine-specific miR-712, transcribed as a part of a spacer element in the pre-rRNA transcript, has been shown to be involved in endothelial inflammation and atherosclerosis (Son et al., 2013). To our knowledge, the RrA, B, F sRNAs described here represent the first report of sRNAs transcribed as part of rRNA primary transcripts in a prokaryote. In conclusion, three out of seven rRNA operons in *E. coli* contains an arrangement of dual terminators with small defined RNAs encoded in between, and these RNAs are conserved both in structure and sequence among species belonging to different genera of Enterobacteriales. We have found that these RNAs interact with both Hfq and CsrA but has been unable to demonstrate clear phenotypes of

both deletion and overexpression mutants. We presume that the conservation among species indicate a function for the RNAs but that this function is still not fully understood.

DATA AVAILABILITY STATEMENT

The datasets presented in this study can be found in online repositories. The names of the repository/repositories and accession number(s) can be found below: <http://www.ebi.ac.uk/pride/archive/projects/PXD013749>.

AUTHOR CONTRIBUTIONS

TS, MK, SS, and MS wrote the manuscript, conceived and designed the research. TS, MK, BK, EH, SS, and MS designed the experiments. MK (Hfq) and TS (CsrA) performed the experiments. All authors contributed to the article and approved the submitted version.

REFERENCES

- Aiba, H., Adhya, S., and de Crombrughe, B. (1981). Evidence for two functional gal promoters in intact *Escherichia coli* cells. *J. Biol. Chem.* 256, 11905–11910.
- Altier, C., Suyemoto, M., Ruiz, A. I., Burnham, K. D., and Maurer, R. (2002). Characterization of two novel regulatory genes affecting *Salmonella* invasion gene expression. *Mol. Microbiol.* 35, 635–646. doi: 10.1046/j.1365-2958.2000.01734.x
- Andrews, B., Adari, H., Hannig, G., Lahue, E., Gosselin, M., Martin, S., et al. (1996). A tightly regulated high level expression vector that utilizes a thermosensitive lac repressor: production of the human T cell receptor V β 5.3 in *Escherichia coli*. *Gene* 182, 101–109. doi: 10.1016/S0378-1119(96)00523-9
- Asha, S., and Soniya, E. V. (2017). The sRNAome mining revealed existence of unique signature small RNAs derived from 5.8SrRNA from *Piper nigrum* and other plant lineages. *Sci. Rep.* 7:41052. doi: 10.1038/srep41052
- Baglio, S. R., Rooijers, K., Koppers-Lalic, D., Verweij, F. J., Pérez Lanzón, M., Zini, N., et al. (2015). Human bone marrow- and adipose-mesenchymal stem cells secrete exosomes enriched in distinctive miRNA and tRNA species. *Stem Cell Res. Ther.* 6:127. doi: 10.1186/s13287-015-0116-z
- Baker, C. S., Morozov, I., Suzuki, K., Romeo, T., and Babitzke, P. (2002). CsrA regulates glycogen biosynthesis by preventing translation of glgC in *Escherichia coli*. *Mol. Microbiol.* 44, 1599–1610. doi: 10.1046/j.1365-2958.2002.02982.x
- Baracchini, E., and Bremer, H. (1991). Control of rRNA synthesis in *Escherichia coli* at increased RRN gene dosage. Role of guanosine tetraphosphate and ribosome feedback. *J. Biol. Chem.* 266, 11753–11760. doi: 10.1016/S0021-9258(18)99021-6
- Bardwell, V. J., and Wickens, M. (1990). Purification of RNA and RNA-protein complexes by an R17 coat protein affinity method. *Nucleic Acids Res.* 18, 6587–6594.
- Beckett, D., Kovaleva, E., and Schatz, P. J. (2008). A minimal peptide substrate in biotin holoenzyme synthetase-catalyzed biotinylation. *Protein Sci.* 8, 921–929. doi: 10.1110/ps.8.4.921
- Beisel, C. L., and Storz, G. (2011). The base-pairing RNA Spot 42 participates in a multioutput feedforward loop to help enact catabolite repression in *Escherichia coli*. *Mol. Cell* 41, 286–297. doi: 10.1016/j.molcel.2010.12.027
- Berk, A. J., and Sharp, P. A. (1977). Sizing and mapping of early adenovirus mRNAs by gel electrophoresis of S1 endonuclease-digested hybrids. *Cell* 12, 721–732. doi: 10.1016/0092-8674(77)90272-0
- Bernstein, J. A., Khodursky, A. B., Lin, P.-H., Lin-Chao, S., and Cohen, S. N. (2002). Global analysis of mRNA decay and abundance in *Escherichia coli* at single-gene

FUNDING

This work was supported by the Lundbeck Foundation [R108-A10583 to MS], the Danish council for Independent Research | Natural Sciences [1323-00343B to SS] and the Danish National Research Foundation [DNRF120 to SS; MS].

ACKNOWLEDGMENTS

The authors thank Marit Warrer, Bertil Gummeson, and Pilar Menéndez Gil for excellent technical assistance. The authors thank Jörg Vogel for help and support to TS during his visit in Würzburg. The authors also thank Anders Boysen for the kind supply of purified Hfq.

SUPPLEMENTARY MATERIAL

The Supplementary Material for this article can be found online at: <https://www.frontiersin.org/articles/10.3389/fmicb.2021.625585/full#supplementary-material>

- resolution using two-color fluorescent DNA microarrays. *Proc. Natl. Acad. Sci. U.S.A.* 99, 9697–9702. doi: 10.1073/pnas.112318199
- Bilusic, I., Popitsch, N., Rescheneder, P., Schroeder, R., and Lybecker, M. (2014). Revisiting the coding potential of the *E. coli* genome through Hfq co-immunoprecipitation. *RNA Biol.* 11, 641–654. doi: 10.4161/rna.29299
- Bordeau, V., and Felden, B. (2014). Curli synthesis and biofilm formation in enteric bacteria are controlled by a dynamic small RNA module made up of a pseudoknot assisted by an RNA chaperone. *Nucleic Acids Res.* 42, 4682–4696. doi: 10.1093/nar/gku098
- Bösl, M., and Kersten, H. (1991). A novel RNA product of the tyrT operon of *Escherichia coli*. *Nucleic Acids Res.* 19, 5863–5870. doi: 10.1093/nar/19.21.5863
- Bösl, M., and Kersten, H. (1994). Organization and functions of genes in the upstream region of tyrT of *Escherichia coli*: phenotypes of mutants with partial deletion of a new gene (tgs). *J. Bacteriol.* 176, 221–231. doi: 10.1128/jb.176.1.221-231.1994
- Brantl, S., and Jahn, N. (2015). sRNAs in bacterial type I and type III toxin-antitoxin systems. *FEMS Microbiol. Rev.* 39, 413–427.
- Brosius, J. (1984). Toxicity of an overproduced foreign gene product in *Escherichia coli* and its use in plasmid vectors for the selection of transcription terminators. *Gene* 27, 161–172. doi: 10.1016/0378-1119(84)90137-9
- Brosius, J., Cate, R. L., and Perlmutter, A. P. (1982). Precise location of two promoters for the beta-lactamase gene of pBR322. S1 mapping of ribonucleic acid isolated from *Escherichia coli* or synthesized *in vitro*. *J. Biol. Chem.* 257, 9205–9210.
- Brosius, J., Dull, T. J., Sleeter, D. D., and Noller, H. F. (1981). Gene organization and primary structure of a ribosomal RNA operon from *Escherichia coli*. *J. Mol. Biol.* 148, 107–127. doi: 10.1016/0022-2836(81)90508-8
- Chak, L. L., Mohammed, J., Lai, E. C., Tucker-Kellogg, G., and Okamura, K. (2015). A deeply conserved, noncanonical miRNA hosted by ribosomal DNA. *RNA* 21, 375–384. doi: 10.1261/rna.049098.114
- Chao, Y., Papenfort, K., Reinhardt, R., Sharma, C. M., and Vogel, J. (2012). An atlas of Hfq-bound transcripts reveals 3' UTRs as a genomic reservoir of regulatory small RNAs. *EMBO J.* 31, 4005–4019. doi: 10.1038/emboj.2012.229
- Ciesiolka, J., Michałowski, D., Wrzesinski, J., Krajewski, J., and Krzyżosiak, W. J. (1998). Patterns of cleavages induced by lead ions in defined RNA secondary structure motifs 1 Edited by I. Tinoco. *J. Mol. Biol.* 275, 211–220. doi: 10.1006/jmbi.1997.1462
- Corcoran, C. P., Rieder, R., Podkaminski, D., Hofmann, B., and Vogel, J. (2012). “Use of aptamer tagging to identify *in vivo* protein binding partners of small

- regulatory RNAs," in *Bacterial Regulatory RNA*, ed. K. C. Keiler (Totowa, NJ: Humana Press), 177–200. doi: 10.1007/978-1-61779-949-5_11
- Culviner, P. H., and Laub, M. T. (2018). Global analysis of the *E. coli* Toxin MazF reveals widespread cleavage of mRNA and the inhibition of rRNA maturation and ribosome biogenesis. *Mol. Cell* 70, 868–880.e10. doi: 10.1016/j.molcel.2018.04.026
- Dalebroux, Z. D., and Swanson, M. S. (2012). ppGpp: magic beyond RNA polymerase. *Nat. Rev. Microbiol.* 10, 203–212. doi: 10.1038/nrmicro2720
- Das, H. K., Goldstein, A., and Kanner, L. C. (1966). Inhibition by chloramphenicol of the growth of nascent protein chains in *Escherichia coli*. *Mol. Pharmacol.* 2, 158–170.
- Denèfle, P., Kovarik, S., Guitton, J.-D., Cartwright, T., and Mayaux, J.-F. (1987). Chemical synthesis of a gene coding for human angiogenin, its expression in *Escherichia coli* and conversion of the product into its active form. *Gene* 56, 61–70. doi: 10.1016/0378-1119(87)90158-2
- Dubey, A. K., Baker, C. S., Romeo, T., and Babitzke, P. (2005). RNA sequence and secondary structure participate in high-affinity CsrA-RNA interaction. *RNA* 11, 1579–1587. doi: 10.1261/rna.2990205
- Duss, O., Michel, E., Diarra dit Konté, N., Schubert, M., and Allain, F. H.-T. (2014). Molecular basis for the wide range of affinity found in Csr/Rsm protein–RNA recognition. *Nucleic Acids Res.* 42, 5332–5346. doi: 10.1093/nar/gku141
- Egan, J., and Landy, A. (1978). Structural analysis of the tRNA^{1Tyr} gene of *Escherichia coli*. A 178 base pair sequence that is repeated 3.14 times. *J. Biol. Chem.* 253, 3607–3622.
- Emara, M. M., Ivanov, P., Hickman, T., Dawra, N., Tisdale, S., Kedersha, N., et al. (2010). Angiogenin-induced tRNA-derived Stress-induced RNAs promote stress-induced stress granule assembly. *J. Biol. Chem.* 285, 10959–10968. doi: 10.1074/jbc.M109.077560
- Engstrom, M. D., and Pfeiffer, B. F. (2017). Transcription control engineering and applications in synthetic biology. *Synth. Syst. Biotechnol.* 2, 176–191. doi: 10.1016/j.synbio.2017.09.003
- Fakhry, C. T., Kulkarni, P., Chen, P., Kulkarni, R., and Zarringhalam, K. (2017). Prediction of bacterial small RNAs in the RsmA (CsrA) and ToxT pathways: a machine learning approach. *BMC Genomics* 18:645. doi: 10.1186/s12864-017-4057-z
- Fessler, M., Gummesson, B., Charbon, G., Svenningsen, S. L., and Sørensen, M. A. (2020). Short-term kinetics of rRNA degradation in *Escherichia coli* upon starvation for carbon, amino acid or phosphate. *Mol. Microbiol.* 113, 951–963. doi: 10.1111/mmi.14462
- Geissmann, T. A., and Touati, D. (2004). Hfq, a new chaperoning role: binding to messenger RNA determines access for small RNA regulator. *EMBO J.* 23, 396–405. doi: 10.1038/sj.emboj.7600058
- Ghosh, B., Grzadzińska, E., Bhattacharya, P., Peralta, E., DeVito, J., and Das, A. (1991). Specificity of antitermination mechanisms. *J. Mol. Biol.* 222, 59–66. doi: 10.1016/0022-2836(91)90737-Q
- Gonzalez Chavez, R., Alvarez, A. F., Romeo, T., and Georgellis, D. (2010). The physiological stimulus for the BarA Sensor Kinase. *J. Bacteriol.* 192, 2009–2012. doi: 10.1128/JB.01685-09
- Green, M. R., and Roeder, R. G. (1980). Definition of a novel promoter for the major adenovirus-associated virus mRNA. *Cell* 22, 231–242. doi: 10.1016/0092-8674(80)90171-3
- Hoekzema, M., Romilly, C., Holmqvist, E., and Wagner, E. G. H. (2019). Hfq-dependent mRNA unfolding promotes sRNA-based inhibition of translation. *EMBO J.* 38:e101199. doi: 10.15252/embj.2018101199
- Holmqvist, E., and Wagner, E. G. H. (2017). Impact of bacterial sRNAs in stress responses. *Biochem. Soc. Trans.* 45, 1203–1212. doi: 10.1042/BST20160363
- Holmqvist, E., Wright, P. R., Li, L., Bischoff, T., Barquist, L., Reinhardt, R., et al. (2016). Global RNA recognition patterns of post-transcriptional regulators Hfq and CsrA revealed by UV crosslinking *in vivo*. *EMBO J.* 35, 991–1011. doi: 10.15252/embj.201593360
- Jackson, D. W., Suzuki, K., Oakford, L., Simecka, J. W., Hart, M. E., and Romeo, T. (2002). Biofilm formation and dispersal under the influence of the global regulator CsrA of *Escherichia coli*. *J. Bacteriol.* 184, 290–301. doi: 10.1128/JB.184.1.290-301.2002
- Jørgensen, M. G., Nielsen, J. S., Boysen, A., Franch, T., Møller-Jensen, J., and Valentin-Hansen, P. (2012). Small regulatory RNAs control the multi-cellular adhesive lifestyle of *Escherichia coli*. *Mol. Microbiol.* 84, 36–50. doi: 10.1111/j.1365-2958.2012.07976.x
- Jørgensen, M. G., Thomason, M. K., Havelund, J., Valentin-Hansen, P., and Storz, G. (2013). Dual function of the McaS small RNA in controlling biofilm formation. *Genes Dev.* 27, 1132–1145. doi: 10.1101/gad.214734.113
- Kawano, M., Reynolds, A. A., Miranda-Rios, J., and Storz, G. (2005). Detection of 5'- and 3'-UTR-derived small RNAs and cis-encoded antisense RNAs in *Escherichia coli*. *Nucleic Acids Res.* 33, 1040–1050. doi: 10.1093/nar/gki256
- Kay, B. K., Thai, S., and Volgina, V. V. (2009). High-throughput biotinylation of proteins. *Methods Mol. Biol.* 498, 185–198. doi: 10.1007/978-1-59745-196-3_13
- Kitamoto, S., Nagao-Kitamoto, H., Kuffa, P., and Kamada, N. (2016). Regulation of virulence: the rise and fall of gastrointestinal pathogens. *J. Gastroenterol.* 51, 195–205. doi: 10.1007/s00535-015-1141-5
- Kurland, C. G., and Maaløe, O. (1962). Regulation of ribosomal and transfer RNA synthesis. *J. Mol. Biol.* 4, 193–210. doi: 10.1016/S0022-2836(62)80051-5
- Lalaouna, D., Carrier, M. C., Semsey, S., Brouard, J. S., Wang, J., Wade, J. T., et al. (2015). A 3' external transcribed spacer in a tRNA transcript acts as a sponge for small RNAs to prevent transcriptional noise. *Mol. Cell* 58, 393–405. doi: 10.1016/j.molcel.2015.03.013
- Lawhon, S. D., Maurer, R., Suyemoto, M., and Altier, C. (2002). Intestinal short-chain fatty acids alter *Salmonella typhimurium* invasion gene expression and virulence through BarA/SirA. *Mol. Microbiol.* 46, 1451–1464. doi: 10.1046/j.1365-2958.2002.03268.x
- Lesnik, E. A., Sampath, R., Levene, H. B., Henderson, T. J., McNeil, J. A., and Ecker, D. J. (2001). Prediction of rho-independent transcriptional terminators in *Escherichia coli*. *Nucleic Acids Res.* 29, 3583–3594. doi: 10.1093/nar/29.17.3583
- Li, S. H.-J., Li, Z., Park, J. O., King, C. G., Rabinowitz, J. D., Wingreen, N. S., et al. (2018). *Escherichia coli* translation strategies differ across carbon, nitrogen and phosphorus limitation conditions. *Nat. Microbiol.* 3, 939–947. doi: 10.1038/s41564-018-0199-2
- Li, Z., and Deutscher, M. P. (1995). The tRNA processing enzyme RNase T is essential for maturation of 5S RNA. *Proc. Natl. Acad. Sci. U.S.A.* 92, 6883–6886. doi: 10.1073/pnas.92.15.6883
- Liu, M. Y., Gui, G., Wei, B., Preston, J. F., Oakford, L., Yüksel, Ü., et al. (1997). The RNA molecule CsrB binds to the global regulatory protein CsrA and antagonizes its activity in *Escherichia coli*. *J. Biol. Chem.* 272, 17502–17510. doi: 10.1074/jbc.272.28.17502
- Liu, M. Y., Yang, H., and Romeo, T. (1995). The product of the pleiotropic *Escherichia coli* gene *csrA* modulates glycogen biosynthesis via effects on mRNA stability. *J. Bacteriol.* 177, 2663–2672. doi: 10.1128/jb.177.10.2663-2672.1995
- Mackie, G. A. (2013). RNase E: at the interface of bacterial RNA processing and decay. *Nat. Rev. Microbiol.* 11, 45–57. doi: 10.1038/nrmicro2930
- Martinez, G., Choudury, S. G., and Slotkin, R. K. (2017). tRNA-derived small RNAs target transposable element transcripts. *Nucleic Acids Res.* 45, 5142–5152.
- McGrath, P. T. (2011). Characterizing cDNA Ends by Circular RACE. *Methods Mol. Biol.* 772, 257–265. doi: 10.1007/978-1-61779-228-1_15
- Miller, J. H. (1972). *Experiments in Molecular Genetics*. New York, NY: Plenum Press.
- Miyakoshi, M., Chao, Y., and Vogel, J. (2015). Regulatory small RNAs from the 3' regions of bacterial mRNAs. *Curr. Opin. Microbiol.* 24, 132–139. doi: 10.1016/j.mib.2015.01.013
- Møller, T., Franch, T., Udesen, C., Gerdes, K., and Valentin-Hansen, P. (2002). Spot 42 RNA mediates discoordination expression of the *E. coli* galactose operon. *Genes Dev.* 16, 1696–1706. doi: 10.1101/gad.231702
- Moon, K., and Gottesman, S. (2009). A PhoQ/P-regulated small RNA regulates sensitivity of *Escherichia coli* to antimicrobial peptides. *Mol. Microbiol.* 74, 1314–1330. doi: 10.1111/j.1365-2958.2009.06944.x
- Morin, M., Ropers, D., Letisse, F., Laguerre, S., Portais, J.-C., Coccagn-Bousquet, M., et al. (2016). The post-transcriptional regulatory system CSR controls the balance of metabolic pools in upper glycolysis of *Escherichia coli*. *Mol. Microbiol.* 100, 686–700. doi: 10.1111/mmi.13343
- Muto, A., Kimura, A., and Osawa, S. (1975). Effects of some antibiotics on the stringent control of RNA synthesis in *Escherichia coli*. *Mol. Gen. Genet.* 139, 321–327. doi: 10.1007/BF00267972
- Neidhardt, F. C., Bloch, P. L., and Smith, D. F. (1974). Culture medium for enterobacteria. *J. Bacteriol.* 119, 736–747.
- Opdyke, J. A., Kang, J.-G., and Storz, G. (2004). GadY, a Small-RNA regulator of acid response genes in *Escherichia coli*. *J. Bacteriol.* 186, 6698–6705. doi: 10.1128/JB.186.20.6698-6705.2004

- Orosz, A., Boros, I., and Venetianer, P. (1991). Analysis of the complex transcription termination region of the *Escherichia coli* rrn B gene. *Eur. J. Biochem.* 201, 653–659. doi: 10.1111/j.1432-1033.1991.tb16326.x
- Parker, A., Cureoglu, S., De Lay, N., Majdalan, N., and Gottesman, S. (2017). Alternative pathways for *Escherichia coli* biofilm formation revealed by sRNA overproduction. *Mol. Microbiol.* 105, 309–325. doi: 10.1111/mmi.13702
- Piir, K., Paier, A., Liiv, A., Tenson, T., and Maiväli, Ü. (2011). Ribosome degradation in growing bacteria. *EMBO Rep.* 12, 458–462. doi: 10.1038/embor.2011.47
- Potrykus, K., Murphy, H., Philippe, N., and Cashel, M. (2011). ppGpp is the major source of growth rate control in *E. coli*. *Environ. Microbiol.* 13, 563–575. doi: 10.1111/j.1462-2920.2010.02357.x
- Potts, A. H., Vakulskas, C. A., Pannuri, A., Yakhnin, H., Babitzke, P., and Romeo, T. (2017). Global role of the bacterial post-transcriptional regulator CsrA revealed by integrated transcriptomics. *Nat. Commun.* 8:1596. doi: 10.1038/s41467-017-01613-1
- Raden, M., Ali, S. M., Alkhnbashi, O. S., Busch, A., Costa, F., Davis, J. A., et al. (2018). Freiburg RNA tools: a central online resource for RNA-focused research and teaching. *Nucleic Acids Res.* 46, 25–29. doi: 10.1093/nar/gky329
- Rasmussen, A. A., Johansen, J., Nielsen, J. S., Overgaard, M., Kallipolitis, B., and Valentin-Hansen, P. (2009). A conserved small RNA promotes silencing of the outer membrane protein YbfM. *Mol. Microbiol.* 72, 566–577. doi: 10.1111/j.1365-2958.2009.06688.x
- Robertson, H. D. (1990). *Escherichia coli* ribonuclease III. *Methods Enzymol.* 181, 189–202. doi: 10.1016/0076-6879(90)81121-A
- Rogers, J. K., Guzman, C. D., Taylor, N. D., Raman, S., Anderson, K., and Church, G. M. (2015). Synthetic biosensors for precise gene control and real-time monitoring of metabolites. *Nucleic Acids Res.* 43, 7648–7660. doi: 10.1093/nar/gkv616
- Romeo, T., and Babitzke, P. (2018). “Global regulation by CsrA and its RNA antagonists,” in *Regulating with RNA in Bacteria and Archaea*, eds G. Storz and K. Papenfort (Washington, DC: ASM Press), 339–354. doi: 10.1128/9781683670247.ch19
- Romeo, T., Gong, M., Liu, M. Y., and Brun-Zinkernagel, A.-M. (1993). Identification and molecular characterization of csrA, a pleiotropic gene from *Escherichia coli* that affects glycogen biosynthesis, gluconeogenesis, cell size, and surface properties. *J. Bacteriol.* 175, 4744–4755. doi: 10.1128/JB.175.15.4744-4755.1993
- Roy, M. K., Singh, B., Ray, B. K., and Apirion, D. (1983). Maturation of 5S RNA: ribonuclease E cleavage and their dependence on precursor sequences. *Eur. J. Biochem.* 131, 119–127.
- Rudd, K. E. (1999). Novel intergenic repeats of *Escherichia coli* K-12. *Res. Microbiol.* 150, 653–664.
- Said, N., Rieder, R., Hurwitz, R., Deckert, J., Urlaub, H., and Vogel, J. (2009). *In vivo* expression and purification of aptamer-tagged small RNA regulators. *Nucleic Acids Res.* 37:e133. doi: 10.1093/nar/gkp719
- Saikia, M., Jobava, R., Parisien, M., Putnam, A., Krokowski, D., Gao, X.-H., et al. (2014). Angiogenin-Cleaved tRNA halves interact with cytochrome c, protecting cells from apoptosis during osmotic stress. *Mol. Cell. Biol.* 34, 2450–2463. doi: 10.1128/MCB.00136-14
- Santiago-Frangos, A., and Woodson, S. A. (2018). Hfq chaperone brings speed dating to bacterial sRNA. *Wiley Interdiscip. Rev. RNA* 9:e1475. doi: 10.1002/wrna.1475
- Sawitzke, J. A., Thomason, L. C., Costantino, N., Bubunencko, M., Datta, S., and Court, D. L. (2007). Recombineering: *in vivo* genetic engineering in *E. coli*, *S. enterica*, and beyond. *Methods Enzymol.* 421, 171–199. doi: 10.1016/S0076-6879(06)21015-2
- Schorn, A. J., Gutbrod, M. J., LeBlanc, C., and Martienssen, R. (2017). LTR-retrotransposon control by tRNA-derived small RNAs. *Cell* 170, 61–71.e11. doi: 10.1016/j.cell.2017.06.013
- Shenk, T. E., Rhodes, C., Rigby, P. W., and Berg, P. (1975). Biochemical method for mapping mutational alterations in DNA with S1 nuclease: the location of deletions and temperature-sensitive mutations in simian virus 40. *Proc. Natl. Acad. Sci. U.S.A.* 72, 989–993. doi: 10.1073/pnas.72.3.989
- Son, D. J., Kumar, S., Takabe, W., Woo Kim, C., Ni, C.-W., Alberts-Grill, N., et al. (2013). The atypical mechanosensitive microRNA-712 derived from pre-ribosomal RNA induces endothelial inflammation and atherosclerosis. *Nat. Commun.* 4:3000. doi: 10.1038/ncomms4000
- Soper, T. J., and Woodson, S. A. (2008). The rpoS mRNA leader recruits Hfq to facilitate annealing with DsrA sRNA. *RNA* 14, 1907–1917. doi: 10.1261/rna.1110608
- Sørensen, M. A. (2001). Charging levels of four tRNA species in *Escherichia coli* Rel+ and Rel- strains during amino acid starvation: a simple model for the effect of ppGpp on translational accuracy. Edited by D. E. Draper. *J. Mol. Biol.* 307, 785–798. doi: 10.1006/jmbi.2001.4525
- Steen, R., Jemiolo, D. K., Skinner, R. H., Dunn, J. J., and Dahlberg, A. E. (1986). Expression of plasmid-coded mutant ribosomal RNA in *E. coli*: choice of plasmid vectors and gene expression systems. *Prog. Nucleic Acid Res. Mol. Biol.* 33, 1–18. doi: 10.1016/S0079-6603(08)60018-5
- Stenum, T. S., Sørensen, M. A., and Svenningsen, S. L. (2017). Quantification of the abundance and charging levels of transfer RNAs in *Escherichia coli*. *J. Vis. Exp.* 126:e56212. doi: 10.3791/56212
- Thomason, M. K., Fontaine, F., De Lay, N., and Storz, G. (2012). A small RNA that regulates motility and biofilm formation in response to changes in nutrient availability in *Escherichia coli*. *Mol. Microbiol.* 84, 17–35. doi: 10.1111/j.1365-2958.2012.07965.x
- Wagner, E. G. H., and Romby, P. (2015). Small RNAs in Bacteria and Archaea: who they are, what they do, and how they do it. *Adv. Genet.* 90, 133–208. doi: 10.1016/bs.adgen.2015.05.001
- Wang, X., Dubey, A. K., Suzuki, K., Baker, C. S., Babitzke, P., and Romeo, T. (2005). CsrA post-transcriptionally represses pgaABCD, responsible for synthesis of a biofilm polysaccharide adhesin of *Escherichia coli*. *Mol. Microbiol.* 56, 1648–1663. doi: 10.1111/j.1365-2958.2005.04648.x
- Wei, B. L., Brun-Zinkernagel, A.-M., Simecka, J. W., Prüß, B. M., Babitzke, P., and Romeo, T. (2001). Positive regulation of motility and flhDC expression by the RNA-binding protein CsrA of *Escherichia coli*. *Mol. Microbiol.* 40, 245–256. doi: 10.1046/j.1365-2958.2001.02380.x
- Wei, H., Zhou, B., Zhang, F., Tu, Y., Hu, Y., Zhang, B., et al. (2013). Profiling and identification of Small rDNA-Derived RNAs and their potential biological functions. *PLoS One* 8:e56842. doi: 10.1371/journal.pone.0056842
- Weilbacher, T., Suzuki, K., Dubey, A. K., Wang, X., Gudapaty, S., Morozov, I., et al. (2003). A novel sRNA component of the carbon storage regulatory system of *Escherichia coli*. *Mol. Microbiol.* 48, 657–670. doi: 10.1046/j.1365-2958.2003.03459.x
- Will, S., Joshi, T., Hofacker, I. L., Stadler, P. F., and Backofen, R. (2012). LocARNA-P: accurate boundary prediction and improved detection of structural RNAs. *RNA* 18, 900–914. doi: 10.1261/rna.029041.111
- Will, S., Reiche, K., Hofacker, I. L., Stadler, P. F., and Backofen, R. (2007). Inferring noncoding RNA families and classes by means of genome-scale structure-based clustering. *PLoS Comput. Biol.* 3:e65. doi: 10.1371/journal.pcbi.0030065
- Wille, T., Barlag, B., Jakovljevic, V., Hensel, M., Sourjik, V., and Gerlach, R. G. (2015). A gateway-based system for fast evaluation of protein-protein interactions in bacteria. *PLoS One* 10:e0123646. doi: 10.1371/journal.pone.0123646
- Yeung, M. L., Bennasser, Y., Watashi, K., Le, S.-Y., Houzet, L., and Jeang, K.-T. (2009). Pyrosequencing of small non-coding RNAs in HIV-1 infected cells: evidence for the processing of a viral-cellular double-stranded RNA hybrid. *Nucleic Acids Res.* 37, 6575–6586. doi: 10.1093/nar/gkp707
- Zhang, X., and Bremer, H. (1995). Control of the *Escherichia coli* rrnB P1 promoter strength by ppGpp. *J. Biol. Chem.* 270, 11181–11189.
- Zhou, J., and Rudd, K. E. (2012). EcoGene 3.0. *Nucleic Acids Res.* 41, D613–D624. doi: 10.1093/nar/gks1235
- Zuker, M. (2003). Mfold web server for nucleic acid folding and hybridization prediction. *Nucleic Acids Res.* 31, 3406–3415.

Conflict of Interest: The authors declare that the research was conducted in the absence of any commercial or financial relationships that could be construed as a potential conflict of interest.

Copyright © 2021 Stenum, Kongstad, Holmqvist, Kallipolitis, Svenningsen and Sørensen. This is an open-access article distributed under the terms of the Creative Commons Attribution License (CC BY). The use, distribution or reproduction in other forums is permitted, provided the original author(s) and the copyright owner(s) are credited and that the original publication in this journal is cited, in accordance with accepted academic practice. No use, distribution or reproduction is permitted which does not comply with these terms.



Transfer RNA-Derived Fragments, the Underappreciated Regulatory Small RNAs in Microbial Pathogenesis

Zhongyou Li and Bruce A. Stanton*

Department of Microbiology and Immunology, Geisel School of Medicine at Dartmouth, Hanover, NH, United States

OPEN ACCESS

Edited by:

Florence Hommais,
Université Claude Bernard Lyon 1,
France

Reviewed by:

Norbert Polacek,
University of Bern, Switzerland
David Lalaouna,
UPR9002 Architecture et Réactivité
de l'arN, France

*Correspondence:

Bruce A. Stanton
bas@dartmouth.edu

Specialty section:

This article was submitted to
Microbial Physiology and Metabolism,
a section of the journal
Frontiers in Microbiology

Received: 29 March 2021

Accepted: 26 April 2021

Published: 17 May 2021

Citation:

Li Z and Stanton BA (2021) Transfer
RNA-Derived Fragments, the
Underappreciated Regulatory Small
RNAs in Microbial Pathogenesis.
Front. Microbiol. 12:687632.
doi: 10.3389/fmicb.2021.687632

In eukaryotic organisms, transfer RNA (tRNA)-derived fragments have diverse biological functions. Considering the conserved sequences of tRNAs, it is not surprising that endogenous tRNA fragments in bacteria also play important regulatory roles. Recent studies have shown that microbes secrete extracellular vesicles (EVs) containing tRNA fragments and that the EVs deliver tRNA fragments to eukaryotic hosts where they regulate gene expression. Here, we review the literature describing microbial tRNA fragment biogenesis and how the fragments secreted in microbial EVs suppress the host immune response, thereby facilitating chronic infection. Also, we discuss knowledge gaps and research challenges for understanding the pathogenic roles of microbial tRNA fragments in regulating the host response to infection.

Keywords: transfer RNA fragments, regulatory RNA, extracellular vesicles, outer membrane vesicles, microbial small RNAs, host-pathogen interaction

INTRODUCTION

To thrive in harsh conditions, micro-organisms must respond to changes in the environment, including iron deprivation, nutrient starvation, and host immune responses. The transcriptional and post-transcriptional regulation by small RNAs (sRNAs) is a highly efficient mechanism to reshape microbial transcriptomes and metabolism in response to changes in the environment. Conventional microbial sRNAs are heterogeneous in size, ranging from 50 to 500 nt, and regulate gene expression by base-pairing with the translation initiation region or coding sequence of target mRNAs or by acting as sRNA sponges (Carrier et al., 2018). In the past decade, microbial non-coding sRNAs (ncRNAs) originating from intergenic regions have been characterized and reviewed extensively (Wagner and Romby, 2015; Carrier et al., 2018). Usually, ncRNAs from the intergenic regions have their promoters, and hence their expression is dictated by promoter activity and transcriptional regulators. Recently, it has become evident that intergenic regions are not the only source of microbial sRNAs. For example, sRNAs cleaved from 5' or 3' untranslated regions of mRNAs with regulatory roles have been reported (Ren et al., 2017; Manna et al., 2018).

Advancements in sRNA sequencing technologies and bioinformatics tools have led to the discovery of transfer RNA (tRNA)-derived fragments, leading to functional studies that have elucidated the regulatory roles of these fragments (Su et al., 2020). In eukaryotes and prokaryotes, tRNAs are the most abundant RNA species by the number of molecules (Neidhardt, 1996; Palazzo and Lee, 2015) and are evolutionarily conserved. Although most studies examining the role of tRNA-derived fragments have been conducted in mammals, in this mini-review, we focus on studies describing the biogenesis and cell-autonomous effects of microbial tRNA fragments. Also, we review papers that report the role of microbial tRNA fragments secreted in extracellular vesicles (EVs) and how they regulate gene expression in the host.

Extracellular vesicles secreted by microbes serve various functions, including intra-kingdom and inter-kingdom transfer of toxins, virulence factors, DNA, sRNAs, and tRNA fragments (Wang and Fu, 2019; Ahmadi Badi et al., 2020). There are several categories of EVs based on their origin, biogenesis, size (10–1,000 nm), and composition (Théry et al., 2018; Toyofuku et al., 2019). One of the main functions of EVs is to protect their RNA content from RNases present in the extracellular environment. In bacteria, the most studied EVs secreted by Gram-negative bacteria are outer membrane vesicles (OMVs) with a single bilayer derived from the outer membrane (Jan, 2017). Also, outer-inner membrane vesicles (O-IMVs), having a double bilayer composed of the outer and inner membranes, are secreted by Gram-negative bacteria, but only represent a very small fraction of EVs (Pérez-Cruz et al., 2015). OMVs and O-IMVs are ~100 nm vesicles that subserve various functions, including pathogen-pathogen interactions, and delivering virulence factors, sRNAs and tRNA fragments into host cells to modulate the host immune response (Kaparakis-Liaskos and Ferrero, 2015; Koeppen et al., 2016; Vitse and Devreese, 2020). Gram-positive bacteria and fungal pathogens also secrete EVs that contain sRNAs, tRNAs, and tRNA fragments (Peres da Silva et al., 2015; Resch et al., 2016; Alves et al., 2019; Rodriguez and Kuehn, 2020; Joshi et al., 2021). In sum, microbial EVs containing sRNAs and tRNA fragments deliver their contents to recipient cells, and a few studies have shown by transfecting synthetic RNA oligos and making sRNA-deletion mutants, that sRNAs and tRNAs regulate gene expression in eukaryotic host cells (Garcia-Silva et al., 2014a; Koeppen et al., 2016; Choi et al., 2017; Zhang et al., 2020).

This article summarizes the current stage of knowledge regarding the biogenesis of microbial tRNA fragments and their regulatory roles in pathogens and host cells. In addition, important knowledge gaps and research challenges regarding their roles in microbial pathogenesis will be discussed.

MICROBIAL tRNA FRAGMENTS AND THEIR BIOGENESIS

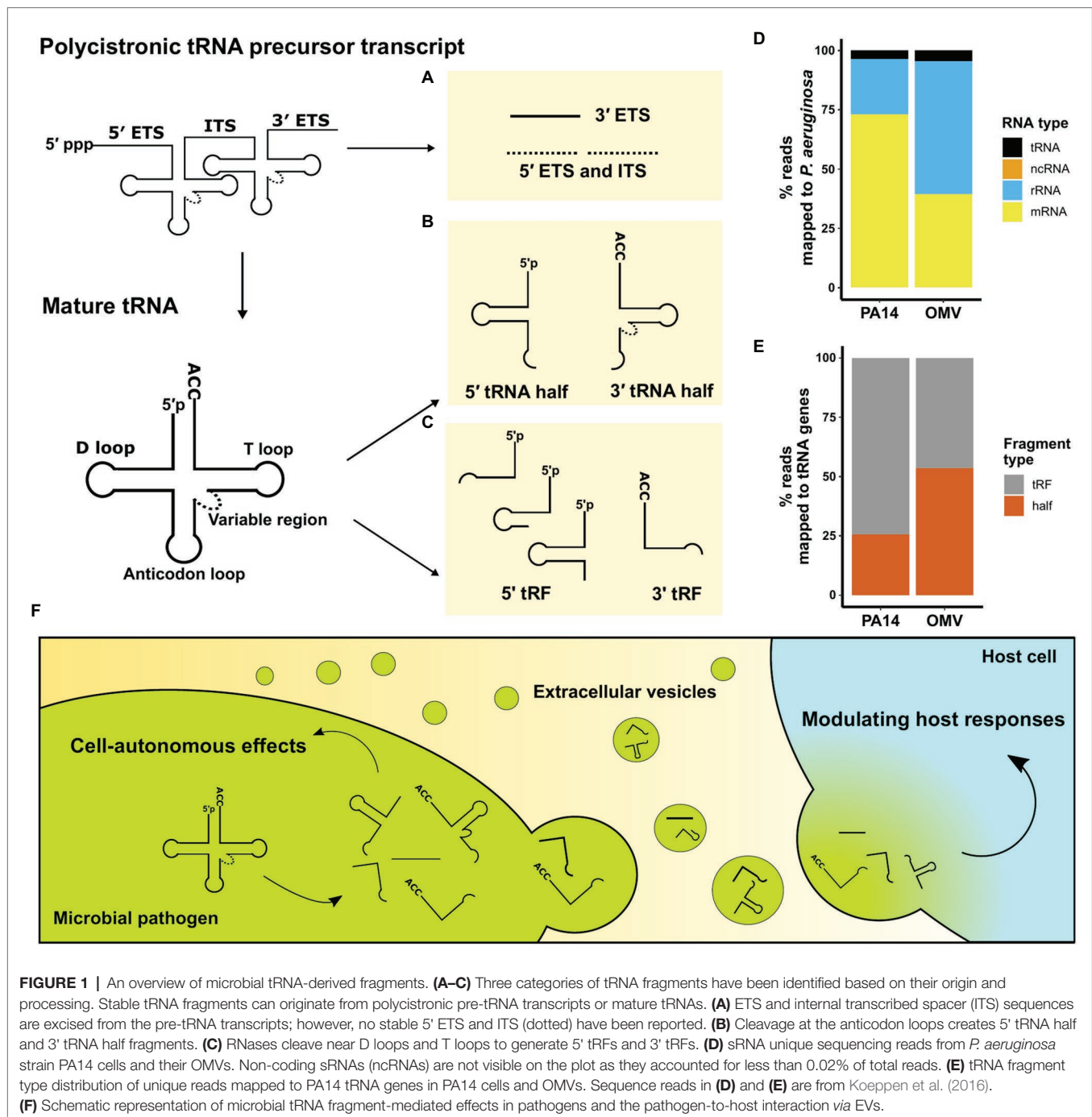
Transfer RNAs are 70–100 nucleotides (nt) long molecules with highly conserved sequences that form secondary cloverleaf and L-shaped three-dimensional structures (Fujishima and Kanai, 2014). Besides their well-known function as amino acid carriers to decode mRNA sequences in eukaryotes, numerous non-canonical

roles of tRNAs have been identified, including tRNA fragment mediated gene silencing through an Argonaute-microRNA like mechanism (Maute et al., 2013) and both negative and positive effects on global regulation of protein translation (Yamasaki et al., 2009; Kim et al., 2017). The roles of tRNA fragments in eukaryotes have been extensively reviewed (Keam and Hutvagner, 2015; Su et al., 2020). tRNA fragments were first described in *Escherichia coli* in response to bacteriophage infection (Levitz et al., 1990). Over the past decades, using northern blot analysis and sRNA sequencing techniques, tRNA fragments have been found in all domains of life and are not random degradation products (Kumar et al., 2014). This article summarizes identified microbial tRNA fragments into three categories (**Figures 1A–C**). They are either derived from a polycistronic tRNA precursor transcript or a mature tRNA and include: (1) external transcribed spacer (ETS) and internal transcribed spacer (ITS) sequences, (2) 5' and 3' tRNA halves, and (3) 5' tRNA-derived fragments (5' tRFs) and 3' tRNA-derived fragments (3' tRFs).

The first category of tRNA fragments is the spacer RNAs arising from the tRNA maturation process (**Figure 1A**). tRNA precursors contain a 5' ETS and a 3' ETS. Prokaryotic tRNA precursors from operons have ITS to separate tRNAs. Multiple ribonucleases, including RNase P and E, are required to generate mature tRNAs and release ETS and ITS (Esakova and Krasilnikov, 2010; Shepherd and Ibba, 2015).

The second category of tRNA fragments consists of 5' tRNA halves and 3' tRNA halves, which are products of endoribonuclease-mediated cleavage in the anticodon loop of mature tRNAs (**Figure 1B**). 5' tRNA halves are 32–40 nucleotides from the 5' terminus of mature tRNAs, while 3' halves are 40–50 bases from the anticodon loop to the 3' terminus due to the variable region and 3'-CCA. Various anticodon ribonucleases (ACNases) targeting the anticodon loop have been identified. In *E. coli*, T4 phage infection activates PrrC, a tRNA^{Lys}-specific ACNase, as one of the suicidal events to protect the population from infection (Morad et al., 1993). Colicin E5 and Colicin D secreted from *E. coli* are ACNases that cleave multiple tRNAs of competing *E. coli* strains in half (Ogawa et al., 1999; Tomita et al., 2000). Ogawa et al. (2020) revealed that the anticodon-loop sequence of tRNA^{Arg} determines its susceptibility to colicin D, and they also demonstrated that the cleaved tRNA^{Arg} occupies the ribosome A-site leading to the impairment of translation. Similarly, fungi secrete different ribotoxins that generate 5' tRNA halves and 3' tRNA halves which inhibit cell growth of nonself yeast cells (Lu et al., 2005; Chakravarty et al., 2014). *Mycobacterium tuberculosis* produces MazF-mt9 that cleaves tRNA^{Lys} in half, which downregulates bacterial growth (Schifano et al., 2016). Ribotoxins including VapCs in *M. tuberculosis*, *Shigella flexneri*, and *Salmonella enterica* target the anticodon loop of different tRNAs to modulate translation (Winther and Gerdes, 2011; Winther et al., 2016).

The third category of tRNA fragments includes 5' tRFs and 3' tRFs. These tRFs are cleavage products near the D loop or in the T loop of mature tRNAs (**Figure 1C**). 5' tRFs start from the extreme 5' end into the D stem, D loop, or anticodon stem; hence, 5' tRFs usually range from 18 to 31 nt. 3' tRFs are defined as sRNAs derived from cleavage in the T loop with a



3'-CCA end and about 18–22 nt in length. MazF-mt9 toxin in *M. tuberculosis* has been reported to cleave tRNA^{Pro} to generate 5' tRFs (Schifano et al., 2016). Due to the size similarity between microRNAs (miRNAs) in eukaryotes and tRFs, the miRNA generation machinery has been implicated in generating 5' tRFs and 3' tRFs. Dicer, which plays a major role in the maturation of miRNAs, also cleaves several mature tRNAs to generate tRFs in vertebrates (Cole et al., 2009; Shigematsu and Kirino, 2015). sRNA sequencing analyses comparing wildtype and Dicer knockout cells in different eukaryotes reveal that Dicer is dispensable for

the biogenesis of the majority of 5' tRFs and 3' tRFs (Li et al., 2012; Kumar et al., 2014); however, in prokaryotes, the biogenesis of tRFs remains largely unknown at this time.

MICROBIAL tRNA FRAGMENTS AND THEIR CELL-AUTONOMOUS EFFECTS

Lalaouna et al. (2015) identified the first functional tRNA fragment from an ETS in *E. coli* and demonstrated that the

3' ETS of *leuZ* (3' ETS^{leuZ}) is an sRNA sponge that inhibits the activity of target sRNAs, RyhB, and RybB. RyhB and RybB regulate iron homeostasis and outer membrane integrity, respectively. To demonstrate the physiological role of 3' ETS^{leuZ} in *E. coli*, the authors reported that it prevents cells from using succinate as the sole carbon source and decreases antibiotic colicin sensitivity. Importantly, they demonstrated that Hfq, a conserved bacterial RNA-binding protein, is required to form the tRNA fragment-sRNA target complex.

Gebetsberger et al. (2012) sequenced sRNAs co-purified with ribosomes of *Haloferax volcanii*, a halophilic archaeon, and identified multiple 5' tRFs. They found that cells grown under elevated pH have abundant 5' tRNA^{Val} fragment, which binds to small ribosomal subunits to inhibit translation globally. In addition, the 5' tRNA^{Val} fragment of *H. volcanii* also attenuates protein synthesis by *S. cerevisiae* and *E. coli*'s ribosomes (Gebetsberger et al., 2017). Also the 3' tRNA^{Thr} half from *Trypanosoma brucei* has a similar effect in *H. volcanii* and *S. cerevisiae* to mediate translation stimulation (Fricker et al., 2019). These reports suggest a functionally conserved mode of action across life domains. Similar regulatory roles of 5' tRFs and 3' tRFs in *S. cerevisiae* have also been identified. Several tRFs in yeast bind to the small ribosomal subunits and aminoacyl-tRNA synthetases to reduce global translation (Mlecenko et al., 2018).

Although 5' and 3' tRNA halves have been identified in many studies, the cell-autonomous effects of tRNA halves are largely unknown. Studies in *M. tuberculosis* and *Aspergillus fumigatus* suggest that micro-organisms maintain their persistence in host cells or remain in a life stage by cleaving tRNAs in half (Jöchl et al., 2008; Winther et al., 2016). Selective human 5' tRNA halves identified in saliva have high sequence similarity to tRNAs of *Fusobacterium nucleatum*, an oral opportunistic pathogen. Co-culture of human 5' tRNA halves with *F. nucleatum* inhibits bacterial growth, likely through interference with bacterial protein biosynthesis (He et al., 2018). Several studies have also demonstrated that environmental stress increases cytosolic tRNA halves in microbes (Thompson et al., 2008; Garcia-Silva et al., 2010; Fricker et al., 2019; Raad et al., 2021); however, the function of 5' and 3' tRNA halves induced by stress remains elusive.

Taken together, these initial reports describing the ubiquity and the function of cytosolic tRNA fragments in microbial cells and the differential expression of specific tRNA fragments (summarized in **Table 1**) suggest their possible roles in bacterial homeostasis and in regulating the expression of virulence factors.

EXTRACELLULAR VESICLES ARE IMPORTANT MEDIATORS OF INTERCELLULAR COMMUNICATION AND DELIVERY OF tRNA FRAGMENTS TO THE HOST

Intercellular communication mediated by EVs is an important aspect of host-pathogen interaction without direct cell-cell

contact (Yáñez-Mó et al., 2015). Secretion of EVs as a mechanism of inter-kingdom and intra-kingdom communication is evolutionarily conserved, as organisms from prokaryotes, plants, and animal cells release EVs into the surrounding environment (Deatherage and Cookson, 2012; Gill et al., 2019; Woith et al., 2019). Identification of regulatory tRNA fragments in EVs has recently garnered attention and led to extensive sRNA content profiling of EVs secreted by Gram-negative and Gram-positive bacteria, fungi, and intracellular parasites (summarized in **Table 1**). Ghosal et al. (2015) performed the first comprehensive sRNA profiling comparing *E. coli* and their secreted OMVs. In *E. coli* OMVs, over 90% of sequence reads were mapped to tRNA fragments, and the authors reported differential packaging of tRNA fragments in OMVs. In a study sequencing sRNA in *Pseudomonas aeruginosa* (Koeppen et al., 2016), we found that tRNA fragments are more abundant than canonical ncRNAs (**Figure 1D**), and those tRNA fragments are differentially packaged in OMVs (**Figure 1E**). Moreover, we exposed human primary bronchial epithelial (HBE) cells to OMVs and used sRNA sequencing to demonstrate that tRNA fragments are the main *P. aeruginosa* sRNAs transferred from OMVs to host cells after exposure. Although tRNA fragments are only a small fraction of sRNAs in OMVs, their predominance in host cells suggests that tRNA fragments may have longer half-lives than other more abundant sRNAs. Moreover, EVs produced by *Trichomonas vaginalis* encapsulate abundant 5' tRNA halves and fuse with benign prostate hyperplasia (BPH-1) cells to deliver sRNAs (Artuyants et al., 2020). In addition, EVs secreted by Gram-positive bacteria, fungi, and even intracellular parasites also deliver protein toxins and sRNA products to host cells to modulate the host immune response (Rodrigues et al., 2008; Rivera et al., 2010; Silverman et al., 2010; Resch et al., 2016; Munhoz da Rocha et al., 2020).

Several studies have reported that tRNA fragments secreted in OMVs are involved in host-pathogen interactions. We demonstrated that sRNA52320, a 24-nt long 5' tRNA^{Met} fragment, is secreted by *P. aeruginosa* in OMVs that fuse with primary HBE cells and attenuates OMV-induced IL-8 secretion and recruitment of neutrophils into mouse lung by reducing the expression of mitogen-activated protein kinases (MAPK; Koeppen et al., 2016). In our study, we used miRanda, a miRNA target prediction algorithm, to reveal that the 5' tRNA^{Met} fragment has specific targets in the MAPK signaling pathway in the host, including MAP2K2, MAP2K3, MAP2K4, MAP3K7, and PIK3R2. An unbiased proteomics approach confirmed our target predictions. In addition, sR-2509025, a 31-nt 5' tRNA^{Met} fragment, is secreted by *Helicobacter pylori* in OMVs and is delivered to human gastric adenocarcinoma cells and diminish LPS-induced IL-8 secretion (Zhang et al., 2020). Intriguingly, the 5' tRNA^{Met} fragments identified from these two independent studies have a high sequence similarity, with only four nucleotides difference in the 24-nt long overlapping region. Moreover, Garcia-Silva et al. (2014a,b) demonstrated that tRNA halves in *Trypanosoma cruzi* EVs are delivered into HeLa cells where the 5' tRNA^{Thr} half modulates the immune response, including upregulating CXCL2 gene expression.

TABLE 1 | Studies identifying and characterizing microbial transfer RNA (tRNA) fragments.

Microbial species	Description of identified tRNA fragments	Proposed function and relevant findings of tRNA fragments	Reference
<i>Aspergillus fumigatus</i> (ATCC46645)	5' and 3' tRNA halves from multiple tRNAs during conidiogenesis were detected by northern blot analysis.	The cleavage of tRNAs into halves causes conidial tRNA depletion leading to the resting stage of <i>A. fumigatus</i> .	Jöchl et al., 2008
<i>Saccharomyces cerevisiae</i>	5' and 3' tRNA halves from multiple tRNAs were detected by northern blot analysis during oxidative stress and stationary phase.	tRNA cleavage is not a function of quality control and unlikely to inhibit protein synthesis.	Thompson et al., 2008; Thompson and Parker, 2009
<i>Trypanosoma cruzi</i>	About 25% of small RNAs (sRNAs) sequenced in the unicellular parasites were 5' tRNA halves from three specific tRNA isoacceptors.	Nutritional stress induces a significant increase of tRNA halves.	Garcia-Silva et al., 2010
<i>Trypanosoma cruzi</i>	tRNA fragments were the second most abundant class in extracellular vesicles (EVs). A high level of tRNA halves from specific tRNA isoacceptors suggests differential packaging.	5' tRNA halves are transferred between parasites to host cells via EVs. 5' tRNA halves affect gene expression patterns in host cells.	Bayer-Santos et al., 2014; Garcia-Silva et al., 2014a,b
<i>Escherichia coli</i> (MG1655)	Abundant tRNA fragments were found in both <i>E. coli</i> cells and outer membrane vesicles (OMVs). Over 90% of sRNA reads in OMVs were mapped to tRNA fragments.	The first report providing detailed profiling of the RNA content in <i>E. coli</i> cells and their OMVs and suggesting selective tRFs are packed into EVs.	Ghosal et al., 2015
<i>Escherichia coli</i> (MG1655)	Excised 3' external transcribed spacer (ETS) of <i>leuZ</i> (3' ETS _{leuZ} , 53 nt-long) was co-purified with sRNAs RyhB, and RybB.	3' ETS _{leuZ} is excised from the pre-tRNA transcript and acts as an sRNA sponge in <i>E. coli</i> to suppress the activity of sRNAs modulating tricarboxylic acid cycle fluxes and antibiotic sensitivity.	Lalaouna et al., 2015, 2017
<i>Candida albicans</i> , <i>Cryptococcus neoformans</i> , <i>Paracoccidioides brasiliensis</i> , <i>Saccharomyces cerevisiae</i>	A high abundance of 3' tRF Arginine (CCU) was found in fungal EVs. sRNA reads mapped to tRNAs account for 20–60% of all reads.	Arginine tRNA (CCU) is required to synthesize the heat shock protein at high temperatures through the regulation of translational frameshift. The production of 3' tRF from this tRNA is suggested to affect fungal gene expression.	Peres da Silva et al., 2015
<i>Leishmania donovani</i> , <i>Leishmania braziliensis</i>	About 25–45% of all reads in the <i>Leishmania</i> EVs were mapped to tRNA fragments. Among those, 5' tRNA halves from a small subset of the same tRNA isoacceptors accounted for the majority of reads.	tRNA fragments and other sRNAs in EVs are delivered into macrophages.	Lambertz et al., 2015
<i>Pseudomonas aeruginosa</i>	Multiple tRNA fragments were detected in microbes and OMVs. sRNA52320, a 5' tRNA ^{Met} fragment and a 5' tRNA ^{Met} half were differentially enriched in the OMVs compared to the cells.	A 5' tRNA ^{Met} fragment is transferred into host cells where it targets the LPS-induced MAPK pathway to reduce IL-8 secretion.	Koeppen et al., 2016
<i>Escherichia coli</i> (UPEC) strain 536	In EVs, 27% of sRNA reads were mapped to tRNA fragments, and only 0.23% reads were mapped to mature intact tRNAs.	Detailed profiling of total RNA in EVs secreted by uropathogenic <i>E. coli</i> adds to the growing evidence of host-pathogen interactions mediated by sRNAs in EVs.	Blenkiron et al., 2016
<i>Mycobacterium tuberculosis</i>	Multiple tRNA halves were identified by using deep sequencing and northern blot analyses.	Twelve anticodon nucleases cleave essential tRNAs to halt protein synthesis leading to survival in host cells.	Winther et al., 2016
<i>Mycobacterium tuberculosis</i>	MazF-mt9 toxin cleaves tRNA ^{Phe14} and tRNA ^{Lys43} in the D loop and anticodon loop, respectively.	The cleavage of specific tRNAs arrests translation and bacterial growth.	Schifano et al., 2016
<i>Haloferax volcanii</i>	Multiple 5' tRNA-derived fragments (tRFs) were co-purified with ribosomes and detected by sRNA sequencing and northern blot analyses.	5' tRNA ^{Val} fragment production is induced at elevated pH, and the fragment binds to small ribosomal subunits to attenuate global translation.	Gebetsberger et al., 2012, 2017
<i>Saccharomyces cerevisiae</i>	Multiple 5' tRFs and 3' tRFs were co-purified with ribosomes and detected by northern blot analyses.	tRFs binds to small ribosomal subunit and aminoacyl-tRNA synthetases to attenuate global translation.	Mleczo et al., 2018

(Continued)

TABLE 1 | Continued

Microbial species	Description of identified tRNA fragments	Proposed function and relevant findings of tRNA fragments	Reference
<i>Trypanosoma brucei</i>	tRNA halves were significantly induced during nutrient deprivation. 3' tRNA ^{Thr} half was the most abundant sRNAs.	3' tRNA ^{Thr} half associates with ribosomes to stimulate translation during the recovery from nutritional stress.	Fricker et al., 2019
<i>Bradyrhizobium japonicum</i> (rhizobium)	Rhizobial tRFs were identified in soybean nodules.	Rhizobial 5' and 3' tRFs are positive regulators of plant nodulation mediated by AGO1.	Ren et al., 2019
<i>Escherichia coli</i>	The susceptibility of four <i>E. coli</i> tRNA ^{Arg} isoacceptors to colicin D, an anticodon nuclease, was tested.	Cleaved tRNA ^{Arg} occupies ribosomal A-site and thus impairs protein translation.	Ogawa et al., 2020
<i>Helicobacter pylori</i> J99	3' tRNA ^{Asn} half and 5' tRNA ^{Met} fragment were identified as the most abundant and differentially packed sRNAs in EVs.	sR-2509025, a 5' tRNA ^{Met} fragment, is transferred from OMVs into human gastric adenocarcinoma cells and reduced the OMV-induced IL-8 secretion.	Zhang et al., 2020
<i>Trichomonas vaginalis</i>	Around 88.2% of sRNA reads in EVs were mapped to tRNA fragments.	5' tRNA halves are the most abundant sRNAs in EVs. The delivery of RNA cargo from EVs to host cells is via lipid raft-dependent endocytosis.	Artuyants et al., 2020
<i>Escherichia coli</i> (MG1655)	Multiple tRNA fragments were detected in total RNA of cells from different growth stages.	Multiple tRFs are enriched in the stationary but not exponential phase suggesting the possible role of maintaining the stationary phase as well as the bacterial stress response.	Raad et al., 2021

Considering the findings discussed above, we propose that tRNA fragments delivered by microbial EVs to host cells are a widespread mechanism utilized to hijack the host immune response to enhance survival (Figure 1F). Additional studies are required to test this hypothesis, including studies on how microbes regulate the biogenesis of tRNA fragments in response to different environmental stimuli, the molecular mechanisms of differential packaging of tRNA fragments in EVs, and the molecular mechanisms whereby microbial tRNA fragments regulate the eukaryotic host response to infection. It will be informative to determine if microbial tRNA fragments delivered to eukaryotic hosts utilize the same mechanisms that mammalian tRNA fragments utilize (Chen and Shen, 2020).

CONCLUSION AND PERSPECTIVES

Recent studies have demonstrated that tRNA fragments secreted by microbes in EVs regulate gene expression in various hosts, thus representing an important but underappreciated mechanism of host-pathogen interactions. Although progress has been made in elucidating the role of tRNA fragments in regulating gene expression in microbes and their hosts, there is much to be learned. For example, although sRNA sequencing has identified tRNA fragments in microbes and EVs, it is important to note current sequencing limitations and biases. First, most of the current approaches of preparing sRNA sequencing libraries rely on adaptor ligation, which requires 5' monophosphate and 3' OH of RNA molecules. This requirement limits the tRNA fragments that can be identified. For example, 5' ETS with 5' triphosphates and

tRNA halves with 2-3-cyclic phosphate at the 3' end or 5' OH created by ACNases are not amenable to adaptor ligation. However, there are methods that use different enzymes to treat RNA samples before adaptor ligation to enrich RNA molecules with different end chemistries (Thomason et al., 2015; Shigematsu et al., 2018). Second, there are more than 90 post-transcriptional modifications found in tRNAs, which are required for their activity, and some of them impede reverse transcription during library preparation and RT-PCR experiments, which could lead to inaccurate profiling of tRNA fragments (Kellner et al., 2010; Lorenz et al., 2017). Also, the stable structure of tRNAs interferes with cDNA synthesis (Zheng et al., 2015; Behrens et al., 2021). Thus, new approaches are needed to identify tRNA fragments more thoroughly. In addition, better algorithms are needed to predict targets of tRNA fragments. Although tRNA fragments regulate gene expression by base-pairing with target genes in host cells, which is reminiscent of microRNA-mRNA interactions in eukaryotes, targeting algorithms for tRNA fragments should be improved due to a variety of factors. For example, sRNAs base-pair to targets with limited complementarity and conserved sequences called seed regions; however, the seed regions of tRFs and tRNA halves have not been fully characterized; thus, a better understanding of seed regions in tRNA fragments is required for a more accurate target prediction. With a better understanding of the targeting rules of tRNA fragments, it would be possible to generalize experiment findings on one tRNA fragment to other pathogens, given the highly conserved tRNA sequences in microbes (Saks and Conery, 2007).

Additional outstanding questions regarding the role of tRNA fragments in mediating host-pathogen interactions are worthy

of note. Is the production and packaging of tRNA fragments into microbial EVs regulated? Does the nucleotide sequence or secondary structure determine differential packaging? How is the secretion of EVs regulated? How do microbial tRNA fragments regulate gene expression in eukaryotic cells? To what extent do microbial EVs in plasma regulate multiple organs? Do differences in EV isolation methods affect EV cargo and the effect of EVs on host cell biology? In this regard, the International Society of Extracellular Vesicles (ISEV) has published a suggested set of standards to increase rigor and reproducibility in EV research (Théry et al., 2018).

In conclusion, despite numerous publications demonstrating the existence of tRNA fragments in microbes and in secreted EVs, many details on the immunoregulatory role of tRNA fragments in regulating the host are unknown. We postulate that tRNA fragments are underappreciated molecules in microbial physiology and host-pathogen interactions (Figure 1F). We anticipate that a greater focus on these molecules in future investigations will lead to a more complete understanding of their roles in mediating host-pathogen interactions.

REFERENCES

- Ahmadi Badi, S., Bruno, S. P., Moshiri, A., Tarashi, S., Siadat, S. D., and Masotti, A. (2020). Small RNAs in outer membrane vesicles and their function in host-microbe interactions. *Front. Microbiol.* 11:1209. doi: 10.3389/fmicb.2020.01209
- Alves, L. R., da Silva, R. P., Sanchez, D. A., Zamith-Miranda, D., Rodrigues, M. L., Goldenberg, S., et al. (2019). Extracellular vesicle-mediated RNA release in *Histoplasma capsulatum*. *mSphere* 4, e00176–e00119. doi: 10.1128/mSphere.00176-19
- Artuyants, A., Campos, T. L., Rai, A. K., Johnson, P. J., Dauros-Singorenko, P., Phillips, A., et al. (2020). Extracellular vesicles produced by the protozoan parasite *Trichomonas vaginalis* contain a preferential cargo of tRNA-derived small RNAs. *Int. J. Parasitol.* 50, 1145–1155. doi: 10.1016/j.ijpara.2020.07.003
- Bayer-Santos, E., Lima, F. M., Ruiz, J. C., Almeida, I. C., and da Silva, J. F. (2014). Characterization of the small RNA content of *Trypanosoma cruzi* extracellular vesicles. *Mol. Biochem. Parasitol.* 193, 71–74. doi: 10.1016/j.molbiopara.2014.02.004
- Behrens, A., Rodschinka, G., and Nedialkova, D. D. (2021). High-resolution quantitative profiling of tRNA abundance and modification status in eukaryotes by mim-tRNAseq. *Mol. Cell* 81, 1802–1815.e7. doi: 10.1016/j.molcel.2021.01.028
- Blenkiron, C., Simonov, D., Muthukaruppan, A., Tsai, P., Dauros, P., Green, S., et al. (2016). Uropathogenic *Escherichia coli* releases extracellular vesicles that are associated with RNA. *PLoS One* 11:e0160440. doi: 10.1371/journal.pone.0160440
- Carrier, M. -C., Lalaouna, D., and Massé, E. (2018). Broadening the definition of bacterial small RNAs: characteristics and mechanisms of action. *Annu. Rev. Microbiol.* 72, 141–161. doi: 10.1146/annurev-micro-090817-062607
- Chakravarty, A. K., Smith, P., Jalan, R., and Shuman, S. (2014). Structure, mechanism, and specificity of a eukaryal tRNA restriction enzyme involved in self-nonspecific discrimination. *Cell Rep.* 7, 339–347. doi: 10.1016/j.celrep.2014.03.034
- Chen, Y., and Shen, J. (2020). Mucosal immunity and tRNA, tRF, and tiRNA. *J. Mol. Med.* 99, 47–56. doi: 10.1007/s00109-020-02008-4
- Choi, J. -W., Kim, S. -C., Hong, S. -H., and Lee, H. -J. (2017). Secreted small RNAs via outer membrane vesicles in periodontal pathogens. *J. Dent. Res.* 96, 458–466. doi: 10.1177/0022034516685071
- Cole, C., Sobala, A., Lu, C., Thatcher, S. R., Bowman, A., Brown, J. W. S., et al. (2009). Filtering of deep sequencing data reveals the existence of abundant dicer-dependent small RNAs derived from tRNAs. *RNA* 15, 2147–2160. doi: 10.1261/rna.1738409
- Deatherage, B. L., and Cookson, B. T. (2012). Membrane vesicle release in bacteria, eukaryotes, and archaea: a conserved yet underappreciated aspect of microbial life. *Infect. Immun.* 80, 1948–1957. doi: 10.1128/IAI.06014-11

AUTHOR CONTRIBUTIONS

ZL and BS conceived and contributed to the writing of the manuscript. All authors contributed to the article and approved the submitted version.

FUNDING

Grants from the NIH (P30 DK117469 and R01 HL151385) and the Cystic Fibrosis Foundation (STANTO19R0 and STANTO19GO) supported the research described in the authors' laboratory.

ACKNOWLEDGMENTS

We thank Katja Koeppen and Thomas H. Hampton for reviewing this mini review and their collaboration on studies examining the role of tRNA fragments in host-pathogen interactions.

- Esakova, O., and Krasilnikov, A. S. (2010). Of proteins and RNA: The RNase P/MRP family. *RNA* 16, 1725–1747. doi: 10.1261/rna.2214510
- Fricker, R., Brogli, R., Luidalepp, H., Wyss, L., Fasnacht, M., Joss, O., et al. (2019). A tRNA half modulates translation as stress response in *Trypanosoma brucei*. *Nat. Commun.* 10:118. doi: 10.1038/s41467-018-07949-6
- Fujishima, K., and Kanai, A. (2014). tRNA gene diversity in the three domains of life. *Front. Genet.* 5:142. doi: 10.3389/fgene.2014.00142
- Garcia-Silva, M. R., Cabrera-Cabrera, F., Cura das Neves, R. F., Souto-Padrón, T., de Souza, W., and Cayota, A. (2014a). Gene expression changes induced by *Trypanosoma cruzi* shed microvesicles in mammalian host cells: relevance of tRNA-derived halves. *Biomed. Res. Int.* 2014:e305239. doi: 10.1155/2014/305239
- Garcia-Silva, M. R., Cura das Neves, R. F., Cabrera-Cabrera, F., Sanguinetti, J., Medeiros, L. C., Robello, C., et al. (2014b). Extracellular vesicles shed by *Trypanosoma cruzi* are linked to small RNA pathways, life cycle regulation, and susceptibility to infection of mammalian cells. *Parasitol. Res.* 113, 285–304. doi: 10.1007/s00436-013-3655-1
- Garcia-Silva, M. R., Frugier, M., Tosar, J. P., Correa-Dominguez, A., Ronalte-Alves, L., Parodi-Talice, A., et al. (2010). A population of tRNA-derived small RNAs is actively produced in *Trypanosoma cruzi* and recruited to specific cytoplasmic granules. *Mol. Biochem. Parasitol.* 171, 64–73. doi: 10.1016/j.molbiopara.2010.02.003
- Gebetsberger, J., Wyss, L., Mleczo, A. M., Reuther, J., and Polacek, N. (2017). A tRNA-derived fragment competes with mRNA for ribosome binding and regulates translation during stress. *RNA Biol.* 14, 1364–1373. doi: 10.1080/15476286.2016.1257470
- Gebetsberger, J., Zywicki, M., Künzi, A., and Polacek, N. (2012). tRNA-derived fragments target the ribosome and function as regulatory non-coding RNA in *Haloferax volcanii*. *Archaea* 2012:e260909. doi: 10.1155/2012/260909
- Ghosal, A., Upadhyaya, B. B., Fritz, J. V., Heintz-Buschart, A., Desai, M. S., Yusuf, D., et al. (2015). The extracellular RNA complement of *Escherichia coli*. *Microbiology* 4, 252–266. doi: 10.1002/mbio.3.235
- Gill, S., Catchpole, R., and Forterre, P. (2019). Extracellular membrane vesicles in the three domains of life and beyond. *FEMS Microbiol. Rev.* 43, 273–303. doi: 10.1093/femsre/fuy042
- He, X., Li, F., Bor, B., Koyano, K., Cen, L., Xiao, X., et al. (2018). Human tRNA-derived small RNAs modulate host–Oral microbial interactions. *J. Dent. Res.* 97, 1236–1243. doi: 10.1177/0022034518770605
- Jan, A. T. (2017). Outer membrane vesicles (OMVs) of gram-negative Bacteria: A perspective update. *Front. Microbiol.* 8:1053. doi: 10.3389/fmicb.2017.01053
- Jöchl, C., Rederstorff, M., Hertel, J., Stadler, P. F., Hofacker, I. L., Schrettl, M., et al. (2008). Small ncRNA transcriptome analysis from *Aspergillus fumigatus* suggests a novel mechanism for regulation of protein synthesis. *Nucleic Acids Res.* 36, 2677–2689. doi: 10.1093/nar/gkn123

- Joshi, B., Singh, B., Nadeem, A., Askarian, F., Wai, S. N., Johannessen, M., et al. (2021). Transcriptome profiling of *Staphylococcus aureus* associated extracellular vesicles reveals presence of small RNA-cargo. *Front. Mol. Biosci.* 7:566207. doi: 10.3389/fmolb.2020.566207
- Kaparakis-Liaskos, M., and Ferrero, R. L. (2015). Immune modulation by bacterial outer membrane vesicles. *Nat. Rev. Immunol.* 15, 375–387. doi: 10.1038/nri3837
- Keam, S. P., and Hutvagner, G. (2015). tRNA-derived fragments (tRFs): emerging new roles for an ancient RNA in the regulation of gene expression. *Life* 5, 1638–1651. doi: 10.3390/life5041638
- Kellner, S., Burhenne, J., and Helm, M. (2010). Detection of RNA modifications. *RNA Biol.* 7, 237–247. doi: 10.4161/rna.7.2.11468
- Kim, H. K., Fuchs, G., Wang, S., Wei, W., Zhang, Y., Park, H., et al. (2017). A transfer-RNA-derived small RNA regulates ribosome biogenesis. *Nature* 552, 57–62. doi: 10.1038/nature25005
- Koeppen, K., Hampton, T. H., Jarek, M., Scharfe, M., Gerber, S. A., Mielcarz, D. W., et al. (2016). A novel mechanism of host-pathogen interaction through sRNA in bacterial outer membrane vesicles. *PLoS Pathog.* 12:e1005672. doi: 10.1371/journal.ppat.1005672
- Kumar, P., Anaya, J., Mudunuri, S. B., and Dutta, A. (2014). Meta-analysis of tRNA derived RNA fragments reveals that they are evolutionarily conserved and associate with AGO proteins to recognize specific RNA targets. *BMC Biol.* 12:78. doi: 10.1186/s12915-014-0078-0
- Lalaouna, D., Carrier, M.-C., Semsey, S., Brouard, J.-S., Wang, J., Wade, J. T., et al. (2015). A 3' external transcribed spacer in a tRNA transcript acts as a sponge for small RNAs to prevent transcriptional noise. *Mol. Cell* 58, 393–405. doi: 10.1016/j.molcel.2015.03.013
- Lalaouna, D., Prévost, K., Eyraud, A., and Massé, E. (2017). Identification of unknown RNA partners using MAPS. *Methods* 117, 28–34. doi: 10.1016/j.mymeth.2016.11.011
- Lambert, U., Oviedo Ovando, M. E., Vasconcelos, E. J., Unrau, P. J., Myler, P. J., and Reiner, N. E. (2015). Small RNAs derived from tRNAs and rRNAs are highly enriched in exosomes from both old and new world *Leishmania* providing evidence for conserved exosomal RNA packaging. *BMC Genomics* 16:151. doi: 10.1186/s12864-015-1260-7
- Levitz, R., Chapman, D., Amitsur, M., Green, R., Snyder, L., and Kaufmann, G. (1990). The optional *E. coli* prr locus encodes a latent form of phage T4-induced anticodon nuclease. *EMBO J.* 9, 1383–1389. doi: 10.1002/j.1460-2075.1990.tb08253.x
- Li, Z., Ender, C., Meister, G., Moore, P. S., Chang, Y., and John, B. (2012). Extensive terminal and asymmetric processing of small RNAs from rRNAs, snRNAs, and tRNAs. *Nucleic Acids Res.* 40, 6787–6799. doi: 10.1093/nar/gks307
- Lorenz, C., Lünse, C. E., and Mörl, M. (2017). tRNA modifications: impact on structure and thermal adaptation. *Biomol. Ther.* 7:35. doi: 10.3390/biom7020035
- Lu, J., Huang, B., Esberg, A., Johansson, M. J. O., and Byström, A. S. (2005). The *Kluyveromyces fragilis* γ-toxin targets tRNA anticodons. *RNA* 11, 1648–1654. doi: 10.1261/rna.2172105
- Manna, A. C., Kim, S., Cengher, L., Corvaglia, A., Leo, S., Francois, P., et al. (2018). Small RNA teg49 is derived from a sarA transcript and regulates virulence genes independent of SarA in *Staphylococcus aureus*. *Infect. Immun.* 86, e00635–e00617. doi: 10.1128/IAI.00635-17
- Maute, R. L., Schneider, C., Sumazin, P., Holmes, A., Califano, A., Basso, K., et al. (2013). tRNA-derived microRNA modulates proliferation and the DNA damage response and is down-regulated in B cell lymphoma. *PNAS* 110, 1404–1409. doi: 10.1073/pnas.1206761110
- Mleczo, A. M., Celichowski, P., and Bąkowska-Żywicka, K. (2018). Transfer RNA-derived fragments target and regulate ribosome-associated aminoacyl-transfer RNA synthetases. *Biochim. Biophys. Acta Gene Regul. Mech.* 1861, 647–656. doi: 10.1016/j.bbargm.2018.06.001
- Morad, I., Chapman-Shimshoni, D., Amitsur, M., and Kaufmann, G. (1993). Functional expression and properties of the tRNA(Lys)-specific core anticodon nuclease encoded by *Escherichia coli* prrC. *J. Biol. Chem.* 268, 26842–26849. doi: 10.1016/S0021-9258(19)74188-X
- Munhoz da Rocha, I. F., Amatuzzi, R. F., Lucena, A. C. R., Faoro, H., and Alves, L. R. (2020). Cross-kingdom extracellular vesicles EV-RNA communication as a mechanism for host–pathogen interaction. *Front. Cell. Infect. Microbiol.* 10:593160. doi: 10.3389/fcimb.2020.593160
- Neidhardt, F. C. (1996). *Escherichia coli and Salmonella: Cellular and Molecular Biology*. 2nd Edn. Washington, D.C: ASM Press.
- Ogawa, T., Takahashi, K., Ishida, W., Aono, T., Hidaka, M., Terada, T., et al. (2020). Substrate recognition mechanism of tRNA-targeting ribonuclease, colicin D, and an insight into tRNA cleavage-mediated translation impairment. *RNA Biol.* 1–13. doi: 10.1080/15476286.2020.1838782 [Epub ahead of print]
- Ogawa, T., Tomita, K., Ueda, T., Watanabe, K., Uozumi, T., and Masaki, H. (1999). A cytotoxic ribonuclease targeting specific transfer RNA anticodons. *Science* 283, 2097–2100. doi: 10.1126/science.283.5410.2097
- Palazzo, A. F., and Lee, E. S. (2015). Non-coding RNA: what is functional and what is junk? *Front. Genet.* 6:2. doi: 10.3389/fgene.2015.00002
- Peres da Silva, R., Puccia, R., Rodrigues, M. L., Oliveira, D. L., Joffe, L. S., César, G. V., et al. (2015). Extracellular vesicle-mediated export of fungal RNA. *Sci. Rep.* 5:7763. doi: 10.1038/srep07763
- Pérez-Cruz, C., Delgado, L., López-Iglesias, C., and Mercade, E. (2015). Outer-inner membrane vesicles naturally secreted by gram-negative pathogenic bacteria. *PLoS One* 10:e0116896. doi: 10.1371/journal.pone.0116896
- Raad, N., Luidalepp, H., Fasnacht, M., and Polacek, N. (2021). Transcriptome-wide analysis of stationary phase small ncRNAs in *E. coli*. *Int. J. Mol. Sci.* 22:1703. doi: 10.3390/ijms22041703
- Ren, G. -X., Guo, X. -P., and Sun, Y. -C. (2017). Regulatory 3' Untranslated regions of bacterial mRNAs. *Front. Microbiol.* 8:1276. doi: 10.3389/fmicb.2017.01276
- Ren, B., Wang, X., Duan, J., and Ma, J. (2019). Rhizobial tRNA-derived small RNAs are signal molecules regulating plant nodulation. *Science* 365, 919–922. doi: 10.1126/science.aav8907
- Resch, U., Tsatsaronis, J. A., Rhun, A. L., Stübiger, G., Rohde, M., Kasvandik, S., et al. (2016). A two-component regulatory system impacts extracellular membrane-derived vesicle production in group A *Streptococcus*. *MBio* 7, e00207–e00216. doi: 10.1128/mBio.00207-16
- Rivera, J., Cordero, R. J. B., Nakouzi, A. S., Frases, S., Nicola, A., and Casadevall, A. (2010). *Bacillus anthracis* produces membrane-derived vesicles containing biologically active toxins. *PNAS* 107, 19002–19007. doi: 10.1073/pnas.1008843107
- Rodrigues, M. L., Nakayasu, E. S., Oliveira, D. L., Nimrichter, L., Nosanchuk, J. D., Almeida, I. C., et al. (2008). Extracellular vesicles produced by *Cryptococcus neoformans* contain protein components associated with virulence. *Eukaryot. Cell* 7, 58–67. doi: 10.1128/EC.00370-07
- Rodriguez, B. V., and Kuehn, M. J. (2020). *Staphylococcus aureus* secretes immunomodulatory RNA and DNA via membrane vesicles. *Sci. Rep.* 10:18293. doi: 10.1038/s41598-020-75108-3
- Saks, M. E., and Conery, J. S. (2007). Anticodon-dependent conservation of bacterial tRNA gene sequences. *RNA* 13, 651–660. doi: 10.1261/rna.345907
- Schifano, J. M., Cruz, J. W., Vvedenskaya, I. O., Edifor, R., Ouyang, M., Husson, R. N., et al. (2016). tRNA is a new target for cleavage by a MazF toxin. *Nucleic Acids Res.* 44, 1256–1270. doi: 10.1093/nar/gkv1370
- Shepherd, J., and Ibba, M. (2015). Bacterial transfer RNAs. *FEMS Microbiol. Rev.* 39, 280–300. doi: 10.1093/femsre/fuv004
- Shigematsu, M., Kawamura, T., and Kirino, Y. (2018). Generation of 2',3'-cyclic phosphate-containing RNAs as a hidden layer of the transcriptome. *Front. Genet.* 9:562. doi: 10.3389/fgene.2018.00562
- Shigematsu, M., and Kirino, Y. (2015). tRNA-derived short non-coding RNA as interacting Partners of Argonaute Proteins. *Gene Regul. Syst. Bio.* 9:GRSB.S29411. doi: 10.4137/GRSB.S29411
- Silverman, J. M., Clos, J., deOliveira, C. C., Shirvani, O., Fang, Y., Wang, C., et al. (2010). An exosome-based secretion pathway is responsible for protein export from *Leishmania* and communication with macrophages. *J. Cell Sci.* 123, 842–852. doi: 10.1242/jcs.056465
- Su, Z., Wilson, B., Kumar, P., and Dutta, A. (2020). Noncanonical roles of tRNAs: tRNA fragments and beyond. *Annu. Rev. Genet.* 54, 47–69. doi: 10.1146/annurev-genet-022620-101840
- Théry, C., Witwer, K. W., Aikawa, E., Alcaraz, M. J., Anderson, J. D., Andriantsitohaina, R., et al. (2018). Minimal information for studies of extracellular vesicles 2018 (MISEV2018): a position statement of the International Society for Extracellular Vesicles and update of the MISEV2014 guidelines. *J. Extracell. Vesicles* 7:1535750. doi: 10.1080/20013078.2018.1535750
- Thomason, M. K., Bischler, T., Eisenbart, S. K., Förstner, K. U., Zhang, A., Herbig, A., et al. (2015). Global transcriptional start site mapping using differential RNA sequencing reveals novel antisense RNAs in *Escherichia coli*. *J. Bacteriol.* 197, 18–28. doi: 10.1128/JB.02096-14

- Thompson, D. M., Lu, C., Green, P. J., and Parker, R. (2008). tRNA cleavage is a conserved response to oxidative stress in eukaryotes. *RNA* 14, 2095–2103. doi: 10.1261/rna.1232808
- Thompson, D. M., and Parker, R. (2009). The RNase Rny1p cleaves tRNAs and promotes cell death during oxidative stress in *Saccharomyces cerevisiae*. *J. Cell Biol.* 185, 43–50. doi: 10.1083/jcb.200811119
- Tomita, K., Ogawa, T., Uozumi, T., Watanabe, K., and Masaki, H. (2000). A cytotoxic ribonuclease which specifically cleaves four isoaccepting arginine tRNAs at their anticodon loops. *PNAS* 97, 8278–8283. doi: 10.1073/pnas.140213797
- Toyofuku, M., Nomura, N., and Eberl, L. (2019). Types and origins of bacterial membrane vesicles. *Nat. Rev. Microbiol.* 17, 13–24. doi: 10.1038/s41579-018-0112-2
- Vitse, J., and Devreese, B. (2020). The contribution of membrane vesicles to bacterial pathogenicity in cystic fibrosis infections and healthcare associated pneumonia. *Front. Microbiol.* 11:630. doi: 10.3389/fmicb.2020.00630
- Wagner, E. G. H., and Romby, P. (2015). Small RNAs in bacteria and archaea: who they are, what they do, and how they do it. *Adv. Genet.* 90, 133–208. doi: 10.1016/bs.adgen.2015.05.001
- Wang, Y. F., and Fu, J. (2019). Secretory and circulating bacterial small RNAs: a mini-review of the literature. *ExRNA* 1:14. doi: 10.1186/s41544-019-0015-z
- Winther, K. S., and Gerdes, K. (2011). Enteric virulence associated protein VapC inhibits translation by cleavage of initiator tRNA. *PNAS* 108, 7403–7407. doi: 10.1073/pnas.1019587108
- Winther, K., Tree, J. J., Tollervey, D., and Gerdes, K. (2016). VapCs of *Mycobacterium tuberculosis* cleave RNAs essential for translation. *Nucleic Acids Res.* 44, 9860–9871. doi: 10.1093/nar/gkw781
- Woith, E., Fuhrmann, G., and Melzig, M. F. (2019). Extracellular vesicles—connecting kingdoms. *Int. J. Mol. Sci.* 20:5695. doi: 10.3390/ijms20225695
- Yamasaki, S., Ivanov, P., Hu, G., and Anderson, P. (2009). Angiogenin cleaves tRNA and promotes stress-induced translational repression. *J. Cell Biol.* 185, 35–42. doi: 10.1083/jcb.200811106
- Yáñez-Mó, M., Siljander, P. R.-M., Andreu, Z., Zavec, A. B., Borràs, F. E., Buzas, E. I., et al. (2015). Biological properties of extracellular vesicles and their physiological functions. *J. Extracell. Vesicles* 4:27066. doi: 10.3402/jev.v4.27066
- Zhang, H., Zhang, Y., Song, Z., Li, R., Ruan, H., Liu, Q., et al. (2020). sncRNAs packaged by *Helicobacter pylori* outer membrane vesicles attenuate IL-8 secretion in human cells. *Int. J. Med. Microbiol.* 310:151356. doi: 10.1016/j.ijmm.2019.151356
- Zheng, G., Qin, Y., Clark, W. C., Dai, Q., Yi, C., He, C., et al. (2015). Efficient and quantitative high-throughput tRNA sequencing. *Nat. Methods* 12, 835–837. doi: 10.1038/nmeth.3478

Conflict of Interest: The authors declare that the research was conducted in the absence of any commercial or financial relationships that could be construed as a potential conflict of interest.

Copyright © 2021 Li and Stanton. This is an open-access article distributed under the terms of the Creative Commons Attribution License (CC BY). The use, distribution or reproduction in other forums is permitted, provided the original author(s) and the copyright owner(s) are credited and that the original publication in this journal is cited, in accordance with accepted academic practice. No use, distribution or reproduction is permitted which does not comply with these terms.



OmpA, a Common Virulence Factor, Is Under RNA Thermometer Control in *Yersinia pseudotuberculosis*

Daniel Scheller[†], Christian Twittenhoff[†], Franziska Becker, Marcel Holler and Franz Narberhaus*

Department of Microbial Biology, Ruhr University Bochum, Bochum, Germany

OPEN ACCESS

Edited by:

Olga Soutourina,
Institut de Biologie Intégrative de la
Cellule (I2BC), France

Reviewed by:

Pierre Mandin,
Laboratoire de chimie bactérienne
(LCB), France
Ombeline Rossier,
Université Paris-Saclay, France

*Correspondence:

Franz Narberhaus
franz.narberhaus@rub.de

[†]These authors have contributed
equally to this work and share first
authorship

Specialty section:

This article was submitted to
Microbial Physiology and Metabolism,
a section of the journal
Frontiers in Microbiology

Received: 29 March 2021

Accepted: 21 April 2021

Published: 14 May 2021

Citation:

Scheller D, Twittenhoff C, Becker F,
Holler M and Narberhaus F (2021)
OmpA, a Common Virulence Factor,
Is Under RNA Thermometer Control
in *Yersinia pseudotuberculosis*.
Front. Microbiol. 12:687260.
doi: 10.3389/fmicb.2021.687260

The outer membrane protein OmpA is a virulence factor in many mammalian pathogens. In previous global RNA structure probing studies, we found evidence for a temperature-modulated RNA structure in the 5'-untranslated region (5'-UTR) of the *Yersinia pseudotuberculosis* *ompA* transcript suggesting that opening of the structure at host-body temperature might relieve translational repression. Here, we support this hypothesis by quantitative reverse transcription PCR, translational reporter gene fusions, enzymatic RNA structure probing, and toeprinting assays. While *ompA* transcript levels decreased at 37°C compared to 25°C, translation of the transcript increased with increasing temperature. Biochemical experiments show that this is due to melting of the RNA structure, which permits ribosome binding to the 5'-UTR. A point mutation that locks the RNA structure in a closed conformation prevents translation by impairing ribosome access. Our findings add another common virulence factor to the growing list of pathogen-associated genes that are under RNA thermometer control.

Keywords: gene expression, thermosensor, RNA structure, pathogen, virulence, outer membrane protein, porin

INTRODUCTION

OmpA is a highly abundant and conserved outer membrane protein in Gram-negative bacteria (Smith et al., 2007). It has a barrel-like structure that confers porin activity. Apart from its function in the influx and efflux of various compounds, OmpA is a multifaceted protein with various other functions, hence its designation as a molecular Swiss army knife. For instance, it plays an important role in envelope stability. In *Acinetobacter baumannii*, it was shown that two highly conserved residues anchor OmpA to the peptidoglycan layer (Park et al., 2012). In addition, OmpA forms complexes with the outer membrane protein Pal, which also associates with the peptidoglycan layer via a conserved α -helical interaction motif (Clavel et al., 1998).

OmpA and OmpA-like proteins have been recognized as virulence factors and are considered as potential vaccine candidates (Confer and Ayalew, 2013). The mode of action by which OmpA contributes to virulence ranges from adherence to epithelial cells and invasion (Smith et al., 2007; Gaddy et al., 2009) to biofilm formation (Weiser and Gotschlich, 1991; Azghani et al., 2002). In *Escherichia coli*, OmpA contributes to the resistance against serum killing by binding to the C4b-binding protein, which inhibits excessive activation of the complement system (Weiser and Gotschlich, 1991; Prasadarao et al., 2002). *A. baumannii* OmpA confers serum resistance through the acquisition of factor H to the cell surface (Kim et al., 2009).

In addition, secreted *A. baumannii* OmpA is able to facilitate apoptosis by inducing mitochondrial damage and the release of proapoptotic molecules, leading to epithelial cell death (Choi et al., 2005). In a mouse model, *A. baumannii* OmpA is important to induce death as demonstrated by a killing defect of an *ompA* deletion strain (Sánchez-Encinales et al., 2017). In *E. coli* K1, OmpA is required to cause neonatal meningitis by enabling invasion of brain microvascular endothelial cells and crossing the blood-brain barrier (Prasadarao et al., 1996). OmpA in *Yersinia pestis* and *Yersinia pseudotuberculosis* is important for intracellular survival within macrophages as shown by reduced survival of strains lacking *ompA* (Bartra et al., 2012).

The amount of OmpA and other porins in the outer membrane is tightly regulated in response to numerous external conditions. Like many other genes coding for outer membrane proteins, *E. coli ompA* is subject to posttranscriptional regulation by small RNAs (sRNAs; Guillier et al., 2006). The paradigm of this type of control is the regulation of the *ompF* mRNA by the MicF sRNA (Mizuno et al., 1984). The 5'-untranslated region (5'-UTR) of *ompA* base-pairs with the sRNA MicA, which destabilizes the *ompA* transcript and requires the help of the RNA chaperone Hfq (Rasmussen et al., 2005; Udekwi et al., 2005). A second Hfq-dependent sRNA involved in *ompA* regulation in *E. coli* is RseX, which also regulates the expression of another outer membrane protein gene called *ompC* (Douchin et al., 2006).

A fundamentally different mode of riboregulation was recently reported for the *Shigella dysenteriae ompA* gene, which is regulated by a fourU-type RNA thermometer (RNAT; Murphy et al., 2020). *Shigella dysenteriae* is a serious foodborne pathogen causing the diarrheal disease shigellosis, and the OmpA protein is involved in intracellular spreading of the pathogen (Ambrosi et al., 2012). The last 20 residues of the 133-nucleotides long 5'-UTR of the *ompA* transcript fold into a simple hairpin structure, in which four uridines pair with GGAG, a part of the Shine-Dalgarno (SD) sequence. This structure is sufficiently strong to inhibit ribosome access at environmental temperatures but labile enough to denature at a host-body temperature in order to facilitate efficient translation resulting in an elevated level of the virulence factor (Murphy et al., 2020).

Regulating the production of virulence factors like OmpA in response to temperature is a sensible strategy since a shift to 37°C is among the most consistent changes upon arrival in the warm-blooded host. Therefore, many pathogens have established various mechanisms to measure the ambient temperature at the DNA, RNA, or protein level (Steinmann and Dersch, 2013; Mandin and Johansson, 2020). A widely used strategy in numerous pathogenic bacteria is the translational control of virulence-associated genes by RNATs (Loh et al., 2018). The sequence and structure of these regulatory elements are surprisingly diverse. Even orthologous genes in related organisms are controlled by unrelated RNATs, and this is also the case for the *ompA* gene. While the *Shigella ompA* transcript is regulated by a fourU thermometer (Murphy et al., 2020), the RNAT upstream of *ompA* in *Y. pseudotuberculosis* presented here is structurally disparate but functionally equivalent.

Like *Shigella*, *Y. pseudotuberculosis* is a notorious foodborne pathogen causing gut-associated diseases. A considerable number of *Yersinia* virulence genes are temperature regulated, often by riboregulatory processes (Knittel et al., 2018). We identified a very promising RNAT upstream of *ompA* by a global RNA structuromics approach, in which *Y. pseudotuberculosis* RNA structures were probed at three different temperatures (Righetti et al., 2016). Here, we set out to study the structure-function relationship of this temperature-labile element and show that it is a functional RNAT allowing induction of OmpA levels at increasing temperature.

MATERIALS AND METHODS

Bacterial Strains and Plasmids

Bacterial strains used in this study are listed in Table 1. Cells were grown in lysogeny broth (LB; 1% NaCl, 1% tryptone, and 0.5% yeast extract) at indicated temperatures. Cultures were supplemented with 150 µg/ml ampicillin when necessary. For the induction of the P_{BAD} promoter, the medium was supplemented with L-arabinose to a final concentration of 0.01% (*E. coli*) or 0.1% (*Y. pseudotuberculosis*), respectively.

Plasmid Construction

All utilized oligonucleotides and plasmids are summarized in Tables 2 and 3, respectively. Point mutations were generated by site-directed mutagenesis according to the instruction manual of the QuikChange® mutagenesis kit (Agilent Technologies).

The *ompA* RNAT-*bgaB* fusion plasmid (pBO4435) was constructed by first amplifying the YPK_2630 (*ompA*) 5'-UTR including 30 bp of the *ompA* coding region (108 bp) with primer pairs *ompA*_UTR_fw/*ompA*_UTR_rev, digested with NheI and EcoRI and ligated into pBAD2-*bgaB*-His. The repressed *ompA* RNAT-*bgaB* (U38UC) fusion was constructed by site-directed mutagenesis with primer pair *ompA*_rep_fw/*ompA*_rep_rev using pBO4435 as a template.

The runoff plasmid for *in vitro* transcription of the *ompA* RNAT (pBO4920) was constructed by blunt-end ligation of a PCR-amplified DNA fragment (primer pair *ompA*_ro_fw/*ompA*_ro_rev), comprising the T7 RNA polymerase promoter, and the *ompA* RNAT including 30 bp of the *ompA* coding region, into the EcoRV restriction site of pUC18. Insertion of the repressive mutation (U38UC) into pBO4920 was achieved by site-directed mutagenesis (primer pair *ompA*_rep_fw/*ompA*_rep_rev).

TABLE 1 | Bacterial strains.

Strain	Relevant characteristics	Reference
<i>Yersinia pseudotuberculosis</i> YPIII	pIB1, wild type	Bölin et al., 1982
<i>Escherichia coli</i> DH5α	<i>supE44</i> , Δ <i>lacU169</i> (ψ 80 <i>lacZ</i> Δ <i>M15</i>), <i>hsdR17</i> , <i>recA1</i> , <i>gyrA96</i> , <i>thi1</i> , and <i>relA1</i>	Hanahan, 1983

TABLE 2 | Oligonucleotide list.

Name	Purpose	Plasmid	Sequence (5' → 3')
ompA_UTR_fw	Forward primer to amplify the 5' UTR of YPK_2630 (<i>ompA</i>) plus 30 bp of <i>ompA</i> coding region (−62 to +30 bp from ATG)	pBO4435	TTGCTAGCATTTTAACCAAGGGCTTAGC
ompA_UTR_rev	Reverse primer to amplify the 5' UTR of YPK_2630 (<i>ompA</i>) plus 30 bp of <i>ompA</i> coding region (−62 to +30 bp from ATG)	pBO4435	TTGAATCCACTGCTAATGCGATAGCT
ompA_rep_fw	Mutagenesis forward primer to introduce the mutation U38UC into YPK_2630 (<i>ompA</i>) 5' UTR	pBO4451 pBO4921	GCTTTTAAAGCTCATTGCCTCATTGGATGATAATGAGG
ompA_rep_rev	Mutagenesis forward primer to introduce the mutation U38UC into YPK_2630 (<i>ompA</i>) 5' UTR	pBO4451 pBO4921	CCTCATTATCATCCAAATGAGGCAATGAGCTTTAAAGC
ompA_ro_fw	Forward primer to amplify YPK_2630 (<i>ompA</i>) 5' UTR with a T7 promoter for the construction of the runoff plasmids	pBO4920	AGAAATTAATACGACTCACTATAGGGATTTTAACCAAGGGCTTAGC
ompA_ro_rev	YPK_2630 (<i>ompA</i>) 5' UTR +30 bp from ATG; reverse primer with EcoRV site for the construction of the runoff plasmid for structure probing and primer extension inhibition	pBO4920	AAGATATCCACTGCTAATGCGATAGCT
RT_ompA_fw	Forward primer for detection of YPK_2630 (<i>ompA</i>) by qRT-PCR	–	CTGTAGTTGTTCTGGGCTTTGCTGAC
RT_ompA_rev	Reverse primer for detection of YPK_2630 (<i>ompA</i>) by qRT-PCR	–	CTTTAGAAACCAGGTAGTCACGCACG
RT_bgaB_fw	Forward primer for detection of <i>bgaB</i> by qRT-PCR	–	GACTGCAACTACTCCAGCTTGGTTTG
RT_bgaB_rev	Reverse primer for detection of <i>bgaB</i> by qRT-PCR	–	CTACTGCCAAACGAGAGAATGACACC
RT_nuoB_fw	Forward primer for detection of YPK_1561 (<i>nuoB</i>) by qRT-PCR	–	GATCCTCTCGAGCAACATG
RT_nuoB_rev	Reverse primer for detection of YPK_1561 (<i>nuoB</i>) by qRT-PCR	–	TAAAGCAGGTTCCGGCCA
RT_gyrB_fw	Forward primer for detection of YPK_0004 (<i>gyrB</i>) by qRT-PCR	–	TCGCCGTGAAGGTAAGTTC
RT_gyrB_rev	Reverse primer for detection of YPK_0004 (<i>gyrB</i>) by qRT-PCR	–	CGTAATGGAAGTGGTCTTCT

TABLE 3 | Plasmid list.

Plasmid	Relevant characteristics	Reference
pUC18	Cloning vector; Ap ^r	Yanisch-Perron et al., 1985
pBAD2- <i>bgaB</i> -His	<i>bgaB</i> reporter gene vector, Ap ^r , araC, P _{BAD} promoter, His-Tag at the C-terminal of BgaB	Righetti et al., 2016
pBO3146	pBAD2- <i>bgaB</i> -His; ICR between pYV0075(<i>yscW</i>) and pYV0076(<i>lcrF</i>) plus 9 bp of <i>lcrF</i> coding region (123 to +9 bp from <i>lcrF</i> ATG)	Righetti et al., 2016
pBO4435	pBAD2- <i>bgaB</i> -His; 5' UTR of YPK_2630 (<i>ompA</i>) plus 30 bp of <i>ompA</i> coding region (−62 to +30 bp from <i>ompA</i> ATG)	This study
pBO4451	pBAD2- <i>bgaB</i> -His; 5' UTR of YPK_2630 (<i>ompA</i>) plus 30 bp of <i>cnfY</i> coding region (−62 to +30 bp from <i>ompA</i> ATG), mutant Rep U38UC	This study
pBO4920	pUC18; YPK_2630 (<i>ompA</i>) 5' UTR plus coding region (−62 to +30 bp from <i>ompA</i> ATG); runoff plasmid for structure probing and primer extension inhibition	This study
pBO4921	pUC18; YPK_2630 (<i>ompA</i>) 5' UTR plus coding region (−62 to +30 bp from <i>ompA</i> ATG), mutant Rep U38UC; runoff plasmid for structure probing and primer extension inhibition	This study

Reporter Gene Activity Assay

Escherichia coli DH5 α or *Y. pseudotuberculosis* YPIII cells carrying the *ompA* RNAT-*bgaB* fusion plasmids were grown overnight in LB supplemented with ampicillin at 25°C. Before being inoculated with an overnight culture to an optical density at 600 nm (OD₆₀₀) of 0.1, LB media supplemented with ampicillin were pre-warmed to 25°C. After growth to an OD₆₀₀ of 0.5, transcription was induced with 0.01% (*E. coli*) or 0.1% for (*Y. pseudotuberculosis*) L-arabinose, respectively. The culture was split and shifted to pre-warmed 100 ml flasks.

After incubation for 30 min, 400 μ l samples was subsequently taken for β -galactosidase assay, 2 ml samples for Western blotting, and 4 ml samples for RNA isolation. The β -galactosidase assay was carried out as described previously (Gaubig et al., 2011; Righetti et al., 2016).

Western Blot Analysis

Cell pellets were resuspended in 1 \times SDS sample buffer (2% SDS, 0.1% bromophenol blue, 1% 2-mercaptoethanol, 25% glycerol, 50 mM Tris/HCl, and pH 6.8) according to their

optical density (100 μ l per OD₆₀₀ of 1). After boiling for 10 min at 95°C, samples were centrifugated (10 min, 13,000 rpm) and the supernatant was separated by SDS gel electrophoresis in 5% stacking and 12% separating gels. Size-separated proteins were transferred by tank blotting onto a nitrocellulose membrane (Hybond-C Extra, GE Healthcare). An anti-His-HRP conjugate antibody (Bio-Rad) was used in a 1:4,000 dilution. Luminescence signals were detected by incubating membranes with Immobilon Forte Western HRP substrate (Millipore) and the FluorChem SP (Alpha Innotec).

RNA Extraction and Quantitative Reverse Transcription PCR

Total RNA was extracted using the peqGOLD TriFast reagent according to the manufacturer's protocol. RNA samples were treated with Turbo™ DNase (TURBO DNA-free™ Kit, Invitrogen) to remove DNA contamination. cDNA synthesis was performed using the iScript™ cDNA synthesis Kit (Bio-Rad) according to the manufacturer's protocol with 1 μ g RNA per reaction. 2 μ l of 1:10 diluted cDNA was mixed with 250 nM of each primer, 5 μ l of 2 \times iTaq Universal SYBR Green Supermix, and 2.5 μ l sterile water (Carl Roth). Amplification and detection were performed in a CFX Connect™ Real-Time System (Bio-Rad). Standard curves were used to calculate primer efficiency and determine the linear range of amplification. Relative transcript amounts were calculated using the primer efficiency corrected method (Pfaffl, 2001). The non-thermoregulated reference genes *gyrB* and *nuoB* were used for normalization.

In vitro Transcription

RNA for RNA structure probing and primer extension inhibition experiments were synthesized *in vitro* by runoff transcription with T7 RNA polymerase (Thermo Scientific) from EcoRV-linearized plasmids (listed in Table 3) as previously described (Righetti et al., 2016).

Enzymatic RNA Structure Probing

RNA structure probing of the 5'-UTR and 30 nt of *ompA* was performed as described previously (Twittenhoff et al., 2020b). Briefly, *in vitro* transcribed and 5'-[³²P]-labeled RNA (3,000 cpm) was mixed with buffer and tRNAs, preincubated for 5 min at the respective temperature, and treated with T1 (0.0017U; Invitrogen) or T2 (0.056U; MoBiTec) RNases for 5 min. For digestion with RNase T1 and RNase T2, a 5 \times TN buffer (100 mM Tris acetate, pH 7, and 500 mM NaCl) was used. An alkaline hydrolysis ladder was prepared as described in Brantl and Wagner (1994), meaning 60,000 cpm of labeled RNA was mixed with tRNAs and ladder buffer (1M Na₂CO₃ and 1M NaHCO₃; pH 9) incubated for 2 min at 90°C. The T1 ladder was generated by using 30,000 cpm-labeled RNA. The samples were heated with 2 μ l sequencing buffer (provided with RNase T1) at 90°C. Afterward, the RNA was incubated with the T1 RNase for 5 min at 37°C. All reactions were stopped by the addition of formamide loading dye and denaturation at 95°C.

Primer Extension Inhibition Analysis (Toeprinting)

Toeprinting analysis was performed with 30S ribosomal subunits, *in vitro* transcribed RNA, and tRNA^{Met} (Sigma-Aldrich) according to a protocol as described before (Hartz et al., 1988). The 5'-[³²P]-labeled oligonucleotide *ompA_ro_rv*, complementary to the 3' end of the *ompA* mRNA, was used as a primer for cDNA synthesis. The radiolabeled primer (0.16 pmol) was annealed to the *ompA* mRNA (0.08 pmol) and incubated with 30S ribosomal subunits (24 pmol) or Watanabe buffer [60 mM HEPES/KOH, 10.5 mM Mg(CH₃COO)₂, 690 mM NH₄COO, 12 mM 2-mercaptoethanol, 10 mM spermidine, and 0.25 mM spermine] in the presence of tRNA^{Met} (8 pmol) at 25, 37, or 42°C for 10 min. After the addition of 2 μ l MMLV-Mix [VD+Mg²⁺ buffer, BSA, dNTPs, and 800 U MMLV reverse transcriptase (Invitrogen)], cDNA synthesis was performed for 10 min at 37°C. The reaction was stopped by the addition of formamide loading dye, and the samples were separated on an 8% denaturing polyacrylamide gel. The Thermo Sequenase Cycle Sequencing Kit (Applied Biosystems) was used for sequencing reactions with plasmid pBO4920 as a template and radiolabeled primer *ompA_ro_rv*.

RESULTS

The *ompA* 5'-UTR Contains a Thermoresponsive RNA Structure, Which Facilitates Temperature-Dependent Regulation

A previously conducted global *in vitro* RNA structure probing analysis (Righetti et al., 2016) provided strong evidence for the existence of temperature-sensitive RNA structures in the 5'-UTRs of numerous mRNAs. One of the top candidates (rank #3 of chromosomally encoded mRNAs) discovered by this parallel analysis of RNA structures approach was the 5'-UTR of *ompA*. The RNA structure observed at 25°C was destabilized at higher temperatures (Figure 1A). This was especially prominent in the region around the SD sequence and in the early coding region. Here, the PARS profile dropped from positive to negative values indicative of a transition from a double-stranded (ds) to single-stranded (ss) conformation. This behavior is typical of zipper-like RNAs that facilitate ribosome binding at elevated temperatures (Kortmann and Narberhaus, 2012). The PARS analysis revealed an almost completely folded *ompA* 5'-UTR that is engaged in several stem-loop structures (Figure 1B). Strikingly, the SD sequence (53-GGAG-56) is imperfectly paired and contains a bulged adenine. It is very likely that this mismatched nucleotide in concert with four unpaired nucleotides (58-GUAA-61) between the SD sequence and the AUG start codon is key to the temperature sensitivity of this 5'-UTR.

To examine the regulation of *ompA* in detail, we first checked, whether transcription of the gene is temperature-controlled by performing qRT-PCR on total RNA samples from *Y. pseudotuberculosis* YPIII after growth at 25 and 37°C (Figure 1C). Consistent with already existing RNA-seq results (Nuss et al., 2015),

we observed a fold change around 0.6 (37 vs. 25°C) showing a reduction in *ompA* mRNA at a higher temperature.

The RNA structurome data, in contrast, suggested an upregulation of OmpA protein at 37°C due to the thermoresponsive nature of the *ompA* 5'-UTR. To test this hypothesis, we translationally fused the *ompA* 5'-UTR to the *bgaB* gene coding for a heat-stable His-tagged β -galactosidase downstream of the arabinose-inducible P_{BAD} promoter and measured the β -galactosidase activity and protein amounts at 25°C and after a shift to 37 or 42°C. The well-studied *lcrF* RNAT of *Y. pseudotuberculosis* served as a positive control (Figure 1D).

A clear increase in β -galactosidase activity and protein amount after the temperature shift supported the existence of a functional RNAT upstream of *ompA* able to confer translational repression at 25°C and induction at 37 or 42°C.

A Stabilizing Point Mutation Prevents RNAT Regulation

One way of verifying the contribution of a temperature-sensitive RNA structure in translational control is the construction of a stabilized version. Based on the PARS-derived secondary structure, the

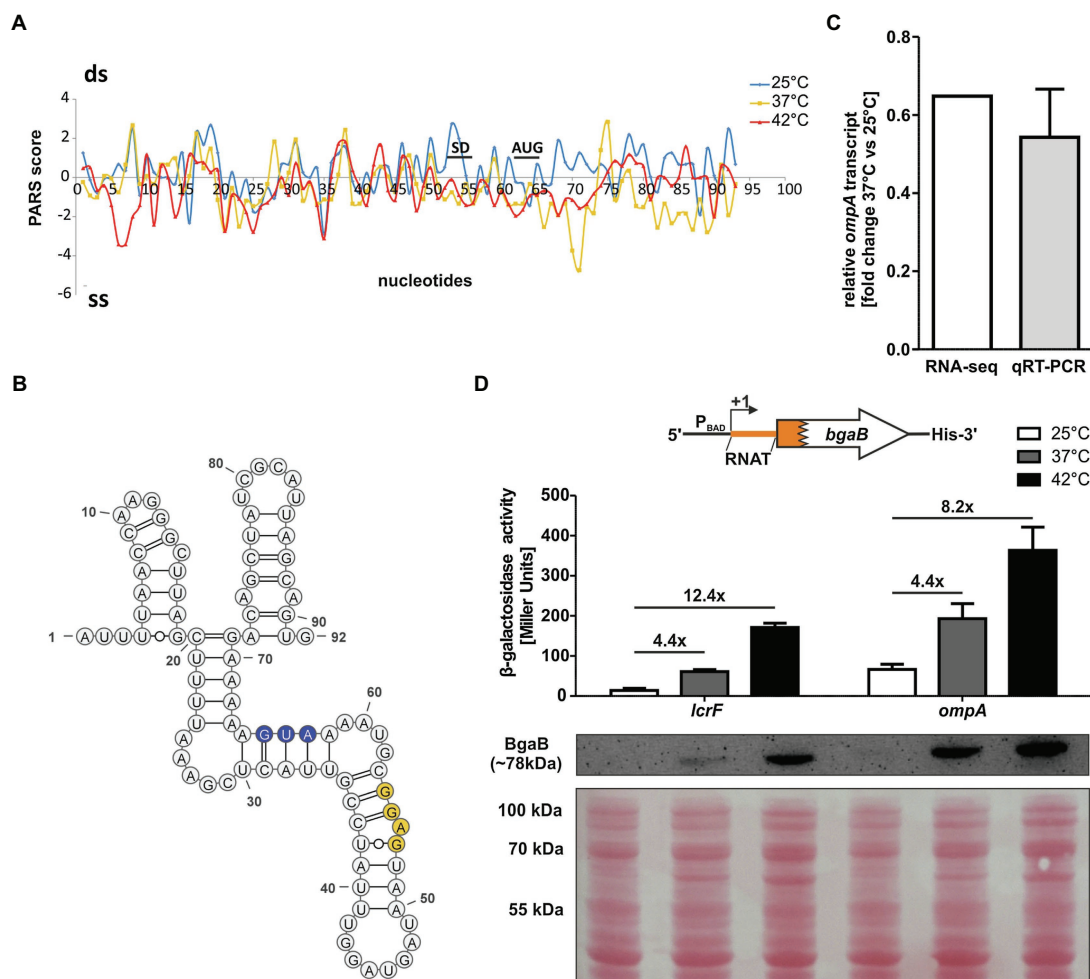


FIGURE 1 | The *ompA* 5'-UTR contains a thermoresponsive RNA structure. **(A)** PARS profiles of the *ompA* RNAT (-62 nt to +30 nt from AUG) at 25, 37, and 42°C (Righetti et al., 2016). The potential SD sequence and the AUG are shown. A positive PARS score is indicative of a double-stranded (ds) conformation, whereas a negative PARS score suggests a single-stranded (ss) conformation. A drop from a positive score at 25°C to a negative score at 37°C suggests melting of a secondary structure. **(B)** PARS-derived secondary structure of the *ompA* RNAT at 25°C. The potential SD sequence is highlighted in yellow and its corresponding AUG in blue. —, AU pair; =, GC pair; O, GU pair. **(C)** Comparison of *ompA* transcript amount between 37 and 25°C by RNA sequencing (Nuss et al., 2015) and qRT-PCR (this study) of exponentially grown YPIII cells at 25 and 37°C, respectively. For qRT-PCR, the obtained data were normalized to *gyrB* and *nuoB*. qRT-PCR was prepared in biological triplicates and technical triplicates. **(D)** Translational control was measured by *bgaB* fusions. A schematic representation of the reporter gene fusion is displayed. The *ompA* RNAT was translationally fused to *bgaB* under control of the P_{BAD} promoter. As a control, the *lcrF* RNAT fusion was used. The fusion plasmids were introduced into *E. coli* cells and grown to an OD₆₀₀ of 0.5 at 25°C. Subsequently, transcription was induced by the addition of 0.01% L-arabinose and the cultures were split and transferred into pre-warmed flask at 25, 37, and 42°C, respectively. After 30 min of incubation, samples were taken for β -galactosidase assays and Western blot analysis. Experiments were carried out in biological triplicates. Mean and corresponding standard deviations are shown. Western blot membranes were stained with Ponceau S as a loading control. One representative Western blot is shown. Analysis was carried out in biological triplicates.

we introduced a cytosine between U38 and A39 (called U38UC or “rep” for repressed variant) in the anti-SD sequence leading to a perfectly paired SD sequence without any mismatches (**Figure 2A**). The increased thermodynamic stability should prevent the RNA structure from melting at higher temperatures and thereby abolish RNAT functionality. Indeed, reporter gene assays revealed the absence of β -galactosidase protein and activity at 25 and 37°C in *E. coli* as well as in *Y. pseudotuberculosis* (**Figure 2B**). Apparently, the introduction of just one additional base pair was sufficient to abolish the temperature regulation. To solidify our claim that the 5'-UTR regulates translation (and not transcription or mRNA degradation), we analyzed the *bgaB* mRNA levels in all three tested *Y. pseudotuberculosis* strains by qRT-PCR and found that the transcript levels were the same at 25 and 37°C (**Figure 2C**).

The *ompA* RNAT Opens at Higher Temperatures Around the SD Region

Next, we examined the structure and temperature-induced conformational changes in the RNAT by enzymatic RNA structure probing using *in vitro* transcribed and 5' end-labeled *ompA* RNA at 25, 37, and 42°C treated with RNases T1 (preferentially cleaves at unpaired guanines) and T2 (preferentially cleaves at unpaired adenines but also other ss residues; **Figure 3A**). The cleavage pattern supported the overall structure of the *ompA* 5'-UTR by prominent cleavage at 25°C in apical loops (e.g., C80 and G81). In accordance with the dynamic PARS-derived secondary structure (**Figures 1A, 3B**), residues around the SD sequence were sensitized against RNase cleavage at higher temperatures due to melting of the secondary structure. For example, nucleotides G53 and G55

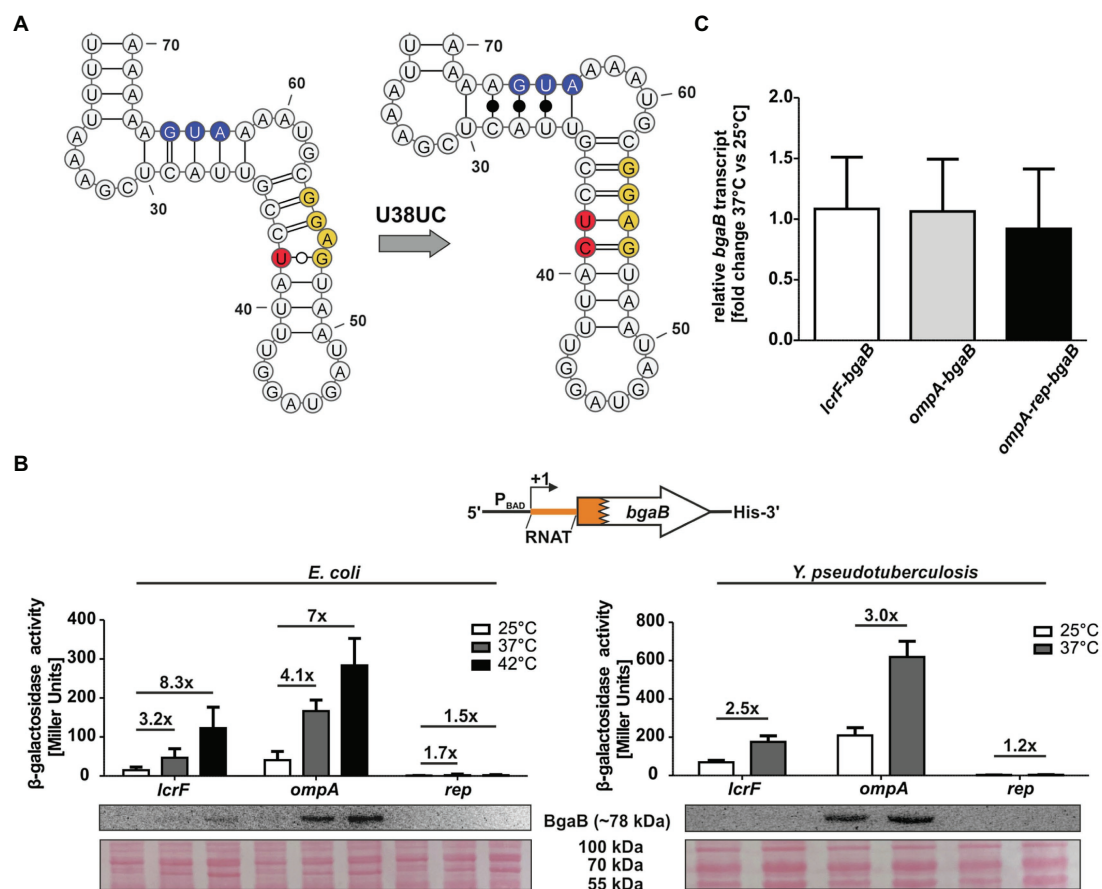


FIGURE 2 | Mutation of the anti-SD sequence locks the RNAT in a closed conformation. **(A)** PARS-derived secondary structure of the *ompA* RNAT stem and the predicted stabilized structure at 25°C. The potential SD sequence is highlighted in yellow, the mutation site of the anti-SD sequence in red and the AUG in blue. **(B)** Translational control was measured by *bgaB* fusions. A schematic representation of the reporter gene fusion is displayed. The *ompA* RNAT was translationally fused to *bgaB* under control of the P_{BAD} promoter. Additionally, a point mutation (U38UC) was introduced to stabilize the RNAT (rep). As a control, the *lcrF* RNAT fusion was used. The fusion plasmids were introduced into *E. coli* and *Y. pseudotuberculosis* YPIII cells and grown to an OD₆₀₀ of 0.5 at 25°C. Subsequently, transcription was induced by the addition of 0.01% for *E. coli* or 0.1% for *Y. pseudotuberculosis* L-arabinose and the cultures were split and transferred into pre-warmed flask at 25 and 37°C, respectively. After 30 min of incubation, samples were taken for β -galactosidase assays, Western blot analysis, and qRT-PCR. Experiments were carried out in biological triplicates. Mean and corresponding standard deviations are shown. Western blot membranes were stained with Ponceau S as a loading control. One representative Western blot is shown. Analysis was carried out in biological triplicates. **(C)** Comparison of *bgaB* transcript amount between 37 and 25°C by qRT-PCR of exponentially grown YPIII cells harboring the *ompA* RNAT-*bgaB* fusion plasmids at 25 and 37°C, respectively. For qRT-PCR, the obtained data were normalized to *gyrB* and *nuoB*. qRT-PCR was prepared in biological triplicates and technical triplicates.

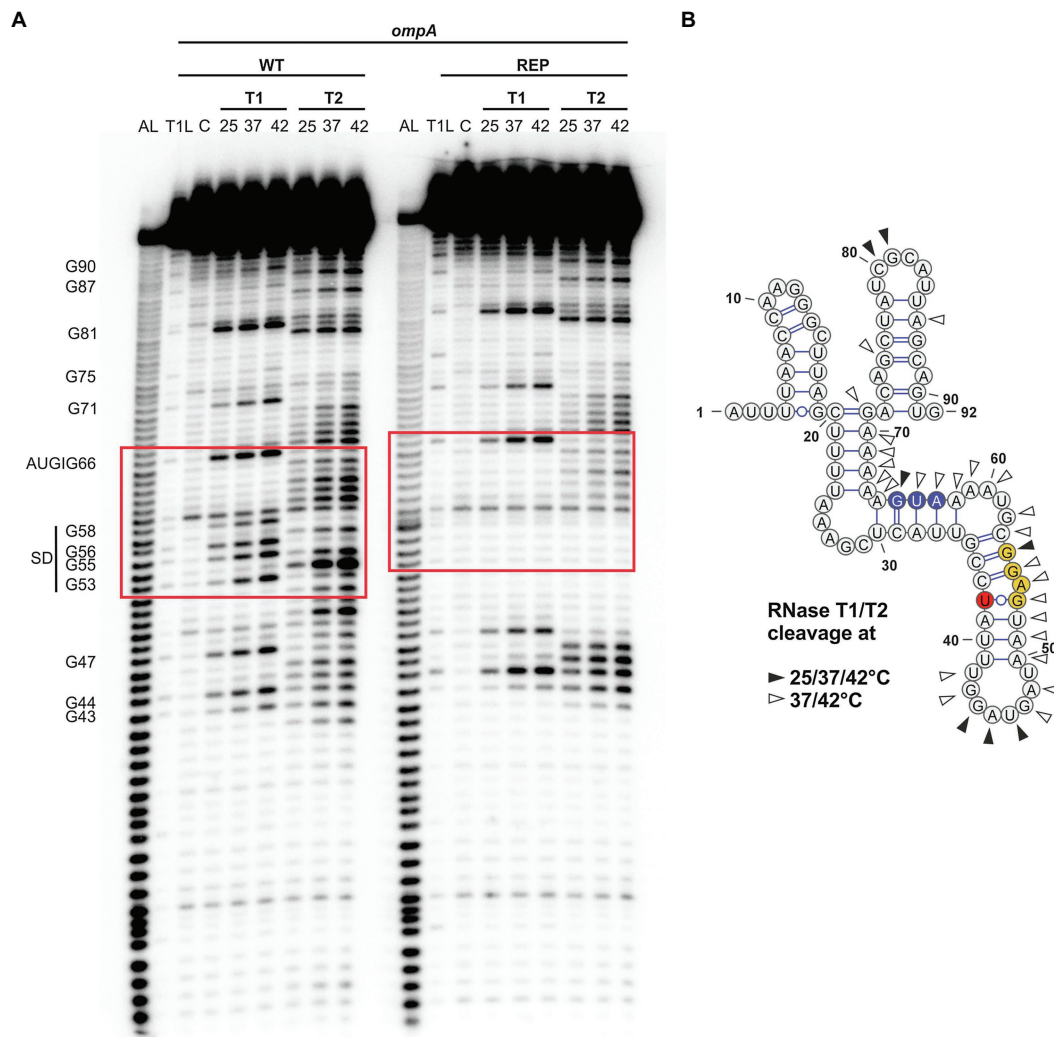


FIGURE 3 | Accessibility of the ribosome-binding site of *ompA* is increased at higher temperatures. **(A)** Enzymatic structure probing of the *ompA* RNAT (WT) and its stabilized version (REP) at 25, 37, and 42°C. *In vitro* transcribed RNA was 5'-[32 P] labeled and treated with RNases T1 and T2, respectively. AL, alkaline ladder; T1L, RNase T1 cleavage ladder in sequencing buffer at 37°C; C, RNA treated with water instead of RNases – cleavage control. Ribosome-binding site is highlighted by a red box. Experiment was carried out at least three times. **(B)** PARS-derived secondary structure of the *ompA* RNAT at 25°C. The potential SD sequence is highlighted in yellow, the mutation site of the anti-SD sequence in red, and the AUG in blue. Distinctive nucleotide cleavage is indicated by black and white arrows.

were almost untouched by T1 at 25°C but efficiently cleaved at 37 and 42°C. Residual cleavage of the bulged A54 by T2 at 25°C massively increased at 37 and 42°C making it the most prominent cleavage product at high temperatures. Fully consistent with the reporter gene assays (Figure 2), the SD sequence of the rep variant was almost completely inaccessible to RNase cleavage demonstrating that melting of the RNAT is prevented by the point mutation, which locks the structure in a closed conformation.

The Ribosome Gains Access to the *ompA* Transcript at 37°C

The observed melting of the *ompA* 5'-UTR at higher temperatures (Figures 1A, 3) together with the reporter gene studies (Figures 1D, 2) strongly suggested increased translation initiation

at higher temperatures. We employed primer extension inhibition assays (toeprinting) to demonstrate ribosome binding. *In vitro* transcribed *ompA* RNA was reversely transcribed from a radiolabeled oligonucleotide in the presence or absence of 30S ribosomal subunits at 25 and 37°C. Ribosomes bound to the mRNA are stabilized in a ternary complex with tRNA^{Met} and act as a roadblock for reverse transcription. This leads to premature termination of reverse transcription and thus shorter fragments (toeprints). As expected, in the presence of ribosomes, the toeprint signals in the appropriate distance from the AUG start codon were weak at 25°C but strong at 37°C (Figure 4). No toeprint signal, i.e., no ribosome binding, was found when the stabilized rep version was assayed. Instead, termination products independent of the presence of ribosomes appeared within the codon sequence, a phenomenon frequently observed downstream (considering the

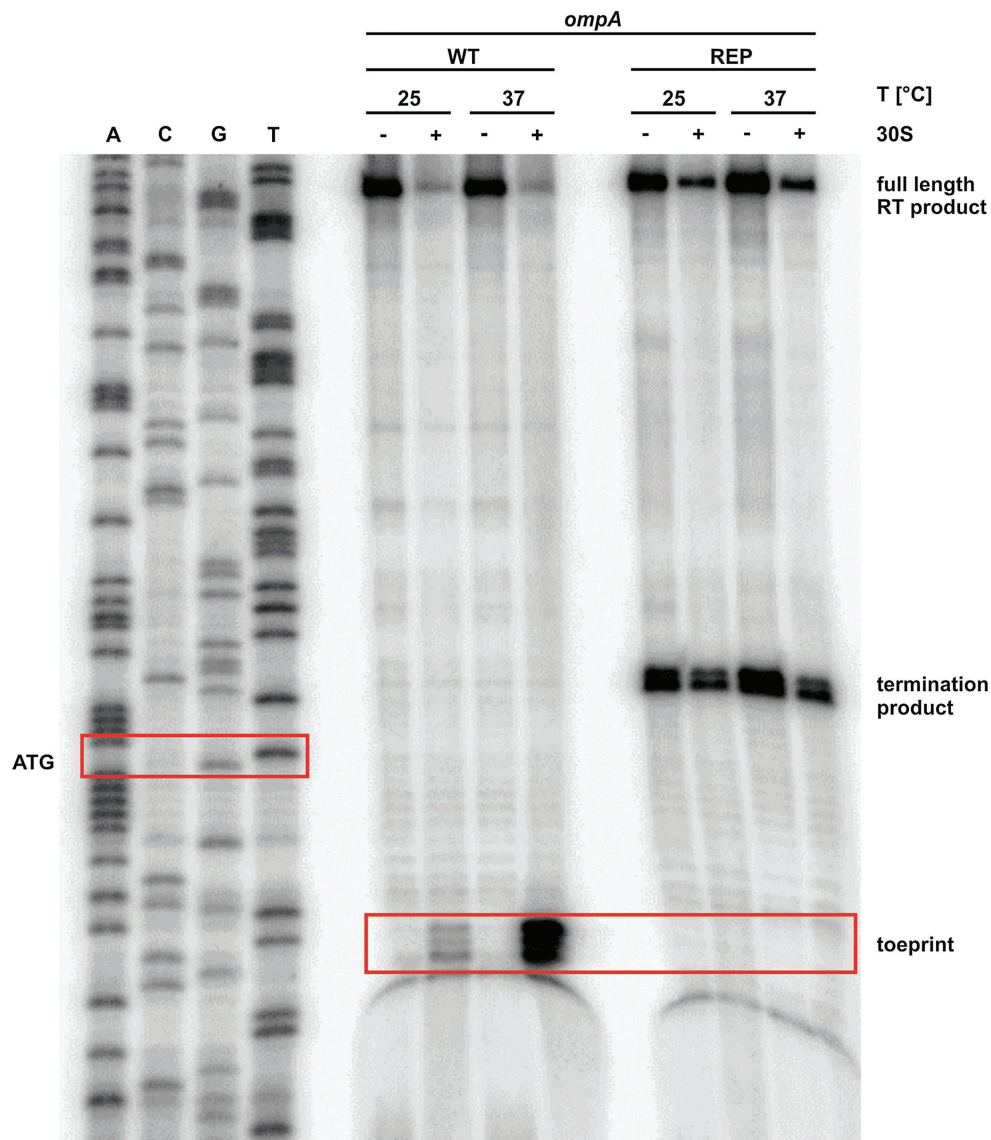


FIGURE 4 | The ribosome binds to the *ompA* transcript at 37°C. Primer extension inhibition of the *ompA* RNAT (WT) and its stabilized version (REP) at 25 and 37°C with (+) and without (-) the addition of 30S ribosomal subunits. The signals represent the full-length reverse transcription (RT) product, the premature termination product, and the toeprint signal (caused by ribosome binding). ACGT lanes indicate sequencing reactions. Position of ATG and the toeprint signal is highlighted by red boxes. Experiment was carried out at least three times.

direction of the reverse transcriptase) of stable structures in stabilized RNATs (Böhme et al., 2012; Twittenhoff et al., 2020b).

DISCUSSION

Sensing of and rapidly responding to the sudden external changes associated with host infection is crucial for enteric pathogens like *Y. pseudotuberculosis*. One parameter that predictably and reversibly changes during the transitions from the environment to a warm-blooded host and back into the environment is temperature. A fast and efficient way to reversibly modulate gene expression in response to temperature

shifts is zipper-like RNATs because the mRNA is already available for translation (Grosso-Becerra et al., 2015; Wei and Murphy, 2016; Loh et al., 2018). This is certainly the reason why RNATs are extremely widespread posttranscriptional control elements in numerous bacterial pathogens (Hoe and Goguen, 1993; Johansson et al., 2002; Böhme et al., 2012; Kouse et al., 2013; Loh et al., 2013; Weber et al., 2014; Wei et al., 2017; Twittenhoff et al., 2020a,b; Brewer et al., 2021).

Here, we describe the structural and functional features of an RNAT in the *Y. pseudotuberculosis ompA* transcript that was one of the prime candidates in our previous PARS study (Righetti et al., 2016). We were particularly interested in this candidate because a recent report demonstrated

RNAT-controlled translation of *ompA* in *S. dysenteriae* (Murphy et al., 2020). Despite regulating the same gene, it is important to note that the *Yersinia* and *Shigella* RNATs are very different with respect to length, sequence, and structure. First, the *S. dysenteriae ompA* 5'-UTR is 133 nucleotides long, and the last 35 residues are sufficient to confer translational control. In contrast, the RNAT from *Y. pseudotuberculosis* is 92 nucleotides long and more densely folded. Second, the *S. dysenteriae* RNAT belongs to the fourU family showing the characteristic complementarity of the SD sequence to four consecutive uracil residues (Waldminghaus et al., 2007). The *Y. pseudotuberculosis* RNAT is not a member of this family. The inherent temperature lability is due to a bulged adenine residue in the center of the SD sequence, which pairs imperfectly with an anti-SD sequence comprised of CCUA. Introducing one additional residue that pairs with the exposed adenine completely eliminated the expression and heat induction even when sufficient *ompA* mRNA was present. This demonstrates the relevance of precisely balanced structural features in a functional RNAT to respond within the virulence-relevant temperature regime. Overall, the *ompA* thermometer is another interesting example of convergent evolution of RNATs as has previously been proposed for the regulation of CnfY-type toxins (Twittenhoff et al., 2020b).

Many enterobacterial outer membrane protein genes are under tight posttranscriptional regulation (Guillier et al., 2006; Vogel and Papenfort, 2006). A highly conserved sRNA also believed to control *ompA* in *Yersinia* species is MicA (Udekwi et al., 2005). It binds across the SD sequence and prevents ribosome binding, which facilitates RNaseE-mediated cleavage. The temperature-induced structural transition of the *ompA* 5'-UTR from a closed to an open conformation potentially adds another layer of posttranscriptional control. Under circumstances when MicA is abundant, the sRNA might interfere with translation initiation. The exact interplay between the *ompA* thermosensor, MicA (and maybe other sRNAs), the RNA chaperone Hfq, and RNases is not yet understood. The situation, however, is somewhat reminiscent of the *Listeria prfA* thermometer that – in its open form – is able to interact with the two sRNAs, SreA and SreB, which decreases the level of PrfA and thereby links virulence gene expression to nutrient availability (Loh et al., 2009).

Having OmpA under temperature regulation supports its role as a virulence factor. There is growing evidence that the outer membrane protein is involved in many pathogenesis-related processes in diverse Gram-negative bacteria (Krishnan and Prasadara, 2012). It is involved in adherence to epithelial cells (Smith et al., 2007; Gaddy et al., 2009), mouse mortality (Sánchez-Encinales et al., 2017), and biofilm formation (Weiser and Gotschlich, 1991; Azghani et al., 2002). OmpA of pathogenic *Yersinia* species is a highly immunogenic protein and may be an excellent vaccine candidate, due to its cross-immunogenicity and intense immune response among *Yersinia* species (Chen et al., 2015). Furthermore, *Y. pestis* and *Y. pseudotuberculosis ompA* mutants are defective in surviving in macrophages, and the *Y. pestis* mutant is outcompeted by the wild-type strain in a mouse-infection model (Bartra et al., 2012).

Given the importance of OmpA for efficient pathogenesis, it may be a promising target for treatment of infections

caused by Gram-negative bacteria. A recently identified OmpA inhibitor, cyclic hexapeptide AOA-2, inhibits adherence to eukaryotic cells and biofilm formation (Vila-Farrés et al., 2017). The compound attenuates virulence by reducing the dissemination between organs and decreases mouse mortality after *A. baumannii*, *E. coli*, and *Pseudomonas aeruginosa* infections. In combination with other antimicrobial agents, OmpA inhibitors might be helpful for combating multidrug-resistant bacteria and thereby reducing mortality caused by infections with Gram-negative pathogens.

A recent study on OmpA in *Acinetobacter* sp. linked *ompA* expression to oxidative stress (Shahryari et al., 2021). The authors suggested a protective effect by the poor permeability of the slow OmpA porin compared to other outer membrane proteins, such as OmpC, which is known to produce larger pores, at least in *Salmonella* (van der Heijden et al., 2016). A connection between OmpA and oxidative stress is interesting since pathogens are typically exposed to a multitude of reactive oxygen species (ROS) upon infection of a host. An intriguing finding of our RNA structurome analyses is the presence of potential RNATs upstream of various oxidative stress response genes (Righetti et al., 2016; Twittenhoff et al., 2020a). This is unlikely to be a coincidence and suggests parallel ways of host-body temperature-induced protective measures against ROS attack. Following up on RNAT-mediated control of genes combating ROS in pathogenic bacteria might be a worthwhile subject of future studies.

DATA AVAILABILITY STATEMENT

The raw data supporting the conclusions of this article will be made available by the authors, without undue reservation.

AUTHOR CONTRIBUTIONS

DS: conceptualization, data curation, formal analysis, investigation, validation, supervision, methodology, and writing original draft. CT: conceptualization, data curation, formal analysis, investigation, validation, supervision, and methodology. FB and MH: investigation, formal analysis, and methodology. FN: conceptualization, data curation, formal analysis, supervision, funding acquisition, project administration, writing original draft, review, and editing. All authors contributed to the article and approved the submitted version.

FUNDING

This study was financially supported by the German Research Foundation (DFG, NA240/10–2). We acknowledge support by the Open Access publication funds of the Ruhr-Universität Bochum.

ACKNOWLEDGMENTS

We thank the RNA group for continuous discussions and reading earlier versions of the manuscript.

REFERENCES

- Ambrosi, C., Pompili, M., Scribano, D., Zagaglia, C., Ripa, S., and Nicoletti, M. (2012). Outer membrane protein A (OmpA): a new player in *Shigella flexneri* protrusion formation and inter-cellular spreading. *PLoS One* 7:e49625. doi: 10.1371/journal.pone.0049625
- Azghani, A. O., Idell, S., Bains, M., and Hancock, R. E. (2002). *Pseudomonas aeruginosa* outer membrane protein F is an adhesin in bacterial binding to lung epithelial cells in culture. *Microb. Pathog.* 33, 109–114. doi: 10.1006/mpat.2002.0514
- Bartra, S. S., Gong, X., Lorica, C. D., Jain, C., Nair, M. K. M., Schifferli, D., et al. (2012). The outer membrane protein A (OmpA) of *Yersinia pestis* promotes intracellular survival and virulence in mice. *Microb. Pathog.* 52, 41–46. doi: 10.1016/j.micpath.2011.09.009
- Böhme, K., Steinmann, R., Kortmann, J., Seekircher, S., Heroven, A. K., Berger, E., et al. (2012). Concerted actions of a thermo-labile regulator and a unique intergenic RNA thermosensor control *Yersinia* virulence. *PLoS Pathog.* 8:e1002518. doi: 10.1371/journal.ppat.1002518
- Bölin, I., Norlander, L., and Wolf-Watz, H. (1982). Temperature-inducible outer membrane protein of *Yersinia pseudotuberculosis* and *Yersinia enterocolitica* is associated with the virulence plasmid. *Infect. Immun.* 37, 506–512. doi: 10.1128/IAI.37.2.506-512.1982
- Brantl, S., and Wagner, E. G. (1994). Antisense RNA-mediated transcriptional attenuation occurs faster than stable antisense/target RNA pairing: an *in vitro* study of plasmid pIP501. *EMBO J.* 13, 3599–3607. doi: 10.1002/j.1460-2075.1994.tb06667.x
- Brewer, S. M., Twittenhoff, C., Kortmann, J., Brubaker, S. W., Honeycutt, J., Massis, L. M., et al. (2021). A *Salmonella* Typhi RNA thermosensor regulates virulence factors and innate immune evasion in response to host temperature. *PLoS Pathog.* 17:e1009345. doi: 10.1371/journal.ppat.1009345
- Chen, Y., Duan, R., Li, X., Li, K., Liang, J., Liu, C., et al. (2015). Homology analysis and cross-immunogenicity of OmpA from pathogenic *Yersinia enterocolitica*, *Yersinia pseudotuberculosis* and *Yersinia pestis*. *Mol. Immunol.* 68, 290–299. doi: 10.1016/j.molimm.2015.09.016
- Choi, C. H., Lee, E. Y., Lee, Y. C., Park, T. I., Kim, H. J., Hyun, S. H., et al. (2005). Outer membrane protein 38 of *Acinetobacter baumannii* localizes to the mitochondria and induces apoptosis of epithelial cells. *Cell. Microbiol.* 7, 1127–1138. doi: 10.1111/j.1462-5822.2005.00538.x
- Clavel, T., Germon, P., Vianney, A., Portalier, R., and Lazzaroni, J. C. (1998). TolB protein of *Escherichia coli* K-12 interacts with the outer membrane peptidoglycan-associated proteins Pal, Lpp and OmpA. *Mol. Microbiol.* 29, 359–367. doi: 10.1046/j.1365-2958.1998.00945.x
- Confer, A. W., and Ayalew, S. (2013). The OmpA family of proteins: roles in bacterial pathogenesis and immunity. *Vet. Microbiol.* 163, 207–222. doi: 10.1016/j.vetmic.2012.08.019
- Douchin, V., Bohn, C., and Boulou, P. (2006). Down-regulation of porins by a small RNA bypasses the essentiality of the regulated intramembrane proteolysis protease RseP in *Escherichia coli*. *J. Biol. Chem.* 281, 12253–12259. doi: 10.1074/jbc.M600819200
- Gaddy, J. A., Tomaras, A. P., and Actis, L. A. (2009). The *Acinetobacter baumannii* 19606 OmpA protein plays a role in biofilm formation on abiotic surfaces and in the interaction of this pathogen with eukaryotic cells. *Infect. Immun.* 77, 3150–3160. doi: 10.1128/IAI.00096-09
- Gaubig, L. C., Waldminghaus, T., and Narberhaus, F. (2011). Multiple layers of control govern expression of the *Escherichia coli* *ibpAB* heat-shock operon. *Microbiology* 157, 66–76. doi: 10.1099/mic.0.043802-0
- Grosso-Becerra, M. V., Servin-González, L., and Soberón-Chávez, G. (2015). RNA structures are involved in the thermoregulation of bacterial virulence-associated traits. *Trends Microbiol.* 23, 509–518. doi: 10.1016/j.tim.2015.04.004
- Guillier, M., Gottesman, S., and Storz, G. (2006). Modulating the outer membrane with small RNAs. *Genes Dev.* 20, 2338–2348. doi: 10.1101/gad.1457506
- Hanahan, D. (1983). Studies on transformation of *Escherichia coli* with plasmids. *J. Mol. Biol.* 166, 557–580. doi: 10.1016/S0022-2836(83)80284-8
- Hart, D., McPheeters, D. S., Traut, R., and Gold, L. (1988). Extension inhibition analysis of translation initiation complexes. *Methods Enzymol.* 164, 419–425. doi: 10.1016/s0076-6879(88)64058-4
- Hoe, N. P., and Goguen, J. D. (1993). Temperature sensing in *Yersinia pestis*: translation of the LcrF activator protein is thermally regulated. *J. Bacteriol.* 175, 7901–7909. doi: 10.1128/JB.175.24.7901-7909.1993
- Johansson, J., Mandin, P., Renzoni, A., Chiaruttini, C., Springer, M., and Cossart, P. (2002). An RNA thermosensor controls expression of virulence genes in *Listeria monocytogenes*. *Cell* 110, 551–561. doi: 10.1016/S0092-8674(02)00905-4
- Kim, S. W., Choi, C. H., Moon, D. C., Jin, J. S., Lee, J. H., Shin, J. H., et al. (2009). Serum resistance of *Acinetobacter baumannii* through the binding of factor H to outer membrane proteins. *FEMS Microbiol. Lett.* 301, 224–231. doi: 10.1111/j.1574-6968.2009.01820.x
- Knittel, V., Vollmer, I., Volk, M., and Dersch, P. (2018). Discovering RNA-based regulatory systems for *Yersinia* virulence. *Front. Cell. Infect. Microbiol.* 8:378. doi: 10.3389/fcimb.2018.00378
- Kortmann, J., and Narberhaus, F. (2012). Bacterial RNA thermometers: molecular zippers and switches. *Nat. Rev. Microbiol.* 10, 255–265. doi: 10.1038/nrmicro2730
- Kouse, A. B., Righetti, F., Kortmann, J., Narberhaus, F., and Murphy, E. R. (2013). RNA-mediated thermoregulation of iron-acquisition genes in *Shigella dysenteriae* and pathogenic *Escherichia coli*. *PLoS One* 8:e63781. doi: 10.1371/journal.pone.0063781
- Krishnan, S., and Prasadara, N. V. (2012). Outer membrane protein A and OprF: versatile roles in gram-negative bacterial infections. *FEBS J.* 279, 919–931. doi: 10.1111/j.1742-4658.2012.08482.x
- Loh, E., Dussurget, O., Gripenland, J., Vaitkevicius, K., Tiensuu, T., Mandin, P., et al. (2009). A trans-acting riboswitch controls expression of the virulence regulator PrfA in *Listeria monocytogenes*. *Cell* 139, 770–779. doi: 10.1016/j.cell.2009.08.046
- Loh, E., Kugelberg, E., Tracy, A., Zhang, Q., Gollan, B., Ewles, H., et al. (2013). Temperature triggers immune evasion by *Neisseria meningitidis*. *Nature* 502, 237–240. doi: 10.1038/nature12616
- Loh, E., Righetti, F., Eichner, H., Twittenhoff, C., and Narberhaus, F. (2018). RNA thermometers in bacterial pathogens. *Microbiol. Spectr.* 6. doi: 10.1128/microbiolspec.RWR-0012-2017
- Mandin, P., and Johansson, J. (2020). Feeling the heat at the millennium: thermosensors playing with fire. *Mol. Microbiol.* 113, 588–592. doi: 10.1111/mmi.14468
- Mizuno, T., Chou, M. Y., and Inouye, M. (1984). A unique mechanism regulating gene expression: translational inhibition by a complementary RNA transcript (micRNA). *Proc. Natl. Acad. Sci. U. S. A.* 81, 1966–1970. doi: 10.1073/pnas.81.7.1966
- Murphy, E. R., Roßmanith, J., Sieg, J., Fris, M. E., Hussein, H., Kouse, A. B., et al. (2020). Regulation of OmpA translation and *Shigella dysenteriae* virulence by an RNA thermometer. *Infect. Immun.* 88:e00871-19. doi: 10.1128/IAI.00871-19
- Nuss, A. M., Heroven, A. K., Waldmann, B., Reinkensmeier, J., Jarek, M., Beckstette, M., et al. (2015). Transcriptomic profiling of *Yersinia pseudotuberculosis* reveals reprogramming of the Crp regulon by temperature and uncovers Crp as a master regulator of small RNAs. *PLoS Genet.* 11:e1005087. doi: 10.1371/journal.pgen.1005087
- Park, J. S., Lee, W. C., Yeo, K. J., Ryu, K. S., Kumarasiri, M., Heseck, D., et al. (2012). Mechanism of anchoring of OmpA protein to the cell wall peptidoglycan of the gram-negative bacterial outer membrane. *FASEB J.* 26, 219–228. doi: 10.1096/fj.11-188425
- Pfaffl, M. W. (2001). A new mathematical model for relative quantification in real-time RT-PCR. *Nucleic Acids Res.* 29:e45. doi: 10.1093/nar/29.9.e45
- Prasadara, N. V., Blom, A. M., Villoutreix, B. O., and Linsangan, L. C. (2002). A novel interaction of outer membrane protein A with C4b binding protein mediates serum resistance of *Escherichia coli* K1. *J. Immunol.* 169, 6352–6360. doi: 10.4049/jimmunol.169.11.6352
- Prasadara, N. V., Wass, C. A., Weiser, J. N., Stins, M. F., Huang, S. H., and Kim, K. S. (1996). Outer membrane protein A of *Escherichia coli* contributes to invasion of brain microvascular endothelial cells. *Infect. Immun.* 64, 146–153. doi: 10.1128/IAI.64.1.146-153.1996
- Rasmussen, A. A., Eriksen, M., Gilany, K., Udesen, C., Franch, T., Petersen, C., et al. (2005). Regulation of *ompA* mRNA stability: the role of a small regulatory RNA in growth phase-dependent control. *Mol. Microbiol.* 58, 1421–1429. doi: 10.1111/j.1365-2958.2005.04911.x

- Righetti, F., Nuss, A. M., Twittenhoff, C., Beele, S., Urban, K., Will, S., et al. (2016). Temperature-responsive *in vitro* RNA structurome of *Yersinia pseudotuberculosis*. *Proc. Natl. Acad. Sci. U. S. A.* 113, 7237–7242. doi: 10.1073/pnas.1523004113
- Sánchez-Encinales, V., Álvarez-Marín, R., Pachón-Ibáñez, M. E., Fernández-Cuenca, F., Pascual, A., et al. (2017). Overproduction of outer membrane protein A by *Acinetobacter baumannii* as a risk factor for nosocomial pneumonia, bacteremia, and mortality rate increase. *J. Infect. Dis.* 215, 966–974. doi: 10.1093/infdis/jix010
- Shahryari, S., Talaei, M., Haghbeen, K., Adrian, L., Vali, H., Shahbani Zahiri, H., et al. (2021). New provisional function of OmpA from *Acinetobacter* sp. strain SA01 based on environmental challenges. *mSystems* 6:e01175-20. doi: 10.1128/mSystems.01175-20
- Smith, S. G., Mahon, V., Lambert, M. A., and Fagan, R. P. (2007). A molecular Swiss army knife: OmpA structure, function and expression. *FEMS Microbiol. Lett.* 273, 1–11. doi: 10.1111/j.1574-6968.2007.00778.x
- Steinmann, R., and Dersch, P. (2013). Thermosensing to adjust bacterial virulence in a fluctuating environment. *Future Microbiol.* 8, 85–105. doi: 10.2217/fmb.12.129
- Twittenhoff, C., Brandenburg, V. B., Righetti, F., Nuss, A. M., Mosig, A., Dersch, P., et al. (2020a). Lead-seq: transcriptome-wide structure probing *in vivo* using lead(II) ions. *Nucleic Acids Res.* 48:e71. doi: 10.1093/nar/gkaa404
- Twittenhoff, C., Heroven, A. K., Mühlen, S., Dersch, P., and Narberhaus, F. (2020b). An RNA thermometer dictates production of a secreted bacterial toxin. *PLoS Pathog.* 16:e1008184. doi: 10.1371/journal.ppat.1008184
- Udekwi, K. I., Darfeuille, F., Vogel, J., Reimegård, J., Holmqvist, E., and Wagner, E. G. (2005). Hfq-dependent regulation of OmpA synthesis is mediated by an antisense RNA. *Genes Dev.* 19, 2355–2366. doi: 10.1101/gad.354405
- van der Heijden, J., Reynolds, L. A., Deng, W., Mills, A., Scholz, R., Imami, K., et al. (2016). *Salmonella* rapidly regulates membrane permeability to survive oxidative stress. *MBio* 7:e01238. doi: 10.1128/mBio.01238-16
- Vila-Farrés, X., Parra-Millán, R., Sánchez-Encinales, V., Varese, M., Ayerbe-Algaba, R., Bayó, N., et al. (2017). Combating virulence of gram-negative bacilli by OmpA inhibition. *Sci. Rep.* 7:14683. doi: 10.1038/s41598-017-14972-y
- Vogel, J., and Papenfort, K. (2006). Small non-coding RNAs and the bacterial outer membrane. *Curr. Opin. Microbiol.* 9, 605–611. doi: 10.1016/j.mib.2006.10.006
- Waldminghaus, T., Heidrich, N., Brantl, S., and Narberhaus, F. (2007). FourU: a novel type of RNA thermometer in *Salmonella*. *Mol. Microbiol.* 65, 413–424. doi: 10.1111/j.1365-2958.2007.05794.x
- Weber, G. G., Kortmann, J., Narberhaus, F., and Klose, K. E. (2014). RNA thermometer controls temperature-dependent virulence factor expression in *Vibrio cholerae*. *Proc. Natl. Acad. Sci. U. S. A.* 111, 14241–14246. doi: 10.1073/pnas.1411570111
- Wei, Y., Kouse, A. B., and Murphy, E. R. (2017). Transcriptional and posttranscriptional regulation of *Shigella shuT* in response to host-associated iron availability and temperature. *Microbiology* 6:e00442. doi: 10.1002/mbo3.442
- Wei, Y., and Murphy, E. R. (2016). “Temperature-dependent regulation of bacterial gene expression by RNA thermometers” in *Nucleic Acids – From Basic Aspects to Laboratory Tools*. eds. M. Larramendy and S. Soloneski (London: IntechOpen).
- Weiser, J. N., and Gotschlich, E. C. (1991). Outer membrane protein A (OmpA) contributes to serum resistance and pathogenicity of *Escherichia coli* K-1. *Infect. Immun.* 59, 2252–2258. doi: 10.1128/IAI.59.7.2252-2258.1991
- Yanisch-Perron, C., Vieira, J., and Messing, J. (1985). Improved M13 phage cloning vectors and host strains: nucleotide sequences of the M13mp18 and pUC19 vectors. *Gene* 33, 103–119. doi: 10.1016/0378-1119(85)90120-9

Conflict of Interest: The authors declare that the research was conducted in the absence of any commercial or financial relationships that could be construed as a potential conflict of interest.

Copyright © 2021 Scheller, Twittenhoff, Becker, Holler and Narberhaus. This is an open-access article distributed under the terms of the Creative Commons Attribution License (CC BY). The use, distribution or reproduction in other forums is permitted, provided the original author(s) and the copyright owner(s) are credited and that the original publication in this journal is cited, in accordance with accepted academic practice. No use, distribution or reproduction is permitted which does not comply with these terms.



An Inventory of CiaR-Dependent Small Regulatory RNAs in *Streptococci*

Nancy Jabbour¹ and Marie-Frédérique Lartigue^{1,2*}

¹ Université de Tours, INRAE, ISP, Tours, France, ² Centre Hospitalier Universitaire de Tours, Service de Bactériologie, Virologie, et Hygiène Hospitalière, Tours, France

OPEN ACCESS

Edited by:

Olga Soutourina,
UMR 9198 Institut de Biologie
Intégrative de la Cellule (I2BC), France

Reviewed by:

Nadja Patenge,
University of Rostock, Germany
Luchang Zhu,
Houston Methodist Research
Institute, United States

*Correspondence:

Marie-Frédérique Lartigue
lartigue@univ-tours.fr

Specialty section:

This article was submitted to
Microbial Physiology and Metabolism,
a section of the journal
Frontiers in Microbiology

Received: 18 February 2021

Accepted: 30 March 2021

Published: 25 May 2021

Citation:

Jabbour N and Lartigue M-F
(2021) An Inventory
of CiaR-Dependent Small Regulatory
RNAs in *Streptococci*.
Front. Microbiol. 12:669396.
doi: 10.3389/fmicb.2021.669396

Bacteria adapt to the different environments encountered by rapid and tightly controlled regulations involving complex networks. A first line of control is transcriptional with regulators such as two-component systems (TCSs) that respond to physical and chemical perturbations. It is followed by posttranscriptional regulations in which small regulatory RNAs (sRNAs) may affect RNA translation. *Streptococci* are opportunistic pathogens for humans and farm animals. The TCS CiaRH is highly conserved among this genus and crucial in bacterial survival under stressful conditions. In several streptococcal species, some sRNAs belong to the CiaRH regulon and are called csRNAs for cia-dependent sRNAs. In this review, we start by focusing on the *Streptococcus* species harboring a CiaRH TCS. Then the role of CiaRH in streptococcal pathogenesis is discussed in the context of recent studies. Finally, we give an overview of csRNAs and their functions in *Streptococci* with a focus on their importance in bacterial adaptation and virulence.

Keywords: *Streptococci*, regulation, CiaRH, regulatory RNAs, csRNAs

INTRODUCTION

Due to their importance in the regulation of gene expression, small non-coding regulatory RNAs (sRNAs) are present in all kingdoms of life. The sRNAs were discovered in prokaryotes long before the first short interfering RNAs (siRNAs) and microRNAs (miRNAs) in eukaryotes. Adaptation to the environment involves a complex regulatory network in which sRNAs play an essential role. A decade ago, the high number of sRNAs discovered in various bacterial species was surprising (Brantl, 2009). Interestingly, these sRNAs differ in length, structure, and mode of action (Gottesman and Storz, 2011). However, sRNAs, 50–500 nucleotides long molecules, are often involved in the regulation of several cellular pathways and allow bacteria to adapt and survive under stressful conditions. All sRNAs are classified in several groups according to their location in the genome and their modes of action (Storz et al., 2011). In 1984, the first chromosomally encoded sRNA was discovered in *Escherichia coli*: MicF. This sRNA inhibits the translation of OmpF messenger RNA (mRNA) encoding the major membrane porin, OmpF (Mizuno et al., 1984). To respond to environmental changes, bacteria must first sense these changes, and two-component regulatory systems (TCS) are known to perform this function (Stock et al., 2000).

Streptococcal species infect humans and farm animals. Although some of them are commensal, other are responsible for severe infections in humans (Krzyściak et al., 2013). In *Streptococci*, many TCSs have been found. The TCS CiaRH was identified to be involved in natural competence and general virulence (Patenge et al., 2013). It is widespread among *Streptococci* but not found in another bacterial genus. Interestingly, it controls the expression of sRNAs called *cia*-dependent sRNAs (csRNAs) (Halfmann et al., 2007). This review concerns csRNAs identified in *streptococci*. It starts by highlighting the most important streptococcal species harboring a CiaRH and then analyzes the CiaRH TCS roles. Finally, this review focuses on all csRNAs identified until now and their functions.

STREPTOCOCCUS SPECIES HARBORING A TCS CIARH

The *Streptococcus* genus is composed of chain-forming gram-positive bacteria including a large number of species (>100). Although this genus includes beneficial species such as *Streptococcus thermophilus*, used in the food industry for the production of yogurt (Blomqvist et al., 2006), streptococci are opportunistic pathogens, often involved in severe diseases in humans and farm animals. The major species in human infections are *Streptococcus pneumoniae*, *S. pyogenes*, and *S. agalactiae* (Krzyściak et al., 2013). *S. pneumoniae* is the main cause of community-acquired pneumonia, meningitis, and acute otitis media. *S. pyogenes* (Group A *Streptococcus*), an exclusively human pathogen, is involved in mild (pharyngitis, skin infections) to severe fatal invasive infections, such as necrotizing fasciitis and streptococcal toxic shock syndrome. Groups C and G *Streptococci*, such as *Streptococcus dysgalactiae* subsp. *equisimilis* and *Streptococcus equi*, are microbiologically similar to *S. pyogenes* (Baracco, 2019). *S. agalactiae* (Group B *Streptococcus*), a commensal bacterium of the gastrointestinal and genitourinary tracts, is the leading cause of neonatal infections, causing pneumonia, bacteremia, and meningitis via maternal transmission. As *S. pneumoniae*, *Streptococcus mutans*, *Streptococcus sanguinis*, *Streptococcus gordonii*, *Streptococcus mitis*, *Streptococcus oralis*, and *Streptococcus infantis* belong to the physiological flora in the human oral cavity. *S. mutans* is an opportunistic commensal species responsible for biofilm formation causing dental caries but also infective endocarditis. Conversely, *S. gordonii* and *S. sanguinis* are non-cariogenic colonizers. *Streptococcus gallolyticus* (and less frequently *Streptococcus lutetiensis*), an opportunistic bacterium inhabiting the gastrointestinal tract, is one of the main causes of infective endocarditis and is strongly associated with colorectal cancer (Pasquereau-Kotula et al., 2018). Among *Streptococci*, including *S. agalactiae* and *S. equi* mentioned above, some species can also infect animals, as *Streptococcus suis*, responsible for severe invasive, and often lethal diseases in swine and humans and *Streptococcus uberis*, main agent of mastitis in dairy cows (Keane, 2019). These bacteria must colonize, invade, and persist in the host. But above all, they must adapt to environmental

changes and the various types of stress they encounter. One of the mechanisms that bacteria use to adapt and survive is the regulation of gene expression through the sRNA-mediated two-component regulatory systems.

CIARH: A STREPTOCOCCAL TWO-COMPONENT REGULATORY SYSTEM

TCS CiaRH was first identified in *S. pneumoniae* while selecting for cefotaxime resistance in spontaneous laboratory mutants. CiaH is a histidine protein kinase anchored in the cytoplasmic membrane that receives information from the environment. It transmits the information to CiaR, a cytoplasmic response regulator that translates the signal into a cellular response by regulating the expression of targeted genes (Figure 1; Guenzi et al., 1994). The amino-acid sequence identity of CiaH and CiaR from different species ranges between 48–71 and 77–85%, respectively (Riani et al., 2007). In several species, CiaRH is involved in biofilm formation. In fact, the presence of SpeA (streptococcal pyogenic exotoxin A) in *S. pyogenes* leads to down-regulation of CiaRH expression genes and attenuates the biofilm-forming capacity, suggesting a link between TCS expression and biofilm formation (Babbar et al., 2019). In *S. sanguinis*, the deletion of the *ciaR* gene up-regulates the expression of arginine biosynthesis genes resulting in the formation of a fragile biofilm (Zhu et al., 2017). In *S. gordonii*, the inactivation of SdbA, a thiol-disulfide oxidoreductase, up-regulates CiaRH, which in turn leads to enhanced biofilm formation (Davey et al., 2016a). In *S. mutans*, the inactivation of CiaH gene affects the dental biofilm formation, abolishes bacteriocin production and competence development, suggesting the involvement of CiaRH in these phenotypes (Qi et al., 2004). Actually, the up-regulation of CiaRH in *sdbA* mutant *S. gordonii* strain leads to bacteriocin expression shutdown whereas inactivation of CiaRH restores bacteriocin production. Involvement of the TCS in bacteriocin expression indicates its importance in bacterial competition in order to colonize the host (Davey et al., 2016b). CiaRH is also known to influence streptococcal stress tolerance. TCS is involved in tolerance to acid and thermal stress in *S. mutans* (Liu and Burne, 2009b). In *S. gordonii*, mutation of the TCS leads a greater susceptibility of the mutant to low pH and oxidative stress than the wild type (Liu and Burne, 2009a). Moreover, CiaRH is involved in resistance to the immune system, intracellular survival, and virulence. Actually, in CiaR-deficient *S. agalactiae* strains, resistance to the immune system and intracellular survival are affected (Quach et al., 2009; Mu et al., 2016). The deletion of CiaRH in *S. suis* enhances the bactericidal activity of macrophages and attenuates bacterial virulence in animal models (Li et al., 2011; Zaccaria et al., 2016). Furthermore, the transcription level of the TCS is significantly higher in virulent than in strains of low virulence (Dong et al., 2015). As for *S. pneumoniae*, the CiaRH system prevents autolysis triggered by different conditions and allows the maintenance of a stationary growth phase (Mascher et al., 2006). In *S. pyogenes*, a *ciaH* mutant strain binds more efficiently

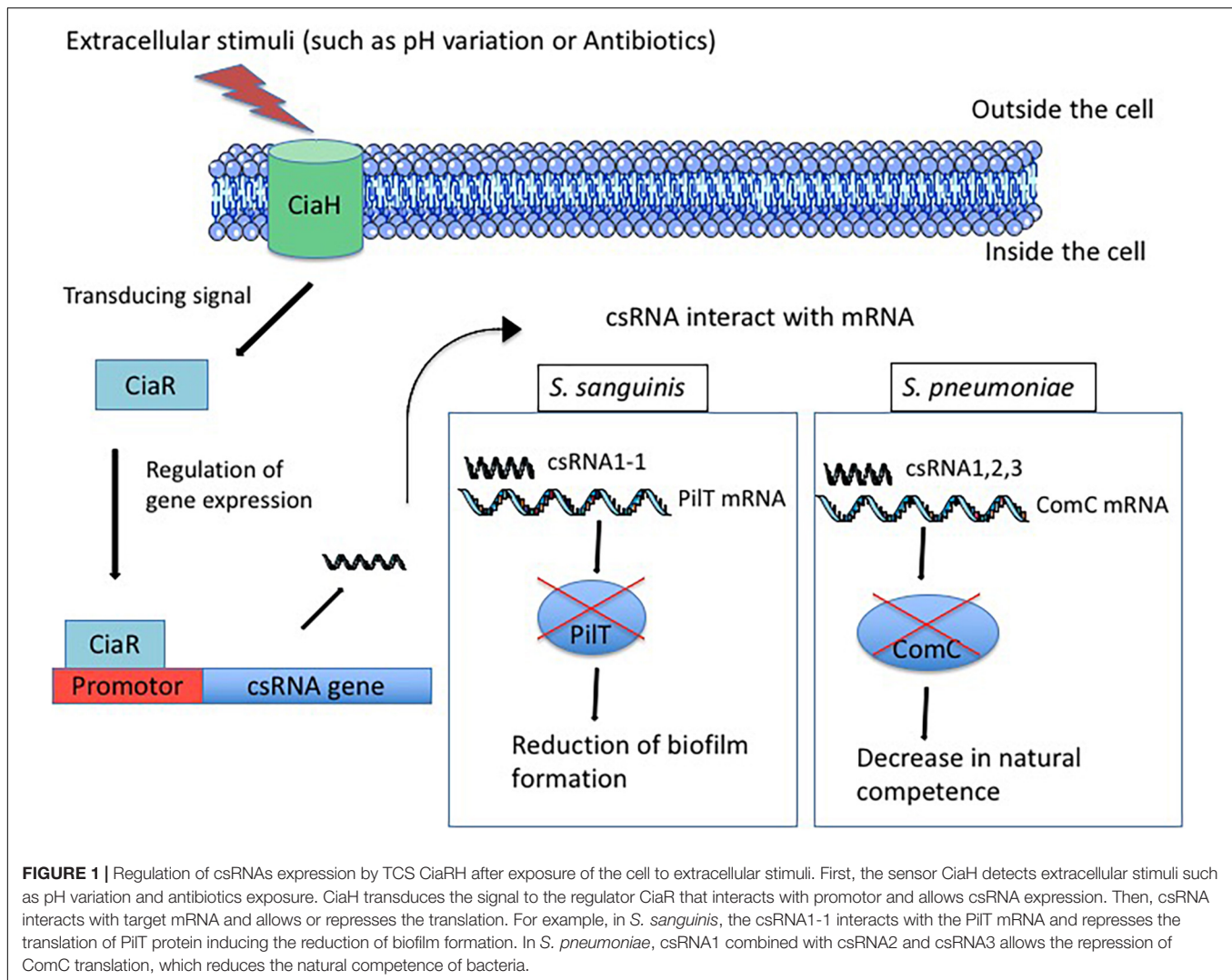


FIGURE 1 | Regulation of csRNAs expression by TCS CiaRH after exposure of the cell to extracellular stimuli. First, the sensor CiaH detects extracellular stimuli such as pH variation and antibiotics exposure. CiaH transduces the signal to the regulator CiaR that interacts with promoter and allows csRNA expression. Then, csRNA interacts with target mRNA and allows or represses the translation. For example, in *S. sanguinis*, the csRNA1-1 interacts with the PiIT mRNA and represses the translation of PiIT protein inducing the reduction of biofilm formation. In *S. pneumoniae*, csRNA1 combined with csRNA2 and csRNA3 allows the repression of ComC translation, which reduces the natural competence of bacteria.

to HEp-2 epithelial cells than the wild type. The internalization rate of the mutant is increased within the same range (Riani et al., 2007). Conversely, the deletion of CiaRH in *S. suis* exhibits a decrease in adherence to HEp-2 epithelial cells (Li et al., 2011). These conflicting results could be explained in two different ways. First, CiaRH-mediated regulation can be different between streptococcal species and under different conditions. Second, inactivation of only one gene of the TCS (*ciaH*) does not allow for obtaining the same phenotype as when both are inactive. In fact, when *ciaH* is inactive, *ciaR* may respond to other regulators whereas when only *ciaR* is inactive, *ciaH* may regulate other sensors. To summarize, CiaRH is involved in many cellular processes, including β -lactam resistance, lytic processes, biofilm formation, bacteriocin production, natural competence, virulence, and resistance to the immune system (Dagkessamanskaia et al., 2004; Seibert et al., 2005; Quach et al., 2009; Li et al., 2011). In *S. pneumoniae*, a direct repeat sequence, TTTAAG-N5-TTTAAG, has been identified by *in vitro* and *in vivo* transcriptional mapping as essential for the binding of CiaR. Fifteen promoters are controlled by

CiaR, five of them (the strongest) drive the expression of sRNAs, which are designated csRNAs for *cia*-dependent sRNAs (Halfmann et al., 2007).

INVENTORY OF CSRNAs IDENTIFIED SO FAR

The sRNAs are classified into four major groups: CRISPRs (clustered regulatory interspaced, short palindromic repeats), riboswitches, protein-binding RNAs, and *trans*-acting RNAs. And the csRNAs belong to the *trans*-acting class and more precisely to the *trans*-encoded subclass. *Trans*-encoded RNAs are often expressed by genes located at a different locus from their target genes and thus share only a short and imperfect complementarity sequence with their target mRNAs. This imperfect complementarity allows *trans*-encoded RNAs to control more than one target mRNA and, therefore, to be part of complex regulatory networks. *Trans*-encoded RNAs, by forming a base association, affect the translation or the stability of the

TABLE 1 | csRNAs predicted in streptococcal species.

Species	Strain	csRNA	Screening method	Confirmed by	Length (nt)	Direct target	Mechanism of action	Regulatory function	References
<i>S. pneumoniae</i>	R6 D39	csRNA1	PredictRegulon server	Northern blot	93	<i>comC</i> , <i>spr0081</i> , <i>spr0159</i> , <i>bmQ</i> , and <i>spr1097</i>	Translational repression by base pairing	Autolysis and competence modulation	Halfmann et al., 2007; Marx et al., 2010; Tsui et al., 2010; Schnorpfeil et al., 2013
		csRNA2			96				
		csRNA3			98				
		csRNA4			92				
		csRNA4			148				
<i>S. agalactiae</i>	NEM316	csRNA10	Non-coding RNA gene finder	RNA-seq, Northern blot	145	ND	ND	ND	Marx et al., 2010; Pichon et al., 2012; Rosinski-Chupin et al., 2015
		csRNA11			96				
		csRNA12			118				
		csRNA13			218				
<i>S. mitis</i>	B6	csRNA1	Non-coding RNA gene finder	Northern blot	94	ND	ND	ND	Marx et al., 2010
		csRNA2			97				
		csRNA3			99				
		csRNA4			96				
		csRNA5			146				
<i>S. mitis</i>	SF100	csRNA2	Non-coding RNA gene finder	NC	98	ND	ND	ND	Marx et al., 2010
		csRNA6			200				
<i>S. oralis</i>	Uo5	csRNA1	Non-coding RNA gene finder	Northern blot	95	ND	ND	ND	Marx et al., 2010
		csRNA2			98				
		csRNA3			100				
		csRNA4			93				
		csRNA6			200				
<i>S. sanguinis</i>	SK36	csRNA1-1	Non-coding RNA gene finder	Northern blot	89	<i>pilT</i>	Putative translational repression by base pairing	Inhibition of biofilm formation	Marx et al., 2010; Ota et al., 2017
		csRNA1-2	Non-coding RNA gene finder	Northern blot	93	ND	ND	ND	Marx et al., 2010
		csRNA1-3			87				
		csRNA2			96				
		csRNA7			85				
		csRNA8			176				
<i>S. pyogenes</i>	MGAS315	csRNA14	Non-coding RNA gene finder	RNA seq	68	ND	ND	ND	Marx et al., 2010; Le Rhun et al., 2016
		csRNA15			142				
		csRNA25			129				
<i>S. gordonii</i>	str. Challis substr. CH1	csRNA1	Non-coding RNA gene finder	NC	87	ND	ND	ND	Marx et al., 2010
		csRNA2-1			96				
		csRNA2-2			94				
		csRNA7			90				
		csRNA21			58				
		csRNA22			202				

(Continued)

TABLE 1 | Continued

Species	Strain	csRNA	Screening method	Confirmed by	Length (nt)	Direct target	Mechanism of action	Regulatory function	References
<i>S. mutans</i>	UA159	csRNA23-1 csRNA23-2 csRNA24	Non-coding RNA gene finder	NC	79 81 152	ND	ND	ND	Marx et al., 2010
<i>S. gallolyticus</i>	UCN34	csRNA9 csRNA18 csRNA38 csRNA39 csRNA40-1 csRNA40-2	Non-coding RNA gene finder	NC	63 66 138 118 65 71	ND	ND	ND	Marx et al., 2010
<i>S. dysgalactiae</i> subsp. <i>Equisimilis</i>	GGS_124	csRNA14 csRNA15 csRNA16 csRNA17	Non-coding RNA gene finder	NC	68 141 127 117	ND	ND	ND	Marx et al., 2010
<i>S. equi</i> subsp. <i>equi</i>	4047	csRNA18 csRNA17	Non-coding RNA gene finder	NC	50 105	ND	ND	ND	Marx et al., 2010
<i>S. equi</i> subsp. <i>zooepidemicus</i>	MGCS10565	csRNA18 csRNA19 csRNA20	Non-coding RNA gene finder	NC	67 105 108	ND	ND	ND	Marx et al., 2010
<i>S. suis</i>	05ZYH33	csRNA26 csRNA27 csRNA28	Non-coding RNA gene finder	NC	172 73 58	ND	ND	ND	Marx et al., 2010
<i>S. uberis</i>	0140J	csRNA29 csRNA30 csRNA31 csRNA32	Non-coding RNA gene finder	NC	84 83 67 140	ND	ND	ND	Marx et al., 2010
<i>S. thermophilus</i>	St0 plasmid pSt0	csRNA9	Non-coding RNA gene finder	NC	60	ND	ND	ND	Marx et al., 2010
<i>S. thermophilus</i>	CNRZ1066	csRNA33 csRNA34 csRNA35 csRNA36 csRNA37	Non-coding RNA gene finder	NC	66 85 64 97 127	ND	ND	ND	Marx et al., 2010
<i>S. lutetiensis</i>	033	csRNA9 csRNA18 csRNA38 csRNA39	BLAST analysis	NC	63 66 137 119	ND	ND	ND	Denapaité et al., 2016
<i>S. infantis</i>	GTC849	csRNA2 csRNA3 csRNA4 csRNA6	BLAST analysis	NC	98 100 93 200	ND	ND	ND	Denapaité et al., 2016

NC, Not confirmed; ND, Not determined.

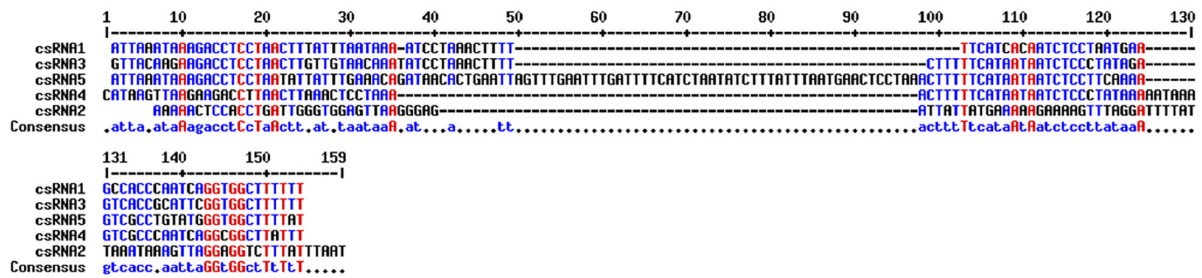
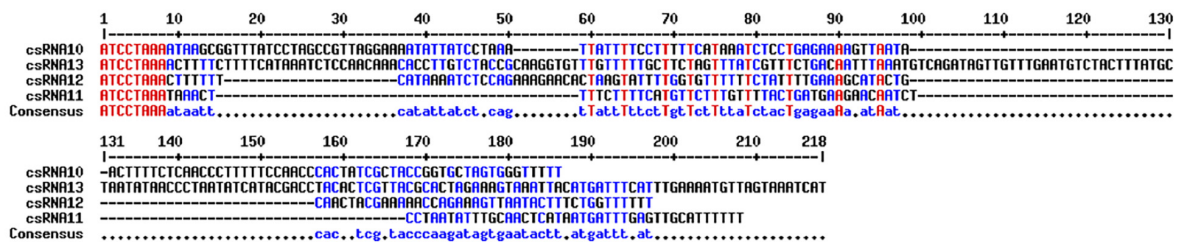
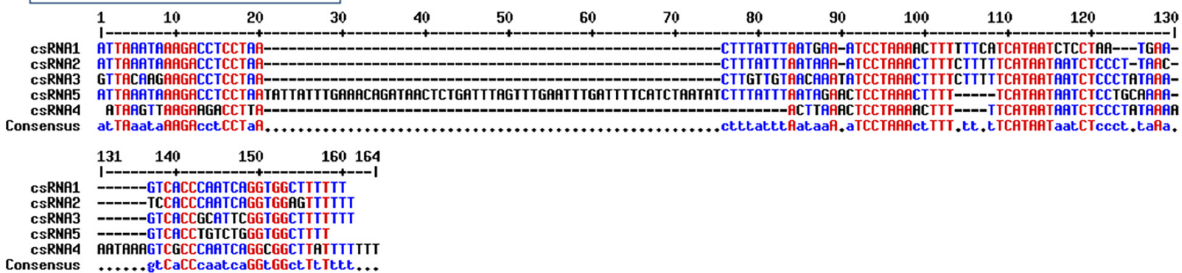
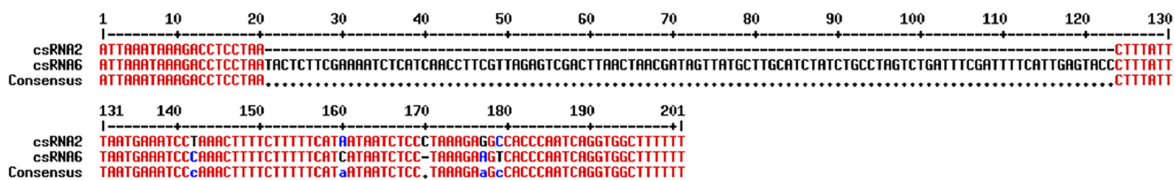
S. pneumoniae R6*S. agalactiae* NEM316*S. mitis* B6*S. mitis* SF100

FIGURE 2 | (Continued)

mRNAs. The interaction between an sRNA and its target mRNA leads to the inhibition of protein translation by blocking the ribosome binding site (RBS) or by inducing the degradation of the sRNA-mRNA duplex by RNases (Hui et al., 2014). Trans-encoded RNAs can also prevent mRNA degradation or activate mRNA translation by preventing the formation of an inhibitory

structure that hides the RBS (Prévost et al., 2007). The FasX sRNA of *S. pyogenes* allows bacterial dissemination through two different mechanisms: first, by increasing ska mRNA stability, allowing the overexpression of streptokinase, and second, by hiding the RBS and decreasing pilus mRNA translation (Ramirez-Peña et al., 2010; Danger et al., 2015).

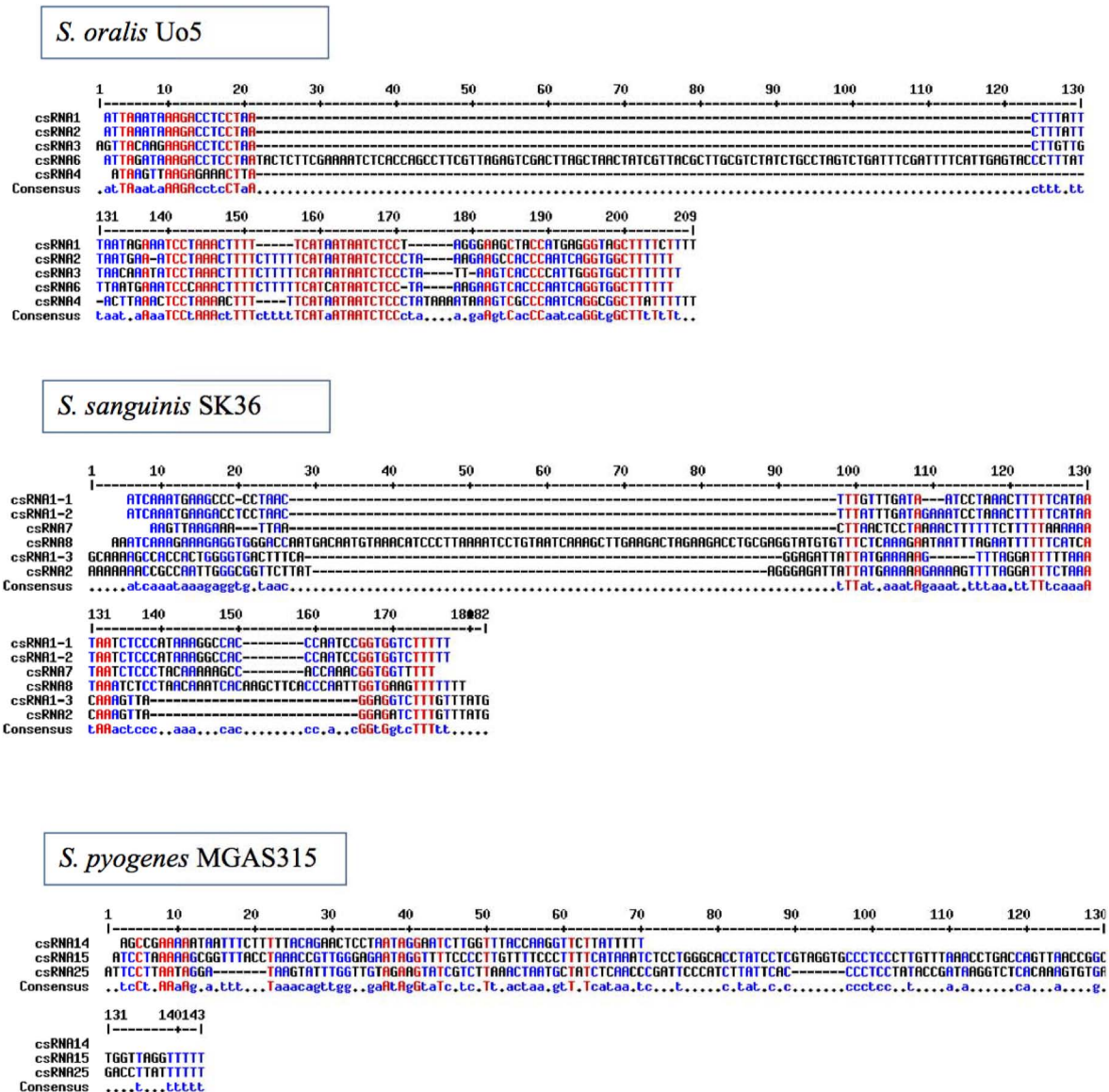


FIGURE 2 | (Continued)

The five csRNAs, discovered in *S. pneumoniae* and validated by Northern blot analyses, are between 87 and 151 nucleotides long and have a high degree of similarity to each other. The presence of sequences complementary to RBS in these csRNAs indicates that they may control the initiation of translation. csRNA1 was shown to be a negative regulator of competence development (Tsui et al., 2010). The deletion of csRNA4 and csRNA5 revealed their role in autolysis control (Halfmann et al., 2007), and a mutant of csRNA5 was defective in a lung infection (Mann et al., 2012). The targets of these csRNAs were investigated by computational predictions with targetRNA and IntaRNA (Tjaden et al., 2006; Busch et al., 2008). Thirty-three predicted genes were tested by translational fusion, and six of them are possibly regulated by *S. pneumoniae* csRNAs

(Schnorpfel et al., 2013). The *spr0081*, *spr0371*, *spr0551*, and *spr1097* genes encode membrane-spanning proteins that belong to different transporter families. The *spr0159* gene encodes a protein harboring a DNA-binding domain and therefore is most likely to be a transcriptional regulator. The last one, *spr2043* (*ComC*), encodes the competence-stimulating peptide precursor (CSP), suggesting a link between CiaRH and competence control, mediated by csRNAs (Figure 1; Håvarstein et al., 1995; Schnorpfel et al., 2013). It has been shown that each of the csRNAs down-regulates the *comC* gene, but they are not as effective alone as they are all together (Schnorpfel et al., 2013). However, the combination of three csRNAs, csRNA1, 2, 3, or csRNA1, 2, 4, is sufficient to decrease the competence of *S. pneumoniae* (Laux et al., 2015). Interestingly, duplicated

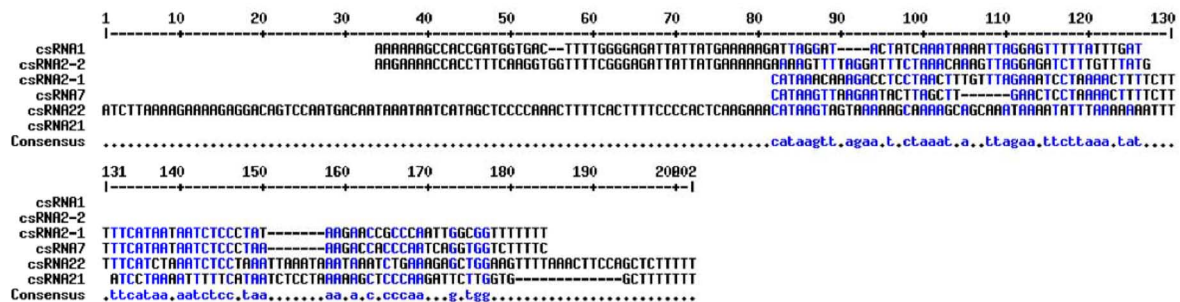
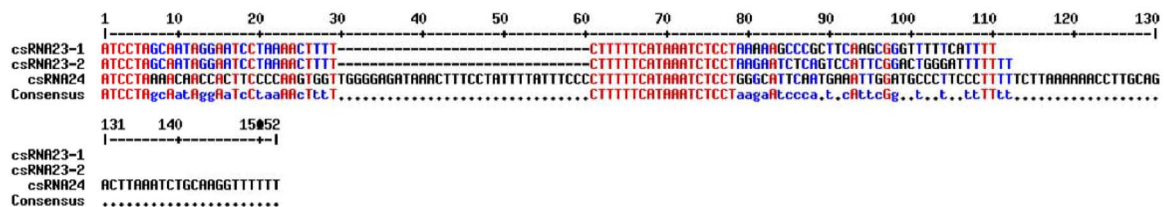
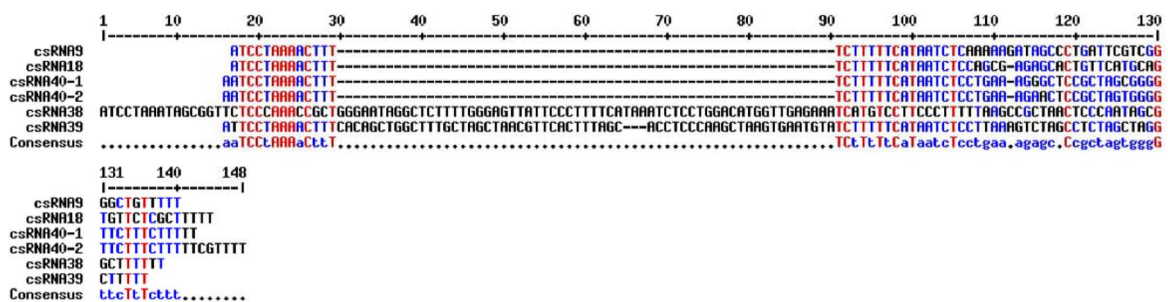
S. gordonii str. Challis substr. CH1*S. mutans* UA159*S. gallolyticus* UCN34

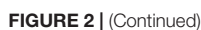
FIGURE 2 | (Continued)

csRNA was observed in Hungarian *S. pneumoniae* serotype 19A isolate. Indeed, an internal sequence duplication is the cause of the carriage and expression of longer version of csRNA5 (Brantl and Brückner, 2014).

In the study of Marx et al. (2010), the presence of the CiaR binding site located in the intergenic regions and followed by transcriptional terminator was investigated in 14 streptococcal genomes. Thus, 61 candidate genes potentially express csRNAs. Among them, four were predicted in all *S. agalactiae* strains: csRNA10, csRNA11, csRNA12, and csRNA13. Their expression was confirmed in NEM316 by RNA sequencing and the first three were also validated by

Northern blot. The genes were renamed *srn015*, *srn024*, *srn070*, and *srn085*, respectively. The corresponding csRNAs were overexpressed at low pH (5.2), suggesting they could contribute to acid stress resistance (Rosinski-Chupin et al., 2015). However, no function and no targets have been assigned to them yet.

In *S. sanguinis* SK36, six csRNAs were predicted (csRNA1-1, csRNA1-2, csRNA1-3, csRNA2, csRNA7, and csRNA8) and confirmed by Northern blot (Marx et al., 2010). Target prediction and a luciferase reporter assay allowed the identification of the *pilT* gene, a constituent of the type IV pilus gene cluster, to be the target of *S. sanguinis* csRNA1-1. The interaction



Five csRNAs in *S. mitis* B6 (csRNA1, csRNA2, csRNA3, csRNA4, and csRNA5) and five other csRNAs in *S. oralis* Uo5 (csRNA1, csRNA2, csRNA3, csRNA4, and csRNA6) were predicted and confirmed by Northern blot (Marx et al., 2010).

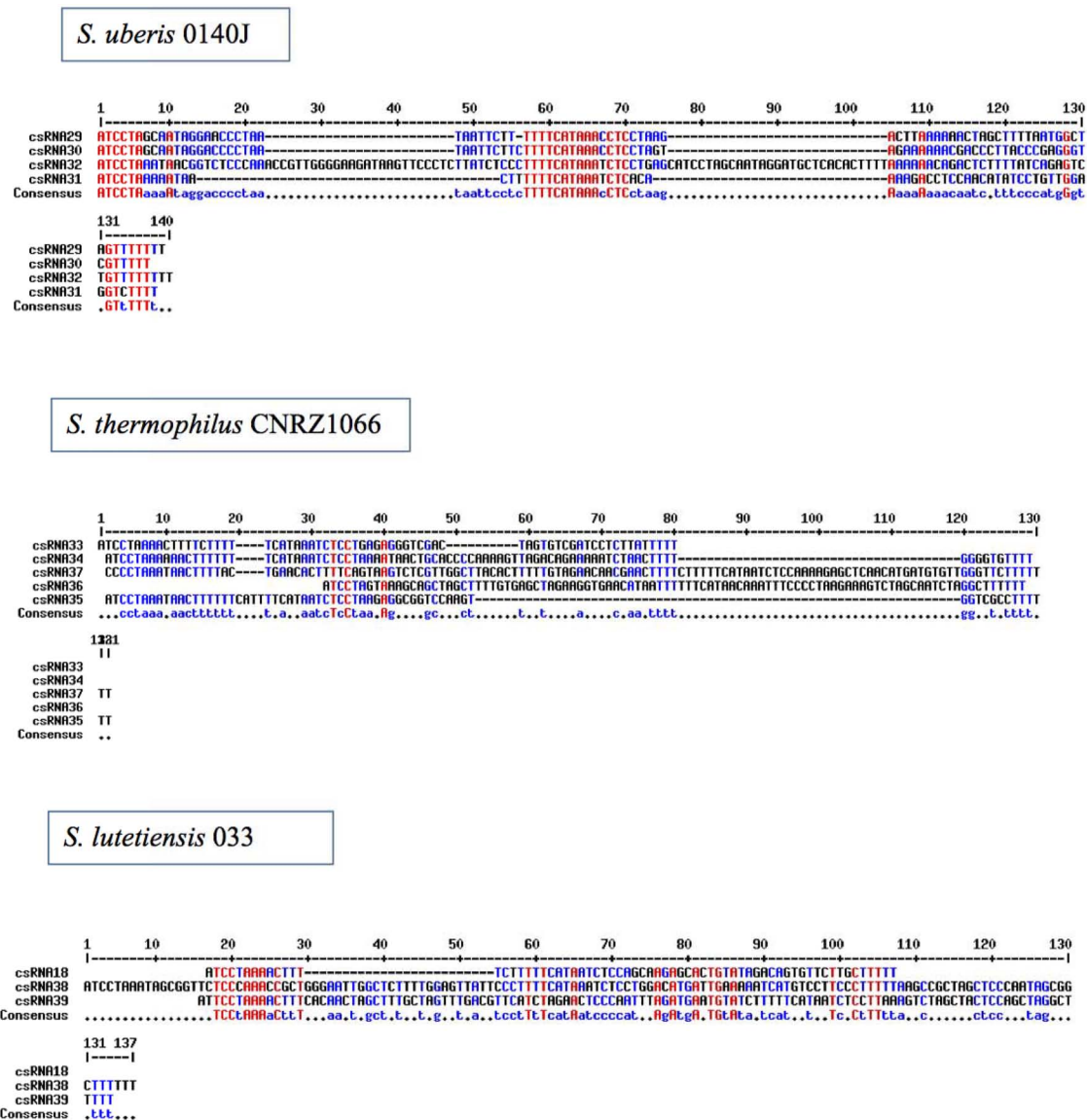


FIGURE 2 | Alignments of csRNAs sequences by species by MultAlin. Nucleotides in red correspond to highly conserved sequences. Nucleotides in blue correspond to conserved sequences. Nucleotides in black correspond to non-conserved sequences.

Other csRNAs have been predicted in *S. mutans* UA159, *S. suis* 05ZYH33, *S. gordonii*, *S. gallolyticus*, *S. dysgalactiae*, *S. equi*, *S. uberis*, and *S. thermophilus* but not confirmed so far (Marx et al., 2010; Table 1 and Supplementary Table 1). The identification of csRNAs of new viridans streptococci obtained from primates indicates that all csRNAs predicted previously in *S. mitis*, *S. gallolyticus*, *S. gordonii*, and *S. oralis* are present in the new strains studied. Two species with unknown csRNAs contain csRNAs from other species. Indeed, *S. infantis* harbors four of the five *S. oralis* Uo5 csRNAs, and *S. lutetiensis* harbors the *S. gallolyticus* UCN34 csRNAs except for csRNA40 (Denapate et al., 2016).

Except for *S. pneumoniae* and *S. sanguinis*, few studies regarding the role and targets of these csRNAs in other

streptococci were conducted, although the importance of RNAs is highlighted.

DISCUSSION

The aim of this review is to carry out an inventory of the sRNAs regulated by the two-component regulatory system CiaRH present in streptococci. CiaRH TCS is conserved in all streptococci and controls many cellular processes including natural competence, virulence, and resistance to the immune system (Dagkessamanskaia et al., 2004; Sebert et al., 2005; Quach et al., 2009; Li et al., 2011). The csRNAs increase the regulatory networks of CiaR, which already directly controls

more than 20 other genes (Halfmann et al., 2007). Promoters that drive the expression of the five csRNAs of *S. pneumoniae* are strongest in the CiaR regulon (Halfmann et al., 2007). The high proportion of sRNAs compared with other genes controlled by CiaRH indicates the importance of these csRNAs in bacterial regulation. Although csRNAs are predicted in various *Streptococcus* species and their importance highlighted, for most of them, no role or target has been identified until now. So far, only the csRNAs of *S. pneumoniae* and *S. sanguinis* have been investigated (Schnorpfel et al., 2013; Laux et al., 2015; Ota et al., 2017). The study of csRNAs in those species has allowed the identification of different metabolic pathways in which csRNAs may be involved. Indeed, *S. pneumoniae* harbors five csRNAs, all implicated in competence development and thus, probably in horizontal transfer (Halfmann et al., 2007; Tsui et al., 2010). Moreover, two *S. pneumoniae* csRNAs (csRNA4 and csRNA5) seem to control bacterial autolysis (Halfmann et al., 2007). The involvement of csRNA5 in lung infection as well shows that each csRNA may be involved in different regulatory pathways (Mann et al., 2012). In this case, csRNA5 is on the one hand involved in competence development and on the other hand in virulence.

The investigation of *S. pneumoniae* csRNAs targets also allowed identifying different regulation pathways. According to the competence regulation previously mentioned, one target (*ComC*), encoding the competence-stimulating peptide precursor (CSP) was identified. This identification adds a proof concerning the involvement of *S. pneumoniae* csRNAs in horizontal transmission pathways. The Spr0159 target is most likely a transcriptional regulator: this suggests the involvement of the csRNAs in complex regulatory networks. Other identified targets (*spr0081*, *spr0371*, *spr0551*, and *spr1097*), encoding membrane spanning, belonging to different transporter families, indicate the possible involvement of csRNAs in stress resistance (Schnorpfel et al., 2013). The four csRNAs identified in *S. agalactiae* NEM316 strain (*srn015*, *srn024*, *srn070*, and *srn085*) are overexpressed at low pH (5.2), suggesting their role in acid stress resistance (Rosinski-Chupin et al., 2015). Thus, the possible implication of csRNAs in stress tolerance in *S. pneumoniae* and *S. agalactiae* reveals a new regulation pathway in which csRNAs may play a role. In *S. sanguinis*, csRNAs are involved in host colonization by biofilm formation (Ota et al., 2017). This regulation of colonization by csRNAs has not yet been observed in other streptococcal species. Analysis of *S. pneumoniae*, *S. agalactiae*, and *S. sanguinis* csRNAs demonstrates that they are involved in a wide range of regulatory pathways. Indeed, the colonization, the virulence, the horizontal transfer, and maybe the resistance to environmental stress is affected by csRNAs. The various regulatory pathways in which csRNAs are involved can be explained by the diversity of csRNAs in each species and between streptococcus species. Moreover, as observed in *S. pneumoniae*, one csRNA can be involved in different regulatory pathways, thus increasing the complexity of regulatory networks.

The diversity of csRNAs between streptococcus species is remarkable (Table 1 and Supplementary Table 1). However, some species contain csRNAs from other species (*S. infantis*

harbors csRNAs of *S. oralis* Uo5 and *S. lutetiensis* harbors the *S. gallolyticus* UCN34 csRNAs) (Denapaite et al., 2016). Moreover, *S. oralis* strains contain duplicated csRNAs genes. A genetic island of four genes is present between them but absent in strains without csRNAs gene duplication. Furthermore, this genetic island is integrated in *S. infantis* DD18 between two csRNAs (Denapaite et al., 2016). These data suggest that csRNAs are not only involved in gene regulation but may also contribute to horizontal gene transfers improving bacterial adaptation.

In some species, csRNAs display a high degree of similarity to each other (Figure 2). This similarity is observed more particularly in regions complementary to RBSs and AUG start codons, suggesting that csRNAs bind to mRNA target and inhibit translational initiation. This would be fully consistent with the regulatory mechanism most commonly associated with sRNAs (Gottesman and Storz, 2011; Storz et al., 2011).

Other bacterial regulators also control multiple sRNA genes. For example, LuxO of *Vibrio harveyi* controls the expression of five sRNA genes (Tu and Bassler, 2007). The presence of regulators involved in sRNA regulation in various species suggests the importance of these sRNAs in bacterial adaptation and, beyond that, in bacterial survival.

Virulence and resistance to antibiotics and to the immune system mediated by CiaRH are possibly carried out through csRNAs. The discovery of Cbf1 protein that stabilizes all csRNAs in *S. pneumoniae* provides additional proof of the importance of csRNAs (Hör et al., 2020). In conclusion, understanding the csRNA-dependent regulatory network may contribute to the development of strategies against bacterial infections by targeting these sRNAs (Warner et al., 2018).

AUTHOR CONTRIBUTIONS

NJ and M-FL wrote the manuscript. Both authors contributed to the article and approved the submitted version.

FUNDING

NJ was supported by a doctoral fellowship of the Région Centre (France).

ACKNOWLEDGMENTS

We are grateful to Philippe Bouloc for his critical reading of the manuscript and helpful discussion. We thank the reviewers for their critical reading of the manuscript.

SUPPLEMENTARY MATERIAL

The Supplementary Material for this article can be found online at: <https://www.frontiersin.org/articles/10.3389/fmicb.2021.669396/full#supplementary-material>

Supplementary Table 1 | *Streptococcus* csRNAs sequences.

REFERENCES

- Babbar, A., Barrantes, I., Pieper, D. H., and Itzek, A. (2019). Superantigen SpeA attenuates the biofilm forming capacity of *Streptococcus pyogenes*. *J. Microbiol.* 57, 626–636. doi: 10.1007/s12275-019-8648-z
- Baracco, G. J. (2019). Infections caused by group C and G *Streptococcus* (*Streptococcus dysgalactiae* subsp. *equisimilis* and others): epidemiological and clinical aspects. *Microbiol. Spectr.* 7, 1–2. doi: 10.1128/microbiolspec.GPP3-0016-2018
- Blomqvist, T., Steinmoen, H., and Håvarstein, L. S. (2006). Natural genetic transformation: a novel tool for efficient genetic engineering of the dairy bacterium *Streptococcus thermophilus*. *Appl. Environ. Microbiol.* 72, 6751–6756. doi: 10.1128/AEM.01156-06
- Brantl, S. (2009). Bacterial chromosome-encoded small regulatory RNAs. *Future Microbiol.* 4, 85–103. doi: 10.2217/17460913.4.1.85
- Brantl, S., and Brückner, R. (2014). Small regulatory RNAs from low-GC gram-positive bacteria. *RNA Biol.* 11, 443–456. doi: 10.4161/rna.28036
- Busch, A., Richter, A. S., and Backofen, R. (2008). IntaRNA: efficient prediction of bacterial sRNA targets incorporating target site accessibility and seed regions. *Bioinforma* 24, 2849–2856. doi: 10.1093/bioinformatics/btn544
- Dagkessamanskaia, A., Moscoso, M., Hénard, V., Guiral, S., Overweg, K., Reuter, M., et al. (2004). Interconnection of competence, stress and CiaR regulons in *Streptococcus pneumoniae*: competence triggers stationary phase autolysis of ciaR mutant cells. *Mol. Microbiol.* 51, 1071–1086. doi: 10.1111/j.1365-2958.2003.03892.x
- Danger, J. L., Makthal, N., Kumaraswami, M., and Paul Sumby, P. (2015). The FasX small regulatory RNA negatively regulates the expression of two fibronectin-binding proteins in group A *Streptococcus*. *J. Bacteriol.* 197, 3720–3730. doi: 10.1128/JB.00530-15
- Davey, L., Halperin, S. A., and Lee, S. F. (2016a). Mutation of the *Streptococcus gordonii* thiol-disulfide oxidoreductase SdbA leads to enhanced biofilm formation mediated by the CiaRH two-component signaling system. *PLoS One* 11:e0166656. doi: 10.1371/journal.pone.0166656
- Davey, L., Halperin, S. A., and Lee, S. F. (2016b). Mutation of the Thiol-Disulfide Oxidoreductase SdbA Activates the CiaRH two-component system, leading to bacteriocin expression shutdown in *Streptococcus gordonii*. *J. Bacteriol.* 198, 321–331. doi: 10.1128/JB.00800-15
- Denapaite, D., Rieger, M., Köndgen, S., Brückner, R., Ochigava, I., Kappeler, P., et al. (2016). Highly variable *Streptococcus oralis* strains are common among viridans Streptococci isolated from primates. *mSphere* 1:e00041-15. doi: 10.1128/mSphere.00041-15
- Dong, W., Ma, J., Zhu, Y., Zhu, J., Yuan, L., Wang, Y., et al. (2015). Virulence genotyping and population analysis of *Streptococcus suis* serotype 2 isolates from China. *Infect. Genet. Evol.* 36, 483–489. doi: 10.1016/j.meegid.2015.08.021
- Gottesman, S., and Storz, G. (2011). Bacterial small RNA regulators: versatile roles and rapidly evolving variations. *Cold Spring Harb. Perspect. Biol.* 3:a003798. doi: 10.1101/cshperspect.a003798
- Guenzi, E., Gasc, A. M., Sicard, M. A., and Hakenbeck, R. (1994). A two-component signal-transducing system is involved in competence and penicillin susceptibility in laboratory mutants of *Streptococcus pneumoniae*. *Mol. Microbiol.* 12, 505–515. doi: 10.1111/j.1365-2958.1994.tb01038.x
- Halfmann, A., Kovács, M., Hakenbeck, R., and Brückner, R. (2007). Identification of the genes directly controlled by the response regulator CiaR in *Streptococcus pneumoniae*: five out of 15 promoters drive expression of small non-coding RNAs. *Mol. Microbiol.* 66, 110–126. doi: 10.1111/j.1365-2958.2007.05900.x
- Håvarstein, L. S., Coomaraswamy, G., and Morrison, D. A. (1995). An unmodified heptadecapeptide pheromone induces competence for genetic transformation in *Streptococcus pneumoniae*. *Proc. Natl. Acad. Sci. U.S.A.* 92, 11140–11144. doi: 10.1073/pnas.92.24.11140
- Hör, J., Garriss, G., Di Giorgio, S., Hack, L. M., Vanselow, J. T., Förstner, K. U., et al. (2020). Grad-seq in a Gram-positive bacterium reveals exonucleolytic sRNA activation in competence control. *EMBO J.* 39:e103852. doi: 10.15252/embj.2019103852
- Hui, M. P., Foley, P. L., and Belasco, J. G. (2014). Messenger RNA degradation in bacterial cells. *Annu. Rev. Genet.* 48, 537–559. doi: 10.1146/annurev-genet-120213-092340
- Keane, O. M. (2019). Symposium review: Intramammary infections-Major pathogens and strain-associated complexity. *J. Dairy Sci.* 102, 4713–4726. doi: 10.3168/jds.2018-15326
- Krzyściak, W., Pluskwa, K. K., Jurczak, A., and Kościelniak, D. (2013). The pathogenicity of the *Streptococcus* genus. *Eur. J. Clin. Microbiol. Infect. Dis.* 32, 1361–1376. doi: 10.1007/s10096-013-1914-9
- Laux, A., Sexauer, A., Sivaselvarajah, D., Kaysen, A., and Brückner, R. (2015). Control of competence by related non-coding csRNAs in *Streptococcus pneumoniae* R6. *Front. Genet.* 6:246. doi: 10.3389/fgene.2015.00246
- Le Rhun, A., Beer, Y. Y., Reimegård, J., Chylinski, K., and Charpentier, E. (2016). RNA sequencing uncovers antisense RNAs and novel small RNAs in *Streptococcus pyogenes*. *RNA Biol.* 13, 177–195. doi: 10.1080/15476286.2015.1110674
- Li, J., Tan, C., Zhou, Y., Fu, S., Hu, L., Hu, J., et al. (2011). The two-component regulatory system CiaRH contributes to the virulence of *Streptococcus suis* 2. *Vet. Microbiol.* 148, 99–104. doi: 10.1016/j.vetmic.2010.08.005
- Liu, Y., and Burne, R. A. (2009a). Multiple two-component systems modulate alkali generation in *Streptococcus gordonii* in response to environmental stresses. *J. Bacteriol.* 191, 7353–7362. doi: 10.1128/JB.01053-09
- Liu, Y., and Burne, R. A. (2009b). Multiple two-component systems of *Streptococcus mutans* regulate agmatine deiminase gene expression and stress tolerance. *J. Bacteriol.* 191, 7363–7366. doi: 10.1128/JB.01054-09
- Mann, B., van Opijnen, T., Wang, J., Obert, C., Wang, Y.-D., Carter, R., et al. (2012). Control of virulence by small RNAs in *Streptococcus pneumoniae*. *PLoS Pathog.* 8:e1002788. doi: 10.1371/journal.ppat.1002788
- Marx, P., Nuhn, M., Kovács, M., Hakenbeck, R., and Brückner, R. (2010). Identification of genes for small non-coding RNAs that belong to the regulon of the two-component regulatory system CiaRH in *Streptococcus*. *BMC Genomics* 11:661. doi: 10.1186/1471-2164-11-661
- Mascher, T., Heintz, M., Zähler, D., Merai, M., and Hakenbeck, R. (2006). The CiaRH system of *Streptococcus pneumoniae* prevents lysis during stress induced by treatment with cell wall inhibitors and by mutations in pbp2x involved in beta-lactam resistance. *J. Bacteriol.* 188, 1959–1968. doi: 10.1128/JB.188.5.1959-1968.2006
- Mizuno, T., Chou, M. Y., and Inouye, M. (1984). A unique mechanism regulating gene expression: translational inhibition by a complementary RNA transcript (micRNA). *Proc. Natl. Acad. Sci. U.S.A.* 81, 1966–1970. doi: 10.1073/pnas.81.7.1966
- Mu, R., Cutting, A. S., Del Rosario, Y., Villarino, N., Stewart, L., Weston, T. A., et al. (2016). Identification of CiaR regulated genes that promote group B Streptococcal virulence and interaction with brain endothelial cells. *PLoS One* 11:e153891. doi: 10.1371/journal.pone.0153891
- Ota, C., Morisaki, H., Nakata, M., Arimoto, T., Fukamachi, H., Kataoka, H., et al. (2017). *Streptococcus sanguinis* noncoding cia-dependent small RNAs negatively regulate expression of Type IV Pilus retraction ATPase PilT and biofilm formation. *Infect. Immun.* 86:e00894-17. doi: 10.1128/IAI.00894-17
- Pasquereau-Kotula, E., Martins, M., Aymeric, L., and Dramsi, S. (2018). Significance of *Streptococcus gallolyticus* subsp. *gallolyticus* association with colorectal cancer. *Front. Microbiol.* 9:614. doi: 10.3389/fmicb.2018.00614
- Patenge, N., Fiedler, T., and Kreikemeyer, B. (2013). Common regulators of virulence in streptococci. *Curr. Top. Microbiol. Immunol.* 368, 111–153. doi: 10.1007/82_2012_295
- Pichon, C., du Merle, L., Caliot, M. E., Trieu-Cuot, P., and Le Bouguéne, C. (2012). An in silico model for identification of small RNAs in whole bacterial genomes: characterization of antisense RNAs in pathogenic *Escherichia coli* and *Streptococcus agalactiae* strains. *Nucleic Acids Res.* 40, 2846–2861. doi: 10.1093/nar/gkr1141
- Prévost, K., Salvail, H., Desnoyers, G., Jacques, J.-F., Phaneuf, E., and Massé, E. (2007). The small RNA RyhB activates the translation of shiA mRNA encoding a permease of shikimate, a compound involved in siderophore synthesis. *Mol. Microbiol.* 64, 1260–1273. doi: 10.1111/j.1365-2958.2007.05733.x
- Qi, F., Merritt, J., Lux, R., and Shi, W. (2004). Inactivation of the ciaH gene in *Streptococcus mutans* diminishes mutacin production and competence development, alters sucrose-dependent biofilm formation, and reduces stress tolerance. *Infect. Immun.* 72, 4895–4899. doi: 10.1128/IAI.72.8.4895-4899.2004
- Quach, D., van Sorge, N. M., Kristian, S. A., Bryan, J. D., Shelver, D. W., and Doran, K. S. (2009). The CiaR response regulator in group B *Streptococcus* promotes

- intracellular survival and resistance to innate immune defenses. *J. Bacteriol.* 191, 2023–2032. doi: 10.1128/JB.01216-08
- Ramirez-Peña, E., Treviño, J., Liu, Z., Perez, N., and Sumbly, P. (2010). The group A *Streptococcus* small regulatory RNA FasX enhances streptokinase activity by increasing the stability of the ska mRNA transcript. *Mol. Microbiol.* 78, 1332–1347. doi: 10.1111/j.1365-2958.2010.07427.x
- Riani, C., Standar, K., Srimuang, S., Lembke, C., Kreikemeyer, B., and Podbielski, A. (2007). Transcriptome analyses extend understanding of *Streptococcus pyogenes* regulatory mechanisms and behavior toward immunomodulatory substances. *Int. J. Med. Microbiol.* 297, 513–523. doi: 10.1016/j.ijmm.2007.04.005
- Rosinski-Chupin, I., Sauvage, E., Sismeiro, O., Villain, A., Da Cunha, V., Caliot, M.-E., et al. (2015). Single nucleotide resolution RNA-seq uncovers new regulatory mechanisms in the opportunistic pathogen *Streptococcus agalactiae*. *BMC Genomics* 16:419. doi: 10.1186/s12864-015-1583-4
- Schnorpfel, A., Kranz, M., Kovács, M., Kirsch, C., Gartmann, J., Brunner, I., et al. (2013). Target evaluation of the non-coding csRNAs reveals a link of the two-component regulatory system CiaRH to competence control in *Streptococcus pneumoniae* R6. *Mol. Microbiol.* 89, 334–349. doi: 10.1111/mmi.12277
- Sebert, M. E., Patel, K. P., Plotnick, M., and Weiser, J. N. (2005). Pneumococcal HtrA protease mediates inhibition of competence by the CiaRH two-component signaling system. *J. Bacteriol.* 187, 3969–3979. doi: 10.1128/JB.187.12.3969-3979.2005
- Stock, A. M., Robinson, V. L., and Goudreau, P. N. (2000). Two-component signal transduction. *Annu. Rev. Biochem.* 69, 183–215. doi: 10.1146/annurev.biochem.69.1.183
- Storz, G., Vogel, J., and Wassarman, K. M. (2011). Regulation by small RNAs in bacteria: expanding frontiers. *Mol. Cell* 43, 880–891. doi: 10.1016/j.molcel.2011.08.022
- Tjaden, B., Goodwin, S. S., Opdyke, J. A., Guillier, M., Fu, D. X., Gottesman, S., et al. (2006). Target prediction for small, noncoding RNAs in bacteria. *Nucleic Acids Res.* 34, 2791–2802. doi: 10.1093/nar/gkl356
- Tsui, H.-C. T., Mukherjee, D., Ray, V. A., Sham, L.-T., Feig, A. L., and Winkler, M. E. (2010). Identification and characterization of noncoding small RNAs in *Streptococcus pneumoniae* serotype 2 strain D39. *J. Bacteriol.* 192, 264–279. doi: 10.1128/JB.01204-09
- Tu, K. C., and Bassler, B. L. (2007). Multiple small RNAs act additively to integrate sensory information and control quorum sensing in *Vibrio harveyi*. *Genes Dev.* 21, 221–233. doi: 10.1101/gad.1502407
- Warner, K. D., Hajdin, C. E., and Weeks, K. M. (2018). Principles for targeting RNA with drug-like small molecules. *Nat. Rev. Drug Discov.* 17, 547–558. doi: 10.1038/nrd.2018.93
- Zaccaria, E., Cao, R., Wells, J. M., and van Baarlen, P. (2016). A Zebrafish larval model to assess virulence of porcine *Streptococcus suis* strains. *PLoS One* 11:e0151623. doi: 10.1371/journal.pone.0151623
- Zhu, B., Ge, X., Stone, V., Kong, X., El-Rami, F., Liu, Y., et al. (2017). ciaR impacts biofilm formation by regulating an arginine biosynthesis pathway in *Streptococcus sanguinis* SK36. *Sci. Rep.* 7, 1–13. doi: 10.1038/s41598-017-17383-1

Conflict of Interest: The authors declare that the research was conducted in the absence of any commercial or financial relationships that could be construed as a potential conflict of interest.

Copyright © 2021 Jabbour and Lartigue. This is an open-access article distributed under the terms of the Creative Commons Attribution License (CC BY). The use, distribution or reproduction in other forums is permitted, provided the original author(s) and the copyright owner(s) are credited and that the original publication in this journal is cited, in accordance with accepted academic practice. No use, distribution or reproduction is permitted which does not comply with these terms.



RNA Chaperones Hfq and ProQ Play a Key Role in the Virulence of the Plant Pathogenic Bacterium *Dickeya dadantii*

Simon Leonard, Camille Villard, William Nasser, Sylvie Reverchon* and Florence Hommais*

Université de Lyon, INSA Lyon, Université Claude Bernard Lyon 1, CNRS, UMR 5240 MAP, Microbiologie, Adaptation, Pathogénie, Villeurbanne, France

OPEN ACCESS

Edited by:

Daniela De Biase,
Sapienza University of Rome, Italy

Reviewed by:

Lucy N. Moleleki,
University of Pretoria, South Africa
Sébastien Bontemps-Gallo,
Institut Pasteur de Lille, France
Marta Potrykus,
Medical University of Gdańsk, Poland

*Correspondence:

Florence Hommais
florence.hommais@univ-lyon1.fr
Sylvie Reverchon
sylvie.reverchon-pescheux@insa-lyon.fr

Specialty section:

This article was submitted to
Microbial Physiology and Metabolism,
a section of the journal
Frontiers in Microbiology

Received: 29 March 2021

Accepted: 31 May 2021

Published: 24 June 2021

Citation:

Leonard S, Villard C, Nasser W, Reverchon S and Hommais F (2021) RNA Chaperones Hfq and ProQ Play a Key Role in the Virulence of the Plant Pathogenic Bacterium *Dickeya dadantii*. *Front. Microbiol.* 12:687484. doi: 10.3389/fmicb.2021.687484

Dickeya dadantii is an important pathogenic bacterium that infects a number of crops including potato and chicory. While extensive works have been carried out on the control of the transcription of its genes encoding the main virulence functions, little information is available on the post-transcriptional regulation of these functions. We investigated the involvement of the RNA chaperones Hfq and ProQ in the production of the main *D. dadantii* virulence functions. Phenotypic assays on the *hfq* and *proQ* mutants showed that inactivation of *hfq* resulted in a growth defect, a modified capacity for biofilm formation and strongly reduced motility, and in the production of degradative extracellular enzymes (proteases, cellulase, and pectate lyases). Accordingly, the *hfq* mutant failed to cause soft rot on chicory leaves. The *proQ* mutant had reduced resistance to osmotic stress, reduced extracellular pectate lyase activity compared to the wild-type strain, and reduced virulence on chicory leaves. Most of the phenotypes of the *hfq* and *proQ* mutants were related to the low amounts of mRNA of the corresponding virulence factors. Complementation of the double mutant *hfq-proQ* by each individual protein and cross-complementation of each chaperone suggested that they might exert their effects via partially overlapping but different sets of targets. Overall, it clearly appeared that the two Hfq and ProQ RNA chaperones are important regulators of pathogenicity in *D. dadantii*. This underscores that virulence genes are regulated post-transcriptionally by non-coding RNAs.

Keywords: *Dickeya dadantii* 3937, ProQ, Hfq, virulence, non-coding RNA (ncRNA)

INTRODUCTION

Dickeya dadantii is a Gram-negative phytopathogenic bacterium responsible for soft rot disease in a wide range of plant species including economically important crops (e.g., potato, chicory, sugar beet) and many ornamental plants (Ma et al., 2007). It causes important production losses (Toth et al., 2011).

Virulence mechanisms of *D. dadantii* have been extensively studied (Ma et al., 2007). The infection process is divided in two distinct phases: (i) an asymptomatic phase when the bacterium penetrates into the host and progresses through intercellular spaces without multiplying

substantially; and (ii) a symptomatic phase associated with strongly increased bacterial fitness and multiplication (Fagard et al., 2007). Globally, the four main steps of plant infection by *Dickeya* are the following: (i) adherence to the plant surface and entry into the plant tissues, via wound sites or through natural openings such as stomata, (ii) colonization of the apoplastic spaces between plant cells, (iii) suppression of the host defense response, and (iv) plant cell wall degradation (through degradative extracellular enzyme production, mainly pectate lyases) resulting in the development of disease symptoms. Each of these disease stages and life-history transitions requires the correct spatio-temporal production of the different adaptive and virulence factors (including those involved in adhesion, motility, stress resistance, and plant cell wall degradation) in response to various signals (changes in cell density, variation in environmental physico-chemical parameters, and host disease reaction) (Reverchon and Nasser, 2013).

To characterize the regulation of this pathogenic process, investigations on *D. dadantii* have mostly focused on its control by DNA-binding transcription factors (Reverchon and Nasser, 2013; Leonard et al., 2017) with a few additional studies about the regulatory role of chromosome dynamics (Ouafa et al., 2012; Jiang et al., 2015; Meyer et al., 2018). Knowledge of the post-transcriptional regulation of virulence factor production by sRNAs in *D. dadantii* is still in its infancy.

Post-transcriptional regulation is defined as the control of gene expression at the RNA level and classically occurs through base-pairing interactions between regulatory RNAs (sRNAs) and mRNAs. This base pairing can have positive or negative effects on the stability and/or the translation of the targeted mRNA. These sRNAs can be broadly divided into two categories according to their genomic location: (i) *cis*-acting antisense sRNAs are transcribed from the opposite strand of their targets and act via extensive base pairing; and (ii) *trans*-acting sRNAs mostly originate from intergenic regions, display partial sequence complementarities with their mRNA targets and can regulate more than one target. The interactions between sRNAs and their targets are often assisted by specialized RNA-binding proteins called RNA chaperones.

A prominent bacterial RNA chaperone is the Hfq protein which contributes to regulation by *trans*-acting sRNAs in many bacteria (Updegrove et al., 2016). Hfq was first discovered in *Escherichia coli* as an essential host factor of the RNA bacteriophage Qbeta. Hfq impacts multiple steps, like changing RNA structure, bringing RNAs into proximity, neutralizing the negative charge of the two pairing RNAs, stimulating the nucleation of the first base pairs as well as facilitating the further annealing of the two RNA strands. While estimates of the number of Hfq vary from $\approx 20,000$ to 60,000 (Kajitani et al., 1994; Ali Azam et al., 1999), it is clear that Hfq is limiting under most conditions (Wagner, 2013).

Other proteins with possible chaperone activity have been reported recently. For example, the monomeric ProQ protein of *Salmonella enterica* is an RNA-binding protein that interacts with and stabilizes over 50 highly structured antisense and *trans*-acting sRNAs (Smirnov et al., 2016). The cellular concentration of ProQ was estimated to be 2,000 copies per cell (Sheidy and

Zielke, 2013). This protein was originally identified as being important for osmolyte accumulation in *E. coli* by increasing cellular levels of the proline transporter ProP (Milner and Wood, 1989; Kunte et al., 1999) and was later shown to possess RNA strand exchange and RNA annealing activities (Chaulk et al., 2011). Thus, ProQ was initially described as an RNA chaperone that controls ProP levels in *E. coli*. In *Legionella pneumophila*, the ProQ equivalent protein (called RocC) interacts with one *trans*-acting sRNA to control the expression of genes involved in natural transformation (Attaiech et al., 2016). ProQ belongs to the RNA-binding proteins of the FinO family. FinO has been studied for its role as an RNA chaperone in antisense regulation of F plasmid conjugation in *E. coli* (Mark Glover et al., 2015). As shown in *S. enterica*, ProQ seems to recognize stable RNA hairpins such as transcriptional terminators and reading the RNA structure rather than its sequence (Holmqvist et al., 2018).

While several recent studies have addressed a potential role of Hfq in the virulence of phytopathogenic bacteria like *Agrobacterium tumefaciens* (Wilms et al., 2012), *Erwinia amylovora* (Zeng et al., 2013), *Pantoea ananatis* (Shin et al., 2019), *Pectobacterium carotovorum* (Wang et al., 2018), and *Xanthomonas campestris* (Lai et al., 2018), nothing is known about the impact of Hfq and ProQ on *D. dadantii* virulence. Moreover, potential links between ProQ and the virulence of plant-pathogenic bacteria have never been established. To address these questions, we constructed and characterized *hfq* and *proQ* mutants. Loss of Hfq or ProQ resulted in drastically reduced virulence. This phenotype was associated with the alteration of several virulence determinants including pectate lyase production, motility, and adhesion. Additionally, analyses of mutants defective in the two proteins suggested that these two RNA chaperones might exert their effects via partially overlapping but different sets of targets.

MATERIALS AND METHODS

Bacterial Strains, Plasmids and Culture Conditions

The bacterial strains, plasmids, phages and primers used in this study are described in **Supplementary Tables 1–3**. *E. coli* and *D. dadantii* strains were grown at 37 and 30°C, respectively, in Lysogeny broth (LB) medium or in M63 minimal medium (Miller, 1972) supplemented with 0.1 mM CaCl₂, 0.2% (w/v) sucrose and 0.25% (w/v) polygalacturonate (PGA, a pectin derivative from Agdia Biofords) as carbon sources. PGA induces the synthesis of pectate lyases, which are the essential virulence factors of *D. dadantii*. Sucrose has been chosen because it is one of the major sugars in the apoplast (Lohaus et al., 2001). When required, the media were supplemented with antibiotics at the following concentrations: ampicillin (Amp) 100 µg/mL, chloramphenicol (Cm) 20 µg/mL, kanamycin (Kan) 50 µg/mL. The media were solidified with 1.5 % (w/v) Difco agar. Liquid cultures were grown in a shaking incubator (220 r.p.m.). Bacterial growth in liquid medium was estimated by measuring turbidity at 600 nm (OD₆₀₀) spectrophotometer Prim' Light Secomam to determine growth rates.

Gene Knockout and Complementation of the Hfq- and ProQ-Encoding Genes in *D. dadantii*

The *hfq* gene was inactivated by introducing a *uidA-Kan* cassette into the unique *BsrGI* restriction site present in its open reading frame. The *uidA-Kan* cassette (Bardonnet and Blanco, 1992) includes a promoterless *uidA* gene that conserves its Shine Dalgarno sequence.

To create a $\Delta\text{proQ}::\text{Cm}$ mutant, segments located 500 bp upstream and 500 bp downstream of *proQ* were amplified by PCR using primer pairs P1-P2 and P3-P4 (Supplementary Table 3). Primers P2 and P3 included a unique restriction site for *BglIII* and were designed to have a short 20-bp overlap of complementary sequences. The two separate PCR fragments were attached together by overlap extension polymerase chain reaction using primers P1 and P4. The resulting $\Delta\text{proQ-BglIII}$ PCR product was cloned into a pGEMT plasmid to create plasmid pGEM-T- $\Delta\text{proQ-BglIII}$. The Cm resistance cassette from plasmid pKD3 (Datsenko and Wanner, 2000) was inserted into the unique *BglIII* site of pGEM-T- $\Delta\text{proQ-BglIII}$ to generate pGEM-T- $\Delta\text{proQ}::\text{Cm}$ (Supplementary Table 2).

We took care to select cassettes without transcription termination signals in order to avoid polar effects on downstream genes for both insertions. The insertions were introduced into the *D. dadantii* chromosome by marker exchange recombination between the chromosomal allele and the plasmid-borne mutated allele. The recombinants were selected after successive cultures in low phosphate medium in the presence of the suitable antibiotic because pGEMT (which is a pBR322 derivative) is very unstable in these conditions (Roeder and Collmer, 1985). Correct recombination was confirmed by PCR. Mutations were transduced into a clean *D. dadantii* 3937 genetic background using phage ΦEC2 (Supplementary Table 1; Resibois et al., 1984).

For complementation of the *hfq* and *proQ* mutations, the promoter and coding sequences of the *proQ* and *hfq* genes were amplified from *D. dadantii* 3937 genomic DNA using primers P5/P6 and P7/P8, respectively (Supplementary Table 3). The forward primers (P5 and P7) included a unique restriction site for *NheI*, and the reverse primers (P6 and P8) included a unique restriction site for *HindIII*. After digestion with *NheI* and *HindIII*, each PCR fragment was ligated into pBBR1-mcs4 previously digested by *NheI* and *HindIII* to generate pBBR1-mcs4::*hfq* and pBBR1-mcs4::*proQ*, respectively (Supplementary Table 2). Correct constructions were confirmed by sequencing.

Agar Plate Detection Tests for Pectate Lyase, Cellulase, Protease and Other Enzyme Assays

Protease activity was detected on medium containing skim milk (12.5 g L^{-1}). Cellulase activity was detected on carboxymethylcellulose agar plates with the Congo red staining procedure (Teather and Wood, 1982). Pectate lyases were assayed on toluenized cell extracts. Pectate lyase activity was measured by recording the degradation of PGA into unsaturated

products that absorb at 230 nm (Moran et al., 1968). Specific activity was expressed as nmol of unsaturated products liberated per min per mg of bacterial dry weight, given that an OD_{600} of 1 corresponded to $10^9 \text{ bacteria mL}^{-1}$ and to 0.47 mg of bacterial dry weight mL^{-1} .

Stress Resistance Assays

Stress resistance assays were performed as previously described (Duprey et al., 2019). Bacteria were cultured at 30°C in 96-well plates using M63S (M63 + 0.2% w/v sucrose), pH 7.0, as minimal medium. Bacterial growth (OD_{600}) was monitored for 48 h using an Infinite®200 PRO – Tecan instrument. Resistance to osmotic stress was analyzed using M63S enriched in 0.05 to 0.5 M NaCl. Resistance to oxidative stress was analyzed in the same medium by adding H_2O_2 concentrations ranging from 25 to 200 μM . The pH effect was analyzed using the same M63S medium buffered with malic acid at different pH values ranging from 3.7 to 7.0.

Biofilm Measurements

Biofilm formation was quantified using the microtiter plate static biofilm model. Bacteria were grown for 48 h at 30°C in 24-well plates in M63 medium supplemented with glycerol as the carbon source. Then, the supernatant was removed, and the biofilm was washed once with 1 mL of M63 medium and resuspended in 1 mL of the same medium. The percentage of adherence was then calculated as the ratio of the number of cells in the biofilm over the total number of cells, i.e., biofilm cells over planktonic cells. The amount of planktonic cells was estimated by measuring the optical density at 600 nm of the supernatant and the washing buffer. The amount of cells in the biofilm was estimated by measuring the OD_{600} of the biofilm resuspended in M63.

Motility and Chemotaxis Assays

For the *proQ* mutant, motility assays were performed on semi-solid LB agar plates. An overnight bacterial culture was prepared as described above, and then inoculated in the center of each of eight Petri dishes with a sterile toothpick. For motility experiments, 0.3 % agar plates were used. Halo sizes were examined after incubation at 30°C for 24 h. Motility indexes were calculated as the ratios of the mutant halo size over the wild type (WT) halo size.

For the *hfq* mutant, motility assays were performed in competition (to avoid the influence of bacterial growth), as previously described (Ashby et al., 1988). Briefly, 10 mL of bacteria in their exponential growth phase were washed twice in sodium-free buffer and then concentrated in 3 mL. Capillary assays were performed in competition in an equal 1:1 ratio. Suspension dilutions of chemotaxis assays were spotted onto LB agar medium supplemented when necessary, with antibiotics to select strains harboring plasmid or cassette. Different bacterial populations were thus enumerated on LB agar plates allowing the growth of both wild-type cells and *hfq::uidA-Kan* mutants and LB agar plates containing kanamycin allowing the growth of *hfq::uidA-Kan* mutants only. Motility indexes were calculated as the ratios of the number of *hfq::uidA-Kan* mutants over the number of wild-type cells. The number of wild-type cells was estimated by subtracting the number of growing cells on LB agar

plates containing kanamycin (*hfq* mutants) from the number of growing cells on LB agar plates containing kanamycin (wild-type and *hfq* mutant).

Virulence Assays

Virulence assays were performed on wounded chicory leaves by depositing a drop of inoculum as previously described (Dellagi et al., 2005). Briefly, chicory leaves were wounded with a 2 cm incision using a sterile scalpel, inoculated with 5×10^6 bacteria and incubated at 30°C in a dew chamber at 100% relative humidity. Disease severity was determined 18 and 48 h after inoculation by collecting and weighing the macerated tissues. The bacteria were estimated by measuring turbidity at 600 nm ($OD_{600} = 1$ corresponds to 10^9 bacteria/mL⁻¹).

Quantitative RT-PCR Analyses

Gene expression analyses were performed using qRT-PCR. Total RNAs were extracted and purified from cultures grown to the late exponential phase ($OD_{600} = 0.8$) as previously described (Maes and Messens, 1992; Hommais et al., 2008). Reverse transcription and quantitative PCR were performed using the REvertAid First Strand cDNA synthesis kit and the Maxima SYBR Green/ROX qPCR Master Mix (Thermo Scientific) with an LC480 Lightcycler (Roche). Primer specificity was verified by melting curve analysis. qPCR primers are listed in **Supplementary Table 4**.

Data Representation and Statistical Analysis

Boxplot representations were generated using R software (R Core Team, 2020) and the beeswarm package (Eklund, 2016). Statistical analysis was performed using Wilcoxon Mann-Whitney tests, and differences were considered significant when the *P* value < 0.05.

RESULTS

Analysis of *D. dadantii* Hfq and ProQ Protein Sequences and Their Genomic Contexts

Escherichia coli and *Dickeya dadantii* Hfq proteins displayed 83% identity. The highest identity level was in the N-terminal region (amino acids 1–74), which forms the core of the protein and contains its RNA-binding sites (Link et al., 2009). Most of the amino acids involved in RNA interactions were conserved except E18, which was K18 in *D. dadantii* (**Supplementary Figure 1**). *D. dadantii* ProQ was 68% identical with *E. coli* ProQ, with also high identity in the N-terminal FinO domain of ProQ, which is the primary determinant of its RNA-binding capacity (Chaulk et al., 2011; Gonzalez et al., 2017). In particular, the regions spanning residues 1–10 and 92–105, shown to interact with RNA, were highly conserved (Gonzalez et al., 2017). All the residues involved in the formation of a basic patch on the protein surface (R32, R69, R80, R100, K101, K107, and R114) – an important structure for interaction with RNAs – were conserved (**Supplementary Figure 1**).

The *hfq* and *proQ* genes are embedded in the same chromosomal context in *D. dadantii* as in other bacteria such as *E. coli* or *S. enterica* (**Supplementary Figure 2**). The *hfq* gene is part of the well conserved *amiB-mutL-miaA-hfq-hflXKC* cluster (Tsui and Winkler, 1994), while *proQ* is localized between *yebR* and *prc*. Inspection of the transcriptomes of *D. dadantii* under various physiological conditions (Reverchon et al., 2021) showed that transcription of *hfq* could be driven by (i) a promoter upstream of *mutL*, (ii) a promoter inside *mutL* and upstream of *miaA*, or (iii) two promoters inside *miaA* and upstream of *hfq* (**Supplementary Figure 2**). Considering the expression level of *mutL-miaA-hfq* genes, it appears that *hfq* was largely transcribed from the two promoters inside *miaA* and rarely co-transcribed with *miaA*. The downstream genes showed similar expression profiles and did not exhibit any promoter activity downstream of *hfq*, suggesting that they may be co-transcribed with *hfq* in the same way as in *E. coli* (RegulonDB¹). Two promoters were found upstream of the *proQ* gene (one between *proQ* and *yebR* and one upstream of *yebR*) (**Supplementary Figure 2B**). Regarding the difference in read coverage obtained from RNA-seq experiments, *yebR* and *proQ* seemed to be largely transcribed separately (**Supplementary Figure 2B**). On the contrary, *prc* and *proQ* had similar coverage, and no transcription start site was found between them, supporting co-transcription similarly to what is observed in *E. coli* (RegulonDB, see text footnote 1). The polycistronic organization and promoters for both *hfq* and *proQ* were confirmed by direct RNA sequencing using the nanopore technology (R. Forquet, personal communication).

Phenotypic Characterization of the *hfq* and *proQ* Mutants

We first analyzed the growth characteristics of the *hfq* and *proQ* mutants. The WT, *hfq* and *proQ* strains were grown in LB rich medium and in M63 minimal medium supplemented with sucrose as the sole carbon source. Sucrose was chosen because it is one of the major sugars of the apoplast (Lohaus et al., 2001). While the *proQ* mutant and the WT grew similarly in both media, the *hfq* mutant exhibited delayed growth. However, in rich medium both the WT strain and *hfq* mutant reached the same optical density after being grown for 26 h (**Figure 1A**). In minimal medium with sucrose as the sole carbon source, the *hfq* mutant grew much more slowly than the WT, and reached the stationary phase at a lower optical density (**Figure 1B**). The growth defect of the *hfq* mutant was fully restored by complementation with plasmid pBBR-mcs4::*hfq* (**Figure 1**), indicating that the *hfq::uidA*-Kan insertion had no polar effects on downstream *hflXKC* genes. In contrast, transformation of the *proQ* mutant and WT strains with the pBBR-mcs4::*proQ* plasmid expressing *proQ* led to a lower growth rate, especially in minimal medium (**Figure 1D**). The two strains grew similarly in the absence of the pBBR-mcs4::*proQ* plasmid. This suggests that slight ProQ overexpression compromises growth irrespective of the genetic background. These data demonstrate that *hfq* mutation retards cellular growth, while *proQ* mutation does not. The effect was more pronounced in minimal medium compared to rich

¹<http://regulondb.ccg.unam.mx/>

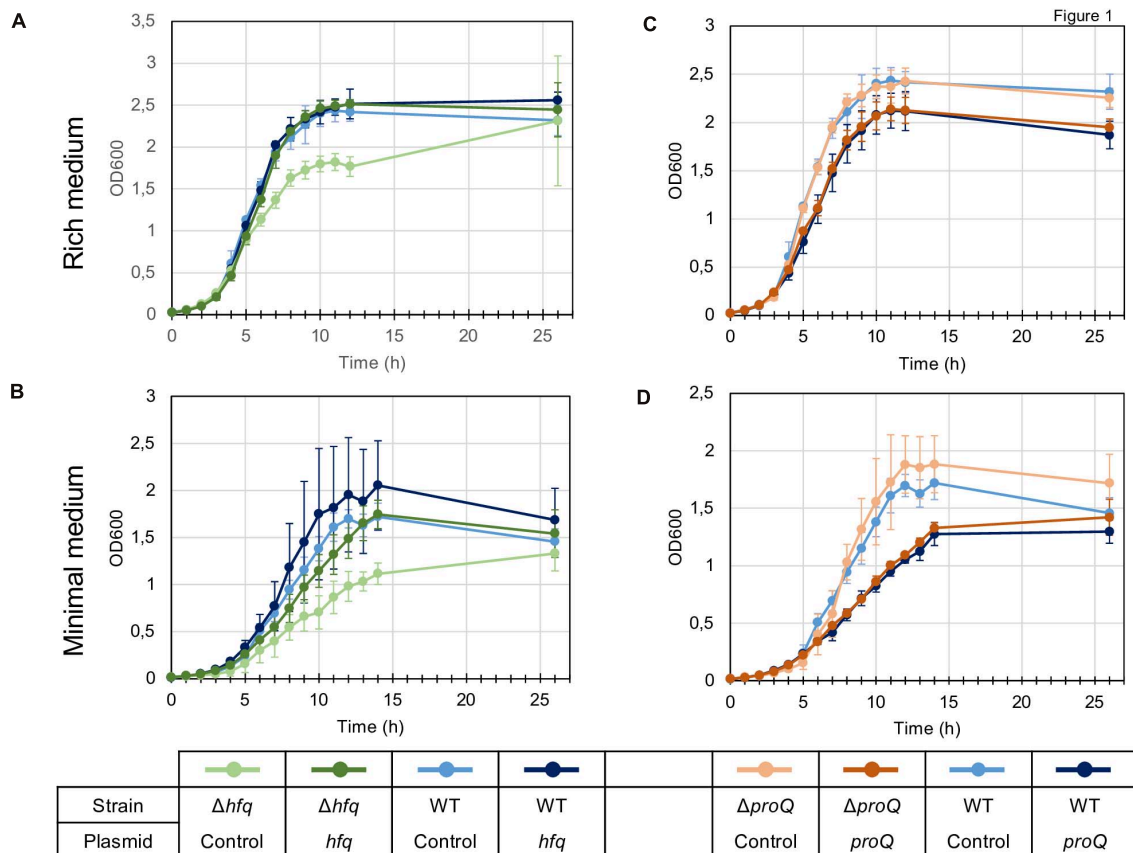


FIGURE 1 | Growth of the wild type, mutant and complemented strains in LB rich medium (A,C) and M63 minimal medium supplemented with sucrose (B,D).

Overnight bacterial precultures were diluted to an OD₆₀₀ of 0.03 in the same growth medium. OD₆₀₀ measurements of the culture were made at regular intervals to determine growth rates. The experiment was repeated three times. The graph shows curves from one representative experiment. Error bars represent deviation of biological replicates.

medium, suggesting that Hfq plays a more important role in the ability of *D. dadantii* to grow under conditions of nutrient limitation. A similar growth defect of *hfq* mutants has been observed in other bacteria such as *P. carotovorum* (Wang et al., 2018), *A. tumefaciens* (Wilms et al., 2012), *X. campestris* (Lai et al., 2018), *P. ananatis* (Shin et al., 2019) or *E. amylovora* (Zeng et al., 2013).

Dickeya encounter various stresses during their pathogenic growth, so we assessed the stress resistance of the *hfq* and *proQ* mutants (Supplementary Figure 3). They both showed behaviors similar to the WT strain regarding pH and H₂O₂ stress resistance, but displayed a higher sensitivity to osmotic stress than the WT strain did. The *hfq* mutant displayed a 50% growth rate reduction on 0.4 M NaCl, while the WT strain was only slightly affected (20% growth rate reduction). This effect was even more pronounced at 0.5 M NaCl, with a growth rate reduction of 90% for *hfq* compared to 60% for the WT. The *proQ* mutant did not grow at 0.3 M NaCl and at higher NaCl concentrations (Supplementary Figure 3). Complementation experiments revealed that expression of *hfq* or *proQ* from an episome (plasmid pBBR-mcs4:*hfq* and pBBR1-mcs4:*proQ*) fully restored the osmotic resistance of the two

mutants to the WT level (Supplementary Figure 3). We inferred that the two chaperones are involved in providing resistance to osmotic stress. Overall, this result is consistent but not identical with previous studies showing that Hfq and ProQ contribute to stress tolerance, including nutrient deprivation, osmotic stress and oxidative stress in *Salmonella* and *E. coli* (Chaulk et al., 2011; Smirnov et al., 2017).

Hfq and ProQ Are Required for Full Virulence of *Dickeya dadantii*

The virulence of the *hfq* and *proQ* mutants was tested on chicory leaves. The *hfq* mutant was severely impaired in virulence, and soft rot symptoms were drastically reduced (Figure 2A). Disease symptoms were observed following inoculation with the *proQ* mutant and the WT strain, but they were less severe in the *proQ* background. Quantitative results obtained by measuring the weight of macerated tissues showed a significant difference between the disease symptoms induced by each strain (p -value = 1.5e-3) (Figures 2B,C). As observed previously, the virulence defect of the *hfq* mutant was more severe than that of the *proQ* mutant, in as far as the *hfq* mutant did not exhibit

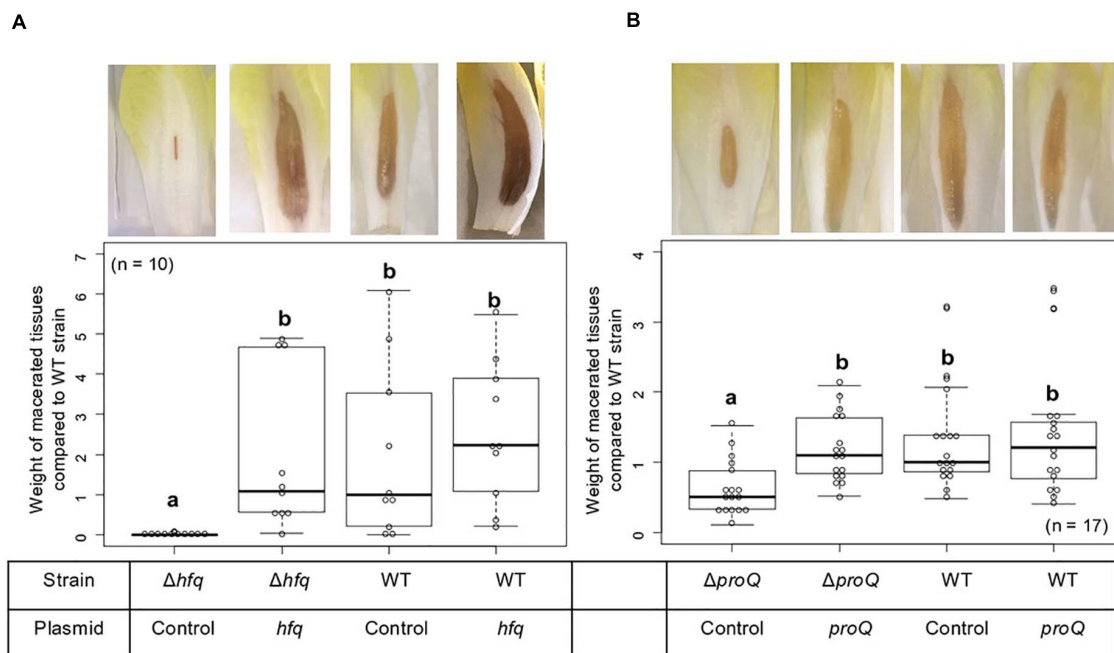


FIGURE 2 | Impact of Hfq and ProQ on *D. dadantii* virulence. Representative examples of symptoms induced by the wild type and mutant strains and weights of macerated tissues following infection by the *hfq* (A) and *proQ* mutants (B), the wild type strain and the respective complemented strains. Data were normalized based on the weights of macerated tissues from the wild-type strain. Chicory leaf assays were performed as described in the Materials and methods section with an incubation time of 18 h, and weights of macerated tissues were measured. The experiments were repeated three times with ten leaves tested in each replicate. Non-capital letters a and b are presented above the boxplots. Groups with the same letter are not detectably different (are in the same set) and groups that are detectably different get different letters (different sets). Note that if the groups have the same letter, this does not mean they are the same, just that there is no evidence of a difference for that pair ($P < 0.05$, Wilcoxon Mann-Whitney test).

any macerated tissue (p -value = $5.7e-4$). Consequently, we did not weigh any macerated tissue in the *hfq* mutant. The soft rot symptoms caused by the *hfq* and *proQ* mutants did not increase over longer incubation times (48 h). The lower virulence of *hfq* and *proQ* was therefore not solely related to retarded cellular growth. Complementation experiments revealed that expression of *hfq* from an episome (plasmid pBBR-mcs4:*hfq*) fully restored the impaired virulence of the *hfq* mutant (Figure 2B). Likewise, expression of *proQ* from an episome (plasmid pBBR-mcs4:*proQ*) restored the impaired virulence of the *proQ* mutant (Figure 2B).

Thus, the *hfq* and *proQ* genes are required for efficient pathogenic growth since both mutants were clearly impaired in initiating maceration and inducing soft rot symptoms, albeit to different extents.

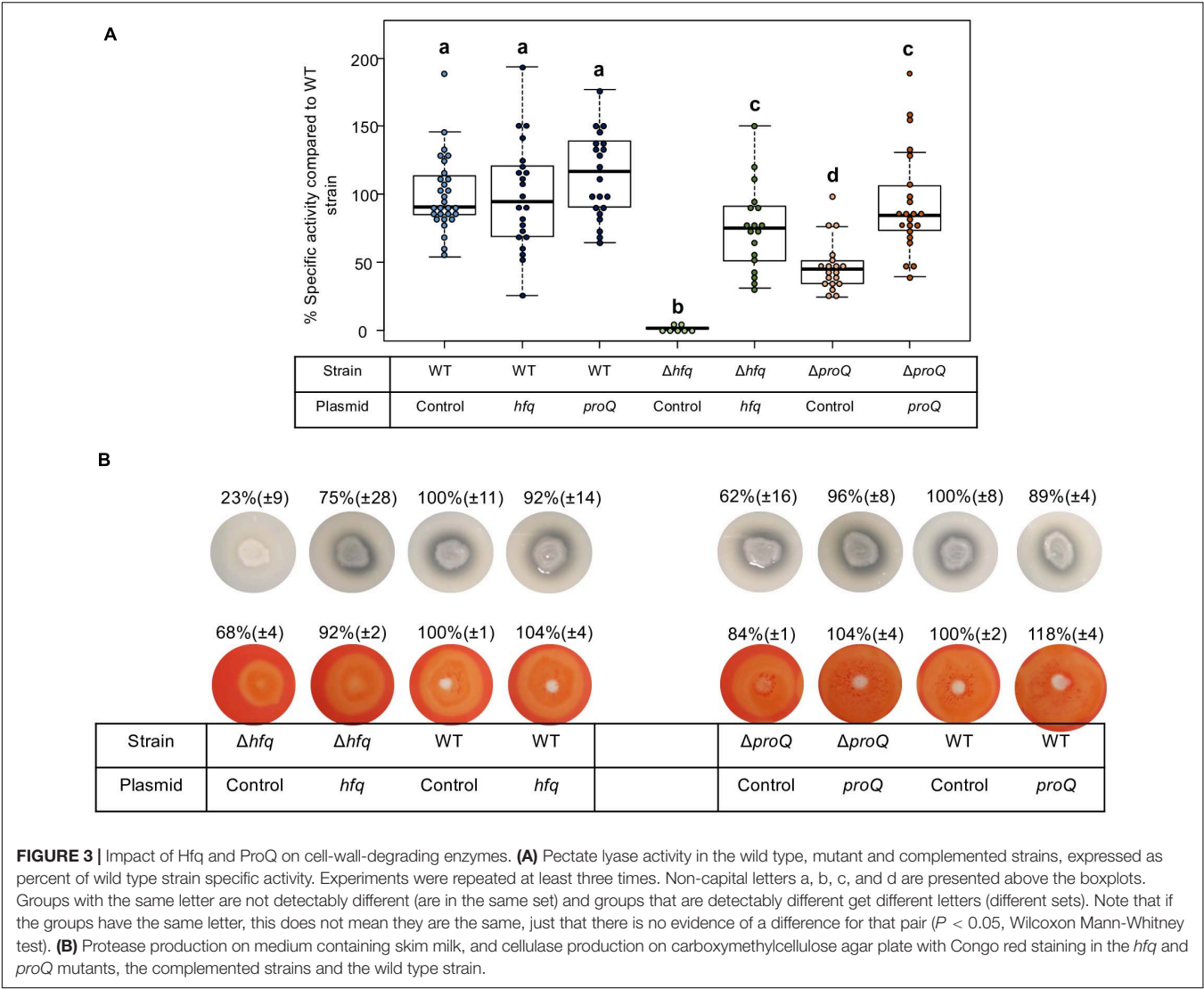
Production of Late Virulence Factors, Pectate Lyase, Protease and Cellulase, Is Abolished in the *hfq* Mutant and Reduced in the *proQ* Mutant

Dickeya dadantii is known to use several essential virulence factors that collectively contribute to its ability to cause disease. These factors include production of cell-wall-degrading enzymes like pectate lyases, proteases and cellulase, which are responsible for soft rot symptoms. To clarify whether Hfq and ProQ have any influence on the production of key virulence factors, we

compared enzyme activity in *hfq* and *proQ* mutant extracts with WT strain extracts (Figure 3A). Pectate lyase activity was abolished in the *hfq* mutant (p -value = $2.4e-7$). This defect in pectate lyase activity was not a consequence of the growth defect of the *hfq* mutant since activities were normalized to cell density. Also, the levels of pectate lyase activity were significantly reduced in the *proQ* mutant compared to the WT (p -value = $2.0e-9$) (Figure 3A). Reduced cellulase and protease activities were also observed on carboxymethylcellulose and skim milk agar plates for each mutant (Figure 3B). Complementation experiments showed that the impaired production of cell-wall-degrading enzymes was restored in *hfq* and *proQ* mutant cells transformed with the pBBR-mcs4:*hfq* and pBBR-mcs4:*proQ* plasmids, respectively (Figure 3). Therefore, the impaired pathogenicity of *D. dadantii* due to *hfq* and *proQ* mutations is linked with reduced production of late virulence factors in these mutant strains.

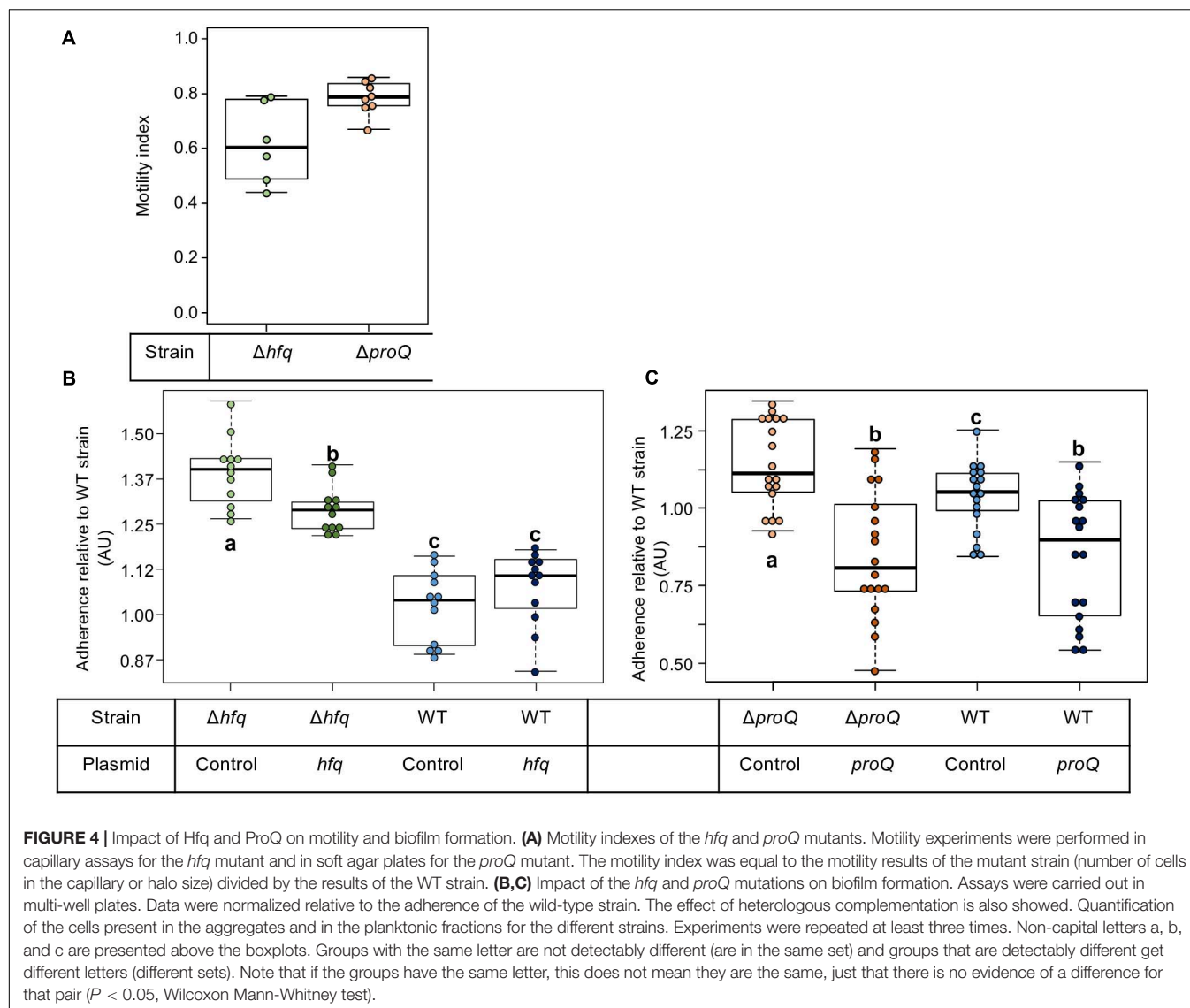
Early Virulence Determinants Such as Biofilm Production and Motility Are Also Impaired in the *hfq* and *proQ* Mutants

At the initial stage of infection, *D. dadantii* must adhere to the plant surface and enter into the apoplast. *D. dadantii* produces cellulose fibrils, which enable it to develop aggregates on the plant surface (Jahn et al., 2011; Prigent-Combaret et al., 2012). These



aggregates are embedded in an extracellular polymeric substance (EPS) that maintains a hydrated surface around the bacteria and thus helps them to survive under conditions of desiccation (Condemine et al., 1999). Motility and chemotaxis are essential for *D. dadantii* when searching for favorable sites to enter into the plant apoplast. Therefore, we evaluated the consequences of the *hfq* or *proQ* mutations on motility and biofilm formation. The ability of the *hfq* and *proQ* mutants to swim was analyzed using capillary and soft agar assays, respectively. Incubation time during the capillary assays was short, so that we were able to overlook the impact of the growth defect between the *hfq* mutant and the WT strain. Soft agar assays were performed to test the motility of the *proQ* mutant, since similar growth rates were obtained for the *proQ* mutant and the WT strain. A motility index was calculated for both experiments (Figure 4A). It was equal to the motility of the mutant strain (number of cells in the capillary or size of the halo) divided by that of the WT strain. Both *hfq* and *proQ* showed reduced motility compared to the WT (−38 and −22%, respectively) and strains complemented

with the respective inactivated gene expressed from an episome restored the ability to swim (90 and 98%, respectively). This reduced cell motility is in agreement with the behavior of *hfq* mutants of most pathogenic bacteria (Chao and Vogel, 2010; Vogel and Luisi, 2011; Sobrero and Valverde, 2012; Wagner, 2013; Updegrove et al., 2016). Flagellar motility negatively affects biofilm formation. Consequently, we monitored the consequences of the *hfq* or *proQ* mutations on the attachment of *D. dadantii* to the plastic coating of the microtiter plate well. From a metabolic point of view, biofilm formation reflects the trade-off between motility and exopolysaccharide (EPS) production. This trade-off was clearly unbalanced in favor of EPS production in the *hfq* mutant (p -value = $7.4e-7$) and less severely so in the *proQ* mutant (p -value = $3.8e-2$) (Figures 4B,C). Complementation experiments demonstrated that *hfq* expressed from an episome did not significantly reduce the increased biofilm forming capacity of the *hfq* mutant (Figure 4B). In contrast, overexpression of *proQ* from the episome slightly decreased the biofilm formation capacity of



the *proQ* mutant and WT strain compared to the *proQ* mutant and to the WT strain without complementation (Figure 4C). These data suggest that the two RNA chaperones play different roles in *D. dadantii* biofilm formation.

Transcripts of Late Virulence Factors and Early Virulence Determinants Are Impaired in the *hfq* and *proQ* Mutants

Hfq and ProQ act post-transcriptionally, so we evaluated the mRNA amounts of various virulence genes in the *hfq* and *proQ* mutants by qRT-PCR. For genes mostly involved in the early stage of infection, we selected *fliC* which encodes flagellin, *rhlA* whose product is involved in the synthesis of a biosurfactant for swarming motility, and *bcsA* which encodes a protein involved in the production of cellulose fibrils important for adherence. Concerning late virulence genes, we retained *pelD* and *pelE* that encode pectate lyases, *prtB* and *prtC* that encode

metalloproteases, *celZ* that encodes a cellulase, *outC* that encodes a compound of the type II secretion system which secretes pectinases and cellulase, *kdgK* that encodes the KDG kinase involved in the catabolism of polygalacturonate, and *hrpN* that encodes harpin which elicits the hypersensitive response. In line with the observed phenotypes, the RNA amounts of most genes were reduced in both mutants, much more drastically so in the *hfq* mutant than in the *proQ* mutant (Figure 5). The greater adherence of the *hfq* mutant was also correlated with the higher *bcsA* RNA amounts compared to the WT (increased by three-fold). However, *celZ* RNA amounts were similar in the *hfq* mutant and in the WT. Therefore, the reduced cellulase activity was not dependent on the *celZ* RNA amount but it could be partially due to reduced cellulase secretion because the *outC* RNA amount was low in the *hfq* mutant (decreased by 70%), or to decreased CelZ translation. In the *proQ* mutant, the amount of *celZ* and *outC* transcripts were slightly reduced (around 40%). Taken together, these results indicate that most of the observed

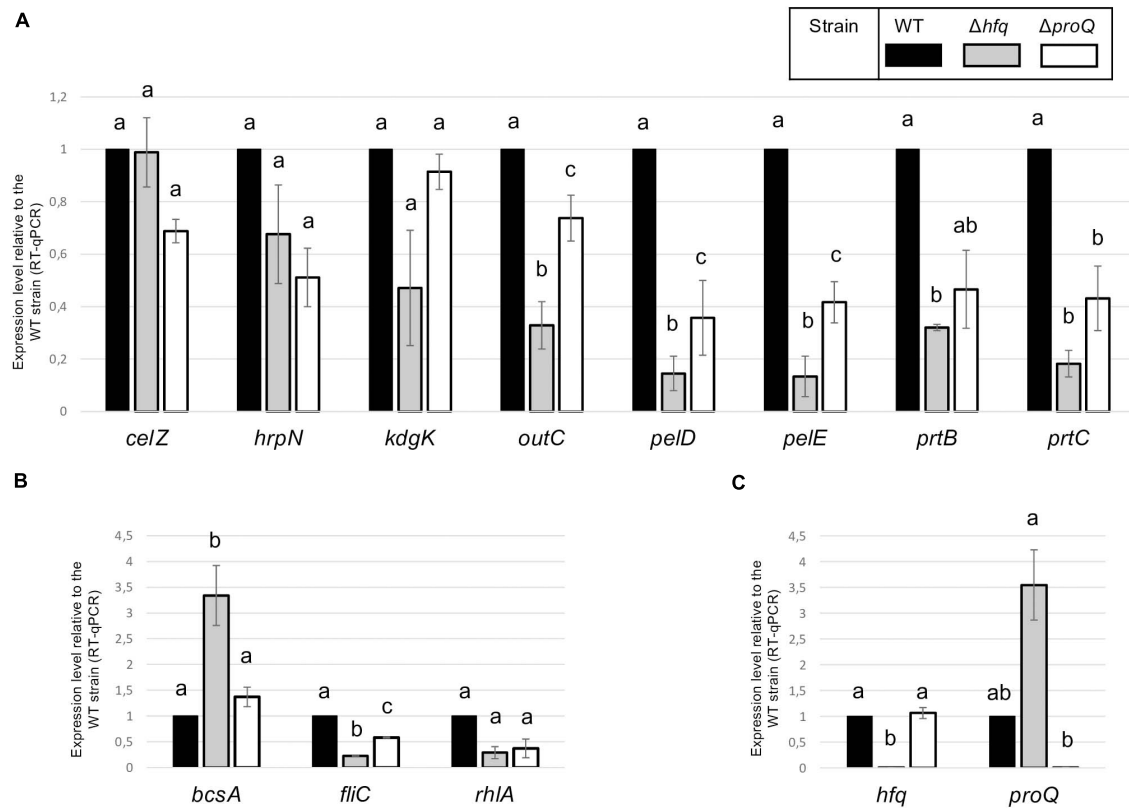


FIGURE 5 | RNA amounts in the *hfq* and *proQ* mutant strains. Gene expression levels relative to the WT strain were evaluated in the two mutants by RT-qPCR. **(A)** Genes encoding late virulence factors or associated with late virulence factors; **(B)** Genes encoding early virulence factors such as adherence and motility factors; **(C)** Expression levels of *hfq* and *proQ* were measured in the different mutants. Non-capital letters a, b, and c are presented above the histograms. Groups with the same letter are not detectably different (are in the same set) and groups that are detectably different get different letters (different sets). Groups can have more than one letter to reflect “overlap” between the sets of groups. Note that if the groups have the same letter, this does not mean they are the same, just that there is no evidence of a difference for that pair ($P < 0.05$, *t*-test).

phenotypes were correlated to a decrease in the mRNA amounts from virulence genes.

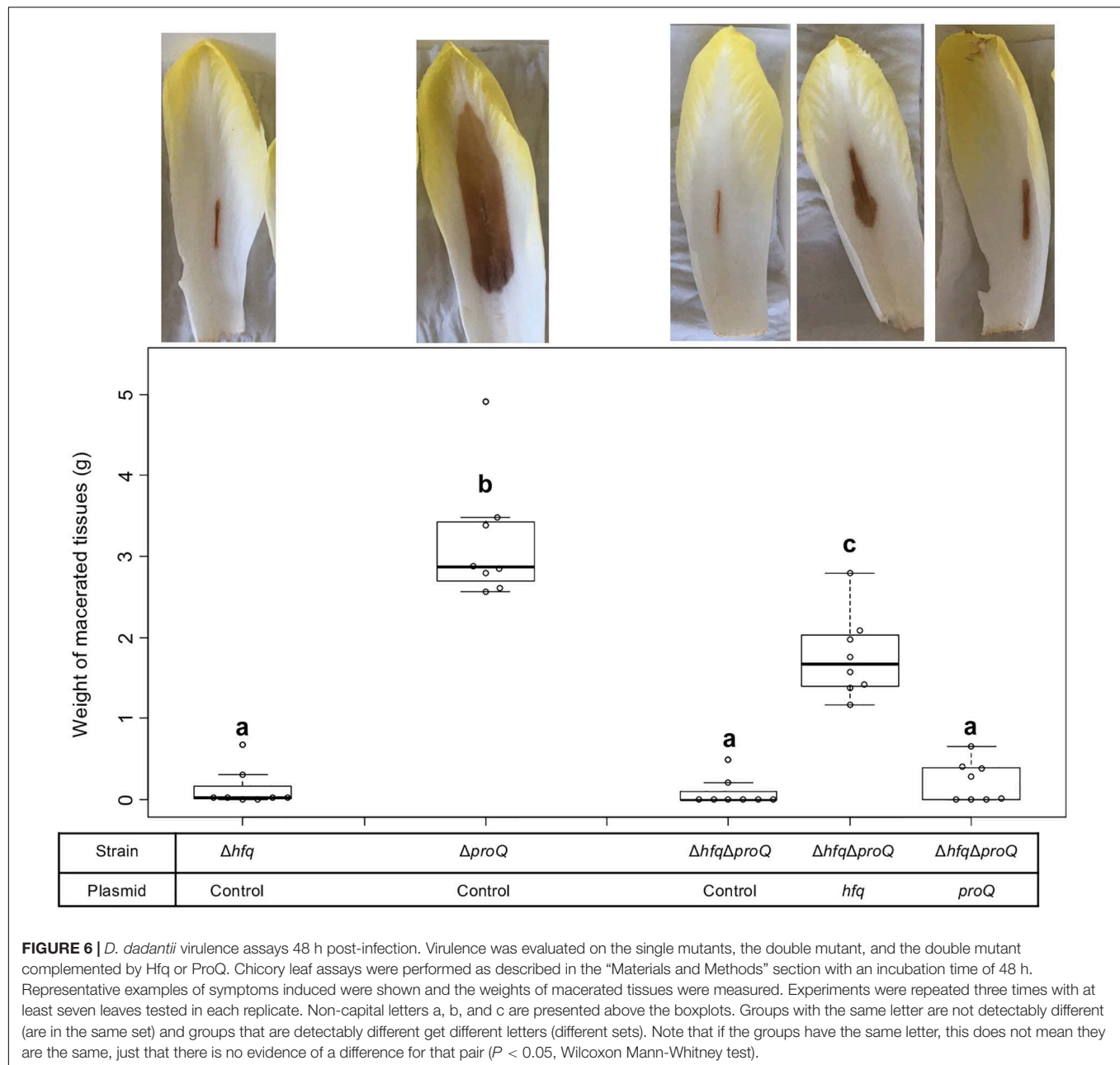
The Effects of RNA Chaperones on Virulence Partially Overlap

The absence of Hfq or ProQ impaired virulence and modified the production of similar virulence factors. Consequently, we evaluated the behavior of a mutant inactivated for both *hfq* and *proQ* and assessed whether *hfq* and *proQ* could restore virulence in the double mutant. The virulence of the *hfq proQ* double mutant and mutant complemented by either *hfq* or *proQ* was tested on chicory leaves. The mutants were asymptomatic whatever the complementation 24 h post-infection, except the mutant *proQ*, that caused reduced soft rot symptoms as noticed earlier (Figure 2). However, 48 h post-infection, the *proQ* gene inserted in the *hfq proQ* mutant produced a weight of macerated tissues similar to the weight observed with the *hfq* mutant, whereas *hfq* complementation of the double mutant only slightly restored soft rot symptoms (Figure 6). Complementation by *proQ* did

not restored virulence while complementation by *hfq* partially restored symptom.

Late and early virulence factors were also impaired in the double mutant, as expected. Compared to the *hfq* mutant, the double mutant showed a similar, perhaps higher reduction of protease, cellulase and pectinase activities (Figure 7A). Motility was also reduced, and adherence was increased compared to the WT (Figures 8A,C). In line with these phenotypes, the expression levels of the corresponding genes were modified: *prtC*, *pelD* and *fliC* RNA amounts decreased by at least five folds in the double mutant, and *hrpN*, *celZ* and *outC* RNA amounts decreased by about two folds (Figures 7B, 8 and Supplementary Figure 4). Overall, the expression levels of *outC*, *pelD*, *bcsA*, and *fliC* were similar in the double mutant and in the *hfq* mutant, whereas the expression levels of *prtC*, *celZ* and *hrpN* decreased more than in the *hfq* mutant (Figures 7B, 8B and Supplementary Figure 4).

The protease, pectinase and motility phenotypes were restored by complementation with Hfq. Accordingly, *prtC*, *pelD*, and *fliC* RNA amounts increased significantly in the double mutant strain complemented by Hfq (Figures 7B, 8B). However, the cellulase phenotype was not complemented by the addition of Hfq, even if the expression level of *celZ* was restored to a



level similar to those measured in the WT or the *hfq* mutant (Figure 7). The adherence phenotype and the expression level of *bcsA* were not complemented by an *hfq* gene expressed from a plasmid (Figure 8). ProQ complementation restored protease, cellulase and pectinase activities and adherence, but not motility. In accordance, the expression level of *fliC* was similar to the levels in the double mutant (Figure 8B), but the expression levels of *bcsA*, *prtC*, *celZ*, and *hrpN* increased in the complemented strain compared to the non-complemented double mutant (Figures 7, 8 and Supplementary Figure 4). Interestingly, the expression levels of genes *outC* and *pelD* were unexpectedly similar to those observed in the double mutant although phenotypes were restored.

We measured the expression levels of *hfq* and *proQ* in the different mutants. As expected, *hfq* and *proQ* expression was not detected in the respective mutant strains or in the double mutant, but a three-fold increase was observed for the gene expressed from the plasmid. *proQ* expression level increased in the strains defective in Hfq production, i.e., 3.5 fold in the single *hfq* mutant and around 12 fold in the double mutant complemented by *proQ*. These results can be explained by an additive effect of the *hfq* mutation and of *proQ* overexpression from the plasmid (Figure 1 and Supplementary Figure 4).

Overall, virulence assays, phenotypes and expression level measurements suggest that the two RNA chaperones Hfq and

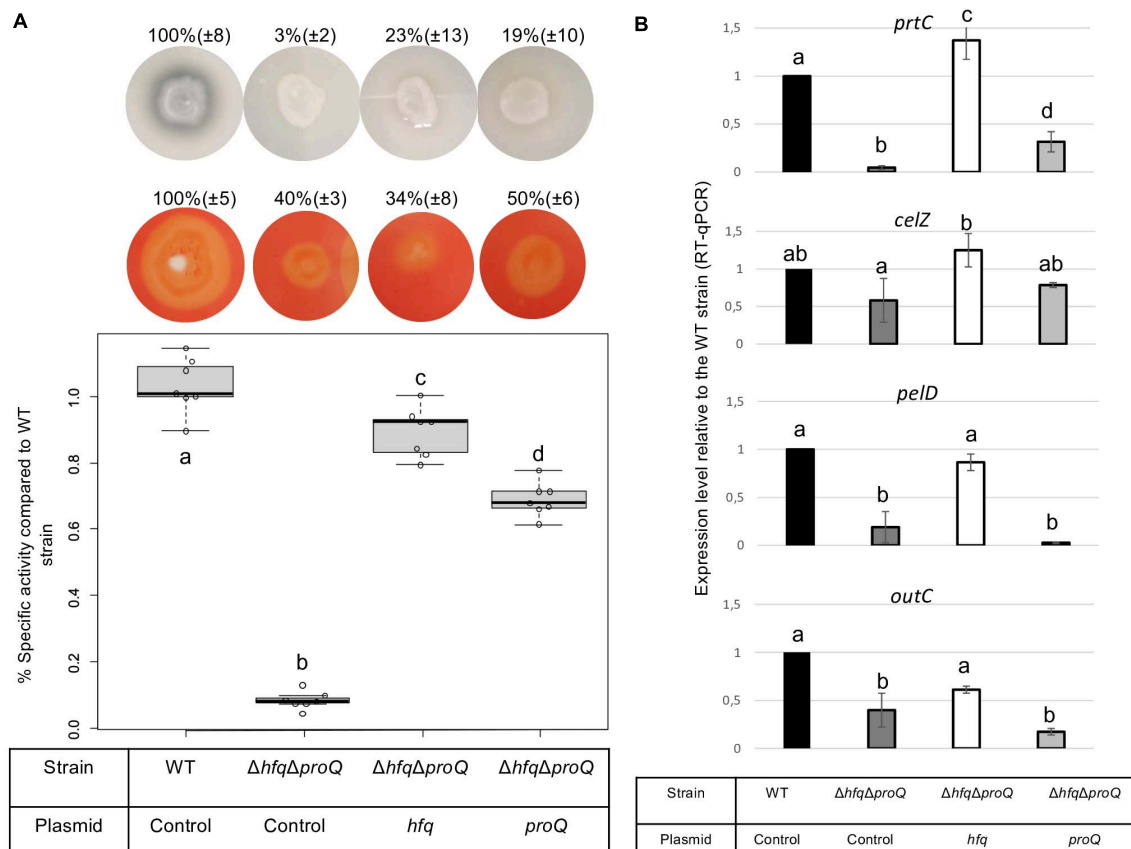


FIGURE 7 | Impact of the double mutant on late virulence factors. **(A)** Protease production on medium containing skim milk, cellulase production on carboxymethylcellulose agar plates with Congo red staining, and pectate lyase activity expressed as percent of wild type strain specific activity were evaluated in the double mutant and in the double mutant complemented by Hfq or ProQ. Experiments were repeated at least three times. Non-capital letters a, b, c, and d are presented above the boxplots and histograms. Groups with the same letter are not detectably different (are in the same set) and groups that are detectably different get different letters (different sets). Groups can have more than one letter to reflect “overlap” between the sets of groups. Note that if the groups have the same letter, this does not mean they are the same, just that there is no evidence of a difference for that pair ($P < 0.05$, Wilcoxon Mann-Whitney test). **(B)** expression levels of *prtC*, *celZ*, *pelD*, and *outC* measured by RT-qPCR in the double mutant and double mutant complemented by Hfq or ProQ. Expression levels were compared with those measured in the WT strain.

ProQ exert their effects via partially overlapping but different sets of targets (Figure 9).

DISCUSSION

We investigated the influence of the two RNA chaperones Hfq and ProQ on the virulence of the bacterial plant pathogen *D. dadantii*. Inactivation of the genes encoding these two chaperones led to lower production of cell-degrading enzymes acting as major virulence factors during *D. dadantii* pathogenic growth, and accordingly lower pathogenicity. Furthermore, both mutations altered osmotic stress tolerance and cell motility. However, the same mutations elicited different effects on cell growth and biofilm formation. Phenotypes were mostly correlated with altered expression of genes encoding virulence factors (*hrpN*, *outC*, *pelD*, *pelE*, *prtC*, *prtB*), motility components (*fliC* and *rhlA*) and adherence components (*bcsA*), except *celZ* expression in the *hfq* mutant (Figure 9). Expression levels

generally decreased less following inactivation of *proQ* than following inactivation of *hfq*, but both RNA chaperones affected similar virulence factors. So far, the involvement of ProQ in virulence has been only reported in *Salmonella* where it regulates motility directly by downregulating *fliC* mRNA and represses or activates the expression of virulence genes (genes localized in SPI and SPII, respectively). Accordingly, infection by a *Salmonella proQ* mutant resulted in a decreased invasion rate in eukaryotic cells (Westermann et al., 2019). The present study reports for the first time the involvement of ProQ in the virulence of a plant-pathogenic bacterium. The expression level of *proQ* does not seem to be significantly modified during the infection (Pédrón et al., 2018). In *D. dadantii*, major virulence genes (*pel*, *prt* and *cel*) were repressed by ProQ, but contrary to what has been observed in *Salmonella*, the amount of *fliC* mRNA decreased in the *proQ* mutant. Differences in *proQ* mutant behavior according to species were also highlighted by comparing mutant strains in *E. coli* and *D. dadantii*: the *proQ* mutant displayed impaired biofilm

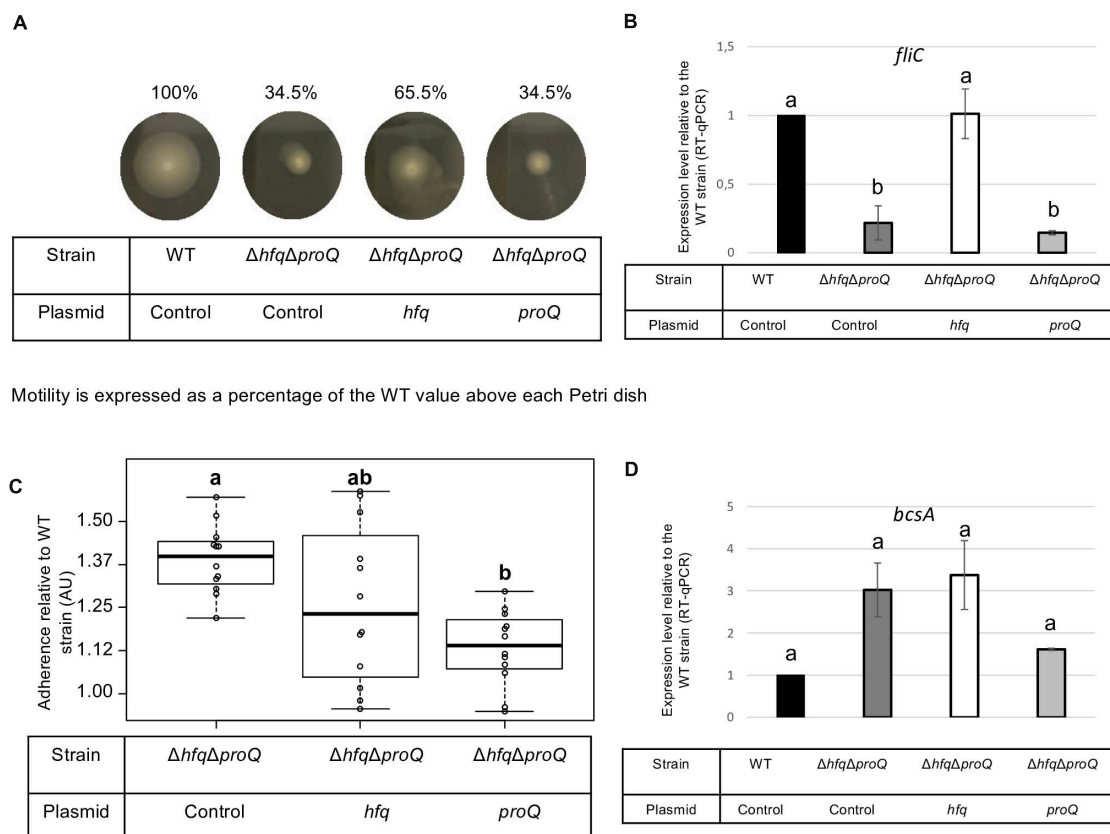


FIGURE 8 | Impact of the double mutant on early virulence factors. Phenotypes and expression levels were analyzed in the double mutant strain and the double mutant strain complemented by Hfq or ProQ. **(A)** Motility was evaluated on semi-solid LB agar plates; **(B,D)** Expression levels of genes were measured by RT-qPCR and compared with the wild type; **(C)** Adherence was evaluated and compared with the wild-type strain. Experiments were repeated at least three times. Non-capital letters a, b, c, and d are presented above the boxplots and histograms. Groups with the same letter are not detectably different (are in the same set) and groups that are detectably different get different letters (different sets). Groups can have more than one letter to reflect “overlap” between the sets of groups. Note that if the groups have the same letter, this does not mean they are the same, just that there is no evidence of a difference for that pair ($P < 0.05$, Wilcoxon Mann-Whitney test).

formation in *E. coli*, whereas it displayed increased adherence in *D. dadantii* (Sheidy and Zielke, 2013). Overall, this illustrates the species specificities of the ProQ regulatory networks, as previously described (Attaiech et al., 2016; Smirnov et al., 2016; Holmqvist et al., 2018; Westermann et al., 2019). Specificities could be a consequence of a rather distinct sRNA landscape produced by these bacterial species, where only small numbers of sRNA homologs overlap (Leonard et al., 2019). In contrast to ProQ, Hfq proteins have already been reported to significantly reduce virulence in several plant-pathogenic bacteria like *A. tumefaciens*, *E. amylovora*, *P. ananatis*, *X. campestris*, and *P. carotovorum*. However, the role of Hfq still remains only partially understood (Wilms et al., 2012; Zeng et al., 2013; Zeng and Sundin, 2014; Lai et al., 2018; Wang et al., 2018; Shin et al., 2019). Additionally, *D. dadantii* strain defective of *hfq* has been shown to present a decreased fitness *in planta* (Royet et al., 2019). The phenotypes of the *D. dadantii hfq* mutant are similar to those of the *P. carotovorum hfq* mutant: *hfq*-defective strains present a decreased growth rate, low cellulase, protease and pectinase production, and altered biofilm formation and motility. Hfq should regulate

directly or indirectly these functions post-transcriptionally using sRNAs. In *D. dadantii*, a recent study highlighted a feed-forward signaling circuit involving Hfq protein which post-transcriptionally regulates RsmB involved in the down-regulation of cell-degrading enzymes and type 3 secretion system (Yuan et al., 2019).

One interesting feature highlighted by this study is the interplay between the two RNA chaperones. The mitigated virulence of the double mutant was only slightly complemented by Hfq or ProQ, so we evaluated the ability of Hfq and ProQ to cross-complement each other regarding mitigation of virulence. ProQ partially complemented the *hfq* mutant, whereas episomal *hfq* did not complement the *proQ* mutant (Supplementary Figure 5). Overall, these results indicate that these two RNA chaperones might exert their effects via partially overlapping but different sets of targets. Although first reports indicate that the RNAs bound by ProQ generally differ from those bound by Hfq, recent studies have demonstrated an unexpected overlap of the sets of Hfq and ProQ targets in *Salmonella* and *E. coli*, with 30% of overlapping interactions (Westermann et al., 2019; Melamed et al., 2020). In line with these results, we identified potential

Strain	WT	Δhfq	Δhfq	$\Delta proQ$	$\Delta proQ$	$\Delta hfq\Delta proQ$	$\Delta hfq\Delta proQ$	$\Delta hfq\Delta proQ$
Plasmid	Control	Control	<i>hfq</i>	Control	<i>proQ</i>	Control	<i>hfq</i>	<i>proQ</i>
Growth	—	↓	—	—	↓	↓	↑	—
Virulence	—	↓	—	↓	—	↓	↑	—
Pectinases	—	↓	—	↓	—	↓	↑	↑
Proteases	—	↓	—	↓	—	↓	↑	↑
Cellulase	—	↓	—	↓	—	↓	—	↑
Mobility	—	↓	—	↓	—	↓	↑	—
Adherence	—	↑	—	↑	—	↑	—	↓
<i>hrpN</i>	—	↓	ND	↓	ND	↓	↑	↑
<i>outC</i>	—	↓	ND	↓	ND	↓	—	↓
<i>pelE/pelD</i>	—	↓	ND	↓	ND	↓	↑	↓
<i>prtB</i>	—	↓	ND	↓	ND	↓	↑	↑
<i>prtC</i>	—	↓	ND	↓	ND	↓	↑	↑
<i>celZ</i>	—	↓	ND	↓	ND	↓	↑	↑
<i>kdgK</i>	—	↓	ND	—	ND	↓	—	↓
<i>fliC</i>	—	↓	ND	↓	ND	↓	↑	—
<i>bcsA</i>	—	↑	ND	↑	ND	↑	—	↓
<i>proQ</i>	—	↑	ND	↓	ND	↓	—	↑
<i>hfq</i>	—	↓	ND	—	ND	↓	↑	—

FIGURE 9 | Overview of phenotypes and variation of expression levels associated with the inactivation of *proQ* and *hfq*. Dash indicates equivalent phenotype (or expression level), up arrow indicates an increase in phenotype (or expression level) and down arrow indicates a decrease in phenotype (or expression level). The double mutant, single mutants and complemented single mutants were compared to the behavior of the wild-type strain whereas double mutant complemented with *proQ* or *hfq* were compared to the behavior of the double mutant without any complementation. Expected behavior is indicated in blue, unexpected behavior is indicated in red. ND: Not determined.

ProQ-specific targets such as *celZ*, but also overlapping targets – the *fliC*, *bcsA*, *pel*, and *prt* genes. Nonetheless, the expression of the target genes was more highly impacted in the double mutant than in each single mutant, indicating putative additive effects of the two proteins. Additionally, analyses of the expression levels of these target genes in the double mutant complemented by each protein highlighted 3 classes of genes: (i) *hrpN*-like genes, whose expression level is restored by Hfq or ProQ, (ii) genes whose expression levels are restored at least partially only by Hfq (e.g., *fliC*, *prtC*, *outC* and *pelE*), and (iii) genes whose expression levels are partially restored only by ProQ (e.g., *bcsA*) (Figure 9). Although further studies aimed at identifying the direct targets of Hfq and ProQ in *D. dadantii* by *in vivo* crosslinking will clarify whether the virulence functions governed by ProQ represent a subset of those governed by Hfq, these data reinforce the assumption that the two proteins could have independent competing or complementary roles. ProQ and Hfq could be involved in different regulatory cascades, with branches converging at identical targets. Alternatively, both proteins could interact with the same mRNA. The site of interaction would not necessarily be identical: ProQ recognizes its targets in a

sequence-independent manner, through RNA structural motifs found in sRNAs and internal to the coding sequence region or at the 3' end of mRNAs (Holmqvist et al., 2018); whereas Hfq interacts with nascent transcripts in the 5'-UTR of the target RNA (Kambara et al., 2018). However, the two proteins could outcompete each other at a given terminator since they both have the propensity to bind intrinsic terminators of RNAs (Holmqvist et al., 2016).

Finally, it is noteworthy that an increased level of *proQ* was measured in the *hfq* mutant and in the double mutant complemented by *proQ*. This is of importance because the impact of ProQ on growth and biofilm production is shown to be highly dependent on the amount of ProQ protein produced in the cells. Here, we showed a correlation between a decrease in growth rate and a increase in the amount of *proQ* and the absence of *hfq*. Furthermore, the decrease level of *proQ* increases with the inactivation of *hfq*. Finally, the growth defect of the double mutant is complemented by *hfq* but not by *proQ*. At this point, we can only speculate, but these observations suggest that in addition to the overlapping, complementary, competing or even

additive roles of these two RNA chaperones, Hfq could indirectly or directly regulate ProQ production. Further analyses of the complex regulatory network of Hfq and ProQ should take this possible regulation into account.

DATA AVAILABILITY STATEMENT

The original contributions presented in the study are included in the article/**Supplementary Material**, further inquiries can be directed to the corresponding authors.

AUTHOR CONTRIBUTIONS

FH and SR contributed to the conception and design of the study. SL performed experiments and the statistical analysis. CV performed the experiments. FH wrote the draft of manuscript. SR and WN contributed to manuscript revision. All authors read and approved the submitted version.

REFERENCES

- Ali Azam, T., Iwata, A., Nishimura, A., Ueda, S., and Ishihama, A. (1999). Growth phase-dependent variation in protein composition of the *Escherichia coli* nucleoid. *J. Bacteriol.* 181, 6361–6370. doi: 10.1128/jb.181.20.6361-6370.1999
- Ashby, A. M., Watson, M. D., Loake, G. J., and Shaw, C. H. (1988). Ti plasmid-specified chemotaxis of *Agrobacterium tumefaciens* C58C1 toward vir-inducing phenolic compounds and soluble factors from monocotyledonous and dicotyledonous plants. *J. Bacteriol.* 170, 4181–4187. doi: 10.1128/jb.170.9.4181-4187.1988
- Attaiach, L., Boughammoura, A., Brochier-Armanet, C., Allatif, O., Peillard-Fiorente, F., Edwards, R. A., et al. (2016). Silencing of natural transformation by an RNA chaperone and a multitarget small RNA. *Proc. Natl. Acad. Sci. U.S.A.* 113, 8813–8818. doi: 10.1073/pnas.1601626113
- Bardonnnet, N., and Blanco, C. (1992). 'uidA'-antibiotic-resistance cassettes for insertion mutagenesis, gene fusions and genetic constructions. *FEMS Microbiol. Lett.* 72, 243–247. doi: 10.1016/0378-1097(92)90469-5
- Chao, Y., and Vogel, J. (2010). The role of Hfq in bacterial pathogens. *Curr. Opin. Microbiol.* 13, 24–33. doi: 10.1016/j.mib.2010.01.001
- Chaulk, S. G., Smith Frieday, M. N., Arthur, D. C., Culham, D. E., Edwards, R. A., Soo, P., et al. (2011). ProQ is an RNA chaperone that controls ProP levels in *Escherichia coli*. *Biochemistry* 50, 3095–3106. doi: 10.1021/bi101683a
- Condemine, G., Castillo, A., Passeri, F., and Enard, C. (1999). The PecT repressor coregulates synthesis of exopolysaccharides and virulence factors in *Erwinia chrysanthemi*. *Mol. Plant-Microbe Interact.* 12, 45–52. doi: 10.1094/MPMI.1999.12.1.45
- Datsenko, K. A., and Wanner, B. L. (2000). One-step inactivation of chromosomal genes in *Escherichia coli* K-12 using PCR products. *Proc. Natl. Acad. Sci. U.S.A.* 97, 6640–6645. doi: 10.1073/pnas.120163297
- Dellagi, A., Rigault, M., Segond, D., Roux, C., Kraepiel, Y., Cellier, F., et al. (2005). Siderophore-mediated upregulation of Arabidopsis ferritin expression in response to *Erwinia chrysanthemi* infection. *Plant J.* 43, 262–272. doi: 10.1111/j.1365-3113.2005.02451.x
- Duprey, A., Taib, N., Leonard, S., Garin, T., Flandrois, J.-P., Nasser, W., et al. (2019). The phytopathogenic nature of *Dickeya aquatica* 174/2 and the dynamic early evolution of *Dickeya* pathogenicity. *Environ. Microbiol.* 21, 2809–2835. doi: 10.1111/1462-2920.14627

FUNDING

This work was supported by a grant from the FR BioEnviS. SL received a doctoral grant from the French Ministère de l'Éducation nationale de l'Enseignement Supérieur, de la Recherche et de l'innovation.

ACKNOWLEDGMENTS

The authors thank Carlos Blanco for providing the *hfq* mutant, Pauline Héritier for helpful technical assistance and Georgi Muskhelishvili for helpful discussion. The authors also thank Annie Buchwalter for her careful correction of English language.

SUPPLEMENTARY MATERIAL

The Supplementary Material for this article can be found online at: <https://www.frontiersin.org/articles/10.3389/fmicb.2021.687484/full#supplementary-material>

- Eklund, A. (2016). *beeswarm: The Bee Swarm Plot, an Alternative to Stripchart. R package version 0.2.3*. Available online at: <https://CRAN.R-project.org/package=beeswarm>
- Fagard, M., Dellagi, A., Roux, C., Périno, C., Rigault, M., Boucher, V., et al. (2007). Arabidopsis thaliana expresses multiple lines of defense to counterattack *Erwinia chrysanthemi*. *Mol. Plant Microbe Interact.* 20, 794–805. doi: 10.1094/MPMI-20-7-0794
- Gonzalez, G. M., Hardwick, S. W., Maslen, S. L., Skehel, J. M., Holmqvist, E., Vogel, J., et al. (2017). Structure of the *Escherichia coli* ProQ RNA-binding protein. *RNA* 23, 696–711. doi: 10.1261/rna.060343.116
- Holmqvist, E., Li, L., Bischler, T., Barquist, L., and Vogel, J. (2018). Global maps of ProQ binding in vivo reveal target recognition via RNA structure and stability control at mRNA 3' ends. *Mol. Cell* 70, 971–982. doi: 10.1016/j.molcel.2018.04.017
- Holmqvist, E., Wright, P. R., Li, L., Bischler, T., Barquist, L., Reinhardt, R., et al. (2016). Global RNA recognition patterns of post-transcriptional regulators Hfq and CsrA revealed by UV crosslinking in vivo. *EMBO J.* 35, 991–1011. doi: 10.15252/emboj.201593360
- Hommais, F., Oger-Desfeux, C., Van Gijsegem, F., Castang, S., Ligor, S., Expert, D., et al. (2008). PecS is a global regulator of the symptomatic phase in the phytopathogenic bacterium *Erwinia chrysanthemi* 3937. *J. Bacteriol.* 190, 7508–7522. doi: 10.1128/JB.00553-08
- Jahn, C. E., Selimi, D. A., Barak, J. D., and Charkowski, A. O. (2011). The *Dickeya dadantii* biofilm matrix consists of cellulose nanofibres, and is an emergent property dependent upon the type III secretion system and the cellulose synthesis operon. *Microbiology* 157, 2733–2744. doi: 10.1099/mic.0.051003-0
- Jiang, X., Sobetzko, P., Nasser, W., Reverchon, S., and Muskhelishvili, G. (2015). Chromosomal "stress-response" domains govern the spatiotemporal expression of the bacterial virulence program. *MBio* 6:e353–15. doi: 10.1128/mBio.00353-15
- Kajitani, M., Kato, A., Wada, A., Inokuchi, Y., and Ishihama, A. (1994). Regulation of the *Escherichia coli* hfq gene encoding the host factor for phage Q beta. *J. Bacteriol.* 176, 531–534. doi: 10.1128/jb.176.2.531-534.1994
- Kambara, T. K., Ramsey, K. M., and Dove, S. L. (2018). Pervasive targeting of nascent transcripts by Hfq. *Cell Rep.* 23, 1543–1552. doi: 10.1016/j.celrep.2018.03.134
- Kunte, H. J., Crane, R. A., Culham, D. E., Richmond, D., and Wood, J. M. (1999). Protein ProQ influences osmotic activation of compatible solute transporter

- ProP in *Escherichia coli* K-12. *J. Bacteriol.* 181, 1537–1543. doi: 10.1128/jb.181.5.1537-1543.1999
- Lai, J.-L., Tang, D.-J., Liang, Y.-W., Zhang, R., Chen, Q., Qin, Z.-P., et al. (2018). The RNA chaperone Hfq is important for the virulence, motility and stress tolerance in the phytopathogen *Xanthomonas campestris*. *Environ. Microbiol. Rep.* 10, 542–554. doi: 10.1111/1758-2229.12657
- Leonard, S., Hommais, F., Nasser, W., and Reverchon, S. (2017). Plant-phytopathogen interactions: bacterial responses to environmental and plant stimuli: Molecular dialog between phytopathogens and plants. *Environ. Microbiol.* 19, 1689–1716. doi: 10.1111/1462-2920.13611
- Leonard, S., Meyer, S., Lacour, S., Nasser, W., Hommais, F., and Reverchon, S. (2019). APERO: a genome-wide approach for identifying bacterial small RNAs from RNA-Seq data. *Nucleic Acids Res.* 47:e88. doi: 10.1093/nar/gkz485
- Link, T. M., Valentin-Hansen, P., and Brennan, R. G. (2009). Structure of *Escherichia coli* Hfq bound to polyribadenylate RNA. *Proc. Natl. Acad. Sci. U.S.A.* 106, 19292–19297. doi: 10.1073/pnas.0908744106
- Lohaus, G., Pennewiss, K., Sattelmacher, B., Hussmann, M., and Hermann Muehling, K. (2001). Is the infiltration-centrifugation technique appropriate for the isolation of apoplastic fluid? A critical evaluation with different plant species. *Physiol. Plant* 111, 457–465. doi: 10.1034/j.1399-3054.2001.1110405.x
- Ma, B., Hibbing, M. E., Kim, H.-S., Reedy, R. M., Yedidia, I., Breuer, J., et al. (2007). Host range and molecular phylogenies of the soft rot enterobacterial genera *Pectobacterium* and *Dickeya*. *Phytopathology* 97, 1150–1163. doi: 10.1094/PHYTO-97-9-1150
- Maes, M., and Messens, E. (1992). Phenol as grinding material in RNA preparations. *Nucleic Acids Res.* 20:4374. doi: 10.1093/nar/20.16.4374
- Mark Glover, J. N., Chaulk, S. G., Edwards, R. A., Arthur, D., Lu, J., and Frost, L. S. (2015). The FinO family of bacterial RNA chaperones. *Plasmid* 78, 79–87. doi: 10.1016/j.plasmid.2014.07.003
- Melamed, S., Adams, P. P., Zhang, A., Zhang, H., and Storz, G. (2020). RNA-RNA interactomes of ProQ and Hfq reveal overlapping and competing roles. *Mol. Cell* 77, 411–425. doi: 10.1016/j.molcel.2019.10.022
- Meyer, S., Reverchon, S., Nasser, W., and Muskhelishvili, G. (2018). Chromosomal organization of transcription: in a nutshell. *Curr. Genet.* 64, 555–565. doi: 10.1007/s00294-017-0785-5
- Miller, J. G. (1972). Living systems: The organization. *Behav. Sci.* 17:182. doi: 10.1002/bs.3830170102
- Milner, J. L., and Wood, J. M. (1989). Insertion proQ220::Tn5 alters regulation of proline porter II, a transporter of proline and glycine betaine in *Escherichia coli*. *J. Bacteriol.* 171, 947–951. doi: 10.1128/jb.171.2.947-951.1989
- Moran, F., Nasuno, S., and Starr, M. P. (1968). Oligogalacturonide trans-eliminase of *Erwinia carotovora*. *Arch. Biochem. Biophys.* 125, 734–741. doi: 10.1016/0003-9861(68)90508-0
- Ouafa, Z.-A., Reverchon, S., Lautier, T., Muskhelishvili, G., and Nasser, W. (2012). The nucleoid-associated proteins H-NS and FIS modulate the DNA supercoiling response of the *pel* genes, the major virulence factors in the plant pathogen bacterium *Dickeya dadantii*. *Nucleic Acids Res.* 40, 4306–4319. doi: 10.1093/nar/gks014
- Pédron, J., Chapelle, E., Alunni, B., and Van Gijsegem, F. (2018). Transcriptome analysis of the *Dickeya dadantii* *PecS* regulon during the early stages of interaction with *Arabidopsis thaliana*. *Mol. Plant Pathol.* 19, 647–663. doi: 10.1111/mpp.12549
- Prigent-Combaret, C., Zghidi-Abouzid, O., Effantin, G., Lejeune, P., Reverchon, S., and Nasser, W. (2012). The nucleoid-associated protein Fis directly modulates the synthesis of cellulose, an essential component of pellicle-biofilms in the phytopathogenic bacterium *Dickeya dadantii*: *Dickeya dadantii* Fis protein and biofilm formation. *Mol. Microbiol.* 86, 172–186. doi: 10.1111/j.1365-2958.2012.08182.x
- R Core Team. (2020). *R: A language and environment for statistical computing*. Vienna, Austria: R Foundation for Statistical Computing. Available online at: <https://www.R-project.org/>
- Resibois, A., Colet, M., Faelen, M., Schoonejans, E., and Toussaint, A. (1984). ϕ IEC2, a new generalized transducing phage of *Erwinia chrysanthemi*. *Virology* 137, 102–112. doi: 10.1016/0042-6822(84)90013-8
- Reverchon, S., Meyer, S., Forquet, R., Hommais, F., Muskhelishvili, G., and Nasser, W. (2021). The nucleoid-associated protein IHF acts as a “transcriptional domainin” protein coordinating the bacterial virulence traits with global transcription. *Nucleic Acids Res.* 49, 776–790. doi: 10.1093/nar/gkaa1227
- Reverchon, S., and Nasser, W. (2013). *Dickeya* ecology, environment sensing and regulation of virulence programme. *Environ. Microbiol. Rep.* 5, 622–636. doi: 10.1111/1758-2229.12073
- Roeder, D. L., and Collmer, A. (1985). Marker-exchange mutagenesis of a pectate lyase isozyme gene in *Erwinia chrysanthemi*. *J. Bacteriol.* 164, 51–56. doi: 10.1128/jb.164.1.51-56.1985
- Royet, K., Parisot, N., Rodrigue, A., Gueguen, E., and Condemine, G. (2019). Identification by Tn-seq of *Dickeya dadantii* genes required for survival in chicory plants. *Mol. Plant Pathol.* 20, 287–306. doi: 10.1111/mpp.12754
- Sheidy, D. T., and Zielke, R. A. (2013). Analysis and Expansion of the Role of the *Escherichia coli* Protein ProQ. *PLoS One* 8:e79656. doi: 10.1371/journal.pone.0079656
- Shin, G. Y., Schachterle, J. K., Shyntum, D. Y., Moleleki, L. N., Coutinho, T. A., and Sundin, G. W. (2019). Functional characterization of a global virulence regulator Hfq and identification of Hfq-Dependent sRNAs in the plant pathogen *Pantoea ananatis*. *Front. Microbiol.* 10:2075. doi: 10.3389/fmicb.2019.02075
- Smirnov, A., Förstner, K. U., Holmqvist, E., Otto, A., Günster, R., Becher, D., et al. (2016). Grad-seq guides the discovery of ProQ as a major small RNA-binding protein. *Proc. Natl. Acad. Sci. U.S.A.* 113, 11591–11596. doi: 10.1073/pnas.1609981113
- Smirnov, A., Wang, C., Drewry, L. L., and Vogel, J. (2017). Molecular mechanism of mRNA repression in trans by a ProQ-dependent small RNA. *EMBO J.* 36, 1029–1045. doi: 10.15252/embj.201696127
- Sobrero, P., and Valverde, C. (2012). The bacterial protein Hfq: much more than a mere RNA-binding factor. *Crit. Rev. Microbiol.* 38, 276–299. doi: 10.3109/1040841X.2012.664540
- Teather, R. M., and Wood, P. J. (1982). Use of Congo red-polysaccharide interactions in enumeration and characterization of cellulolytic bacteria from the bovine rumen. *Appl. Environ. Microbiol.* 43, 777–780. doi: 10.1128/aem.43.4.777-780.1982
- Toth, I., van der Wolf, J. M., Saddler, G., Lojkowska, E., Hélias, V., Pirhonen, M., et al. (2011). *Dickeya* species: an emerging problem for potato production in Europe. *Plant Pathol.* 60, 385–399. doi: 10.1111/j.1365-3059.2011.02427.x
- Tsui, H. C., and Winkler, M. E. (1994). Transcriptional patterns of the *mutL-miaA* superoperon of *Escherichia coli* K-12 suggest a model for posttranscriptional regulation. *Biochimie* 76, 1168–1177. doi: 10.1016/0300-9084(94)90046-9
- Updegrove, T. B., Zhang, A., and Storz, G. (2016). Hfq: the flexible RNA matchmaker. *Curr. Opin. Microbiol.* 30, 133–138. doi: 10.1016/j.mib.2016.02.003
- Vogel, J., and Luisi, B. F. (2011). Hfq and its constellation of RNA. *Nat. Rev. Microbiol.* 9, 578–589. doi: 10.1038/nrmicro2615
- Wagner, E. G. H. (2013). Cycling of RNAs on Hfq. *RNA Biol.* 10, 619–626. doi: 10.4161/rna.24044
- Wang, C., Pu, T., Lou, W., Wang, Y., Gao, Z., Hu, B., et al. (2018). Hfq, a RNA chaperone, contributes to virulence by regulating plant cell wall-degrading enzyme production, type VI secretion system expression, bacterial competition, and suppressing host defense response in *Pectobacterium carotovorum*. *Mol. Plant Microbe Interact.* 31, 1166–1178. doi: 10.1094/MPMI-12-17-0303-R
- Westermann, A. J., Venturini, E., Sellin, M. E., Förstner, K. U., Hardt, W.-D., and Vogel, J. (2019). The major RNA-binding protein ProQ impacts virulence gene expression in *Salmonella enterica* Serovar Typhimurium. *mBio* 10:e02504–18. doi: 10.1128/mBio.02504-18
- Wilms, I., Möller, P., Stock, A.-M., Gurski, R., Lai, E.-M., and Narberhaus, F. (2012). Hfq influences multiple transport systems and virulence in the

- plant pathogen *Agrobacterium tumefaciens*. *J. Bacteriol.* 194, 5209–5217. doi: 10.1128/JB.00510-12
- Yuan, X., Zeng, Q., Khokhani, D., Tian, F., Severin, G. B., Waters, C. M., et al. (2019). A feed-forward signalling circuit controls bacterial virulence through linking cyclic di-GMP and two mechanistically distinct sRNAs, ArcZ and RsmB. *Environ. Microbiol.* 21, 2755–2771. doi: 10.1111/1462-2920.14603
- Zeng, Q., McNally, R. R., and Sundin, G. W. (2013). Global small RNA chaperone Hfq and regulatory small RNAs are important virulence regulators in *Erwinia amylovora*. *J. Bacteriol.* 195, 1706–1717. doi: 10.1128/JB.02056-12
- Zeng, Q., and Sundin, G. W. (2014). Genome-wide identification of Hfq-regulated small RNAs in the fire blight pathogen *Erwinia amylovora* discovered small RNAs with virulence regulatory function. *BMC Genom.* 15:414. doi: 10.1186/1471-2164-15-414
- Conflict of Interest:** The authors declare that the research was conducted in the absence of any commercial or financial relationships that could be construed as a potential conflict of interest.

Copyright © 2021 Leonard, Villard, Nasser, Reverchon and Hommais. This is an open-access article distributed under the terms of the Creative Commons Attribution License (CC BY). The use, distribution or reproduction in other forums is permitted, provided the original author(s) and the copyright owner(s) are credited and that the original publication in this journal is cited, in accordance with accepted academic practice. No use, distribution or reproduction is permitted which does not comply with these terms.



Riboregulation in the Major Gastric Pathogen *Helicobacter pylori*

Alejandro Tejada-Arranz^{1,2†} and Hilde De Reuse^{1*}

¹ Unité Pathogénèse de *Helicobacter*, CNRS UMR 2001, Département de Microbiologie, Institut Pasteur, Paris, France,

² Université de Paris, Sorbonne Paris Cité, Paris, France

OPEN ACCESS

Edited by:

Florence Hommais,
Université Claude Bernard Lyon 1,
France

Reviewed by:

Davide Roncarati,
University of Bologna, Italy
Timothy Cover,
Vanderbilt University, United States

*Correspondence:

Hilde De Reuse
hdereuse@pasteur.fr

†Present address:

Alejandro Tejada-Arranz,
Biozentrum University of Basel, Basel,
Switzerland

Specialty section:

This article was submitted to
Microbial Physiology and Metabolism,
a section of the journal
Frontiers in Microbiology

Received: 21 May 2021

Accepted: 23 June 2021

Published: 16 July 2021

Citation:

Tejada-Arranz A and De Reuse H
(2021) Riboregulation in the Major
Gastric Pathogen *Helicobacter pylori*.
Front. Microbiol. 12:712804.
doi: 10.3389/fmicb.2021.712804

Helicobacter pylori is a Gram-negative bacterial pathogen that colonizes the stomach of about half of the human population worldwide. Infection by *H. pylori* is generally acquired during childhood and this bacterium rapidly establishes a persistent colonization. *H. pylori* causes chronic gastritis that, in some cases, progresses into peptic ulcer disease or adenocarcinoma that is responsible for about 800,000 deaths in the world every year. *H. pylori* has evolved efficient adaptive strategies to colonize the stomach, a particularly hostile acidic environment. Few transcriptional regulators are encoded by the small *H. pylori* genome and post-transcriptional regulation has been proposed as a major level of control of gene expression in this pathogen. The transcriptome and transcription start sites (TSSs) of *H. pylori* strain 26695 have been defined at the genome level. This revealed the existence of a total of 1,907 TSSs among which more than 900 TSSs for non-coding RNAs (ncRNAs) including 60 validated small RNAs (sRNAs) and abundant anti-sense RNAs, few of which have been experimentally validated. An RNA degradosome was shown to play a central role in the control of mRNA and antisense RNA decay in *H. pylori*. Riboregulation, genetic regulation by RNA, has also been revealed and depends both on antisense RNAs and small RNAs. Known examples will be presented in this review. Antisense RNA regulation was reported for some virulence factors and for several type I toxin antitoxin systems, one of which controls the morphological transition of *H. pylori* spiral shape to round coccoids. Interestingly, the few documented cases of small RNA-based regulation suggest that their mechanisms do not follow the same rules that were well established in the model organism *Escherichia coli*. First, the genome of *H. pylori* encodes none of the two well-described RNA chaperones, Hfq and ProQ that are important for riboregulation in several organisms. Second, some of the reported small RNAs target, through “rheostat”-like mechanisms, repeat-rich stretches in the 5'-untranslated region of genes encoding important virulence factors. In conclusion, there are still many unanswered questions about the extent and underlying mechanisms of riboregulation in *H. pylori* but recent publications highlighted original mechanisms making this important pathogen an interesting study model.

Keywords: small RNAs, antisense RNAs, virulence, phase variation, *Helicobacter pylori*, post-transcriptional regulation

INTRODUCTION

Helicobacter pylori is a Gram-negative bacterium belonging to the epsilon-proteobacteria class recently proposed to be renamed as *Campylobacterota* (Waite et al., 2017). *H. pylori* is a microaerophilic and helical shaped microorganism that inhabits the stomach of half of the human population worldwide. *H. pylori* is transmitted between humans and generally acquired before the age of five. Infected individuals suffer from chronic gastritis that can remain asymptomatic throughout their lives in 85% of the cases or can evolve into a range of disorders including peptic ulcers or gastric adenocarcinoma, that is responsible for about 800,000 deaths every year worldwide (Robinson and Atherton, 2021). The severe pathologies associated to *H. pylori* infection, like cancer, generally occur after decades of chronic infection. *H. pylori* has evolved to persistently colonize the stomach, despite the harsh conditions of this hostile environment, such as a very low pH and constantly changing conditions, which indicates that it has a strong adaptation capacity. It was thus surprising to observe that *H. pylori* possesses few [only 16 (De la Cruz et al., 2017)] transcriptional regulators (Tomb et al., 1997). This is consistent with its small genome of only 1.67 Mb that encodes 1,576 open reading frames (ORFs) in the 26695 type strain and its unique human gastric niche. Given the reduced number of transcriptional regulators, post-transcriptional regulation has been proposed to play a major role in the control of gene expression in *H. pylori* (Pernitzsch and Sharma, 2012). *H. pylori* does not possess RNA chaperones like Hfq and ProQ, that are important factors in post-transcriptional regulation in many bacteria, including the model organism *Escherichia coli* (Quendera et al., 2020). This characteristic has been an impediment for rapid regulatory RNAs identification in *H. pylori* but it also hints to original mechanisms for post-transcriptional regulation, that we will address in this review and are summarized in Figures 1, 2.

THE TRANSCRIPTOME OF *H. pylori*

The seminal work by Sharma et al. (2010) revealed the complexity of the transcriptome of this bacterium. They mapped 1,907 transcription start sites (TSSs) in *H. pylori* strain 26695 and revealed that 87.5% of the genes are expressed from 337 primary operons, some of which contain additional internal TSSs. Surprisingly, they also detected massive antisense transcription with at least one antisense TSS associated to approximately 46% of all ORFs, including housekeeping genes like 28% of tRNAs and the 5'-leader regions of the 23S and 16S rRNA precursors. Interestingly, most known riboswitches are absent in *H. pylori*, with the exception of a predicted thiamine pyrophosphate riboswitch upstream of *pnuC*. Riboswitches are elements in an RNA molecule that can alter their structure in response to an environmental signal, such as a temperature shift or the presence of certain metabolites, and as a consequence regulate the translation or degradation of this RNA molecule. Even so, there are 337 untranslated regions (UTRs) that are long enough

to accommodate other *cis*-acting regulatory RNA structures (Sharma et al., 2010).

In addition to tRNAs, rRNAs, transfer-messenger RNA (*tmRNA*, an RNA molecule in charge of ribosome unstalling), RNase P, 6S RNA and the signal recognition particle RNA (SRP RNA), Sharma et al. (2010) detected hundreds of candidate non-coding RNAs (ncRNAs). These ncRNAs are transcribed from intergenic regions (small RNAs or sRNAs), antisense to ORFs (antisense RNAs, asRNAs) and sense within ORFs. The expression of 60 of these intergenic ncRNAs was validated (visualized by Northern blot), and more than 900 asRNAs were detected, a few of them being validated (Sharma et al., 2010). It is interesting to note that, even if such massive amounts of asRNAs were first detected in *H. pylori*, other bacteria have since then been shown to have even more asRNAs (Georg and Hess, 2018). The validated and characterized ncRNAs are summarized in Table 1.

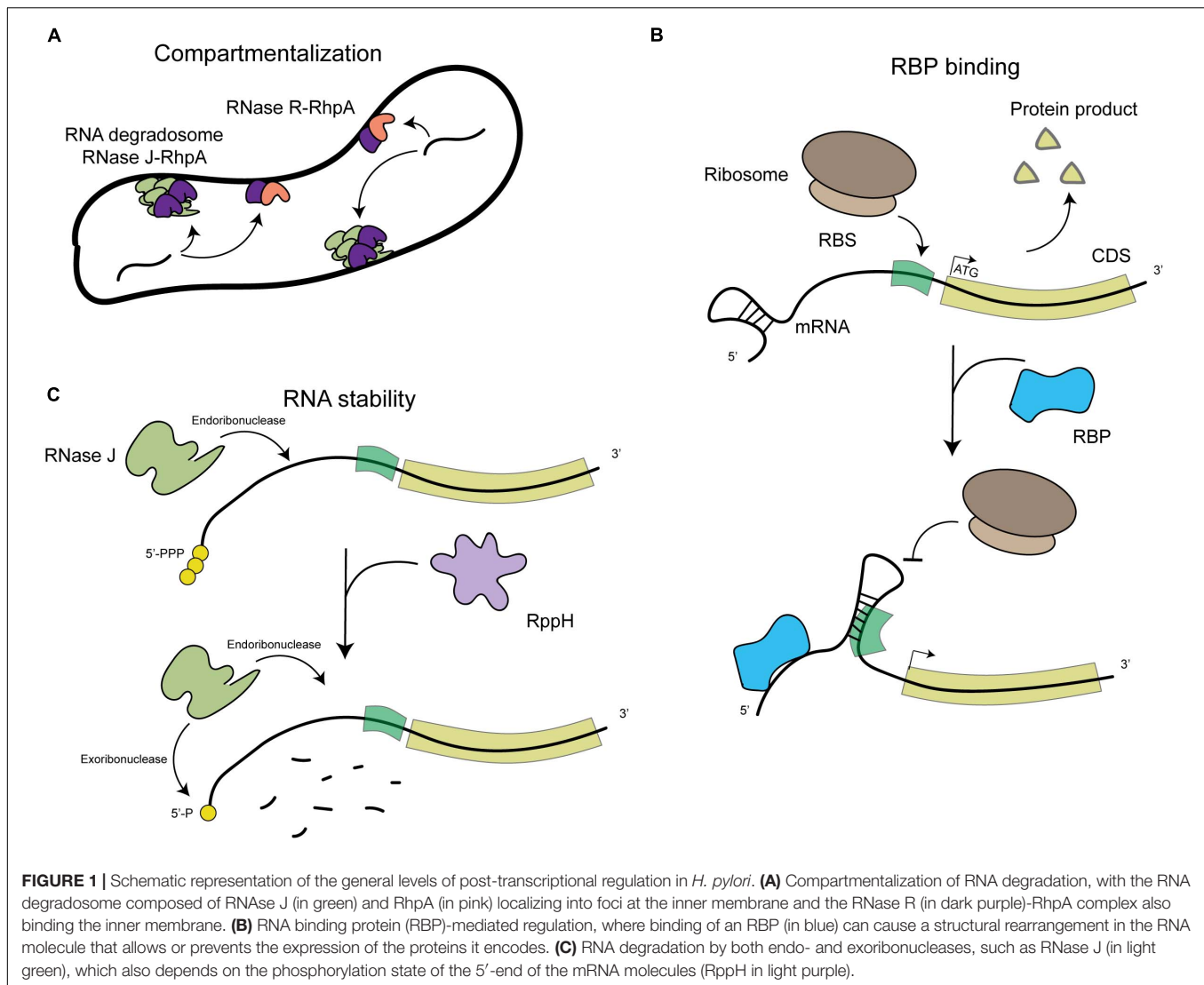
TOOLS TO STUDY THE TRANSCRIPTOME OF *H. pylori*

In the original description of the *H. pylori* transcriptome by Sharma et al. (2010), differential RNA sequencing (dRNA-seq) technologies were used to sequence and define TSSs, and such techniques have been further optimized since then (Bischler et al., 2015). First, in order to detect the widest range of TSSs, RNA was extracted from *H. pylori* grown under different conditions. Then prior to sequencing of cDNA libraries, RNAs were treated or not with terminator exonuclease. This enzyme specifically degrades 5'-P (monophosphate) RNA molecules [that usually result from processing of transcripts by ribonucleases (RNases)] but not 5'-PPP (triphosphate) RNA molecules (that result from transcription), thus allowing the detection of TSSs. Furthermore, the authors developed an online browser for the visualization of TSSs in *H. pylori*¹ (Bischler et al., 2015).

As mentioned earlier, the main *E. coli* RNA-binding proteins (RBPs) participating in ncRNA-mediated regulation of gene expression, Hfq and ProQ, are absent in *H. pylori* (Quendera et al., 2020). Only a homolog of the RBP CsrA (Carbon storage regulator A) has been identified (Barnard et al., 2004). However, the complexity of the transcriptome suggests that other mechanisms and RBPs might be involved in post-transcriptional regulation in this organism.

Tools have been developed in recent years to identify novel RNA-RBP complexes in *H. pylori* (Rieder et al., 2012). One of these approaches was based on the purification of aptamer-tagged sRNAs by chromatography to identify their protein binding partners by mass spectrometry (Rieder et al., 2012). Complementarily, a method to FLAG-tag putative RBPs, co-immunoprecipitate them and sequence the associated RNA molecules was developed. Such tools permitted the detection of interactions between the S1 ribosomal protein and some mRNAs and sRNAs in *H. pylori*, as well as the identification of protein

¹<http://www.imib-wuerzburg.de/research/hpylori/>

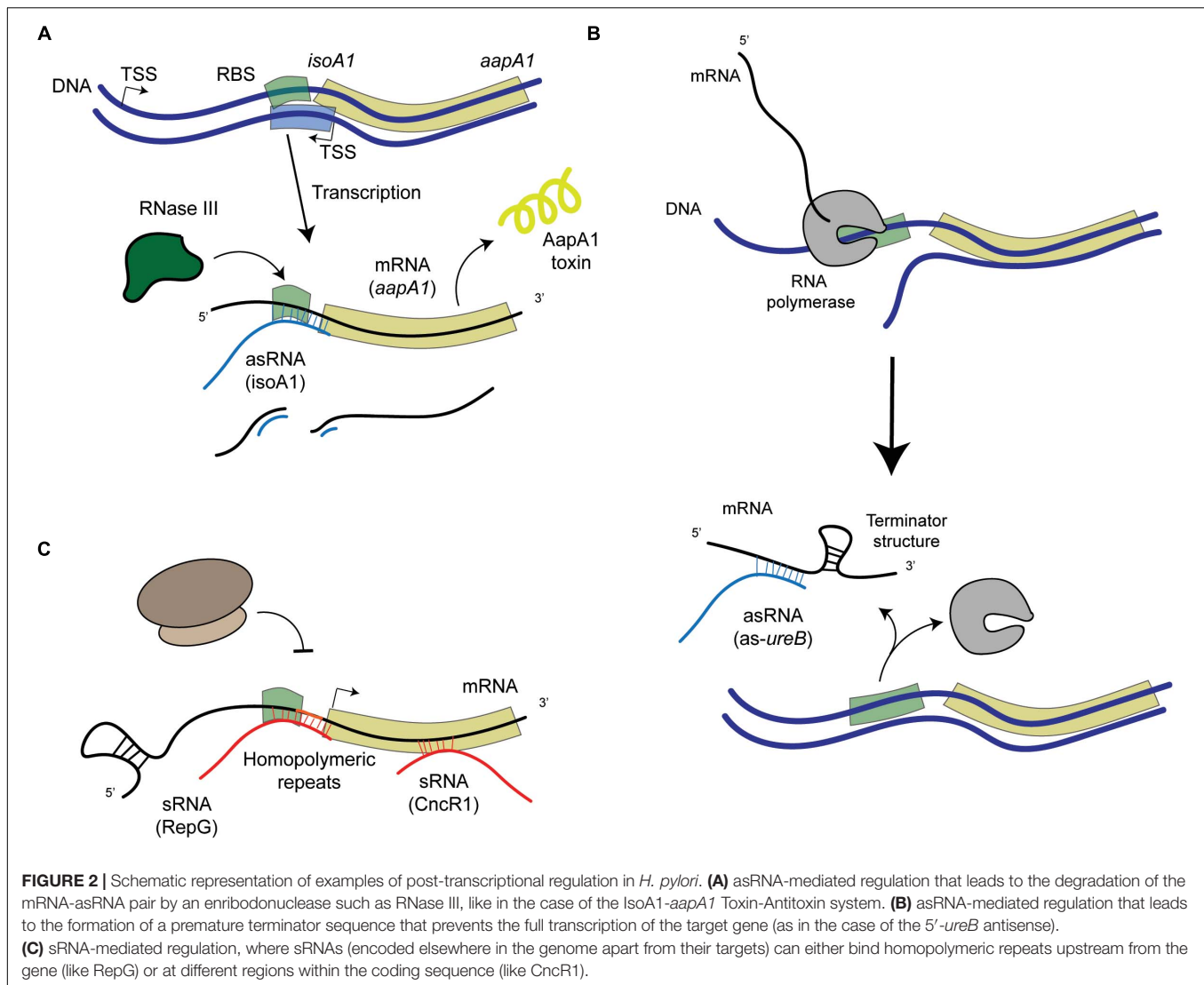


HP1334 as a binding partner of the abundant HPnc6910 sRNA (Rieder et al., 2012).

THE MEMBRANE-ASSOCIATED RNA DEGRADOSOME REGULATES ANTISENSE RNA ABUNDANCE

Despite progress in the detection of RNA species and their putative protein partners, nothing is known about the subcellular distribution of these elements in *H. pylori*. Different RNA molecules from the transcriptome of *E. coli* have been shown to display specific subcellular localization patterns, being targeted to the membrane, the cellular poles or distributed in the cytosol (Kannaiah et al., 2019). This likely plays a role in localizing their protein products and in regulating their expression and stability (Irastortza-Olaziregi and Amster-Choder, 2020). Bacterial RNA degradosomes, that are composed of at least one RNase and one DEAD-box RNA helicase protein that unwinds the target

RNA, are central in the control of RNA decay and maturation (Tejada-Arranz et al., 2020a). The membrane localization of RNA degradosomes has been linked to the rate of degradation of different categories of transcripts including regulatory sRNAs (Moffitt et al., 2016), indicating a compartmentalization of RNA degradation and maturation that plays a role in transcriptome dynamics in prokaryotes. In *H. pylori*, we showed that the RNA degradosome, composed of the essential RNAse J protein and of RhpA, the sole DEAD-box RNA helicase of this bacterium (Redko et al., 2013; El Mortaji et al., 2018), is compartmentalized at the inner membrane where it is assembled into foci whose formation is regulated and likely represent RNA degradation hubs (Tejada-Arranz et al., 2020b; **Figures 1A,C**). In addition, the 3'-5' exoribonuclease RNAse R was also associated to the *H. pylori* inner membrane (Tejada-Arranz et al., 2021; **Figure 1A**). The development of imaging techniques [reviewed in Fei and Sharma (2018)] for the study of the localization of RNA molecules in *H. pylori* is needed in order to assess how the transcriptome is distributed in *H. pylori* cells.



In *H. pylori*, we found that RNase J, the main RNase of its minimal RNA degradosome (Redko et al., 2013), is able to degrade many asRNAs (as well as mRNAs), with about 80% of them being upregulated more than 2-fold in an RNase J-depletion strain, and approximately 50% being regulated more than 4-fold (Redko et al., 2016). This suggests that a major level of regulation of the amount of these asRNAs relies on RNA degradosome-mediated degradation. Interestingly, sRNAs were found not to be preferred targets of this enzyme and are likely regulated through other mechanisms.

REGULATION BY RNA-BINDING PROTEINS (RBPS)

The only RBP that has been extensively studied in other bacteria and that is present in *H. pylori* is CsrA (Quendera et al., 2020). This protein is necessary for full *H. pylori* motility and survival under oxidative stress conditions. Accordingly, a strain lacking

CsrA is defective for virulence in a mouse model (Barnard et al., 2004). More recent studies have found the reduced motility of a Δ *csrA* strain to be associated with a defect in flagellar assembly due to a reduced expression of FlaA and FlaB (Kao et al., 2014) and to the dysregulation of the expression of a putative glycosyltransferase (Kao et al., 2017). In *H. pylori*, no CsrB/D-like sRNAs, which regulate CsrA activity in other organisms, were identified and thus the regulation of the activity of CsrA is not known in this organism. Nevertheless, the role of CsrA in asRNA- and sRNA-mediated regulation remains to be investigated. Other RBPs have been found in *H. pylori*, like the glycolytic enzyme aconitase that was shown to be important for full motility, oxidative stress response and lysozyme resistance (Austin and Maier, 2013; Austin et al., 2015; see Figure 1B).

A homolog of the RNA pyrophosphohydrolase, RppH, was also characterized in *H. pylori*. This enzyme targets the 5'-end of both mRNAs and sRNAs in the cell and cleaves the 5'-triphosphorylated end, yielding a 5'-monophosphorylated molecule that is targeted for degradation (Bischler et al., 2017;

TABLE 1 | List of non-coding RNAs (ncRNAs) validated (visualized by Northern blot) in *Helicobacter pylori*.

ncRNA	sRNA or asRNA	Demonstrated target (when known)	Phenotypes regulated	Expression regulation	References
<i>tmRNA</i>	–	Stalled ribosomes	Competence; oxidative and antibiotic stress tolerance	Induction under acidic conditions	Thibonnier et al. (2008)
6S RNA	–	RNA polymerase	Global regulator of transcription		Sharma et al. (2010)
SRP RNA	–	SRP	Membrane protein targeting		Sharma et al. (2010)
IsoA1	asRNA	<i>aapA1</i> (Type I TA system)	Growth and morphology (coccoid transition)	Repression by hydrogen peroxide	Sharma et al. (2010), Arnion et al. (2017), El Mortaji et al. (2020)
IsoA3	asRNA	<i>aapA3</i> (Type I TA system)	Growth		Sharma et al. (2010), Masachis et al. (2019)
23S asRNA	asRNA	23S-5S rRNA precursor			Iost et al. (2019)
IG-443	asRNA	antisense to <i>flhM</i>			Xiao et al. (2009)
IG-524	asRNA	antisense to <i>fumC</i>			Xiao et al. (2009)
RepG/HPnc5490	sRNA	<i>tlpB-hp0102</i>	Chemotaxis, LPS biosynthesis and resistance to antibiotics	As a function of growth phase, accumulates in coccoid forms	Sharma et al. (2010), Pernitzsch et al. (2014, 2021)
NikS/HPnc4160 (<i>IsoB</i>)	asRNA	<i>cagA</i> , <i>vacA</i> , <i>horF</i> , <i>hofC</i> , <i>horB</i> , <i>hopE</i> , <i>omp14</i> , <i>hpg27_1238</i> , <i>hp1227</i> , <i>hp0410</i> , <i>helpy_1262</i>	Bacterial internalization, colonization and epithelial barrier disruption, production of phosphorylated CagA in host cells	Phase-variable expression and regulated by NikR	Eisenbart et al. (2020), Kinoshita-Daitoku et al. (2021)
5' <i>ureB</i> -sRNA	asRNA	<i>ureB</i>	Urease activity	Expression at neutral pH, negatively regulated by the ArsRS TCS	Wen et al. (2011), Wen et al. (2013)
CncR1/HPnc2630	sRNA	<i>flhK</i>	Motility and adhesion to host cells	Growth phase regulated by HsrA (orphan response regulator)	Sharma et al. (2010), Vannini et al. (2014, 2016)
IsoA2	asRNA	<i>aapA2</i> (Type I TA system)			Sharma et al. (2010)
IsoA4	asRNA	<i>aapA4</i> (Type I TA system)			Sharma et al. (2010)
IsoA5	asRNA	<i>aapA5</i> (Type I TA system)			Sharma et al. (2010)
IsoA6	asRNA	<i>aapA6</i> (Type I TA system)			Sharma et al. (2010)
HPnc1200	asRNA	<i>rplU</i>			Sharma et al. (2010)
HPnc6270	asRNA	<i>cstA</i>			Sharma et al. (2010)
HPnc3200	asRNA	<i>hp0637</i>			Sharma et al. (2010)
HPnc3210	asRNA	<i>hp0637</i>			Sharma et al. (2010)
HPnc2240	asRNA	<i>Hp0488</i>			Sharma et al. (2010)
HPnc2250	asRNA	<i>Hp0488</i>			Sharma et al. (2010)
HPnc5970	asRNA	<i>Hp1116</i>			Sharma et al. (2010)
HPnc6000	asRNA	<i>Hp1116</i>			Sharma et al. (2010)
HPnc2450	asRNA	<i>Hp0513</i>			Sharma et al. (2010)
HPnc1470	asRNA	<i>Hp0357</i>			Sharma et al. (2010)
HPnc7450	asRNA	<i>HPr06</i>			Sharma et al. (2010)
HPnc3320	asRNA	<i>Hp0660</i>			Sharma et al. (2010)
HPnc1810	asRNA	<i>Hp0423</i>			Sharma et al. (2010)
HPnc7520	asRNA	<i>Hp1412</i>			Sharma et al. (2010)
HPnc6910	sRNA				Sharma et al. (2010), Rieder et al. (2012)

Non-characterized sRNAs identified in Sharma et al. (2010)

HPnc6670, HPnc2090, HPnc2420, HPnc4590, HPnc7830, HPnc1810, HPnc6160, HPnc4870, HPnc7430, HPnc1880, HPnc5490, HPnc6670, HPnc2630, HPnc2640, HPnc0260 HPnc0270, HPnc1200, HPnc1820, HPnc7510, HPnc2250, HPnc5970, HPnc2440, HPnc3110, HPnc3200, HPnc3210, HPnc3830, HPnc3840, HPnc4510, HPnc4850, HPnc4870, HPnc5300, HPnc5580, HPnc6160, HPnc6270, HPnc6630, HPnc6620, HPnc7100, HPnc7230, HPnc7430, HPnc7770, HPnc7890, HPnc7830, HPnc4620, HPnc4630, HPnc0580, HPnc7830, HPnc0580, HPnc1990, HPnc1980, HPnc0470, HPnc0480, HPnc0490, HPnc2420, HPnc3560, HPnc5000, HPnc5130, HPnc5140, HPnc5310, HPnc5800, HPnc5810, HPnc6870, HPnc7300, HPnc7700, HPnc7720, HPnc7670, HPnc7680, HPnc0710, HPnc1070, HPnc3020, HPnc3880, HPnc4860, HPnc5960.

An online browser for the visualization of TSSs in *H. pylori* is available at <http://www.imib-wuerzburg.de/research/hpylori/> (Bischler et al., 2015).

Figure 1C). In addition, mutants in this protein are more susceptible to hydrogen peroxide (Lundin et al., 2003) and are less able to invade gastric adenocarcinoma cells (Liu et al., 2012).

NON-CODING RNA-MEDIATED REGULATION OF GENE EXPRESSION

As mentioned above, the transcriptome of *H. pylori* contains >900 asRNA molecules and 60 validated sRNAs, with only one predicted riboswitch. Overall, there is little information about the molecular mechanisms by which asRNAs and sRNAs regulate gene expression and how their expression is regulated in *H. pylori*. Generally, these ncRNAs act by base-pairing with their target mRNAs (that can be transcribed from the opposite strand in the case of asRNAs or from somewhere else in the genome for the sRNAs) and hence altering their secondary structure, which might have consequences regarding their expression (ribosome accessibility) or stability (RNase accessibility). The few examples that have been analyzed in detail in *H. pylori* will be presented below.

Antisense RNA-Mediated Regulation of Gene Expression

Regulation of Type I TA Systems

Toxin-antitoxin (TA) systems are genetic modules that are widespread in prokaryotes. They encode a protein toxin and a cognate antitoxin that prevents the activity or expression of the toxin. The type I TA systems, in which the antitoxin is an asRNA, are highly represented on the *H. pylori* chromosome and several are strongly expressed (Sharma et al., 2010; Masachis and Darfeuille, 2019). Among them, the type I TA *aapA1-isoA1* system has been extensively studied (Arnion et al., 2017; El Mortaji et al., 2020). The corresponding AapA1 toxin is a 30 aa-long hydrophobic peptide that, upon expression, targets the inner membrane and inhibits *H. pylori* growth (El Mortaji et al., 2020; Korkut et al., 2020). We have recently shown that this toxin triggers a morphological transition of *H. pylori* from its typical helical shape to round coccoid cells, that have been observed in response to stress as well as in human biopsies (El Mortaji et al., 2020). Our characterization of the toxin-induced coccoids suggests that they are viable cells that could correspond to dormant bacteria and might be responsible for *H. pylori* infections refractory to treatment.

Under normal growth conditions, different mechanisms that prevent the expression of the AapA1 toxin have been revealed (Arnion et al., 2017). Folding of the *aapA1* full length transcript prevents its translation, unless its 3'-end is processed. This active *aapA1* structure allows the formation of an extended duplex with the *isoA1* asRNA that is degraded by RNase III, thus preventing AapA1 translation (Arnion et al., 2017; **Figure 2A**). The expression of AapA1 occurs under conditions that reduce the activity of the *isoA1* promoter, namely oxidative stress and hence triggers *H. pylori* morphological transition (El Mortaji et al., 2020). Thus, the *isoA1* asRNA is involved in regulating the transition of *H. pylori* cells

into dormant forms that likely play an important role during colonization.

In another TA system from this family, *aapA3-isoA3*, the expression of the toxin is regulated by the formation of metastable structures in the *aapA3* mRNA that transiently form during transcription and result in sequestration of the Shine-Dalgarno sequence, thereby also preventing unwanted toxin synthesis (Masachis et al., 2019).

Regulation of the Expression of the *ureAB* Operon by an asRNA

Urease is a major colonization factor for *H. pylori*. This nickel metalloenzyme catalyzes the hydrolysis of urea into ammonia and bicarbonate (de Reuse et al., 2013). Both compounds allow *H. pylori* to buffer its cytoplasm and thus resist the extremely low pH of its unique niche, the human stomach. Large amounts of urease are produced by *H. pylori*. However, its synthesis requires regulation to avoid a toxic alkalization of the cytoplasm. Urease of *H. pylori* is composed of two structural units, UreA and UreB. These proteins are expressed from an operon that is adjacent to a second one encoding the so-called urease accessory proteins required for nickel incorporation into urease. Expression of *ureAB* is positively controlled by NikR, a nickel-responsive regulator (Muller et al., 2011; Jones et al., 2018) and by a two-component system (TCS) of the OmpR-EnvZ family (Bury-Moné et al., 2004) designated ArsRS in *H. pylori* (Pflock et al., 2006). Under low pH conditions, the ArsRS system activates the urease operons ensuring increased production of this enzyme under the condition where its activity is vital. Wen et al. (2011, 2013) have identified another level of regulation of the *ureAB* operon. At neutral pH, they demonstrated the expression of a 290 nucleotides (nt)-long asRNA to *ureB* that favors the accumulation of a truncated transcript of the *ureAB* operon lacking the *ureB* 3'-end (**Figure 2B**). Interestingly, the expression of this asRNA is negatively regulated by the ArsRS TCS in response to acidic pH. Electrophoretic mobility shift assays (EMSA) showed that unphosphorylated ArsR regulator protein indeed binds to the *ureB*-asRNA promoter region. They determined that the mechanism at play is base-pairing of the antisense 5'*ureB*-asRNA with the *ureAB* transcript and subsequent transcription termination of the sense *ureAB* mRNA that causes diminished urease production. These data highlight a dual control of urease production that is adjusted to the pH of the environment encountered by *H. pylori*, with activation of urease expression at acidic pH and repression at neutral pH.

Other Antisense RNAs

Another example concerns rRNA maturation in *H. pylori*. A strongly expressed asRNA overlapping the leader region of the 23S-5S rRNA precursor has been identified and found to be conserved (Sharma et al., 2010; Iost et al., 2019). It was demonstrated that this asRNA interacts with an rRNA precursor, forming an intermolecular complex that is cleaved by RNase III. This pairing induces further specific cleavages of the rRNA precursor and the degradation of the 23S asRNA.

Whether this asRNA plays a regulatory function in rRNA maturation is still unclear as it is dispensable for *H. pylori* growth and for proper rRNA maturation under laboratory conditions. However, it might have a fine-tuning function by facilitating the degradation of processed fragments or a quality control role by favoring appropriate rRNA folding, that might become more evident under different growth conditions (Iost et al., 2019).

Other asRNAs were first identified *in silico* and then found to be expressed. They were predicted to target the flagellar motor switch gene (*fliM*) and fumarase (*fumC*), potentially regulating the expression of these genes (Xiao et al., 2009).

Trans-Acting Regulatory sRNAs of *H. pylori*

RepG, A sRNA That Targets Simple Repeat Sequences (SRRs)

Besides transcriptional regulators, gene expression can be modulated by variations in the length of repeated nucleotide sequences, the “simple sequence repeats” (SSRs), located in their 5′-UTR that modify the stability or translation of the mRNA; or located in the promoter region, affecting the spacing of promoter elements or transcription factors binding sites. Phase variation of SSRs is due to slipped strand mispairing during replication and is used by many pathogens as an adaptive mechanism in which the most favorable expression is selected. Genes encoding bacterial surface structures or DNA Restriction-Modification enzymes are among the most frequently regulated by SSRs. The group of Sharma et al. (2010) identified and characterized the first sRNA that mediates post-transcriptional regulation by targeting a G-repeat stretch that is located in the 5′-UTR of the bicistronic *tlpB-hp0102* operon (Pernitzsch et al., 2014, 2021; **Figure 2C**). This operon encodes the TlpB chemotaxis receptor and the HP0102 protein that was shown to function as a glycosyltransferase involved in lipopolysaccharide (LPS) O-chain biosynthesis (Pernitzsch et al., 2021). The precise fucosyltransferase activity of HP0102 was shown (Li et al., 2019). The sRNA designated RepG (REGulator of Polymeric G-repeats) is highly conserved in *H. pylori*. In contrast, the length of the G-repeat stretch upstream *tlpB-hp0102* is highly variable among *H. pylori* strains and in sequential isolates from human patients, indicating that this region indeed undergoes phase variation during infection. Direct binding and base pairing of RepG to the 5′-UTR SSR region was demonstrated. Most interestingly, they showed that depending on the length of the G repeat, the binding of RepG can either mediate activation or repression of the *tlpB-hp0102* operon and that this regulation acts at the translational level (Pernitzsch et al., 2014, 2021). In a recent publication, in collaboration with our group (Pernitzsch et al., 2021), the HP0102 glycosyltransferase was shown to be essential for colonization of the mouse model by *H. pylori* and to modulate LPS O-chain synthesis. The gradual modulation of *H. pylori* LPS through RepG regulation impacts bacterial resistance to membrane-targeting antibiotics and the exposure of Lewis antigens that contribute to the host immune recognition of this pathogen. In conclusion, these studies establish an original

mechanism of post-transcriptional regulation by RepG, a trans-acting sRNA, that mediates a gradual rather than ON/OFF switch of the expression of its targets enabling *H. pylori* to adapt to its host.

NikS/HPnc4160, A sRNA Regulating Major Virulence Factors in *H. pylori*

Two recent publications report the characterization of a sRNA (HPnc4160) that regulates the expression of major *H. pylori* virulence factors (Eisenbart et al., 2020; Kinoshita-Daitoku et al., 2021). HPnc4160 was previously identified as a highly transcribed sRNA (IsoB) expressed from the opposite strand of a poorly expressed small ORF (AapB) as a part of a probably “degenerated” type I TA system (Sharma et al., 2010; Vannini et al., 2017). HPnc4160 is strongly conserved in *H. pylori* and harbors a length-variable T stretch upstream its −10 promoter sequence. The expression of HPnc4160 was shown to be repressed by NikR in response to nickel (Eisenbart et al., 2020) through direct binding of this transcriptional regulator to the sRNA promoter (Vannini et al., 2017). Therefore, HPnc4160 was renamed NikS (Eisenbart et al., 2020). The T stretch preceding the HPnc4160/NikS sRNA was variable in length in strains isolated from patients or during Mongolian gerbil colonization (Eisenbart et al., 2020; Kinoshita-Daitoku et al., 2021); this length variation affects the sRNA expression. Both studies identified the targets of this sRNA by mRNA and protein expression analysis. Genes encoding major virulence and colonization factors were found to be targeted by HPnc4160/NikS, [five in Eisenbart et al. (2020) and eight in Kinoshita-Daitoku et al. (2021); see **Table 1**]. Both studies identified *cagA*, encoding the oncoprotein CagA, as a target and found that the expression of several outer membrane proteins, some being potential adhesins, is targeted. Eisenbart et al. identified in addition *vacA*, encoding the vacuolating cytotoxin, as being directly regulated by HPnc4160/NikS. Post-transcriptional repression by HPnc4160/NikS base pairing to five mRNA leaders was demonstrated, which results in translation inhibition (Eisenbart et al., 2020). *In vitro* EMSA and structure probing analysis validated the direct HPnc4160/NikS interaction with several of its targets (Eisenbart et al., 2020; Kinoshita-Daitoku et al., 2021). However, the two publications present divergent data on the targeting site in *cagA*, in the 5′ UTR region for Eisenbart et al. (2020) and intragenic for Kinoshita-Daitoku et al. (2021), which implies different underlying regulatory mechanisms. Both studies validate that the control of *cagA* expression by HPnc4160/NikS indeed impacts *H. pylori* pathogenicity. *In vitro* infection of different cell types by *H. pylori* revealed that HPnc4160/NikS decreases CagA-dependent bacterial internalization, reduces cell colonization and epithelial barrier disruption (Eisenbart et al., 2020) and also decreases the level of phosphorylated CagA, IL8 production and the associated CagA-induced hummingbird phenotype (Kinoshita-Daitoku et al., 2021). During mouse colonization by *H. pylori*, the number of repeats of HPnc4160/NikS varies with a trend to expansion while a deletion of this sRNA favors short term colonization. The selective pressure that drives these variations *in vivo* still needs to be identified. Finally, the T-repeats were found to be significantly longer in strains isolated from patients

with gastric cancer than in “non-cancer” strains. In conclusion, HPnc4160/NikS is a sRNA acting as a master regulator of the adaptation of *H. pylori* to the colonization of its host.

CncR1, A sRNA Regulating Motility and Adhesion to Host Cells

The *H. pylori* *cag* pathogenicity island (*cag* PAI) is a 40 kb DNA element that encodes a type IV secretion system. The *cag* PAI is a major virulence determinant of *H. pylori* that allows for the delivery of bacterial effector molecules into host gastric epithelial cells, in particular the oncoprotein CagA encoded within the *cag* PAI.

Both groups of Sharma et al. (2010) and Vannini et al. (2014) have identified, within the *cag* PAI, a ncRNA expressed within the 5′-UTR of *cagP*. This 213 nt-long sRNA is abundant and conserved in *H. pylori*. It was designated HPnc2630 in strain 26695 (Sharma et al., 2010) and was renamed CncR1 for “*cag* non-coding RNA 1” in strain G27 where it was characterized (Vannini et al., 2016). Vannini et al. (2016) showed that the expression of the CncR1 sRNA is directed by the *cagP* promoter and regulated as a function of growth through direct binding of the essential orphan response regulator HsrA (HP1043). Transcriptomic analysis of a Δ *cncR1* mutant identified 71 deregulated genes. Enrichment in downregulated genes related to host-pathogen interactions was observed in addition to upregulation of genes involved in the assembly and regulation of the flagellar apparatus including FliK, a flagellar hook-length control protein. They validated that CncR1 negatively regulates *H. pylori* motility functions. Using EMSA and RNase T1 footprinting experiments, direct targeting of the sRNA on different regions of the *fliK* mRNA was demonstrated (Figure 2C). Finally, CncR1 is required for full bacterial adhesion to host cells. In conclusion, the CncR1 sRNA modulates *H. pylori* virulence through opposite effects on motility and adhesion which might be relevant to signals related to growth phase or bacterial density where bacteria move to a new colonization site.

CONCLUSION

Relatively few studies have been published on riboregulation in *H. pylori*. However, the established properties make it a

fascinating microorganism to study. The huge number of genes for which a *cis*-asRNA is expressed is still intriguing, some of them certainly have regulatory roles on the expression of the complementary mRNA but many RNAs that are produced by pervasive transcription may have other functions. The post-transcriptional mode of gene regulation where a sRNA targets homopolymeric repeats within 5′-UTR is original. This mechanism and other variations linking RNA-mediated control and SSRs are most probably widespread in *H. pylori* and will certainly be found in other bacteria in the future. In *H. pylori*, RepG has other targets, several antisense TSSs were shown to overlap SSRs and some sRNA candidates have internal repeats (Sharma et al., 2010; Pernitzsch et al., 2014, 2021). These data, together with what is known about the SSR-controlled NikS/HPnc4160 sRNA, reveal that bacterial phase variation, which is associated to host adaptation, impacts gene expression at several levels. Finally, since no RNA chaperone facilitating sRNA-mRNA base-pairing has been reported so far in *H. pylori*, the question of discrimination of the targets, in particular those with low complexity, such as SSRs, remains open.

AUTHOR CONTRIBUTIONS

Both authors wrote and edited the manuscript, contributed to the article and approved the submitted version.

FUNDING

AT-A have been part of the Pasteur - Paris University (PPU) International Ph.D. Program. This project have received funding from the European Union’s Horizon 2020 Research and Innovation Programme under the Marie Skłodowska-Curie grant agreement No 665807 and from the Institut Carnot Pasteur Microbes & Santé. Support was provided by “Fondation pour la Recherche Médicale” for the grant DBF20161136767 to HDR and the Pasteur-Weizmann Consortium of “The Roles of Non-coding RNAs in Regulation of Microbial Life Styles and Virulence” to HDR.

REFERENCES

- Arnion, H., Korkut, D. N., Masachis Gelo, S., Chabas, S., Reignier, J., Iost, I., et al. (2017). Mechanistic insights into type I toxin antitoxin systems in *Helicobacter pylori*: the importance of mRNA folding in controlling toxin expression. *Nucleic Acids Res.* 45:gw1343. doi: 10.1093/nar/gkw1343
- Austin, C. M., and Maier, R. J. (2013). Aconitase-mediated posttranscriptional regulation of *Helicobacter pylori* peptidoglycan deacetylase. *J. Bacteriol.* 195, 5316–5322. doi: 10.1128/JB.00720-13
- Austin, C. M., Wang, G., and Maier, R. J. (2015). Aconitase functions as a pleiotropic posttranscriptional regulator in *Helicobacter pylori*. *J. Bacteriol.* 197, 3076–3086. doi: 10.1128/JB.00529-15
- Barnard, F. M., Loughlin, M. F., Fainberg, H. P., Messenger, M. P., Ussery, D. W., Williams, P., et al. (2004). Global regulation of virulence and the stress response by CsrA in the highly adapted human gastric pathogen *Helicobacter pylori*. *Mol. Microbiol.* 51, 15–32. doi: 10.1046/j.1365-2958.2003.03788
- Bischler, T., Hsieh, P.-K., Resch, M., Liu, Q., Tan, H. S., Foley, P. L., et al. (2017). Identification of the RNA pyrophosphohydrolase RppH of *Helicobacter pylori* and Global analysis of its RNA targets. *J. Biol. Chem.* 292, 1934–1950. doi: 10.1074/jbc.M116.761171
- Bischler, T., Tan, H. S., Nieselt, K., and Sharma, C. M. (2015). Differential RNA-seq (dRNA-seq) for annotation of transcriptional start sites and small RNAs in *Helicobacter pylori*. *Methods* 86, 89–101. doi: 10.1016/j.ymeth.2015.06.012
- Bury-Moné, S., Thiberge, J.-M., Contreras, M., Maitournam, A., Labigne, A., and De Reuse, H. (2004). Responsiveness to acidity via metal ion regulators mediates virulence in the gastric pathogen *Helicobacter pylori*. *Mol. Microbiol.* 53, 623–638. doi: 10.1111/j.1365-2958.2004.04137
- De la Cruz, M. A., Ares, M. A., von Bargen, K., Panunzi, L. G., Martínez-Cruz, J., Valdez-Salazar, H. A., et al. (2017). Gene expression profiling of transcription factors of *Helicobacter pylori* under different environmental conditions. *Front. Microbiol.* 8:615. doi: 10.3389/fmicb.2017.00615

- de Reuse, H., Vinella, D., and Cavazza, C. (2013). Common themes and unique proteins for the uptake and trafficking of nickel, a metal essential for the virulence of *Helicobacter pylori*. *Front. Cell. Infect. Microbiol.* 3:94. doi: 10.3389/fcimb.2013.00094
- Eisenbart, S. K., Alzheimer, M., Pernitzsch, S. R., Dietrich, S., Stahl, S., and Sharma, C. M. (2020). A repeat-associated small RNA controls the major virulence factors of *Helicobacter pylori*. *Mol. Cell* 80, 210.e–226.e. doi: 10.1016/j.molcel.2020.09.009
- El Mortaji, L., Aubert, S., Galtier, E., Schmitt, C., Anger, K., Redko, Y., et al. (2018). The sole DEAD-Box RNA helicase of the gastric pathogen *Helicobacter pylori* is essential for colonization. *mBio* 9:e02071-17. doi: 10.1128/mBio.02071-17
- El Mortaji, L., Tejada-Arranz, A., Rifflet, A., Boneca, I. G., Pehau-Arnaudet, G., Radicella, J. P., et al. (2020). A peptide of a type I toxin-antitoxin system induces *Helicobacter pylori* morphological transformation from spiral shape to coccoids. *Proc. Natl. Acad. Sci. U.S.A.* 117, 31398–31409. doi: 10.1073/pnas.2016195117
- Fei, J., and Sharma, C. M. (2018). RNA localization in bacteria. *Microbiol. Spectr.* 6, 1–19. doi: 10.1128/microbiolspec.RWR-0024-2018
- Georg, J., and Hess, W. R. (2018). “Widespread antisense transcription in prokaryotes,” in *Regulating with RNA in Bacteria and Archaea*, eds G. Storz and K. Papenfort (Washington, DC: ASM Press), 191–210. doi: 10.1128/9781683670247.ch12
- Iost, I., Chabas, S., and Darfeuille, F. (2019). Maturation of atypical ribosomal RNA precursors in *Helicobacter pylori*. *Nucleic Acids Res.* 47, 5906–5921. doi: 10.1093/nar/gkz258
- Irastortza-Olaziregi, M., and Amster-Choder, O. (2020). RNA localization in prokaryotes: where, when, how, and why. *Wiley Interdiscip. Rev. RNA* 12:e1615. doi: 10.1002/wrna.1615
- Jones, M. D., Li, Y., and Zamble, D. B. (2018). Acid-responsive activity of the *Helicobacter pylori* metalloregulator NikR. *Proc. Natl. Acad. Sci. U.S.A.* 115, 8966–8971. doi: 10.1073/pnas.1808393115
- Kannaiah, S., Livny, J., and Amster-Choder, O. (2019). Spatiotemporal organization of the *E. coli* transcriptome: translation independence and engagement in regulation. *Mol. Cell* 76, 574.e–589.e. doi: 10.1016/j.molcel.2019.08.013
- Kao, C.-Y., Chen, J.-W., Wang, S., Sheu, B.-S., and Wu, J.-J. (2017). The *Helicobacter pylori* J99 jhp0106 gene, under the control of the CsrA/RpoN regulatory system, modulates flagella formation and motility. *Front. Microbiol.* 8:483. doi: 10.3389/fmicb.2017.00483
- Kao, C.-Y., Sheu, B.-S., and Wu, J.-J. (2014). CsrA regulates *Helicobacter pylori* J99 motility and adhesion by controlling flagella formation. *Helicobacter* 19, 443–454. doi: 10.1111/hel.12148
- Kinoshita-Daitoku, R., Kiga, K., Miyakoshi, M., Otsubo, R., Ogura, Y., Sanada, T., et al. (2021). A bacterial small RNA regulates the adaptation of *Helicobacter pylori* to the host environment. *Nat. Commun.* 12:2085. doi: 10.1038/s41467-021-22317-7
- Korkut, D. N., Alves, I. D., Vogel, A., Chabas, S., Sharma, C. M., Martinez, D., et al. (2020). Structural insights into the AapA1 toxin of *Helicobacter pylori*. *Biochim. Biophys. Acta. Gen. Subj.* 1864:129423. doi: 10.1016/j.bbagen.2019.129423
- Li, H., Marceau, M., Yang, T., Liao, T., Tang, X., Hu, R., et al. (2019). East-Asian *Helicobacter pylori* strains synthesize heptan-deficient lipopolysaccharide. *PLoS Genet.* 15:e1008497. doi: 10.1371/journal.pgen.1008497
- Liu, H., Semino-Mora, C., and Dubois, A. (2012). Mechanism of *H. pylori* intracellular entry: an in vitro study. *Front. Cell. Infect. Microbiol.* 2:13. doi: 10.3389/fcimb.2012.00013
- Lundin, A., Nilsson, C., Gerhard, M., Andersson, D. I., Krabbe, M., and Engstrand, L. (2003). The NudA protein in the gastric pathogen *Helicobacter pylori* is an ubiquitous and constitutively expressed dinucleoside polyphosphate hydrolase. *J. Biol. Chem.* 278, 12574–12578. doi: 10.1074/JBC.M212542200
- Masachis, S., and Darfeuille, F. (2019). “Type I toxin-antitoxin systems: regulating toxin expression via Shine-Dalgarno sequence sequestration and small RNA binding,” in *Regulating with RNA in Bacteria and Archaea*, eds G. Storz and K. Papenfort (Washington, DC: American Society of Microbiology), 173–190. doi: 10.1128/microbiolspec.RWR-0030-2018
- Masachis, S., Tourasse, N. J., Lays, C., Faucher, M., Chabas, S., Iost, I., et al. (2019). A genetic selection reveals functional metastable structures embedded in a toxin-encoding mRNA. *Elife* 8:e47549. doi: 10.7554/eLife.47549
- Moffitt, J. R., Pandey, S., Boettiger, A. N., Wang, S., and Zhuang, X. (2016). Spatial organization shapes the turnover of a bacterial transcriptome. *Elife* 5:e13065. doi: 10.7554/eLife.13065
- Muller, C., Bahlawane, C., Aubert, S., Delay, C. M., Schauer, K., Michaud-Soret, I., et al. (2011). Hierarchical regulation of the NikR-mediated nickel response in *Helicobacter pylori*. *Nucleic Acids Res.* 39, 7564–7575. doi: 10.1093/nar/gkr460
- Pernitzsch, S. R., Alzheimer, M., Bremer, B. U., Robbe-Saule, M., De Reuse, H., and Sharma, C. M. (2021). Small RNA-mediated gradual lipopolysaccharide biosynthesis control affects antibiotics resistance of *Helicobacter pylori*. *Nat. Comm.* (in press).
- Pernitzsch, S. R., and Sharma, C. M. (2012). Transcriptome complexity and riboregulation in the human pathogen *Helicobacter pylori*. *Front. Cell. Infect. Microbiol.* 2:14. doi: 10.3389/fcimb.2012.00014
- Pernitzsch, S. R., Tirier, S. M., Beier, D., and Sharma, C. M. (2014). A variable homopolymeric G-repeat defines small RNA-mediated posttranscriptional regulation of a chemotaxis receptor in *Helicobacter pylori*. *Proc. Natl. Acad. Sci. U.S.A.* 111, E501–E510. doi: 10.1073/pnas.1315152111
- Pflock, M., Finsterer, N., Joseph, B., Mollenkopf, H., Meyer, T., and Beier, D. (2006). Characterization of the ArsRS regulon of *Helicobacter pylori*, involved in acid adaptation. *J. Bacteriol.* 188, 3449–3462. doi: 10.1128/JB.188.10.3449-3462.2006
- Quendera, A. P., Seixas, A. F., Dos Santos, R. F., Santos, I., Silva, J. P. N., Arraiano, C. M., et al. (2020). RNA-binding proteins driving the regulatory activity of small non-coding RNAs in bacteria. *Front. Mol. Biosci.* 7:78. doi: 10.3389/fmolb.2020.00078
- Redko, Y., Aubert, S., Stachowicz, A., Lenormand, P., Namane, A., Darfeuille, F., et al. (2013). A minimal bacterial RNase J-based degradosome is associated with translating ribosomes. *Nucleic Acids Res.* 41, 288–301. doi: 10.1093/nar/gks945
- Redko, Y., Galtier, E., Arnion, H., Darfeuille, F., Sismeiro, O., Coppée, J.-Y., et al. (2016). RNase J depletion leads to massive changes in mRNA abundance in *Helicobacter pylori*. *RNA Biol.* 13, 243–253. doi: 10.1080/15476286.2015.1132141
- Rieder, R., Reinhardt, R., Sharma, C., and Vogel, J. (2012). Experimental tools to identify RNA-protein interactions in *Helicobacter pylori*. *RNA Biol.* 9, 520–531. doi: 10.4161/rna.20331
- Robinson, K., and Atherton, J. C. (2021). The spectrum of *Helicobacter*-mediated diseases. *Annu. Rev. Pathol.* 16, 123–144. doi: 10.1146/annurev-pathol-032520-024949
- Sharma, C. M., Hoffmann, S., Darfeuille, F., Reignier, J., Findeiß, S., Sittka, A., et al. (2010). The primary transcriptome of the major human pathogen *Helicobacter pylori*. *Nature* 464, 250–255. doi: 10.1038/nature08756
- Tejada-Arranz, A., de Crécy-Lagard, V., and de Reuse, H. (2020a). Bacterial RNA degradosomes: molecular machines under tight control. *Trends Biochem. Sci.* 45, 42–57. doi: 10.1016/j.tibs.2019.10.002
- Tejada-Arranz, A., Galtier, E., El Mortaji, L., Turlin, E., Ershov, D., and De Reuse, H. (2020b). The RNase J-based RNA degradosome is compartmentalized in the gastric pathogen *Helicobacter pylori*. *MBio* 11:e01173-20. doi: 10.1128/mBio.01173-20
- Tejada-Arranz, A., Matos, R. G., Quentin, Y., Bouilloux-Lafont, M., Galtier, E., Briolat, V., et al. (2021). RNase R is associated in a functional complex with the RhpA DEAD-box RNA helicase in *Helicobacter pylori*. *Nucleic Acids Res.* 49, 5249–5264. doi: 10.1093/nar/gkab283
- Thibonnier, M., Thiberge, J.-M., and De Reuse, H. (2008). Trans-translation in *Helicobacter pylori*: essentiality of ribosome rescue and requirement of protein tagging for stress resistance and competence. *PLoS One* 3:e3810. doi: 10.1371/journal.pone.0003810
- Tomb, J. F., White, O., Kerlavage, A. R., Clayton, R. A., Sutton, G. G., Fleischmann, R. D., et al. (1997). The complete genome sequence of the gastric pathogen *Helicobacter pylori*. *Nature* 388, 539–547. doi: 10.1038/41483
- Vannini, A., Pinatel, E., Costantini, P. E., Pellicciari, S., Roncarati, D., Puccio, S., et al. (2017). Comprehensive mapping of the *Helicobacter pylori* NikR regulon provides new insights in bacterial nickel responses. *Sci. Rep.* 7:45458. doi: 10.1038/srep45458
- Vannini, A., Roncarati, D., and Danielli, A. (2016). The cag-pathogenicity island encoded CncR1 sRNA oppositely modulates *Helicobacter pylori* motility and

- adhesion to host cells. *Cell. Mol. Life Sci.* 73, 3151–3168. doi: 10.1007/s00018-016-2151-z
- Vannini, A., Roncarati, D., Spinsanti, M., Scarlato, V., and Danielli, A. (2014). In depth analysis of the *Helicobacter pylori* cag pathogenicity island transcriptional responses. *PLoS One* 9:e98416. doi: 10.1371/journal.pone.0098416
- Waite, D. W., Vanwonterghem, I., Rinke, C., Parks, D. H., Zhang, Y., Takai, K., et al. (2017). Comparative genomic analysis of the class epsilonproteobacteria and proposed reclassification to Epsilonbacteraeota (phyl. nov.). *Front. Microbiol.* 8:682. doi: 10.3389/fmicb.2017.00682
- Wen, Y., Feng, J., and Sachs, G. (2013). *Helicobacter pylori* 5'ureB-sRNA, a cis-encoded antisense small RNA, negatively regulates ureAB expression by transcription termination. *J. Bacteriol.* 195, 444–452. doi: 10.1128/JB.01022-12
- Wen, Y., Feng, J., Scott, D. R., Marcus, E. A., and Sachs, G. (2011). A cis-encoded antisense small RNA regulated by the HP0165-HP0166 two-component system controls expression of ureB in *Helicobacter pylori*. *J. Bacteriol.* 193, 40–51. doi: 10.1128/JB.00800-10
- Xiao, B., Li, W., Guo, G., Li, B., Liu, Z., Jia, K., et al. (2009). Identification of small noncoding RNAs in *Helicobacter pylori* by a bioinformatics-based approach. *Curr. Microbiol.* 58, 258–263. doi: 10.1007/s00284-008-9318-2
- Conflict of Interest:** The authors declare that the research was conducted in the absence of any commercial or financial relationships that could be construed as a potential conflict of interest.

Copyright © 2021 Tejada-Arranz and De Reuse. This is an open-access article distributed under the terms of the Creative Commons Attribution License (CC BY). The use, distribution or reproduction in other forums is permitted, provided the original author(s) and the copyright owner(s) are credited and that the original publication in this journal is cited, in accordance with accepted academic practice. No use, distribution or reproduction is permitted which does not comply with these terms.



Assembling the Current Pieces: The Puzzle of RNA-Mediated Regulation in *Staphylococcus aureus*

Laura Barrientos, Noémie Mercier, David Lalaouna and Isabelle Caldelari*

Université de Strasbourg, CNRS, Architecture et Réactivité de l'ARN, UPR 9002, Strasbourg, France

OPEN ACCESS

Edited by:

Olga Soutourina,
UMR 9198 Institut de Biologie
Intégrative de la Cellule (I2BC), France

Reviewed by:

Shanshan Liu,
The First Affiliated Hospital of Bengbu
Medical College, China
Amy H. Lee,
Simon Fraser University, Canada

*Correspondence:

Isabelle Caldelari
i.caldelari@unistra.fr

Specialty section:

This article was submitted to
Microbial Physiology and Metabolism,
a section of the journal
Frontiers in Microbiology

Received: 07 May 2021

Accepted: 30 June 2021

Published: 21 July 2021

Citation:

Barrientos L, Mercier N,
Lalaouna D and Caldelari I (2021)
Assembling the Current Pieces:
The Puzzle of RNA-Mediated
Regulation in *Staphylococcus aureus*.
Front. Microbiol. 12:706690.
doi: 10.3389/fmicb.2021.706690

The success of the major opportunistic human *Staphylococcus aureus* relies on the production of numerous virulence factors, which allow rapid colonization and dissemination in any tissues. Indeed, regulation of its virulence is multifactorial, and based on the production of transcriptional factors, two-component systems (TCS) and small regulatory RNAs (sRNAs). Advances in high-throughput sequencing technologies have unveiled the existence of hundreds of potential RNAs with regulatory functions, but only a fraction of which have been validated *in vivo*. These discoveries have modified our thinking and understanding of bacterial physiology and virulence fitness by placing sRNAs, alongside transcriptional regulators, at the center of complex and intertwined regulatory networks that allow *S. aureus* to rapidly adapt to the environmental cues present at infection sites. In this review, we describe the recently acquired knowledge of characterized regulatory RNAs in *S. aureus* that are associated with metal starvation, nutrient availability, stress responses and virulence. These findings highlight the importance of sRNAs for the comprehension of *S. aureus* infection processes while raising questions about the interplay between these key regulators and the pathways they control.

Keywords: regulatory RNA, interconnected network, *Staphylococcus aureus*, virulence, metabolism

INTRODUCTION

Staphylococcus aureus is a major opportunistic human pathogen capable of causing an extensive array of human infections, ranging from easy-treatable sinusitis to life-threatening endocarditis or septicemia. Its versatility in colonizing diverse human organs relies on the temporally coordinated expression of numerous virulence factors allowing the bacterium to adhere, invade and disseminate into host tissues. Regulation of virulence factors expression is conducted by two-component systems (TCS), transcriptional regulators and in particular small regulatory RNAs (sRNAs). These include *cis*-acting RNAs such as antisense RNAs or riboswitches, and *trans*-acting RNAs (Carrier et al., 2018; Jørgensen et al., 2020).

The latter generally control multiple messenger RNAs, especially by targeting their Shine-Dalgarno (SD) sequence, which results in translational repression and/or stability modulation. Indeed, many staphylococcal sRNAs contain a characteristic C-rich sequence complementary to the SD sequence of targeted mRNAs (Geissmann et al., 2009). In many bacteria, sRNA:mRNA interactions are mediated by the chaperones Hfq or ProQ. However, the role of Hfq in *S. aureus*

is still controversial and ProQ is not present (Christopoulou and Granneman, 2021). Even though staphylococcal Hfq is able to bind some sRNAs *in vivo* and *in vitro*, it does not facilitate sRNA-mRNA interactions (Bohn et al., 2007). In addition, its deletion has no effect on sRNA-mediated regulation and did not present any specific phenotype. The dispensability of Hfq may result from longer and, consequently more stable, sRNA-mRNA duplexes than the ones requiring Hfq in *Escherichia coli* (Jousselin et al., 2009).

The functions of sRNAs in gene regulation and physiological responses in bacteria are now well established. Their ability to regulate specific metabolic pathways and stress responses makes them ideal candidates to regulate virulence in pathogenic bacteria. Indeed, in *S. aureus* the bi-functional sRNA RNAIII is the main intracellular effector of the quorum sensing system and controls temporal expression of virulence genes, in addition to containing the open reading frame (ORF) for the phenol soluble modulins (PSM) hemolysin delta (Bronesky et al., 2016). Besides, RNAIII, RsaA, SprC, SprD; Teg49 and SSR42 contribute to different facets of virulence regulation in animal models of infection (Desgranges et al., 2019).

DISCOVERY OF sRNA IN *Staphylococcus aureus*

The use of predictive bioinformatic searches, microarrays and expression studies led to the discovery of the first sRNAs in *S. aureus* (Pichon and Felden, 2005; Geissmann et al., 2009; Nielsen et al., 2011). Then, the advances in high-throughput sequencing technologies opened the door to a whole new era in the small RNA field (Desgranges et al., 2020). It not only helped and accelerated the discovery of further RNAs with regulatory functions in *S. aureus* (Abu-Qatouseh et al., 2010; Beaume et al., 2010; Bohn et al., 2010; Howden et al., 2013; Carroll et al., 2016; Mäder et al., 2016), but also facilitated their characterization by promoting global analyses of transcriptional changes they induce. sRNAs are commonly encoded in intergenic regions or are originated from 3' or 5'-UTR of mRNAs and are associated to the regulation of numerous metabolic pathways and virulence. Accessibility of these sequencing techniques accumulated huge transcriptomic data. However, the lack of a consensual and fully annotated *S. aureus* genome added to a missing unified sRNA nomenclature led to numerous redundancies and misannotated sRNAs. To overcome this matter, Sassi et al. (2015) designed the *Staphylococcus* Regulatory RNA Database (SRD) which provides a simple and non-redundant list of sRNAs identified in *S. aureus*. Sequences of transcribed sRNAs were compiled from various RNAseq analyses to yield a non-redundant catalog of ca. 500 sRNAs assigned with a single identifier. This list is drastically reduced to 50 when only *trans*-acting sRNAs are considered (Liu et al., 2018). Unfortunately, most putative 5'/3'-UTR-derived sRNAs are discarded here. Very recently, Carroll's team re-analyzed published RNAseq and ribosome profiling data scrutinizing the expression and stability or capacities to encode peptides of 303 sRNAs in different conditions, showing their diversity in behavior and functions (Sorensen et al., 2020).

Altogether, these studies raise issues about the poor annotation of staphylococcal genome concerning sRNAs. Furthermore, the effort of the scientific community in sequencing genomes of many staphylococcal isolates will considerably improve it.

DIVING INTO sRNA NETWORKS

To unravel the functions of a newly identified sRNA, it is necessary to define its partners. The identification of RNA candidates as direct targets of sRNAs would provide hints of their roles and pathways, in which a specific sRNA might be involved. Several experimental techniques have been recently developed to characterize sRNA targetomes in bacteria, mostly based on the pull-down of chaperone proteins such as Hfq followed by sequencing of associated RNAs (Desgranges et al., 2020). In *S. aureus*, preference was given to a distinct approach, which relies on the co-purification of binding partners with a biotinylated/tagged sRNA. These methods called MAPS (Lalaouna et al., 2015; Mercier et al., 2021) and Hybrid-trap-seq (Rochat et al., 2018) have been used to determine the interactome of various sRNAs in *S. aureus*, generating ever more complex regulatory networks picturing many events: one sRNA involved in different pathways, several sRNA involved in the same pathway or sRNAs associated with one another (Figure 1). This has highlighted the complexity and intertwined nature of sRNA networks in *S. aureus*, which most certainly accounts for the versatility of this pathogen.

Overall, of the numerous sequences for potential sRNAs, only a small fraction has been experimentally confirmed and many more remain to be characterized. In this work we will review the current state of the art of the sRNA world from *S. aureus*, featuring those involved in virulence, nutrient availability, metal starvation and stress responses. We will focus predominantly on recent results deciphering functions of staphylococcal sRNAs, while others were extensively reviewed in Guillet et al. (2013), Tomasini et al. (2013), and Desgranges et al. (2019).

THE QUEST OF POWER: A LARGER ARSENAL OF sRNAs REGULATING VIRULENCE: Teg41 AND SSR42

Besides the well described RNAIII, RsaA, Teg49 and SprC/D (Desgranges et al., 2019), two sRNAs, Teg41 and SSR42, appeared recently to regulate virulence in *S. aureus*. Teg41 is a 205 nt-long sRNA that is divergently transcribed from the locus encoding alpha phenol soluble modulins (α PSM), highly potent pore-forming toxins exhibiting cytolytic activity (Zapf et al., 2019). The deletion of 24 nts in its 3' end is sufficient to lower α PSM production at the protein level, reduce hemolytic activity and attenuate virulence in a murine abscess model. Conversely, Teg41 overexpression enhances hemolytic activity by increasing α PSM protein levels. *In silico* predictions suggest the binding of Teg41 after the start codon of α PSM4, the 4th gene of the operon and most abundant α PSM. However, this interaction remains to be confirmed as well as the activation mechanism of *psma4*. Several

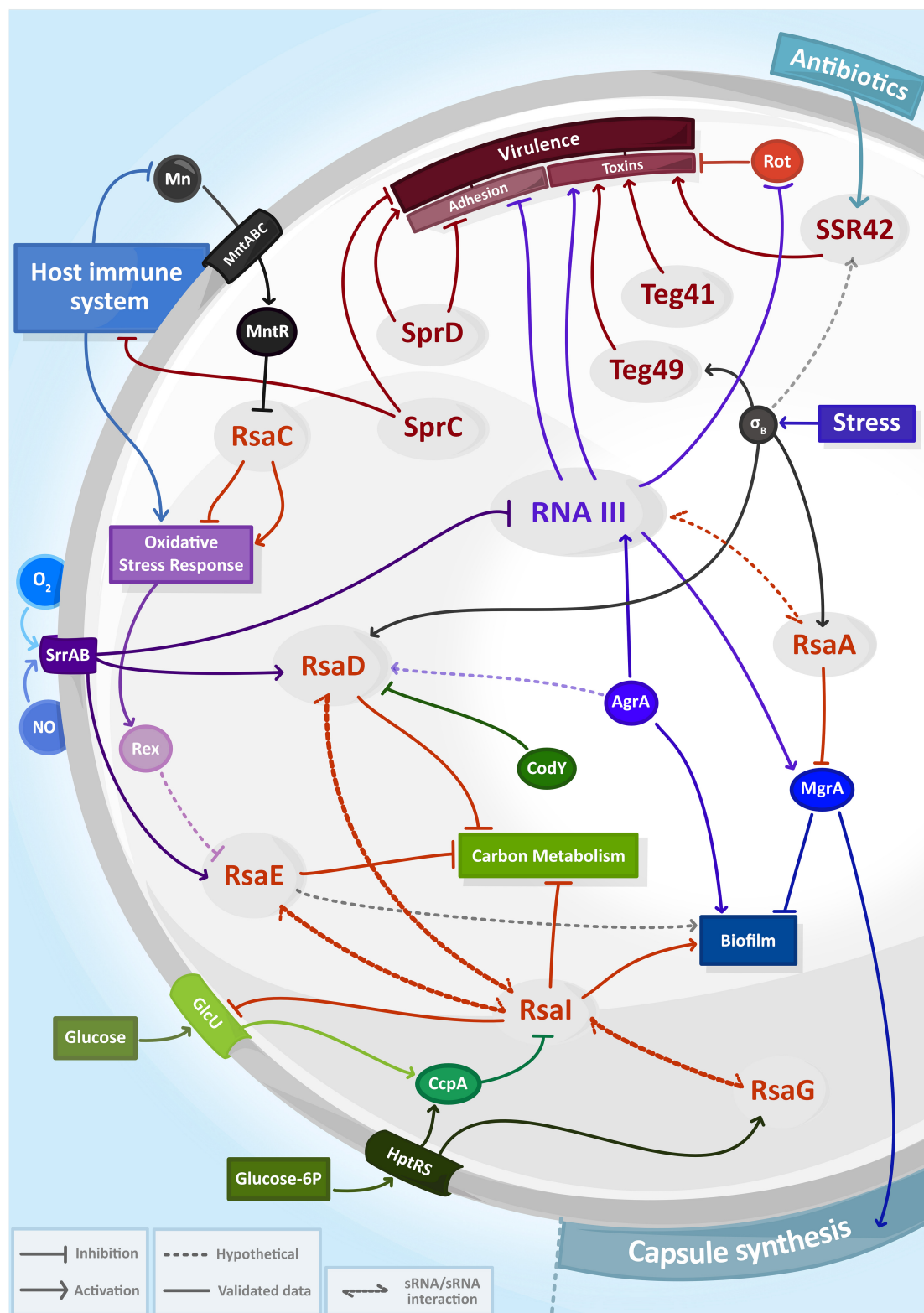


FIGURE 1 | The complexity and entanglement of regulatory RNA (sRNA) networks in *Staphylococcus aureus*. Expression of sRNAs (in gray circles) are induced by environmental signals including antibiotics, host immune system responses, exposure to reactive species (NO, O₂⁻) and nutrient availability. Together with transcriptional factors (solid circle) or two-component systems, sRNAs control capsule synthesis, biofilm production, carbon metabolism, oxidative stress response or virulence and then form intricate regulatory networks.

hypotheses are raised, such as a positive regulation where Teg41 would stabilize the PSM transcript to facilitate its translation or induce conformational changes to free the ribosome binding site (RBS) together with an unknown partner. This would be the first time that an sRNA has been directly linked to the regulation of α PSM, since only protein regulators such as MgrA or AgrA are known to regulate the transcription of mRNA encoding these toxins (Jiang et al., 2018). Interestingly, the *teg41* gene is restricted to *S. aureus* and the very closely related *Staphylococcus argenteus*, and this conservation seems to correlate with the presence of the α PSM locus. This suggests that both might be genetically linked (Zapf et al., 2019).

The 1,232 nt-long SSR42 belongs to the family of small stable RNAs (SSR), a group of regulatory RNAs induced and/or stabilized during stress-related conditions such as log-phase growth, heat/cold shock or stringent response (Anderson et al., 2006; Morrison et al., 2012). SSR42 is stabilized during stationary phase where it mostly represses expression of several virulence genes through an indirect yet undescribed mechanism, probably by regulating transcriptional regulators of these virulence factors (Morrison et al., 2012). This sRNA is also required for hemolysis and for virulence in a murine model of skin infection. SSR42 is located directly upstream and in an antiparallel orientation from the gene encoding Rsp, the repressor of surface proteins, a regulator of hemolysis that positively controls the production of *hla* via the *agr* system (Li et al., 2015). Rsp activates the expression of SSR42 in presence of antibiotics as oxacillin. Consecutively, SSR42 enhances hemolysis by acting indirectly on the *hla* promoter during stationary phase (Horn et al., 2018). SSR42 therefore places itself in line with regulators such as SaeR and SarA for transcriptional activation of *hla* and RNAIII for its translation. Besides, SSR42 stabilizes the *sae* transcript encoding the major transcriptional regulator of *hla* through a yet unknown mechanism (Horn et al., 2018). This suggests that modulation of *sae* transcript impacts Hla production. SSR42 therefore participates in the complex regulation of *hla* transcription in response to antibiotics even though the molecular mechanisms remain elusive.

RsaC, THE MISSING LINK BETWEEN MANGANESE HOMEOSTASIS AND OXIDATIVE STRESS

RsaC length is highly variable across *S. aureus* isolates due to the presence of repeated sequences at its 5' end and, consequently, ranges from 584 to 1,116 nts (Lalaouna et al., 2019). Remarkably, the characterization of RsaC provided the missing link between manganese homeostasis and oxidative stress response. The mutation of *mntABC*, coding for the major manganese ABC transporter, was previously reported as detrimental for Mn acquisition, but also for oxidative stress resistance (Handke et al., 2018). Lalaouna et al. (2019) demonstrated that RsaC derives from the 3' untranslated region of *mntABC* after cleavage by the double-stranded ribonuclease RNase III. In manganese-limiting conditions, RsaC negatively regulates the non-essential Mn-containing superoxide dismutase A (SodA), which is involved

in reactive oxygen species detoxification (O_2^- to H_2O_2). Concurrently, RsaC favors the SodM-dependent oxidative stress response, an alternative SOD enzyme using either Fe or Mn as cofactor. Besides helping maintain the appropriate cellular Mn^{2+} concentration, it restores the ROS detoxification pathway and counteracts Mn sequestration by host immune cells.

Noteworthy, RsaC could also interconnect and balance various metallostasis systems (Fe and Zn) (Lalaouna et al., 2019), but is apparently not involved in the MntABC-mediated increased resistance to copper (Al-Tameemi et al., 2021).

THE BLURRED LINE BETWEEN METABOLISM AND VIRULENCE: RsaD, RsaE, RsaI, AND RsaG

RsaD, a 176 nt-long sRNA, is conserved in multiple staphylococcal species (Geissmann et al., 2009). It accumulates in the late exponential phase of growth and is highly expressed in strains with an active σ_B factor, which is responsible of the regulation of genes involved in stress response in *S. aureus*. Nonetheless, the exact mechanism of *rsaD* regulation by this factor remains uncertain. More recently, Augagneur et al. (2020) observed that expression of *rsaD* is repressed by CodY, a global regulator activated by branched amino-acids and GTP and regulating genes involved in primary metabolism and virulence (Brinsmade, 2017). The promoter region of *rsaD* contains a putative CodY binding motif, which was detected in at least 15 staphylococcal species, indicating that the regulation of *rsaD* by CodY is probably conserved (Augagneur et al., 2020). In addition, RsaD is activated during nitric oxide (NO) stress, sensed by the TCS SrrAB (Bronsky et al., 2019) and possibly by the quorum sensing system Agr (Marroquin et al., 2019). Thus, RsaD seems to assimilate multiple signals from the environment. To determine the physiological functions of RsaD, *in silico* analyses using RNA Predator, TargetRNA2 and IntaRNA identified *alsS*, which is positively regulated by CodY and whose product is involved in carbon metabolism, as a possible target. RsaD binds the RBS of *alsSD* mRNA through its C-rich region and inhibits its translation initiation, leading to a decrease in AlsS enzymatic activity (Augagneur et al., 2020). Thus, by repressing RsaD, CodY permits AlsS synthesis. When glucose is in excess, AlsSD (acetolactate synthase/decarboxylase) generates acetoin (a neutral-pH compound) from pyruvate and therefore protects bacteria from death due to acidification of the cytoplasm by increased acetate production. Then, in these conditions, RsaD must be repressed for survival. This work revealed the *trans*-acting regulatory activity of RsaD on at least one mRNA and highlights the balancing role of this sRNA in carbon overflow and its implications in cell survival (Augagneur et al., 2020). All these mechanisms by which RsaD might be regulated, integrate, and respond to different environmental cues remain to be unveiled. Its place in the complex regulatory RNA networks of *S. aureus* awaits to be established.

RsaE is a highly conserved sRNA among the Firmicute phylum. This striking conservation emphasizes the crucial role of RsaE in metabolism adaptation. First discovered in *S. aureus*,

this 93 nt long sRNA is composed of two UCCCC motifs critical for its interaction with the RBS of its mRNA targets (Geissmann et al., 2009; Rochat et al., 2018). Its expression depends on the activation of the TCS SrrAB that responds to low oxygen concentration and NO exposure (Kinkel et al., 2013). A similar activation pattern is described in *B. subtilis* with its homolog RoxS (Durand et al., 2015). In addition, RoxS is repressed by the NAD⁺/NADH sensor Rex whose binding site is conserved, which suggests that Rex could fulfill a similar role in *S. aureus*.

RsaE is involved in the regulation of central metabolic pathways, in particular by negatively regulating numerous enzymes of the TCA cycle and folate metabolism (Geissmann et al., 2009; Bohn et al., 2010; Rochat et al., 2018). Among its targets, RsaE inhibits the translation of *rocF* mRNA, which encodes an arginase responsible of converting arginine into ornithine (Rochat et al., 2018). Furthermore, the absence of RsaE stimulates growth rate in a medium containing exclusively 18 amino acids (all except glutamine and asparagine) as sole carbon sources, positioning RsaE as a major repressor of amino-acid catabolism.

Surprisingly, RsaE is processed in *S. epidermidis* and *B. subtilis* but apparently not in *S. aureus* (Rochat et al., 2018). In *S. epidermidis*, the processed form of RsaE (RsaEp) expands its targetome with the transcripts of the main biofilm repressor IcaR or of the succinyl-CoA synthetase SucCD, an enzyme involved in TCA cycle (Schoenfelder et al., 2019). Interestingly, both mRNAs only interact with RsaEp. In *B. subtilis*, RNase Y is responsible of RoxS cleavage, however, in a *S. aureus* RNase Y mutant strain, the levels of RsaE or its targets are not impacted (Marincola et al., 2012). Still, a processed RsaE could act on yet unknown mRNAs. Altogether, RsaE interferes with the TCA cycle by directly inhibiting related enzymes and by limiting the production of amino-acid alternative substrates. It has been suggested in *S. aureus* and in *B. subtilis* that RsaE balances NAD⁺/NADH ratio when environmental stimuli (such as O₂ concentration or NO exposure) trigger a metabolism slowdown (Durand et al., 2015).

Additionally, RsaE interacts with another sRNA named RsaI involved in sugar metabolism control (Rochat et al., 2018; Bronesky et al., 2019), that could potentially connect the regulation network of both sRNAs. It cannot be excluded that RsaE or RsaI could behave as an sRNA sponge of one another, promoting the decay or sequestration of the other partner. RsaI is a 144 nt long sRNA conserved among the *Staphylococcaceae* family. The expression of RsaI is repressed by the catabolite control protein A (CcpA) in presence of glucose (Bronesky et al., 2019). When glucose has been metabolized, RsaI inhibits the translation of the main glucose uptake protein GlcU and activates enzymes acting in glucose fermentation. On the other hand, RsaI represses FN3K expression, a protein protecting the bacterium from the damages caused by high glucose concentration, positioning RsaI at the core of regulatory pathways of sugar metabolism. Interestingly, RsaI binds the 3'UTR of *icaR* mRNA and thus promotes biofilm formation by a mechanism which is still unsolved (Bronesky et al., 2019). To note, the *icaR* messenger was pulled out with RsaE *in vitro*, and sequencing suggested that it interacts with the 5'UTR of *icaR* such

as in *S. epidermidis* (Rochat et al., 2018). Knowing that RsaE and RsaI form a duplex, further experiments would be necessary to decipher the intricacy of regulatory lines among all these RNAs.

In addition to RsaE, RsaD (see above) and the glucose-6-phosphate induced sRNA RsaG were enriched with RsaI in MAPS, but the relevant significance of these interactions has not been explained yet (Bronesky et al., 2019). Interestingly, it has been suggested that RsaI promotes the expression of NO detoxification or anaerobic metabolism enzymes as an indirect effect of its interaction with RsaE, RsaD and RsaG. Nevertheless, shared signals and targets between these sRNAs imply tight connections and that all these regulatory networks would rationally impact each other at different levels, connecting sugar metabolism and stress responses.

CONCLUSION

In the recent years, several tools were developed to decipher the functions of staphylococcal sRNAs. They revealed that sRNAs sense and reply to different environmental stimuli and that they mostly control mRNA translation to remodel metabolomic pathways to adapt and survive in harsh environments conditions.

The more the identified sRNAs are studied, the clearer it becomes that there is no isolated node in regulatory network or pathway, but a myriad of interconnections that we are only at the beginning to acknowledge. Exciting discoveries await for us in the years to come, as all these interrelationships will be straightened out and a clearer map of sRNA interactions will be drawn.

In the meantime, many questions about the sRNA world in *S. aureus* remain to be addressed. The significance of RNA-binding proteins in all these networks is still very uncertain, besides the established role of RNase III in sRNA maturation and target degradation. However, there could be holes in the puzzle that might be filled in by some of these proteins, which may help explaining unsolved sRNA-dependent mechanisms of action.

The study of the complex regulatory networks of *S. aureus*, in which sRNAs are at the center, is undoubtedly essential for understanding its virulence and adaptation mechanisms and will ultimately guide us in the design of treatments to fight this pathogen.

AUTHOR CONTRIBUTIONS

LB, NM, DL, and IC contributed to the manuscript writing. All authors contributed to the article and approved the submitted version.

FUNDING

This work was supported by the labEx NetRNA ANR-10-labEx-0036 and of the Interdisciplinary Thematic Institute IMCBio, as part of the ITI 2021-2028 program of the University of Strasbourg, CNRS and Inserm, by IdEx Unistra (ANR-10-IDEX-0002), by SFRI-STRAT'US project and EUR

IMCBio (IMCBio ANR-17-EURE-0023) under the framework of the French Investments for the Future Program. LB was supported by the “Fondation pour la Recherche Médicale” (N° ECO202006011534).

REFERENCES

- Abu-Qatouseh, L. F., Chinni, S. V., Seggewiss, J., Proctor, R. A., Brosius, J., Rozhdestvensky, T. S., et al. (2010). Identification of differentially expressed small non-protein-coding RNAs in *Staphylococcus aureus* displaying both the normal and the small-colony variant phenotype. *J. Mol. Med. (Berl)* 88, 565–575. doi: 10.1007/s00109-010-0597-2
- Al-Tameemi, H., Beavers, W. N., Norambuena, J., Skaar, E. P., and Boyd, J. M. (2021). *Staphylococcus aureus* lacking a functional MntABC manganese import system has increased resistance to copper. *Mol. Microbiol.* 115, 554–573. doi: 10.1111/mmi.14623
- Anderson, K. L., Roberts, C., Disz, T., Vonstein, V., Hwang, K., Overbeek, R., et al. (2006). Characterization of the *Staphylococcus aureus* heat shock, cold shock, stringent, and SOS responses and their effects on log-phase mRNA turnover. *J. Bacteriol.* 188, 6739–6756. doi: 10.1128/jb.00609-06
- Augagneur, Y., King, A. N., Germain-Amiot, N., Sassi, M., Fitzgerald, J. W., Sahukhal, G. S., et al. (2020). Analysis of the CodY RNome reveals RsaD as a stress-responsive riboregulator of overflow metabolism in *Staphylococcus aureus*. *Mol. Microbiol.* 113, 309–325. doi: 10.1111/mmi.14418
- Beaume, M., Hernandez, D., Farinelli, L., Deluen, C., Linder, P., Gaspin, C., et al. (2010). Cartography of methicillin-resistant *S. aureus* transcripts: detection, orientation and temporal expression during growth phase and stress conditions. *PLoS One* 5:e10725. doi: 10.1371/journal.pone.0010725
- Bohn, C., Rigoulay, C., and Boulou, P. (2007). No detectable effect of RNA-binding protein Hfq absence in *Staphylococcus aureus*. *BMC Microbiol.* 7:10. doi: 10.1186/1471-2180-7-10
- Bohn, C., Rigoulay, C., Chabelskaya, S., Sharma, C. M., Marchais, A., Skorski, P., et al. (2010). Experimental discovery of small RNAs in *Staphylococcus aureus* reveals a riboregulator of central metabolism. *Nucleic Acids Res.* 38, 6620–6636. doi: 10.1093/nar/gkq462
- Brinsmade, S. R. (2017). CodY, a master integrator of metabolism and virulence in Gram-positive bacteria. *Curr. Genet.* 63, 417–425. doi: 10.1007/s00294-016-0656-5
- Bronesky, D., Desgranges, E., Corvaglia, A., Francois, P., Caballero, C. J., Prado, L., et al. (2019). A multifaceted small RNA modulates gene expression upon glucose limitation in *Staphylococcus aureus*. *EMBO J.* 38:e99363.
- Bronesky, D., Wu, Z., Marzi, S., Walter, P., Geissmann, T., Moreau, K., et al. (2016). *Staphylococcus aureus* RNAIII and its regulon link quorum sensing, stress responses, metabolic adaptation, and regulation of virulence gene expression. *Annu. Rev. Microbiol.* 70, 299–316. doi: 10.1146/annurev-micro-102215-095708
- Carrier, M. C., Lalaouna, D., and Masse, E. (2018). Broadening the definition of bacterial small RNAs: characteristics and mechanisms of action. *Annu. Rev. Microbiol.* 72, 141–161. doi: 10.1146/annurev-micro-090817-062607
- Carroll, R. K., Weiss, A., Broach, W. H., Wiemels, R. E., Mogen, A. B., Rice, K. C., et al. (2016). Genome-wide annotation, identification, and global transcriptomic analysis of regulatory or small RNA gene expression in *Staphylococcus aureus*. *MBio* 7, e1990–e1915.
- Christopoulou, N., and Granneman, S. (2021). The role of RNA-binding proteins in mediating adaptive responses in Gram-positive bacteria. *Febs J. [Online ahead of print]* doi: 10.1111/febs.15810
- Desgranges, E., Caldelari, I., Marzi, S., and Lalaouna, D. (2020). Navigation through the twists and turns of RNA sequencing technologies: application to bacterial regulatory RNAs. *Biochim. Biophys. Acta - Gene Regulatory Mechan.* 1863:194506. doi: 10.1016/j.bbagr.2020.194506
- Desgranges, E., Marzi, S., Moreau, K., Romby, P., and Caldelari, I. (2019). Noncoding RNA. *Microbiol. Spectr.* 7.
- Durand, S., Tomasini, A., Braun, F., Condon, C., and Romby, P. (2015). sRNA and mRNA turnover in Gram-positive bacteria. *FEMS Microbiol. Rev.* 39, 316–330. doi: 10.1093/femsre/fuv007
- Geissmann, T., Chevalier, C., Cros, M. J., Boisset, S., Fechter, P., Noirot, C., et al. (2009). A search for small noncoding RNAs in *Staphylococcus aureus* reveals a conserved sequence motif for regulation. *Nucleic Acids Res.* 37, 7239–7257. doi: 10.1093/nar/gkp668
- Guillet, J., Hallier, M., and Felden, B. (2013). Emerging functions for the *Staphylococcus aureus* RNome. *PLoS Pathog* 9:e1003767. doi: 10.1371/journal.ppat.1003767
- Handke, L. D., Gribenko, A. V., Timofeyeva, Y., Scully, I. L., and Anderson, A. S. (2018). MntC-dependent manganese transport is essential for *Staphylococcus aureus* oxidative stress resistance and virulence. *mSphere* 3, e336–e318.
- Horn, J., Klepsch, M., Manger, M., Wolz, C., Rudel, T., and Fraunholz, M. (2018). Long noncoding RNA SSR42 controls *Staphylococcus aureus* alpha-toxin transcription in response to environmental stimuli. *J. Bacteriol.* 200, e252–e218.
- Howden, B. P., Beaume, M., Harrison, P. F., Hernandez, D., Schrenzel, J., Seemann, T., et al. (2013). Analysis of the small RNA transcriptional response in multidrug-resistant *Staphylococcus aureus* after antimicrobial exposure. *Antimicrob. Agents Chemother.* 57, 3864–3874. doi: 10.1128/aac.00263-13
- Jiang, Q., Jin, Z., and Sun, B. (2018). MgrA negatively regulates biofilm formation and detachment by repressing the expression of psm operons in *Staphylococcus aureus*. *Appl. Environ. Microbiol.* 84, e1008–e1018.
- Jørgensen, M. G., Pettersen, J. S., and Kallipolitis, B. H. (2020). sRNA-mediated control in bacteria: an increasing diversity of regulatory mechanisms. *Biochim. Biophys. Acta Gene Regul. Mech.* 1863:194504. doi: 10.1016/j.bbagr.2020.194504
- Jousselin, A., Metzinger, L., and Felden, B. (2009). On the facultative requirement of the bacterial RNA chaperone, Hfq. *Trends Microbiol.* 17, 399–405. doi: 10.1016/j.tim.2009.06.003
- Kinkel, T. L., Roux, C. M., Dunman, P. M., and Fang, F. C. (2013). The *Staphylococcus aureus* SrrAB two-component system promotes resistance to nitrosative stress and hypoxia. *mBio* 4, e696–e613.
- Lalaouna, D., Baude, J., Wu, Z., Tomasini, A., Chicher, J., Marzi, S., et al. (2019). RsaC sRNA modulates the oxidative stress response of *Staphylococcus aureus* during manganese starvation. *Nucleic Acids Res.* 47, 9871–9887. doi: 10.1093/nar/gkz728
- Lalaouna, D., Carrier, M. C., Semsey, S., Brouard, J. S., Wang, J., Wade, J. T., et al. (2015). A 3' external transcribed spacer in a tRNA transcript acts as a sponge for small RNAs to prevent transcriptional noise. *Mol. Cell* 58, 393–405. doi: 10.1016/j.molcel.2015.03.013
- Li, T., He, L., Song, Y., Villaruz, A. E., Joo, H. S., Liu, Q., et al. (2015). AraC-Type regulator Rsp adapts *Staphylococcus aureus* gene expression to acute infection. *Infect. Immun.* 84, 723–734. doi: 10.1128/iai.01088-15
- Liu, W., Rochat, T., Toffano-Nioche, C., Le Lam, T. N., Boulou, P., and Morvan, C. (2018). Assessment of bona fide sRNAs in *Staphylococcus aureus*. *Front. Microbiol.* 9:228. doi: 10.3389/fmicb.2018.00228
- Mäder, U., Nicolas, P., Depke, M., Pané-Farré, J., Debarbouille, M., Van Der Kooy, Pol, M. M., et al. (2016). *Staphylococcus aureus* transcriptome architecture: from laboratory to infection-mimicking conditions. *PLoS Genet.* 12:e1005962. doi: 10.1371/journal.pgen.1005962
- Marincola, G., Schäfer, T., Behler, J., Bernhardt, J., Ohlsen, K., Goerke, C., et al. (2012). RNase Y of *Staphylococcus aureus* and its role in the activation of virulence genes. *Mol. Microbiol.* 85, 817–832. doi: 10.1111/j.1365-2958.2012.08144.x
- Marroquin, S., Gimza, B., Tomlinson, B., Stein, M., Frey, A., Keogh, R. A., et al. (2019). MroQ is a novel abi-domain protein that influences virulence gene expression in *Staphylococcus aureus* via modulation of agr activity. *Infect. Immun.* 87, e00002–e00019.
- Mercier, N., Prévost, K., Massé, E., Romby, P., Caldelari, I., and Lalaouna, D. (2021). MS2-Affinity purification coupled with RNA sequencing in gram-positive bacteria. *J. Vis. Exp.* 23.

ACKNOWLEDGMENTS

We would like to thank Pascale Romby for helpful advice and discussions.

- Morrison, J. M., Miller, E. W., Benson, M. A., Alonzo, F. 3rd, Yoong, P., Torres, V. J., et al. (2012). Characterization of SSR42, a novel virulence factor regulatory RNA that contributes to the pathogenesis of a *Staphylococcus aureus* USA300 representative. *J. Bacteriol.* 194, 2924–2938. doi: 10.1128/jb.06708-11
- Nielsen, J. S., Christiansen, M. H., Bonde, M., Gottschalk, S., Frees, D., Thomsen, L. E., et al. (2011). Searching for small σ B-regulated genes in *Staphylococcus aureus*. *Arch. Microbiol.* 193, 23–34. doi: 10.1007/s00203-010-0641-1
- Pichon, C., and Felden, B. (2005). Small RNA genes expressed from *Staphylococcus aureus* genomic and pathogenicity islands with specific expression among pathogenic strains. *Proc. Natl. Acad. Sci. U.S.A.* 102, 14249–14254. doi: 10.1073/pnas.0503838102
- Rochat, T., Bohn, C., Morvan, C., Le Lam, T. N., Razvi, F., Pain, A., et al. (2018). The conserved regulatory RNA RsaE down-regulates the arginine degradation pathway in *Staphylococcus aureus*. *Nucleic Acids Res.* 46, 8803–8816. doi: 10.1093/nar/gky584
- Sassi, M., Augagneur, Y., Mauro, T., Ivain, L., Chabelskaya, S., Hallier, M., et al. (2015). SRD: a *Staphylococcus* regulatory RNA database. *RNA* 21, 1005–1017. doi: 10.1261/rna.049346.114
- Schoenfelder, S. M. K., Lange, C., Prakash, S. A., Marincola, G., Lerch, M. F., Wencker, F. D. R., et al. (2019). The small non-coding RNA RsaE influences extracellular matrix composition in *Staphylococcus epidermidis* biofilm communities. *PLoS Pathog.* 15:e1007618. doi: 10.1371/journal.ppat.1007618
- Sorensen, H. M., Keogh, R. A., Wittekind, M. A., Caillet, A. R., Wiemels, R. E., Laner, E. A., et al. (2020). Reading between the lines: utilizing RNA-Seq data for global analysis of sRNAs in *Staphylococcus aureus*. *mSphere* 5, e439–e420.
- Tomasini, A., François, P., Howden, B. P., Fechter, P., Romby, P., and Caldelari, I. (2013). The importance of regulatory RNAs in *Staphylococcus aureus*. *Infect. Genet. Evol.* 21, 616–626. doi: 10.1016/j.meegid.2013.11.016
- Zapf, R. L., Wiemels, R. E., Keogh, R. A., Holzschu, D. L., Howell, K. M., Trzeciak, E., et al. (2019). The small RNA Teg41 regulates expression of the alpha phenol-soluble modulins and is required for virulence in *staphylococcus aureus*. *mBio* 10, e2484–e2418.

Conflict of Interest: The authors declare that the research was conducted in the absence of any commercial or financial relationships that could be construed as a potential conflict of interest.

Copyright © 2021 Barrientos, Mercier, Lalaouna and Caldelari. This is an open-access article distributed under the terms of the Creative Commons Attribution License (CC BY). The use, distribution or reproduction in other forums is permitted, provided the original author(s) and the copyright owner(s) are credited and that the original publication in this journal is cited, in accordance with accepted academic practice. No use, distribution or reproduction is permitted which does not comply with these terms.



The Small Protein YmoA Controls the Csr System and Adjusts Expression of Virulence-Relevant Traits of *Yersinia pseudotuberculosis*

Katja Böhme^{1†}, Ann Kathrin Heroven^{1†}, Stephanie Lobedann¹, Yuzhu Guo², Anne-Sophie Stolle² and Petra Dersch^{1,2*}

¹ Department of Molecular Infection Biology, Helmholtz Centre for Infection Research, Braunschweig, Germany, ² Institute of Infectiology, Center for Molecular Biology of Inflammation (ZMBE), Medical Faculty Münster, University of Münster, Münster, Germany

OPEN ACCESS

Edited by:

Olga Soutourina,
UMR 9198 Institut de Biologie
Intégrative de la Cellule (I2BC), France

Reviewed by:

Kai Papenfort,
Friedrich Schiller University Jena,
Germany
Eun-Jin Lee,
Korea University, South Korea

*Correspondence:

Petra Dersch
petra.dersch@uni-muenster.de

[†] These authors have contributed
equally to this work

Specialty section:

This article was submitted to
Microbial Physiology and Metabolism,
a section of the journal
Frontiers in Microbiology

Received: 08 May 2021

Accepted: 12 July 2021

Published: 03 August 2021

Citation:

Böhme K, Heroven AK,
Lobedann S, Guo Y, Stolle AS and
Dersch P (2021) The Small Protein
YmoA Controls the Csr System
and Adjusts Expression
of Virulence-Relevant Traits of *Yersinia*
pseudotuberculosis.
Front. Microbiol. 12:706934.
doi: 10.3389/fmicb.2021.706934

Virulence gene expression of *Yersinia pseudotuberculosis* changes during the different stages of infection and this is tightly controlled by environmental cues. In this study, we show that the small protein YmoA, a member of the Hha family, is part of this process. It controls temperature- and nutrient-dependent early and later stage virulence genes in an opposing manner and co-regulates bacterial stress responses and metabolic functions. Our analysis further revealed that YmoA exerts this function by modulating the global post-transcriptional regulatory Csr system. YmoA pre-dominantly enhances the stability of the regulatory RNA CsrC. This involves a stabilizing stem-loop structure within the 5'-region of CsrC. YmoA-mediated CsrC stabilization depends on H-NS, but not on the RNA chaperone Hfq. YmoA-promoted reprogramming of the Csr system has severe consequences for the cell: we found that a mutant deficient of *ymoA* is strongly reduced in its ability to enter host cells and to disseminate to the Peyer's patches, mesenteric lymph nodes, liver and spleen in mice. We propose a model in which YmoA controls transition from the initial colonization phase in the intestine toward the host defense phase important for the long-term establishment of the infection in underlying tissues.

Keywords: *Yersinia*, regulatory RNA, gene regulation, virulence, CsrA, YmoA, Hha

INTRODUCTION

Enteropathogenic yersiniae, *Yersinia enterocolitica* and *Yersinia pseudotuberculosis* are fecal-oral pathogens that can cause food-borne infections in animals and humans with symptoms ranging from self-limiting enteritis, mesenteric lymphadenitis to autoimmune responses (Bottone, 1997; Koornhof et al., 1999; Galindo et al., 2011). Both *Yersinia* species initiate infection after oral uptake in the gastrointestinal tract by tight adhesion to the mucosal surface of the intestine, which is followed by rapid internalization and translocation through M-cells of the intestinal epithelium (Pepe and Miller, 1993; Marra and Isberg, 1997; Koornhof et al., 1999). Migration through M-cells leads to the accumulation of the bacteria in underlying lymphatic tissues (Peyer's patches) and their dissemination to mesenteric lymph nodes, liver and spleen (Barnes et al., 2006; Trülsch et al., 2007).

Upon ingestion, *Yersinia* encounters changing growth conditions including elevated temperature as well as variations of nutrients and ions within the intestinal tract. *Yersinia* senses changes of environmental parameters to determine its localization and adapt expression of pathogenicity factors and survival strategies accordingly (Marceau, 2005; Heroven and Dersch, 2014; Chen et al., 2016). Some of the most important virulence properties are encoded on the virulence plasmid pYV (pIB1). They are predominantly expressed at 37°C upon contact with host immune cells after the bacteria entered the gut-associated lymphatic tissues (Straley and Perry, 1995; Kusmirek et al., 2019; Volk et al., 2019; Schneiders et al., 2021). Among them are the adhesion factor YadA, the structural components of a functional type three secretion system (T3SS) and the antiphagocytic *Yersinia* outer proteins (Yops) - the effectors which are secreted and translocated by the T3S machinery (Cornelis, 2006; Bliska et al., 2013). Expression of these virulence genes is activated by the AraC-type transcriptional regulator LcrF (VirF) (Lambert de Rouvroit et al., 1992; Hoe and Goguen, 1993; Böhme et al., 2012; Schwiesow et al., 2015) (**Figure 1**).

Other virulence factors, including smooth lipopolysaccharides, flagellar motility, iron uptake and storage, enterotoxin (Yst) and the cell internalization factor invasin are predominantly expressed at moderate temperatures during stationary phase, conditions, which are more typical for the environmental life-style of the bacteria (Straley and Perry, 1995; Marceau, 2005; Heroven and Dersch, 2014; Chen et al., 2016). This class of virulence factors appears to be required for the initial stages of infection and seems to assure rapid and efficient colonization and penetration of the intestinal epithelial layer shortly after infection. The molecular mechanisms, regulating the expression of the virulence genes during the different stages of the infection are still far from being understood. However, over the last years it became evident that a complex regulatory network including the carbon storage regulator (Csr) system plays a crucial role in the control of virulence-associated traits initiating intestinal colonization and dissemination into deeper tissues (Heroven et al., 2008, 2012a; Nuss et al., 2014, 2017a,b; Kusmirek and Dersch, 2017; Kusmirek et al., 2019).

The Csr system is a global regulatory system that consists of (i) the dimeric RNA-binding protein CsrA, that binds to and thus regulates translation and stability of target mRNAs, and (ii) the untranslated regulatory Csr-RNAs CsrB and CsrC that antagonize CsrA function (Heroven et al., 2012a; Kusmirek and Dersch, 2017; Romeo and Babitzke, 2018; Pourciau et al., 2020). Both CsrB and CsrC bind multiple CsrA dimers. This sequestration of CsrA reduces the pool of free CsrA which is able to interact with other target mRNAs without changing the overall level of CsrA. The Csr system was first identified to control the expression of the virulence regulator RovA of *Y. pseudotuberculosis* (Heroven et al., 2008). RovA, a member of the SlyA/Hor family of DNA-binding proteins, acts as an activator of the primary cell internalization factor invasin, the PsaA adhesin (pH6 antigen) and many other factors contributing to *Yersinia* virulence in the early stages of the infection (Nagel et al., 2001; Cathelyn et al., 2006, 2007; Yang et al., 2010). CsrA-mediated influence on *rovA* expression occurs through indirect

control of the LysR-type regulator RovM (Heroven and Dersch, 2006; Heroven et al., 2008). Further analysis revealed a complex control system in which the regulatory RNAs CsrC and CsrB are regulated by the global cAMP-binding repressor protein (Crp) and the two-component system BarA/UvrY or PhoQ/PhoP in response to nutrients/metabolites and ions (Heroven et al., 2008, 2012b; Bücker et al., 2014; Nuss et al., 2014).

Virulence-promoting processes are activated by the CsrABC-RovM-RovA cascade in the very early colonization stages of the infection. Once bacteria have reached the lymphatic tissues these virulence traits are no longer needed and hence are downregulated during ongoing infection stages. In this phase, virulence plasmid-encoded LcrF-induced defensive pathogenicity factors are upregulated to protect the pathogen against the attack of the host immune system. How reprogramming of virulence gene expression is controlled in the course of the infection is still unknown, however, it is emerging that the small protein YmoA (*Yersinia* modulator A; 9 kDa, 67 aa) participates in this process. YmoA shares extensive homology with the *Escherichia coli* Hha protein, and belongs to a group of low-molecular-weight proteins involved in the regulation of bacterial pathogenicity and virulence-associated physiological traits (Cornelis et al., 1991; de la Cruz et al., 1992; Mikulskis and Cornelis, 1994; Madrid et al., 2002, 2007; Lawal et al., 2013). YmoA was first identified as a thermosensitive repressor of *lcrF*, encoding the main transcriptional activator of the pYV-encoded later-stage virulence genes, and the *Y. enterocolitica* enterotoxin gene *yst* (Cornelis et al., 1991; de la Cruz et al., 1992; Cornelis, 1993; Mikulskis et al., 1994; Jackson et al., 2004; Böhme et al., 2012). Thermal control is mediated by rapid degradation of YmoA by Lon and Clp proteases at a host temperature of 37°C (Jackson et al., 2004; Böhme et al., 2012). Later on, several studies demonstrated that YmoA interacts with a small portion of the nucleoid-structuring and global regulatory protein H-NS, and this generates YmoA/H-NS heteromeric complexes with somewhat different target specificity (Madrid et al., 2002; Nieto et al., 2002; Ellison and Miller, 2006). This suggests that YmoA has a more global role and evolved to fine-tune the activity of H-NS to adapt expression of virulence-associated traits in response to temperature. More recently, it has been reported that YmoA/Hha together with YmoB/TomB(YbaJ) bears the characteristics of a bonafide type II toxin-antitoxin (TA) system, which is involved in biofilm and persister cell formation in *E. coli* and in persistence and programmed cell death in *Salmonella enterica* serovar Typhimurium (García-Contreras et al., 2008; Marimon et al., 2016).

In this study, we demonstrate that YmoA plays a key role in the control *Yersinia* pathogenesis. YmoA is part of a complex regulatory network and controls more than 289 genes, many of them implicated in virulence. In addition to its inhibitory effect on antiphagocytic T3SS-associated virulence factors, YmoA was found to promote the induction of the CsrABC-RovM-RovA regulatory cascade, which is important for the expression of early-stage virulence genes through control of CsrB and CsrC RNA levels. We postulate that YmoA in *Y. pseudotuberculosis* plays a crucial role switching expression from RovA-activated early-stage

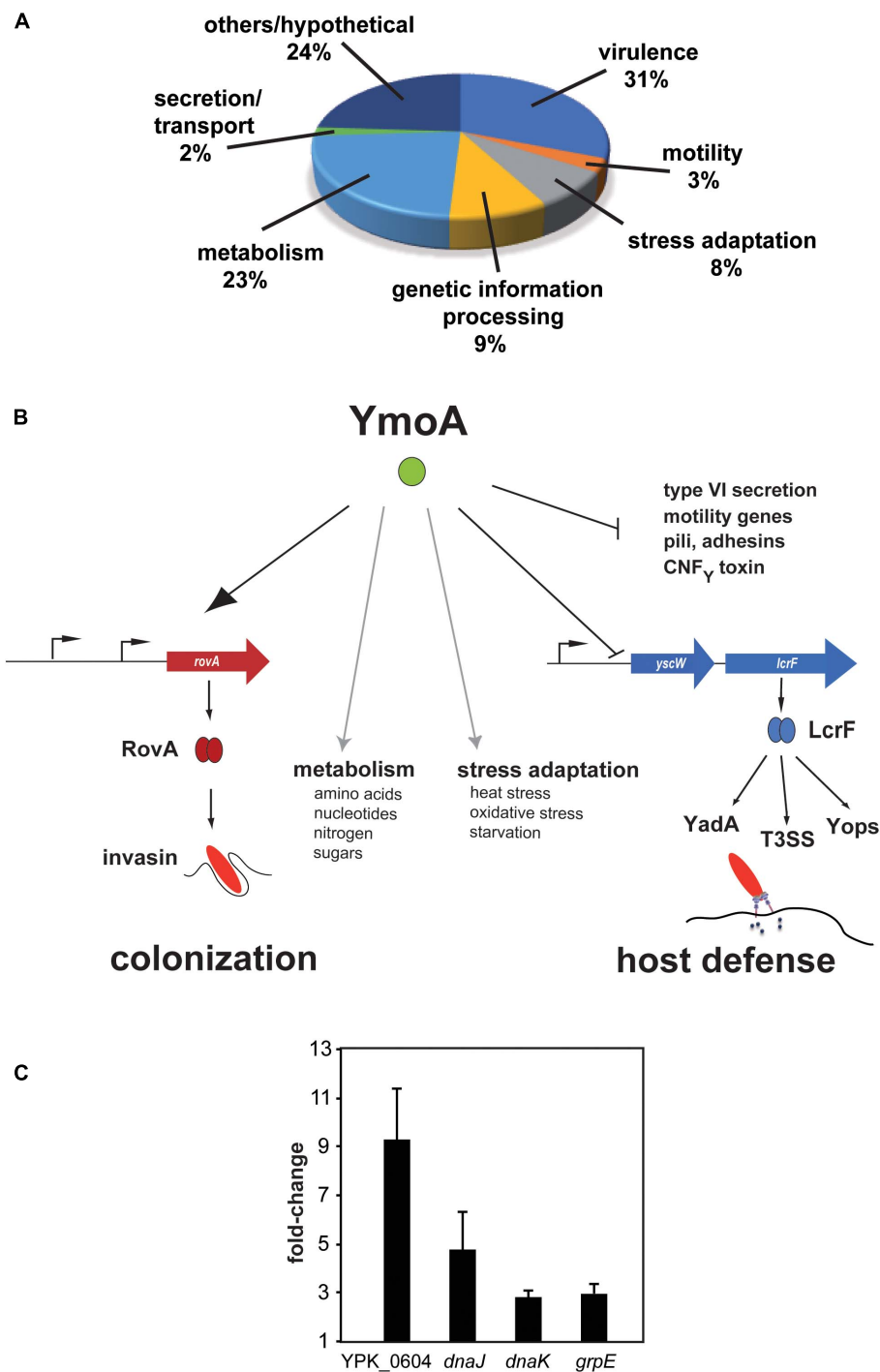


FIGURE 1 | Influence of YmoA on the global gene expression in *Y. pseudotuberculosis*. **(A)** Proportion of gene classes up- or downregulated by YmoA. Genes showing overall fold-changes ≥ 2.0 are included in the displayed diagram of gene classes. **(B)** Schematic scheme of the global influence of YmoA on virulence-relevant genes. YmoA activates the synthesis of the early-phase virulence RovA, leading to expression of colonization factors such as invasins. In contrast, later-stage virulence factors, e.g., YadA, Yops, or T3SS, which are essential to combat triggered immune responses, are silenced by YmoA through repression of the transcriptional activator LcrF. Moreover, YmoA is implicated in many other virulence-relevant metabolic and stress adaptation processes. This control network allows switching of virulence gene expression by variations of YmoA levels. The dark arrow displays activation of the gene expression or protein synthesis; T represents repression or inactivation. Gray arrows indicate control of metabolic and stress adaptation processes by YmoA. **(C)** RNA of early stationary cultures of strains YPIII and YP50 ($\Delta ymoA$) in LB medium at 25°C was prepared and six independent samples were pooled. qRT-PCR was carried out in triplicates. Gene expression levels were normalized to levels of the *sopB* transcript and are given as relative values $\Delta ymoA$ /wild-type. Mean \pm SD of three independent experiments are displayed.

virulence genes toward LcrF-induced virulence genes important for host defense.

MATERIALS AND METHODS

Cell Culture, Media and Growth Conditions

Overnight cultures of *E. coli* were routinely grown at 37°C, *Yersinia* strains were grown at 25°C or 37°C in LB (Luria Bertani) broth if not indicated otherwise. The antibiotics used for bacterial selection were as follows: ampicillin 100 µg ml⁻¹, chloramphenicol 30 µg ml⁻¹, tetracycline 5 µg ml⁻¹, kanamycin 50 µg ml⁻¹, and gentamicin 50 µg ml⁻¹. HEp-2 cells were cultured in RPMI 1640 media (Sigma) supplemented with 5% new-born calf serum (Invitrogen) and 2 mM glutamine at 37°C in the presence of 5% CO₂.

Plasmid Constructions

All DNA manipulations, restriction digestions, ligations and transformations were performed using standard genetic and molecular techniques (Miller, 1992; Sambrook, 2001). Plasmid DNA was purified using a Qiagen kit. Restriction and DNA-modifying enzymes were obtained from Roche, Promega or New England Biolabs. The oligonucleotides used for amplification by PCR, sequencing and primer extension were purchased from Metabion (Martinsried, Germany). PCR reactions were performed routinely in a 100 µl mix for 25 cycles using *Taq* polymerase or Phusion High-Fidelity DNA polymerase (New England Biolabs) according to the manufacturer's instructions. PCR products were purified with the QIAquick PCR purification kit (Qiagen, Germany) before and after digestion of the amplification product. Sequencing reactions were performed by Agowa (Berlin, Germany) or GATC (Konstanz, Germany).

Plasmids used in this study are listed in **Supplementary Table 1** and primers for plasmid generation are listed in **Supplementary Table 2**. Plasmids pAKH106, pAKH107, pKB20, pAKH76 and pAKH104 carry PCR generated fragments harboring *csrC* promoter regions from nucleotide -355 (primer 3) to nucleotide +39 (primer 5), +61 (primer 6), +71 (primer 7), +81 (primer 8) and +254 (primer 9), respectively. The fragments were digested with *EcoRI* and *Sall* and cloned into the corresponding sites of pHT124. The *hfq*⁺ plasmids pAKH115 and pAKH119 were constructed by insertion of a PCR fragment amplified with primer 10 and primer 11 into the vector pACYC184 and pHSG575 digested with *Sall* and *BamHI*.

To generate pKB4, the *ymoA* gene was amplified from chromosomal DNA of YPIII using primer 1 and 2 and inserted into the *Sall/BamHI* sites of pHSG575. To generate pKB17, a *csrC* fragment harboring an internal deletion from nucleotide +24 to +57 was amplified using primers 3 and 12 and cloned into the *EcoRI/Sall* sites of pHT124. To express the *csrC* gene under the control of the *tet* promoter, *csrC* was amplified with primers 13 (including the *tet* promoter sequence) and 14. The resulting fragment was cloned into the *Sall/BamHI* sites of vector pHSG575, generating pKB47. The *csrC* gene, including the 5'-regulatory region, was amplified

with primers 15 and 16 and inserted into the *BamHI/Sall* site of pHSG576, resulting in pKB59. Subsequently, the region from position +24 to +57 within the *csrC* gene was deleted by three-step-PCR. First, the upstream region was amplified by primers 15 and 17 (encoding the deleted region), and the downstream region was amplified with primer 18 (encoding the deleted region) and primer 16. Next, up- and downstream fragments were mixed with primers 15 and 16 to generate the *csrC* deletion fragment, which was inserted into the *Sall/BamHI* sites resulting in pKB49. The *P_{tet}:lacZ* containing vector pTT1 was constructed by the insertion of a DNA fragment amplified with primers 23 and 24 into the *PstI/EcoRV* sites of pTS03. The sequence and the correct orientation of all cloned fragments were proven by DNA sequencing.

Construction of the *Y. pseudotuberculosis* Deletion Mutants

The *Y. pseudotuberculosis* mutant strains were constructed with the RED recombinase system as described previously (Datsenko and Wanner, 2000; Derbise et al., 2003) and are all derived from wild-type strain YPIII. First, a kanamycin cassette was amplified by PCR with primers homologous to the resistance gene encoded on pKD4 followed by homologous sequences of adjacent regions of the target gene (for primer see **Supplementary Table 3**). The PCR fragment was transformed into *Y. pseudotuberculosis* YPIII pKD46. Chromosomal integration of the fragment was selected by plating on LB supplemented with kanamycin. Subsequently, mutant derivatives were cured of the temperature-sensitive plasmid pKD46 by cultivation at 37°C. To remove the resistance gene at its FLP recognition sites the mutants were transformed with the helper plasmid pCP20 encoding the FLP recombinase. For thermal induction of FLP synthesis and subsequent removal of the temperature-sensitive plasmid pCP20, mutants were incubated at 37°C.

To generate YP73 and YP75, a $\Delta ymoA$ fragment was inserted into YP69 (YPIII $\Delta csrB$) and YP72 (YPIII $\Delta rovM$), respectively. First, the kanamycin resistance gene was amplified using primer pairs 25/26 for YP73 and YP75 (see **Supplementary Table 3**). Next, the *Yersinia* genomic DNA was used as a template to amplify 500-bp regions flanking the target genes *ymoA* (see **Supplementary Table 3**). The upstream fragment was amplified with a primer pair of which the reverse primer contained additional 20 nt at the 5'-end which were homologous to the start of the kanamycin resistance gene, the downstream fragment was amplified with a primer pair of which the forward primer contained additional 20 nt at the 5'-end which were homologous to the end of the kanamycin resistance gene (for primer see **Supplementary Table 4**). In the next step, a PCR reaction was performed with the forward primer and the reverse primer using the upstream and downstream PCR products of the target gene and the *kan* gene fragment as templates. The PCR fragment was transformed into *Y. pseudotuberculosis* YPIII pKD46 and chromosomal integration of the fragments was selected by plating on LB supplemented with kanamycin. The selection of the mutants and removal

of the kanamycin resistance gene was performed as described (Datsenko and Wanner, 2000).

RNA Isolation and Northern Detection

Overnight cultures were grown to stationary phase (OD_{600} of 3). 2.5 ml culture were withdrawn, mixed with 0.2 volume of stop solution (5% water-saturated phenol, 95% ethanol) and snap-frozen in liquid nitrogen. After thawing on ice, bacteria were pelleted by centrifugation (2 min, 14,000 rpm, 4°C), and RNA was isolated using the SV total RNA purification kit (Promega) as described by the manufacturer. RNA concentration and quality were determined by measurement of A_{260} and A_{280} . Total cellular RNA (10 µg) was mixed with loading buffer (0.03% bromophenol blue, 4 mM EDTA, 0.1 mg/ml EtBr, 2.7% formaldehyde, 31% formamide, 20% glycerol in 4 × MOPS buffer) and was separated on agarose gels (1.2%), transferred overnight onto positively charged membranes (Roche) in 20 × SSC and UV cross-linked. Prehybridization, hybridization to DIG-labeled DNA probes and membrane washing were conducted using the DIG luminescent Detection kit (Roche) according to the manufacturer's instructions. The *csrC* and *csrB* transcripts were detected with a DIG-labeled PCR fragment (DIG-PCR nucleotide mix, Roche) with primer pair 23/24 and 25/26 (Supplementary Table 2), respectively.

RNA Stability Assay

RNA stability assay was used to compare degradation of the CsrC RNA between wild-type and different mutant strains. A YPIII overnight culture was mixed with rifampicin at a final concentration of 500 µg/ml to inhibit transcription. At certain time points after blockage of transcription, samples were withdrawn and total RNA was prepared for Northern blot analysis as described above. The half-life of CsrC was calculated by least squares analysis of semi-logarithmic plots of RNA concentration versus time.

Primer Extension Analysis to Test CsrB and CsrC Stability

Primer extension analysis was performed to determine the steady-state level and the stability of the CsrB and CsrC RNA from strains YPIII and YP80 (YPIII Δhfq). At an OD_{600} of 2.0 (early stationary phase), rifampicin was added to a final concentration of 500 µg ml⁻¹, after 0, 10, 20, 30, and 60 min, 2 ml aliquots were withdrawn and total RNA was extracted of the samples using the SV total RNA purification kit (Promega) as described by the manufacturer. Annealing was performed with 5 µg extracted RNA and the 5'-Dig-labeled oligonucleotides (primer 5'-CTGAAGACACATCTTCC-3' for CsrB, primer 5'-CCTGAGTAAGTGTGCTCC-3' for CsrC, and primer 5'-CCCACACTACCATCGGCGC-3' for 5S RNA) in 20 µl of 1× First Strand Buffer (Invitrogen) by slow cooling of the sample (0.01°C/sec) including 8 mM dNTPs with 200 U Superscript II reverse transcriptase (Invitrogen) was added and incubated for 1 h at 42°C. The size of the Dig-labeled reaction products was determined on a denaturing 4%

DNA sequencing gel by a detection procedure as described (Heroven et al., 2008).

Expression and Purification of the Y. pseudotuberculosis YmoA and H-NS Protein

KB4 (Δhns , $\Delta stpA$, and Δhha) transformed with pAKH77 or pAKH11 was grown at 37°C in LB broth to an A_{600} of 0.6. Anhydrotetracycline was added (0.2 µg/ml) to induce the expression of YmoA-Strep-Tag and/or 2 mM IPTG was used to induce H-NS-His₆ expression. For purification of the YmoA-H-NS heterodimer KB4 transformed with pAKH77 and pAKH11 was used for overexpression of the YmoA and H-NS protein. The cells were grown for an additional 3 h before being harvested. The purification procedure for the Strep-tagged YmoA protein was performed according to the manufacturer's instructions (IBA GmbH, Germany). H-NS purification was performed as described (Heroven et al., 2004). The purity of the YmoA and the H-NS protein was estimated to be >95%.

RNA/DNA Retardation Assays

For RNA-binding studies the purified YmoA and H-NS proteins were dialyzed against the RNA-binding buffer (10 mM Tris-HCl pH 7.5; 3 mM M DTT; 7.5% glycerol; 100 mM KCl; 100 mM MgCl₂). The CsrC RNA for RNA band shift analysis was obtained by *in vitro* transcription from a PCR fragment as described (Heroven et al., 2008; Böhme et al., 2012). The *csrC* transcript (extending 150 nt downstream of the transcriptional start site of *csrC*) and the control transcript (extending 117 nt downstream of the transcriptional start site of the 5S rRNA gene) were synthesized *in vitro* using the Fermentas TranscriptAid T7 High Yield Transcription Kit from PCR products of the target regions. Primers 29/30 and 31/32 were used for amplification of the *csrC* and 5S RNA control fragment from chromosomal DNA of YPIII. The RNA transcripts were extracted with phenol:chloroform, precipitated with ethanol and stored in DEPC-treated water. The RNA-binding reactions included the CsrC (1.1 µM) and 5S rRNA transcripts (1 µM), 1× RNA-binding buffer and increasing concentrations of the H-NS and YmoA proteins. In the following, they were incubated for 30 min at room temperature and immediately loaded on 8% polyacrylamide gels.

For DNA-binding studies, the purified YmoA and H-NS proteins were dialyzed against the DNA-binding buffer (10 mM Tris-HCl, pH 7.5, 1 mM EDTA, 5 mM dithiothreitol, 5% glycerol, 10 mM NaCl, 1 mM MgCl₂, 100 µg/ml BSA). Defined PCR fragments, carrying portions of the *csrC* regulatory region and the *csiD* region of *E. coli* K-12 CC118λpir (negative control), were mixed in an equimolar ratio and incubated with increasing amounts of purified YmoA and/or H-NS for 20 min at room temperature and used for DNA band shift assays as described by (Böhme et al., 2012).

Microarray Analysis and Data Analysis

Sequences used for the design of the microarrays (Agilent, 8 × 15K format), containing three different 60 nt oligonucleotides for all 4,172 chromosomal genes (ORFs > 30

codons) of the *Y. pseudotuberculosis* YPIII genome and six probes for the 92 genes of the virulence plasmid pYV of *Y. pseudotuberculosis* strain IP32953, were obtained from the NCBI Genome Genbank (NC_010465 and NC_006153). The ORF-specific oligonucleotides were designed using the web design application eArray from Agilent¹. 16 independent cultures of *Y. pseudotuberculosis* YPIII and the *ymoA* mutant strain were grown in LB at 25°C to OD₆₀₀ 0.8, total RNA was isolated from samples using the SV total RNA purification kit (Promega), and RNA concentration and quality was determined with an Agilent 2100 Bioanalyzer using the RNA Nano6000 kit as described by the manufacturers. Total RNA of four independent samples was pooled. 1 µg of the pooled samples was used for RNA-labeling with Cy5 (for wild-type RNA) and Cy3 (for mutant RNA) using the ULSTM Fluorescent Labeling Kit for Agilent Arrays (Kreatech). Non-incorporated Cy5/Cy3 was removed by KREApure purification columns as suggested by the manufacturers. The degree of labeling was determined by a Nanodrop (Peqlab). Subsequently, 300 ng Cy5-labeled RNA and 300 ng Cy3-labeled RNA were mixed, fragmented and hybridized to custom-made Agilent microarray slides (8 × 15K) using the Agilent gene expression hybridization kit as described by the manufacturer. Direct use of labeled RNA for array hybridization was chosen to avoid bias obtained by cDNA library formation. In general, four biological replicates were used for each experiment. After washing and drying of the microarray slide, data were scanned using Axon GenePix Personal 4100A scanner and array images were captured using the software package GenePix Pro 6.015.

The processing of the resulting microarray data was performed using the software package R² in combination with the “Bioconductor” software framework³ (Gentleman et al., 2004). Preprocessing based on the marray package employing the read.GenePix function. Control code for probe selection was adapted to the custom-made Agilent microarray system and a quality control was performed to check for hybridization artifacts and large-scale differences between the microarrays of one experiment. A two-color intensity-dependent normalization (“Lowess” normalization) was applied and if necessary supplemented by scale normalization between different microarrays as described (Yang et al., 2002). Differentially expressed genes were obtained using the limma package and the lmFit function for linear modeling. eBayes was used for significance calculations (Smyth, 2004). The overall fold-changes of a gene represented by at least three probes are given as median values for all probes. A cut-off of fold-change ≥ 2 (*P*-value of >0.001) was chosen to determine YmoA-dependent genes/operons and the set of resulting differential expressed genes was analyzed employing the topGO package for Gene Ontology (GO) term enrichment (Alexa et al., 2006). MIAME compliant array data were deposited in Gene Expression Omnibus (GEO) database and are available via the following accession number: GSE35043.

¹ <http://www.genomics.agilent.com>

² www.r-project.org

³ www.bioconductor.org

Quantitative RT-PCR

One step real-time RT-PCR was performed in triplicate with RNA preparations of six independent cultures using a Rotor-Gene Q thermo cycler (Qiagen). For qRT-PCR analysis RNA was prepared from bacterial cells grown to early stationary phase at 25°C using Qiazol and the chloroform/phenol extraction method. Quantitative RT-PCR was carried out with the SensiFast SYBR No-ROX One-Step Kit (Bioline, Germany) applying the 3-step cycling protocol according to the manufacturer. Gene specific-primers used for qRT-PCR amplification are listed in **Supplementary Table 3** and were designed to produce a 200–250 bp amplicon with *Y. pseudotuberculosis* YPIII cDNA as template. The amount of PCR product was quantified by measuring fluorescence of SYBR Green dye. Reported gene expression levels were normalized to levels of the *sopB* transcript. This gene was used as it exhibited identical expression levels in the wild-type and the *ymoA* mutant under used experimental conditions. Standard curves were detected during every run for each gene tested and established by comparing transcript levels in serial dilutions of total RNA from a control sample. The relative expression of each gene was calculated as described (Pfaffl, 2001).

β-Galactosidase and Alkaline Phosphatase Assays

The activity of the *inv-phoA* fusion encoded on plasmid pPD297 and the β-galactosidase activity of the *lacZ* fusion constructs were measured in permeabilized cells as described previously (Manoil, 1990; Miller, 1992). The activities were calculated as follows: β-galactosidase activity $OD_{420} \cdot 6.75 \cdot OD_{600}^{-1} \cdot \Delta t \text{ (min)}^{-1} \cdot Vol \text{ (ml)}^{-1}$; alkaline phosphatase activity $OD_{420} \cdot 6.46 \cdot OD_{578}^{-1} \cdot \Delta t \text{ (min)}^{-1} \cdot Vol \text{ (ml)}^{-1}$.

Gel Electrophoresis, Preparation of Cell Extracts and Western Blotting

For immunological detection of the YmoA, RovA, RovM, and invasin proteins, *Y. pseudotuberculosis* cultures were grown under specific environmental conditions as described. Cell extracts of equal amounts of the bacteria were prepared and separated on a 15% (RovA, Hfq), 12% (RovM) or 10% (invasin) SDS-PAGE (Sambrook, 2001). The low molecular weight proteins (YmoA and CsrA) were separated by 20% TRICINE-PAGE as described recently (Schagger, 2006).

Subsequently, the samples were transferred onto an Immobilon-P membrane (Millipore) and probed with a polyclonal antibodies directed against RovA, RovM, Hfq, CsrA, and YmoA, or a monoclonal antibody 3A2 directed against invasin as described recently (Heroven and Dersch, 2006). The cell extracts used for Western blotting were also separated by SDS-PAGE and stained with Coomassie blue to ensure that the protein concentrations in the different cell extracts are comparable; about 10 µg protein was applied of each sample.

Cell Invasion Assay

In preparation of the cell adhesion and uptake assay, 5 × 10⁴ HEp-2 cells were seeded and grown overnight in individual wells of 24-well cell culture plates (Nunc). Cell monolayers were

washed three times with phosphate-buffered saline (PBS) and incubated in binding buffer (RPMI 1640 medium supplemented with 20 mM HEPES pH7.0 and 0.4% bovine serum albumin) before infection with bacteria. Approximately 10^6 bacteria were added to the monolayer and incubated at 37°C. Bacterial uptake was assessed 30 min after infection as the percentage of bacteria, which survived a gentamicin treatment versus the input cell number as described previously (Dersch and Isberg, 1999). The experiments were routinely performed in triplicate.

Mouse Infections

Yersinia pseudotuberculosis YPIII (wild-type) and YP50 (*ymoA* mutant) were grown overnight at 25°C, washed in sterile PBS and used for intragastrical inoculation of 6–8 weeks old female BALB/c mice (Janvier, France) using a ball-tipped feeding needle. To assess the impact of an *ymoA* deletion in *Y. pseudotuberculosis* on tissue colonization, different groups of BALB/c mice were infected with 5×10^8 bacteria of each strain. In co-infection experiments mice were orally inoculated with an equal mixture of strains YPIII and YP50, each at a dosage of 5×10^8 CFU. Three days post infection, mice were sacrificed using CO₂. Mesenteric lymph nodes, liver and spleen were recovered. Isolated Peyer's patches were washed with sterile PBS, incubated in 100 µg/ml gentamycin for 30 min and washed intensively with sterile PBS three-times. Organs were weighed and homogenized for 30 s in sterile PBS using a Polytron PT 2100 homogenizer (Kinematica, Switzerland). Subsequently, they were plated on *Yersinia* selective agar (Oxoid, Germany) in three serial dilutions with or without kanamycin. Colony forming units were determined and are given in cfu per gram organ/tissue. The competitive index in comparison to the wild-type strain YPIII was calculated as described (Monk et al., 2008).

Ethics Statements

Animal work was performed in strict accordance with the German regulations of the Society for Laboratory Animal Science (GV-SOLAS) and the European Health Law of the Federation of Laboratory Animal Science Associations (FELASA). The animal study was reviewed and approved by the Niedersächsisches Landesamt für Verbraucherschutz und Lebensmittelsicherheit: animal licensing committee permission no. 33.9.42502-04-055/09.

RESULTS

The Modulator YmoA Has a Global Influence on Gene Expression of *Y. pseudotuberculosis*

In a previous study we showed that YmoA directly represses transcription of the regulator of *lcrF*, which is encoded on the *Yersinia* virulence plasmid (pYV) and controls expression of the antiphagocytic T3SS machinery and effectors (Böhme et al., 2012). However, despite its influence on *lcrF* expression, the overall influence of YmoA on *Y. pseudotuberculosis* virulence was still unknown. In the context of a previous study addressing the

influence of different early-stage virulence regulators (CsrA, Crp, and RovA) on gene expression of *Y. pseudotuberculosis* YPIII (Bücker et al., 2014), we also investigated the effect of YmoA on the *Yersinia* transcriptome. The analysis was performed with *Y. pseudotuberculosis* wildtype strain YPIII and the isogenic *ymoA* mutant (YP50) grown at 25°C to late exponential phase, conditions under which YmoA production was found to be high (Supplementary Figure 1). In total 289 genes showed twofold or greater difference in transcript abundance between the wild-type and the $\Delta ymoA$ strain. Among them, 227 genes (79%) were up-regulated and 62 (21%) were down-regulated in the *ymoA* mutant (Supplementary Table 4), indicating that YmoA is an important global regulator implicated in the control of fitness- and virulence-relevant processes. Classification according to genome annotation of *Y. pseudotuberculosis* YPIII showed that altered genes belong to several functional categories (Figure 1A and Supplementary Table 4). About 31% of all YmoA-dependent transcripts (90 genes) are related to virulence. As expected from previous studies (de la Cruz et al., 1992; Cornelis, 1993), 42 genes of the virulence plasmid encoding the structural components of the type III secretion system (*yscA-L*, *yscO-S*, and *yscU*), the intracellularly delivered Yop effector proteins and their chaperones (*yopE*, *ycyE*, *yopH*, *yopJ*, *yopO*, *ycyO*, *yopK*, and *yopM*), regulators of the secretion system (*yscW-lcrE*, *lcrQ*, *yopN-sycN-tyeA-yscXY*, and *lcrDRGVH-yopBD*), and the adhesin YadA were upregulated in the *ymoA* mutant. Notably, multiple virulence plasmid-encoded putative resolvases and transposase genes were also upregulated in the *ymoA* mutant (Supplementary Table 4), suggesting that YmoA did not only control expression of the T3SS-Yop injectisome via its influence on LcrF (Böhme et al., 2012), but seems to have a more global effect.

In addition, many chromosomally encoded virulence genes were differentially regulated in the absence of YmoA. Among them were genes for potential adhesins (*ail*, *ailB*, *psaA*, *yadC*, and *yadF*) and fimbriae/pili (*ybgP*, *fimA1-3*, *fimC*, *fimD*, *smfA1-2*, and *csgG*), the *cnfY* gene encoding a cytotoxic necrotizing factor and the insecticidal toxin genes *tcaAB*, as well as genes for iron/heme acquisition (*hasA* and *bfr*), LPS/O-antigen synthesis (*wzz*, *manB*, *gne*, *whyL*, *manC*, *fcl*, *gmd*, and *whyK*) and autoinducer synthesis (*lsrRBFG*, *yplI/ytlI*). In addition, genes encoding Hcp1 family effectors and different operons for type VI secretion systems (*hcp1* and *imp* genes), flagella assembly and chemotaxis genes (*flhDC*, *fliETfz*, and *flgDCB*) were upregulated in the *ymoA* deficient strain (Figures 1A,B and Supplementary Table 4). These data were validated with a subset of identified YmoA-dependent genes using qRT-PCR with *sopB* as control as *sopB* was not affected by YmoA according to the microarray analysis [Figure 1C, *YPK_0604* (*l-ppp*; 9.3-fold), *grpE* (3-fold), *dnaJ* (4.8-fold), and *dnaK* (2.8-fold)].

YmoA Controls the CsrABC-RovM-RovA Regulator Signaling Cascade in *Y. pseudotuberculosis*

Among the identified YmoA-dependent virulence genes were early-stage pathogenicity factors of *Yersinia*, which

are predominantly expressed at lower temperature *in vitro*. Several of them, including the virulence regulator gene *rovA* (Supplementary Table 4), have been shown to be controlled by the Csr system (Heroven et al., 2008, 2012a; Bückner et al., 2014). This suggested that YmoA might be implicated in the control of the CsrABC-RovM-RovA regulatory cascade (Figure 2A). To prove this assumption, we first compared intracellular YmoA, RovM and RovA levels between wild-type (YP113), the *ymoA* mutant (YP50) and the complemented strain YP50 ($\Delta ymoA$) pAKH71 (*ymoA*⁺). As shown in Figures 2B–D, expression of the negative regulator RovM is significantly increased in the absence of YmoA, which in turn leads to a strong reduction of the amount of RovA. Influence on RovM and RovA levels could be fully complemented by the *ymoA*⁺ plasmid. Interestingly, the intracellular amount of YmoA is very low in *Y. pseudotuberculosis* YP113 under growth conditions simulating the early-stage of infection (Figure 2B and Supplementary Figure 1), but this concentration seems sufficient to promote RovA synthesis to levels similar to *pymoA*⁺ containing strains (Figure 2D), with significantly higher amounts of YmoA (Figure 2B).

While a deletion of *ymoA* alone abrogated RovA synthesis, it had no influence on *rovA* expression in the *rovM/ymoA* double mutant; in the contrary higher RovA level were detected similar to the *rovM* mutant (Figure 2E). This demonstrated that YmoA exerts its effect mainly via RovM. This was somewhat surprising as YmoA was found to interact with the nucleoid-structuring protein H-NS (Nieto et al., 2002) which is known to control *rovA* expression directly (Heroven et al., 2004) (Figure 2A). In fact, overexpression of a dominant-negative N-terminal H-NS fragment (H-NS*) – a knock-out is deleterious to *Y. pseudotuberculosis* – reduced H-NS-mediated *rovA* silencing as shown previously (Heroven et al., 2004). This led to an increase of RovA levels in the *Y. pseudotuberculosis* wild-type, but not in the *ymoA* mutant (Supplementary Figure 2).

Expression of the *rovM* gene was shown to be under control of the *Yersinia* Csr system, comprising the two regulatory ncRNAs, CsrB, and CsrC, and the RNA-binding protein CsrA (Heroven et al., 2008) (Figure 3A). The CsrB and CsrC RNAs both sequester the CsrA RNA-binding protein resulting in reduced RovM synthesis. To determine whether YmoA acts on *rovM* via the *Yersinia* Csr system, we compared the amount of CsrA and expression of the *csr* RNA genes between wild-type and the *ymoA* mutant. While no changes of CsrA levels were detectable (Figure 3B), a mild increase in CsrB and a strong reduction of CsrC could be observed in a $\Delta ymoA$ strain compared to the wild-type (Figures 3C,D).

YmoA Has a Positive Effect on CsrC Levels

As both Csr-RNAs have a negative influence on each other (Heroven et al., 2008), we first addressed whether YmoA affects only the expression of CsrC RNA, which in turn inhibits the synthesis of CsrB. In fact, identical changes were observed on CsrC and RovM levels in a *ymoA* and a *csrB/ymoA* mutant strain, implying that YmoA exerts its major effect on the Csr regulon through regulation of CsrC (Supplementary Figure 3).

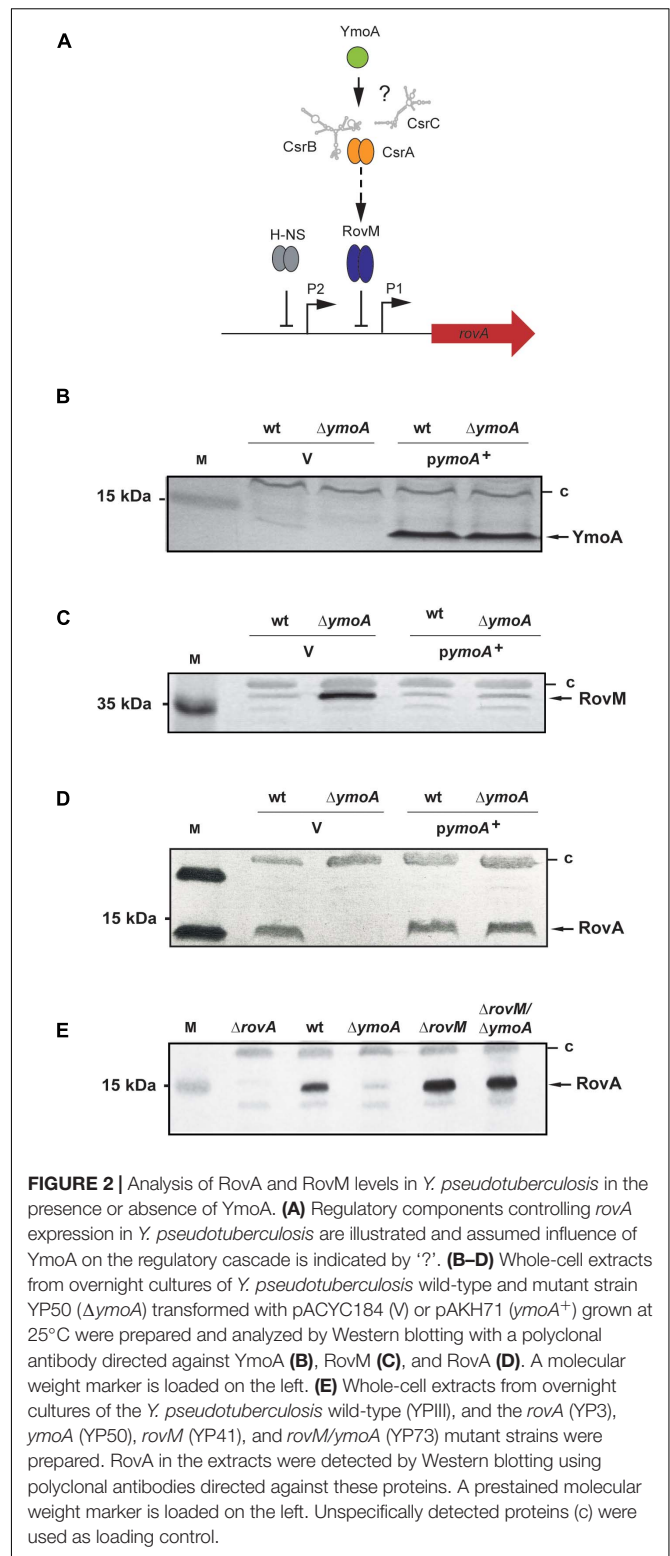
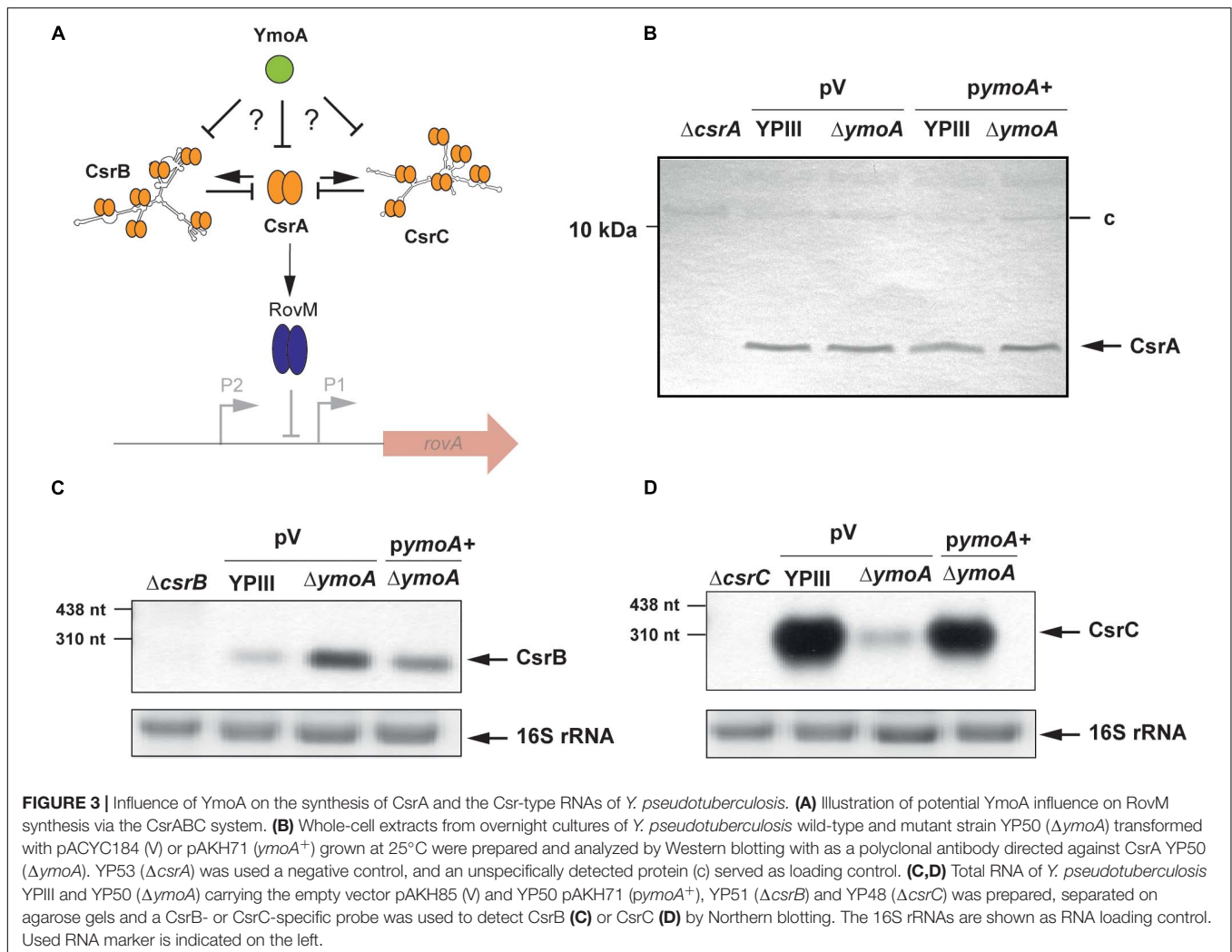


FIGURE 2 | Analysis of RovA and RovM levels in *Y. pseudotuberculosis* in the presence or absence of YmoA. **(A)** Regulatory components controlling *rovA* expression in *Y. pseudotuberculosis* are illustrated and assumed influence of YmoA on the regulatory cascade is indicated by ‘?’. **(B–D)** Whole-cell extracts from overnight cultures of *Y. pseudotuberculosis* wild-type and mutant strain YP50 ($\Delta ymoA$) transformed with pACYC184 (V) or pAKH71 (*ymoA*⁺) grown at 25°C were prepared and analyzed by Western blotting with a polyclonal antibody directed against YmoA **(B)**, RovM **(C)**, and RovA **(D)**. A molecular weight marker is loaded on the left. **(E)** Whole-cell extracts from overnight cultures of the *Y. pseudotuberculosis* wild-type (YP113), and the *rovA* (YP3), *ymoA* (YP50), *rovM* (YP41), and *rovM/ymoA* (YP73) mutant strains were prepared. RovA in the extracts were detected by Western blotting using polyclonal antibodies directed against these proteins. A prestained molecular weight marker is loaded on the left. Unspecifically detected proteins (c) were used as loading control.

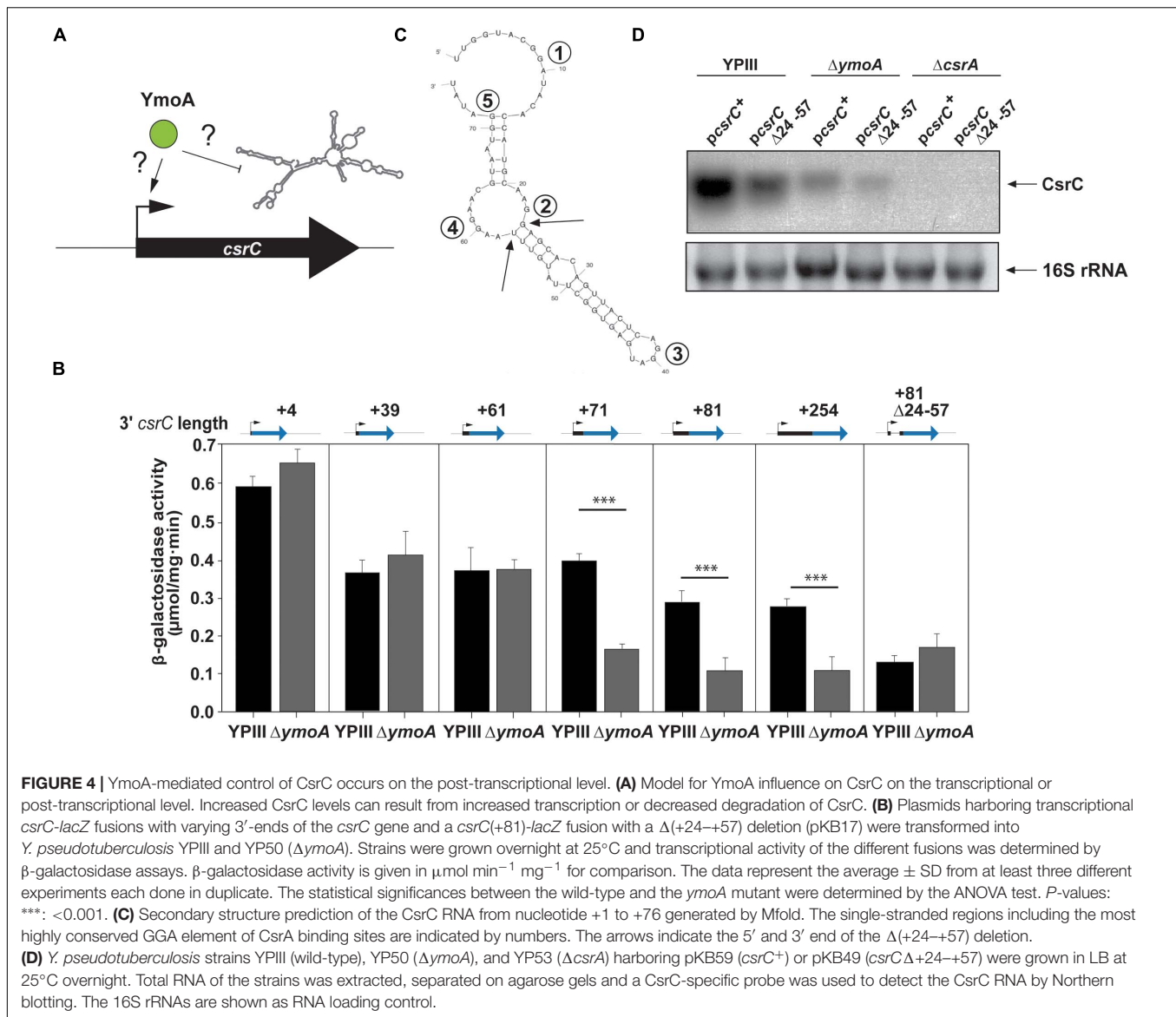
To determine whether this positive effect of YmoA on CsrC occurs on the transcriptional or post-transcriptional level (Figure 4A), we analyzed expression of *csrC-lacZ* transcriptional fusions harboring *csrC* fragments with varying 3' endpoints



(+4, +39, +61, +71, +81, or +254). In general, elongation of the *csrC* fragment led to a continuous decrease of *csrC-lacZ* expression (Figure 4B), suggesting that *csrC* sequences destabilize or reduce translation of the *lacZ* RNA and/or lead to a premature termination of transcription. Furthermore, we found that absence of YmoA had no significantly different effect on *csrC-lacZ* reporter fusions which included the first ≤ 61 nucleotides of *csrC*, whereas expression of fusions, containing the first 71 nucleotides or more, was more than twofold reduced. Computational secondary structure analyses of the *csrC* transcript predict that nucleotides from position +24 to +57 form a hairpin structure (Figure 4C). Expression of mutant variants of *csrC*(+81)-*lacZ* fusion and *csrC* in which nucleotides +24 to +57 were deleted became independent of YmoA (Figures 4B,D). This suggests the presence of (i) a stabilizing element or (ii) a transcriptional terminator within the 5'-sequences of the CsrC RNA which is affected by YmoA. The fact that (i) the 5'-hairpin region has a positive influence on the overall expression of *csrC* and (ii) truncated CsrC species could not be detected in the *ymoA* mutant suggested that YmoA enhances CsrC RNA stability through the stem loop segment. To

confirm YmoA-mediated post-transcriptional control of CsrC, *csrC* was expressed under the control of a plasmid-encoded tetracycline promoter (P_{tet}). To ensure expression was only derived from the plasmid, culturing conditions were chosen under which the chromosomal *csrC* gene is fully repressed (Heroven et al., 2008). While expression of the control gene *lacZ* under P_{tet} control was identical in the wildtype and the *ymoA* mutant (Supplementary Figure 4A), considerably higher levels of CsrC were detectable in the wild-type when expressed from the identical P_{tet} expression plasmid (Supplementary Figure 4B). This also suggested that YmoA acts on CsrC on the post-transcriptional level.

To further analyze the influence of YmoA on CsrC (Figure 5A), CsrC levels were determined by Northern blotting after transcription of $P_{tet}:csrC$ was blocked by rifampicin. As shown in Figure 5B, the CsrC RNA was slowly degraded in the *Y. pseudotuberculosis* wild-type strain with a half-life of about 100 min, whereas CsrC was less stable in the *ymoA* mutant and decayed with a half-life of about 45–50 min. Presence of five potential CsrA-binding sites (GGA motif) within the 5'-hairpin region of the CsrC transcript (Figure 4C), suggested that



the interaction and sequestration of CsrA could also increase the stability of the CsrC RNA. Northern blot analysis further revealed that CsrA is important for CsrC abundance as CsrC is not detectable in the $\Delta csrA$ mutant (Figure 4D). To further characterize CsrA influence on CsrC stability, we induced *csrC* expression under the control of P_{tet} by anhydrotetracycline (AHT). After transcription was blocked by rifampicin, the CsrC transcript was much more rapidly degraded in the *csrA* mutant compared to wildtype (Figure 5C). In comparison, the influence of CsrA on CsrC stability was much more pronounced than that of YmoA (Figures 5B,C). Hence, it seemed possible that presence of YmoA influences the function of CsrA. To test this assumption, we tested whether CsrA overexpression is able to complement a *ymoA* mutant strain or whether YmoA overproduction can complement *csrA* deficiency by comparing CsrC levels in the different recombinant strains. As shown in Figure 5D, overexpression of YmoA was not able to complement

csrA deficiency, whereas CsrC RNA synthesis was partially complemented when CsrA was overproduced in the *ymoA* mutant. This suggested that loss of YmoA can be overcome by an increase of CsrA-binding to the CsrC RNA. Based on these results, it is possible that YmoA has an influence on the activity of CsrA, e.g., by controlling an RNA chaperone assisting in CsrA-binding or folding of the CsrC RNA.

The RNA Chaperone Hfq Acts Differently and Independently of YmoA on CsrC

One molecule that has been shown to assist in folding of Csr/Rsm-type RNAs, CsrA/RsmA binding and increases the stability and abundance of Csr/Rsm-type RNAs in *Pseudomonas aeruginosa* is the ubiquitous hexameric RNA-chaperone Hfq (Sonnleitner et al., 2006; Sorger-Domenigg et al., 2007). Hence, it seemed possible that YmoA exerts its stabilizing influence

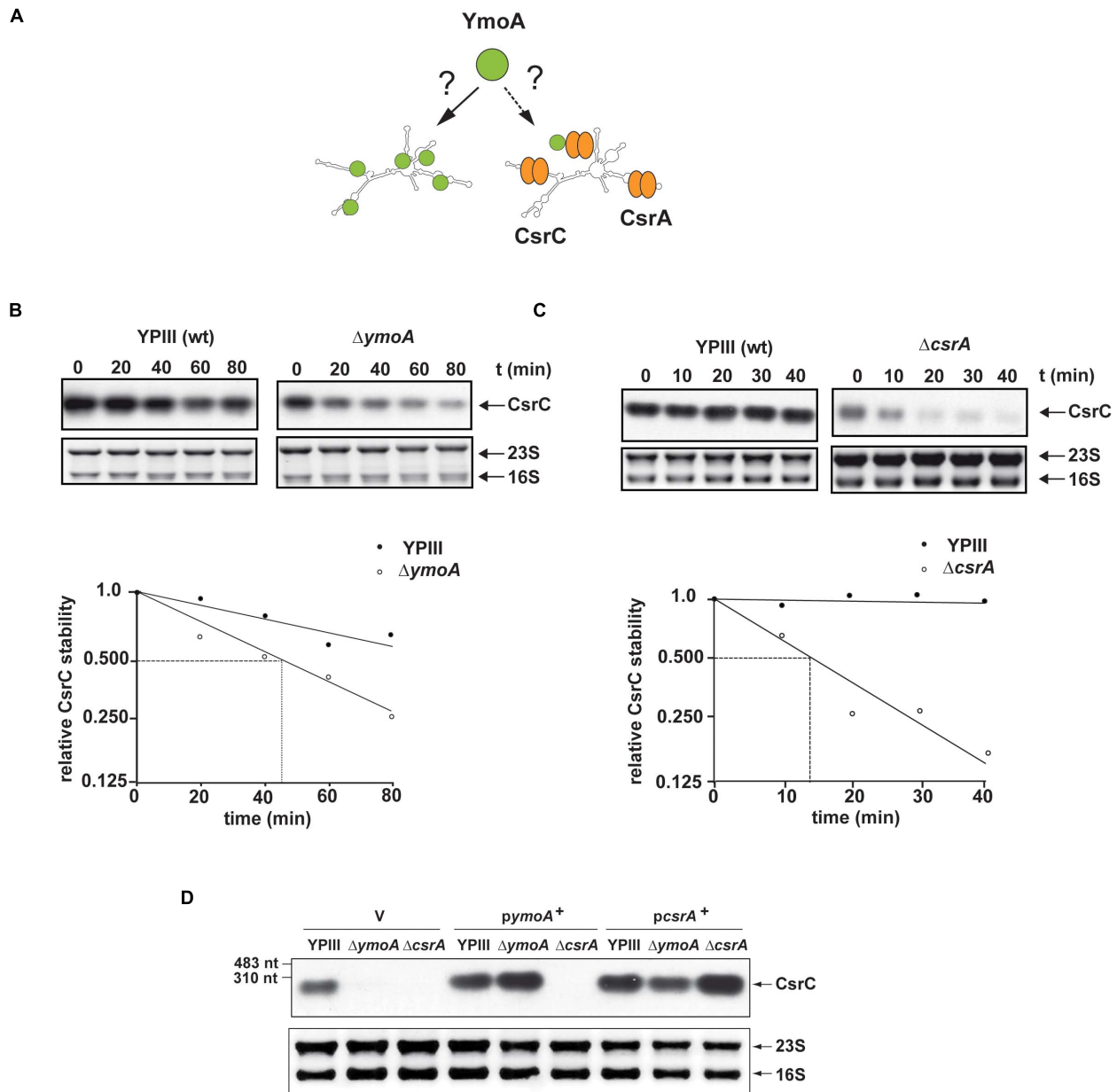


FIGURE 5 | YmoA and CsrA increase the stability of the CsrC RNA. **(A)** Model for YmoA-dependent CsrC stabilization. **(B,C)** The stability of the CsrC RNA expressed under the control of the *tet* promoter was compared between *Y. pseudotuberculosis* strain YP111 (wild-type) and YP50 ($\Delta ymoA$) **(B)** or YP53 ($\Delta csrA$) **(C)** and CsrC RNA stability was analyzed over time by Northern blotting with a CsrC-specific probe. A representative Northern blot of three independent experiments is shown in the upper panel. 16S and 23S rRNA were used as loading controls. The band corresponding to the CsrC transcript was quantified using the BioRAD Image LabTM Software and was plotted versus time of extraction (in minutes) to calculate the half-life of the sRNA indicated by dotted lines (lower panel). **(D)** *Y. pseudotuberculosis* strains YP111, YP50 ($\Delta ymoA$), and YP53 ($\Delta csrA$) harboring vector pHSG576 (V), a *ymoA*⁺ (pKB4) or *csrA*⁺ derivative (pKB60) were cultivated overnight in LB medium at 25°C. Total RNA of the strains was extracted, separated on agarose gels and a CsrC-specific probe was used to detect the CsrC ncRNA by Northern blotting. Used RNA marker is marked on the left. The 16S and 23S rRNAs are shown as RNA loading control.

on CsrC via upregulation of Hfq (Figure 6A). As shown in Figure 6B, no or only very low amounts of the CsrC RNA were detected in an Δhfq mutant strain. This resulted in a dramatic increase of RovM and decrease of RovA levels and all these effects could be complemented by an *hfq*⁺ plasmid (Supplementary Figure 5). To elucidate how Hfq affects the

Csr-RNAs, we performed a primer extension analysis to test whether absence of Hfq affects the abundance of CsrB and CsrC when transcription was blocked. Although slightly more CsrB transcript was found in the *hfq* mutant, the CsrB RNA seemed to be more rapidly degraded in the absence of Hfq (Figure 6C). In contrast, overall CsrC levels were significantly

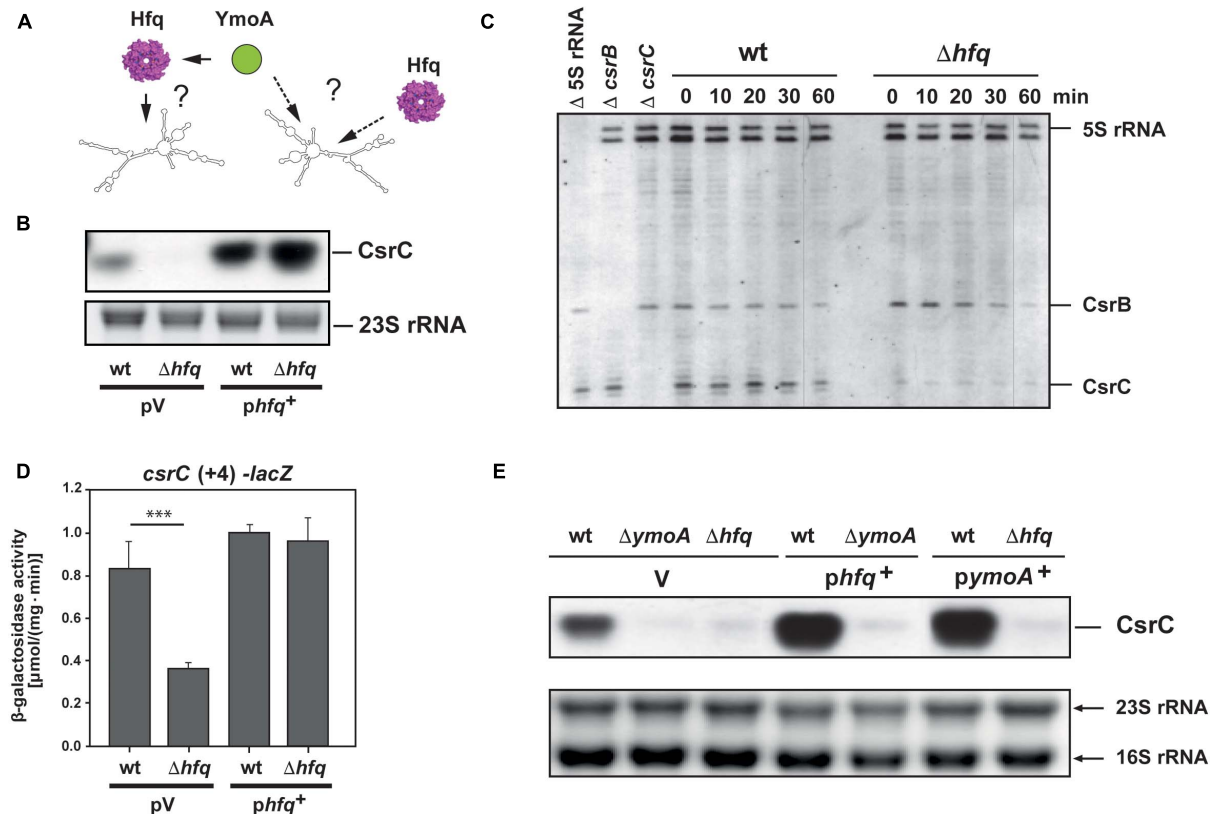


FIGURE 6 | Hfq influence on CsrB and CsrC stability and cooperation with YmoA. **(A)** The model illustrates possible influence of YmoA on CsrC abundance via or independent of Hfq. **(B)** *Y. pseudotuberculosis* strain YPIII (wt) and YP80 (Δhfq) carrying the vector pAKH85 (pV) or its *hfq*⁺ derivative (pAKH115) were grown overnight in LB medium. Total RNA of the samples was isolated, separated on agarose gels and the CsrC RNA was detected by Northern blotting using a CsrC-specific probe. The 23S rRNAs is shown as RNA loading control. **(C)** *Y. pseudotuberculosis* strain YPIII (wt) and YP80 (Δhfq) were grown in LB at 25°C to early stationary phase, rifampicin was added in a final concentration of 500 $\mu\text{g ml}^{-1}$ and aliquots were withdrawn at indicated time points. Total RNA was extracted and used for primer extension analysis. Samples without addition of labeled primers for 5S rRNA (Δ 5S rRNA), *csrB* ($\Delta csrB$), and CsrC ($\Delta csrC$) were used as controls. The reaction products were separated on 4% DNA sequencing gels. The positions of the transcripts are indicated. **(D)** *Y. pseudotuberculosis* strain YPIII (wt) and YP80 (Δhfq) carrying the vector pAKH85 (pV) or its *hfq*⁺ derivative (pAKH115) and the *csrC-lacZ* fusion (pAKH103) were grown in LB at 25°C overnight. β -Galactosidase activity of the cultures was determined (upper panels) and is given in $\mu\text{mol min}^{-1} \text{mg}^{-1}$ for comparison. The data represent the average \pm SD from at least three different experiments each done in duplicate. The statistical significances between the wild-type and the *ymoA* mutant were determined by the ANOVA test. *P*-values: ***: <0.001 . **(E)** *Y. pseudotuberculosis* strains YPIII, YP50 ($\Delta ymoA$) and YP80 (Δhfq) harboring vector pHSG575 (V), a *ymoA*⁺ (pKB4) or *hfq*⁺ derivative (pAKH119) were cultivated overnight in LB medium at 25°C. Total RNA of the strains was prepared, separated on agarose gels and a specific probe was used to detect the CsrC RNAs by Northern blotting. The 16S and 23S rRNAs are shown as RNA loading control.

reduced in the Δhfq strain, but the half-life of the transcript was not influenced by Hfq (Figure 6C). This strongly indicated that Hfq has a positive influence on *csrC* transcription, but not on CsrC RNA stability. In agreement with this assumption we found that expression of the *csrC*(+4)-*lacZ* fusion harboring only the first four nucleotides of the *csrC* gene was downregulated in the *hfq* mutant (Figure 6D). Complementation assays further demonstrated that neither YmoA nor Hfq could compensate the effect of the *hfq* or the *ymoA* knock-out mutation on the abundance of the CsrC RNA (Figure 6E). Based on this observation, we concluded that Hfq and YmoA act differently and independently on CsrC.

H-NS Influences CsrC Stability

As members of the YmoA/Hha protein family are able to form heteromeric complexes with H-NS (Nieto et al., 2002),

we wanted to know whether YmoA acts through H-NS on CsrC. If so, changes in the active amounts of H-NS should influence CsrC RNA levels in *Y. pseudotuberculosis*. As shown in Figure 7A, the intracellular CsrC level was reduced in the presence of the dominant negative *hns*^{*} allele and increased upon *hns* overexpression. Moreover, low abundance of CsrC in the *ymoA* mutant was further reduced by *hns*^{*}, whereas overexpression of H-NS is able to compensate for the loss of YmoA and led to CsrC levels similar to the wild-type strain (Figure 7A). Furthermore, a significant reduction of *csrC*(+81)-*lacZ* expression, was observed in the absence of *ymoA* which could be compensated by overexpression of *hns* (Figure 7B). However, the identical changes of YmoA and H-NS levels had no influence on *csrC*(+4)-*lacZ* expression, indicating that both regulatory factors act through the *csrC* fragment including positions +5 to +81.

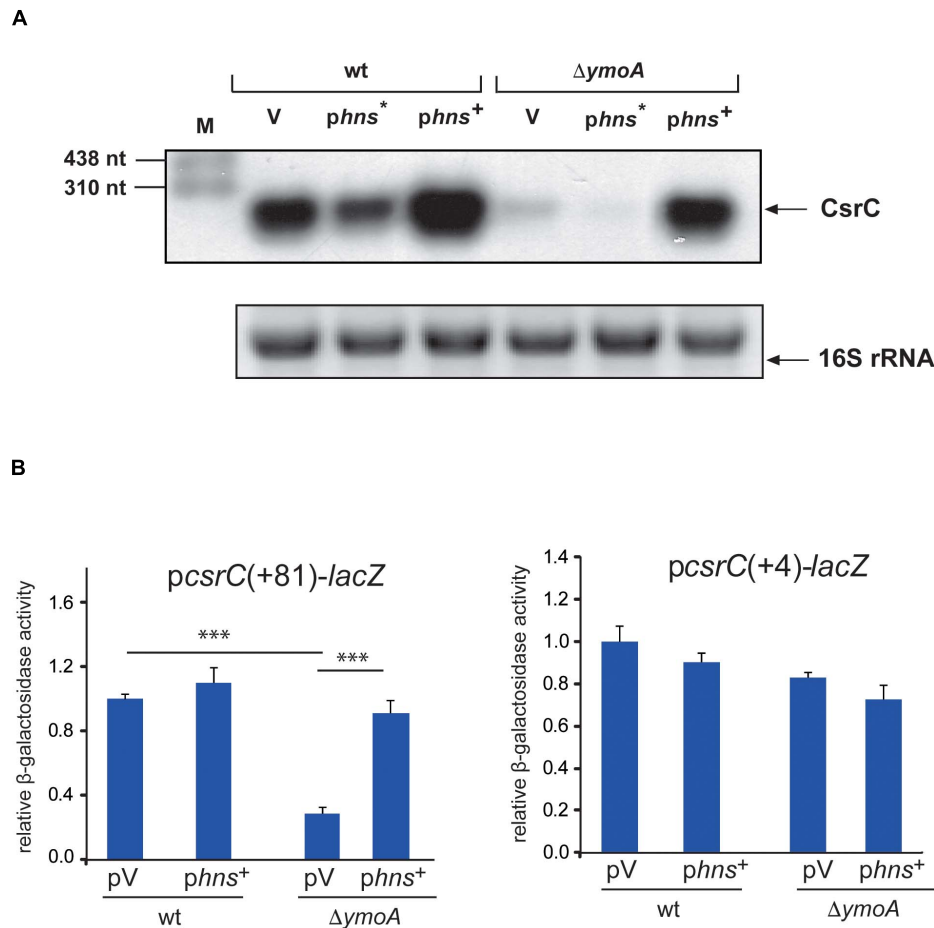


FIGURE 7 | H-NS has a positive influence on *csrC*. **(A)** *Y. pseudotuberculosis* strain YPIII and YP50 ($\Delta ymoA$) harboring the empty vector (V), a *hns*⁺ (pAKH31) or *hns*⁺ (pAKH74) overexpression construct were cultivated overnight in LB medium at 25°C. Total RNA of the strains was prepared, separated on agarose gels and a specific probe was used to detect the CsrC RNA by Northern blotting. The 16S rRNA is shown as RNA loading control. **(B)** Expression of *pcsrC(+4)-lacZ* and *pcsrC(+81)-lacZ* was analyzed in overnight cultures of *Y. pseudotuberculosis* strains YPIII (wild-type) and YP50 ($\Delta ymoA$) harboring vector pACYC184, pAKH85 or its *hns*⁺ derivative pAKH74 grown in LB at 25°C. β -galactosidase activity from the overnight cultures was determined and is given as relative expression for comparison. The data represent the average \pm SD from at least three different experiments each done in duplicate. Data were analyzed by the ANOVA test, *** $P < 0.001$.

As loss of YmoA did not influence H-NS levels (Supplementary Figure 6), we first assumed that YmoA enhances H-NS activity through YmoA-H-NS complex formation, and this could have a positive influence on CsrC level. Although YmoA and H-NS were shown to act predominantly on the transcriptional level, it has also been demonstrated that H-NS and paralogous proteins such as StpA can bind specifically to RNA and affect their folding and/or susceptibility to nuclease cleavage by RNases (Zhang et al., 1996; Mayer et al., 2002; Brescia et al., 2004). We tested whether YmoA and/or H-NS of *Y. pseudotuberculosis* could bind to the CsrC RNA *in vitro*. For this purpose, purified CsrC RNA transcript was incubated with increasing concentrations of the *Yersinia* H-NS and/or YmoA proteins. Both proteins were overexpressed and purified from *E. coli* strain KB4 deficient of all *E. coli* H-NS/Hha family proteins. However, neither H-NS alone nor in complex with YmoA was found to bind specifically to the CsrC RNA (Supplementary Figure 7A), whereas specific H-NS-dependent

high molecular weight complexes were identified with a *yscW* promoter control fragment as reported previously (Böhme et al., 2012), demonstrating that the H-NS protein is active (Supplementary Figure 7B). This strongly suggests that YmoA and H-NS influence on CsrC is indirect, e.g., occurs through a factor controlling CsrC stability.

Regulation of CsrC by YmoA and CsrA Depends on Environmental Parameters

Next, we analyzed how YmoA and CsrA cooperate in the control of CsrC in response to different environmental parameters. To do so, we monitored the amount of CsrA and YmoA in the wild-type under different growth conditions. Synthesis of CsrA was slightly dependent on growth phase control resulting in moderately higher protein levels during stationary phase, but temperature and media composition had no considerable effect (Supplementary Figure 1). In contrast, YmoA protein levels

were strongly dependent on temperature and growth phase, and at 37°C also on nutrient composition of the medium. Maximal amount of YmoA were observed at moderate temperature, in complex medium during exponential growth whereas no YmoA was detectable at 37°C in minimal medium (**Supplementary Figure 1**). To analyze the influence of the two regulatory factors

in more detail, we determined CsrA, YmoA, and CsrC levels along the bacterial growth curve at 25 and 37°C in complex medium. At 25°C, highest CsrC levels were detected during stationary phase (8–12 h), whereas at 37°C CsrC levels were maximal during late exponential phase (6 h), but decreased upon entry into stationary phase (**Figure 8**). As, the intracellular

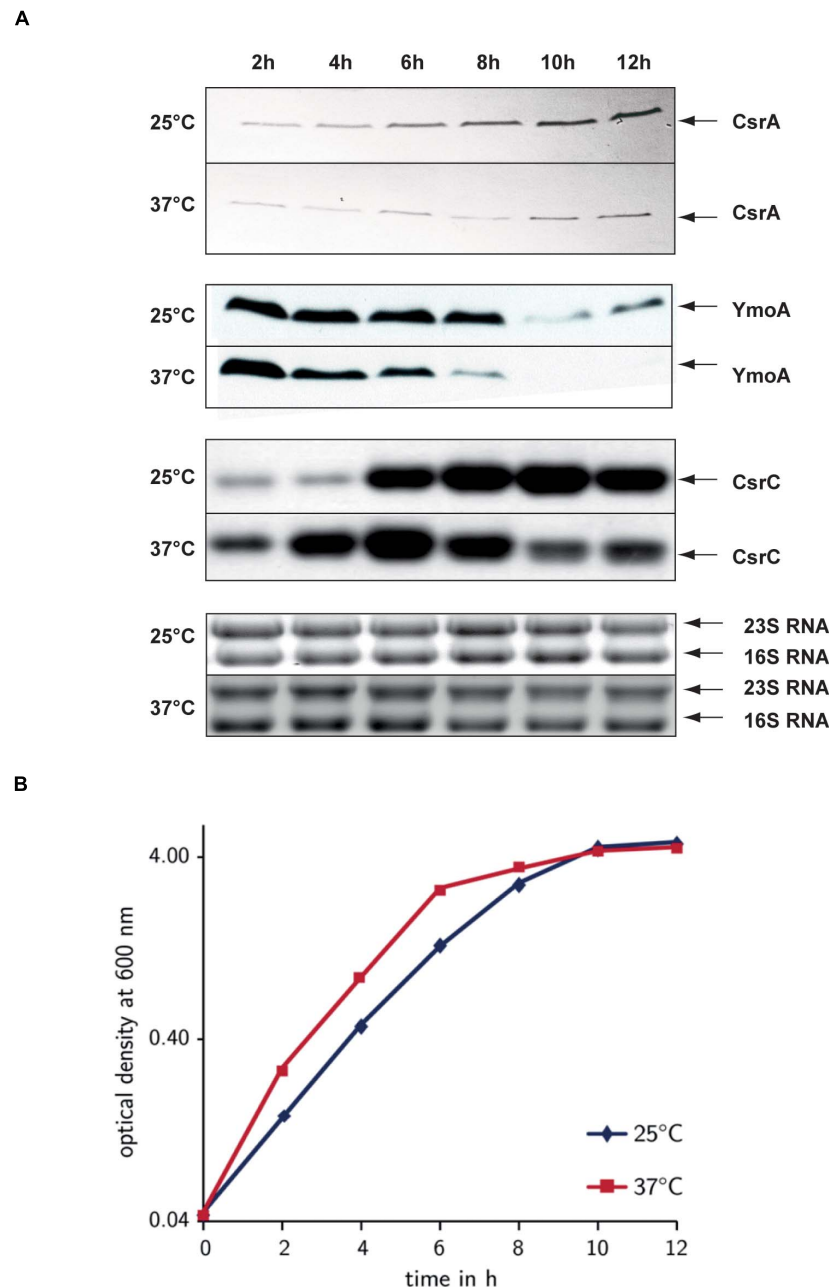


FIGURE 8 | Comparison of the environmental control of CsrA, YmoA, and CsrC synthesis. *Y. pseudotuberculosis* strain YPIII was diluted 1:100 from an overnight culture and was grown in LB at 25 and 37°C. Every 2 h, samples were withdrawn for whole cell extract and total RNA preparations (**A**) and the OD₆₀₀ of the cultures was determined to monitor growth (**B**). (**A**) Total RNA of the samples was separated on agarose gels and the CsrC RNA was detected by Northern blotting using a CsrC-specific probe. Whole cell extracts were separated on 18% TRICINE polyacrylamide gels and analyzed by Western blotting with a polyclonal antibody directed against YmoA and CsrA. The CsrC RNA band and the YmoA and CsrA protein bands are indicated by arrows. (**B**) OD₆₀₀ of the cultures used for the upper analysis was plotted over time to illustrate and compare the different growth phases.

concentration of CsrA remained at the same or even higher level, the decrease of CsrC amounts seems to result mainly from the strong reduction of YmoA levels during stationary phase, which is more pronounced at 37°C than at 25°C. The latter is the result of temperature-regulated proteolysis of YmoA mainly by the Lon protease but to a minor extent also by the ClpP protease (Supplementary Figure 8), similar to what has been described for the YmoA protein of *Yersinia pestis* (Jackson et al., 2004).

The Modulator YmoA Is Crucial for Virulence

Transcriptome analysis and subsequent investigation revealed that YmoA not only inhibits the expression of the pYV-encoded antiphagocytic T3SS-associated virulence factors important to resist innate immune cell attacks through, but also modulates the expression of multiple colonization factors crucial for the

initial infection phase (Supplementary Table 4). In fact, absence of YmoA strongly reduced synthesis of the RovA-dependent internalization factor invasins (InvA) (Figures 9A,B) which decreased the ability of *Y. pseudotuberculosis* to invade human cells by 50% (Figure 9C). This suggested that YmoA acts as a key virulence modulator which supports reprogramming from the initial colonization into the host defense mode.

To further define the overall influence of *ymoA* on bacterial pathogenesis, we compared the ability to colonize lymphatic tissues and organs between the *Y. pseudotuberculosis* wild-type strain YPIII and an isogenic *ymoA*-deficient strain (YP50) in a mouse infection model. First, we examined success of the infection in BALB/c mice 3 days after oral uptake of 5×10^8 bacteria by quantifying the number of bacteria that reached and survived in the Peyer's patches (PP), the mesenteric lymph nodes (MLN), liver and spleen (Figure 9D). Significantly reduced numbers of the *ymoA* mutant bacteria were recovered from

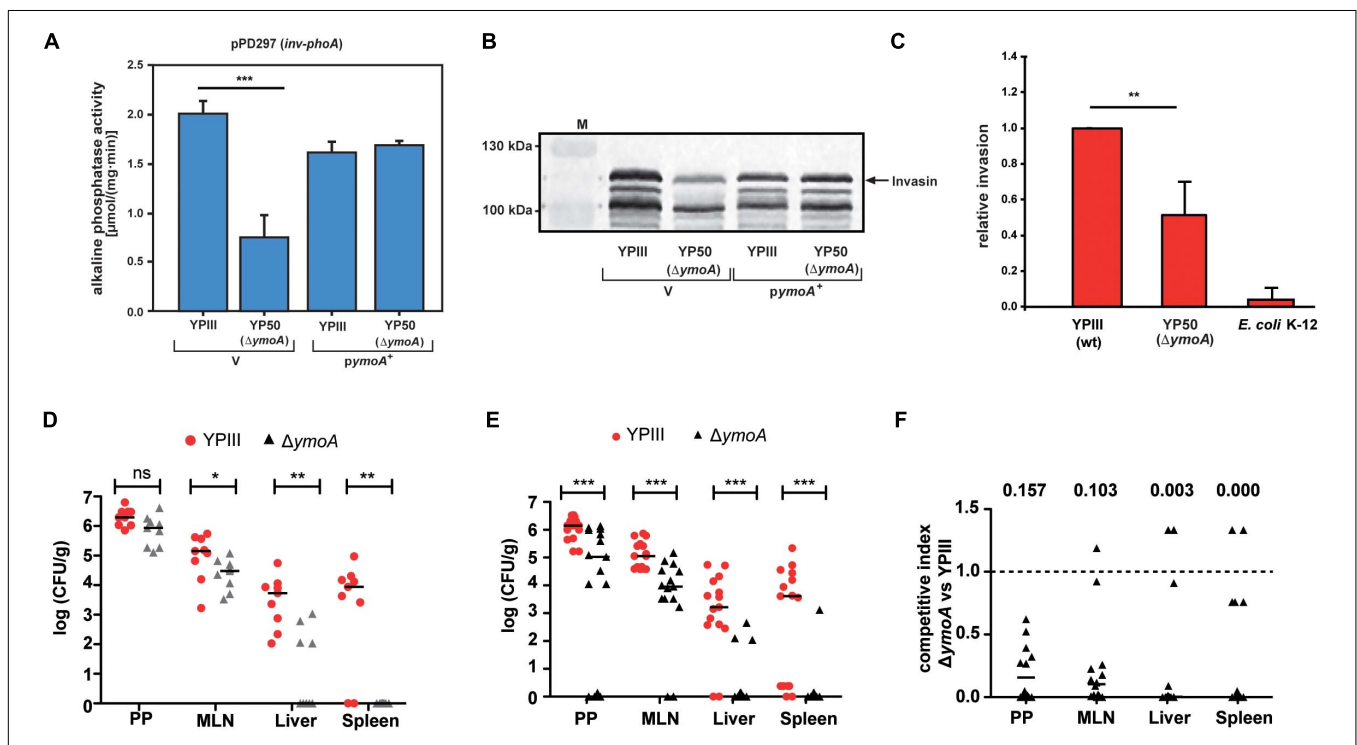


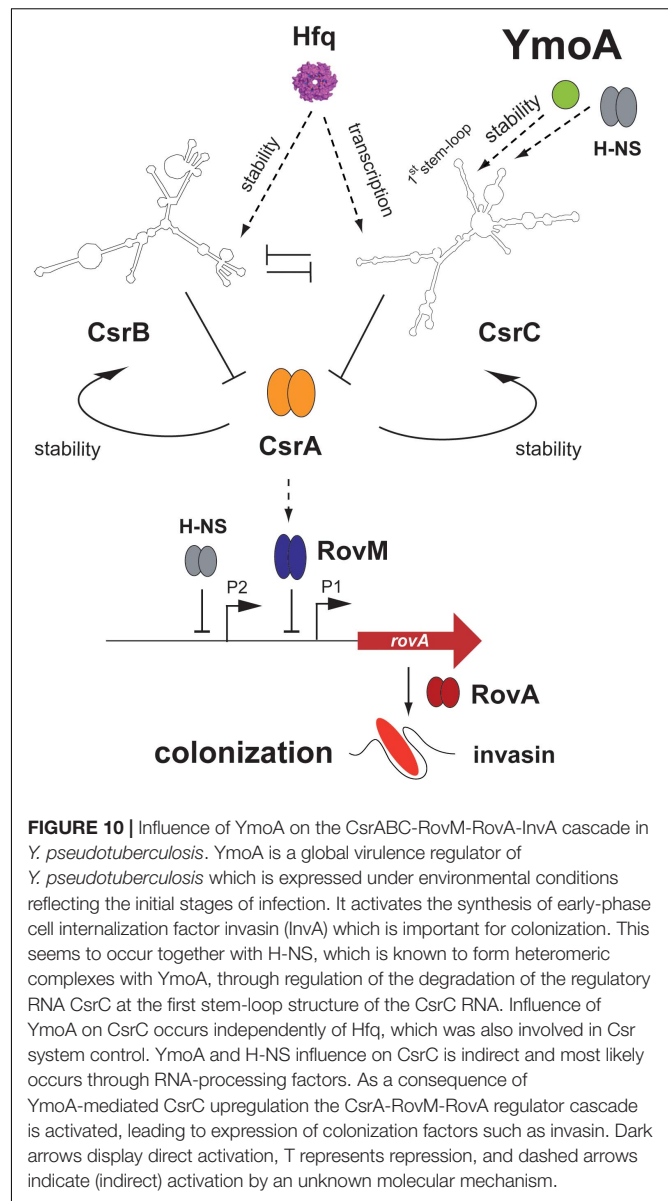
FIGURE 9 | Influence of *ymoA* on the virulence of *Y. pseudotuberculosis*. *Y. pseudotuberculosis* wild-type strain YPIII and the mutant strain YP50 (ΔymoA) harboring the *inv-phoA* fusion plasmid pPD297 and the empty vector control pACYC184 (V) or the *ymoA*+ plasmid pAKH71 were grown overnight in LB medium at 25°C. **(A)** Alkaline phosphatase activity from overnight cultures was determined and is given in $\mu\text{mol min}^{-1} \text{mg}^{-1}$. The data represent the average SD from at least three different experiments each done in duplicate. The statistical significances between the wild-type and the *ymoA* mutant were determined by the ANOVA test. *P*-values: ***: <0.001. **(B)** In parallel, whole cell extracts of the strains were prepared and analyzed by Western blotting with a monoclonal antibody directed against invasins. A molecular weight marker is loaded on the left. **(C)** HEP-2 cells were infected with wild-type *Y. pseudotuberculosis*, ΔymoA *Y. pseudotuberculosis* and *E. coli* K-12 and relative invasion was calculated. Each bar represents the average of three independent experiments relative to the invasion rate promoted by the *Y. pseudotuberculosis* wild-type strain, defined as 1.0. The statistical significances between the wild-type and the *ymoA* mutant were determined by the Students-test. *P*-values: **: <0.01. **(D)** BALB/c mice were infected intragastrically with an inoculum of $5 \cdot 10^8$ CFU of *Y. pseudotuberculosis* wild-type YPIII and the *ymoA* mutant YP50. Colonization of Peyer's patches (PP), mesenteric lymph nodes (MLN), liver and spleen after 3 days of infection is displayed. **(E)** For co-infection experiments, an inoculum with $1 \cdot 10^9$ CFU of an equal mixture comprising *Y. pseudotuberculosis* wild-type YPIII and the *ymoA* mutant strain YP50 was infected into BALB/c mice via the orogastric route. After 3 days of infection, mice were sacrificed and the number of bacteria in homogenized host tissues and organs was determined by plating. Data are represented in scatter plots of numbers of CFU per gram as determined by counts of viable bacteria on plates. The statistical significances between the wild-type and the *ymoA* mutant were determined by the Mann-Whitney-test. *P*-values: *: <0.05; **: <0.01; ***: <0.001. **(F)** Data are graphed as competitive index values for the tissue samples from one mouse. Solid lines indicate median values. A competitive index score of 1 denotes no difference in the virulence compared to YPIII. Underlined values indicated the competitive index scores of the *ymoA* mutant relative to the wild-type.

the MLNs and the organs. Attenuation of the *ymoA* mutant strain was even more evident when competition experiments were performed with 1×10^9 bacteria in an inoculum of an equal mixture of the wild-type and the *ymoA*-deficient strain (Figure 9E). Ten times less bacteria of the mutant were identified in the PPs and the MLNs, and only few numbers of bacteria were able to reach liver and spleen. Calculations of the competitive index of the mutant relative to wild-type clearly indicated that presence of YmoA is advantageous for the colonization of *Y. pseudotuberculosis* in all tested organs (Figure 9F).

DISCUSSION

Rapid adaptation of the gene expression profile by bacterial pathogens to changing environments within their hosts is a prerequisite to persist and establish a successful infection. Complex regulatory networks including global transcriptional and post-transcriptional regulatory factors orchestrate global cellular changes and control expression of virulence factors in close association with stress adaptation and metabolic functions. The carbon storage regulator (Csr) system composed of the RNA-binding protein CsrA and at least two regulatory RNAs (CsrB and CsrC) play a central role in the control of many host-pathogen interactions (Lucchetti-Miganeh et al., 2008; Kusmierek and Dersch, 2017; Romeo and Babitzke, 2018; Pourciau et al., 2020). In this report, we show that the *Yersinia* modulating protein YmoA is crucial for the control of Csr-type regulatory RNAs and reprograms virulence-relevant functions important for different stages of the infection (Figure 1B).

The YmoA protein of *Yersinia* belongs to a class of small proteins which modulate virulence gene expression in *Enterobacteriaceae* in response to environmental changes, e.g., temperature (Madrid et al., 2007). YmoA has a high amino acid sequence identity to and a similar overall fold consisting of four helices to Hha of *E. coli* which was identified as repressor of α -hemolysin production and other virulence genes (Mourino et al., 1996; Sharma and Zuerner, 2004; McFeeters et al., 2007). Also, the *Yersinia* YmoA protein is a key regulator of pathogenicity factors. It was identified as a thermosensitive transcriptional silencer for *lcrF* expression. LcrF is a key regulator for the pYV-encoded temperature-induced T3SS and *yop* effector genes important to prevent the immune defense after entry of the gut-associated lymphatic tissues (Mikulskis et al., 1994; Jackson et al., 2004; Böhme et al., 2012). Hence, by controlling *lcrF* expression, YmoA regulates one of the most crucial pathogenicity factors for infection of the human host. In this study, we show that YmoA also activates expression of virulence genes important for host tissue colonization during early stages of the infection. YmoA induces expression of the virulence regulator gene *rovA* and the RovA-dependent *invA* gene by downregulation of the LysR repressor RovM, and this is mediated through YmoA-dependent changes of the global post-transcriptional Csr system (Figure 10). YmoA was found to enhance the stability of the CsrC RNA and this was shown to involve sequences within the 5'-region of the CsrC RNA predicted to form an extended stem-loop.



Turnover of regulatory RNAs is a highly regulated process. Potential pathways for modulation include recruitment or inhibition of RNA decay enzymes (RNases), formation of stabilizing RNA secondary structures and/or alteration of the expression, activity or localization of RNA-binding factors. In *E. coli* and *Salmonella enterica* serovar Typhimurium, CsrB and CsrC decay involves the essential enzyme RNase E, a single-strand-specific endoribonuclease, which associates with the 3'-5' processive exonuclease polynucleotide phosphorylase (PNPase), the glycolytic enzyme enolase, and an RNA helicase (RhlB/CsdA) to form an RNA-degrading complex (degradosome) (Suzuki et al., 2006; Viegas et al., 2007). Processing of the *Salmonella* CsrC RNA at one of the longer 3' stems is also RNase III-dependent (Viegas et al., 2007). Here, we show that a 5'-terminal segment between nt +24 and +57 of the *Yersinia* CsrC RNA which is able to form a stem-loop structure is important for

its stabilization. It is likely that the accessibility of potential ribonuclease cleavage sites is inhibited by this structured RNA element. However, none of the genes for RNase III (*rnc*), PNPase (*pnp*), and RNase E (*rne*) were differently expressed in the $\Delta ymoA$ mutant (**Supplementary Table 4**). As this part of the RNA varies significantly from *E. coli* and *Salmonella* CsrC and no smaller CsrC transcripts were detectable, it seems that CsrC decay mechanism in *Yersinia* differs from the other CsrC RNAs.

As absence of the hairpin sequence in the *csrC* gene eliminates YmoA influence on CsrC stabilization, it is also possible that YmoA controls RNA-binding proteins, protecting CsrC from decay. Although the abundance of CsrB and CsrC of *Y. pseudotuberculosis* is positively affected by the RNA chaperone Hfq, we show that YmoA acts independently of Hfq. As Hfq is still able to induce *csrC*(+4)-*lacZ* fusion, it is more likely that Hfq activates *csrC* expression indirectly through control of (an)other sensory or regulatory RNA(s). We further found that also the RNA-binding protein CsrA is crucial for CsrC abundance in *Yersinia*, and absence of YmoA could be partly overcome by CsrA overexpression. This implies that stabilization of CsrC by CsrA might either impede the activity of a YmoA-dependent destabilizing factor or CsrA might act as a stabilization factor itself. The most highly conserved element of CsrA binding sites is a GGA sequence. Five GGA motifs are located within the stabilizing 5' region of the CsrC RNA, one in the loop, two at the 5'- and 3'-end of the hairpin structure and one at the start and end of the sequence (**Figure 4C**), which could assist in the formation of the stabilizing RNA element and/or protection of RNase cleavage sites. In this case, sequestration of CsrA to other target sequences would destabilize CsrC. Although overall CsrA levels remain unchanged in the absence of YmoA (**Figure 3B**), it is possible that global transcriptional changes of 289 genes detected in the $\Delta ymoA$ mutant – the great majority (79%) of which were upregulated – are associated with a significant increase of alternative CsrA target transcripts, which would reduce the availability of free CsrA to bind and stabilize the CsrC transcript. Similarly, CsrB and CsrC synthesis in *E. coli* is positively regulated by CsrA, but their stability was essentially identical between wild-type and the *csrA* mutant. This indicated that CsrA does not directly affect CsrB and CsrC RNA degradation in this organism (Gudapaty et al., 2001; Weilbacher et al., 2003).

Several years ago, Saxena and Gowrishankar (2011) showed that overexpression of the YmoA/Hha paralog YdgT suppressed the phenotypes of *rho* and *nusG* mutants. They suggest a model whereby YdgT modulates Rho-dependent transcription termination, by compensating for Rho loss (Saxena and Gowrishankar, 2011). Following the *E. coli* model, YmoA would increase transcriptional termination, what is not observed with *csrC*. Nonetheless, the hairpin structure of CsrC could be involved in premature transcriptional termination which could be inhibited by YmoA. However, no short, truncated CsrC transcripts have been identified with CsrC-specific probes.

Several studies further indicate that the global YmoA/Hha modulators exert their effect through heterocomplex formation with H-NS (Nieto et al., 2002; Madrid et al., 2007). As YmoA was also found to be structurally similar to H-NS, it was further suggested that YmoA may intercalate into higher-order

structures by substituting for an H-NS dimer (McFeeters et al., 2007). H-NS is a highly abundant DNA-binding protein, which binds and polymerizes along AT-rich, curved DNA sites and acts as global regulator of gene expression in response to environmental signals (Bouffartigues et al., 2007; Fang and Rimsky, 2008). Heterocomplex formation with YmoA modifies the biological activity of H-NS and reduces or increases its ability to repress transcription (Nieto et al., 2002; Banos et al., 2008). Alike YmoA, H-NS controls the amount of CsrC and complements the decrease of CsrC levels in an *ymoA* mutant, indicating that YmoA and H-NS most likely acts in a cooperative manner to modulate transcription of factors controlling CsrC decay.

More recently, YmoA/Hha, together with YmoB/TomB(YbaJ) encoded in the same operon, was found to constitute a type II toxin-antitoxin (TA), which is implicated in the formation of persister cells and biofilms by repressing type I fimbriae expression in related *Enterobacteriaceae* (García-Contreras et al., 2008; Marimon et al., 2016). In *E. coli*, TomB(YbaJ) transiently interacts with the YmoA homolog Hha and initiates spontaneous oxidation of a conserved Cys residue leading to a destabilization of Hha. Its function can be replaced by the TomB homolog YmoB of *Yersinia* (Marimon et al., 2016). Interestingly, the abundance of the *ymoB* transcript is strongly (81-fold) increased in the absence of *ymoA* (**Supplementary Table 4**), indicating a negative autoregulatory loop. This reveals also the possibility that enhanced degradation of CsrC and changes of RovM, RovA and InvA levels in the $\Delta ymoA$ mutant could be promoted through upregulation of YmoB. The overall contribution of the TA system is not yet fully understood, but induction of the TA loci by environmental stress conditions led to the idea that these systems enhance bacterial fitness under adverse conditions and play roles in pathogenesis (Norton and Mulvey, 2012). Our work showing that YmoA manipulates the global post-transcriptional Csr system, influences multiple fitness- and virulence-relevant components and has a strong effect on virulence, supports this assumption.

Our transcriptome analysis revealed a global impact of YmoA on early and later stage virulence genes. This includes virulence traits important for host tissue colonization such as cell adhesion and invasion factors (invasin, Ail, PsaA adhesin, and fimbriae), toxins and type VI secretion system components as well as immune cell defense strategies (T3SS-Yops). Moreover, a variety of genes for stress responses experienced in the initial stage of the infection (oxidative stress, starvation, and pH) are activated by YmoA, whereas factors promoting translation and proper folding of proteins (e.g., heat stress/shock genes) are repressed. In addition, metabolic activities related to the amino acid/nitrogen metabolism and assimilation are activated, whereas the metabolism of many carbon sources is repressed by YmoA (**Figures 1B,C** and **Supplementary Table 4**). This reprogramming implicates control of the Csr system which (i) plays a central role coordinating virulence gene expression with adaptative responses functions for different nutritional demands and stress resistance during infections (Lucchetti-Miganeh et al., 2008; Timmermans and Van Melder, 2010; Bückner et al., 2014; Kusmirek and Dersch, 2017) and (ii)

promotes transition between different physiological stages of pathogens, e.g., the switch from an acute to a chronic infection or from a transmission into an intracellular replication state (Molofsky and Swanson, 2003; Goodman et al., 2004; Laskowski and Kazmierczak, 2006; Mulcahy et al., 2008; Brencic and Lory, 2009; Sahr et al., 2009).

One important environmental parameter, which induce global alterations in the gene expression and reprogramming between the different virulence-related stages of *Yersinia*, is temperature (Nuss et al., 2015; Schmühl et al., 2019). As YmoA turnover by the ClpP and Lon proteases is modulated by temperature (Jackson et al., 2004) (Supplementary Figure 8), it is tempting to speculate that YmoA plays a crucial role adjusting the Csr regulon in response to temperature which is pivotal for the establishment of a successful infection.

Based on our analysis we assume that thermosensitive YmoA promotes expression of very early-stage virulence-relevant traits to promote initiation of the infection. Subsequent degradation of YmoA at 37°C within the host will then trigger an upregulation of pathogenicity factors, i.e., toxin CNF γ and the antiphagocytic T3SS/Yop machinery, and improve use of carbon sources, which are crucial for the establishment of the infection in the intestine and underlying lymphoid tissues. Co-induction of mechanisms that promote protein translation and folding may guarantee a rapid and highly efficient production of these virulence traits. This global impact of YmoA on virulence was visible in non-competitive mouse infection studies and was even more noticeable in competitive assays in which the *ymoA* mutant was clearly outcompeted by the wild-type. Many questions concerning the molecular interactions between YmoA and the Csr system, and significance of YmoA-controlled genes for virulence remain to be solved. Yet, it is foreseeable that the YmoA-Csr control network is a valuable target for antibacterial therapeutics to block the bacteria at specific stages during infection.

DATA AVAILABILITY STATEMENT

The datasets generated for this study can be found in online repositories. The names of the repository/repositories and accession number(s) can be found in the article/Supplementary Material.

ETHICS STATEMENT

The animal study was reviewed and approved by Niedersächsisches Landesamt für Verbraucherschutz und Lebensmittelsicherheit: animal licensing committee permission no. 33.9.42502-04-055/09.

AUTHOR CONTRIBUTIONS

AH, KB, and PD designed the research. AH, KB, and SL performed the experiments. AH, KB, SL, PD, ASS, and YG analyzed the data. AH, KB, and PD interpreted the data. AH and PD wrote the manuscript. AH and ASS edited the manuscript.

PD acquired funding. All authors contributed to the article and approved the submitted version.

FUNDING

This work was supported by Deutsche Forschungsgemeinschaft Grant DE616/3 and DE616/7. YG has a stipend of the China Scholarship Council.

ACKNOWLEDGMENTS

We thank Martin Fenner for helpful discussions. Further we thank Tatjana Stolz and Tanja Krause for technical support, Rebekka Steinmann and Janika Viereck for construction of plasmids, and Jana Melzer, Johannes Klein, and Richard Münch for support in the analysis of the microarray data.

SUPPLEMENTARY MATERIAL

The Supplementary Material for this article can be found online at: <https://www.frontiersin.org/articles/10.3389/fmicb.2021.706934/full#supplementary-material>

Supplementary Figure 1 | Influence of the growth medium, growth phase and temperature on YmoA synthesis. *Y. pseudotuberculosis* strain YPIII was grown in LB or minimal medium A (MMA) to exponential ($OD_{600} = 0.8$) or stationary phase at 25 and 37°C. Whole cell extracts of the cultures were prepared, proteins were separated on 18% TRICINE polyacrylamide gels and analyzed by Western blotting with a polyclonal antibody directed against YmoA and CsrA. Cell extracts of an *ymoA* and a *csrA* mutant strain were used as controls. A used prestained molecular weight marker is indicated on the left. Unspecifically detected proteins (c) were used as loading control.

Supplementary Figure 2 | YmoA has no influence on *rovA* expression through H-NS. *Y. pseudotuberculosis* strain YPIII and YP50 ($\Delta ymoA$) harboring the empty vector (V), or a dominant negative *hns** allele (pAKH31) were cultivated overnight in LB medium at 25°C. Whole cell extracts were prepared, separated by SDS-PAGE and analyzed by Western blotting with a polyclonal antibody directed against RovA. Cell extracts of a *rovA* mutant was used as control. Unspecifically detected proteins (c) were used as loading control.

Supplementary Figure 3 | Influence of YmoA on the Csr system occurs through CsrC. *Y. pseudotuberculosis* strains YPIII (wild-type), YP50 ($\Delta ymoA$), YP69 ($\Delta csrB$), and YP75 ($\Delta csrB$ and $\Delta ymoA$) were grown in LB at 25°C overnight. (A) Total RNA of the strains was extracted, and CsrC transcripts were detected by Northern blotting with a CsrC-specific probe. The 16S rRNAs are shown as RNA loading control. (B) In parallel, whole-cell extracts were prepared from the cultures and analyzed by Western blotting with a polyclonal antibody directed against RovM. A molecular weight marker is loaded on the left. Unspecifically detected proteins (c) were used as loading control.

Supplementary Figure 4 | YmoA has a positive effect on CsrC stability. (A) *Y. pseudotuberculosis* strains YPIII (wild-type) and YP50 ($\Delta ymoA$) harboring a $P_{tet}:lacZ$ expression construct (pTT1) were grown to exponential phase in minimal medium at 25°C in the presence of 0.5 nM anhydrotetracycline. β -galactosidase activity from the overnight cultures was determined and is given in $\mu\text{mol min}^{-1} \text{mg}^{-1}$ for comparison. The data represent the average \pm SD from at least three different experiments each done in duplicate. (B) *Y. pseudotuberculosis* strains YPIII (wild-type) and YP50 ($\Delta ymoA$) harboring the empty vector (pHSG576) or a $P_{tet}:csrC$ expression construct (pKB47) were grown to exponential phase in minimal medium at 25°C in the presence of 0.5 nM anhydrotetracycline. Total RNA of the strains was extracted and CsrC was detected by Northern blotting with a CsrC-specific probe. The 16S and 23S rRNAs are shown as RNA loading control.

Supplementary Figure 5 | Hfq influence on RovA and RovM levels.

Y. pseudotuberculosis strain YPIII and YP80 (Δhfq) carrying the vector pAKH85 (pV) or its *hfq*⁺ (pAKH115) were grown in LB at 25°C overnight. Whole-cell extracts from the overnight cultures were prepared and analyzed by Western blotting with polyclonal antibodies directed against RovA or RovM. Unspecifically detected proteins (c) were used as loading control.

Supplementary Figure 6 | YmoA influence on Hfq production.

Y. pseudotuberculosis strain YPIII and YP50 ($\Delta ymoA$) carrying the vector pAKH85 (pV) or its *ymoA*⁺ derivative (pAKH71) were grown in LB at 25°C overnight. Whole-cell extracts from the overnight cultures were prepared and analyzed by Western blotting with a polyclonal antibody directed against Hfq. An unspecifically detected protein (c) was used as loading control.

Supplementary Figure 7 | Analysis of YmoA and H-NS binding to CsrC and *yscW*. (A) CsrC RNA (+1 to +150) and a 5S RNA fragment serving as a negative

control as well as (B) the *yscW-lcrF* promoter fragment and a *csdD* fragment of *E. coli* serving as negative control were incubated without or with increasing amounts of purified *Y. pseudotuberculosis* YmoA in the presence or absence of H-NS or H-NS alone. The samples were separated on 8% polyacrylamide gels. The positions of the gene fragments are indicated, and the formation of higher molecular complexes is shown by an arrow.

Supplementary Figure 8 | Temperature-dependent YmoA degradation.

Whole cell extracts from overnight cultures of *Y. pseudotuberculosis* strains YPIII (wild-type), YP63 ($\Delta clpP$), YP64 (Δlon) and YP67 ($\Delta clpP \Delta lon$) grown in LB at 25 and 37°C were prepared, separated by 20% TRICINE-PAGE and analyzed by Western blotting using a polyclonal anti-YmoA antibody. Whole cell extract of an overnight culture of YP50 ($\Delta ymoA$) was used as negative control. A molecular weight marker was loaded on the left, the YmoA protein is indicated by an arrow. Unspecifically detected proteins (c) were used as loading control.

REFERENCES

- Alexa, A., Rahnenfuhrer, J., and Lengauer, T. (2006). Improved scoring of functional groups from gene expression data by decorrelating GO graph structure. *Bioinformatics* 22, 1600–1607. doi: 10.1093/bioinformatics/btl140
- Banos, R. C., Pons, J. I., Madrid, C., and Juarez, A. (2008). A global modulatory role for the *Yersinia enterocolitica* H-NS protein. *Microbiology* 154, 1281–1289. doi: 10.1099/mic.0.2007/015610-0
- Barnes, P. D., Bergman, M. A., Mecsas, J., and Isberg, R. R. (2006). *Yersinia pseudotuberculosis* disseminates directly from a replicating bacterial pool in the intestine. *J. Exp. Med.* 203, 1591–1601. doi: 10.1084/jem.20060905
- Bliska, J. B., Wang, X., Viboud, G. I., and Brodsky, I. E. (2013). Modulation of innate immune responses by *Yersinia* type III secretion system translocators and effectors. *Cell. Microbiol.* 15, 1622–1631. doi: 10.1111/cmi.12164
- Böhme, K., Steinmann, R., Kortmann, J., Seekircher, S., Heroven, A. K., Berger, E., et al. (2012). Concerted actions of a thermo-labile regulator and a unique intergenic RNA thermosensor control *Yersinia virulence*. *PLoS Pathog.* 8:e1002518. doi: 10.1371/journal.ppat.1002518
- Bottone, E. J. (1997). *Yersinia enterocolitica*: the charisma continues. *Clin. Microbiol. Rev.* 10, 257–276. doi: 10.1128/cmr.10.2.257-276.1997
- Bouffartigues, E., Buckle, A., Badaut, C., Travers, A., and Rimsky, S. (2007). H-NS cooperative binding to high-affinity sites in a regulatory element results in transcriptional silencing. *Nat. Struct. Mol. Biol.* 14, 441–448. doi: 10.1038/nsmb1233
- Brencic, A., and Lory, S. (2009). Determination of the regulon and identification of novel mRNA targets of *Pseudomonas aeruginosa* RsmA. *Mol. Microbiol.* 72, 612–632. doi: 10.1111/j.1365-2958.2009.06670.x
- Brescia, C. C., Kaw, M. K., and Sledjeski, D. D. (2004). The DNA binding protein H-NS binds to and alters the stability of RNA in vitro and in vivo. *J. Mol. Biol.* 339, 505–514. doi: 10.1016/j.jmb.2004.03.067
- Bücker, R., Heroven, A. K., Becker, J., Dersch, P., and Wittmann, C. (2014). The pyruvate-tricarboxylic acid cycle node: a focal point of virulence control in the enteric pathogen *Yersinia pseudotuberculosis*. *J. Biol. Chem.* 289, 30114–30132. doi: 10.1074/jbc.M114.581348
- Cathelyn, J. S., Crosby, S. D., Latham, W. W., Goldman, W. E., and Miller, V. L. (2006). RovA, a global regulator of *Yersinia pestis*, specifically required for bubonic plague. *Proc. Natl. Acad. Sci. U.S.A.* 103, 13514–13519. doi: 10.1073/pnas.0603456103
- Cathelyn, J. S., Ellison, D. W., Hinchliffe, S. J., Wren, B. W., and Miller, V. L. (2007). The RovA regulons of *Yersinia enterocolitica* and *Yersinia pestis* are distinct: evidence that many RovA-regulated genes were acquired more recently than the core genome. *Mol. Microbiol.* 66, 189–205. doi: 10.1111/j.1365-2958.2007.05907.x
- Chen, S., Thompson, K. M., and Francis, M. S. (2016). Environmental regulation of *Yersinia* pathophysiology. *Front. Cell. Infect. Microbiol.* 6:25. doi: 10.3389/fcimb.2016.00025
- Cornelis, G. R. (1993). Role of the transcription activator virF and the histone-like protein YmoA in the thermoregulation of virulence functions in *Yersinia*. *Zentralbl. Bakteriol.* 278, 149–164. doi: 10.1016/s0934-8840(11)80833-9
- Cornelis, G. R. (2006). The type III secretion injectisome. *Nat. Rev. Microbiol.* 4, 811–825. doi: 10.1038/nrmicro1526
- Cornelis, G. R., Sluiter, C., Delor, I., Geib, D., Kaniga, K., Lambert de Rouvroit, C., et al. (1991). *ymoA*, a *Yersinia enterocolitica* chromosomal gene modulating the expression of virulence functions. *Mol. Microbiol.* 5, 1023–1034. doi: 10.1111/j.1365-2958.1991.tb01875.x
- Datsenko, K. A., and Wanner, B. L. (2000). One-step inactivation of chromosomal genes in *Escherichia coli* K-12 using PCR products. *Proc. Natl. Acad. Sci. U.S.A.* 97, 6640–6645. doi: 10.1073/pnas.120163297
- de la Cruz, F., Carmona, M., and Juarez, A. (1992). The Hha protein from *Escherichia coli* is highly homologous to the YmoA protein from *Yersinia enterocolitica*. *Mol. Microbiol.* 6, 3451–3452. doi: 10.1111/j.1365-2958.1992.tb02214.x
- Derbise, A., Lescic, B., Dacheux, D., Ghigo, J. M., and Carniel, E. (2003). A rapid and simple method for inactivating chromosomal genes in *Yersinia*. *FEMS Immunol. Med. Microbiol.* 38, 113–116. doi: 10.1016/s0928-8244(03)00181-0
- Dersch, P., and Isberg, R. R. (1999). A region of the *Yersinia pseudotuberculosis* invasin protein enhances integrin-mediated uptake into mammalian cells and promotes self-association. *EMBO J.* 18, 1199–1213. doi: 10.1093/emboj/18.5.1199
- Ellison, D. W., and Miller, V. L. (2006). H-NS represses *inv* transcription in *Yersinia enterocolitica* through competition with RovA and interaction with YmoA. *J. Bacteriol.* 188, 5101–5112. doi: 10.1128/jb.00862-05
- Fang, F. C., and Rimsky, S. (2008). New insights into transcriptional regulation by H-NS. *Curr. Opin. Microbiol.* 11, 113–120. doi: 10.1016/j.mib.2008.02.011
- Galindo, C. L., Rosenzweig, J. A., Kirtley, M. L., and Chopra, A. K. (2011). Pathogenesis of *Y. enterocolitica* and *Y. pseudotuberculosis* in human yersiniosis. *J. Pathog.* 2011:182051. doi: 10.4061/2011/182051
- García-Contreras, R., Zhang, X.-S., Kim, Y., and Wood, T. K. (2008). Protein translation and cell death: the role of rare tRNAs in biofilm formation and in activating dormant phase killer genes. *PLoS One* 3:e2394. doi: 10.1371/journal.pone.0002394
- Gentleman, R. C., Carey, V. J., Bates, D. M., Bolstad, B., Dettling, M., Dudoit, S., et al. (2004). Bioconductor: open software development for computational biology and bioinformatics. *Genome Biol.* 5:R80.
- Goodman, A. L., Kulasekara, B., Rietsch, A., Boyd, D., Smith, R. S., and Lory, S. (2004). A signaling network reciprocally regulates genes associated with acute infection and chronic persistence in *Pseudomonas aeruginosa*. *Dev. Cell* 7, 745–754. doi: 10.1016/j.devcel.2004.08.020
- Gudapaty, S., Suzuki, K., Wang, X., Babitzke, P., and Romeo, T. (2001). Regulatory interactions of Csr components: the RNA binding protein CsrA activates *csrB* transcription in *Escherichia coli*. *J. Bacteriol.* 183, 6017–6027. doi: 10.1128/jb.183.20.6017-6027.2001
- Heroven, A. K., and Dersch, P. (2006). RovM, a novel LysR-type regulator of the virulence activator gene *rovA*, controls cell invasion, virulence and motility of *Yersinia pseudotuberculosis*. *Mol. Microbiol.* 62, 1469–1483. doi: 10.1111/j.1365-2958.2006.05458.x
- Heroven, A. K., and Dersch, P. (2014). Coregulation of host-adapted metabolism and virulence by pathogenic *Yersinia*. *Front. Cell. Infect. Microbiol.* 4:146. doi: 10.3389/fcimb.2014.00146

- Heroven, A. K., Böhme, K., and Dersch, P. (2012a). The Csr/Rsm system of *Yersinia* and related pathogens: a post-transcriptional strategy for managing virulence. *RNA Biol* 9, 379–391. doi: 10.4161/rna.19333
- Heroven, A. K., Böhme, K., Rohde, M., and Dersch, P. (2008). A Csr-type regulatory system, including small non-coding RNAs, regulates the global virulence regulator RovA of *Yersinia pseudotuberculosis* through RovM. *Mol. Microbiol.* 68, 1179–1195. doi: 10.1111/j.1365-2958.2008.06218.x
- Heroven, A. K., Nagel, G., Tran, H. J., Parr, S., and Dersch, P. (2004). RovA is autoregulated and antagonizes H-NS-mediated silencing of invasin and rovA expression in *Yersinia pseudotuberculosis*. *Mol. Microbiol.* 53, 871–888. doi: 10.1111/j.1365-2958.2004.04162.x
- Heroven, A. K., Sest, M., Pisano, F., Scheb-Wetzel, M., Steinmann, R., Böhme, K., et al. (2012b). Crp induces switching of the CsrB and CsrC RNAs in *Yersinia pseudotuberculosis* and links nutritional status to virulence. *Front. Cell Infect. Microbiol.* 2:158. doi: 10.3389/fcimb.2012.00158
- Hoe, N. P., and Goguen, J. D. (1993). Temperature sensing in *Yersinia pestis*: translation of the LcrF activator protein is thermally regulated. *J. Bacteriol.* 175, 7901–7909. doi: 10.1128/jb.175.24.7901-7909.1993
- Jackson, M. W., Silva-Herzog, E., and Plano, G. V. (2004). The ATP-dependent ClpXP and Lon proteases regulate expression of the *Yersinia pestis* type III secretion system via regulated proteolysis of YmoA, a small histone-like protein. *Mol. Microbiol.* 54, 1364–1378. doi: 10.1111/j.1365-2958.2004.04353.x
- Koornhof, H. J., Smego, R. A., and Nicol, M. (1999). Yersiniosis. II: The pathogenesis of *Yersinia* infections. *Eur. J. Clin. Microbiol. Infect. Dis.* 18, 87–112. doi: 10.1007/s100960050237
- Kusmieriek, M., and Dersch, P. (2017). Regulation of host-pathogen interactions via the post-transcriptional Csr/Rsm system. *Curr. Opin. Microbiol.* 41, 58–67. doi: 10.1016/j.mib.2017.11.022
- Kusmieriek, M., Hofmann, J., Witte, R., Opitz, W., Vollmer, I., Volk, M., et al. (2019). A bacterial secreted translocator hijacks riboregulators to control type III secretion in response to host cell contact. *PLoS Pathog.* 15:e1007813. doi: 10.1371/journal.ppat.1007813
- Lambert de Rouvroit, C., Sluiter, C., and Cornelis, G. R. (1992). Role of the transcriptional activator, VirF, and temperature in the expression of the pYV plasmid genes of *Yersinia enterocolitica*. *Mol. Microbiol.* 6, 395–409. doi: 10.1111/j.1365-2958.1992.tb01483.x
- Laskowski, M. A., and Kazmierczak, B. I. (2006). Mutational analysis of RetS, an unusual sensor kinase-response regulator hybrid required for *Pseudomonas aeruginosa* virulence. *Infect. Immun.* 74, 4462–4473. doi: 10.1128/iai.00575-06
- Lawal, A., Kirtley, M. L., van Lier, C. J., Erova, T. E., Kozlova, E. V., Sha, J., et al. (2013). The effects of modeled microgravity on growth kinetics, antibiotic susceptibility, cold growth, and the virulence potential of a *Yersinia pestis* ymoA-deficient mutant and its isogenic parental strain. *Astrobiology* 13, 821–832. doi: 10.1089/ast.2013.0968
- Lucchetti-Miganeh, C., Burrows, E., Baysse, C., and Ermel, G. (2008). The post-transcriptional regulator CsrA plays a central role in the adaptation of bacterial pathogens to different stages of infection in animal hosts. *Microbiology* 154, 16–29. doi: 10.1099/mic.0.2007/012286-0
- Madrid, C., Balsalobre, C., Garcia, J., and Juarez, A. (2007). The novel Hha/YmoA family of nucleoid-associated proteins: use of structural mimicry to modulate the activity of the H-NS family of proteins. *Mol. Microbiol.* 63, 7–14. doi: 10.1111/j.1365-2958.2006.05497.x
- Madrid, C., Nieto, J. M., and Juarez, A. (2002). Role of the Hha/YmoA family of proteins in the thermoregulation of the expression of virulence factors. *Int. J. Med. Microbiol.* 291, 425–432. doi: 10.1078/1438-4221-00149
- Manoil, C. (1990). Analysis of protein localization by use of gene fusions with complementary properties. *J. Bacteriol.* 172, 1035–1042. doi: 10.1128/jb.172.2.1035-1042.1990
- Marceau, M. (2005). Transcriptional regulation in *Yersinia*: an update. *Curr. Issues Mol. Biol.* 7, 151–177.
- Marimon, O., Teixeira, J. M. C., Cordeiro, T. N., Soo, V. W. C., Wood, T. L., Mayzel, M., et al. (2016). An oxygen-sensitive toxin-antitoxin system. *Nat. Commun.* 7:13634.
- Marra, A., and Isberg, R. R. (1997). Invasin-dependent and invasin-independent pathways for translocation of *Yersinia pseudotuberculosis* across the Peyer's patch intestinal epithelium. *Infect. Immun.* 65, 3412–3421. doi: 10.1128/iai.65.8.3412-3421.1997
- Mayer, O., Waldsich, C., Grossberger, R., and Schroeder, R. (2002). Folding of the td pre-RNA with the help of the RNA chaperone StpA. *Biochem. Soc. Trans.* 30, 1175–1180. doi: 10.1042/bst0301175
- McFeeters, R. L., Altieri, A. S., Cherry, S., Tropea, J. E., Waugh, D. S., and Byrd, R. A. (2007). The high-precision solution structure of *Yersinia* modulating protein YmoA provides insight into interaction with H-NS. *Biochemistry* 46, 13975–13982. doi: 10.1021/bi701210j
- Mikulskis, A. V., and Cornelis, G. R. (1994). A new class of proteins regulating gene expression in enterobacteria. *Mol. Microbiol.* 11, 77–86. doi: 10.1111/j.1365-2958.1994.tb00291.x
- Mikulskis, A. V., Delor, I., Thi, V. H., and Cornelis, G. R. (1994). Regulation of the *Yersinia enterocolitica* enterotoxin Yst gene. Influence of growth phase, temperature, osmolarity, pH and bacterial host factors. *Mol. Microbiol.* 14, 905–915. doi: 10.1111/j.1365-2958.1994.tb01326.x
- Miller, J. H. (1992). *A Short Course In Bacterial Genetic: A Laboratory Manual And Handbook For Escherichia Coli And Related Bacteria*. Cold Spring Harbor, New York: Cold Spring Harbor Laboratory Press.
- Molofsky, A. B., and Swanson, M. S. (2003). *Legionella pneumophila* CsrA is a pivotal repressor of transmission traits and activator of replication. *Mol. Microbiol.* 50, 445–461. doi: 10.1046/j.1365-2958.2003.03706.x
- Monk, I. R., Casey, P. G., Cronin, M., Gahan, C. G., and Hill, C. (2008). Development of multiple strain competitive index assays for *Listeria monocytogenes* using pIMC; a new site-specific integrative vector. *BMC Microbiol.* 8:96. doi: 10.1186/1471-2180-8-96
- Mourino, M., Madrid, C., Balsalobre, C., Prenafeta, A., Munoa, F., Blanco, J., et al. (1996). The Hha protein as a modulator of expression of virulence factors in *Escherichia coli*. *Infect. Immun.* 64, 2881–2884. doi: 10.1128/iai.64.7.2881-2884.1996
- Mulcahy, H., O'Callaghan, J., O'Grady, E. P., Macia, M. D., Borrell, N., Gomez, C., et al. (2008). *Pseudomonas aeruginosa* RsmA plays an important role during murine infection by influencing colonization, virulence, persistence, and pulmonary inflammation. *Infect. Immun.* 76, 632–638. doi: 10.1128/iai.01132-07
- Nagel, G., Lahrz, A., and Dersch, P. (2001). Environmental control of invasin expression in *Yersinia pseudotuberculosis* is mediated by regulation of RovA, a transcriptional activator of the SlyA/Hor family. *Mol. Microbiol.* 41, 1249–1269. doi: 10.1046/j.1365-2958.2001.02522.x
- Nieto, J. M., Madrid, C., Miquel, E., Parra, J. L., Rodriguez, S., and Juarez, A. (2002). Evidence for direct protein-protein interaction between members of the enterobacterial Hha/YmoA and H-NS families of proteins. *J. Bacteriol.* 184, 629–635. doi: 10.1128/jb.184.3.629-635.2002
- Norton, J. P., and Mulvey, M. A. (2012). Toxin-Antitoxin systems are important for niche-specific colonization and stress resistance of uropathogenic *Escherichia coli*. *PLoS Pathog.* 8:e1002954. doi: 10.1371/journal.ppat.1002954
- Nuss, A. M., Beckstette, M., Pimenova, M., Schmöhl, C., Opitz, W., Pisano, F., et al. (2017a). Tissue dual RNA-seq: a fast discovery path for infection-specific functions and riboregulators shaping host-pathogen transcriptomes. *Proc. Natl. Acad. Sci. U.S.A.* 114, E791–E800.
- Nuss, A. M., Heroven, A. K., and Dersch, P. (2017b). RNA regulators: formidable modulators of *Yersinia* virulence. *Trends Microbiol.* 25, 19–34. doi: 10.1016/j.tim.2016.08.006
- Nuss, A. M., Heroven, A. K., Waldmann, B., Reinkensmeier, J., Jarek, M., Beckstette, M., et al. (2015). Transcriptomic profiling of *Yersinia pseudotuberculosis* reveals reprogramming of the Crp regulon by temperature and uncovers Crp as a master regulator of small RNAs. *PLoS Genet.* 11:e1005087. doi: 10.1371/journal.pgen.1005087
- Nuss, A. M., Schuster, F., Kathrin Heroven, A., Heine, W., Pisano, F., and Dersch, P. (2014). A direct link between the global regulator PhoP and the Csr regulon in *Y. pseudotuberculosis* through the small regulatory RNA CsrC. *RNA Biol.* 11, 580–593. doi: 10.4161/rna.28676
- Pepe, J. C., and Miller, V. L. (1993). *Yersinia enterocolitica* invasin: a primary role in the initiation of infection. *Proc. Natl. Acad. Sci. U.S.A.* 90, 6473–6477. doi: 10.1073/pnas.90.14.6473
- Pfaffl, M. W. (2001). A new mathematical model for relative quantification in real-time RT-PCR. *Nucleic Acids Res.* 29:e45.
- Pourciau, C., Lai, Y.-J., Gorelik, M., Babitzke, P., and Romeo, T. (2020). Diverse mechanisms and circuitry for global regulation by the RNA-Binding protein CsrA. *Front. Microbiol.* 11:601352. doi: 10.3389/fmicb.2020.601352

- Romeo, T., and Babitzke, P. (2018). Global regulation by CsrA and its RNA antagonists. *Microbiol. Spectr.* 6:2. doi: 10.1128/microbiolspec.RWR-0009-2017
- Sahr, T., Bruggemann, H., Jules, M., Lomma, M., Albert-Weissenberger, C., Cazalet, C., et al. (2009). Two small ncRNAs jointly govern virulence and transmission in *Legionella pneumophila*. *Mol. Microbiol.* 72, 741–762. doi: 10.1111/j.1365-2958.2009.06677.x
- Sambrook, J. (2001). *Molecular Cloning: A Laboratory Manual*. Cold Spring Harbor, NY: Cold Spring Harbor Laboratories.
- Saxena, S., and Gowrishankar, J. (2011). Compromised factor-dependent transcription termination in a nusA mutant of *Escherichia coli*: spectrum of termination efficiencies generated by perturbations of Rho, NusG, NusA, and H-NS family proteins. *J. Bacteriol.* 193, 3842–3850. doi: 10.1128/JB.00221-11
- Schagger, H. (2006). Tricine-SDS-PAGE. *Nat. Protoc.* 1, 16–22. doi: 10.1038/nprot.2006.4
- Schmühl, C., Beckstette, M., Heroven, A. K., Bunk, B., Spröer, C., McNally, A., et al. (2019). Comparative transcriptomic profiling of *Yersinia enterocolitica* O:3 and O:8 reveals major expression differences of fitness- and virulence-relevant genes indicating ecological separation. *mSystems* 4:e00239–18. doi: 10.1128/mSystems.00239-18
- Schneiders, S., Hechard, T., Edgren, T., Avican, K., Fällman, M., Fahlgren, A., et al. (2021). Spatiotemporal variations in growth rate and virulence plasmid copy number during *Yersinia pseudotuberculosis* infection. *Infect. Immun.* 89, e710–e720. doi: 10.1128/IAI.00710-20
- Schwiesow, L., Lam, H., Dersch, P., and Auerbuch, V. (2015). *Yersinia* type III secretion system master regulator LcrF. *J. Bacteriol.* 198, 604–614. doi: 10.1128/JB.00686-15
- Sharma, V. K., and Zuercher, R. L. (2004). Role of hha and ler in transcriptional regulation of the esp operon of enterohemorrhagic *Escherichia coli* O157:H7. *J. Bacteriol.* 186, 7290–7301. doi: 10.1128/jb.186.21.7290-7301.2004
- Smyth, G. K. (2004). Linear models and empirical bayes methods for assessing differential expression in microarray experiments. *Stat. Appl. Genet. Mol. Biol.* 3:3. doi: 10.2202/1544-6115.1027
- Sonnleitner, E., Schuster, M., Sorger-Domenigg, T., Greenberg, E. P., and Blasi, U. (2006). Hfq-dependent alterations of the transcriptome profile and effects on quorum sensing in *Pseudomonas aeruginosa*. *Mol. Microbiol.* 59, 1542–1558. doi: 10.1111/j.1365-2958.2006.05032.x
- Sorger-Domenigg, T., Sonnleitner, E., Kaberdin, V. R., and Blasi, U. (2007). Distinct and overlapping binding sites of *Pseudomonas aeruginosa* Hfq and RsmA proteins on the non-coding RNA RsmY. *Biochem. Biophys. Res. Commun.* 352, 769–773. doi: 10.1016/j.bbrc.2006.11.084
- Straley, S. C., and Perry, R. D. (1995). Environmental modulation of gene expression and pathogenesis in *Yersinia*. *Trends Microbiol.* 3, 310–317. doi: 10.1016/s0966-842x(00)88960-x
- Suzuki, K., Babitzke, P., Kushner, S. R., and Romeo, T. (2006). Identification of a novel regulatory protein (CsrD) that targets the global regulatory RNAs CsrB and CsrC for degradation by RNase E. *Genes Dev.* 20, 2605–2617. doi: 10.1101/gad.1461606
- Timmermans, J., and Van Melder, L. (2010). Post-transcriptional global regulation by CsrA in bacteria. *Cell Mol. Life Sci.* 67, 2897–2908. doi: 10.1007/s00181-010-0381-z
- Trülsch, K., Oellerich, M. F., and Heesemann, J. (2007). Invasion and dissemination of *Yersinia enterocolitica* in the mouse infection model. *Adv. Exp. Med. Biol.* 603, 279–285. doi: 10.1007/978-0-387-72124-8_25
- Viegas, S. C., Pfeiffer, V., Sittka, A., Silva, I. J., Vogel, J., and Arraiano, C. M. (2007). Characterization of the role of ribonucleases in *Salmonella* small RNA decay. *Nucleic Acids Res.* 35, 7651–7664. doi: 10.1093/nar/gkm916
- Volk, M., Vollmer, I., Heroven, A. K., and Dersch, P. (2019). Transcriptional and post-transcriptional regulatory mechanisms controlling type III secretion. *Curr. Top. Microbiol. Immunol.* 427, 11–33. doi: 10.1007/82_2019_168
- Weilbacher, T., Suzuki, K., Dubey, A. K., Wang, X., Gudapaty, S., Morozov, I., et al. (2003). A novel sRNA component of the carbon storage regulatory system of *Escherichia coli*. *Mol. Microbiol.* 48, 657–670. doi: 10.1046/j.1365-2958.2003.03459.x
- Yang, F., Ke, Y., Tan, Y., Bi, Y., Shi, Q., Yang, H., et al. (2010). Cell membrane is impaired, accompanied by enhanced type III secretion system expression in *Yersinia pestis* deficient in RovA regulator. *PLoS One* 5:e12840. doi: 10.1371/journal.pone.0012840
- Yang, Y. H., Dudoit, S., Luu, P., Lin, D. M., Peng, V., Ngai, J., et al. (2002). Normalization for cDNA microarray data: a robust composite method addressing single and multiple slide systematic variation. *Nucleic Acids Res.* 30:e15.
- Zhang, A., Rimsky, S., Reaban, M. E., Buc, H., and Belfort, M. (1996). *Escherichia coli* protein analogs StpA and H-NS: regulatory loops, similar and disparate effects on nucleic acid dynamics. *EMBO J.* 15, 1340–1349. doi: 10.1002/j.1460-2075.1996.tb00476.x

Conflict of Interest: The authors declare that the research was conducted in the absence of any commercial or financial relationships that could be construed as a potential conflict of interest.

Publisher's Note: All claims expressed in this article are solely those of the authors and do not necessarily represent those of their affiliated organizations, or those of the publisher, the editors and the reviewers. Any product that may be evaluated in this article, or claim that may be made by its manufacturer, is not guaranteed or endorsed by the publisher.

Copyright © 2021 Böhme, Heroven, Lobedann, Guo, Stolle and Dersch. This is an open-access article distributed under the terms of the Creative Commons Attribution License (CC BY). The use, distribution or reproduction in other forums is permitted, provided the original author(s) and the copyright owner(s) are credited and that the original publication in this journal is cited, in accordance with accepted academic practice. No use, distribution or reproduction is permitted which does not comply with these terms.



Diversity and Versatility in Small RNA-Mediated Regulation in Bacterial Pathogens

Brice Felden[†] and Yoann Augagneur^{*}

Inserm, Bacterial Regulatory RNAs and Medicine (BRM) - UMR_S 1230, Rennes, France

OPEN ACCESS

Edited by:

Olga Soutourina,
UMR9198 Institut de Biologie
Intégrative de la Cellule (I2BC),
France

Reviewed by:

Teppei Morita,
Keio University, Japan
Young Min Kwon,
University of Arkansas, United States

*Correspondence:

Yoann Augagneur
yoann.augagneur@univ-rennes1.fr

[†]Deceased

Specialty section:

This article was submitted to
Microbial Physiology and Metabolism,
a section of the journal
Frontiers in Microbiology

Received: 03 June 2021

Accepted: 20 July 2021

Published: 10 August 2021

Citation:

Felden B and Augagneur Y (2021)
Diversity and Versatility in Small
RNA-Mediated Regulation in
Bacterial Pathogens.
Front. Microbiol. 12:719977.
doi: 10.3389/fmicb.2021.719977

Bacterial gene expression is under the control of a large set of molecules acting at multiple levels. In addition to the transcription factors (TFs) already known to be involved in global regulation of gene expression, small regulatory RNAs (sRNAs) are emerging as major players in gene regulatory networks, where they allow environmental adaptation and fitness. Developments in high-throughput screening have enabled their detection in the entire bacterial kingdom. These sRNAs influence a plethora of biological processes, including but not limited to outer membrane synthesis, metabolism, TF regulation, transcription termination, virulence, and antibiotic resistance and persistence. Almost always noncoding, they regulate target genes at the post-transcriptional level, usually through base-pair interactions with mRNAs, alone or with the help of dedicated chaperones. There is growing evidence that sRNA-mediated mechanisms of actions are far more diverse than initially thought, and that they go beyond the so-called *cis*- and *trans*-encoded classifications. These molecules can be derived and processed from 5' untranslated regions (UTRs), coding or non-coding sequences, and even from 3' UTRs. They usually act within the bacterial cytoplasm, but recent studies showed sRNAs in extracellular vesicles, where they influence host cell interactions. In this review, we highlight the various functions of sRNAs in bacterial pathogens, and focus on the increasing examples of widely diverse regulatory mechanisms that might compel us to reconsider what constitute the sRNA.

Keywords: bacterial regulatory RNAs, noncoding RNAs, pathogens, small regulatory RNAs, small RNAs, sRNAs

INTRODUCTION: A HISTORICAL OVERVIEW OF REGULATORY RNA DISCOVERIES

The central dogma of molecular biology states that DNA is replicated or transcribed into RNA, and that RNA is translated into proteins (Crick, 1958, 1970). This has contributed to the understanding (or perhaps widespread belief) that RNAs are just unstable intermediates (Pennisi, 2010). However, extensive research into these molecules has revealed that their purpose is not always to be translated. This has resulted in the identification of a new class called noncoding RNAs, which have gradually been shown to have a seemingly infinite range of biological functions and mechanisms of action (Cech and Steitz, 2014).

The first discoveries and characterizations of noncoding RNAs appeared in the late 1950s with the publication of studies on tRNA (Hoagland et al., 1958) and then rRNA (Cotter et al., 1967), both involved in protein translation. Various small noncoding RNAs (sRNAs) were subsequently identified in prokaryotes, with some being defined as regulatory RNAs due to their involvement in modulating bacterial metabolism (Wassarman et al., 1999). This was the case for 4.5S, transfer-messenger RNA (tmRNA), ribonuclease P (RNaseP) RNA, and 6S, all initially identified by fractionation in the late 1960s (Hindley, 1967). 4.5S is a 114-nucleotide (nt) component of the signal recognition particle (SRP) involved in protein secretion (Luirink and Dobberstein, 1994). It is essential, normally associates with ribosomes, and processed to be functional. tmRNA is a highly stable RNA that requires processing at the 5' and 3' ends by RNaseP and RNaseIII, respectively (Wassarman et al., 1999). It has sequential tRNA- and mRNA-like properties, and is involved in *trans*-translation for rescue of stalled ribosomes and protein degradation promotion (Janssen and Hayes, 2012). Initially identified as “10Sb” (Hindley, 1967), RNaseP is an essential RNA processed at the 3' end by RNaseE, and it forms a ribonucleoprotein complex with the RNaseP protein (Altman et al., 1989). RNaseP is responsible for the maturation of tRNA 5' termini, an essential step preceding the aminoacylation of mature tRNAs. *In vitro* studies on RNaseP revealed that the RNA moiety is the catalytic subunit (Guerrier-Takada et al., 1983), paving the way for the concept of ribozyme and later to that of the RNA world (Gilbert, 1986). One distinctive feature of RNaseP is that the RNA moiety recognizes a tRNA-like structure rather than Watson-Crick complexes, thus permitting the cleavage and maturation of 4.5S RNA or tmRNA or else the development of RNaseP-mediated RNA therapeutics through gene-selective mRNA cleavage (Augagneur et al., 2012; Kole et al., 2012; Derksen et al., 2015). The first non-rRNA, non-tRNA to be sequenced was 6S RNA from *Escherichia coli* (Brownlee, 1971), although it took almost 30 years for its role in sequestering the $\sigma 70$ subunit of RNA polymerase to be demonstrated (Wassarman et al., 1999).

Meanwhile, other sRNAs including Spot42 and MicF were being discovered in *E. coli* (Ikemura and Dahlberg, 1973; Mizuno et al., 1984), and RNAI and RNAIII were soon thereafter discovered in the pathogen *Staphylococcus aureus* (Novick et al., 1989, 1993). As sRNAs were being discovered in virtually all bacteria, their regulatory mechanisms and biological functions began to be elucidated, bringing this class into the spotlight. Typically, sRNAs bind their target(s) (most often other RNAs by base-pairing and in a limited number of cases proteins) to modulate their expression at post-transcriptional level by influencing their stability and/or translation. However, it turns out that as a great variety of mechanisms was unraveled, a profusion of sRNA sub-categories emerged, and these regulatory RNAs began to be characterized as *cis*-encoded, *trans*-encoded, *cis*-acting, *trans*-acting, or even as sRNA-binding proteins. In eukaryotes, a similar abundance of non-mRNAs have been described. These include microRNAs, small interfering RNAs, Piwi-interacting RNAs, small noncoding RNAs, long noncoding RNAs, and circular RNAs, with these last ones acting as

microRNA sponges in the cytoplasm (Chen et al., 2015; Burenina et al., 2017). It is therefore clear that the term “RNA” encompasses molecules that have a plethora of biological traits and mechanisms in both prokaryotes and eukaryotes (Cech and Steitz, 2014). In this review, we summarize, in a non-exhaustive manner, the current knowledge on sRNAs in bacterial pathogens, with a particular focus on *S. aureus*, *Listeria monocytogenes*, and *Salmonella*. We use specific examples to describe some usual and unusual features of this heterogeneous group of transcripts whose precise categorization appears to be much more complicated than initially expected.

SRNA REGULATION IS REQUIRED FOR A VARIETY OF BIOLOGICAL FUNCTIONS

Small regulatory RNAs are often described according to categories based on genome localization and their featured regulatory mechanisms. In this review, we take an opposite view, and start by discussing the diversity of biological functions in which sRNAs play a role. They are not constitutively expressed, but instead respond to environmental variations to modulate the gene expression of numerous targets (Wagner and Romby, 2015). These specific conditions include transition to the stationary phase, thermal shock, oxidative stress, and many other environmental challenges. Although, there are few sRNAs conserved over the bacterial kingdom (structural “housekeeping” sRNAs such as 6S, tmRNA, and RNaseP), they are often species- or order-specific. They have substantial advantages over transcription factors (TFs); they require less energy for production since translation initiation is unnecessary; they can act faster and reversibly; and they can still bind to multiple targets, which allow them to regulate a wide range of biological functions.

sRNAs and Their Involvement in Virulence

In bacterial pathogens, it was an open question whether sRNAs were required for regulating virulence, either as activators or repressors. As sRNA molecular targets were being identified and regulatory functions in multiple pathways revealed, evidence has progressively emerged regarding their role in the direct or indirect control of virulence factors or the TFs that regulate virulence.

In *S. aureus*, the main sRNA involved in the commitment to virulence and quorum-sensing (QS) is RNAIII, an unusual 514-nt RNA that has an internal sequence coding for δ -hemolysin (Novick et al., 1993). RNAIII responds to cell density through the *agr* QS system and its TF, AgrA. The sRNA accumulates during bacterial growth, reaching a maximal concentration during the post-exponential phase (Singh and Ray, 2014). In doing this, it coordinates the transition from colonization to infection by directly or indirectly reprogramming the expression of a large set of genes (Bronesky et al., 2016; **Table 1**). Among the various virulence factors, RNAIII represses the expression of the TF Rot (Geisinger et al., 2006; Boisset et al., 2007),

TABLE 1 | Targets regulated by RNAIII.

Target	RNAIII effect	Encoded target function	Mechanism of action
<i>spa</i>	Repression	Adhesion and immune evasion	Translation inhibition and degradation by RNaseIII
<i>coa</i>		Adhesion	
<i>sa1000</i>		Adhesion	
<i>rot</i>		Transcription factor and toxin repressor	
<i>sbi</i>	Activation	Adhesion and immune evasion	Translation inhibition
<i>lytM</i>		Cell-wall metabolism and release of Spa	Translation inhibition
<i>hla</i>		Alpha toxin	Translation activator
<i>mgrA</i>		Transcription factor, inhibitor of surface proteins and autolysis, and activator of capsule synthesis	Stabilization of mRNA

a repressor of numerous exotoxins that positively controls surface proteins such as Spa (Saïd-Salim et al., 2003; Oscarsson et al., 2006). By inhibiting this TF, RNAIII indirectly activates exotoxin production and inhibits surface protein expression. RNAIII and Rot inverted effects allow an effective switch between defense and offensive mode called Double Selector Switch (DSS; Nitzan et al., 2015). RNAIII also represses the expression of Spa, Coa, LytM, and Sbi by inhibiting ribosome binding or sometimes by promoting mRNA degradation (Table 1). Conversely, it upregulates the expression of α -hemolysin (Hla; α -toxin; Morfeldt et al., 1995) and MgrA TF, which inhibits surface protein expression (Luong et al., 2006; Gupta et al., 2015). We describe the actual mechanisms of actions against these targets later on in this review.

Other *S. aureus* sRNAs participate in virulence gene regulation, including SprD, the sRNA expressed from a pathogenicity island (Pichon and Felden, 2005). SprD downregulates the expression of Sbi, an immune evasion factor, at translational level (Chabelskaya et al., 2010). In the same study, the authors showed that the deletion of SprD resulted in the generation of a less-virulent strain in the mouse model of infection. This suggests that SprD controls the expression of other factors through yet-unknown mechanisms. Interestingly, Sbi is tightly controlled by both SprD and RNAIII, which are not expressed in *S. aureus* under the same conditions, and this suggests complementary roles for these two sRNAs in Sbi expression (Chabelskaya et al., 2014). Several other examples of sRNAs that positively or negatively control virulence exist in this bacterium, including SSR42, SprC, and RsaA (Morrison et al., 2012; Romilly et al., 2014; Le Pabic et al., 2015; Das et al., 2016).

In another low GC-content human pathogen *L. monocytogenes*, several sRNAs contribute to virulence (Toledo-Arana et al., 2007, 2009; Gripenland et al., 2010; Mellin and Cossart, 2012; Quereda and Cossart, 2017). First line of evidences came out

with the deletions of blood-induced *rli38* and *rliB*, which resulting in attenuated or increased tissue colonization in a mouse model of infection, respectively. A study of *Listeria's* intracellular transcriptome during growth in macrophages identified a large set of sRNAs, three of which (Rli31, Rli33-1, and Rli50) are directly associated with virulence (Mraheil et al., 2011). In addition, during intracellular growth, the blood-induced sRNA Rli27 upregulates the expression of Lmo0514, a cell-wall protein that has a pivotal role in virulence, as it is required for survival in plasma and for virulence in mice (Quereda et al., 2014, 2016).

In Gram-negative pathogens, most studies have focused on *Salmonella* Typhimurium and enterohemorrhagic *E. coli* (EHEC). In *Salmonella*, IsrM is a pathogenicity island-encoded sRNA with interesting features (Gong et al., 2011). Although, non-essential during growth *in vitro*, it is upregulated during infection, with high levels in the ileum. IsrM targets the SpoA and HilE mRNAs, which control the expression of *Salmonella* pathogenicity island 1 (SPI-1) genes. Deletion of *isrM* affects the bacterial invasion of epithelial cells, intracellular replication/survival in macrophages, and virulence in mice. In *E. coli* O157:H7 strain, several sRNAs are involved in virulence (Sauder and Kendall, 2018). Interestingly, the functions regulated by sRNAs differ in nonpathogenic *E. coli* and in EHEC, where core genome-encoded sRNAs can regulate virulence factors carried in pathogenicity islands. These include GlmY and GlmZ, sRNAs which control amino-sugar metabolism in nonpathogenic *E. coli* (Gruber and Sperandio, 2015) as well as being involved in type III secretion machinery in EHEC (Gruber and Sperandio, 2014). Similar to *S. aureus*, EHEC contains pathogenicity island-encoded sRNAs such as the antisense sRNAs Arl and sRNA350, both of which regulate bacterial virulence (Tobe et al., 2014; Bhatt et al., 2016). Additionally, some sRNAs such as DicF have both core genome-encoded and pathogenicity island-encoded copies (Melson and Kendall, 2019). When oxygen is limited, DicF binds *pchA* mRNAs, which encode a transcriptional activator of the type III secretion system. This allows access to the *pchA* ribosome binding site (RBS), promoting the expression of the activator and thereby increasing virulence (Melson and Kendall, 2019). Recent work on the sRNA, RyfA revealed its roles in virulence (mouse model) and survival (in human primary macrophages), both carried out by regulating genes coding for cell surface proteins and biofilm formation (Bessaiah et al., 2021). Other examples of sRNAs involved in virulence were reported in *Pseudomonas aeruginosa*, *Vibrio cholerae*, and *Helicobacter pylori*, and these have been thoroughly discussed in several articles and reviews (Pitman and Cho, 2015; Svensson and Sharma, 2016; Vannini et al., 2016; Ferrara et al., 2017; Quereda and Cossart, 2017; Zhao et al., 2018; Kinoshita-Daitoku et al., 2021).

The Role of sRNAs in Host-Pathogen Interactions

In most of the examples discussed above, researchers began by identifying sRNAs and their targets in laboratory conditions or using *in silico* strategies before moving on to testing sRNA-deleted strains in animal models. These laboratory conditions

only partially reproduce environmental cues, so some sRNA functions may be underestimated. Recently, the advent of deep-sequencing technologies filled in many blanks, enabling the study of sRNA expression and functions directly during host-pathogen interactions. Originally, the sRNA EsrF was predicted from transcriptomic data generated during EHEC infection of HeLa cells (Yang et al., 2015). EsrF senses high ammonium concentrations in the colon and promotes bacterial motility, host cell adhesion, and virulence in the colon (Jia et al., 2021). In *Salmonella*, dual RNA sequencing (RNA-seq) analysis revealed an activation of PinT during infection (Westermann et al., 2016). Similar to RNAIII, this sRNA plays an important role in chronological control of virulence factor expression in order to push the bacteria from the invasive to the virulent mode. PinT controls the SPI-1 and SPI-2 effectors required for intracellular survival, and causes pervasive changes in ~10% of the host's coding and noncoding transcripts. A recent study using a novel MS2 affinity purification coupled with RNA sequencing (MAPS) technique (Lalaouna et al., 2017) in macrophages elegantly identified SteC, a novel PinT ligand that affects host actin rearrangement during infection (Correia Santos et al., 2021). The use of such new techniques should be extended to other pathogens, paving the way for the discovery of more sRNAs and new and better knowledge about their biological functions.

Another interesting thing about sRNAs is that their delivery into host cells from outer membrane vesicles allows them to modulate host-pathogen communications. While the characterization of sRNA content in extracellular vesicles is quite recent, links between sRNAs and host immune response were reported in *P. aeruginosa*, *H. pylori*, and *Vibrio fischeri* (Koeppen et al., 2016; Moriano-Gutierrez et al., 2020; Zhang et al., 2020). The RNA cargo of *S. aureus* was also recently characterized, revealing that the sRNAs RNAIII, RsaC, and SsrA (tmRNA) predominate. This suggests additional functions for these sRNAs in the control of immune host response (Joshi et al., 2020; Luz et al., 2021), as suggested in earlier reviews (Ellis and Kuehn, 2010; Avila-Calderón et al., 2015).

sRNA-Mediated Antimicrobial Responses and Resistance

Although, the study of sRNAs and their roles in pathogenicity has inspired growing interest and uncovered new features, the biological functions of sRNAs go far beyond virulence. Besides being pathogenic, the emergence of bacterial strains resistant to antibiotic treatments is a serious public health issue, and several studies have therefore looked for correlations between sRNA expression and antibiotic challenges. These contributions to a better understanding of bacterial resistance and the role of sRNAs in these networks were recently reviewed (Felden and Cattoir, 2018).

In *Salmonella*, four sRNAs (sYJ5, SroA, sYJ75, and sYJ118) are upregulated when subjected to half the MIC of tigecycline (Yu and Schneiders, 2012), and the genetic deletion of *sroA* leads to reduced viability in the presence of that antibiotic. SroA exhibits the structural characteristics of a riboswitch, although its mechanism of action has not yet been characterized.

In *E. coli*, RyhB is induced upon iron starvation, and it represses the expression of a large set of genes as well as participating in iron homeostasis (Massé and Gottesman, 2002; Chareyre and Mandin, 2018). During iron starvation, it is also involved in sensitivity to colicin Ia, an *E. coli*-specific bacteriocin produced to kill other *E. coli* strains (Salvail et al., 2013). To do this, RyhB binds *cirA* mRNAs, thereby activating its translation. CirA is a colicin Ia receptor and allows its translocation into the cell. Another study reported on the role of RyhB in antibiotic resistance after testing four classes of antibiotics (aminoglycosides, β -lactams, fluoroquinolones, and tetracycline; Chareyre et al., 2019). The authors showed that during iron starvation *ryhB* mutants were more susceptible to the aminoglycoside gentamicin as a result of the derepression of respiratory complexes Nuo and Sdh.

In *P. aeruginosa*, at least three sRNAs are known to be required for carbapenem resistance (Zhang et al., 2017; Sonnleitner et al., 2020). In the first study, Hi-GRIL-seq identified Sr0161 and ErsA as sRNA repressors of OprD, a porin involved in carbapenem antibiotic uptake. Their roles were functionally demonstrated in their respective deleted strains, in which meropenem susceptibility was significantly increased (Zhang et al., 2017). In the same article, Sr006 was shown to be involved in resistance to polymyxin B through the translation activation of PagL, an enzyme involved in lipopolysaccharide synthesis. In the second study, the sRNA CrcZ was shown to regulate carbapenem susceptibility through an indirect mechanism (Sonnleitner et al., 2020). By sequestering the Hfq protein when the preferred carbon source is exhausted, CrcZ prevents Hfq-mediated translational repression of OprP, another porin involved in carbapenem entry. Other studies have emphasized the role of sRNAs in *P. aeruginosa* and other Enterobacteriaceae, and are summarized in a recent review (Mediati et al., 2021).

In *S. aureus*, antibiotic exposure causes the specific expression of several sRNAs in the multidrug-resistant strain JKD6008 (Howden et al., 2013). Recently, the same authors identified a set of 18 sRNAs whose expressions vary under linezolid treatment (Gao et al., 2020). Although, no phenotypic variations were observed after genetic deletions of these sRNAs, which questions their actual roles in antibiotic resistance/adaptation, other studies have given direct evidence of direct sRNA involvement in antibiotic resistance. Depending on the strain, the sRNA SprX is encoded in one or more copies, and it inhibits translation of the SpoVG TF involved in glycopeptide and oxacillin resistance (Eyraud et al., 2014). The direct role of this sRNA was confirmed, as its deletion leads to moderately increased resistance, while its overexpression results in glycopeptide susceptibility. Antibiotic treatment failure is also largely attributed to the formation of persister cells, a subpopulation which is transiently tolerant of various antibiotic classes following entry into dormancy. A recent work identified the RNA antitoxin SprF1 in *S. aureus* as an RNA factor promoting persistence when challenged by ciprofloxacin and vancomycin at high doses (20x and 80x the MIC, respectively; Pinel-Marie et al., 2021). The authors demonstrated that this sRNA binds 70S ribosomes to slow translation and favor the

entry into persistence, allowing survival until the antibiotic treatment is discontinued.

sRNAs Span Many Other Functions

Studies of sRNAs in bacterial pathogens spotlight those involved in virulence or antibiotic resistance. However, many are involved in the regulation of other biological functions, especially fitness and adaptation. This is the case for instance for RsaE, RsaI, and RsaD in *S. aureus*. RsaE is the sRNA of about 100 nt which was identified by bioinformatics in intergenic regions (Geissmann et al., 2009), and which is conserved in Bacillales (Bohn et al., 2010). Transcriptomic and 2D-DIGE analysis of an *rsaE* mutant showed that this sRNA is involved in the regulation of several pathways connected to central metabolism, including the TCA cycle and metabolism of folate and malate. The first two targets to be characterized were the operon-encoded mRNAs *oppA* and *oppB* (Geissmann et al., 2009; Bohn et al., 2010). A subsequent search for molecular targets uncovered its role in arginine catabolism, with the arginase RocF downregulated when RsaE binds the mRNA (Rochat et al., 2018). In *Staphylococcus epidermidis*, a species which could become a threat due to spreading multidrug-resistant strains (Lee et al., 2018), RsaE participates in the regulation of the composition of the extracellular matrix (Schoenfelder et al., 2019). To do so, the sRNA undergoes processing which results in two forms regulating different targets (Lee et al., 2018). While the longer transcript interacts with *lrgA* mRNA (Rice et al., 2005) to cause both RNA decay and translational attenuation, the shorter species binds *icaR* mRNA (Cue et al., 2012) to inhibit translation. *Staphylococcus aureus* RsaI is the sRNA whose expression is tightly controlled by CcpA, a global regulator of carbon catabolite repression (Seidl et al., 2009; Bronesky et al., 2019). It is inhibited under high concentrations of glucose, and this is alleviated during the growth stationary phase (Geissmann et al., 2009). An in-depth characterization of the targetome using MAPS uncovered mRNA targets involved in sugar metabolism, glucose uptake, and biofilm formation, including mRNA transcription factors and remarkably, other sRNAs such as RsaE, RsaD, and RsaG (Bronesky et al., 2019). Among the target characterized, RsaI primarily acts as a post-transcriptional repressor. RsaD was discovered at the same time with other Rsa sRNAs (Geissmann et al., 2009). It might be part of the RsaI regulon, and is induced upon nitric oxide challenge (Bronesky et al., 2019). A study of the CodY regulon identified RsaD as a direct molecular target, and computational tools enabled the authors to find various RsaD mRNA targets including *alsS*, which encodes α -acetolactate synthase (Augagneur et al., 2020). Through post-transcriptional repression of *alsS*, RsaD redirects carbon overflow metabolism and regulates cell death during exposure to a weak acid stress.

In *Salmonella* Typhimurium, RydC was the first sRNA characterized as a regulator of membrane stability, binding *cfa* mRNAs and encoding cyclopropane fatty-acid (CFA) synthase (Fröhlich et al., 2013). Unlike most of the sRNAs discussed above, RydC upregulates CFA synthase by stabilization its mRNA. Other sRNAs such as RybB and MicA maintain envelope homeostasis (Papenfort et al., 2006), with RybB spurring the

degradation of *omp* mRNAs upon activation of the envelope stress response, while MicA controls their decay.

SgrS is another sRNA that promotes the expression of some of its targets (Papenfort et al., 2013). This sRNA is involved in glucose homeostasis through the activation and repression of several targets (Vanderpool and Gottesman, 2004). SgrS was first identified as a repressor of the phosphotransferase system (PTS), preventing the translocation of sugars into cells when the intracellular concentration of phosphorylated sugars is too high (Vanderpool and Gottesman, 2004). The sRNA also activates the translation of YigL, a phosphatase involved in detoxification of phosphosugars, thereby allowing diffusion of dephosphorylated sugars outside the cell membrane (Papenfort et al., 2013). While GlmY and GlmZ are both involved in virulence in EHEC (see section above on sRNAs and Their Involvement in Virulence), they also have other conserved regulatory activities in nonpathogenic *E. coli*, including amino sugar metabolism and cell envelope synthesis (Urban and Vogel, 2008; Göpel et al., 2014; Sauder and Kendall, 2018).

Initially identified in nonpathogenic *E. coli*, RyhB is involved in iron homeostasis, a critical factor in cellular processes (Massé and Gottesman, 2002). It is under the control of Fur, the TF that represses iron acquisition genes and RyhB when iron is abundant. RyhB downregulates iron-storing and iron-using proteins and these are therefore indirectly activated when Fur represses RyhB. In *Salmonella*, two paralogs have been identified: RyhB-1 and RyhB-2 (Kim, 2016). These share a 33-bp sequence with perfect identity, and can thus regulate the same targets (Kim and Kwon, 2013). Although their promoters are recognized by Fur, their expression profiles vary (Padalon-Brauch et al., 2008): *ryhB-1* is induced under iron-depleted conditions or oxidative stress, while maximal *ryhB-2* expression is seen during the stationary phase. Additional roles for RyhB paralogs were reported in *Salmonella* (Kim, 2016). These include involvement in nitrate homeostasis (Teixidó et al., 2010), oxidative stress, intracellular survival in macrophages, and control of SPI-1 and Type III secretion system gene expression (Leclerc et al., 2013; Calderón et al., 2014; Peñaloza et al., 2021).

DapZ is an 80-nt sRNA identified in *Salmonella* and transcribed from the 3' region of *dapB* (Chao et al., 2012). It is involved in the uptake of nutrient and signaling molecules. *Via* base-pairing, DapZ modulates the synthesis of ABC transporters Opp and Dpp, which encode oligopeptide and dipeptide permeases, respectively.

The ensemble of sRNA studies highlights their roles in many biological functions ranging from virulence to antibiotic resistance, and even including the regulation of TF expression and transcription termination. While sRNA research involving bacterial pathogens has often concentrated on virulence or antibiotic resistance because of public health issues, they are actually involved in all aspects of bacterial biology. There are about as many sRNAs discovered as TFs factors inventoried, which indicates that sRNAs are among the key players in transcriptional and post-transcriptional regulation of gene expression.

Just as there has been a large number of biological functions identified, the functional categorization of their mechanisms

of production or regulation is broad and diverse, with new features constantly unraveled. sRNAs are a heterogeneous group of transcripts with lengths usually ranging from 50 to 500 nucleotides. They are usually highly structured, have greater stability than mRNAs, and use their base-pairing abilities to interact with and regulate their targets. To promote interaction with a target, a chaperone is sometimes necessary (Kavita et al., 2018). Based on their features, they can be categorized in multiple manners. In the following sections, we will first present the canonical features and mechanisms of action, then use selected examples to illustrate original features to showcase the diversity and versatility uncovered at the same time as the discovery of sRNAs exploded, suggesting that more surprises are in store.

sRNAs THAT INTERACT WITH PROTEINS

While most sRNAs use base-pairing to activate or repress the expression of their targets, some bind proteins to form ribonucleoprotein complexes (Pichon and Felden, 2007). These complexes are involved in the metabolism of DNA (regulation of plasmids and DNA transfers), RNAs, and proteins. When it comes to RNA metabolism, sRNAs can be involved in transcription through 6S sRNAs, in RNA maturation *via* RNaseP, or subject to decay when recognized by endo- or exo-ribonucleases (Wassarman et al., 1999; Hausmann et al., 2017; Redder, 2018; Le Scornet and Redder, 2019). In addition, some are assisted by *trans*-acting chaperones to facilitate recognition of “bait” and “prey” (Pichon and Felden, 2007). At protein level, they are important for global translation machinery and quality control (including tmRNAs involved in ribosome rescue), for protein trafficking with SRP and 4.5S RNA, and for sequestration of global regulators. Most of these characteristics are beyond the scope of this review, and we will just discuss the need for protein chaperones to stabilize interactions as well as the role of sRNAs in protein sequestration, both usually found in Gram-negative bacteria.

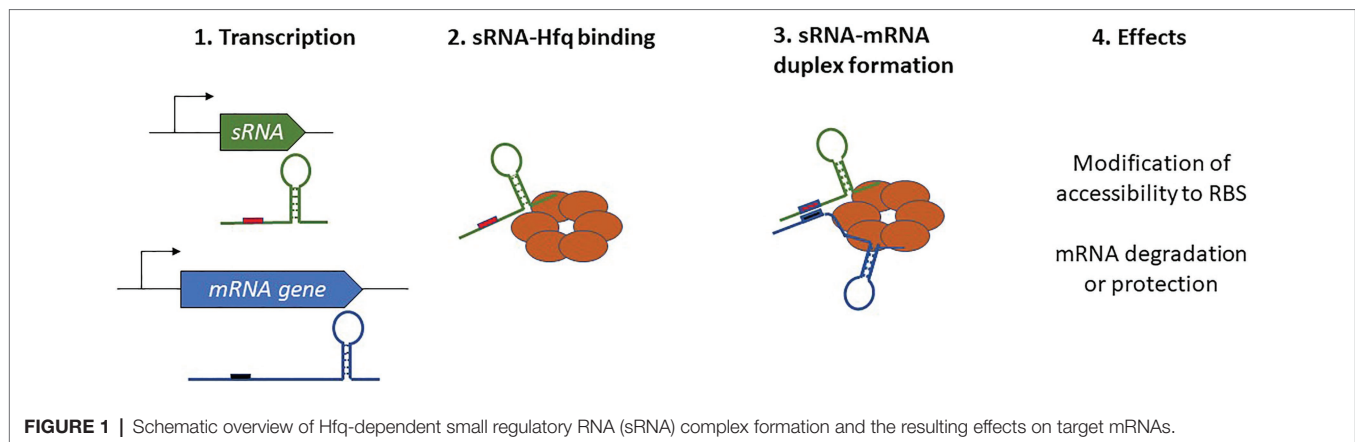
The Role of Protein Chaperones in Stabilizing RNA–RNA Interactions

In Gram-negative bacteria, the activity of numerous sRNAs relies on them acting in concert with a RNA chaperone protein. The most prevalent of these is Hfq, often referred to as the “RNA matchmaker” (Updegrave et al., 2016). Hfq is a homohexameric ring-shaped protein with at least three different RNA-binding domains shared between the rim and the proximal and distal faces of the hexamer (Gorski et al., 2017; Carrier et al., 2018). The proximal face specifically recognizes U-rich tracts, often associated with *rho*-independent transcription terminators, whereas the distal face anneals sRNAs through A-rich regions. Similar to the proximal face, the rim of the hexamer also binds U-rich regions. Not only does the binding with Hfq stabilize the sRNA and protect it from RNases, but

also its ability to bind simultaneously with mRNAs and favors the formation of mRNA-sRNA duplexes. Indeed, this feature allows for the appropriate presentation of the sRNA seed region to an mRNA target, which in turn affects mRNA stability or translation (Figure 1). With the help of Hfq, only a short and conserved sRNA seed sequence is necessary for annealing with the target and promotion of regulatory activity. For instance, just seven nucleotides are responsible for the degradation of *omp* mRNAs by RybB (Balbontín et al., 2010; Papenfort et al., 2010). In addition to its RNA chaperone activity, Hfq can also directly influence translation by binding the 5' UTR of *cirA* mRNAs as well as participate in RNaseE recruitment to induce the rapid degradation of target mRNAs (Ikeda et al., 2011; Salvail et al., 2013). This indicates a novel role and mechanisms of action for this sRNA, and these are extensively discussed in a recent review by Ng Kwan Lim et al. (2021).

Whether Hfq was the sole RNA chaperone, which was answered using a Grad-seq, technology first used in *Salmonella* (Smirnov et al., 2016). This enabled the discovery of several sRNAs such as RaiZ, associated with ProQ RNA-binding protein. The authors demonstrated that RaiZ represses the expression of the histone-like protein HU- α and that ProQ acts as a chaperone in RaiZ transcription stabilization rather than facilitating base-pairing. RIL-seq then enabled a redefinition of the interactomes of Hfq and ProQ, revealing their overlapping and competing roles (Melamed et al., 2020). In other Gram-negative bacteria such as *Legionella* and meningococcus, identification and exploration of ProQ and ProQ-like proteins has demonstrated that Hfq is not the only player in the RNA-binding hub (Attaiech et al., 2016; Bauriedl et al., 2020).

Conversely, the need for the RNA chaperone to enhance sRNA-mRNA interactions seems marginal in Gram-positive bacteria, as no Hfq homologs exist in streptococci or lactobacilli (Mellin and Cossart, 2012). Investigations into Hfq functions in *S. aureus* and *Bacillus subtilis* using deleted strains did not result in any significant phenotypes, and several Hfq-independent sRNAs have now been described (Bohn et al., 2007; Rochat et al., 2015). However, studies in *L. monocytogenes* did reveal a functional albeit sometimes minor role for Hfq in sRNA-mediated regulation or tolerance to stress and virulence (Christiansen et al., 2004; Mandin et al., 2007). Co-immunoprecipitation coupled to enzymatic RNA sequencing produced the first evidence of interaction between Hfq and three sRNAs (Christiansen et al., 2006). Among these, LhtA regulates the translation and degradation of its mRNA targets through an Hfq-dependent antisense mechanism (Nielsen et al., 2010, 2011). In contrast, the multicopy sRNA LhrC identified in the same screen (Christiansen et al., 2006) does not require Hfq to stabilize its interaction with *lapB*, its target mRNA (Sievers et al., 2014). Together, these results indicate a controversial and probably dispensable role for Hfq in post-transcriptional control of gene expression in several Gram-positive species. This points to major differences in sRNA-mediated regulation between Gram-negative and Gram-positive bacteria, or perhaps to the existence of other RNA chaperones (Jørgensen et al., 2020) yet to be discovered.



Sequestration of Proteins by sRNAs

Small regulatory RNAs do not necessarily anneal to the RNA chaperone to enhance target recognition. They can bind proteins to inhibit their action by mimicking the structures of their target mRNAs, although examples of this are limited, and mostly restricted to Gram-negative bacteria. For instance, the homodimeric RNA-binding protein CsrA is sequestered by CsrB and CsrC sRNAs, which antagonize its activity (Liu et al., 1997; Weilbacher et al., 2003). This CsrA carbon storage regulator normally represses gene expression by direct binding with the translation initiation region of its mRNA targets, and only a few examples of gene activation have been reported (Pourciau et al., 2020). This sRNA is associated with post-transcriptional control of its targets rather than the transcriptional control usually described for TFs, and it affects translation initiation, RNA stabilization, and transcription termination. For optimal sequestration of the protein, CsrB and CsrC sRNAs contain multiple CsrA-binding sites, with ~18 in CsrB. That sRNA harbors repeated sequence elements, including a GGA motif present in the loop of hairpin structures or in single-stranded regions (Romeo, 1998). These GGA seeds decoy the CsrA target motifs usually present near the SD sequence of target sRNAs. Similar decoy seed regions are found in several CsrB homologs in various bacterial species (Babitzke and Romeo, 2007; Janssen et al., 2018; Müller et al., 2019; Sonnleitner et al., 2020). sRNAs in the CsrB family have an impact on the CsrA regulon and on various physiological functions such as biofilm formation, host-microbe interaction, and virulence (Vakulskas et al., 2015). Their expression relies on the BarA/UvrY two-component system, increasing under nutrient limitation or cellular stress, and decreasing through RNA degradation in the presence of the preferred carbon source (Pourciau et al., 2020). In addition, a reciprocal regulation was also revealed, as free CsrA is mandatory for CsrB/C synthesis. Unusually, sRNAs in the Csr family have short half-lives, allowing for the rapid adjustment of CsrA activity in response to environmental cues. Ultimately, it has been shown that CsrB homologs do not necessarily sequester CsrA. In *P. aeruginosa*, CsrZ antagonizes Hfq, resulting in differential carbapenem susceptibility during growth on different carbon sources (Sonnleitner et al., 2020). More roles were reported

for CsrA in *B. subtilis*, where it allows the formation of complexes between the sRNA and its mRNA target, therefore, working as an Hfq-like or ProQ-like RNA chaperone (Müller et al., 2019). Additionally, some sRNAs belong to type III toxin-antitoxin (TA) systems in which the regulatory RNA binds and sequesters its cognate toxin (Brantl and Jahn, 2015).

CLASSIFICATION OF BASE-PAIRING ACTING sRNAs ACCORDING TO THEIR ORIGINS AND MECHANISMS OF ACTION

Base-pairing sRNAs are expressed from a large variety of loci, and they can be generated from the genome or plasmids (Tomizawa et al., 1981). Within the genome, they are transcribed from both the core genome and accessory genomes such as pathogenicity islands (Pichon and Felden, 2005), and either antisense to their target or *trans*-encoded from a locus distant to their cognate targets.

Antisense-Encoded sRNAs and Their Mechanisms of Action

Antisense-encoded sRNAs (asRNAs), also called *cis*-encoded antisense RNAs, are encoded on the DNA strand opposite to their mRNA target. They share extensive and perfect complementarity with part of their mRNA target, allowing efficient regulation without usually requiring the RNA chaperone. They were originally discovered in plasmids and other genetic mobile elements such as phages and transposons (Tomizawa et al., 1981; Brantl, 2002), but we now know that they are present throughout in the genome. For some asRNAs, additional targets transcribed from distant loci have been reported, indicating that they can also act as *trans*-encoded sRNAs. asRNAs have a large range of lengths, from ~50 to several thousand nucleotides. They can be transcribed from a DNA strand whose coordinates are within the coding region (CDS) of the opposite strand, overlapping with a CDS (at the 5' or 3' UTR), or in the case of the very long RNAs (lasRNAs), antisense to a complete operon (Dühning et al., 2006;

Figures 2A–D). Their identification is challenging, as wide antisense transcription was reported in several pathogens including *S. aureus*, making it difficult to distinguish between “true” asRNAs (having their own promoters) and transcriptional noise (Lasa et al., 2011). Of the thousands of asRNAs identified in a single species, only a tiny subset has been functionally characterized. Plasmid-encoded asRNAs are often constitutively expressed and involved in specific biological functions such as plasmid replication, conjugation, post-segregational killing, and transposition (Wagner et al., 2002). Conversely, genome-encoded asRNAs are primarily linked to the functions of the protein encoded from the opposite strand, and their expression is modulated under specific conditions (Brantl, 2007). Most often, asRNAs are responsible for post-transcriptional regulation and they exhibit a large array of mechanisms of actions that include transcription attenuation or inhibition, modification of mRNA decay, RNA pseudoknot formation, and primer maturation inhibition (Brantl, 2007; **Figure 3**). In a few cases, activating mechanisms have been reported. Similar mechanisms of action have also been described for *trans*-encoded sRNAs. We will not discuss the inhibition of primer maturation here, as this mechanism of action is mostly restricted to plasmid replication and is not generally applicable to most asRNAs or *trans*-encoded sRNAs.

Transcription Attenuation

Transcription attenuation occurs when a termination structure is formed in the target mRNA after asRNA annealing (**Figure 3A**). This was first observed as a means to control copy numbers

in staphylococcal and streptococcal plasmids (Novick et al., 1989; Brantl et al., 1993; Brantl, 2002). In these bacteria, *rep* mRNAs can adopt two mutually exclusive conformations depending on the presence or absence of the asRNA. Expression of the asRNA induces a terminating stem-loop that causes the premature termination of *rep* transcription upstream from the RBS, thereby preventing translation initiation. Conversely, in the absence of the asRNA, the natural conformation of *rep* mRNA prevents stem-loops from forming. This structure enables the transcription of full-length *rep* mRNA, permitting translation and therefore plasmid replication. Such a mechanism of action has been reported in the post-transcriptional control of the virulence gene *icsA* in *Shigella flexneri* (Giangrossi et al., 2010), as well as in iron transport in the fish pathogen *Vibrio anguillarum* (Stork et al., 2007). That first study identified RnaG, an asRNA expressed from the opposite strand of *iscA*. Upon RnaG expression, the formation of a heteroduplex induces the formation of an intrinsic terminator, thus leads to transcription termination (Giangrossi et al., 2010). In the second study, the expression of the asRNA Rna β enabled transcription termination within the *fatDCBA-angRT* transport and siderophore biosynthesis operon, resulting in approximately 17-fold higher expression levels of *fatDCBA* genes than *angRT* ones (Stork et al., 2007).

Translation Inhibition

Translation inhibition is probably the most well-known RNA-mediated mechanism employed to post-transcriptionally regulate gene expression (**Figure 3B**). Here, the asRNA presents perfect complementarity with the RBS of the mRNA transcribed

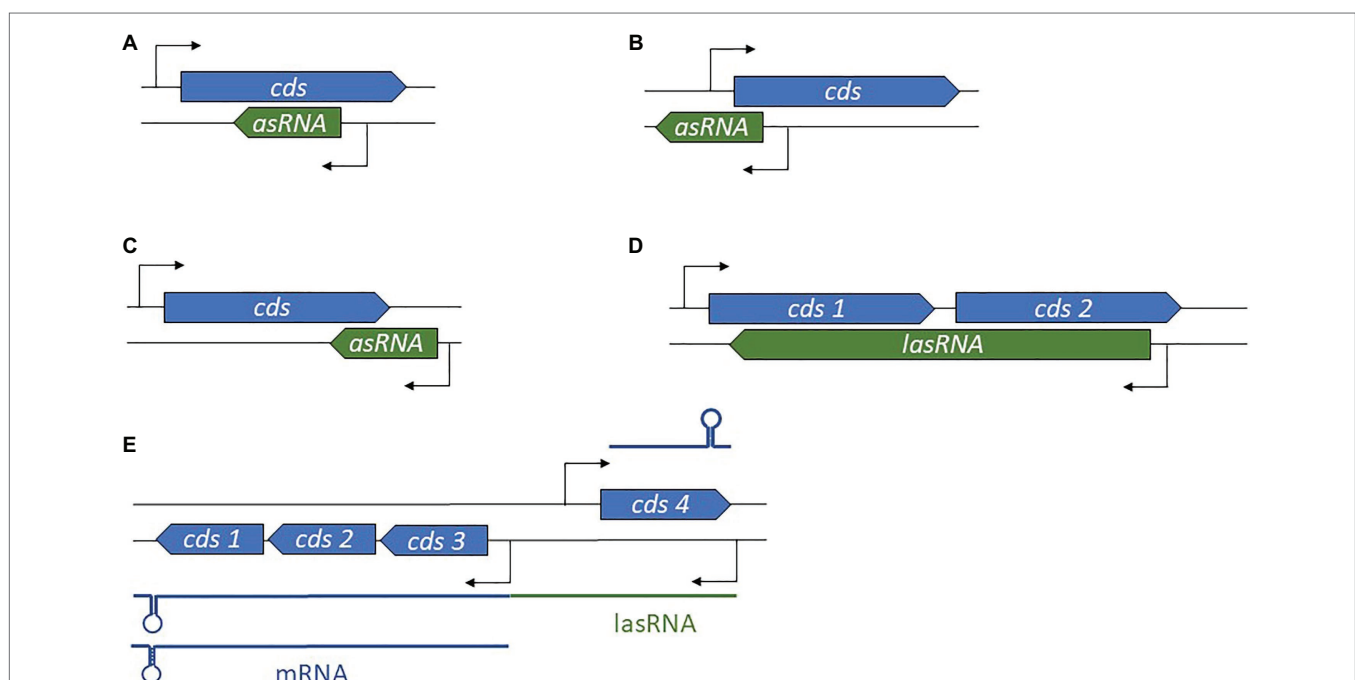
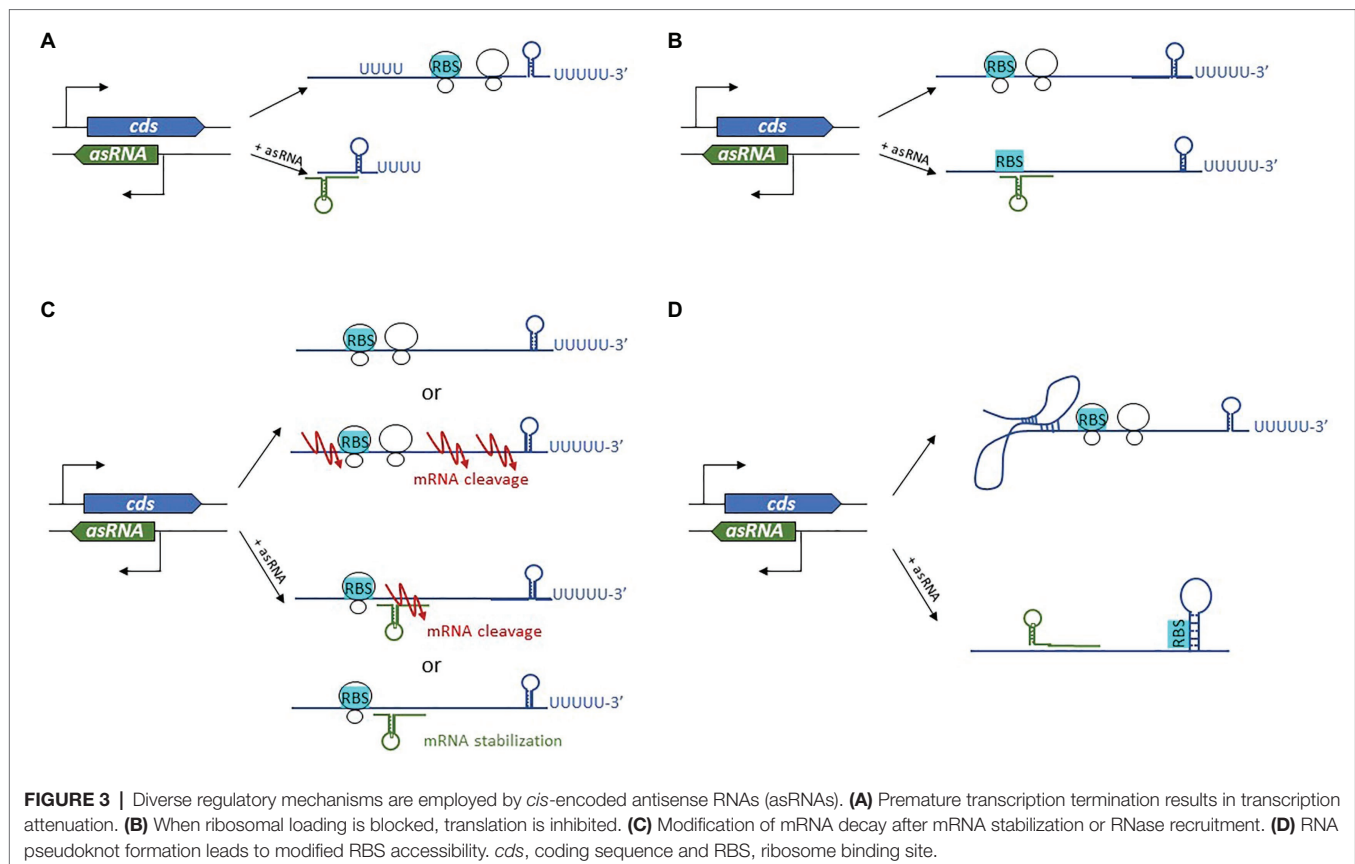


FIGURE 2 | Diversity in antisense RNA (asRNA) genomic locations and lengths. **(A)** Position of an intragenic asRNA. **(B)** An asRNA complementary to and overlapping the 5' untranslated region (UTR). **(C)** An asRNA complementary to and overlapping the 3' UTR. **(D)** A long asRNA (lasRNA) covers multiple genes. **(E)** In the concept of the excludon, an lasRNA controls the expression of an mRNA expressed from the opposite strand, and also encodes mRNA. *cds*, coding sequence.



from the opposite strand, so it competes with ribosome loading. Several examples have been described in plasmidic asRNAs, such as RNAII which controls plasmid pLS1 replication by binding the *repB* RBS (Brantl, 2007). A similar mechanism was reported in FinP, an asRNA which represses the expression of TraJ by blocking ribosomal access to *traJ* mRNA, inhibiting conjugation. For optimal regulation in this case, the FinO RNA chaperone is necessary to facilitate RNA–RNA duplex formation and to protect FinP against RNaseE-mediated RNA degradation (Arthur et al., 2003).

Modification of mRNA Decay

The binding of the asRNA to its complementary mRNA target also modifies mRNA decay (Brantl, 2007; **Figure 3C**). Most often, repression is observed through endoribonuclease cleavage of RNA. Indeed, double-stranded RNAs and the asRNA-mRNA heteroduplex are substrates of RNase III. This enzyme preferentially recognizes long dsRNA segments, which are then cleaved. In *S. aureus*, genome-wide antisense transcription activity was shown to be coupled with RNase III processing of mRNA/asRNA duplexes (Lasa et al., 2011). Such a mechanism may be involved in the post-transcriptional modulation of mRNA counts, as this duplex formation causes at least 75% of the mRNAs to be specifically cleaved by RNase III. In the same study, the authors reported similar trends in *B. subtilis*, *Enterococcus faecalis*, and *L. monocytogenes*. RNase E is another RNase that participates

in mRNA decay. A good example is that of the *Salmonella* asRNA AmgR, expressed from the opposite strand of *mgtC* (Lee and Groisman, 2010; **Figure 4A**). During phagocytosis, the PhoPQ two-component system senses low concentrations of Mg^{2+} , leading to signal transduction and the induction of the expression of several genes including the *mgtCBR* operon (Alix and Blanc-Potard, 2008). In addition, PhoP activates the expression of AmgR, which binds *mgtC* mRNAs, and favors its degradation *via* RNase E but not RNase III. In the absence of AmgR, the operon is transcribed, promoting bacterial virulence (Lee and Groisman, 2010). Although, the preferred mode of action is the promotion of RNA degradation, there have also been reports of inhibition of mRNA degradation and therefore of positive post-transcriptional effects of asRNAs (Sesto et al., 2013; Svensson and Sharma, 2016).

In bacterial pathogens, several examples of asRNAs overlapping an RBS have been described, and they go beyond plasmid replication-related functions (Thomason and Storz, 2010; Lejars and Hajnsdorf, 2020). This is the case in *Pseudomonas*, *Salmonella*, *Shigella*, *Clostridioides difficile*, *L. monocytogenes*, and *S. aureus*, although precise demonstrations of this mechanism of action are lacking, and it is often linked to transcript abundance variations, as recently reviewed (Lejars and Hajnsdorf, 2020). This indicates that translation inhibition and mRNA decay are often concomitant, as we will see for RNAIII in the next section.

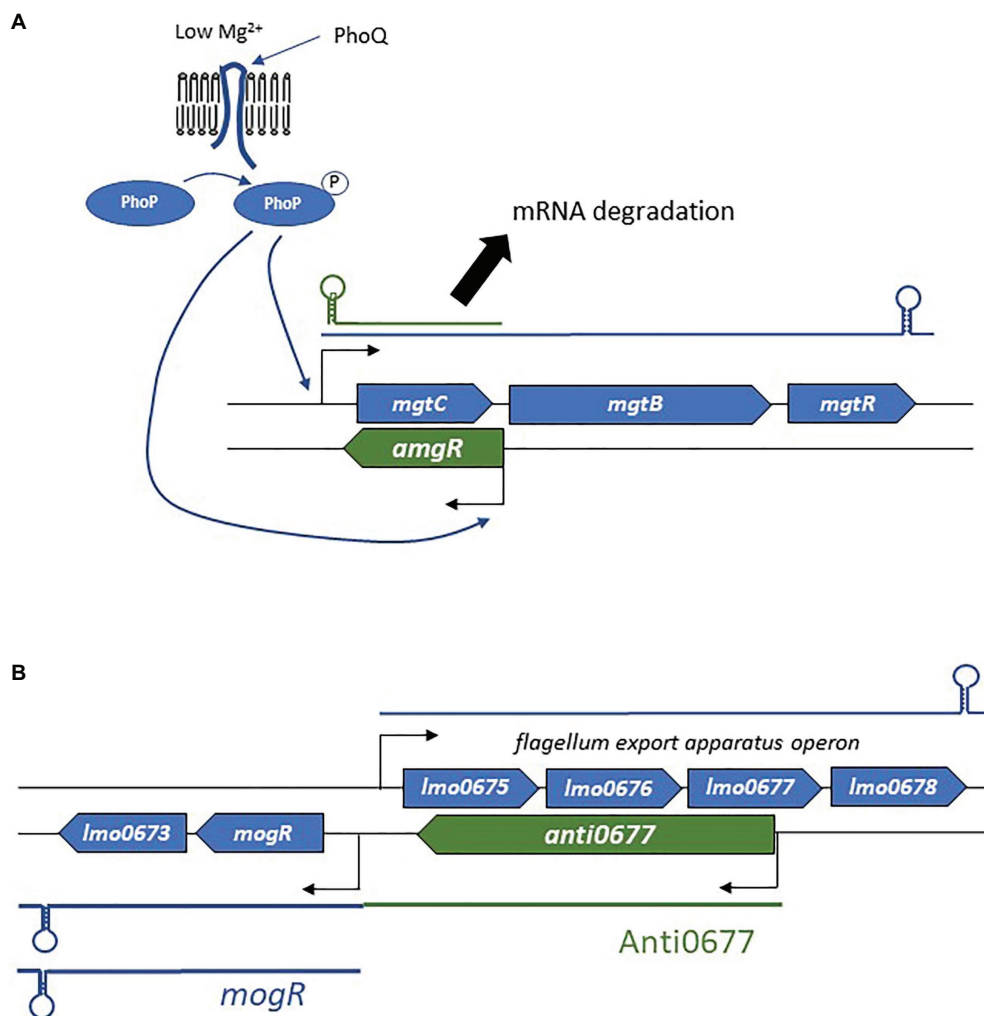


FIGURE 4 | Examples of the mechanism of actions employed by asRNAs. **(A)** Regulation of the *mgtCBA* operon and the role of AmgR in degradation of *mgtC* mRNA. **(B)** Schematic representation of the flagellum biosynthesis exclusion downregulated by the long asRNA Anti0677.

RNA Pseudoknot Formation

RNA pseudoknot formation can be altered by the presence of asRNAs (Asano and Mizobuchi, 1998a,b). In this case, conformational changes are responsible for regulation as well as for transcription attenuation (Figure 3D), with the translation of *repZ* dependent on the formation of a pseudoknot upstream of the RBS. Binding of the asRNA Inc. to *repZ* mRNA blocks the formation of this pseudoknot and thus prevents translation (Brantl, 2007).

The Excludon

In addition to the canonical localizations and mechanisms of action, a novel concept in bacterial asRNA-mediated gene regulation has also emerged: the excludon (Sesto et al., 2013; Toledo-Arana and Lasa, 2020). This was first delineated in *L. monocytogenes* soon after the identification of a group of lasRNAs (Wurtzel et al., 2012). In an excludon, transcription of lasRNAs is initiated from a promoter located on the opposite

strand of the CDS (Figure 2E). One interesting feature of the excludon is that transcription continues beyond the overlapping region, also encompassing the coding regions located downstream from the actual asRNA locus. Through this atypical mode of biogenesis, the transcript possesses dual functions, with the 5' antisense regulator of the gene(s) expressed from the opposite strand, while the 3' moiety encodes one or more proteins. Several excludons are reported in *L. monocytogenes*, and the functions encoded within the locus (i.e., lasRNA and mRNA) are closely related (Sesto et al., 2013). In that pathogen, excludons were shown (or predicted) to be involved in flagellum biosynthesis, a permease-efflux pump, or utilization of carbon sources. As these examples have already been well-described (Sesto et al., 2013), we will just discuss the mechanism of action employed in the biosynthesis of flagella (Figure 4B), extracellular appendages important for cell motility, biofilm formation, and host cell invasion (O'Neil and Marquis, 2006; Lemon et al., 2007). The excludon is composed of four genes

expressed from the positive strand that encodes the flagellum export apparatus, *lmo0675*, *lmo0676*, *lmo0677*, and *lmo0678*. Two genes of this operon are encoded divergently, including the *mogR* transcriptional regulator of the flagellum export apparatus (**Figure 4B**). The *lasRNA* Anti0677 is expressed from a σ^B -dependent promoter far upstream from *mogR* and as an antisense of *lmo0677*. When bacteria are not subjected to stress, the flagellum export apparatus operon is under the sole control of the transcriptional repressor MogR. Under stress conditions, σ^B promotes transcription of Anti0677, leading to an efficient switch-off of the flagellum production through direct antisense inhibition of the operon and increased MogR expression in both *mogR* mRNAs and Anti0667 *lasRNAs*. Recently, a similar “noncontiguous operon” organization leading to transcriptional interference coupled with endoribonuclease-mediated cleavage was reported in *S. aureus* (Sáenz-Lahoya et al., 2019).

sRNAs in Type I Toxin-Antitoxin Systems

Several asRNAs belong to type I TA systems. Type I TA modules are composed of a stable toxic peptide and a labile asRNA that inhibits toxin expression, although the existence of divergently expressed genes leading to the expression of a *trans*-encoded sRNA has also been reported (Brantl and Jahn, 2015). Initially discovered on plasmids, where their role in post-segregational killing prevents plasmid loss during cell division, overexpression of these systems induces small membrane-damaging peptides, which leads to cell death, global translation inhibition, and commitment to persistence. Their mechanisms of action often rely on a perfect complementarity between the RNA antitoxin and the mRNA target, and are associated with translation inhibition and dsRNA-degradation of the heteroduplex through RNase III recruitment (Wen and Fozo, 2014). However, several new features have also been reported, particularly in *S. aureus*.

The type I TA SprA/SprA_{AS} system identified in a pathogenicity island (Pichon and Felden, 2005), exemplified the fact that an asRNA regulates in *trans* the translation of its cognate antitoxin (Sayed et al., 2012). Here, the two genes overlap at their 3' ends, suggesting that the putative mechanism of action is not the annealing of the RNA antitoxin onto the RBS. Structural probing of SprA1 RNAs showed the presence of two pseudoknots and a 5' stem-loop that disfavored RBS accessibility. Upon SprA1_{AS} binding, an internal RNA pseudoknot of SprA1 unfolds and forms a helix with SprA1_{AS}. Surprisingly, gel retardation assays and mutational analysis revealed that by imperfect base-pairing, the non-overlapping region of SprA1_{AS} binds the antitoxin to the RBS, preventing ribosome loading and translation. Therefore, in a *trans*-encoded manner, the *cis*-encoded asRNA SprA1_{AS} negatively regulates the translation of its cognate antitoxin. A similar *cis-trans* mechanism of action was also reported in the SprA2/SprA2_{AS} type I TA module (Germain-Amiot et al., 2019).

The SprG/F TA module is another intriguing example of the TA system, in which, the RNA antitoxin can act in *trans* and exert several functions. This system was originally characterized by its perfect base complementarity between the 3' end of each RNA and for not competing with ribosome loading (Pinel-Marie et al., 2014). However, the authors showed

that this was sufficient to destabilize mRNA and toxic peptide levels, even if the mechanism was not precisely defined. In a more recent study, SprF1 was demonstrated to have a novel *trans*-effect on ribosomes and polysomes (Pinel-Marie et al., 2021). A purine-rich sequence in the antitoxin is responsible for binding ribosomes, which results in global translation initiation interference and increased tolerance to antibiotics, thereby enabling the formation of persister cells. This new finding suggests that type I antitoxin RNA functions are not restricted to regulation of their cognate toxins.

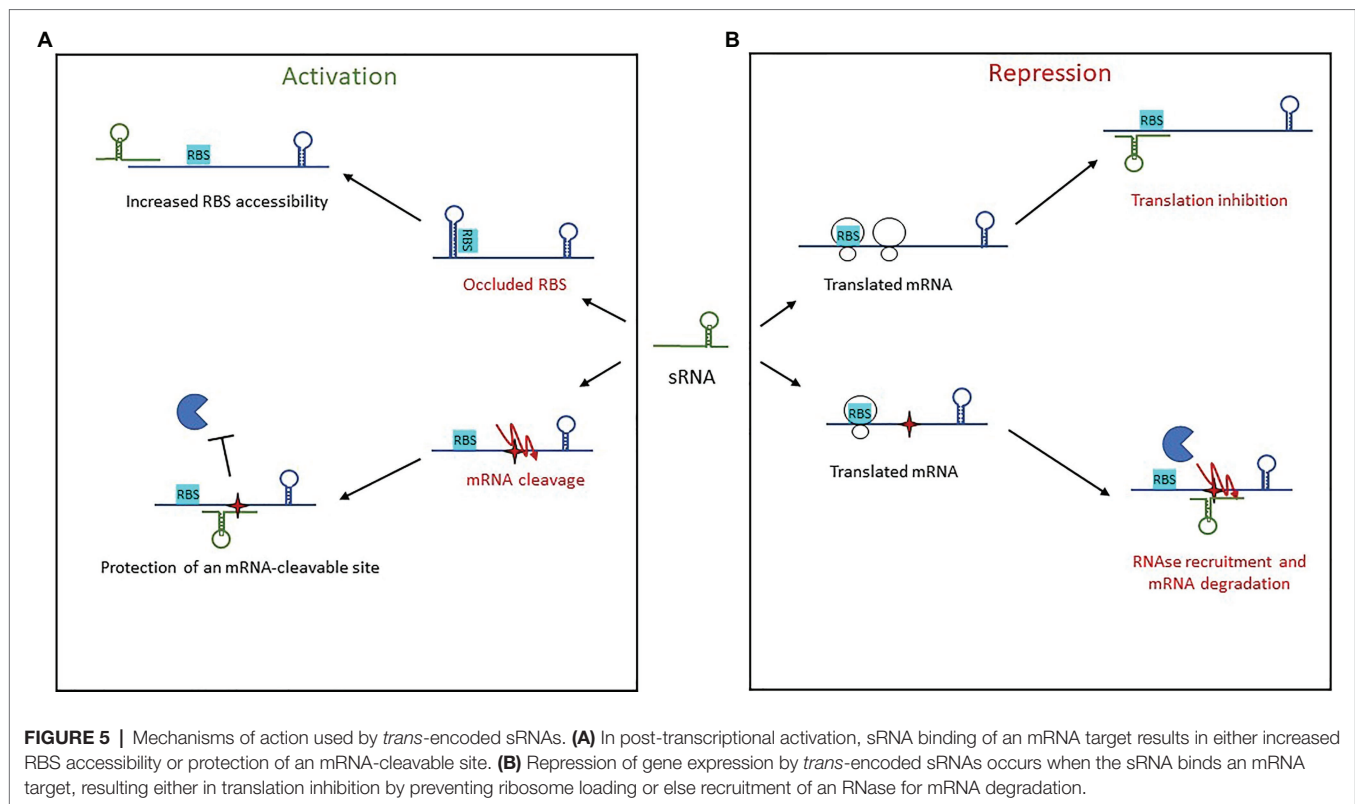
Trans-Encoded sRNAs

Trans-encoded sRNAs are associated with intergenic regions and are relatively easy to identify experimentally or *via* predictive tools, since they have distinctive features including a consensus promoter region and U-tract following inverted repeated sequences (intrinsic terminator). Their biogenesis occurs at a locus distant from their targets, so their seed sequences share partial complementarity with them. These sRNAs thus usually regulate more than one mRNA through some of the mechanisms detailed for asRNAs. This partial complementarity, which could represent an apparent weakness, is in the most cases circumvented with the help of RNA chaperones. These sRNAs transcribed from intergenic regions represent the largest set of functionally characterized molecules in the bacterial kingdom. They are expressed under specific conditions to fine-tune gene expression and are highly structured, which may contribute to their increased stability (Waters and Storz, 2009). Typically, they have one or more stem-loops, some of which have cytosine-rich motifs that favor interaction with the RBSs of their targets (Geissmann et al., 2009). As mentioned above, *trans*-encoded sRNAs are involved in a large set of functions, with repression the most common outcome, although examples of activation have also been reported.

Trans-Encoded sRNA Activators

While considered marginal, there are growing examples of *trans*-encoded sRNAs that permit increased translation and/or mRNA stabilization (**Figure 5A**). Activation of sRNA base-pairing is typically associated with the 5' UTR, although targeting of the coding sequence is also possible (Papenfert and Vanderpool, 2015).

Activation *via* the 5' UTR involves two mechanisms of action. The first is an anti-antisense mechanism that induces structural modifications to enable the unfolding of an intrinsic structure that inhibits translation. This leads to the release of the occluded RBS, thus enhanced ribosomal access. This has been observed with RNAIII in *S. aureus* (Morfeldt et al., 1995), further discussed below, as well as with Rli27 in *L. monocytogenes* (Quereda et al., 2014). Rli27 is involved in cell-wall formation during a pathogen's intracellular lifestyle. It activates the cell wall-encoding protein Lmo0514 *via* binding of its 5' UTR, thus unmasking the RBS and promoting Lmo0514 production inside eukaryotic cells. The second mechanism of 5' UTR-activation is mRNA stabilization, an even a less-described phenomenon in which sRNA target-binding protects it from



RNases and therefore from cleavage. This is seen with RydC in *Salmonella* (Fröhlich et al., 2013). There, RydC adopts a pseudoknot structure at its 5' end that contains a seed sequence involved in recognizing a 5' UTR located far upstream from the RBS of *cfa* mRNA, which encodes CFA synthase. This seed pairing activates Cfa expression by mRNA stabilization through the mRNA cleavage protection provided by RNase E. In *Clostridium perfringens*, another mechanism of action was reported for the stabilization of the mRNA *colA*, which encodes collagenase toxin (Obana et al., 2010). In this pathogen, the 3' region of VR-RNA binds *colA* to mediate cleavage of the mRNA 78 nt upstream the A of initiation codon, resulting in the release of a more stable mRNA.

Other sRNAs activate translation by base-pairing with the coding sequence. In *E. coli* and *Salmonella*, the sRNA SgrS involved in sugar homeostasis displays several distinctive features (Papenfort et al., 2013). Like RNAIII, it has dual functions, acting both as a *trans*-encoded sRNA as well as encoding the small protein SgrT. Among the known targets of SgrS is the second gene of the bicistronic operon *pldB-yigL*, which is under its positive control and encodes a phosphatase. Under normal conditions, the transcript is processed by RNase E, resulting in *yigL* transcript level adjustments. When the concentration of phosphorylated sugars increases, regulation is needed to avoid cell toxicity, so SgrS is expressed. It binds the coding sequence to stabilize the *yigL* transcript by masking a cleavage site recognized by RNase E, thereby preventing its degradation. The increased phosphatase activity lowers sugar phosphate levels and causes the excretion of non-phosphorylated sugars. At the

same time, SgrS effectively controls sugar phosphate levels by repressing the expression of three other targets involved in sugar transport, once again demonstrating the versatility of sRNAs as regulators.

Trans-Encoded sRNA Repressors

Repression by *trans*-encoded sRNAs involves transcription attenuation, translation repression, and mRNA degradation (Figure 5B). Regulatory signals are often contained within the 5' UTR of target mRNAs. The most common mechanism of action in this group is the repression of translation initiation, with sRNAs binding the RBS to prevent loading by the 30S ribosomal subunit. This binding sometimes encompasses the AUG codon, although any interaction surrounding the RBS and AUG up to five codons into the coding sequence is inhibitory (Hüttenhofer and Noller, 1994; Bouvier et al., 2008). Several seed regions/sequence patterns have been described for these *trans*-encoded sRNAs, and the association of single-stranded RNAs to form heteroduplexes is not the only one. The patterns usually reflect the structural shape of RNAs and include several hairpin loops that require additional features. For instance, "kissing complexes" (loop-loop interactions between sRNAs and mRNAs) can occur when GC-rich sequences present in the sRNA loop associate with the RBS of their target (Lioliou et al., 2010).

To facilitate complex formation, sRNAs (and sometimes mRNAs) have to unfold to generate double-stranded heteroduplexes, which are thermodynamically favorable. C-rich conserved sequences were identified in stem-loops and shown

to be involved in the recognition of G-rich sequences such as the RBSs of mRNA targets. This was first proved in *E. coli* for the repression of *fhlA* by OxyS (Altuvia et al., 1998), then later on in multiple pathogens including *L. monocytogenes*, *Salmonella*, *H. pylori*, *V. cholerae*, and *S. aureus* (Papenfort et al., 2008, 2015; Geissmann et al., 2009; Pernitzsch et al., 2014; Sievers et al., 2014). In *S. aureus*, bioinformatic and phylogenetic analyses were used to identify a conserved unpaired UCCC motif present in the apical loop of several sRNAs, and this was interpreted to be the potential signature of Hfq-independent sRNAs in Gram-positive bacteria (Geissmann et al., 2009; Jørgensen et al., 2020). The role of this motif in the repression of translation was demonstrated for the sRNA RsaE (Geissmann et al., 2009). In *L. monocytogenes*, LhrC sRNAs contain three redundant CU-rich motifs, with one in a stem-loop, another on a single-strand region, and the last occurring in the terminator (Sievers et al., 2014). These sites are important for the translational repression of LapB at the RBS, and another study showed that LhrC translationally represses OppA via RBS binding of two of the three CU-rich motifs (Sievers et al., 2015). However, there are also examples of sRNAs blocking translation by masking the RBS with seed sequences that do not exhibit strong C-rich motifs. In *Salmonella*, IsrM, the sRNA involved in virulence, represses the expression of *hilE* and *sopA* mRNAs using two different seeds, which seem to have random C-distributions although they still sequester the RBS (Gong et al., 2011). The presence of two seeds in IsrM indicates that sRNAs can have several regulatory domains. In *S. aureus*, the multifaceted sRNA RsaI expressed under glucose-limited conditions displays similar properties, with two distinct regulatory domains (Bronsky et al., 2019). The first is a typical unpaired CU-rich sequence that base pairs with the RBSs of most of the identified mRNA targets (sugar uptake and metabolism). The second is a G-rich sequence that binds the CU-rich tracts of other sRNAs such as RsaD, RsaG, RsaH, and RsaE, indicating the potential existence of other mechanisms of actions for controlling sRNA functions.

Apart from the ribosome binding site, other target regions do exist. For instance, sRNAs can bind their mRNA targets upstream from the RBS, within the coding region or at the 3' UTR. The *Salmonella* sRNA GcvB contains the GU-rich sequence that interacts with the CA-rich sequences of its target mRNAs (Sharma et al., 2007). For at least one target, *gltI* mRNA, the sRNA specifically recognizes a sequence far upstream from the RBS (~50 nt) that actually acts as a translational enhancer sequence. Still in *Salmonella*, examples of sRNAs binding coding sequences several nucleotides downstream from the RBS were also reported. In that bacterium, MicC sRNAs repress *ompD* mRNAs via binding to codons 23–26, which is sufficient for repression (Pfeiffer et al., 2009). By doing so, MicC increases RNase E-dependent *ompD* mRNA decay rather than repressing translation. Interestingly, the SdsR sRNA also represses *ompD* using a similar mechanism between the 15th and 26th codons (Fröhlich et al., 2012).

The sRNA can also bind the 3' UTR of an mRNA to modulate its expression. For instance, *S. aureus* RsaI binds the 3' UTR of the mRNA *icaR*, which encodes a transcriptional

repressor of exopolysaccharide production (Bronsky et al., 2019). Although the mechanism of action is yet not understood, this binding contributes to the translational repression of IcaR either by preventing the action of *trans*-acting activators (proteins or RNAs) or by indirectly stabilizing the interaction between the 5' and 3' UTRs of *icaR* mRNAs, known to sequester the RBS.

Along with translation inhibition, sRNA-mediated regulation often involves degradation by RNases. Untranslated mRNAs are subjected to RNA degradation since the absence of polysomes does not protect RNAs from RNases (Deana and Belasco, 2005). Furthermore, the sRNA-mRNA duplex can be used to recruit RNaseE as the means to control RNA decay (Morita et al., 2005; Bandyra et al., 2012). Some sRNAs are then co-degraded with their targets, some are recycled like enzymes, and the fate of the others depends on their molecular target (Massé et al., 2003; Feng et al., 2015). In addition to RNase E, roles for RNase III and RNase Z were also reported in target RNA degradation (Dutta and Srivastava, 2018).

Altogether, study of *trans*-encoded sRNAs reveals that they can act anywhere on their mRNA targets and that any parts of their sequences can have regulatory functions, implying unlimited possibilities for their mechanisms of action.

Cis-Acting Regulatory Elements of mRNAs: Riboswitches, Thermosensors, and T Boxes

Although not considered to be sRNAs, riboswitches are pivotal players in RNA-mediated regulation of gene expression, and as we will see later, their extraordinary versatility lets them closely link with sRNAs. Riboswitches are natural aptamers usually identified in the 5' UTR of some mRNAs in both Gram-positive and Gram-negative bacteria. They are *cis*-acting elements regulating at the transcriptional and/or translational levels the expression of their downstream genes. To do this, they sense by physical interaction metabolite variations, then modify their secondary structures to form two mutually exclusive RNA conformations (Mironov et al., 2002; Winkler et al., 2002; McDaniel et al., 2003; Nudler, 2006). They contain two distinct functional domains: a metabolite-sensing domain, and an expression platform. Ligand binding induces conformational changes that lead to transcription termination or inhibition of translation initiation. One interesting feature of riboswitches is their conserved sensing domain and the variability of their expression platform. This is the case for the riboswitch that senses thiamine pyrophosphate (TPP): its sensing domain specifically and selectively binds TPP, while its expression platform induces transcription termination in Gram-positive bacteria and suppresses translation initiation in Gram-negative bacteria (Serganov et al., 2004; Nudler, 2006). Another specific feature of riboswitches is their ability to bind ligands without the need to establish Watson-Crick base pairs. The riboswitch folds into a very specific configuration that allows target metabolite recognition and sequestration due to the hydrogen bonds of RNA bases and ribose sugars. Riboswitches are

widespread and diverse, as a plethora of effectors have been identified (TPP, SAM, FMN, sugars, divalent ions, etc.). Usually, they control the expression of genes that have functional links with their effector.

The canonical description of the riboswitch mode of action was overturned by the discovery that they can act as RNA thermometers and pH meters, thus they can be active without necessarily requiring metabolite sensing. RNA thermometers generally fold in a temperature-dependent manner to generate alternative conformations that affect translation (Kortmann and Narberhaus, 2012). The first example of an RNA thermometer was identified in the pathogen *L. monocytogenes* (Johansson et al., 2002). In this study, the authors showed that the switch into virulence orchestrated by PrfA, the master regulator of virulence, is actually dependent on a conformational change of the 5' UTR of its cognate mRNA. At 30°C, the *prfA* 5' UTR adopts a secondary structure that masks the RBS, acting as a translation repressor. At 37°C, the energy provided by the increased temperature is sufficient to cause a structural switch that enables translation of the TF. Additional thermometers are found in many pathogens such as *Salmonella* Typhi and *S. aureus* (Hussein et al., 2019; Brewer et al., 2021; Catalan-Moreno et al., 2021), and have been extensively reviewed (Loh et al., 2018).

The first 5' UTR element to be identified in the late 1990s was the T-box, which controls the expression of genes involved in amino acid biosynthesis or use. They are typically upstream aminoacyl-tRNA synthetase transcripts, are widely distributed in Gram-positive bacteria, and they respond to the accumulation of uncharged tRNAs when cognate amino acid concentrations are too low. Contrary to metabolite-sensing riboswitches, T-boxes bind uncharged tRNAs by base-pairing with their anticodons and with the acceptor-end T/D loops to stabilize an anti-terminator element, allowing synthesis of full-length mRNA. In *Clostridium acetobutylicum* (André et al., 2008) and later in *L. monocytogenes* (Mellin et al., 2013), exploration of T-box riboswitches led to the discovery of a novel mechanism of action, with *cis* elements involved in antisense RNA control located downstream (these turned out to be SAM riboswitches) and on the opposite strand of the gene. Other unexpected riboswitch mechanisms of action is reviewed here (Mellin and Cossart, 2015).

UNCONVENTIONAL REGULATORY RNA BIOGENESIS AND FUNCTIONS

The term “sRNA” was often restricted to those species transcribed from intergenic regions, or as antisense to a coding sequence. Ongoing efforts to identify novel sRNAs and to decipher their mechanisms of action has demonstrated that they harbor an even broader than expected variety of structural traits, biological functions (and even sometimes dual functions), and modes of biogenesis. For instance, studies have shown that RNA regulators are also produced from 5' to 3' UTRs (Miyakoshi et al., 2015b; Heidrich et al., 2017; Carrier et al., 2018).

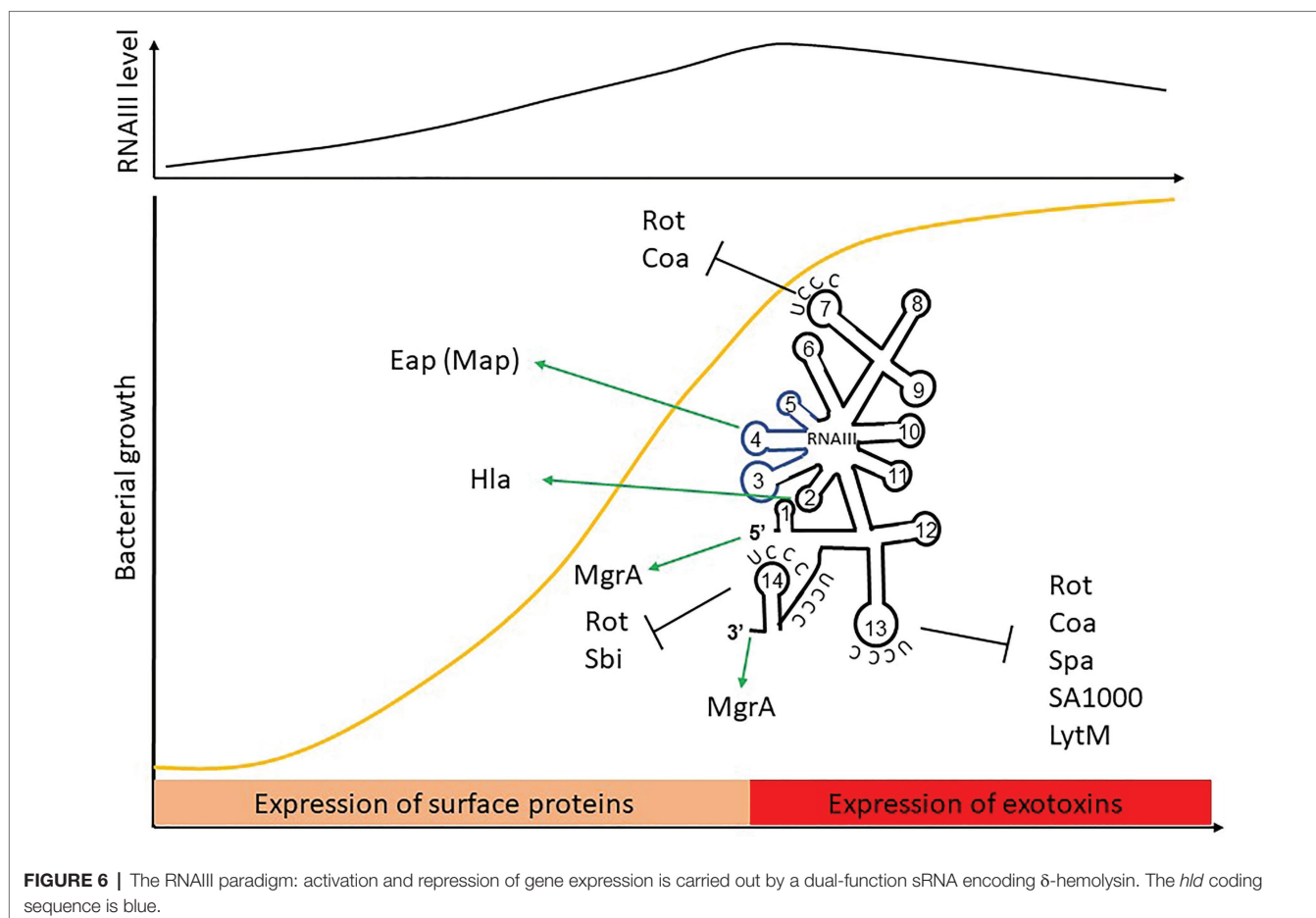
The Fascinating Case of RNAIII in *Staphylococcus aureus*

RNAIII is one of the best-characterized sRNAs in pathogens and probably even in bacteria. It was first described in 1993, when it was defined as the intracellular effector of the Agr system (Novick et al., 1993). It is one of the most representative examples of the sRNA with distinctive futures. RNAIII is a 514-nt long dual-function sRNA whose expression is regulated by growth phase and cell density through QS. RNAIII acts at a post-transcriptional level by using antisense mechanisms, which lead to translation inhibition and/or modification of target RNA stability (Figure 6). RNAIII positively or negatively regulates a large number of targets through various mechanisms, and has a complex structure with 14 stem-loops (Benito et al., 2000) of which three contain C-rich sequences. These three hairpins, H7, H13, and H14, are involved in translation repression, preventing ribosomes from loading onto target RBSs. The first stem-loop (H1) is required for RNAIII stability, while H14 acts as an intrinsic transcription terminator. H3, H4, and H5 are responsible for the definition of this sRNA as dual-function, another sRNA subgroup which has been extensively reviewed (Gimpel and Brantl, 2017; Raina et al., 2018). These three stem-loops encode δ -hemolysin (Hld), which is a toxin made of 26 amino acids arranged into an α -helix structure, and which permeabilizes host cells (Figure 6). Interestingly, there is not a perfect transcription-translation coupling between *hld* mRNA biogenesis and translation of the Hld peptide. Although the cause for this is not completely understood, it was reported that deletion of the 3' end of RNAIII abolishes this delay, suggesting either that a third party is involved (Balaban and Novick, 1995) or that the 5' and 3' regions of RNAIII are (or serve as) *cis*-regulatory elements. RNAIII is under the positive transcriptional control of AgrA and accumulates in bacteria over the course of the growth phase, reaching its maximal transcript levels during the post-exponential phase (Dunman et al., 2001). With its versatile effects, RNAIII orchestrates the transition between colonization and infection by repressing early virulence genes and activating other virulence factors (Table 1).

RNAIII Target Repression

RNAIII represses the expression of several genes involved in virulence (adhesion or immune evasion), including Rot TF (Table 1). The mechanism of action is always translation repression, with RBS binding in order to prevent ribosome loading and translation initiation. In most cases, duplex formation is followed by rapid degradation of the mRNA target through the recruitment of RNase III (Bronesky et al., 2016), although the mechanism differs for the regulation of Sbi and perhaps also for LytM (Boisset et al., 2007; Chabelskaya et al., 2014).

Repression of Spa involves the 3' end domain of RNAIII (Huntzinger et al., 2005). Spa is one of the major surface proteins involved in host interactions as well as virulence (Foster, 2005). Based on sequence complementarity, the deletion of RNAIII's H13 stem-loop abolishes regulation by RNAIII. This repressive hairpin sequesters the *spa* RBS to prevent translation initiation, although efficient repression requires RNase III. A similar repression mechanism involving H13 and



RNase III was reported for SA1000, which encodes a fibrinogen-binding protein (Boisset et al., 2007). Repression of Rot, the repressor of toxin Rot requires hairpins H7, H13, and H14, who form kissing complexes to permit translation repression and RNase III cleavage (Boisset et al., 2007). To do this, H7 and H13 enable the formation of a loop-loop interaction with the 5' UTR of *rot*, while H14 is involved in a loop-loop interaction with the mRNA RBS. Two loop-loop interactions are needed for efficient translation inhibition, and binding of RNAIII with *rot* induces a specific signature for RNase III cleavage. Rot is known to inhibit the production of several exotoxins after their transcription as well as to enhance Spa expression. Therefore, RNAIII inhibition of Rot indirectly promotes exotoxin expression and represses surface protein production.

As with Rot, RNAIII repression of Coa involves two stem-loops (H7 and H13), although the structural conformations differ between these examples (Chevalier et al., 2010). In this case, H13 sequesters the *coa* RBS through canonical imperfect double-strand base-pairing and this is sufficient to block the formation of ribosomal initiation complexes. Additionally, H7 forms a loop-loop interaction with the 3' end of *coa*, and both RNAIII-*coa* complexes serve as templates for RNase III.

RNAIII regulation of LytM is less documented. While bioinformatic predictions suggest that stem-loop H13 is involved

(Boisset et al., 2007), and it is known that the *lytM* RBS is an RNAIII target (Chunhua et al., 2012), the precise mechanism of action and the putative involvement of RNase have not yet been determined.

Sbi is another target repressed by RNAIII (Chabelskaya et al., 2014), and it is negatively regulated by SprD sRNAs (Chabelskaya et al., 2010). Sbi protein participates in anti-opsonization effects by binding immunoglobulins (Foster, 2005). Three distant RNAIII domains interact with *sbi* mRNAs, with two annealing regions located within the *sbi* coding region and one on the RBS to block translation initiation. Since RNAIII and SprD are not expressed at the same time, these studies highlight a cooperative role of these two sRNAs to precisely control Sbi expression suggesting the presence of complex sRNA control networks in bacteria.

RNAII Activation of Gene Expression

In addition to its inhibitory roles, RNAIII can also directly activate several targets. This is true in the case of Hla, whose expression is reduced in a mutant lacking RNAIII (Morfeldt et al., 1995). RNAIII binds *hla* mRNAs to prevent the formation of a structure that would sequester the RBS, thereby promoting RBS accessibility and translation. Unlike the mechanism involving repression, here the 5' end (H2 in RNAIII) is required for base-pairing with *hla*. Map (also known as Eap) is another

target that is stimulated by RNAIII (Liu et al., 2011). To activate Map expression, RNAIII binds the 5' UTR of *map* using its hairpin H4, which suggests a structural modification that enables ribosomal loading, although the mechanism of action has not yet been unraveled. RNAIII was also shown to positively regulate MgrA (Gupta et al., 2015), the TF which inhibits surface proteins, autolysis, and biofilm formation, as well as promoting capsule synthesis (Bronesky et al., 2016). Interestingly, MgrA also activates the expression of Agr and thus indirectly RNAIII (Ingavale et al., 2005). RNAIII stabilizes *mgrA* RNAs by double-strand base-pairing using both its 5' and 3' ends (Bronesky et al., 2016), with each end interacting simultaneously with the 5' UTR of *mgrA* mRNA to allow mRNA stabilization and translation.

RNAIII thus differs from the conventional dogma about sRNAs in many ways. It contains a coding sequence, and is therefore considered as a dual-function sRNA. It is longer than most sRNAs, and has a complex structure containing several hairpins, which are crucial for gene repression. Its gene repression mechanism involves translation initiation control and is often associated with RNase III cleavage. The 5' end is thought to be involved in gene activation *via* mRNA stabilization and translation activation, while the 3' end is involved in both activation and the repression mechanisms. The 3' end is also important for RNAIII's own stability, and therefore may be a key *cis* element for Hld production. Finally, little is known regarding the role of the other hairpins, suggesting that there may be additional features left to discover.

5' UTR-Derived sRNAs

5' UTRs are normally considered to be riboswitches, *cis*-acting elements. The first major evidence of the sRNA produced from a 5' UTR was the cleavage of the two SAM riboswitches SreA and SreB in *L. monocytogenes* (Loh et al., 2009). In that report, the biogenesis of SreA and that sRNA's mechanism of action were described extensively. During methionine starvation, SAM concentrations are relatively low, leading to the formation of an anti-terminator structure that enables the transcription of the downstream gene. When the concentrations of this ligand increase along with methionine biosynthesis, SAM binds the riboswitch. This allows structural rearrangement and transcription termination, and results in the accumulation of SreA, an sRNA transcript of 229 nts which has *trans*-acting features. Remarkably, SreA controls the expression of the virulence TF PrfA by binding the 5' UTR of its mRNA, while PrfA exerts a positive control on SreA expression. This shows that some *cis*-acting regulators can be cleaved to act in *trans* in response to environmental cues. Another example of a riboswitch-producing *trans*-acting sRNA was reported in *L. monocytogenes* (Mellin et al., 2014). The authors showed that in the absence of the ligand, a riboswitch binding vitamin B12 is cleaved and releases Rli55. In turn, Rli55 expression prevents the expression of the *eut* genes involved in ethanolamine use and whose expression depends on vitamin B12 availability. To do this, Rli55 sequesters EutV, a regulatory protein which binds *eut* mRNAs to prevent premature termination of transcription. A similar mechanism for regulating *eut* *via* protein sequestration was described in

E. faecalis, although there an adenosyl cobalamine-binding riboswitch releases EutX *trans*-acting sRNAs (DebRoy et al., 2014). In *S. aureus*, the sRNA Teg49 is derived from the 5' UTR region of TF *sarA* mRNA (Beaume et al., 2010; Kim et al., 2014). The expression of *sarA* is under the control of the three promoters P1 through P3, with P3 important for expression during the post-exponential growth phase. Teg49 is transcribed from P3 and is probably the result of RNase III processing. Another study indicated a role of Teg49 in virulence, although the mechanism of action is not clearly understood (Manna et al., 2018).

Based on the first discoveries, 5' UTR-derived sRNAs are probably more present in Gram-positive pathogens. It was proposed that the relative absence of such sRNAs in Gram-negative pathogens is explained by the fact that most sRNAs studies have been designed based on Hfd-binding. This binding usually occurs with the 3' poly(U) tail of sRNAs located downstream from intrinsic terminators, and these are likely to be absent in 5' UTR-derived sRNAs. Additionally, the need for Hfq-binding was questioned (Carrier et al., 2018). The mystery was solved in *P. aeruginosa* with a screen that attempted to map transcription termination sites affected by homoserine lactone quorum sensing (Thomason et al., 2019). Term-seq analysis identified RhlS as a novel Hfq-dependent sRNA expressed from the 5' UTR of *rhII*, an actor in the Rhl two-component system related to quorum sensing. Interestingly, RhlS is not derived from a riboswitch, but is induced when homoserine lactone concentrations increase. RhlS not only controls the translation of its downstream gene (*rhII*), but also regulates the translation of *fvpA* mRNAs transcribed from a distant locus and which encode a siderophore pyoverdine receptor, although the mechanism of action here is still unclear. Finally, recent work on *E. coli* focusing on the identification of 3' ends from 5' UTRs revealed the presence of *trans*-acting sRNA sponges (Adams et al., 2021).

3' UTR Is a Reservoir of *Trans*-Acting sRNAs

Expression of 3' UTR-derived sRNAs occurs frequently in bacteria, and the number of examples is growing quickly. Over the past few years, their identification has become easier with the development of high-throughput screenings such as Term-seq, RIL-seq, RIP-seq, and CLASH (Dar et al., 2016; Melamed et al., 2016; Hoyos et al., 2020). These sRNAs act in various physiological regulons including amino acid transport and biogenesis. They are categorized into two classes depending on whether they have their own promoters (type I) or if they are produced by mRNA processing (type II; Miyakoshi et al., 2015b). While type I sRNAs seem completely independent of the gene encoded upstream when it comes to biogenesis the functions they regulate, the expression of type II sRNAs depends on the initial mRNA transcription. So far, more type II molecules have been discovered, and most 3' UTR-derived sRNAs have been discovered in Gram-negative bacteria. Post-transcriptional regulation by 3' UTR elements was recently reviewed (Menendez-Gil and Toledo-Arana, 2020).

Type I 3' UTR-Derived sRNAs

This type of 3' UTR-derived sRNA contains its own promoter, located either within the coding sequence or immediately downstream. In 2012, Hfq co-immunoprecipitation of transcripts followed by RNA-seq analysis enabled the discovery of novel sRNAs whose RNA sequences mapped with the 3' region of mRNAs (Chao et al., 2012). During this screen, the authors identified DapZ, an 80-nt sRNA transcribed from its own promoter and that overlaps the *dapB* 3' UTR. Although they share the same terminator, their transcription is independent of each other. DapZ modulates the synthesis of ABC transporters of Opp and Dpp by base-pairing with their cognate mRNAs. One interesting feature of DapZ is that it contains a repressing seed sequence (G/U-rich domain) similar to that of GcvB sRNA, a global regulator of amino acid transport and biosynthesis genes, so they recognize the same targets. This indicates that despite being independent, the two sRNAs can have complementary functions.

In *S. aureus*, a search for novel transcripts uncovered an intricate organization in the Newman strain, with an unusual condensed sRNA cluster (Srn_9342 to Srn_9346; Bronsard et al., 2017). Using 5' RACE mapping combined with TEX and polyphosphatase treatments, the authors were able to show that the Srn_9342 transcription start site is located within the coding region of the upstream gene. This was supported by the identification of a putative sigma B binding site (Mader et al., 2016). Interestingly, Srn_9342 is expressed in two forms having different lengths and sharing the same 5' extremity, although the mechanism of biogenesis of each form and their respective functions remain to be elucidated. In this specific example, two terminators were predicted (Bronsard et al., 2017), with one sharing the upstream coding sequence as occurs in typical type I 3' UTR-derived sRNAs, and the other specific to the long sRNA species, indicating another variation in sRNA biogenesis within this category.

Type II 3' UTR-Derived sRNAs

This type of sRNA is derived from RNase E cleavage of an mRNA. An example is CpxQ, a ~60 nt-long transcript generated through cleavage of the 3' UTR of *cpxP* mRNA and which requires Hfq for optimal maturation as well as protection from further RNA decay (Chao and Vogel, 2016). Both CpxQ sRNAs and CpxP proteins are involved in inner membrane homeostasis, with the protein acting as a chaperone for misfolded proteins in the periplasm, and the sRNA controlling their expression in the cytosol. Thus, unlike with type I 3' UTR-derived sRNAs, CpxQ synthesis depends on *cpxP* transcription, and these two elements cooperate to carry out the same function. In *S. aureus*, after cleavage by the double-stranded RNase III, the sRNA RsaC is released from the 3' UTR of the *mntABC* operon, which encodes the major manganese ABC transporter (Lalaouna et al., 2019). This sRNA is intriguing, as its length varies between isolates due to the presence of a variable number of repeats within its internal RNA sequence. The 3' domain of RsaC was found to be involved in translational repression of *sodA* mRNA during manganese starvation, thereby modulating the response to oxidative stress.

The regulatory functions of these 3' UTR-derived sRNAs are often linked to the biological roles of their associated upstream genes (Menendez-Gil and Toledo-Arana, 2020). They therefore autoregulate the expression of their associated genes at the post-transcriptional level, inhibit translation by base-pairing, and serve as negative feedback controls (Chao and Vogel, 2016; Miyakoshi et al., 2019; Hoyos et al., 2020; Wang et al., 2020). As the description of this sub-class of sRNAs is relatively new, it is expected that its ranks will increase in the future.

sRNAs Excised/Expressed From Coding Sequences

While the examples cited above pertain to biogenesis from the 3' UTR or at least from the 3' end of mRNA coding regions, in-depth study of the transcriptomes of *E. coli*, *Enterobacter aerogenes*, and *Salmonella Typhimurium* uncovered the biogenesis of decay-generated noncoding RNAs (decRNAs) from coding regions situated far from mRNA 3' ends (Dar and Sorek, 2018). The authors identified a set of conserved sequences generated through RNase E activity and predicted to interact with the RNA chaperones Hfq and ProQ. A search for transcriptional start sites using 5' RNA-seq mapping uncovered numerous sRNAs transcribed from within coding sequences in several species including *Borrelia burgdorferi* and *Leptospira interrogans* (Adams et al., 2017; Zhukova et al., 2017). However, the functions of this novel type of sRNAs remain to be elucidated.

sRNA Processing to Produce Novel sRNAs or Additional Functions

In *S. aureus*, Srn_9342 is not the only sRNA transcribed into two forms (Bronsard et al., 2017), and similar properties were observed for both RsaA (Romilly et al., 2014) and RsaE (Schoenfelder et al., 2019). While transcriptional readthrough was just hypothesized for Srn_9342 and RsaA, post-transcriptional modification was actually demonstrated for RsaE. In *S. epidermidis*, RsaE is normally transcribed as a transcript ~110-nt long, but it can undergo processing to release a transcript of ~80 nt which lacks the 5' end. Biogenesis of this second form enables the expansion of the original RsaE targetome. The full-length sRNA specifically regulates antiholin-encoding *lrgA* mRNA by binding the RBS, preventing ribosome loading, and influencing mRNA levels. Conversely, the processed RsaE interacts with the 5' UTR of *icaR* and *sucCD* mRNAs, which encode the IcaR repressor of biofilm formation and the succinyl-CoA synthetase of the TCA cycle, respectively.

sRNA Sequestration by Other RNAs (Sponge RNAs)

As for any genes, we expect sRNA genes and transcripts to require fine regulation. Several TFs were identified as regulators of sRNA transcription, but regulation or sequestration of sRNAs by other RNAs is a relatively new topic of investigation. Research into type II 3' UTR-derived sRNAs engendered the concept of bacterial sponge RNAs, which soak up other sRNAs rather than just proteins in

order to suppress their regulatory functions (Azam and Vanderpool, 2015). The first sponge to be characterized was *chb*, which sequesters the sRNA ChiX (Figueroa-Bossi et al., 2009). ChiX represses the expression of ChiP, a porin involved in the uptake of chitosugars. In the absence of chitosugars, ChiX represses ChiP since it is not needed. When chitosugars are present, the *chBCARFG* operon is transcribed, and an intercistronic spacer sequence between *chbB* and *chbC* acts as a sponge for ChiX, allowing ChiP expression. Later on, a study reported the case of SroC, a type II 3' UTR-derived sRNA that activates up to 26 targets, while repressing 14, an unusually high number of targets (Miyakoshi et al., 2015a). The authors showed that SroC acts as a sponge of GcvB, the sRNA involved in amino-acid metabolism, and the most repressed of the SroC targets. The intriguing feature is that SroC is produced from the *gltJKL* operon, an mRNA target of GcvB, indicating an elegant cross-talk mechanism. When produced, SroC binds GcvB by base-pairing, allowing the recruitment of RNase E and subsequent GcvB degradation and derepression of its targetome. In other words, GcvB sequestration permits the indirect activation of most of the 26 targets identified in the screen, indicating that sRNAs can function using mechanisms similar to some TFs that repress other repressors to activate gene expression. In a second study, SroC was shown to sequester another sRNA, MgrR, by binding its seed sequence (Acuña et al., 2016). In addition to this sponge activity, SroC also indirectly regulates the expression of other targets functionally related to the GcvB targetome (Miyakoshi et al., 2015a). Interestingly, GcvB is also controlled by the AgvB bacteriophage-encoded sponge RNA (Tree et al., 2014), which adds another layer of complexity: a sponge RNA can mitigate several sRNAs, and a single sRNA can be sequestered by more than one sponge RNA.

Besides 3' UTR mRNA-related biogenesis, sRNA sponges can also be generated from diverse loci such as tRNA transcripts, either mature or precursor tRNA (Lalaouna et al., 2015). During the maturation of the *glyW-cystT-leuZ* polycistronic pre-tRNA, a 3' external transcribed spacer sequence (3' ETS^{leuZ}) is released and acts as a sponge for RyhB and RybB sRNAs to reduce transcriptional noise during non-inducing conditions. RybB is also sponged by RbsZ, the sRNA associated with Hfq and ProQ (Melamed et al., 2020). Recent studies in the model organism *E. coli* demonstrated the presence of sRNA sponges ChiZ and IspZ deriving from 5' UTRs (Adams et al., 2021), suggesting that sponge RNAs can be produced from any part of the genome. They can thus be produced independently since they contain their own promoters, they can be processed from an existing transcript, they may belong to intergenic spacer regions or intergenic tRNA spacers, or they can be generated from 3' UTRs (Denham, 2020).

With the concept of sponge, it appears that the bioavailability of the mRNA target and the presence of a sponge RNA are important parts of sRNA-mediated gene regulation. The discovery of sRNA sponges is still recent, and more breakthroughs are expected in the near future, which should help us understand their importance in regulatory networks.

Mediation of Transcription Termination

In *E. coli* (and perhaps in all bacteria), sRNAs can affect gene expression through a variety of mechanisms of action. Another example of this extraordinary diversity is the ability of some sRNAs to mediate transcription termination. Study of the transcriptional regulation of the *chiPQ* operon by ChiX sRNAs revealed that by pairing with the 5' end of its mRNA target, the sRNA induces Rho-dependent transcription termination (Bossi et al., 2012). The actual mechanism of action relies on the inhibition of ribosome binding, decreasing ribosomes at the Rho utilization site thus increasing Rho-dependent transcription termination. Conversely, other examples of positive regulation have been reported, with DsrA, ArcZ, and RprA regulating *rpoS* expression by preventing Rho from binding to the mRNA, while the sRNAs continue to bind the 5' UTRs (Sedlyarova et al., 2016). Transcription termination regulation by sRNAs was recently reviewed (Chen et al., 2019; Bossi et al., 2020).

Clusters of Regularly Interspaced Short Palindromic Repeat

Although, there has been an explosion of information about sRNA modes of action and expression, the general rule was that since RNA is the product of DNA transcription, it only rarely retroactively affects DNA. This dogma has been overturned with the discovery of clusters of regularly interspaced short palindromic repeats (CRISPRs), which provide immunity to bacteria by recognizing any re-invasion of nucleic acids (Barrangou et al., 2007). In CRISPR, a guide RNA (crRNA) is crucial for the recognition of foreign DNA or RNA (from bacteriophages, plasmids, or mobile genetic elements), enabling its cleavage by the Cas9 nuclease (Brouns et al., 2008). Following processing, the foreign sequence is integrated into the genome in a CRISPR array usually located close to the Cas system. The CRISPR array is composed of spacer sequences corresponding to foreign DNAs serving as immune memory, and which are flanked by DNA repeats. The DNA-encoded CRISPR system thus involves RNA-mediated recognition of foreign nucleic acids, and functions as a defense system.

CONCLUDING REMARKS

Over the past few decades, a tremendous shift has taken place in how we define RNA species. Although, they were long dismissed as simple messengers, the first in-depth characterizations of non-coding RNAs have paved the way for fascinating discoveries about their functions, which range from essential roles in translation machinery to global regulatory functions. Genome-wide and high-throughput screenings have enabled a rapid evolution in knowledge, and the establishment of new rules. They helped reveal an extraordinary diversity in types of non-coding RNAs and showed that they use an abundance of mechanisms of action. Non-coding RNAs include rRNAs, tRNAs, 6S RNA, ribozymes, riboswitches, CRISPRs, and sRNAs. In terms

of viability, sRNAs are often non-essential, but they are valuable for rapid and cost-effective regulation of gene expression in response to environmental cues. Therefore, they appear to be key players, adding another layer to gene expression control. Within sRNAs, a large number of classes and sub-classes have been created as a result of novel discoveries about their genomic locations, biogenesis, and modes of action, and these go way beyond protein classifications based solely on function and domain presence. In each sRNA category, there are a variety of mechanisms of action (with some appearing in several categories), and a large diversity of functions. The boundaries between sub-classes, between sRNAs and riboswitches or CRISPRs, sometimes appear very thin, particularly as novel mechanisms of action or biogenesis are constantly discovered. It is now accepted that their biogenesis can occur from any locus in the genome or in plasmids, and from any type of RNA molecule. Although categorization into multiple and highly specific types permits the organization of information, it may be detrimental for a rapid and simple presentation of what constitutes the sRNA. Cech and Steitz (2014) attempted to summarize the definition of sRNAs based on their most general function, base-pairing with mRNAs to regulate gene expression. However, this definition is limited, as it does not include protein-binding sRNAs. Perhaps just minor adjustments are enough to ensure consensus around a definition expansive enough to avoid

obsolescence. Bacterial sRNAs are any RNA molecules that interact with other actors to regulate gene expression.

AUTHOR CONTRIBUTIONS

BF and YA planned the outline of the manuscript. YA wrote the review. All authors contributed to the article and approved the submitted version.

FUNDING

This work was funded by the University of Rennes 1 and the Institut National de la Santé et de la Recherche Médicale.

ACKNOWLEDGMENTS

This manuscript is dedicated to Brice Felden and to his passion for the RNA world and the multifaceted roles of bacterial sRNAs. The authors would like to thank Astrid Rouillon and Marie-Laure Pinel-Marie for reading the manuscript, and to Svetlana Chabelskaya for sharing the drawing of the structure of RNAIII.

REFERENCES

- Acuña, L. G., Barros, M. J., Peñaloza, D., Rodas, P. I., Paredes-Sabja, D., Fuentes, J. A., et al. (2016). A feed-forward loop between SroC and MgrR small RNAs modulates the expression of eptB and the susceptibility to polymyxin B in *Salmonella* Typhimurium. *Microbiology* 162, 1996–2004. doi: 10.1099/mic.0.000365
- Adams, P. P., Baniulyte, G., Esnault, C., Chegiredy, K., Singh, N., Monge, M., et al. (2021). Regulatory roles of *Escherichia coli* 5' UTR and ORF-internal RNAs detected by 3' end mapping. *elife* 10:e62438. doi: 10.7554/eLife.62438
- Adams, P. P., Flores Avile, C., Popitsch, N., Bilusic, I., Schroeder, R., Lybecker, M., et al. (2017). In vivo expression technology and 5' end mapping of the *Borrelia burgdorferi* transcriptome identify novel RNAs expressed during mammalian infection. *Nucleic Acids Res.* 45, 775–792. doi: 10.1093/nar/gkw1180
- Alix, E., and Blanc-Potard, A.-B. (2008). Peptide-assisted degradation of the *Salmonella* MgtC virulence factor. *EMBO J.* 27, 546–557. doi: 10.1038/sj.emboj.7601983
- Altman, S., Baer, M. F., Bartkiewicz, M., Gold, H., Guerrier-Takada, C., Kirsebom, L. A., et al. (1989). Catalysis by the RNA subunit of RNase P—a mini review. *Gene* 82, 63–64. doi: 10.1016/0378-1119(89)90030-9
- Altuvia, S., Zhang, A., Argaman, L., Tiwari, A., and Storz, G. (1998). The *Escherichia coli* OxyS regulatory RNA represses hflA translation by blocking ribosome binding. *EMBO J.* 17, 6069–6075. doi: 10.1093/emboj/17.20.6069
- André, G., Even, S., Putzer, H., Burguière, P., Croux, C., Danchin, A., et al. (2008). S-box and T-box riboswitches and antisense RNA control a sulfur metabolic operon of *Clostridium acetobutylicum*. *Nucleic Acids Res.* 36, 5955–5969. doi: 10.1093/nar/gkn601
- Arthur, D. C., Ghetu, A. F., Gubbins, M. J., Edwards, R. A., Frost, L. S., and Glover, J. N. M. (2003). FinO is an RNA chaperone that facilitates sense-antisense RNA interactions. *EMBO J.* 22, 6346–6355. doi: 10.1093/emboj/cdg607
- Asano, K., and Mizobuchi, K. (1998a). An RNA pseudoknot as the molecular switch for translation of the repZ gene encoding the replication initiator of IncIalpha plasmid ColIb-P9. *J. Biol. Chem.* 273, 11815–11825. doi: 10.1074/jbc.273.19.11815
- Asano, K., and Mizobuchi, K. (1998b). Copy number control of IncIalpha plasmid ColIb-P9 by competition between pseudoknot formation and antisense RNA binding at a specific RNA site. *EMBO J.* 17, 5201–5213. doi: 10.1093/emboj/17.17.5201
- Attaiech, L., Boughammoura, A., Brochier-Armanet, C., Allatif, O., Peillard-Fiorente, F., Edwards, R. A., et al. (2016). Silencing of natural transformation by an RNA chaperone and a multitarget small RNA. *Proc. Natl. Acad. Sci. U. S. A.* 113, 8813–8818. doi: 10.1073/pnas.1601626113
- Augagneur, Y., King, A. N., Germain-Amiot, N., Sassi, M., Fitzgerald, J. W., Sahukhal, G. S., et al. (2020). Analysis of the CodY RNome reveals RsaD as a stress-responsive riboregulator of overflow metabolism in *Staphylococcus aureus*. *Mol. Microbiol.* 113, 309–325. doi: 10.1111/mmi.14418
- Augagneur, Y., Wesolowski, D., Tae, H. S., Altman, S., and Ben Mamoun, C. (2012). Gene selective mRNA cleavage inhibits the development of *Plasmodium falciparum*. *Proc. Natl. Acad. Sci. U. S. A.* 109, 6235–6240. doi: 10.1073/pnas.1203516109
- Avila-Calderón, E. D., Araiza-Villanueva, M. G., Cancino-Díaz, J. C., López-Villegas, E. O., Sriranganathan, N., Boyle, S. M., et al. (2015). Roles of bacterial membrane vesicles. *Arch. Microbiol.* 197, 1–10. doi: 10.1007/s00203-014-1042-7
- Azam, M. S., and Vanderpool, C. K. (2015). Talk among yourselves: RNA sponges mediate cross talk between functionally related messenger RNAs. *EMBO J.* 34, 1436–1438. doi: 10.15252/emboj.201591492
- Babitzke, P., and Romeo, T. (2007). CsrB sRNA family: sequestration of RNA-binding regulatory proteins. *Curr. Opin. Microbiol.* 10, 156–163. doi: 10.1016/j.mib.2007.03.007
- Balaban, N., and Novick, R. P. (1995). Translation of RNAIII, the *Staphylococcus aureus* agr regulatory RNA molecule, can be activated by a 3'-end deletion. *FEMS Microbiol. Lett.* 133, 155–161. doi: 10.1111/j.1574-6968.1995.tb07877.x
- Balbontin, R., Fiorini, F., Figueroa-Bossi, N., Casadesús, J., and Bossi, L. (2010). Recognition of heptameric seed sequence underlies multi-target regulation by RybB small RNA in *Salmonella enterica*. *Mol. Microbiol.* 78, 380–394. doi: 10.1111/j.1365-2958.2010.07342.x
- Bandrya, K. J., Said, N., Pfeiffer, V., Góna, M. W., Vogel, J., and Luisi, B. F. (2012). The seed region of a small RNA drives the controlled destruction of the target mRNA by the endoribonuclease RNase E. *Mol. Cell* 47, 943–953. doi: 10.1016/j.molcel.2012.07.015

- Barrangou, R., Fremaux, C., Deveau, H., Richards, M., Boyaval, P., Moineau, S., et al. (2007). CRISPR provides acquired resistance against viruses in prokaryotes. *Science* 315, 1709–1712. doi: 10.1126/science.1138140
- Bauriedl, S., Gerovac, M., Heidrich, N., Bischler, T., Barquist, L., Vogel, J., et al. (2020). The minimal meningococcal ProQ protein has an intrinsic capacity for structure-based global RNA recognition. *Nat. Commun.* 11:2823. doi: 10.1038/s41467-020-16650-6
- Beaume, M., Hernandez, D., Farinelli, L., Deluen, C., Linder, P., Gaspin, C., et al. (2010). Cartography of methicillin-resistant *S. aureus* transcripts: detection, orientation and temporal expression during growth phase and stress conditions. *PLoS One* 5:e10725. doi: 10.1371/journal.pone.0010725
- Benito, Y., Kolb, F. A., Romby, P., Lina, G., Etienne, J., and Vandenesch, F. (2000). Probing the structure of RNAIII, the *Staphylococcus aureus* agr regulatory RNA, and identification of the RNA domain involved in repression of protein A expression. *RNA* 6, 668–679. doi: 10.1017/S1355838200992550
- Bessaiah, H., Pokharel, P., Loucif, H., Kulbay, M., Sasseville, C., Habouria, H., et al. (2021). The RyfA small RNA regulates oxidative and osmotic stress responses and virulence in uropathogenic *Escherichia coli*. *PLoS Pathog.* 17:e1009617. doi: 10.1371/journal.ppat.1009617
- Bhatt, S., Egan, M., Jenkins, V., Muche, S., and El-Fenei, J. (2016). The tip of the iceberg: on the roles of regulatory small RNAs in the virulence of enterohemorrhagic and enteropathogenic *Escherichia coli*. *Front. Cell. Infect. Microbiol.* 6:105. doi: 10.3389/fcimb.2016.00105
- Bohn, C., Rigoulay, C., and Boulou, P. (2007). No detectable effect of RNA-binding protein Hfq absence in *Staphylococcus aureus*. *BMC Microbiol.* 7:10. doi: 10.1186/1471-2180-7-10
- Bohn, C., Rigoulay, C., Chabelskaya, S., Sharma, C. M., Marchais, A., Skorski, P., et al. (2010). Experimental discovery of small RNAs in *Staphylococcus aureus* reveals a riboregulator of central metabolism. *Nucleic Acids Res.* 38, 6620–6636. doi: 10.1093/nar/gkq462
- Boisset, S., Geissmann, T., Huntzinger, E., Fechter, P., Bendridi, N., Possedko, M., et al. (2007). *Staphylococcus aureus* RNAIII coordinately represses the synthesis of virulence factors and the transcription regulator rot by an antisense mechanism. *Genes Dev.* 21, 1353–1366. doi: 10.1101/gad.423507
- Bossi, L., Figueroa-Bossi, N., Boulou, P., and Boudvillain, M. (2020). Regulatory interplay between small RNAs and transcription termination factor rho. *Biochim. Biophys. Acta Gene Regul. Mech.* 1863:194546. doi: 10.1016/j.bbagr.2020.194546
- Bossi, L., Schwartz, A., Guillemardet, B., Boudvillain, M., and Figueroa-Bossi, N. (2012). A role for rho-dependent polarity in gene regulation by a noncoding small RNA. *Genes Dev.* 26, 1864–1873. doi: 10.1101/gad.195412.112
- Bouvier, M., Sharma, C. M., Mika, F., Nierhaus, K. H., and Vogel, J. (2008). Small RNA binding to 5' mRNA coding region inhibits translational initiation. *Mol. Cell* 32, 827–837. doi: 10.1016/j.molcel.2008.10.027
- Brantl, S. (2002). Antisense-RNA regulation and RNA interference. *Biochim. Biophys. Acta* 1575, 15–25. doi: 10.1016/s0167-4781(02)00280-4
- Brantl, S. (2007). Regulatory mechanisms employed by cis-encoded antisense RNAs. *Curr. Opin. Microbiol.* 10, 102–109. doi: 10.1016/j.mib.2007.03.012
- Brantl, S., Birch-Hirschfeld, E., and Behnke, D. (1993). RepR protein expression on plasmid pIP501 is controlled by an antisense RNA-mediated transcription attenuation mechanism. *J. Bacteriol.* 175, 4052–4061. doi: 10.1128/jb.175.13.4052-4061.1993
- Brantl, S., and Jahn, N. (2015). sRNAs in bacterial type I and type III toxin-antitoxin systems. *FEMS Microbiol. Rev.* 39, 413–427. doi: 10.1093/femsre/fuv003
- Brewer, S. M., Twittenhoff, C., Kortmann, J., Brubaker, S. W., Honeycutt, J., Massis, L. M., et al. (2021). A *Salmonella* Typhi RNA thermosensor regulates virulence factors and innate immune evasion in response to host temperature. *PLoS Pathog.* 17:e1009345. doi: 10.1371/journal.ppat.1009345
- Bronesky, D., Desgranges, E., Corvaglia, A., François, P., Caballero, C. J., Prado, L., et al. (2019). A multifaceted small RNA modulates gene expression upon glucose limitation in *Staphylococcus aureus*. *EMBO J.* 38:e99363. doi: 10.15252/embj.201899363
- Bronesky, D., Wu, Z., Marzi, S., Walter, P., Geissmann, T., Moreau, K., et al. (2016). *Staphylococcus aureus* RNAIII and its regulon link quorum sensing, stress responses, metabolic adaptation, and regulation of virulence gene expression. *Annu. Rev. Microbiol.* 70, 299–316. doi: 10.1146/annurev-micro-102215-095708
- Bronsard, J., Pascreau, G., Sassi, M., Mauro, T., Augagneur, Y., and Felden, B. (2017). sRNA and cis-antisense sRNA identification in *Staphylococcus aureus* highlights an unusual sRNA gene cluster with one encoding a secreted peptide. *Sci. Rep.* 7:4565. doi: 10.1038/s41598-017-04786-3
- Brouns, S. J. J., Jore, M. M., Lundgren, M., Westra, E. R., Slijkhuys, R. J. H., Snijders, A. P. L., et al. (2008). Small CRISPR RNAs guide antiviral defense in prokaryotes. *Science* 321, 960–964. doi: 10.1126/science.1159689
- Brownlee, G. G. (1971). Sequence of 6S RNA of *E. coli*. *Nat. New Biol.* 229, 147–149. doi: 10.1038/newbio229147a0
- Burenina, O. Y., Oretskaya, T. S., and Kubareva, E. A. (2017). Non-coding RNAs as transcriptional regulators in eukaryotes. *Acta Nat.* 9, 13–25. doi: 10.32607/20758251-2017-9-4-13-25
- Calderón, I. L., Morales, E. H., Collao, B., Calderón, P. F., Chahuán, C. A., Acuña, L. G., et al. (2014). Role of *Salmonella* Typhimurium small RNAs RyhB-1 and RyhB-2 in the oxidative stress response. *Res. Microbiol.* 165, 30–40. doi: 10.1016/j.resmic.2013.10.008
- Carrier, M.-C., Lalaouna, D., and Massé, E. (2018). Broadening the definition of bacterial small RNAs: characteristics and mechanisms of action. *Annu. Rev. Microbiol.* 72, 141–161. doi: 10.1146/annurev-micro-090817-062607
- Catalan-Moreno, A., Cela, M., Menendez-Gil, P., Irurzun, N., Caballero, C. J., Caldelari, I., et al. (2021). RNA thermoswitches modulate *Staphylococcus aureus* adaptation to ambient temperatures. *Nucleic Acids Res.* 49, 3409–3426. doi: 10.1093/nar/gkab117
- Cech, T. R., and Steitz, J. A. (2014). The noncoding RNA revolution-trashing old rules to forge new ones. *Cell* 157, 77–94. doi: 10.1016/j.cell.2014.03.008
- Chabelskaya, S., Bordeau, V., and Felden, B. (2014). Dual RNA regulatory control of a *Staphylococcus aureus* virulence factor. *Nucleic Acids Res.* 42, 4847–4858. doi: 10.1093/nar/gku119
- Chabelskaya, S., Gaillot, O., and Felden, B. (2010). A *Staphylococcus aureus* small RNA is required for bacterial virulence and regulates the expression of an immune-evasion molecule. *PLoS Pathog.* 6:e1000927. doi: 10.1371/journal.ppat.1000927
- Chao, Y., Papenfort, K., Reinhardt, R., Sharma, C. M., and Vogel, J. (2012). An atlas of Hfq-bound transcripts reveals 3' UTRs as a genomic reservoir of regulatory small RNAs. *EMBO J.* 31, 4005–4019. doi: 10.1038/emboj.2012.229
- Chao, Y., and Vogel, J. (2016). A 3' UTR-derived small RNA provides the regulatory noncoding arm of the inner membrane stress response. *Mol. Cell* 61, 352–363. doi: 10.1016/j.molcel.2015.12.023
- Chareyre, S., Barras, F., and Mandin, P. (2019). A small RNA controls bacterial sensitivity to gentamicin during iron starvation. *PLoS Genet.* 15:e1008078. doi: 10.1371/journal.pgen.1008078
- Chareyre, S., and Mandin, P. (2018). Bacterial iron homeostasis regulation by sRNAs. *Microbiol. Spectr.* 6. doi: 10.1128/microbiolspec.RWR-0010-2017
- Chen, L., Huang, C., Wang, X., and Shan, G. (2015). Circular RNAs in eukaryotic cells. *Curr. Genomics* 16, 312–318. doi: 10.2174/1389202916666150707161554
- Chen, J., Morita, T., and Gottesman, S. (2019). Regulation of transcription termination of small RNAs and by small RNAs: molecular mechanisms and biological functions. *Front. Cell. Infect. Microbiol.* 9:201. doi: 10.3389/fcimb.2019.00201
- Chevalier, C., Boisset, S., Romilly, C., Masquida, B., Fechter, P., Geissmann, T., et al. (2010). *Staphylococcus aureus* RNAIII binds to two distant regions of coa mRNA to arrest translation and promote mRNA degradation. *PLoS Pathog.* 6:e1000809. doi: 10.1371/journal.ppat.1000809
- Christiansen, J. K., Larsen, M. H., Ingmer, H., Sogaard-Andersen, L., and Kallipolitis, B. H. (2004). The RNA-binding protein Hfq of *Listeria monocytogenes*: role in stress tolerance and virulence. *J. Bacteriol.* 186, 3355–3362. doi: 10.1128/JB.186.11.3355-3362.2004
- Christiansen, J. K., Nielsen, J. S., Ebersbach, T., Valentin-Hansen, P., Sogaard-Andersen, L., and Kallipolitis, B. H. (2006). Identification of small Hfq-binding RNAs in *Listeria monocytogenes*. *RNA* 12, 1383–1396. doi: 10.1261/rna.49706
- Chunhua, M., Yu, L., Yaping, G., Jie, D., Qiang, L., Xiaorong, T., et al. (2012). The expression of LytM is down-regulated by RNAIII in *Staphylococcus aureus*. *J. Basic Microbiol.* 52, 636–641. doi: 10.1002/jobm.201100426
- Correia Santos, S., Bischler, T., Westermann, A. J., and Vogel, J. (2021). MAPS integrates regulation of actin-targeting effector SteC into the virulence control network of *Salmonella* small RNA PinT. *Cell Rep.* 34:108722. doi: 10.1016/j.celrep.2021.108722

- Cotter, R. I., McPhie, P., and Gratzer, W. B. (1967). Internal organization of the ribosome. *Nature* 216, 864–868. doi: 10.1038/216864a0
- Crick, F. H. (1958). On protein synthesis. *Symp. Soc. Exp. Biol.* 12, 138–163.
- Crick, F. (1970). Central dogma of molecular biology. *Nature* 227, 561–563. doi: 10.1038/227561a0
- Cue, D., Lei, M. G., and Lee, C. Y. (2012). Genetic regulation of the intercellular adhesion locus in staphylococci. *Front. Cell. Infect. Microbiol.* 2:38. doi: 10.3389/fcimb.2012.00038
- Dar, D., Shamir, M., Mellin, J. R., Koutero, M., Stern-Ginossar, N., Cossart, P., et al. (2016). Term-seq reveals abundant ribo-regulation of antibiotics resistance in bacteria. *Science* 352:aad9822. doi: 10.1126/science.aad9822
- Dar, D., and Sorek, R. (2018). Bacterial noncoding RNAs excised from within protein-coding transcripts. *MBio* 9, e01730–e01818. doi: 10.1128/mBio.01730-18
- Das, S., Lindemann, C., Young, B. C., Muller, J., Osterreich, B., Ternette, N., et al. (2016). Natural mutations in a *Staphylococcus aureus* virulence regulator attenuate cytotoxicity but permit bacteremia and abscess formation. *Proc. Natl. Acad. Sci. U. S. A.* 113, E3101–E3110. doi: 10.1073/pnas.1520255113
- Deana, A., and Belasco, J. G. (2005). Lost in translation: the influence of ribosomes on bacterial mRNA decay. *Genes Dev.* 19, 2526–2533. doi: 10.1101/gad.1348805
- DeRoy, S., Gebbie, M., Ramesh, A., Goodson, J. R., Cruz, M. R., van Hoof, A., et al. (2014). Riboswitches. A riboswitch-containing sRNA controls gene expression by sequestration of a response regulator. *Science* 345, 937–940. doi: 10.1126/science.1255091
- Denham, E. L. (2020). The sponge RNAs of bacteria—how to find them and their role in regulating the post-transcriptional network. *Biochim. Biophys. Acta Gene Regul. Mech.* 1863:194565. doi: 10.1016/j.bbagr.2020.194565
- Derksen, M., Mertens, V., and Pruijn, G. J. M. (2015). RNase P-mediated sequence-specific cleavage of RNA by engineered external guide sequences. *Biomol. Ther.* 5, 3029–3050. doi: 10.3390/biom5043029
- Dühring, U., Axmann, I. M., Hess, W. R., and Wilde, A. (2006). An internal antisense RNA regulates expression of the photosynthesis gene *isiA*. *Proc. Natl. Acad. Sci. U. S. A.* 103, 7054–7058. doi: 10.1073/pnas.0600927103
- Dunman, P. M., Murphy, E., Haney, S., Palacios, D., Tucker-Kellogg, G., Wu, S., et al. (2001). Transcription profiling-based identification of *Staphylococcus aureus* genes regulated by the *agr* and/or *sarA* loci. *J. Bacteriol.* 183, 7341–7353. doi: 10.1128/JB.183.24.7341-7353.2001
- Dutta, T., and Srivastava, S. (2018). Small RNA-mediated regulation in bacteria: a growing palette of diverse mechanisms. *Gene* 656, 60–72. doi: 10.1016/j.gene.2018.02.068
- Ellis, T. N., and Kuehn, M. J. (2010). Virulence and immunomodulatory roles of bacterial outer membrane vesicles. *Microbiol. Mol. Biol. Rev.* 74, 81–94. doi: 10.1128/MMBR.00031-09
- Eyraud, A., Tattevin, P., Chabelskaya, S., and Felden, B. (2014). A small RNA controls a protein regulator involved in antibiotic resistance in *Staphylococcus aureus*. *Nucleic Acids Res.* 42, 4892–4905. doi: 10.1093/nar/gku149
- Felden, B., and Cattoir, V. (2018). Bacterial adaptation to antibiotics through regulatory RNAs. *Antimicrob. Agents Chemother.* 62, e02503–e02517. doi: 10.1128/AAC.02503-17
- Feng, L., Rutherford, S. T., Papenfort, K., Bagert, J. D., van Kessel, J. C., Tirrell, D. A., et al. (2015). A *qrr* noncoding RNA deploys four different regulatory mechanisms to optimize quorum-sensing dynamics. *Cell* 160, 228–240. doi: 10.1016/j.cell.2014.11.051
- Ferrara, S., Falcone, M., Macchi, R., Bragonzi, A., Girelli, D., Cariani, L., et al. (2017). The PAPI-1 pathogenicity island-encoded small RNA *PesA* influences *Pseudomonas aeruginosa* virulence and modulates pyocin S3 production. *PLoS One* 12:e0180386. doi: 10.1371/journal.pone.0180386
- Figuerola-Bossi, N., Valentini, M., Malleret, L., Fiorini, F., and Bossi, L. (2009). Caught at its own game: regulatory small RNA inactivated by an inducible transcript mimicking its target. *Genes Dev.* 23, 2004–2015. doi: 10.1101/gad.541609
- Foster, T. J. (2005). Immune evasion by staphylococci. *Nat. Rev. Microbiol.* 3, 948–958. doi: 10.1038/nrmicro1289
- Fröhlich, K. S., Papenfort, K., Berger, A. A., and Vogel, J. (2012). A conserved RpoS-dependent small RNA controls the synthesis of major porin OmpD. *Nucleic Acids Res.* 40, 3623–3640. doi: 10.1093/nar/gkr1156
- Fröhlich, K. S., Papenfort, K., Fekete, A., and Vogel, J. (2013). A small RNA activates CFA synthase by isoform-specific mRNA stabilization. *EMBO J.* 32, 2963–2979. doi: 10.1038/emboj.2013.222
- Gao, W., Guérillot, R., Lin, Y. H., Tree, J., Beaume, M., François, P., et al. (2020). Comparative transcriptomic and functional assessments of linezolid-responsive small RNA genes in *Staphylococcus aureus*. *mSystems* 5, e00665–e00719. doi: 10.1128/mSystems.00665-19
- Geisinger, E., Adhikari, R. P., Jin, R., Ross, H. F., and Novick, R. P. (2006). Inhibition of rot translation by RNAIII, a key feature of *agr* function. *Mol. Microbiol.* 61, 1038–1048. doi: 10.1111/j.1365-2958.2006.05292.x
- Geissmann, T., Chevalier, C., Cros, M. J., Boisset, S., Fechter, P., Noirot, C., et al. (2009). A search for small noncoding RNAs in *Staphylococcus aureus* reveals a conserved sequence motif for regulation. *Nucleic Acids Res.* 37, 7239–7257. doi: 10.1093/nar/gkp668
- Germain-Amiot, N., Augagneur, Y., Camberlein, E., Nicolas, I., Lecureur, V., Rouillon, A., et al. (2019). A novel *Staphylococcus aureus* cis-trans type I toxin-antitoxin module with dual effects on bacteria and host cells. *Nucleic Acids Res.* 47, 1759–1773. doi: 10.1093/nar/gky1257
- Giangrossi, M., Prosseda, G., Tran, C. N., Brandi, A., Colonna, B., and Falconi, M. (2010). A novel antisense RNA regulates at transcriptional level the virulence gene *icsA* of *Shigella flexneri*. *Nucleic Acids Res.* 38, 3362–3375. doi: 10.1093/nar/gkq025
- Gilbert, W. (1986). Origin of life: the RNA world. *Nature* 319:618. doi: 10.1038/319618a0
- Gimpel, M., and Brantl, S. (2017). Dual-function small regulatory RNAs in bacteria. *Mol. Microbiol.* 103, 387–397. doi: 10.1111/mmi.13558
- Gong, H., Vu, G.-P., Bai, Y., Chan, E., Wu, R., Yang, E., et al. (2011). A *Salmonella* small non-coding RNA facilitates bacterial invasion and intracellular replication by modulating the expression of virulence factors. *PLoS Pathog.* 7:e1002120. doi: 10.1371/journal.ppat.1002120
- Göpel, Y., Khan, M. A., and Görke, B. (2014). Ménage à trois: post-transcriptional control of the key enzyme for cell envelope synthesis by a base-pairing small RNA, an RNase adaptor protein, and a small RNA mimic. *RNA Biol.* 11, 433–442. doi: 10.4161/rna.28301
- Gorski, S. A., Vogel, J., and Doudna, J. A. (2017). RNA-based recognition and targeting: sowing the seeds of specificity. *Nat. Rev. Mol. Cell Biol.* 18, 215–228. doi: 10.1038/nrm.2016.174
- Gripenland, J., Netterling, S., Loh, E., Tiensuu, T., Toledo-Arana, A., and Johansson, J. (2010). RNAs: regulators of bacterial virulence. *Nat. Rev. Microbiol.* 8, 857–866. doi: 10.1038/nrmicro2457
- Gruber, C. C., and Sperandio, V. (2014). Posttranscriptional control of microbe-induced rearrangement of host cell actin. *MBio* 5, e01025–e01113. doi: 10.1128/mBio.01025-13
- Gruber, C. C., and Sperandio, V. (2015). Global analysis of posttranscriptional regulation by GlmY and GlmZ in enterohemorrhagic *Escherichia coli* O157:H7. *Infect. Immun.* 83, 1286–1295. doi: 10.1128/IAI.02918-14
- Guerrier-Takada, C., Gardiner, K., Marsh, T., Pace, N., and Altman, S. (1983). The RNA moiety of ribonuclease P is the catalytic subunit of the enzyme. *Cell* 35, 849–857. doi: 10.1016/0092-8674(83)90117-4
- Gupta, R. K., Luong, T. T., and Lee, C. Y. (2015). RNAIII of the *Staphylococcus aureus* *agr* system activates global regulator MgrA by stabilizing mRNA. *Proc. Natl. Acad. Sci. U. S. A.* 112, 14036–14041. doi: 10.1073/pnas.1509251112
- Hausmann, S., Guimarães, V. A., Garcin, D., Baumann, N., Linder, P., and Redder, P. (2017). Both exo- and endo-nucleolytic activities of RNase J1 from *Staphylococcus aureus* are manganese dependent and active on triphosphorylated 5'-ends. *RNA Biol.* 14, 1431–1443. doi: 10.1080/15476286.2017.1300223
- Heidrich, N., Bauriedl, S., Barquist, L., Li, L., Schoen, C., and Vogel, J. (2017). The primary transcriptome of *Neisseria meningitidis* and its interaction with the RNA chaperone Hfq. *Nucleic Acids Res.* 45, 6147–6167. doi: 10.1093/nar/gkx168
- Hindley, J. (1967). Fractionation of 32P-labelled ribonucleic acids on polyacrylamide gels and their characterization by fingerprinting. *J. Mol. Biol.* 30, 125–136. doi: 10.1016/0022-2836(67)90248-3
- Hoagland, M. B., Stephenson, M. L., Scott, J. F., Hecht, L. I., and Zamecnik, P. C. (1958). A soluble ribonucleic acid intermediate in protein synthesis. *J. Biol. Chem.* 231, 241–257. doi: 10.1016/S0021-9258(19)77302-5
- Howden, B. P., Beaume, M., Harrison, P. F., Hernandez, D., Schrenzel, J., Seemann, T., et al. (2013). Analysis of the small RNA transcriptional response in multidrug-resistant *Staphylococcus aureus* after antimicrobial exposure. *Antimicrob. Agents Chemother.* 57, 3864–3874. doi: 10.1128/AAC.00263-13

- Hoyos, M., Huber, M., Förstner, K. U., and Papenfort, K. (2020). Gene autoregulation by 3' UTR-derived bacterial small RNAs. *elife* 9:e58836. doi: 10.7554/eLife.58836
- Huntzinger, E., Boisset, S., Saveanu, C., Benito, Y., Geissmann, T., Namane, A., et al. (2005). *Staphylococcus aureus* RNAIII and the endoribonuclease III coordinately regulate spa gene expression. *EMBO J.* 24, 824–835. doi: 10.1038/sj.emboj.7600572
- Hussein, H., Fris, M. E., Salem, A. H., Wiemels, R. E., Bastock, R. A., Righetti, E., et al. (2019). An unconventional RNA-based thermosensor within the 5' UTR of *Staphylococcus aureus* cidA. *PLoS One* 14:e0214521. doi: 10.1371/journal.pone.0214521
- Hüttenhofer, A., and Noller, H. F. (1994). Footprinting mRNA-ribosome complexes with chemical probes. *EMBO J.* 13, 3892–3901. doi: 10.1002/j.1460-2075.1994.tb06700.x
- Ikedo, Y., Yagi, M., Morita, T., and Aiba, H. (2011). Hfq binding at RhlB-recognition region of RNase E is crucial for the rapid degradation of target mRNAs mediated by sRNAs in *Escherichia coli*. *Mol. Microbiol.* 79, 419–432. doi: 10.1111/j.1365-2958.2010.07454.x
- Ikemura, T., and Dahlberg, J. E. (1973). Small ribonucleic acids of *Escherichia coli*. I. Characterization by polyacrylamide gel electrophoresis and fingerprint analysis. *J. Biol. Chem.* 248, 5024–5032. doi: 10.1016/S0021-9258(19)43666-1
- Ingavale, S., van Wamel, W., Luong, T. T., Lee, C. Y., and Cheung, A. L. (2005). Rat/MgrA, a regulator of autolysis, is a regulator of virulence genes in *Staphylococcus aureus*. *Infect. Immun.* 73, 1423–1431. doi: 10.1128/IAI.73.3.1423-1431.2005
- Janssen, K. H., Diaz, M. R., Gode, C. J., Wolfgang, M. C., and Yahr, T. L. (2018). RsmV, a small noncoding regulatory RNA in *Pseudomonas aeruginosa* that sequesters RsmA and RsmF from target mRNAs. *J. Bacteriol.* 200, e00277–e00318. doi: 10.1128/JB.00277-18
- Janssen, B. D., and Hayes, C. S. (2012). The tmRNA ribosome-rescue system. *Adv. Protein Chem. Struct. Biol.* 86, 151–191. doi: 10.1016/B978-0-12-386497-0.00005-0
- Jia, T., Liu, B., Mu, H., Qian, C., Wang, L., Li, L., et al. (2021). A novel small RNA promotes motility and virulence of enterohemorrhagic *Escherichia coli* O157:H7 in response to ammonium. *MBio* 12, e03605–e03620. doi: 10.1128/mBio.03605-20
- Johansson, J., Mandin, P., Renzoni, A., Chiaruttini, C., Springer, M., and Cossart, P. (2002). An RNA thermosensor controls expression of virulence genes in *Listeria monocytogenes*. *Cell* 110, 551–561. doi: 10.1016/S0092-8674(02)00905-4
- Jørgensen, M. G., Pettersen, J. S., and Kallipolitis, B. H. (2020). sRNA-mediated control in bacteria: an increasing diversity of regulatory mechanisms. *Biochim. Biophys. Acta Gene Regul. Mech.* 1863:194504. doi: 10.1016/j.bbaggm.2020.194504
- Joshi, B., Singh, B., Nadeem, A., Askarian, F., Wai, S. N., Johannessen, M., et al. (2020). Transcriptome profiling of *Staphylococcus aureus* associated extracellular vesicles reveals presence of small RNA-cargo. *Front. Mol. Biosci.* 7:566207. doi: 10.3389/fmolb.2020.566207
- Kavita, K., de Mets, F., and Gottesman, S. (2018). New aspects of RNA-based regulation by Hfq and its partner sRNAs. *Curr. Opin. Microbiol.* 42, 53–61. doi: 10.1016/j.mib.2017.10.014
- Kim, J. N. (2016). Roles of two RyhB paralogs in the physiology of *Salmonella enterica*. *Microbiol. Res.* 186–187, 146–152. doi: 10.1016/j.micres.2016.04.004
- Kim, J. N., and Kwon, Y. M. (2013). Identification of target transcripts regulated by small RNA RyhB homologs in *Salmonella*: RyhB-2 regulates motility phenotype. *Microbiol. Res.* 168, 621–629. doi: 10.1016/j.micres.2013.06.002
- Kim, S., Reyes, D., Beaume, M., Francois, P., and Cheung, A. (2014). Contribution of teg49 small RNA in the 5' upstream transcriptional region of sarA to virulence in *Staphylococcus aureus*. *Infect. Immun.* 82, 4369–4379. doi: 10.1128/IAI.02002-14
- Kinoshita-Daitoku, R., Kiga, K., Miyakoshi, M., Otsubo, R., Ogura, Y., Sanada, T., et al. (2021). A bacterial small RNA regulates the adaptation of *helicobacter pylori* to the host environment. *Nat. Commun.* 12:2085. doi: 10.1038/s41467-021-22317-7
- Koeppen, K., Hampton, T. H., Jarek, M., Scharfe, M., Gerber, S. A., Mielcarz, D. W., et al. (2016). A novel mechanism of host-pathogen interaction through sRNA in bacterial outer membrane vesicles. *PLoS Pathog.* 12:e1005672. doi: 10.1371/journal.ppat.1005672
- Kole, R., Krainer, A. R., and Altman, S. (2012). RNA therapeutics: beyond RNA interference and antisense oligonucleotides. *Nat. Rev. Drug Discov.* 11, 125–140. doi: 10.1038/nrd3625
- Kortmann, J., and Narberhaus, F. (2012). Bacterial RNA thermometers: molecular zippers and switches. *Nat. Rev. Microbiol.* 10, 255–265. doi: 10.1038/nrmicro2730
- Lalaouna, D., Baude, J., Wu, Z., Tomasini, A., Chicher, J., Marzi, S., et al. (2019). RsaC sRNA modulates the oxidative stress response of *Staphylococcus aureus* during manganese starvation. *Nucleic Acids Res.* 47, 9871–9887. doi: 10.1093/nar/gkz728
- Lalaouna, D., Carrier, M.-C., Semsey, S., Brouard, J.-S., Wang, J., Wade, J. T., et al. (2015). A 3' external transcribed spacer in a tRNA transcript acts as a sponge for small RNAs to prevent transcriptional noise. *Mol. Cell* 58, 393–405. doi: 10.1016/j.molcel.2015.03.013
- Lalaouna, D., Prevost, K., Eyraud, A., and Masse, E. (2017). Identification of unknown RNA partners using MAPS. *Methods* 117, 28–34. doi: 10.1016/j.ymeth.2016.11.011
- Lasa, I., Toledo-Arana, A., Dobin, A., Villanueva, M., de los Mozos, I. R., Vergara-Irigaray, M., et al. (2011). Genome-wide antisense transcription drives mRNA processing in bacteria. *Proc. Natl. Acad. Sci. U. S. A.* 108, 20172–20177. doi: 10.1073/pnas.1113521108
- Leclerc, J.-M., Dozois, C. M., and Daigle, F. (2013). Role of the *Salmonella enterica* serovar Typhi Fur regulator and small RNAs RfrA and RfrB in iron homeostasis and interaction with host cells. *Microbiology* 159, 591–602. doi: 10.1099/mic.0.064329-0
- Lee, E.-J., and Groisman, E. A. (2010). An antisense RNA that governs the expression kinetics of a multifunctional virulence gene. *Mol. Microbiol.* 76, 1020–1033. doi: 10.1111/j.1365-2958.2010.07161.x
- Lee, J. Y. H., Monk, I. R., Gonçalves da Silva, A., Seemann, T., Chua, K. Y. L., Kearns, A., et al. (2018). Global spread of three multidrug-resistant lineages of *Staphylococcus epidermidis*. *Nat. Microbiol.* 3, 1175–1185. doi: 10.1038/s41564-018-0230-7
- Lejars, M., and Hajnsdorf, E. (2020). The world of asRNAs in gram-negative and gram-positive bacteria. *Biochim. Biophys. Acta Gene Regul. Mech.* 1863:194489. doi: 10.1016/j.bbaggm.2020.194489
- Lemon, K. P., Higgins, D. E., and Kolter, R. (2007). Flagellar motility is critical for *Listeria monocytogenes* biofilm formation. *J. Bacteriol.* 189, 4418–4424. doi: 10.1128/JB.01967-06
- Le Pabic, H., Germain-Amiot, N., Bordeau, V., and Felden, B. (2015). A bacterial regulatory RNA attenuates virulence, spread and human host cell phagocytosis. *Nucleic Acids Res.* 43, 9232–9248. doi: 10.1093/nar/gkv783
- Le Scornet, A., and Redder, P. (2019). Post-transcriptional control of virulence gene expression in *Staphylococcus aureus*. *Biochim. Biophys. Acta Gene Regul. Mech.* 1862, 734–741. doi: 10.1016/j.bbaggm.2018.04.004
- Lioliou, E., Romilly, C., Romby, P., and Fechter, P. (2010). RNA-mediated regulation in bacteria: from natural to artificial systems. *New Biotechnol.* 27, 222–235. doi: 10.1016/j.nbt.2010.03.002
- Liu, M. Y., Gui, G., Wei, B., Preston, J. F., Oakford, L., Yüksel, U., et al. (1997). The RNA molecule CsrB binds to the global regulatory protein CsrA and antagonizes its activity in *Escherichia coli*. *J. Biol. Chem.* 272, 17502–17510. doi: 10.1074/jbc.272.28.17502
- Liu, Y., Mu, C., Ying, X., Li, W., Wu, N., Dong, J., et al. (2011). RNAIII activates map expression by forming an RNA-RNA complex in *Staphylococcus aureus*. *FEBS Lett.* 585, 899–905. doi: 10.1016/j.febslet.2011.02.021
- Loh, E., Dussurget, O., Gripenland, J., Vaitkevicius, K., Tiensuu, T., Mandin, P., et al. (2009). A trans-acting riboswitch controls expression of the virulence regulator PrfA in *Listeria monocytogenes*. *Cell* 139, 770–779. doi: 10.1016/j.cell.2009.08.046
- Loh, E., Righetti, E., Eichner, H., Twittenhoff, C., and Narberhaus, F. (2018). RNA thermometers in bacterial pathogens. *Microbiol. Spectr.* 6. doi: 10.1128/microbiolspec.RWR-0012-2017
- Luirink, J., and Dobberstein, B. (1994). Mammalian and *Escherichia coli* signal recognition particles. *Mol. Microbiol.* 11, 9–13. doi: 10.1111/j.1365-2958.1994.tb00284.x
- Luong, T. T., Dunman, P. M., Murphy, E., Projan, S. J., and Lee, C. Y. (2006). Transcription profiling of the mgrA regulon in *Staphylococcus aureus*. *J. Bacteriol.* 188, 1899–1910. doi: 10.1128/JB.188.5.1899-1910.2006
- Luz, B. S. R. D., Nicolas, A., Chabelskaya, S., Rodovalho, V., de Rezende Rodovalho, V., Le Loir, Y., et al. (2021). Environmental plasticity of the RNA content of *Staphylococcus aureus* extracellular vesicles. *Front. Microbiol.* 12:634226. doi: 10.3389/fmicb.2021.634226
- Mader, U., Nicolas, P., Depke, M., Pane-Farre, J., Debarbouille, M., van der Kooi-Pol, M. M., et al. (2016). *Staphylococcus aureus* transcriptome

- architecture: from laboratory to infection-mimicking conditions. *PLoS Genet.* 12:e1005962. doi: 10.1371/journal.pgen.1005962
- Mandin, P., Repoila, F., Vergassola, M., Geissmann, T., and Cossart, P. (2007). Identification of new noncoding RNAs in *Listeria monocytogenes* and prediction of mRNA targets. *Nucleic Acids Res.* 35, 962–974. doi: 10.1093/nar/gkl1096
- Manna, A. C., Kim, S., Cengher, L., Corvaglia, A., Leo, S., Francois, P., et al. (2018). Small RNA teg49 is derived from a sarA transcript and regulates virulence genes independent of SarA in *Staphylococcus aureus*. *Infect. Immun.* 86, e00635–e00717. doi: 10.1128/IAI.00635-17
- Massé, E., Escorcía, F. E., and Gottesman, S. (2003). Coupled degradation of a small regulatory RNA and its mRNA targets in *Escherichia coli*. *Genes Dev.* 17, 2374–2383. doi: 10.1101/gad.1127103
- Massé, E., and Gottesman, S. (2002). A small RNA regulates the expression of genes involved in iron metabolism in *Escherichia coli*. *Proc. Natl. Acad. Sci. U. S. A.* 99, 4620–4625. doi: 10.1073/pnas.032066599
- McDaniel, B. A. M., Grundy, F. J., Artsimovitch, I., and Henkin, T. M. (2003). Transcription termination control of the S box system: direct measurement of S-adenosylmethionine by the leader RNA. *Proc. Natl. Acad. Sci. U. S. A.* 100, 3083–3088. doi: 10.1073/pnas.0630422100
- Mediati, D. G., Wu, S., Wu, W., and Tree, J. J. (2021). Networks of resistance: small RNA control of antibiotic resistance. *Trends Genet.* 37, 35–45. doi: 10.1016/j.tig.2020.08.016
- Melamed, S., Adams, P. P., Zhang, A., Zhang, H., and Storz, G. (2020). RNA-RNA interactomes of ProQ and Hfq reveal overlapping and competing roles. *Mol. Cell* 77, 411.e7–425.e7. doi: 10.1016/j.molcel.2019.10.022
- Melamed, S., Peer, A., Faigenbaum-Romm, R., Gatt, Y. E., Reiss, N., Bar, A., et al. (2016). Global mapping of small RNA-target interactions in bacteria. *Mol. Cell* 63, 884–897. doi: 10.1016/j.molcel.2016.07.026
- Mellin, J. R., and Cossart, P. (2012). The non-coding RNA world of the bacterial pathogen *Listeria monocytogenes*. *RNA Biol.* 9, 372–378. doi: 10.4161/rna.19235
- Mellin, J. R., and Cossart, P. (2015). Unexpected versatility in bacterial riboswitches. *Trends Genet.* 31, 150–156. doi: 10.1016/j.tig.2015.01.005
- Mellin, J. R., Kouter, M., Dar, D., Nahori, M.-A., Sorek, R., and Cossart, P. (2014). Riboswitches. Sequestration of a two-component response regulator by a riboswitch-regulated noncoding RNA. *Science* 345, 940–943. doi: 10.1126/science.1255083
- Mellin, J. R., Tiensuu, T., Bécavin, C., Gouin, E., Johansson, J., and Cossart, P. (2013). A riboswitch-regulated antisense RNA in *Listeria monocytogenes*. *Proc. Natl. Acad. Sci. U. S. A.* 110, 13132–13137. doi: 10.1073/pnas.1304795110
- Melson, E. M., and Kendall, M. M. (2019). The sRNA DicF integrates oxygen sensing to enhance enterohemorrhagic *Escherichia coli* virulence via distinctive RNA control mechanisms. *Proc. Natl. Acad. Sci. U. S. A.* 116, 14210–14215. doi: 10.1073/pnas.1902725116
- Menendez-Gil, P., and Toledo-Arana, A. (2020). Bacterial 3'UTRs: a useful resource in post-transcriptional regulation. *Front. Mol. Biosci.* 7:617633. doi: 10.3389/fmolb.2020.617633
- Mironov, A. S., Gusarov, I., Rafikov, R., Lopez, L. E., Shatalin, K., Krenova, R. A., et al. (2002). Sensing small molecules by nascent RNA: a mechanism to control transcription in bacteria. *Cell* 111, 747–756. doi: 10.1016/S0092-8674(02)01134-0
- Miyakoshi, M., Chao, Y., and Vogel, J. (2015a). Cross talk between ABC transporter mRNAs via a target mRNA-derived sponge of the GcvB small RNA. *EMBO J.* 34, 1478–1492. doi: 10.15252/embj.201490546
- Miyakoshi, M., Chao, Y., and Vogel, J. (2015b). Regulatory small RNAs from the 3' regions of bacterial mRNAs. *Curr. Opin. Microbiol.* 24, 132–139. doi: 10.1016/j.mib.2015.01.013
- Miyakoshi, M., Matera, G., Maki, K., Sone, Y., and Vogel, J. (2019). Functional expansion of a TCA cycle operon mRNA by a 3' end-derived small RNA. *Nucleic Acids Res.* 47, 2075–2088. doi: 10.1093/nar/gky1243
- Mizuno, T., Chou, M. Y., and Inouye, M. (1984). A unique mechanism regulating gene expression: translational inhibition by a complementary RNA transcript (micRNA). *Proc. Natl. Acad. Sci. U. S. A.* 81, 1966–1970.
- Morfeldt, E., Taylor, D., von Gabain, A., and Arvidson, S. (1995). Activation of alpha-toxin translation in *Staphylococcus aureus* by the trans-encoded antisense RNA, RNAIII. *EMBO J.* 14, 4569–4577. doi: 10.1002/j.1460-2075.1995.tb00136.x
- Moriano-Gutierrez, S., Bongrand, C., Essock-Burns, T., Wu, L., McFall-Ngai, M. J., and Ruby, E. G. (2020). The noncoding small RNA SsrA is released by *Vibrio fischeri* and modulates critical host responses. *PLoS Biol.* 18:e3000934. doi: 10.1371/journal.pbio.3000934
- Morita, T., Maki, K., and Aiba, H. (2005). RNase E-based ribonucleoprotein complexes: mechanical basis of mRNA destabilization mediated by bacterial noncoding RNAs. *Genes Dev.* 19, 2176–2186. doi: 10.1101/gad.1330405
- Morrison, J. M., Miller, E. W., Benson, M. A., Alonzo, F. 3rd., Yoong, P., Torres, V. J., et al. (2012). Characterization of SSR42, a novel virulence factor regulatory RNA that contributes to the pathogenesis of a *Staphylococcus aureus* USA300 representative. *J. Bacteriol.* 194, 2924–2938. doi: 10.1128/JB.06708-11
- Mraheil, M. A., Billion, A., Mohamed, W., Mukherjee, K., Kuenne, C., Pischmarov, J., et al. (2011). The intracellular sRNA transcriptome of *Listeria monocytogenes* during growth in macrophages. *Nucleic Acids Res.* 39, 4235–4248. doi: 10.1093/nar/gkr033
- Müller, P., Gimpel, M., Wildenhain, T., and Brantl, S. (2019). A new role for CsrA: promotion of complex formation between an sRNA and its mRNA target in *Bacillus subtilis*. *RNA Biol.* 16, 972–987. doi: 10.1080/15476286.2019.1605811
- Ng Kwan Lim, E., Sasseville, C., Carrier, M.-C., and Massé, E. (2021). Keeping up with RNA-based regulation in bacteria: new roles for RNA binding proteins. *Trends Genet.* 37, 86–97. doi: 10.1016/j.tig.2020.09.014
- Nielsen, J. S., Larsen, M. H., Lillebæk, E. M. S., Bergholz, T. M., Christiansen, M. H. G., Boor, K. J., et al. (2011). A small RNA controls expression of the chitinase ChiA in *Listeria monocytogenes*. *PLoS One* 6:e19019. doi: 10.1371/journal.pone.0019019
- Nielsen, J. S., Lei, L. K., Ebersbach, T., Olsen, A. S., Klitgaard, J. K., Valentin-Hansen, P., et al. (2010). Defining a role for Hfq in gram-positive bacteria: evidence for Hfq-dependent antisense regulation in *Listeria monocytogenes*. *Nucleic Acids Res.* 38, 907–919. doi: 10.1093/nar/gkp1081
- Nitzan, M., Fechter, P., Peer, A., Altuvia, Y., Bronesky, D., Vandenesch, F., et al. (2015). A defense-offense multi-layered regulatory switch in a pathogenic bacterium. *Nucleic Acids Res.* 43, 1357–1369. doi: 10.1093/nar/gkv001
- Novick, R. P., Iordanescu, S., Projan, S. J., Kornblum, J., and Edelman, I. (1989). pT181 plasmid replication is regulated by a countertranscript-driven transcriptional attenuator. *Cell* 59, 395–404. doi: 10.1016/0092-8674(89)90300-0
- Novick, R. P., Ross, H. F., Projan, S. J., Kornblum, J., Kreiswirth, B., and Moghazeh, S. (1993). Synthesis of staphylococcal virulence factors is controlled by a regulatory RNA molecule. *EMBO J.* 12, 3967–3975. doi: 10.1002/j.1460-2075.1993.tb06074.x
- Nudler, E. (2006). Flipping riboswitches. *Cell* 126, 19–22. doi: 10.1016/j.cell.2006.06.024
- Obana, N., Shirahama, Y., Abe, K., and Nakamura, K. (2010). Stabilization of *Clostridium perfringens* collagenase mRNA by VR-RNA-dependent cleavage in 5' leader sequence. *Mol. Microbiol.* 77, 1416–1428. doi: 10.1111/j.1365-2958.2010.07258.x
- O'Neil, H. S., and Marquis, H. (2006). *Listeria monocytogenes* flagella are used for motility, not as adhesins, to increase host cell invasion. *Infect. Immun.* 74, 6675–6681. doi: 10.1128/IAI.00886-06
- Oscarsson, J., Tegmark-Wisell, K., and Arvidson, S. (2006). Coordinated and differential control of aureolysin (aur) and serine protease (sspA) transcription in *Staphylococcus aureus* by sarA, rot and agr (RNAIII). *Int. J. Med. Microbiol.* 296, 365–380. doi: 10.1016/j.ijmm.2006.02.019
- Padalon-Brauch, G., Hershberg, R., Elgrably-Weiss, M., Baruch, K., Rosenshine, I., Margalit, H., et al. (2008). Small RNAs encoded within genetic islands of *Salmonella* Typhimurium show host-induced expression and role in virulence. *Nucleic Acids Res.* 36, 1913–1927. doi: 10.1093/nar/gkn050
- Papenfert, K., Bouvier, M., Mika, F., Sharma, C. M., and Vogel, J. (2010). Evidence for an autonomous 5' target recognition domain in an Hfq-associated small RNA. *Proc. Natl. Acad. Sci. U. S. A.* 107, 20435–20440. doi: 10.1073/pnas.1009784107
- Papenfert, K., Förstner, K. U., Cong, J.-P., Sharma, C. M., and Bassler, B. L. (2015). Differential RNA-seq of *Vibrio cholerae* identifies the VqmR small RNA as a regulator of biofilm formation. *Proc. Natl. Acad. Sci. U. S. A.* 112, E766–E775. doi: 10.1073/pnas.1500203112
- Papenfert, K., Pfeiffer, V., Lucchini, S., Sonawane, A., Hinton, J. C. D., and Vogel, J. (2008). Systematic deletion of *Salmonella* small RNA genes identifies CyaR, a conserved CRP-dependent riboregulator of OmpX synthesis. *Mol. Microbiol.* 68, 890–906. doi: 10.1111/j.1365-2958.2008.06189.x

- Papenfort, K., Pfeiffer, V., Mika, F., Lucchini, S., Hinton, J. C., and Vogel, J. (2006). SigmaE-dependent small RNAs of *Salmonella* respond to membrane stress by accelerating global omp mRNA decay. *Mol. Microbiol.* 62, 1674–1688. doi: 10.1111/j.1365-2958.2006.05524.x
- Papenfort, K., Sun, Y., Miyakoshi, M., Vanderpool, C. K., and Vogel, J. (2013). Small RNA-mediated activation of sugar phosphatase mRNA regulates glucose homeostasis. *Cell* 153, 426–437. doi: 10.1016/j.cell.2013.03.003
- Papenfort, K., and Vanderpool, C. K. (2015). Target activation by regulatory RNAs in bacteria. *FEMS Microbiol. Rev.* 39, 362–378. doi: 10.1093/femsre/fuv016
- Peñaloza, D., Acuña, L. G., Barros, M. J., Núñez, P., Montt, F., Gil, F., et al. (2021). The small RNA RyhB homologs from *Salmonella* Typhimurium restrain the intracellular growth and modulate the SPI-1 gene expression within RAW264.7 macrophages. *Microorganisms* 9:635. doi: 10.3390/microorganisms9030635
- Pennisi, E. (2010). Shining a light on the genome's "dark matter." *Science* 330:1614. doi: 10.1126/science.330.6011.1614
- Pernitzsch, S. R., Tirier, S. M., Beier, D., and Sharma, C. M. (2014). A variable homopolymeric G-repeat defines small RNA-mediated posttranscriptional regulation of a chemotaxis receptor in *Helicobacter pylori*. *Proc. Natl. Acad. Sci. U. S. A.* 111, E501–E510. doi: 10.1073/pnas.1315152111
- Pfeiffer, V., Papenfort, K., Lucchini, S., Hinton, J. C. D., and Vogel, J. (2009). Coding sequence targeting by MicC RNA reveals bacterial mRNA silencing downstream of translational initiation. *Nat. Struct. Mol. Biol.* 16, 840–846. doi: 10.1038/nsmb.1631
- Pichon, C., and Felden, B. (2005). Small RNA genes expressed from *Staphylococcus aureus* genomic and pathogenicity islands with specific expression among pathogenic strains. *Proc. Natl. Acad. Sci. U. S. A.* 102, 14249–14254. doi: 10.1073/pnas.0503838102
- Pichon, C., and Felden, B. (2007). Proteins that interact with bacterial small RNA regulators. *FEMS Microbiol. Rev.* 31, 614–625. doi: 10.1111/j.1574-6976.2007.00079.x
- Pinel-Marie, M. L., Brielle, R., and Felden, B. (2014). Dual toxic-peptide-coding *Staphylococcus aureus* RNA under antisense regulation targets host cells and bacterial rivals unequally. *Cell Rep.* 7, 424–435. doi: 10.1016/j.celrep.2014.03.012
- Pinel-Marie, M. L., Brielle, R., Riffaud, C., Germain-Amiot, N., Polacek, N., and Felden, B. (2021). RNA antitoxin SprF1 binds ribosomes to attenuate translation and promote persister cell formation in *Staphylococcus aureus*. *Nat. Microbiol.* 6, 209–220. doi: 10.1038/s41564-020-00819-2
- Pitman, S., and Cho, K. H. (2015). The mechanisms of virulence regulation by small noncoding RNAs in low GC gram-positive pathogens. *Int. J. Mol. Sci.* 16, 29797–29814. doi: 10.3390/ijms161226194
- Pourciau, C., Lai, Y.-J., Gorelik, M., Babitzke, P., and Romeo, T. (2020). Diverse mechanisms and circuitry for global regulation by the RNA-binding protein CsrA. *Front. Microbiol.* 11:601352. doi: 10.3389/fmicb.2020.601352
- Quereda, J. J., and Cossart, P. (2017). Regulating bacterial virulence with RNA. *Annu. Rev. Microbiol.* 71, 263–280. doi: 10.1146/annurev-micro-030117-020335
- Quereda, J. J., García-Del Portillo, F., and Pucciarelli, M. G. (2016). *Listeria monocytogenes* remodels the cell surface in the blood-stage. *Environ. Microbiol. Rep.* 8, 641–648. doi: 10.1111/1758-2229.12416
- Quereda, J. J., Ortega, A. D., Pucciarelli, M. G., and García-Del Portillo, F. (2014). The *Listeria* small RNA Rli27 regulates a cell wall protein inside eukaryotic cells by targeting a long 5'-UTR variant. *PLoS Genet.* 10:e1004765. doi: 10.1371/journal.pgen.1004765
- Raina, M., King, A., Bianco, C., and Vanderpool, C. K. (2018). Dual-function RNAs. *Microbiol. Spectr.* 6:10. doi: 10.1128/microbiolspec.RWR-0032-2018
- Redder, P. (2018). Molecular and genetic interactions of the RNA degradation machineries in Firmicute bacteria. *Wiley Interdiscip. Rev. RNA* 9. doi: 10.1002/wrna.1460
- Rice, K. C., Nelson, J. B., Patton, T. G., Yang, S.-J., and Bayles, K. W. (2005). Acetic acid induces expression of the *Staphylococcus aureus* cidABC and lrgAB murein hydrolase regulator operons. *J. Bacteriol.* 187, 813–821. doi: 10.1128/JB.187.3.813-821.2005
- Rochat, T., Bohn, C., Morvan, C., Le Lam, T. N., Razvi, F., Pain, A., et al. (2018). The conserved regulatory RNA RsaE down-regulates the arginine degradation pathway in *Staphylococcus aureus*. *Nucleic Acids Res.* 46, 8803–8816. doi: 10.1093/nar/gky584
- Rochat, T., Delumeau, O., Figueroa-Bossi, N., Noirot, P., Bossi, L., Dervyn, E., et al. (2015). Tracking the elusive function of *Bacillus subtilis* Hfq. *PLoS One* 10:e0124977. doi: 10.1371/journal.pone.0124977
- Romeo, T. (1998). Global regulation by the small RNA-binding protein CsrA and the non-coding RNA molecule CsrB. *Mol. Microbiol.* 29, 1321–1330. doi: 10.1046/j.1365-2958.1998.01021.x
- Romilly, C., Lays, C., Tomasini, A., Caldeleri, I., Benito, Y., Hammann, P., et al. (2014). A non-coding RNA promotes bacterial persistence and decreases virulence by regulating a regulator in *Staphylococcus aureus*. *PLoS Pathog.* 10:e1003979. doi: 10.1371/journal.ppat.1003979
- Sáenz-Lahoya, S., Bitarte, N., García, B., Burgui, S., Vergara-Irigaray, M., Valle, J., et al. (2019). Noncontiguous operon is a genetic organization for coordinating bacterial gene expression. *Proc. Natl. Acad. Sci. U. S. A.* 116, 1733–1738. doi: 10.1073/pnas.1812746116
- Saïd-Salim, B., Dunman, P. M., McAleese, F. M., Macapagal, D., Murphy, E., McNamara, P. J., et al. (2003). Global regulation of *Staphylococcus aureus* genes by rot. *J. Bacteriol.* 185, 610–619. doi: 10.1128/JB.185.2.610-619.2003
- Salvail, H., Caron, M.-P., Bélanger, J., and Massé, E. (2013). Antagonistic functions between the RNA chaperone Hfq and an sRNA regulate sensitivity to the antibiotic colicin. *EMBO J.* 32, 2764–2778. doi: 10.1038/emboj.2013.205
- Sauder, A. B., and Kendall, M. M. (2018). After the fact(or): posttranscriptional gene regulation in enterohemorrhagic *Escherichia coli* O157:H7. *J. Bacteriol.* 200, e00228–e00318. doi: 10.1128/JB.00228-18
- Sayed, N., Jousselin, A., and Felden, B. (2012). A cis-antisense RNA acts in trans in *Staphylococcus aureus* to control translation of a human cytolytic peptide. *Nat. Struct. Mol. Biol.* 19, 105–112. doi: 10.1038/nsmb.2193
- Schoenfelder, S. M. K., Lange, C., Prakash, S. A., Marincola, G., Lerch, M. F., Wencker, F. D. R., et al. (2019). The small non-coding RNA RsaE influences extracellular matrix composition in *Staphylococcus epidermidis* biofilm communities. *PLoS Pathog.* 15:e1007618. doi: 10.1371/journal.ppat.1007618
- Sedlyarova, N., Shamovsky, I., Bharati, B. K., Epshtein, V., Chen, J., Gottesman, S., et al. (2016). sRNA-mediated control of transcription termination in *E. coli*. *Cell* 167, 111.e13–121.e13. doi: 10.1016/j.cell.2016.09.004
- Seidl, K., Müller, S., François, P., Kriebitzsch, C., Schrenzel, J., Engelmann, S., et al. (2009). Effect of a glucose impulse on the CcpA regulon in *Staphylococcus aureus*. *BMC Microbiol.* 9:95. doi: 10.1186/1471-2180-9-95
- Serganov, A., Yuan, Y.-R., Pikovskaya, O., Polonskaia, A., Malinina, L., Phan, A. T., et al. (2004). Structural basis for discriminative regulation of gene expression by adenine- and guanine-sensing mRNAs. *Chem. Biol.* 11, 1729–1741. doi: 10.1016/j.chembiol.2004.11.018
- Sesto, N., Wurtzel, O., Archambaud, C., Sorek, R., and Cossart, P. (2013). The excludon: a new concept in bacterial antisense RNA-mediated gene regulation. *Nat. Rev. Microbiol.* 11, 75–82. doi: 10.1038/nrmicro2934
- Sharma, C. M., Darfeuille, F., Plantinga, T. H., and Vogel, J. (2007). A small RNA regulates multiple ABC transporter mRNAs by targeting C/A-rich elements inside and upstream of ribosome-binding sites. *Genes Dev.* 21, 2804–2817. doi: 10.1101/gad.447207
- Sievers, S., Lund, A., Menendez-Gil, P., Nielsen, A., Storm Møllerup, M., Lambert Nielsen, S., et al. (2015). The multicopy sRNA LhrC controls expression of the oligopeptide-binding protein OppA in *Listeria monocytogenes*. *RNA Biol.* 12, 985–997. doi: 10.1080/15476286.2015.1071011
- Sievers, S., Sternkopf Lillebæk, E. M., Jacobsen, K., Lund, A., Møllerup, M. S., Nielsen, P. K., et al. (2014). A multicopy sRNA of *Listeria monocytogenes* regulates expression of the virulence adhesin LapB. *Nucleic Acids Res.* 42, 9383–9398. doi: 10.1093/nar/gku630
- Singh, R., and Ray, P. (2014). Quorum sensing-mediated regulation of staphylococcal virulence and antibiotic resistance. *Future Microbiol.* 9, 669–681. doi: 10.2217/fmb.14.31
- Smirnov, A., Förstner, K. U., Holmqvist, E., Otto, A., Günster, R., Becher, D., et al. (2016). Grad-seq guides the discovery of ProQ as a major small RNA-binding protein. *Proc. Natl. Acad. Sci. U. S. A.* 113, 11591–11596. doi: 10.1073/pnas.1609981113
- Sonnleitner, E., Pusic, P., Wolfinger, M. T., and Bläsi, U. (2020). Distinctive regulation of carbapenem susceptibility in *Pseudomonas aeruginosa* by Hfq. *Front. Microbiol.* 11:1001. doi: 10.3389/fmicb.2020.01001
- Stork, M., Di Lorenzo, M., Welch, T. J., and Crosa, J. H. (2007). Transcription termination within the iron transport-biosynthesis operon of *Vibrio anguillarum* requires an antisense RNA. *J. Bacteriol.* 189, 3479–3488. doi: 10.1128/JB.00619-06

- Svensson, S. L., and Sharma, C. M. (2016). Small RNAs in bacterial virulence and communication. *Microbiol. Spectr.* 4. doi: 10.1128/microbiolspec.VMBF-0028-2015
- Teixidó, L., Cortés, P., Bigas, A., Alvarez, G., Barbé, J., and Campoy, S. (2010). Control by Fur of the nitrate respiration regulators NarP and NarL in *Salmonella enterica*. *Int. Microbiol.* 13, 33–39. doi: 10.2436/20.1501.01.108
- Thomason, M. K., and Storz, G. (2010). Bacterial antisense RNAs: how many are there, and what are they doing? *Annu. Rev. Genet.* 44, 167–188. doi: 10.1146/annurev-genet-102209-163523
- Thomason, M. K., Voichek, M., Dar, D., Addis, V., Fitzgerald, D., Gottesman, S., et al. (2019). A rhlI 5' UTR-derived sRNA regulates RhlR-dependent quorum sensing in *Pseudomonas aeruginosa*. *MBio* 10, e02253–e02319. doi: 10.1128/mBio.02253-19
- Tobe, T., Yen, H., Takahashi, H., Kagayama, Y., Ogasawara, N., and Oshima, T. (2014). Antisense transcription regulates the expression of the enterohemorrhagic *Escherichia coli* virulence regulatory gene ler in response to the intracellular iron concentration. *PLoS One* 9:e101582. doi: 10.1371/journal.pone.0101582
- Toledo-Arana, A., Dussurget, O., Nikitas, G., Sesto, N., Guet-Revillet, H., Balestrino, D., et al. (2009). The *Listeria* transcriptional landscape from saprophytism to virulence. *Nature* 459, 950–956. doi: 10.1038/nature08080
- Toledo-Arana, A., and Lasa, I. (2020). Advances in bacterial transcriptome understanding: from overlapping transcription to the exclusion concept. *Mol. Microbiol.* 113, 593–602. doi: 10.1111/mmi.14456
- Toledo-Arana, A., Repoila, F., and Cossart, P. (2007). Small noncoding RNAs controlling pathogenesis. *Curr. Opin. Microbiol.* 10, 182–188. doi: 10.1016/j.mib.2007.03.004
- Tomizawa, J., Itoh, T., Selzer, G., and Som, T. (1981). Inhibition of ColE1 RNA primer formation by a plasmid-specified small RNA. *Proc. Natl. Acad. Sci. U. S. A.* 78, 1421–1425. doi: 10.1073/pnas.78.3.1421
- Tree, J. J., Granneman, S., McAtter, S. P., Tollervy, D., and Gally, D. L. (2014). Identification of bacteriophage-encoded anti-sRNAs in pathogenic *Escherichia coli*. *Mol. Cell* 55, 199–213. doi: 10.1016/j.molcel.2014.05.006
- Updegrove, T. B., Zhang, A., and Storz, G. (2016). Hfq: the flexible RNA matchmaker. *Curr. Opin. Microbiol.* 30, 133–138. doi: 10.1016/j.mib.2016.02.003
- Urban, J. H., and Vogel, J. (2008). Two seemingly homologous noncoding RNAs act hierarchically to activate glmS mRNA translation. *PLoS Biol.* 6:e64. doi: 10.1371/journal.pbio.0060064
- Vakulskas, C. A., Potts, A. H., Babitzke, P., Ahmer, B. M. M., and Romeo, T. (2015). Regulation of bacterial virulence by Csr (Rsm) systems. *Microbiol. Mol. Biol. Rev.* 79, 193–224. doi: 10.1128/MMBR.00052-14
- Vanderpool, C. K., and Gottesman, S. (2004). Involvement of a novel transcriptional activator and small RNA in post-transcriptional regulation of the glucose phosphoenolpyruvate phosphotransferase system. *Mol. Microbiol.* 54, 1076–1089. doi: 10.1111/j.1365-2958.2004.04348.x
- Vannini, A., Roncarati, D., and Danielli, A. (2016). The cag-pathogenicity island encoded CncR1 sRNA oppositely modulates *Helicobacter pylori* motility and adhesion to host cells. *Cell. Mol. Life Sci.* 73, 3151–3168. doi: 10.1007/s00018-016-2151-z
- Wagner, E. G. H., Altuvia, S., and Romby, P. (2002). Antisense RNAs in bacteria and their genetic elements. *Adv. Genet.* 46, 361–398. doi: 10.1016/s0065-2660(02)46013-0
- Wagner, E. G., and Romby, P. (2015). Small RNAs in bacteria and archaea: who they are, what they do, and how they do it. *Adv. Genet.* 90, 133–208. doi: 10.1016/bs.adgen.2015.05.001
- Wang, C., Chao, Y., Matera, G., Gao, Q., and Vogel, J. (2020). The conserved 3' UTR-derived small RNA NarS mediates mRNA crossregulation during nitrate respiration. *Nucleic Acids Res.* 48, 2126–2143. doi: 10.1093/nar/gkz1168
- Wassarman, K. M., Zhang, A., and Storz, G. (1999). Small RNAs in *Escherichia coli*. *Trends Microbiol.* 7, 37–45. doi: 10.1016/S0966-842X(98)01379-1
- Waters, L. S., and Storz, G. (2009). Regulatory RNAs in bacteria. *Cell* 136, 615–628. doi: 10.1016/j.cell.2009.01.043
- Weilbacher, T., Suzuki, K., Dubey, A. K., Wang, X., Gudapaty, S., Morozov, I., et al. (2003). A novel sRNA component of the carbon storage regulatory system of *Escherichia coli*. *Mol. Microbiol.* 48, 657–670. doi: 10.1046/j.1365-2958.2003.03459.x
- Wen, J., and Fozo, E. M. (2014). sRNA antitoxins: more than one way to repress a toxin. *Toxins* 6, 2310–2335. doi: 10.3390/toxins6082310
- Westermann, A. J., Förstner, K. U., Amman, F., Barquist, L., Chao, Y., Schulte, L. N., et al. (2016). Dual RNA-seq unveils noncoding RNA functions in host-pathogen interactions. *Nature* 529, 496–501. doi: 10.1038/nature16547
- Winkler, W., Nahvi, A., and Breaker, R. R. (2002). Thiamine derivatives bind messenger RNAs directly to regulate bacterial gene expression. *Nature* 419, 952–956. doi: 10.1038/nature01145
- Wurtzel, O., Sesto, N., Mellin, J. R., Karunker, I., Edelheit, S., Bécavin, C., et al. (2012). Comparative transcriptomics of pathogenic and non-pathogenic *Listeria* species. *Mol. Syst. Biol.* 8:583. doi: 10.1038/msb.2012.11
- Yang, B., Feng, L., Wang, F., and Wang, L. (2015). Enterohemorrhagic *Escherichia coli* senses low biotin status in the large intestine for colonization and infection. *Nat. Commun.* 6:6592. doi: 10.1038/ncomms7592
- Yu, J., and Schneiders, T. (2012). Tigecycline challenge triggers sRNA production in *Salmonella enterica* serovar Typhimurium. *BMC Microbiol.* 12:195. doi: 10.1186/1471-2180-12-195
- Zhang, Y. F., Han, K., Chandler, C. E., Tjaden, B., Ernst, R. K., and Lory, S. (2017). Probing the sRNA regulatory landscape of *P. aeruginosa*: post-transcriptional control of determinants of pathogenicity and antibiotic susceptibility. *Mol. Microbiol.* 106, 919–937. doi: 10.1111/mmi.13857
- Zhang, H., Zhang, Y., Song, Z., Li, R., Ruan, H., Liu, Q., et al. (2020). sncRNAs packaged by *Helicobacter pylori* outer membrane vesicles attenuate IL-8 secretion in human cells. *Int. J. Med. Microbiol.* 310:151356. doi: 10.1016/j.ijmm.2019.151356
- Zhao, X., Zhang, Y., and Huang, X. (2018). Pathogenicity-island-encoded regulatory RNAs regulate bacterial virulence and pathogenesis. *Microb. Pathog.* 125, 196–204. doi: 10.1016/j.micpath.2018.09.028
- Zhukova, A., Fernandes, L. G., Hugon, P., Pappas, C. J., Sismeiro, O., Coppée, J.-Y., et al. (2017). Genome-wide transcriptional start site mapping and sRNA identification in the pathogen *Leptospira interrogans*. *Front. Cell. Infect. Microbiol.* 7:10. doi: 10.3389/fcimb.2017.00010

Conflict of Interest: The authors declare that the research was conducted in the absence of any commercial or financial relationships that could be construed as a potential conflict of interest.

Publisher's Note: All claims expressed in this article are solely those of the authors and do not necessarily represent those of their affiliated organizations, or those of the publisher, the editors and the reviewers. Any product that may be evaluated in this article, or claim that may be made by its manufacturer, is not guaranteed or endorsed by the publisher.

Copyright © 2021 Felden and Augagneur. This is an open-access article distributed under the terms of the Creative Commons Attribution License (CC BY). The use, distribution or reproduction in other forums is permitted, provided the original author(s) and the copyright owner(s) are credited and that the original publication in this journal is cited, in accordance with accepted academic practice. No use, distribution or reproduction is permitted which does not comply with these terms.



The Small RNA ErsA Impacts the Anaerobic Metabolism of *Pseudomonas aeruginosa* Through Post-Transcriptional Modulation of the Master Regulator Anr

Silvia Ferrara*, Riccardo Carrubba, Silvia Santoro and Giovanni Bertoni*

Department of Biosciences, Università degli Studi di Milano, Milan, Italy

OPEN ACCESS

Edited by:

Olga Soutourina,
Institut de Biologie Intégrative de la
Cellule (I2BC), France

Reviewed by:

Hiroyuki Arai,
The University of Tokyo, Japan
Amy H. Lee,
Simon Fraser University, Canada

*Correspondence:

Silvia Ferrara
silvia.ferrara@unimi.it
Giovanni Bertoni
giovanni.bertoni@unimi.it

Specialty section:

This article was submitted to
Microbial Physiology and Metabolism,
a section of the journal
Frontiers in Microbiology

Received: 06 April 2021

Accepted: 27 July 2021

Published: 20 August 2021

Citation:

Ferrara S, Carrubba R,
Santoro S and Bertoni G (2021) The
Small RNA ErsA Impacts the
Anaerobic Metabolism of
Pseudomonas aeruginosa Through
Post-Transcriptional Modulation of
the Master Regulator Anr.
Front. Microbiol. 12:691608.
doi: 10.3389/fmicb.2021.691608

Pseudomonas aeruginosa is one of the most critical opportunistic pathogens in humans, able to cause both lethal acute and chronic lung infections. In previous work, we indicated that the small RNA ErsA plays a role in the regulatory network of *P. aeruginosa* pathogenicity in airways infection. To give further insight into the lifestyle functions that could be either directly or indirectly regulated by ErsA during infection, we reanalyzed the categories of genes whose transcription appeared dysregulated in an *ersA* knock-out mutant of the *P. aeruginosa* PAO1 reference strain. This preliminary analysis indicated ErsA as a candidate co-modulator of denitrification and in general, the anaerobiosis response, a characteristic physiologic state of *P. aeruginosa* during chronic infection of the lung of cystic fibrosis (CF) patients. To explain the pattern of dysregulation of the anaerobic-lifestyle genes in the lack of ErsA, we postulated that ErsA regulation could target the expression of Anr, a well-known transcription factor that modulates a broad regulon of anoxia-responsive genes, and also Dnr, required for the transcription activation of the denitrification machinery. Our results show that ErsA positively regulates Anr expression at the post-transcriptional level while no direct ErsA-mediated regulatory effect on Dnr was observed. However, Dnr is transcriptionally downregulated in the absence of ErsA and this is consistent with the well-characterized regulatory link between Anr and Dnr. Anr regulatory function is critical for *P. aeruginosa* anaerobic growth, both through denitrification and fermentation of arginine. Interestingly, we found that, differently from the laboratory strain PAO1, ErsA deletion strongly impairs the anaerobic growth by both denitrification and arginine fermentation of the RP73 clinical isolate, a multi-drug resistant *P. aeruginosa* CF-adapted strain. This suggests that *P. aeruginosa* adaptation to CF lung might result in a higher dependence on ErsA for the transduction of the multiple signals to the regulatory network of key functions for survival in such a complex environment. Together, our results suggest that ErsA takes an upper place in the regulatory network of airways infection, transducing host inputs to biofilm-related factors, as underlined in our previous reports, and to functions that allow *P. aeruginosa* to thrive in low-oxygen conditions.

Keywords: *Pseudomonas aeruginosa*, small RNA, Anr, cystic fibrosis, anoxia adaptation

INTRODUCTION

The small RNA (sRNA) ErsA of *Pseudomonas aeruginosa* is associated with the regulation of bacterium-host interaction traits, such as biofilm maturation, motility (Falcone et al., 2018), and resistance to carbapenem antibiotics (Zhang et al., 2017; Sonnleitner et al., 2020). A key role of ErsA in the regulatory network of *P. aeruginosa* pathogenicity was recently assessed (Ferrara et al., 2020). The deletion of ErsA leads to *P. aeruginosa* virulence attenuation both *in vitro* and *in vivo* (Ferrara et al., 2020). The significant impairment of *P. aeruginosa* in biofilm formation and maturation resulting from ErsA deletion can explain the involvement of ErsA in acute infection and immune response activation (Ferrara et al., 2020). The ErsA role in biofilm regulation is supposed to involve the downregulation of the AlgC enzyme (Ferrara et al., 2015) and the activation of the AmrZ regulon (Falcone et al., 2018). However, the ErsA role in the host-pathogen interaction is not only limited to biofilm regulation but influences also the envelope composition of *P. aeruginosa* by direct negative regulation of *oprD* mRNA (Zhang et al., 2017; Sonnleitner et al., 2020). Moreover, recent transcriptomics data (Falcone et al., 2018) suggest a broader regulatory network influenced by ErsA since the ErsA deletion can affect other aspects of *P. aeruginosa* lifestyle when coping with, for example, an oxygen-restricted environment, such as the airways of cystic fibrosis (CF) patients (Govan and Deretic, 1996; Worlitzsch et al., 2002).

The complex matrix of biofilm structure and thick mucus in CF lungs impede oxygen diffusion and generate a hypoxic microenvironment. It was shown that microaerophilic and anaerobic conditions are predominant in the sputum of CF patients (Yoon et al., 2002; Alvarez-Ortega and Harwood, 2007; Hassett et al., 2009). It has been known for a long time that *P. aeruginosa*, being a facultative anaerobe, can thrive in such CF environment within mucus plugs and biofilm (Schobert and Jahn, 2010) and besides anoxia and hypoxia are thought to be essential for full biofilm establishment (Stewart and Franklin, 2008).

In case of limiting or no oxygen availability, denitrification allows *P. aeruginosa* to respire nitrates or nitrites (Carlson and Ingraham, 1983; Davies et al., 1989; Zumft, 1997). When these are also absent, *P. aeruginosa* can moderately support anaerobic growth and survival through the activation of the arginine fermentation pathway (Vander Wauven et al., 1984; Luthi et al., 1990) and pyruvate fermentation (Eschbach et al., 2004; **Supplementary Figure S1**, schematizing the complex anaerobic metabolism of *P. aeruginosa*).

The expression of the enzymes for growth and survival in anaerobic environments is coordinated by the transcriptional factor Anr, a global oxygen-sensing transcription factor that plays the role of the master regulator of anaerobiosis-related genes (Galimand et al., 1991; Zimmermann et al., 1991; Ye et al., 1995; Platt et al., 2008; Trunk et al., 2010). Anr is essential for *P. aeruginosa* anaerobic growth on both nitrate and arginine (Filiatrault et al., 2006) and responsible for the activation of the *ackA-pta* operon for pyruvate fermentation in response to oxygen limitation (Eschbach et al., 2004; Filiatrault et al., 2006). Moreover, it controls the expression of *dnr* and *narL* genes, encoding two transcription factors required for

the activation of the denitrification machinery and the regulation of other genes linked to anaerobic metabolism (Schreiber et al., 2007; Arai, 2011; Tribelli et al., 2019).

In this work, we expand the knowledge on the regulatory network of ErsA and show its additional role in the regulation of Anr and consequently of anaerobic metabolism and denitrification processes. Therefore, ErsA is not only correlated to anaerobiosis as transcriptionally activated under reduced oxygen conditions (Ferrara et al., 2015), but it also transduces the low-oxygen cue toward the Anr regulon acting as a positive post-transcriptional regulator of the *anr* mRNA. Furthermore, we show that, beyond a certain threshold of ErsA abundance, the RNA-binding protein Hfq cooperates with ErsA in Anr activation. This role of Hfq is added to the one exercised post-transcriptionally *per se* by Hfq on Anr. Finally, ErsA deletion strongly impairs the anaerobic growth by both denitrification and arginine fermentation of the RP73 clinical isolate, a multi-drug resistant *P. aeruginosa* CF-adapted strain. This suggests that *P. aeruginosa* adaptation to CF lung might result in a higher dependence on ErsA for the regulation of anaerobic metabolism.

MATERIALS AND METHODS

Bacterial Strains and Culture Conditions

Bacterial strains and plasmids used in this study are listed in **Supplementary Table S1**. *P. aeruginosa* and *E. coli* strains were routinely grown in Luria-Bertani broth (LB) at 37°C. For selective *E. coli* growth, ampicillin, gentamicin, and chloramphenicol were added at 100, 20, and 25 µg/ml, respectively. For selective *Pseudomonas* growth, carbenicillin and gentamicin were added at 300 and 60 µg/ml, respectively. For P_{BAD} induction in vector plasmid pGM931, arabinose was added to a final concentration of 10 mM.

Anaerobic cultivations of *P. aeruginosa* strains were performed in Oxoid anaerobiosis jars at 37°C, using agar plates prepared with Brain Heart Infusion (BHI)-rich medium supplemented with 100 mM KNO₃ to allow anaerobic respiration or without KNO₃ to test arginine fermentation. For the anaerobic growth assay, cell cultures of *P. aeruginosa* RP73 (Bianconi et al., 2015) and RP73 Δ ersA (Ferrara et al., 2020), PAO1 (Stover et al., 2000), and PAO1 Δ ersA (Ferrara et al., 2015) with an OD₆₀₀ of 1 (corresponding to 1 × 10⁹ CFU/ml) were serially diluted until 10⁻⁶; 2 µl of each dilution was spotted and incubated for 72 h. For total RNA extraction from anaerobically grown cell cultures of PAO1 and PAO1 Δ ersA (Ferrara et al., 2015), the strains were plated at the confluence and incubated for 72 h. The anaerobic atmosphere was induced by the Oxoid AnaeroGen sachet. Control testing of anaerobiosis was performed using the Oxoid Anaerobic indicator in the jar as a visual check that anaerobic conditions have been achieved and maintained.

Plasmid Constructions

The oligonucleotides used in this study are listed in **Supplementary Table S2**. Plasmids pBBR1-*anr::sfGFP* and pBBR1-*dnr::sfGFP* expressing *anr::sfGFP* and *dnr::sfGFP*

translational fusions, respectively, under the $P_{LtetO-1}$ constitutive promoter were constructed as follows. A DNA fragment including the 31-nt UTR along with the first 22 codons (66 nt) of the *anr* open reading frame (66 nt) was PCR amplified from PAO1 genomic DNA with oligos 2/3, digested with *NsiI/NheI*, and cloned into the sfGFP reporter vector pXG10-SF (Corcoran et al., 2012) giving rise to plasmid pXG10-*anr::sfGFP*. With the same procedure, a DNA fragment including the 116-nt UTR and the first 32 codons (96 nt) of the *dnr* open reading frame was amplified with oligos 4/5, digested *NsiI/NheI*, and cloned into the sfGFP reporter vectors pXG10-SF giving rise to plasmid pXG10-*dnr::sfGFP*. The DNA fragments spanning from the $P_{LtetO-1}$ promoter to the end of the sfGFP reporter gene were amplified by PCR, respectively, from pXG10-*anr::sfGFP* and pXG10-*dnr::sfGFP* with oligos 6/7, digested *ClaI/XbaI*, and cloned into the low-copy number shuttle vector pBBR1-MCS5 (Kovach et al., 1995) giving rise to constructs pBBR1-*anr::sfGFP* and pBBR1-*dnr::sfGFP*, respectively. All constructs were verified by sequencing (Eurofins Genomics) using either oligos 7 or 8.

In vitro Assays of sRNA/mRNA Interactions

Purified RNA for RNA/RNA interaction assays was prepared by T7 RNA polymerase transcription of gel-purified DNA fragments. DNA fragments for *anr* mRNA and ErsA RNA preparations were amplified from *P. aeruginosa* PAO1 genomic DNA with oligo pairs 9/10 and 11/12, respectively. Each transcription reaction was performed with the Riboprobe® System-T7 (Promega) with 300 ng of DNA template. Synthesized RNA was purified using the RNeasy MinElute Cleanup Kit (Qiagen). Purified RNA was checked by denaturing polyacrylamide gel electrophoresis and quantified using Eppendorf Biospectrometer. Electrophoretic Mobility Shift Assay to analyze ErsA/*anr* mRNA interactions was performed in 10 µl of reactions containing 1×RNA-binding buffer (10 mM Tris-HCl, pH 7, 100 mM KCl, 10 mM MgCl₂, and 10% glycerol), purified ErsA RNA and increasing amounts of purified *anr* mRNA, or yeast tRNA (Ambion). Binding reactions were incubated at 37°C for 20 min, then loaded into a native 6% polyacrylamide gel (acrylamide-bis ratio 29:1) in 0.5×TBE buffer (45 mM Tris-borate, pH 8.0, 1 mM EDTA), and electrophoresed using a Mini-Protean Electrophoresis System (Bio-Rad) at 4°C and 180 V for 90 min. RNAs were transferred into a GeneScreen plus nylon hybridization transfer membrane (Perkin Elmer) using a semi-dry electroblotting (Fastblot B33, Biometra) set at 25 V, 400 mA for 1 h, and UV-crosslinked to the membrane with a Stratilinker 1800 UV Crosslinker (Stratagene). The blotting membrane was hybridized with a biotinylated anti-ErsA probe (oligo 1) using the North2South Chemiluminescent Hybridization and Detection kit (Thermo Scientific) according to the manufacturer's instructions. After the addition of the Streptavidin-HRP conjugate, the ErsA bands were visualized by mixing equal volumes of luminol/enhancer solution and stable peroxide solution and acquiring images with a ChemiDoc Touch Imaging System (Bio-Rad) using ImageLab analysis software.

In vivo Assays of sRNA/mRNA Interactions

Fluorescence measurements in *P. aeruginosa* strains PAO1 wild type (Stover et al., 2000), PAO1 Δ ersA (Ferrara et al., 2015), and PAO1 *hfq*[−] (Sonnleitner et al., 2003) carrying the sfGFP translational fusions with target genes were carried out as follows. To test the sRNA/target interaction in planktonic cells of aerobically grown cultures, strains carrying the reporter pBBR1-*anr::sfGFP* or pBBR1-*dnr::sfGFP* alone, or combined with either pGM931 (Qiu et al., 2008; Delvillani et al., 2014; Ferrara et al., 2020) or pGM-ersA (Ferrara et al., 2015), were inoculated in 15 ml tubes filled with 5 ml of LB at an OD₆₀₀ of 0.1 and grown at 37°C in a rotatory shaker. Samples were taken after 6 and 24 h (Ferrara et al., 2015). For the testing of anaerobically grown cultures, strains were inoculated at an OD₆₀₀ of 0.4 in 50 ml flasks filled with 10 ml of LB medium supplemented with 100 mM KNO₃. The anaerobic atmosphere was induced by Oxoid AnaeroGen sachet. Control testing of anaerobiosis was assessed by the Oxoid Anaerobic Indicator. Samples were taken after 2 days of static anaerobic growth at 37°C. The collected samples were centrifuged, washed twice, and resuspended in PBS (10 mM Na₃PO₄, 150 mM NaCl) to OD₆₀₀ of 1. Samples were then serially diluted 1.33-fold (corresponding to OD₆₀₀ of 0.75, 0.5, and 0.25). 200 µl of aliquots was transferred to black polystyrene 96-well microplates with a clear, flat bottom (Corning). At least three biological replicates were used for every experimental set. The absorbance (Abs₅₉₅) and fluorescence polarization (FP_{485/535}) were measured in an EnSight Multimode Plate Reader (PerkinElmer) using Kaleido data acquiring software. GFP activity was expressed in arbitrary units (AU) as FP_{485/535}/Abs₅₉₅.

To test fluorescence in surface-grown cells, the strains were spotted on agar plates of BHI supplemented with or without 100 mM KNO₃ and incubated at 37°C for 72 h. Cells were collected from spots, resuspended in PBS, and assayed as described above.

RNA Isolation and Quantitative RT-PCR Analysis

Quantitative RT-PCR analysis (qRT-PCR) was performed on total RNA extracted from *P. aeruginosa* PAO1 wild type and Δ ersA surface-grown cells under anaerobic conditions for 72 h. Immediately after opening the jar, cells were removed from plates, resuspended in RNAProtect Cell Reagent (Qiagen), incubated, for 5 min at room temperature, pelleted by centrifugation, and stored at −80°C until use. RNA extraction was performed as described previously in Ferrara et al. (2015). The quality and concentration of the extracted RNA were assessed by a Biospectrometer (Eppendorf).

cDNA was synthesized from 1 µg of total purified RNA using Superscript III Reverse Transcriptase (Invitrogen) according to the manufacturer's instructions. qRT-PCR was performed in triplicate using SYBR Green PCR Master Mix (Bio-Rad) on a CFX Connect Real-Time System (Bio-Rad). Oligo pairs 13/14 (Vitale et al., 2008), 15/16 (Tribelli et al., 2019), and 17/18 (Jackson et al., 2013) were used for amplification of 16S, *anr*, and *dnr*, respectively. The reaction procedure involved incubation at 95°C for 5 min

and 39 cycles of amplification at 95°C for 15s, 58°C for 20s, and 72.5°C for 30s. The calculation of the relative expression of *anr* and *dnr* genes in the PAO1 Δ ersA mutant vs. the wild-type strain was performed first normalizing mRNA amounts to 16S ribosome RNA (ΔC_T) and then relating the ΔC_T in the Δ ersA mutant to the wild type ($\Delta\Delta C_T$).

RESULTS

The Regulation of Denitrification and Anaerobiosis in *P. aeruginosa* Is a Target of ErsA RNA

The transcriptome profiling of the aerobically grown PAO1 wild-type strain vs. the corresponding Δ ersA mutant showed more than 160 differentially expressed genes (DEGs) (Falcone et al., 2018). These data were collected from bacterial cells incubated at 37°C until the onset of the stationary phase ($OD_{600} = 2.7$; Falcone et al., 2018).

For a more comprehensive understanding of the ErsA-dependent regulatory networks, we performed a new functional categorization of the above-mentioned DEGs. This analysis revealed 52 DEGs associated with growth or survival under anaerobic conditions (Table 1). Among these, some genes belong to the denitrification and nitrate metabolism (*narK1*, *narH*, *narI*, *narJ*, *narL*, and *nirN*), the fermentation pathways of arginine and pyruvate (*arcD*, *ackA*), and the universal stress response (*uspL*/PA1789, *uspM*/PA4328, *uspN*/PA4352, and *uspO*/PA5027). Out of 52 anaerobiosis-linked DEGs, 44 and 5 were already known to be up- or downregulated under anaerobic growth, respectively (Alvarez-Ortega and Harwood, 2007; Platt et al., 2008; Trunk et al., 2010; Crespo et al., 2017; Tribelli et al., 2019).

The majority of the DEGs known to be induced by anaerobic conditions was downregulated in the Δ ersA strain. Vice versa, DEGs repressed in anaerobiosis and appeared upregulated in the Δ ersA strain. Exceptions are the *nirN* gene for nitrite respiration, and the last genes of the *nar* operon (*narH*, *J*, and *I*) for nitrate respiration, which are upregulated by anaerobiosis, and appear also upregulated in the Δ ersA mutant strain. Besides, as evidenced in Tables 1, 23 and 3 DEGs induced and repressed by anoxia, respectively, are under the transcriptional control of the master regulator of anaerobiosis, Anr (Trunk et al., 2010). Finally, the heat-shock protein IbpA and the transcription regulator PsrA (involved in the positive regulation of RpoS and the TTSS) were included among DEGs not belonging to the Anr regulon.

Taken together, this more accurate analysis of the comparative transcriptional profiling between PAO1 wild-type and Δ ersA mutant strains suggested that the overall anaerobic metabolism in *P. aeruginosa* and particularly the denitrification processes could be co-regulated by ErsA. Despite the list of anaerobically regulated DEGs in Table 1 is reasonably not exhaustive since bacterial cells were grown in aerobic conditions before RNA extraction (Falcone et al., 2018), this evidenced that ErsA influences a peculiar set of genes belonging to the regulon of the transcription factor Anr. Specifically, the pattern of upregulated and downregulated genes in the PAO1 Δ ersA strain

seemed to be consistent with positive post-transcriptional regulation of *anr* mRNA by ErsA. This suggested that Anr expression could be directly targeted by ErsA. Furthermore, since Anr is the master regulator in anaerobiosis of a broad regulon of anoxia-responsive genes (Platt et al., 2008; Trunk et al., 2010) including also the transcription factor DNR (Supplementary Figure S1), which is indeed responsible for the transcription activation of the denitrification machinery (Trunk et al., 2010), we speculated that ErsA might additionally regulate DNR expression.

ErsA Targets *Anr* mRNA and Positively Regulates Anr Expression

The results of the analysis described above suggested that *anr* and *dnr* mRNAs could be targeted by ErsA. To assess preliminarily the interaction between ErsA RNA and the two candidate target mRNAs, the web tool IntaRNA (Wright et al., 2014) was used. The modeling of the interaction between the full-length ErsA and *anr* mRNA comprehensive of 5' untranslated region (5'-UTR) predicted that the 34-nt long U-rich unstructured domain II of ErsA (Ferrara et al., 2015) could, from nt 31 to 54, extensively base-pair with the open reading frame region of *anr* mRNA, from nt +28 to +49 relative to the translational start site AUG (Figure 1A). To validate this sRNA/mRNA interaction *in vivo*, we used a robust two-plasmid reporter system suited for *P. aeruginosa* in our previous works (Ferrara et al., 2015, 2017). To this end, we generated a translational fusion between the first 22 codons of *anr* open reading frame linked to its 5'-UTR and the *superfolder* variant gene of the green fluorescent protein (*sfGFP*; Corcoran et al., 2012) under the control of the heterologous constitutive promoter $P_{LtetO-1}$. We comparatively assayed the *anr::sfGFP* fusion in planktonic cells, grown in aerobic conditions, of wild-type and Δ ersA mutant strains and observed no significant differences in fluorescence levels. Then, the fluorescence expressed by the *anr::sfGFP* fusion was assayed in *P. aeruginosa* PAO1 strains, still grown in planktonic and aerobic conditions, in the absence and presence of ErsA overexpression from the arabinose inducible pGM-ersA vector (Ferrara et al., 2015). As shown in Figure 1B, ErsA overexpression by pGM-ersA conferred an approximately 2-fold increase in GFP activity compared to the strain harboring the control vector pGM931 (Qiu et al., 2008; Delvillani et al., 2014). Since spurious activating interactions of ErsA with the *sfGFP* open reading frame were ruled out (Ferrara et al., 2015), these results strongly suggested a positive direct modulation of *anr* mRNA by ErsA. Since a non-planktonic growth, e.g., adherent to a surface in form of either biofilm or colony can strongly influence *P. aeruginosa* physiology and gene expression, we assayed the *anr::sfGFP* fusion in *P. aeruginosa* cells grown as extended colonies on agar plates, either in aerobic or anaerobic conditions. As shown in Figure 2A, no significant differences in fluorescence levels of the *anr::sfGFP* fusion between wild-type and Δ ersA mutant strains were observed in both conditions. However, ErsA overexpression from the arabinose inducible pGM-ersA vector resulted in a significantly higher magnitude of induction of the *anr::sfGFP* fusion (Figure 2B) than the

TABLE 1 | Differentially expressed genes (DEGs) in the PAO1 wild-type vs. the Δ ersA mutant strains belonging to regulons responsive to anoxic conditions.

Locus	Description	Δ ersA effect ^a	Log ₂ (FC) ^b	Anaerobic response by ^c		References
				Anr	Low O ₂	
Transcription regulators						
PA1196	probable transcription regulator	D	−2.53	U	U	Alvarez-Ortega and Harwood, 2007; Tribelli et al., 2019
PA2127	<i>cgrA</i> , cupA gene regulator A CgrA	D	−1.57		U	Alvarez-Ortega and Harwood, 2007; Tribelli et al., 2019
PA2663	<i>ppyR</i> , psl and pyoverdine operon regulator PpyR	D	−2.18	U	U	Trunk et al., 2010
PA3006	<i>psrA</i> , transcription regulator PsrA	D	−1.35	U	U	Trunk et al., 2010
PA3458	probable transcription regulator	D	−1.97		U	Trunk et al., 2010
PA3879	<i>narL</i> , two-component response regulator NarL	D	−1.67		U	Trunk et al., 2010
PA3973	probable transcriptional regulator	D	−1.64		U	Trunk et al., 2010
PA4596	<i>esrC</i> , EsrC	D	−2.53		U/D	Alvarez-Ortega and Harwood, 2007; Tribelli et al., 2019
Energy metabolism						
PA3613	D-xylulose 5-phosphate phosphoketolase	D	−1.77		U	Alvarez-Ortega and Harwood, 2007; Tribelli et al., 2019
PA0509	<i>nirN</i> , NirN	U	2.22	U (and U in response to nitrate)		Alvarez-Ortega and Harwood, 2007; Platt et al., 2008
PA3872	<i>narI</i> , respiratory nitrate reductase gamma chain	U	3.08	U (and U in response to nitrate)		Alvarez-Ortega and Harwood, 2007; Platt et al., 2008
PA3873	<i>narJ</i> , respiratory nitrate reductase delta chain	U	2.19	U (and U in response to nitrate)		Alvarez-Ortega and Harwood, 2007; Platt et al., 2008
PA3874	<i>narH</i> , respiratory nitrate reductase beta chain	U	1.65	U (and U in response to nitrate)		Alvarez-Ortega and Harwood, 2007; Platt et al., 2008
Transport						
PA3465	major facilitator superfamily transporter	D	−1.57	U	U	Alvarez-Ortega and Harwood, 2007; Tribelli et al., 2019
PA3877	<i>narK1</i> , nitrite extrusion protein 1	D	−3.06		U	Alvarez-Ortega and Harwood, 2007; Platt et al., 2008; Tribelli et al., 2019
PA4610	copper transporter	D	−1.86	U	U	Trunk et al., 2010; Tribelli et al., 2019
PA5170	<i>arcD</i> , arginine/ornithine antiporter	D	−2.09	U	U	(Trunk et al., 2010; Tribelli et al., 2019)
PA5232	secretion protein HlyD family; glycoside hydrolase family 43	D	−1.29	U	U	Trunk et al., 2010; Tribelli et al., 2019
Cell wall/LPS/capsule						
PA3337	<i>rfaD</i> , ADP-L-glycero-D-mannoheptose 6-epimerase	D	−2.02	U	U	Trunk et al., 2010; Tribelli et al., 2019
Membrane proteins						
PA0563	membrane protein	U	1.50	D	D	Trunk et al., 2010
PA1429	probable cation-transporting P-type ATPase	D	−2.27		U	Alvarez-Ortega and Harwood, 2007; Tribelli et al., 2019
PA1337	<i>ansB</i> , glutaminase-asparaginase	D	−1.28		U	Alvarez-Ortega and Harwood, 2007; Tribelli et al., 2019
PA1546	<i>hemN</i> , oxygen-independent coproporphyrinogen III oxidase	D	−1.58	U	U	Trunk et al., 2010; Tribelli et al., 2019
PA1920	<i>nrdD</i> , class III (anaerobic) ribonucleoside-triphosphate reductase subunit, NrdD	D	−2.06		U	Alvarez-Ortega and Harwood, 2007; Crespo et al., 2017; Tribelli et al., 2019
Antibiotic resistance						
PA3614	metallo-β-lactamase superfamily protein	D	−1.56		U	Trunk et al., 2010; Tribelli et al., 2019
Binding proteins						
PA1673	Bacteriohemerythrin	D	−1.29	U	U	Trunk et al., 2010; Tribelli et al., 2019

(Continued)

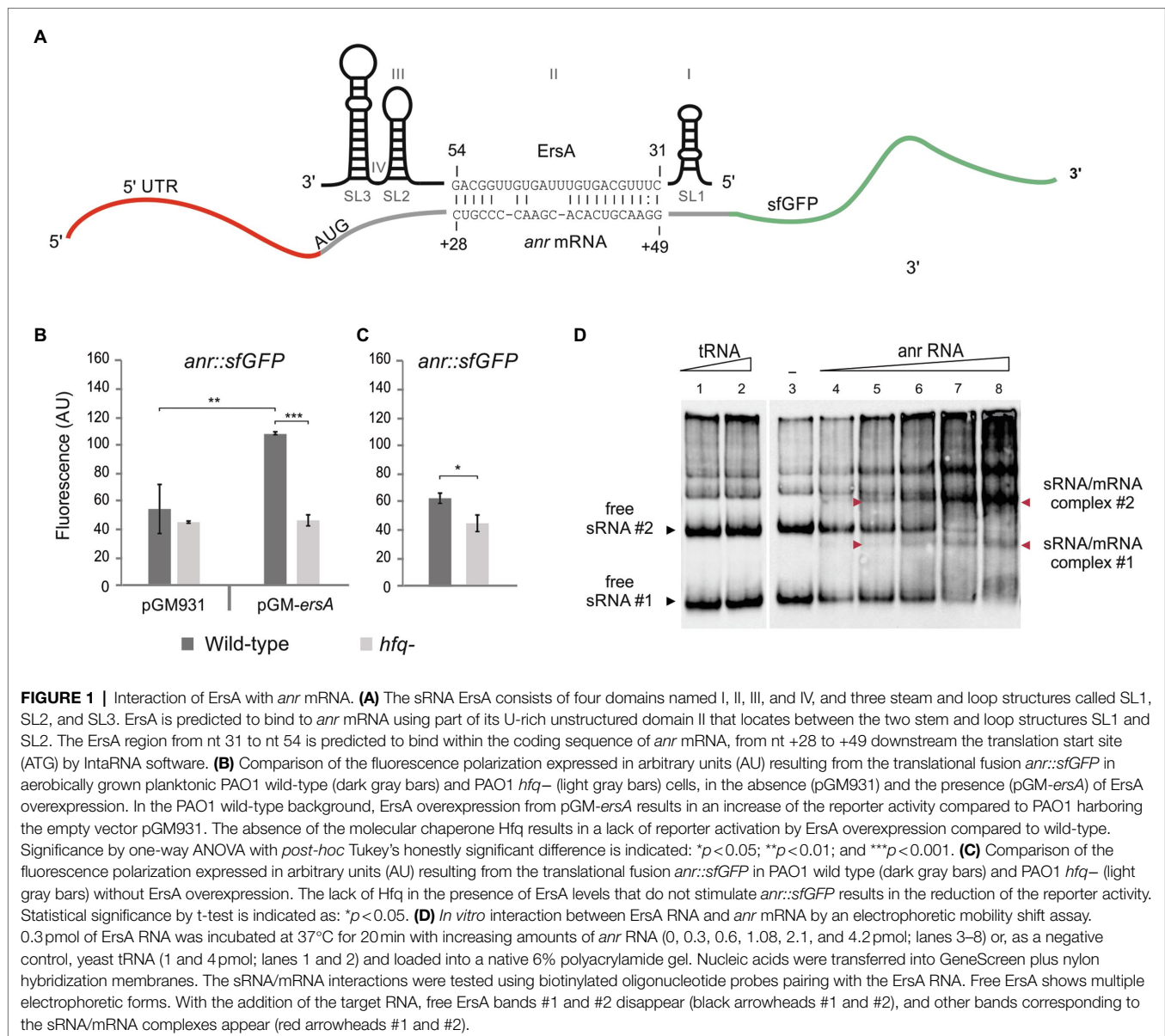
TABLE 1 | Continued

Locus	Description	Δ ersA effect ^a	Log ₂ (FC) ^b	Anaerobic response by ^c		References
				Anr	Low O ₂	
PA4577	transfer protein TraR	D	-1.59	U	U	Trunk et al., 2010; Tribelli et al., 2019
Degradation of chloroaromatic compounds						
PA1597	dienelactone hydrolase	D	-1.52		U	Alvarez-Ortega and Harwood, 2007; Tribelli et al., 2019
Chaperones and heat-shock proteins						
PA3126	<i>ibpA</i> , heat-shock protein IbpA	D	-2.64		U	Trunk et al., 2010
PA4385	<i>groEL</i> , GroEL protein	D	-1.37		D	Alvarez-Ortega and Harwood, 2007; Tribelli et al., 2019
PA4760	<i>dnaJ</i> , DnaJ protein	D	-1.23		D	Alvarez-Ortega and Harwood, 2007; Tribelli et al., 2019
PA4761	<i>dnaK</i> , DnaK protein	D	-1.72		D	Alvarez-Ortega and Harwood, 2007; Tribelli et al., 2019
Translation, post-translational modification, degradation						
PA0579	<i>rpsU</i> , 30S ribosomal protein S21	U	1.41	D	D	Trunk et al., 2010
PA2619	<i>infA</i> , initiation factor	U	1.43	D	D	Trunk et al., 2010
PA4542	<i>clpB</i> , ClpB protein	D	-2.16		U/D	Alvarez-Ortega and Harwood, 2007; Tribelli et al., 2019
Putative enzymes						
PA0506	probable acyl-CoA dehydrogenase	D	-1.95	U	U	Trunk et al., 2010
PA0836	<i>ackA</i> , acetate kinase	D	-1.57		U	Trunk et al., 2010; Tribelli et al., 2019
PA2119	alcohol dehydrogenase (Zn-dependent)	D	-1.70	U	U	Trunk et al., 2010; Tribelli et al., 2019
PA2662	short-chain dehydrogenase	D	-2.03	U	U	Trunk et al., 2010
PA5475	Acetyltransferase	D	-1.65	U	U	Trunk et al., 2010; Tribelli et al., 2019
Hypothetical proteins						
PA0200	hypothetical protein	D	-1.26	U	U	Trunk et al., 2010; Tribelli et al., 2019
PA0526	DnrP	D	-1.96		U	Alvarez-Ortega and Harwood, 2007; Tribelli et al., 2019
PA1789	hypothetical protein	D	-1.57	U	U	Trunk et al., 2010; Tribelli et al., 2019
PA2753	hypothetical protein	D	-1.84	U	U	Trunk et al., 2010
PA2754	conserved hypothetical protein	D	-1.90	U	U	Trunk et al., 2010
PA2937	hypothetical protein	D	-1.93	U	U	Trunk et al., 2010
PA3572	hypothetical protein	D	-1.93		U	Trunk et al., 2010
PA4328	hypothetical protein	D	-1.44	U	U	Trunk et al., 2010; Tribelli et al., 2019
PA4352	conserved hypothetical protein	D	-1.42	U	U	Trunk et al., 2010; Tribelli et al., 2019
PA4387	<i>fxsA</i> , cytoplasmic membrane protein	D	-1.39		U	Trunk et al., 2010
PA5027	hypothetical protein	D	-2.00	U	U	Trunk et al., 2010
PA5446	hypothetical protein	D	-2.17		U	Trunk et al., 2010

^aD, downregulation; U, upregulation^bLog₂ of Fold Change (FC) calculated as ratio of expression in Δ ersA vs. wt^cD, downregulated; U, upregulated.

planktonic conditions (Figure 1B), namely, 5- (surface-grown cells) vs. 2-fold (planktonic cells). This enhanced effect of ErsA overexpression was independent of the presence of oxygen (Figure 2B). Overall, these results suggested that, above a certain abundance threshold, ErsA can enhance Anr mRNA translatability and the ErsA-mediated stimulation is more efficient when cells grow aggregated on a surface.

Furthermore, we aimed to evaluate whether the activity of the RNA chaperone Hfq could influence the ErsA-mediated activation of *anr* expression. This is because the regulatory activity of ErsA was shown to be dependent on Hfq for other targets (e.g., *algC*, *amrZ*, and *oprD*; Ferrara et al., 2015; Falcone et al., 2018; Sonnleitner et al., 2020) and it has been deduced that Hfq stimulates the expression of *anr* by an unknown



mechanism since Anr was less expressed in an *hfq*⁻ mutant of *P. aeruginosa* than in the corresponding wild type (Sonnleitner et al., 2011). The positive influence of Hfq on Anr expression was reconfirmed in our experimental system. As shown in **Figure 1C**, the fluorescence levels expressed by the translational fusion *anr::sfGFP* were significantly lower in the *hfq*⁻ than in the wild-type background. These results suggested that Hfq plays *per se* a direct and positive post-transcriptional regulatory role on *anr*.

Besides, differently from the wild type, the overexpression of ErsA from pGM-*ersA* in an *hfq*⁻ background (Sonnleitner et al., 2003) showed no effects on fluorescence levels generated by the *anr::sfGFP* fusion (**Figure 1B**). Despite Hfq contributes to ErsA stability (Ferrara et al., 2015), overexpression of ErsA from pGM-*ersA* in an *hfq*⁻ strain reaches levels similar to those of the wild type (Ferrara et al., 2015). Therefore, the

Anr activation failure by ErsA in the absence of effective Hfq was a genuine effect which strongly indicated that the ErsA-mediated activation of *anr* expression is an Hfq-dependent mechanism.

To assess *in vitro* the ErsA/*anr* mRNA interaction, the whole ErsA RNA and the *anr* mRNA region spanning -31 (5'-UTR) to +66 were synthesized *in vitro*, mixed, and analyzed on native polyacrylamide gels. We mixed fixed amounts of ErsA RNA with increasing concentrations of target *anr* mRNA. As shown in **Figure 1D**, ErsA showed multiple electrophoretic forms, with two prevalent fast-migrating bands, #1 and #2. After the addition of increasing amounts of the target *anr* mRNA, bands #1 and #2 progressively decreased in intensity, and bands corresponding to the sRNA/mRNA complexes appeared accordingly. No extra-bands formed when increasing amounts of control tRNAs preparation were mixed with ErsA

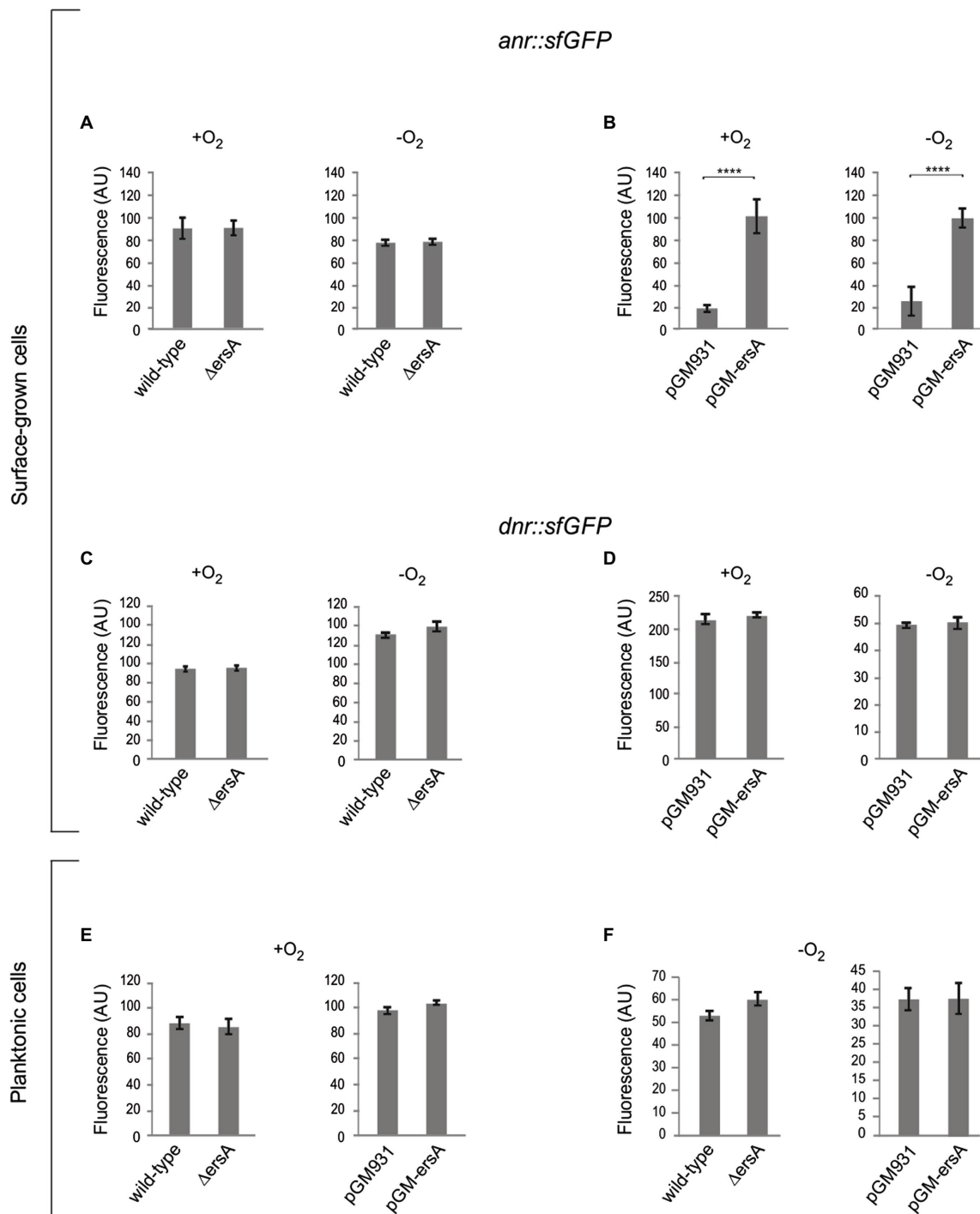


FIGURE 2 | Analysis of the ErsA-mediated modulation of the *anr::sfGFP* and *dnr::sfGFP* translational fusions in surface-grown and planktonic cells, in both aerobic and anaerobic conditions. Fluorescence polarization in arbitrary units (AU) resulting from the translational fusions in PAO1 wild-type and Δ ersA strains, and in PAO1 strains with wild-type background harboring the pGM-ersA vector for ErsA overexpression, or the empty vector pGM931 are reported. **(A)** Comparison of the fluorescence resulting from the translational fusion *anr::sfGFP* in surface-grown PAO1 wild-type and Δ ersA mutant cells. **(B)** Comparison of the fluorescence resulting from the translational fusion *anr::sfGFP* in surface-grown PAO1 wild type harboring the pGM-ersA vector for ErsA overexpression, or the empty vector pGM931. **(C)** Comparison of the fluorescence resulting from the translational fusion *dnr::sfGFP* in surface-grown PAO1 wild-type and Δ ersA mutant cells. **(D)** Comparison of the fluorescence resulting from the translational fusion *dnr::sfGFP* in surface-grown PAO1 wild type harboring the pGM-ersA vector for ErsA overexpression, or the empty vector pGM931. **(E)** and **(F)** Comparison of the fluorescence resulting from the translational fusion *dnr::sfGFP* in planktonic PAO1 wild-type and Δ ersA mutant cells, and PAO1 wild type harboring the pGM-ersA vector for ErsA overexpression, or the empty vector pGM931, respectively. Statistical significance by t-test is indicated as: **** $p < 0.0001$.

RNA. This indicated that ErsA and *anr* RNAs can specifically interact.

We also modeled a possible interaction of ErsA with *dnr* mRNA. The IntaRNA tool predicted that an interval similar to the above nt of the unstructured region of ErsA could couple with the open read frame of *dnr*, from nt 16 to 38 downstream AUG start codon (Supplementary Figure S2). To test *in vivo* this prediction, we generated a *dnr::sfGFP* translational fusion cloning the whole 5'-UTR of the *dnr* gene and 96 nt of its open reading frame, corresponding to the first 32 amino acids of Dnr, fused to *sfGFP*. As in the case of *anr*, we compared the fluorescence of the *dnr::sfGFP* reporter in surface-grown cells of the wild-type and Δ *ersA* strains under aerobic and anaerobic conditions, and no relevant differences were detected between the two strains (Figure 2C). However, differently from *anr::sfGFP*, ErsA overexpression had no effects on *sfGFP* expression (Figure 2D). We performed the same experiments with planktonic cells either in either aerobic or anaerobic conditions and again no effects of ErsA deletion or overexpression were detected, respectively (Figures 2E,F). Overall, these assays did not evidence any regulatory activity of ErsA on the translational fusion *dnr::sfGFP*.

Effects of ErsA Regulation on Anr and Dnr Genes at the Transcription Level in Denitrification Conditions

The results presented above with the *anr::sfGFP* translational fusion revealed no decrease in the translation of Anr in the Δ *ersA* background under any oxygen conditions tested, either in planktonic or surface-grown cells. However, these tests may suffer from sensitivity when evaluating downregulations due to the stability of the reporter gene product vs. the detection of upregulation which is less affected by the half-life of the reporter. Therefore, to evaluate the ErsA-mediated regulation of Anr in physiological conditions of denitrification, we assessed whether the loss of ErsA and the ensuing expected decrease of translation rate could influence negatively the *anr* mRNA abundance in anaerobiosis. According to the well-characterized regulatory link between Anr and Dnr during anaerobic growth, i.e., the *dnr* gene is transcriptionally activated by Anr, the *dnr* mRNA levels were also expected to decrease in the Δ *ersA* background. On these bases, we evaluated the mRNA levels of both *anr* and *dnr* expressed under anaerobic conditions in surface-grown cells of the PAO1 wild-type and Δ *ersA* strains. Total RNAs were extracted from cell cultures grown for 3 days in agar plates with BHI supplemented with 100 mM KNO₃ in a jar for anaerobiosis and analyzed by qRT-PCR. As shown in Table 2, the expression of *anr* showed a 1.26-fold decrease in the Δ *ersA* mutant relative to the wild-type strain. This was accompanied by a 1.53-fold decrease in *dnr* expression again in the Δ *ersA* mutant.

These results are consistent with positive ErsA-mediated regulation of Anr in denitrification conditions. According to the well-known effect that translation potential affects mRNA stability, it is conceivable that the *anr* mRNA is more prone

to degradation because of lower translatability in the absence of ErsA. Lower levels of Anr would lead to a lower degree of activation of the transcription of *dnr* and thus to a decrease in the abundance of *dnr* mRNA.

ErsA Plays a Critical Role in the Growth of a CF-Adapted *P. aeruginosa* Strain in Denitrification and Arginine Fermentation Conditions

Although it was possible to detect the regulatory effects of ErsA on Anr and, subsequently, on Dnr during anaerobic respiration (Table 2), this ErsA role did not appear to be critical for *P. aeruginosa* PAO1 growth in these conditions. Since the experiments described above were not suited to quantitatively compare the growth efficiency between PAO1 wild-type and the Δ *ersA* mutants, we repeated the bacterial cell plating on BHI supplemented with KNO₃ and incubated in anaerobiosis by spotting calibrated volumes of serial dilutions of quantified cell suspensions. We aimed also to assay in this way the other more virulent reference *P. aeruginosa* PA14 strain and the corresponding Δ *ersA* mutant (Ferrara et al., 2015). As anticipated, no substantial differences in growth rate and efficiency under denitrification conditions were detected between both PAO1 (Figure 3) and PA14 and their corresponding Δ *ersA* mutants. However, some important metabolic pathways occurring in low-oxygen conditions, such for instance denitrification, are perturbed by the competition for Hfq by the sRNA CrcZ, which can result in diminished anoxic growth and biofilm formation in *P. aeruginosa* (Pusic et al., 2016). It was indeed speculated that the Hfq sequestration-mediated function of CrcZ in limiting biofilm formation might be associated with the adaptive microevolution of *P. aeruginosa* for long-term persistence in the harsh environment of the CF airways (Pusic et al., 2016). Therefore, we wondered whether the regulatory effects of ErsA on Anr might be critical for the growth of a clinical strain of *P. aeruginosa* adapted for CF. To this end, we performed the calibrated bacterial cell plating on BHI supplemented with KNO₃ and incubation in anaerobiosis comparing the *P. aeruginosa* multi-drug resistant clinical isolate RP73 (Bianconi et al., 2015) with the corresponding Δ *ersA* mutant strain (Ferrara et al., 2020).

TABLE 2 | Relative expression of *anr* and *dnr* in wild-type vs. Δ *ersA* PAO1 strains determined by qRT-PCR.

Strain	Relative expression ^a (2 ^{-ΔΔCT})	
	<i>anr</i>	<i>dnr</i>
PAO1 wild type	1.00	1.00
PAO1 Δ <i>ersA</i>	0.79	0.65

^aThe calculation of the relative expression of the *anr* and *dnr* genes in the Δ *ersA* mutant vs. the WT strain was performed as described by the 2^{-ΔΔCT} method (Livak and Schmittgen, 2001; Vitale et al., 2008). Values represent the average of two independent experiments where qRT-PCR amplification of each sample was performed in (technical) triplicate reactions.

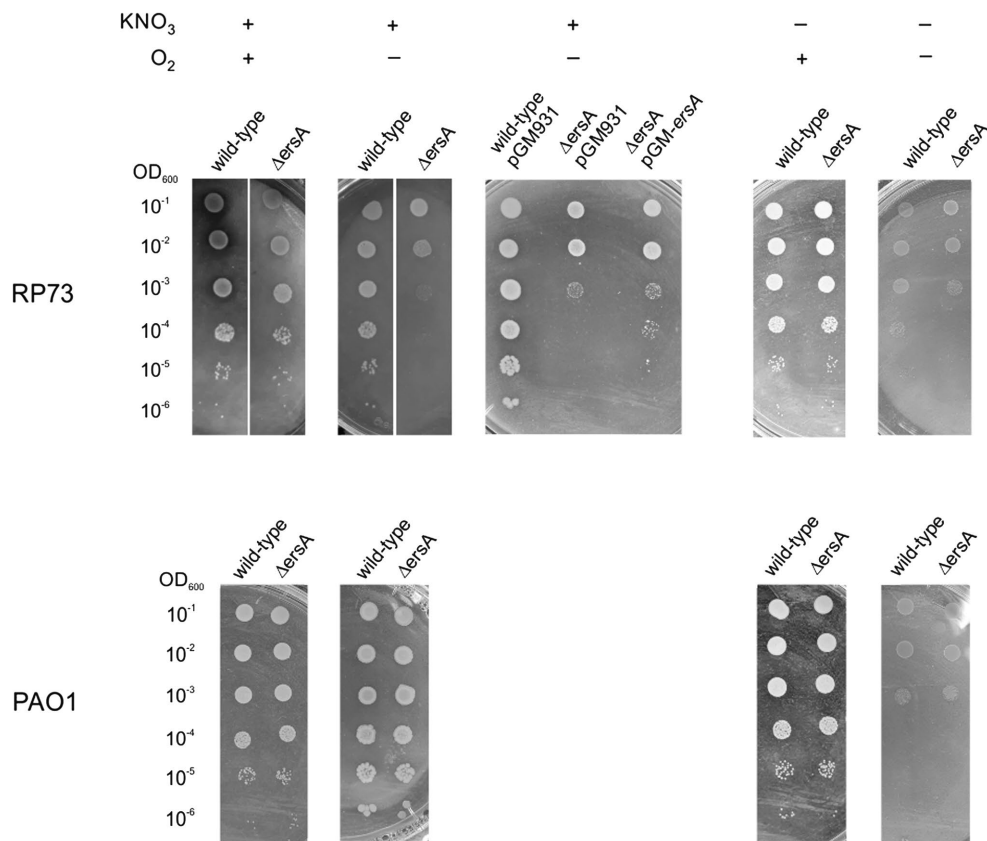


FIGURE 3 | ErsA deletion impairs anaerobic growth in the RP73 clinical isolate. 2 μ l of cultures of the wild-type *P. aeruginosa* clinical isolate RP73 and PAO1 along with the corresponding Δ ersA mutants, serially diluted 10-fold, were spotted into BHI agar plates supplemented with 100 mM KNO_3 to allow anaerobic respiration or without KNO_3 addition to assess arginine fermentation capacity. Plates were incubated under aerobic (+O₂) or anaerobic (-O₂) conditions. The presented results are representative of three independent experiments.

As shown in **Figure 3**, RP73 Δ ersA is strongly impaired in growing under denitrification conditions compared to wild type as evidenced by colonies extremely smaller and plating efficiency at least 10-fold lower. In the absence of KNO_3 without oxygen, we also evaluated arginine fermentation for both PAO1 and RP73 and the corresponding Δ ersA mutants. As shown in **Figure 3**, differently from PAO1, the loss of ErsA in RP73 strongly impairs also arginine fermentation, the other energy process for which Anr is critical. Despite the *ersA* gene deletion in the *polA-engB* intergenic region shows no polar effects on flanking genes (Falcone et al., 2018) and the mutagenesis protocols that we used to generate it are suited to hinder secondary off-site mutations (Ferrara et al., 2015), we evaluated the effects on denitrification capacity of the RP73 Δ ersA strain following the reintroduction of the *ersA* gene expressed from pGM-ersA. As shown in **Figure 3**, pGM-ersA could complement the nitrate respiration in the RP73 Δ ersA, further supporting the notion that ErsA regulation is key for denitrification in the RP73 *CF*-adapted strain. Taken together, this suggested that *P. aeruginosa* adaptation to *CF* lung might result in a higher dependence on ErsA for the regulation of anaerobic energy metabolism.

DISCUSSION

The sRNA ErsA is inducible by different cues relevant for airway infection, such as, for instance, envelope stress and shift from aerobic to anaerobic conditions (**Figure 4**). This environmental response is translated by ErsA in the modulation of biofilm dynamics through the activation of the AmrZ regulon (Falcone et al., 2018), the repression of a crossroad, the enzyme AlgC, of important pathways for the biosynthesis of sugar precursor leading to exopolysaccharides production (Ferrara et al., 2015), and of carbapenem resistance, via the negative regulation of porin OprD (Zhang et al., 2017). For its role in biofilm regulation, ErsA has been implicated as an important player in the regulatory network of *P. aeruginosa* pathogenicity in airway infection (Ferrara et al., 2020). With this work, we add a new piece to the ErsA role of transducing environmental signals into physiological responses showing that ErsA positively regulates Anr levels. Since Anr is the master regulator of the anaerobic response of *P. aeruginosa*, with a regulon of approximately 170 predicted transcription units (Trunk et al., 2010), ErsA rises to the role of a key co-mediator of the *P. aeruginosa* anaerobic metabolism.

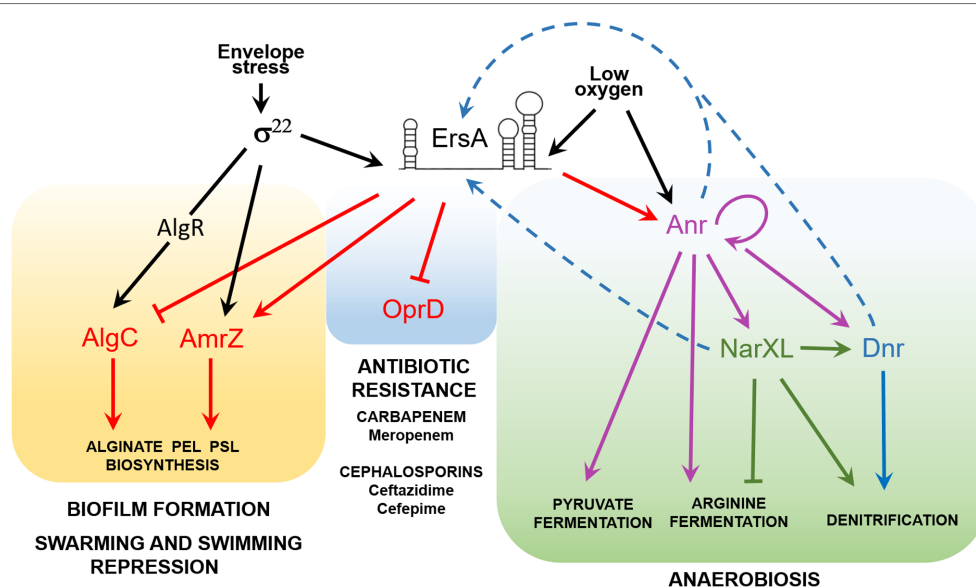


FIGURE 4 | The ErsA regulatory network in *P. aeruginosa*. Acting as a post-transcriptional modulator, ErsA influences several virulence traits of *P. aeruginosa*, related to biofilm formation, repression of swarming and twitching motility, antibiotic resistance, and metabolic adaptation to low-oxygen environments typical of CF lung infection. ErsA modulates alginate and exopolysaccharides (Pel and Psl) production by activating the AmrZ regulon and through the fine-tuning of AlgC levels. The regulatory circuit is mediated by the envelope stress-responsive sigma factor σ^{22} , which in *P. aeruginosa* triggers ErsA levels and is responsible for the transcription of *amrZ* mRNA and the activation of *algC* through the regulator AlgR. ErsA negatively regulates the expression of the major porin *oprD*, responsible for the uptake of carbapenem antibiotics, thus leading to increased resistance to meropenem. By unknown mechanisms, ErsA contributes also to ceftazidime and cefepime resistance, two antibiotics that belong to the class of cephalosporins. ErsA modulates the expression of genes for anaerobic growth and survival. Low-oxygen levels trigger the transcription of ErsA, which positively modulates the expression of the transcription factor Anr, the master regulator of anaerobiosis. Activation of Anr by dimerization is also promoted by low-oxygen tension. Other genes involved in anaerobic adaptation are also regulated by ErsA by an unknown mechanism. The signal that activates ErsA expression under an anaerobic or low-oxygen environment is still unknown. We speculate that ErsA expression can be controlled by transcription factors like Anr, Dnr, or NarXL (blue dotted arrows). A putative NarL box (TACCGCT) is present from 179 to 173nt upstream of the *ersA* transcription start site.

Furthermore, this work highlights how ErsA can constitute a flexible regulatory node linked to the adaptive plasticity of *P. aeruginosa*. This is evidenced by the fact that the lack of ErsA dramatically impacts the possibility to grow by anaerobic nitrate respiration and arginine fermentation of a strain adapted to the CF lung environment, RP73, and not of reference strains, such as PAO1 and PA14. This phenomenon is coupled with the results of our previous work where the lack of ErsA in RP73 induced sensitivity to the antibiotics ceftazidime, cefepime, meropenem, and ciprofloxacin, suggesting that ErsA could contribute to *P. aeruginosa* adaptation to long-term antibiotic treatment undergone by CF patients. Dynamicity of the regulatory networks of bacterial functions for long-term persistence in the CF lung environment is frequently observed during the adaptive radiation of *P. aeruginosa* in such context where bacteria endure various attacks, encompassing oxidative stresses, immune responses, and prolonged antibiotic treatments. Our results suggest that the genetic adaptation to CF lung occurred in the strain RP73 might have led to a higher dependence on ErsA for the transduction of the multiple signals to the regulatory network of key functions for survivance in such a complex environment. In addition, other factors linked to ErsA might be critical for denitrification

regulation in the CF-adapted RP73 and not in the reference strain PAO1.

From a mechanistic point of view, we can speculate that ErsA expression in response to environmental factors, such as anaerobiosis and possibly other cues in CF lungs, can be modulated to compensate for physiological adaptations involving a decrease in the amounts of effective Hfq, which is known to have a large regulon (Sonnleitner et al., 2006) and a pivotal role in *P. aeruginosa* physiology (anaerobic metabolism included) and virulence (Sonnleitner et al., 2003; Pusic et al., 2016). A key regulator impacting the abundance of effective Hfq is the sRNA CrcZ that acts as a decoy to abrogate Hfq-mediated translational repression of catabolic genes (Sonnleitner and Blasi, 2014) and indeed mediating the carbon catabolite repression (CCR) mechanism in *P. aeruginosa* but also implementing Hfq sequestration for the cross-regulation of the panoply of Hfq-dependent physiological processes (Pusic et al., 2016). For example, high levels of CrcZ and therefore low abundance of active Hfq were evoked to explain the limitation of anoxic biofilm formation and this scenario could occur in the adaptation of *P. aeruginosa* to the CF lung (Pusic et al., 2016). In this context, the regulatory node of ErsA could co-adapt and become critical to compensate for the limiting amount of effective Hfq.

The mediating role of Hfq in anaerobic metabolism appears to be large and important. The absence of Hfq results in an increased abundance of transcripts encoded by the *nar*, *nap*, and *nor* operons, encoding enzymes required for denitrification. Besides, several *nuo* transcripts, encoding subunits of the NADH dehydrogenase, were downregulated in the absence of Hfq (Pusic et al., 2016). Incidentally, the NADH dehydrogenase is required for anaerobic growth in the presence of nitrate, contributes to the intracellular redox balance, i.e., the NADH/NAD⁺ ratio, and is linked to the energizing processes of the membrane and ATP synthesis. Furthermore, it was reported that Hfq stimulates the expression of *anr* by an unknown mechanism (Sonnleitner et al., 2011).

Our results strongly suggest that this regulation is directly given by Hfq at the post-transcriptional level. Furthermore, beyond a certain threshold of abundance, we show that ErsA participates in the positive regulation of Anr through an Hfq-dependent mechanism. Also for *anr* mRNA, the role of Hfq chaperone could be that of favoring the ErsA/*anr* mRNA interaction pathway which may result in enhanced translatability of the *anr* mRNA due, for example, to the increased accessibility of the translation start site. This positive ErsA-mediated effect would be a component of the *anr* mRNA stabilization and consistent with the decrease in *anr* mRNA abundance in the lack of ErsA. Besides, we can postulate an additional interplay between ErsA and Hfq in the post-transcriptional regulation of Anr based on reciprocal recruitment on *anr* mRNA which might stabilize the transcript and participates further in the positive effects on Anr translation.

Therefore, this work suggests the correlation between the property of ErsA of being transcriptionally activated under reduced oxygen conditions (Ferrara et al., 2015), and its role in participating in the transduction of the low-oxygen cue toward the Anr regulon, acting as a positive post-transcriptional regulator of the *anr* mRNA. However, other environmental signals modulating ErsA could be important in the fine-tuning of the Anr regulon.

From the point of view of the *P. aeruginosa* anaerobic lifestyle during airways infection, it was shown that a Δanr mutant is attenuated in a mouse pneumonia model of acute infection (Jackson et al., 2013). Besides, the *anr* gene deletion leads to defective biofilm formation, while increased Anr activity results in enhanced biofilm formation (Jackson et al., 2013). Despite the differences in the experimental setting of infections, the strong attenuation of acute infection that we reported for the PAO1 $\Delta ersA$ mutant (Ferrara et al., 2020) is consistent with the *P. aeruginosa* behavior in the absence of Anr described previously. The lack of ErsA-mediated regulation of several factors, including Anr, could prevent the formation of biofilm-like aggregates that assemble on airway surfaces (Tran et al., 2014) and promote mucosal colonization leading to bypassing the epithelial barrier and thus invasion and systemic dissemination (Sadikot et al., 2005).

In this work, we also propose that the role of ErsA in regulating the anaerobic physiology of *P. aeruginosa* is broader than the upstream co-modulation of Anr regulon, whose

most important regulatory member is undoubtedly Dnr. Indeed, the transcriptional profile of the *ersA* mutant also shows a dysregulation of genes not belonging to Anr regulon but still involved in anaerobic metabolism (Falcone et al., 2018). It is therefore plausible that ErsA exerts other regulatory functions, acting as a direct or indirect regulator of the genes listed in **Table 1**. Other unlisted genes may also be direct targets that have not been detected due to a “below-threshold” concentration of ErsA in the wild-type strain or to unimpaired mRNA stability in the *ersA* mutant. The *algC* gene is a representative example of the second case, whose mRNA levels are comparable in the *ersA* mutant and the wild type (Ferrara et al., 2015).

In summary, the list of known ErsA-regulated genes is becoming more and more populated (**Figure 4**) and with this work, it has extended to anaerobic metabolism. It is evident that important ErsA-modulated *P. aeruginosa* phenotypes are related to both acute and chronic airway infection and, associated with the latter, to adaptive microevolution in the CF environment.

DATA AVAILABILITY STATEMENT

The raw data supporting the conclusions of this article will be made available by the authors, without undue reservation.

AUTHOR CONTRIBUTIONS

GB and SF conceived, designed the study, and wrote the paper. SF, RC, SS, and GB conceived the experiments and analyzed the data. SF, RC, and SS designed and performed the experiments. All authors contributed to the article and approved the submitted version.

FUNDING

This work has been supported by the European Commission grant NABATIVI-223670 EUFP7-HEALTH-2007-B (to GB) and Italian Cystic Fibrosis Research Foundation grant FFC#13/2015 (to GB) with the contribution of Gruppo di Sostegno FFC di Sassari Castelsardo and Delegazione FFC di Boschi Sant'Anna Minerbe, grant FFC#14/2016 (to GB) with the contribution of Delegazione FFC di Reggio Calabria and Gruppo di Sostegno FFC di Vigevano, and grant FFC#10/2020 (to GB) with the contribution of Delegazione FFC di Firenze and Delegazione FFC di Prato.

SUPPLEMENTARY MATERIAL

The Supplementary material for this article can be found online at <https://www.frontiersin.org/articles/10.3389/fmicb.2021.691608/full#supplementary-material>

REFERENCES

- Alvarez-Ortega, C., and Harwood, C. S. (2007). Responses of *Pseudomonas aeruginosa* to low oxygen indicate that growth in the cystic fibrosis lung is by aerobic respiration. *Mol. Microbiol.* 65, 153–165. doi: 10.1111/j.1365-2958.2007.05772.x
- Arai, H. (2011). Regulation and function of versatile aerobic and anaerobic respiratory metabolism in *Pseudomonas aeruginosa*. *Front. Microbiol.* 2:103. doi: 10.3389/fmicb.2011.00103
- Bianconi, I., Jeukens, J., Freschi, L., Alcalá-Franco, B., Facchini, M., Boyle, B., et al. (2015). Comparative genomics and biological characterization of sequential *Pseudomonas aeruginosa* isolates from persistent airways infection. *BMC Genomics* 16:1105. doi: 10.1186/s12864-015-2276-8
- Carlson, C. A., and Ingraham, J. L. (1983). Comparison of denitrification by *Pseudomonas stutzeri*, *Pseudomonas aeruginosa*, and *Paracoccus denitrificans*. *Appl. Environ. Microbiol.* 45, 1247–1253. doi: 10.1128/aem.45.4.1247-1253.1983
- Corcoran, C. P., Podkaminski, D., Papenfort, K., Urban, J. H., Hinton, J. C., and Vogel, J. (2012). Superfolder GFP reporters validate diverse new mRNA targets of the classic porin regulator, MicF RNA. *Mol. Microbiol.* 84, 428–445. doi: 10.1111/j.1365-2958.2012.08031.x
- Crespo, A., Gavalda, J., Julian, E., and Torrents, E. (2017). A single point mutation in class III ribonucleotide reductase promoter renders *Pseudomonas aeruginosa* PAO1 inefficient for anaerobic growth and infection. *Sci. Rep.* 7:13350. doi: 10.1038/s41598-017-14051-2
- Davies, K. J., Lloyd, D., and Boddy, L. (1989). The effect of oxygen on denitrification in *Paracoccus denitrificans* and *Pseudomonas aeruginosa*. *J. Gen. Microbiol.* 135, 2445–2451. doi: 10.1099/00221287-135-9-2445
- Delvillani, F., Sciadrone, B., Peano, C., Petiti, L., Berens, C., Georgi, C., et al. (2014). Tet-trap, a genetic approach to the identification of bacterial RNA thermometers: application to *Pseudomonas aeruginosa*. *RNA* 20, 1963–1976. doi: 10.1261/rna.044354.114
- Eschbach, M., Schreiber, K., Trunk, K., Buer, J., Jahn, D., and Schobert, M. (2004). Long-term anaerobic survival of the opportunistic pathogen *Pseudomonas aeruginosa* via pyruvate fermentation. *J. Bacteriol.* 186, 4596–4604. doi: 10.1128/JB.186.14.4596-4604.2004
- Falcone, M., Ferrara, S., Rossi, E., Johansen, H. K., Molin, S., and Bertoni, G. (2018). The small RNA ErsA of *Pseudomonas aeruginosa* contributes to biofilm development and motility through post-transcriptional modulation of AmrZ. *Front. Microbiol.* 9:238. doi: 10.3389/fmicb.2018.00238
- Ferrara, S., Carloni, S., Fulco, R., Falcone, M., Macchi, R., and Bertoni, G. (2015). Post-transcriptional regulation of the virulence-associated enzyme AlgC by the σ_{22} -dependent small RNA ErsA of *Pseudomonas aeruginosa*. *Environ. Microbiol.* 17, 199–214. doi: 10.1111/1462-2920.12590
- Ferrara, S., Falcone, M., Macchi, R., Bragonzi, A., Girelli, D., Cariani, L., et al. (2017). The PAPI-1 pathogenicity island-encoded small RNA PesA influences *Pseudomonas aeruginosa* virulence and modulates pyocin S3 production. *PLoS One* 12:e0180386. doi: 10.1371/journal.pone.0180386
- Ferrara, S., Rossi, A., Ranucci, S., De Fino, I., Bragonzi, A., Cigana, C., et al. (2020). The small RNA ErsA plays a role in the regulatory network of *Pseudomonas aeruginosa* pathogenicity in airway infections. *mSphere* 5:00909–20. doi: 10.1128/mSphere.00909-20
- Filiatrault, M. J., Picardo, K. F., Ngai, H., Passador, L., and Iglewski, B. H. (2006). Identification of *Pseudomonas aeruginosa* genes involved in virulence and anaerobic growth. *Infect. Immun.* 74, 4237–4245. doi: 10.1128/IAI.02014-05
- Galimand, M., Gamper, M., Zimmermann, A., and Haas, D. (1991). Positive FNR-like control of anaerobic arginine degradation and nitrate respiration in *Pseudomonas aeruginosa*. *J. Bacteriol.* 173, 1598–1606. doi: 10.1128/jb.173.5.1598-1606.1991
- Govan, J. R., and Deretic, V. (1996). Microbial pathogenesis in cystic fibrosis: mucoid *Pseudomonas aeruginosa* and *Burkholderia cepacia*. *Microbiol. Rev.* 60, 539–574. doi: 10.1128/mr.60.3.539-574.1996
- Hassett, D. J., Sutton, M. D., Schurr, M. J., Herr, A. B., Caldwell, C. C., and Matu, J. O. (2009). *Pseudomonas aeruginosa* hypoxic or anaerobic biofilm infections within cystic fibrosis airways. *Trends Microbiol.* 17, 130–138. doi: 10.1016/j.tim.2008.12.003
- Jackson, A. A., Gross, M. J., Daniels, E. F., Hampton, T. H., Hammond, J. H., Vallet-Gely, I., et al. (2013). Anr and its activation by PlcH activity in *Pseudomonas aeruginosa* host colonization and virulence. *J. Bacteriol.* 195, 3093–3104. doi: 10.1128/JB.02169-12
- Kovach, M. E., Elzer, P. H., Hill, D. S., Robertson, G. T., Farris, M. A., Roop, R. M. 2nd, et al. (1995). Four new derivatives of the broad-host-range cloning vector pBBR1MCS, carrying different antibiotic-resistance cassettes. *Gene* 166, 175–176. doi: 10.1016/0378-1119(95)00584-1
- Livak, K. J., and Schmittgen, T. D. (2001). Analysis of relative gene expression data using real-time quantitative PCR and the 2⁻(Delta C(T)) method. *Methods* 25, 402–408. doi: 10.1006/meth.2001.1262
- Luthi, E., Baur, H., Gamper, M., Brunner, F., Villeval, D., Mercenier, A., et al. (1990). The arc operon for anaerobic arginine catabolism in *Pseudomonas aeruginosa* contains an additional gene, arcD, encoding a membrane protein. *Gene* 87, 37–43. doi: 10.1016/0378-1119(90)90493-B
- Platt, M. D., Schurr, M. J., Sauer, K., Vazquez, G., Kukavica-Ibrulj, I., Potvin, E., et al. (2008). Proteomic, microarray, and signature-tagged mutagenesis analyses of anaerobic *Pseudomonas aeruginosa* at pH 6.5, likely representing chronic, late-stage cystic fibrosis airway conditions. *J. Bacteriol.* 190, 2739–2758. doi: 10.1128/JB.01683-07
- Pusic, P., Tata, M., Wolfinger, M. T., Sonnleitner, E., Haussler, S., and Blasi, U. (2016). Cross-regulation by CrcZ RNA controls anoxic biofilm formation in *Pseudomonas aeruginosa*. *Sci. Rep.* 6:39621. doi: 10.1038/srep39621
- Qiu, D., Damron, F. H., Mima, T., Schweizer, H. P., and Yu, H. D. (2008). PBAD-based shuttle vectors for functional analysis of toxic and highly regulated genes in *Pseudomonas* and *Burkholderia* spp. and other bacteria. *Appl. Environ. Microbiol.* 74, 7422–7426. doi: 10.1128/AEM.01369-08
- Sadikot, R. T., Blackwell, T. S., Christman, J. W., and Prince, A. S. (2005). Pathogen-host interactions in *Pseudomonas aeruginosa* pneumonia. *Am. J. Respir. Crit. Care Med.* 171, 1209–1223. doi: 10.1164/rccm.200408-1044SO
- Schobert, M., and Jahn, D. (2010). Anaerobic physiology of *Pseudomonas aeruginosa* in the cystic fibrosis lung. *Int. J. Med. Microbiol.* 300, 549–556. doi: 10.1016/j.ijmm.2010.08.007
- Schreiber, K., Krieger, R., Benkert, B., Eschbach, M., Arai, H., Schobert, M., et al. (2007). The anaerobic regulatory network required for *Pseudomonas aeruginosa* nitrate respiration. *J. Bacteriol.* 189, 4310–4314. doi: 10.1128/JB.00240-07
- Sonnleitner, E., and Blasi, U. (2014). Regulation of Hfq by the RNA CrcZ in *Pseudomonas aeruginosa* carbon catabolite repression. *PLoS Genet.* 10:e1004440. doi: 10.1371/journal.pgen.1004440
- Sonnleitner, E., Gonzalez, N., Sorger-Domenig, T., Heeb, S., Richter, A. S., Backofen, R., et al. (2011). The small RNA PhrS stimulates synthesis of the *Pseudomonas aeruginosa* quinolone signal. *Mol. Microbiol.* 80, 868–885. doi: 10.1111/j.1365-2958.2011.07620.x
- Sonnleitner, E., Hagens, S., Rosenau, F., Wilhelm, S., Habel, A., Jager, K. E., et al. (2003). Reduced virulence of a Hfq mutant of *Pseudomonas aeruginosa* O1. *Microb. Pathog.* 35, 217–228. doi: 10.1016/S0882-4010(03)00149-9
- Sonnleitner, E., Pusic, P., Wolfinger, M. T., and Blasi, U. (2020). Distinctive regulation of Carbapenem susceptibility in *Pseudomonas aeruginosa* by Hfq. *Front. Microbiol.* 11:1001. doi: 10.3389/fmicb.2020.01001
- Sonnleitner, E., Schuster, M., Sorger-Domenig, T., Greenberg, E. P., and Blasi, U. (2006). Hfq-dependent alterations of the transcriptome profile and effects on quorum sensing in *Pseudomonas aeruginosa*. *Mol. Microbiol.* 59, 1542–1558. doi: 10.1111/j.1365-2958.2006.05032.x
- Stewart, P. S., and Franklin, M. J. (2008). Physiological heterogeneity in biofilms. *Nat. Rev. Microbiol.* 6, 199–210. doi: 10.1038/nrmicro1838
- Stover, C. K., Pham, X. Q., Erwin, A. L., Mizoguchi, S. D., Warrenner, P., Hickey, M. J., et al. (2000). Complete genome sequence of *Pseudomonas aeruginosa* PAO1, an opportunistic pathogen. *Nature* 406, 959–964. doi: 10.1038/35023079
- Tran, C. S., Rangel, S. M., Almblad, H., Kierbel, A., Givskov, M., Tolker-Nielsen, T., et al. (2014). The *Pseudomonas aeruginosa* type III translocon is required for biofilm formation at the epithelial barrier. *PLoS Pathog.* 10:e1004479. doi: 10.1371/journal.ppat.1004479
- Tribelli, P. M., Lujan, A. M., Pardo, A., Ibarra, J. G., Fernandez Do Porto, D., Smania, A., et al. (2019). Core regulon of the global anaerobic regulator Anr targets central metabolism functions in *Pseudomonas* species. *Sci. Rep.* 9:9065. doi: 10.1038/s41598-019-45541-0
- Trunk, K., Benkert, B., Quack, N., Munch, R., Scheer, M., Garbe, J., et al. (2010). Anaerobic adaptation in *Pseudomonas aeruginosa*: definition of the Anr and Dnr regulons. *Environ. Microbiol.* 12, 1719–1733. doi: 10.1111/j.1462-2920.2010.02252.x

- Vander Wauven, C., Pierard, A., Kley-Raymann, M., and Haas, D. (1984). *Pseudomonas aeruginosa* mutants affected in anaerobic growth on arginine: evidence for a four-gene cluster encoding the arginine deiminase pathway. *J. Bacteriol.* 160, 928–934. doi: 10.1128/jb.160.3.928-934.1984
- Vitale, E., Milani, A., Renzi, F., Galli, E., Rescalli, E., De Lorenzo, V., et al. (2008). Transcriptional wiring of the TOL plasmid regulatory network to its host involves the submission of the σ 54-promoter Pu to the response regulator PprA. *Mol. Microbiol.* 69, 698–713. doi: 10.1111/j.1365-2958.2008.06321.x
- Worlitzsch, D., Tarran, R., Ulrich, M., Schwab, U., Cekici, A., Meyer, K. C., et al. (2002). Effects of reduced mucus oxygen concentration in airway *pseudomonas* infections of cystic fibrosis patients. *J. Clin. Invest.* 109, 317–325. doi: 10.1172/JCI0213870
- Wright, P. R., Georg, J., Mann, M., Sorescu, D. A., Richter, A. S., Lott, S., et al. (2014). CopraRNA and IntaRNA: predicting small RNA targets, networks and interaction domains. *Nucleic Acids Res.* 42, W119–W123. doi: 10.1093/nar/gku359
- Ye, R. W., Haas, D., Ka, J. O., Krishnapillai, V., Zimmermann, A., Baird, C., et al. (1995). Anaerobic activation of the entire denitrification pathway in *Pseudomonas aeruginosa* requires Anr, an analog of Fnr. *J. Bacteriol.* 177, 3606–3609. doi: 10.1128/jb.177.12.3606-3609.1995
- Yoon, S. S., Hennigan, R. F., Hilliard, G. M., Ochsner, U. A., Parvatiyar, K., Kamani, M. C., et al. (2002). *Pseudomonas aeruginosa* anaerobic respiration in biofilms: relationships to cystic fibrosis pathogenesis. *Dev. Cell* 3, 593–603. doi: 10.1016/S1534-5807(02)00295-2
- Zhang, Y. F., Han, K., Chandler, C. E., Tjaden, B., Ernst, R. K., and Lory, S. (2017). Probing the sRNA regulatory landscape of *P. aeruginosa*: post-transcriptional control of determinants of pathogenicity and antibiotic susceptibility. *Mol. Microbiol.* 106, 919–937. doi: 10.1111/mmi.13857
- Zimmermann, A., Reimann, C., Galimand, M., and Haas, D. (1991). Anaerobic growth and cyanide synthesis of *Pseudomonas aeruginosa* depend on anr, a regulatory gene homologous with fnr of *Escherichia coli*. *Mol. Microbiol.* 5, 1483–1490. doi: 10.1111/j.1365-2958.1991.tb00794.x
- Zumft, W. G. (1997). Cell biology and molecular basis of denitrification. *Microbiol. Mol. Biol. Rev.* 61, 533–616. doi: 10.1128/mmbr.61.4.533-616.1997

Conflict of Interest: The authors declare that the research was conducted in the absence of any commercial or financial relationships that could be construed as a potential conflict of interest.

Publisher's Note: All claims expressed in this article are solely those of the authors and do not necessarily represent those of their affiliated organizations, or those of the publisher, the editors and the reviewers. Any product that may be evaluated in this article, or claim that may be made by its manufacturer, is not guaranteed or endorsed by the publisher.

Copyright © 2021 Ferrara, Carrubba, Santoro and Bertoni. This is an open-access article distributed under the terms of the Creative Commons Attribution License (CC BY). The use, distribution or reproduction in other forums is permitted, provided the original author(s) and the copyright owner(s) are credited and that the original publication in this journal is cited, in accordance with accepted academic practice. No use, distribution or reproduction is permitted which does not comply with these terms.

Advantages of publishing in Frontiers



OPEN ACCESS

Articles are free to read
for greatest visibility
and readership



FAST PUBLICATION

Around 90 days
from submission
to decision



HIGH QUALITY PEER-REVIEW

Rigorous, collaborative,
and constructive
peer-review



TRANSPARENT PEER-REVIEW

Editors and reviewers
acknowledged by name
on published articles

Frontiers

Avenue du Tribunal-Fédéral 34
1005 Lausanne | Switzerland

Visit us: www.frontiersin.org

Contact us: frontiersin.org/about/contact



REPRODUCIBILITY OF RESEARCH

Support open data
and methods to enhance
research reproducibility



DIGITAL PUBLISHING

Articles designed
for optimal readership
across devices



FOLLOW US

@frontiersin



IMPACT METRICS

Advanced article metrics
track visibility across
digital media



EXTENSIVE PROMOTION

Marketing
and promotion
of impactful research



LOOP RESEARCH NETWORK

Our network
increases your
article's readership